Molecular Modelling of EF-Tu

Julie Davey Dalsgaard Lund

Master's Thesis

September 2006

Department of Chemistry
University of Aarhus
Denmark

Abstract

More and more resistant bacteria are found today and it becomes increasingly difficult to treat the infections they cause. Therefore, it is essential that there is a constant development of new and improved antibiotics. Unfortunately, the process of finding lead compounds is long and difficult using traditional laboratory-based methods. *De novo* design methods and computer-aided docking simulations are promising and novel ways of speeding up the design and test process. This thesis presents rational drug design for the inhibition of the elongation factor Tu (EF-Tu) and shows that it is possible to design lead compounds that have an inhibitory effect on EF-Tu. There are already known inhibitors of EF-Tu and two of these, kirromycin and enacyloxin IIa, are examined in this thesis. The most promising of the lead compounds fulfills Lipinski's rule of five and docks even better than cutoffs of both kirromycin and enacyloxin IIa. Furthermore, the molecule stays in place and keeps the binding site open during a molecular dynamics simulation.

Resumé

I dag opdages flere og flere resistente bakterier og det bliver sværere og sværere at behandle de infektioner, de giver anledning til. Derfor er det essentielt at der er en konstant udvikling af nye og forbedrede antiobiotika. Uheldigvis er det en meget tidskrævende og besværlig proces at finde nye præparat kandidater ved hjælp af traditionelle laboratorie-baserede metoder. *De novo* design metoder og docking simuleringer ved hjælp af computere er lovende og nye måder at fremskynde design og test processen. Denne afhandling præsenterer rationelt præparat design for blokering af elongationsfaktor Tu (EF-Tu) og viser at det er muligt at designe lovende, nye præparater, der har en hæmmende effekt på EF-Tu. Der findes allerede kendte hæmmere af EF-Tu, og to af disse, kirromycin og enacyloxin IIa, behandles og undersøges ligeledes i denne afhandling. Det mest lovende af de designede præparater opfylder Lipinskis fem-regel og dock'er bedre end afskæringer af såvel kirromycin som enacyloxin IIa. Molekylet bliver også på plads i og holder bindingsstedet åbent under en molekyle dynamik simulering.

Preface

For the past three years, I have been part of Birgit Schiøtt's bio-modelling group at the Department of Chemistry at the University of Aarhus. During the last year, I have been involved in the elongation factor Tu project, which I continued when PhD student Mette Lie went on maternity leave. I have worked with professor Troels Skydstrup and one of his PhD students, Rolf Taaning, who are from the Department of Organic Chemistry and professor Poul Nissen at the Department of Molecular Biology. It has been a very interesting and educational process and I have enjoyed it very much. I would like to thank associate professor Birgit Schiøtt for her help and guidance during my time in her group. I would like to give a special thanks to all the people that have taken time to read my thesis and give me constructive criticism, and equally I have appreciated Mette Lie's assistance and the tea breaks we had at her home. Thanks to my husband Kasper for his patience and all his help during the last year and to my family for their support and understanding.

Aarhus, September 2006

Abbreviations

aa-tRNA	aminoacyl-tRNA
AMBER	Assisted Model Building with Energy Refinement
A-site	aminoacyl site
ATP	adenosine triphosphate
CHARMM	Chemistry at HARvard Macromolecular Mechanics
co-pep	co-activator peptide for the estrogen receptor
DNA	deoxyribonucleic acid
E2	estradiol
E. coli	Escherichia coli
EF-G	elongation factor G
EF-Ts	elongation factor Ts
EF-Tu	elongation factor Tu
E-model	energy model score
Enx	enacyloxin IIa
E-site	exit site
ESP	electrostatic potential
fMet-tRNA	formylmethionine-tRNA
GDP	guanosine diphosphate
GDPNP	guanylyl iminodiphosohate
G-score	GlideScore
GTP	guanosine triphosphate
GTPase	guanosine triphosphatase
HTS	high-throughput screening
IF	initiation factor
IFD	Induced Fit Docking
Kir	kirromycin
LBD	ligand binding domain
MD	molecular dynamics

MM	molecular mechanics
mRNA	messenger RNA
NAMD	Not Another Molecular Dynamics program
NR	nuclear receptor
OPLS	Optimized Potential for Liquid Simulations
PASS	Putative Active Site with Spheres
PME	particle mesh Ewald
P-site	peptidyl site
Pul	pulvomycin
QM	quantum mechanics
RESP	restrained ESP
RF	release factor
RMSD	root mean square deviation
RNA	ribonucleic acid
SCREEN	Surface Cavity REcognition and EvaluatioN
rRNA	ribosomal RNA
tRNA	transfer RNA
vdW	van der Waal
VMD	Visual Molecular Dynamics

Contents

Chapter 1

Introduction

This thesis presents rational drug design for the inhibition of the elongation factor Tu (EF-Tu). EF-Tu is part of the protein synthesis and it is present in bacteria cell. The inhibition of EF-Tu stops the protein synthesis in the bacteria cells, thereby preventing the cell from synthesizing new bacteria. In this thesis, the complexes of EF-Tu with known antibiotics bound are examined and the binding of antibiotics and the behavior of the EF-Tu is studied. As part of the thesis work, several lead compounds have been identified and tested using different programs.

1.1 Motivation

More and more resistant bacteria are found today and it becomes increasingly difficult to treat the infections they cause. Therefore, it is essential that there is a constant development of new and improved antibiotics. Unfortunately, the process of finding lead compounds is long and difficult using traditional laboratory-based methods. *De novo* design methods and computer-aided docking simulations are promising and novel ways of speeding up the design and test process. These modelling methods open new roads to finding ways of treating infections and fighting the ever-growing risk of new resistant bacteria. The programs available today are under constant development to improve the process by making the programs faster and more accurate. Finding lead compounds is also helped by the computer industry and its continuous development of faster computers.

1.2 Goals

The purpose of this thesis is to design lead compounds and show that they have an inhibitory effect on EF-Tu. I want to demonstrate that it is possible to develop antibiotic compounds using computer calculations and show that these have an effect comparable to the existing antibiotics. I also want to indicate that the programs used are able to find the known effects of the known ligands, thereby establishing a basis for comparison of the lead compounds designed. Furthermore, I want to highlight the qualitative differences between versions 3.5 and 4.0 of Glide, the docking program used in the thesis.

1.3 Overview

Chapter 2 gives an overview of the protein synthesis and describes the different steps that occur during the protein synthesis. This includes a description of the elongation factors focusing on EF-Tu. In this chapter, the known antibiotics that block the effects of EF-Tu are also described.

Chapter 3 describes the theory of molecular mechanics and gives a detailed description of the different aspects of the computer calculations used in the thesis. There is also a detailed description of the specific programs used for the calculations on the protein structures of EF-Tu.

Chapter 4 describes the methods and setup of the different programs used in the thesis.

Chapter 5 describes the results of the thesis work and gives a systematic review of the work from *de novo* design through docking to molecular dynamics studies.

Chapter 6 concludes my thesis by summarizing the contributions and the conclusions from the preceding chapters. In this chapter, I also provide a glimpse of possible future work and research directions.

Chapter 7 gives a general introduction to the estrogen receptor project that I have been involved in. The work was done in collaboration with PhD student Leyla Celik and associate professor Birgit Schiøtt.

Chapter 2

System

In living organisms, DNA carries the genetic information of the cells and consists of thousands of genes. DNA acts like an instruction manual inside the cell that tells how to build a protein molecule. Proteins perform important tasks for the function of the cell or serve as building blocks. DNA is found in the nucleus of the cell and it is organized into chromosomes. Every cell contains the genetic information and for that reason, the DNA is duplicated before the cells divide. This process is called the replication process. The building of proteins is started with the transcription of RNA from DNA. The RNA is transported out of the cell where the translation is performed and proteins are constructed. There are different RNAs and they have different functions in the translation. The different RNAs are mRNA, tRNA, and rRNA; mRNA is messenger RNA which contains the information on how the proteins are made, tRNA is transfer RNA which is used to transport the different amino acids to the growing protein chains and rRNA is ribosomal RNA which catalyzes the formation of peptide bonds between the individual amino acids [17]. The protein synthesis described in this chapter takes place in a prokaryote.

2.1 Protein Synthesis

Protein synthesis is a translation process, where the four letter alphabet of nucleic acids is translated into the twenty letter alphabet of amino acids. The protein synthesis takes place on the ribosomes. As shown in figure 2.1 on the following page, the protein synthesis occurs in the amino-to-carboxyl direction by adding the amino acids to the carboxyl end of the growing polypeptide chain [17].

Figure 2.1 Polypeptide chain growth

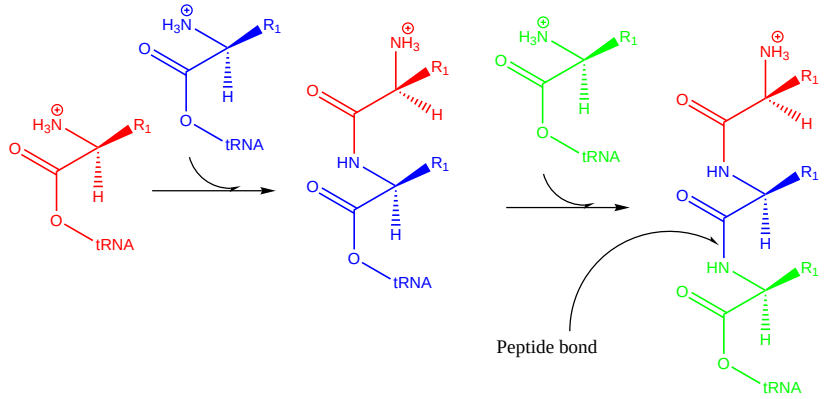

The mRNA consists of bases that are divided into codons, sequences of three bases that code for one specific amino acid. With help from ribosomes, the mRNA can be translated to amino acids and because of this the protein can be made. The tRNA brings the amino acids to the ribosome where they are connected by a peptide bond (see figure 2.1) and the polypeptide chain is made. The tRNA recognizes the codon on mRNA by Watson-Crick base pairing [11, 17]. The Watson-Crick base pairing is a codon/anti-codon pairing where the anti-codon is found on the tRNA. The tRNA functions as an adaptor molecule that binds to a specific codon and brings an amino acid to be incorporated in the polypeptide chain.

2.1.1 Initiation

The ribosome is an essential part of the protein synthesis, and it must be formed before the cycle can start. Figure 2.2 on the next page shows the translation initiation and in this process the mRNA and formylmethionine-tRNA (fMet-tRNA) is brought to the ribosome. For the ribosome to bind to the mRNA, a start codon and a so-called Shine-Delgarno sequence must be found on the mRNA. The ribosome has a sedimentation coefficient of 70S and can dissociate into a large subunit 50S and a smaller subunit 30S. By cleaving the 30S subunit, the ribosomal RNAs 5S, 16S, and 23S are found and these play important roles in the protein synthesis. The 16S subunit has a region which is complementary to the purine rich region of the sequence on the mRNA, called the Shine-Delgarno sequence [17, 95]. This sequence is on the 5′ end of the initial codon. The initial codon is an AUG (methionine) or less frequently a GUG (valine). The 16S subunit will bind to the Shine-Delgarno sequence and the initial tRNA will bind to

the start codon. The translation initiation is aided by initiation factors (IF1, IF2, and IF3). The 30S subunit of the ribosome binds to two initiation factors IF1 and IF3. The factors stop the 30S from joining the 50S subunit too early and in this way they prevent the formation of a 70S complex without mRNA, which would not allow the protein synthesis to start. IF2 binds to GTP and forms a complex with fMet-tRNA$_f$. This complex binds with mRNA to the 30S subunit. Then a hydrolysis of GTP bound to IF2 occurs at the same time as the 50S subunit enters. When the 50S subunit enters, the initiations factors are released, the 70S initiation complex is formed, and the ribosome is ready for the protein synthesis [17, 95].

Figure 2.2 Translation initiation

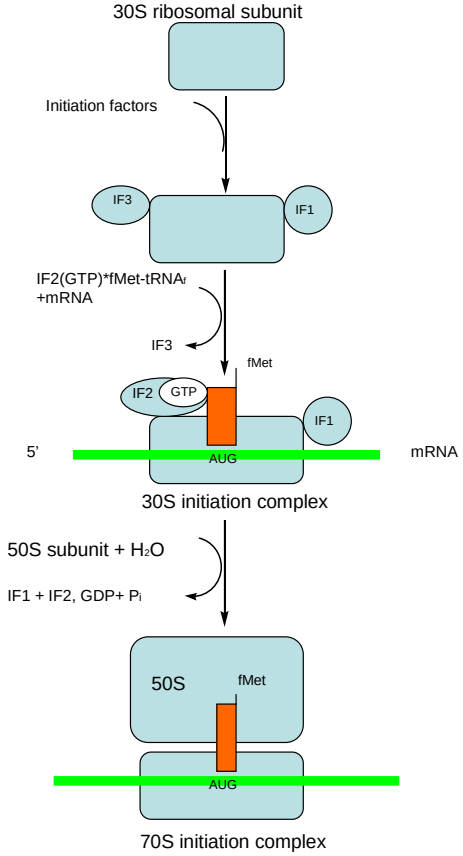

2.1.2 Elongation

The central step in the protein synthesis is the elongation. The elongation cycle starts with the insertion of aminoacyl-tRNA (aa-tRNA) in the empty aminoacyl (A) site on the ribosome; see figure 2.3 on the following page. The specific amino

acid inserted depends on the mRNA codon in the A-site. The cognate aa-tRNA does not leave the synthase and diffuse to the A-site on its own. It is brought to the A-site by the unstable translation elongation factor, EF-Tu. EF-Tu only binds the aa-tRNA in its GTP form. The binding has two functions: It protects the delicate ester linkage in the aa-tRNA from hydrolysis, and it allows hydrolysis of GTP in EF-Tu to GDP when an appropriate complex between the EF-Tu*aa-tRNA and the ribosome is formed. If the anti-codon does not fit, the hydrolysis will not take place and the aa-tRNA will not be transferred to the ribosome. EF-Tu is reset by the stable translation elongation factor EF-Ts, which joins EF-Tu and promotes the dissociation of GDP. After the dissociation of GDP, GTP binds to EF-Tu and the protein is reactivated. EF-Tu does not interact with fMet-tRNA$_f$, because the initiator tRNA is not brought to the A-site like the rest of the aa-tRNA [11, 17, 85, 95].

Figure 2.3 EF-Tu cycle

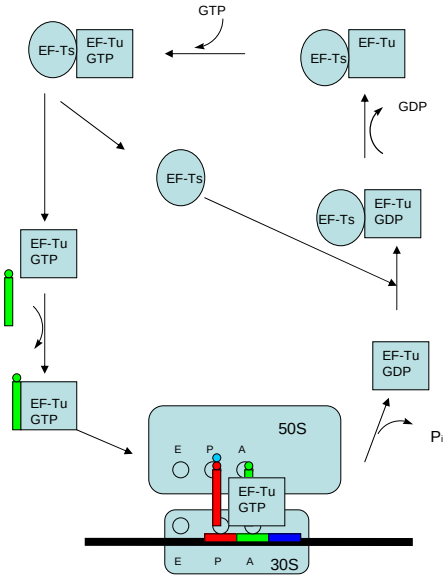

The cycle of the protein synthesis starts with a peptidyl-tRNA in the peptidyl (P) site on the ribosome; see figure 2.4 on the next page. A loaded tRNA with an anti-codon, which matches the codon in the A-site, enters and binds here, and a peptide bond is formed between the two amino acids. The formylmethionine (fMet) molecule bound on tRNA is transfered to the amino group of the amino acid in the A-site. This happens in the ribosome site called the peptidyl transferase center. When the peptide bond is formed, the peptide chain is connected to the tRNA in the A-site on the 30S subunit, while an interaction with the 50S subunit has placed the tRNA and amino acid in the P-site. The tRNA in the P-site

on the 30S subunit is now uncharged. For the cycle to continue, the mRNA must be moved three bases so that the codon for the next amino acid can be added to the A-site. Translation takes place through a protein called elongation factor G (EF-G) which is driven by GTP hydrolysis. EF-G binds to the ribosome in its GTP form on the 50S subunit which interacts with the 30S subunit. The binding stimulates the GTPase activity. When GTP is hydrolyzed, the EF-G undergoes a conformational change which forces the arm of EF-G further into the A-site on the 30S subunit. To accommodate this change, the peptidyl-tRNA moves into the P-site carrying the mRNA and the deacylated tRNA with it. When this step is completed, the tRNA is completely in the P-site and the uncharged tRNA is in the E-site where it is released from mRNA. The EF-G*GDP complex is released from the ribosome, and the high level of GTP in the cell and the relative low affinity for GDP causes EF-G to be reactivated to EF-G*GTP spontaneously. Now the cycle is ready to start again [17, 85, 95].

Figure 2.4 Protein synthesis

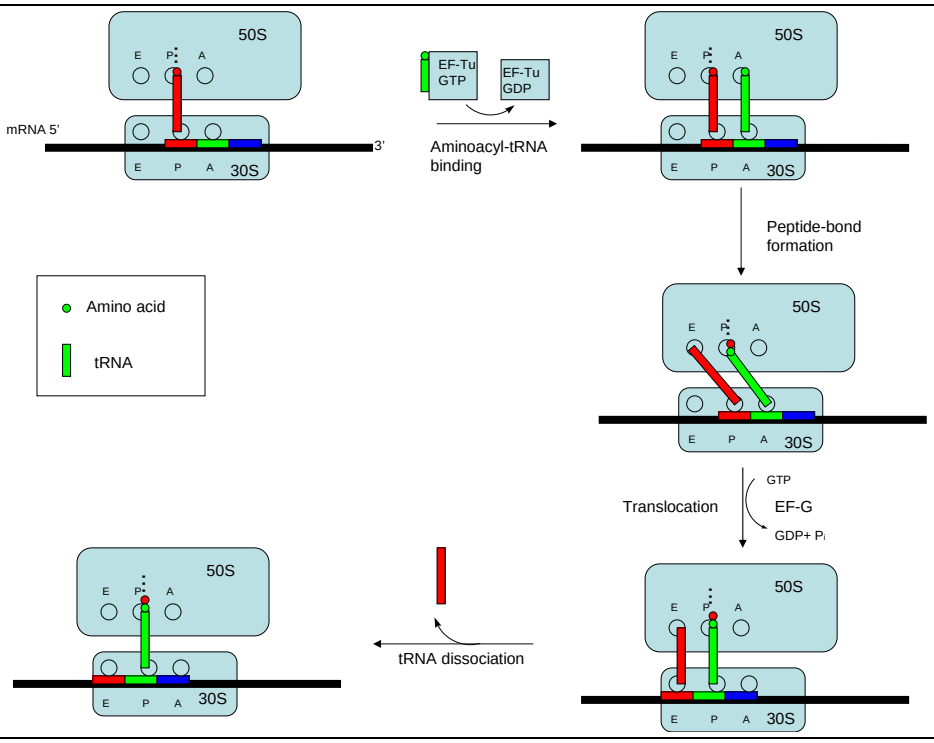

2.1.3 Termination

The termination of the protein synthesis begins when a stop codon is incorporated in the A-site on the mRNA. The stop codon is recognized by a release factor

(RF) and not by the aminoacyl-tRNA. There are two release factors in bacteria, RF1 and RF2. They both recognize the stop codon UAA while RF1 recognizes UAG and RF2 recognizes UGA. When the appropriate codon is in the A-site and is recognized by a release factor, a hydrolysis is triggered and the peptide is released from the tRNA in the P-site [51, 95].

2.2 Elongation Factor Tu

Several crystal structures of the elongation factor Tu in its different states have been solved and can be found in the Protein Data Bank [19] . The states, EF-Tu*GTP, EF-Tu*GDP, and EF-Tu*EF-Ts are shown in figure 2.5 on page 10, which is similar in structure to a figure shown in [11]. The most stable conformation is the EF-Tu*GDP complex. The biologically active form of the complex EF-Tu*GTP is solved with a GTP-analog bound instead of GTP, and the analog is often the non-hydrolysable GDPNP, where the oxygen atom between β and γ phosphate in GTP is replaced with an amide group. EF-Tu consists of 400 amino acids and can be subdivided into three domains. Domain 1 (residues 1-199) is also called domain G and this is where the nucleotide and an Mg^{2+} ion bind. Domains 2 (residues 209-299) and 3 (residues 300-393) both have a β barrel structure and they are held together by a single structural unit. The three domains are positioned differently depending on the nucleotide bound in domain G. The nucleotide is, in this case, either GTP or GDP based on the state of EF-Tu. The G domain has the same basic structure as G domains in other G-proteins, and it consists of a central β sheet surrounded by α helices. The domain also contains all the consensus sequences which are typical for a GTP-binding protein. This includes a P-loop, GXXXXGK(S/T), and a DXXG sequence motif, which is found in many ATP-binding proteins, where they are called the Walker A and B motifs [11, 85]. The consensus sequence also has an NKXD sequence motif, which is involved in the specific recognition of the guanine base in GTP and a threonine residue in the switch I region (residues 50-63 using E. coli numbering), which is known to be involved in the Mg^{2+} binding and in the conformational change in EF-Tu from GTP to GDP state. A domain similar to this is found in all known G-proteins, such as GTPase, and in the $\alpha-$subunit of hetrotrimeric G-proteins involved in cellular response to external signals [64].

The Mg^{2+} ion is placed in a deep cleft in the G domain between two β strands, and the presence of the ion is essential to the GTPase activity. In the GDP state, the Mg^{2+} is placed in the center of the cleft where it separates the

GDP/GTP binding site from the loop containing the amino acids Asp80 to His84. The Mg^{2+} ion is octahedral coordinated to two water molecules, one β phosphate oxygen and the hydroxyl-group from Thr25. The last two interactions occur via water molecules from the carboxyl oxygen of Pro82 and the side chain oxygen of Asp80. In the GTP state, one of the water molecules is replaced by a γ phosphate oxygen [63, 64, 66].

There is a significant structural difference between the biologically active form EF-Tu*GTP and the inactive form EF-Tu*GDP. The change between the two forms is catalyzed by a second factor called EF-Ts. The inactive form of EF-Tu is stretched out, whereas the active form has its three domains more packed [1]. Figure 2.5 on the next page shows the structures of three complexes with EF-Tu and illustrates the structural differences. Like all G-proteins, EF-Tu has a switch region in the G domain. This region has very different structures in GDP and GTP conformations.

In the large conformational change from the GDP to the GTP bound state, domains 2 and 3 move together as one rigid unit. This leads to a displacement of certain residues with as much as 40 Å [16, 66, 93]. The structure elements, that are affected the most by the change, are the switch regions. Switch region I in the effector region consists of two short α helices, 1* and 1**, where 1* unwinds to an extended β hairpin structure in the GDP state and forms a bridge to domain 3. The γ phosphate attracts the DXXG sequence motif from domain G which makes the peptide bond between the Gly residue and the preceding Pro residue rotate 150 degrees, and the amid group of the peptide bond forms a hydrogen bond with the γ phosphate. In EF-Tu, the DXPGH motif is in the beginning of the switch II region (residues 81-98 using E. coli numbering), which is included in the α helix in both the GDP and GTP form. Between the two forms, the helix will move four residues along the sequence and the axis will rotate 45 degrees. As this helix is an essential part of the interface towards domain 3, this change will result in an overall 90 degrees rotation of the G domain relative to domains 2 and 3 [56, 66, 85].

The structure of the complex between EF-Tu and the nucleotide exchange factor EF-Ts is also known; see figure 2.5. EF-Ts interacts with the G domain in EF-Tu by the loops, and is responsible for the nucleotide binding and changes the GTP binding pocket. EF-Ts also interacts with the top of domain 3 and causes the G domain and domain 3 to separated. This separation represents an intermediate in the large conformational change in EF-Tu, and is also part of the catalysis of the nucleotide exchange [56, 85].

Figure 2.5 Different conformations of EF-Tu

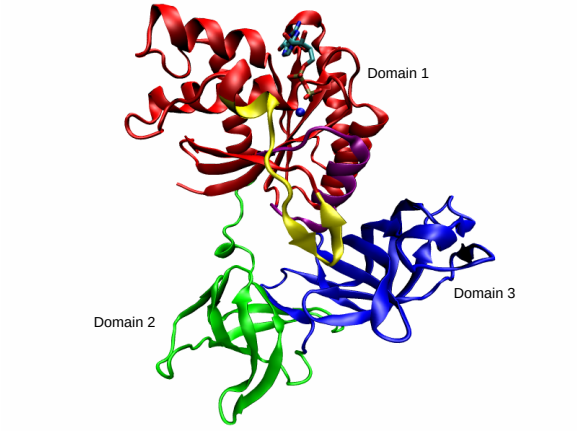

(a) EF-Tu*GDP

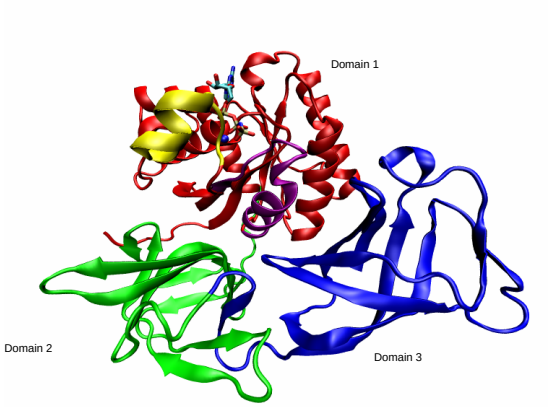

(b) EF-Tu*GTP

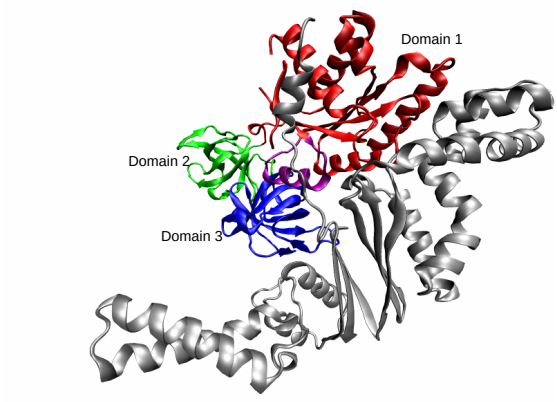

(c) EF-Tu*EF-Ts

Structures of bacterial elongation factor in the different states. Domain 1 is shown in red, domain 2 is shown in green, and domain 3 is shown in blue. The switch region I is shown in yellow and the switch region II is shown in purple. The nucleotide is shown in licorice representation and the magnesium ion is shown in blue. The elongation factor Ts in (c) is shown in gray. (a) is made from crystal structure 1TUI [93], (b) is made from crystal structure 1EXM [55], and (c) is made from crystal structure 1EFU [62].

The last structure of the EF-Tu is the ternary complex and it is shown in figure 2.6 on the following page. The ternary complex is where tRNA is bound to EF-Tu*GTP. The first structures of the ternary complex were solved with a yeast phenylalanyl-tRNA, but fortunately the structure is very similar in the bacterial state. The three domains all take part in the binding of tRNA when EF-Tu is in its GTP state. In the GDP state, there is no strong binding between aminoacyl-tRNA and EF-Tu*GDP. The reason for this is that the intermolecular contact sites are not properly aligned, so the binding site for aminoacyl-tRNA cannot be formed. This is because of the orientation of domains 2 and 3 with respect to domain 1. The acylated form of tRNA fits better than the non-acylated form. There are four regions that interact with EF-Tu*GTP: The aminoacyl group, the 3′-CCA acceptor stem, the adjacent helix of the 5′ end of tRNA, and the T-stem. When the amino acid binds in a pocket formed between domains 1 and 2, hydrogen bonds between the amino acid and EF-Tu are formed. The 3′-CCA stem interacts with EF-Tu primarily through ionic interaction with the phosphate groups. In this case, the bases are pointing away from the protein. The primary interaction with the acceptor stem helix is at the interface of domains 1 and 3 of EF-Tu and includes interaction with switch regions I and II. One side of the backbone of the T-stem helix forms contact with domain 3, and the 5′ end binds close to a junction of the three domains. The binding is described in more details in [1, 84, 86].

2.3 Elongation Factor G

The elongation factor G (EF-G) is also a G-protein and it has a single binding site which binds both GDP and GTP. EF-G does not need any outer factors to change from the GDP state to the GTP state, and this is probably because the conformational differences are not too big [1]. There have only been solved crystal structures for the EF-G*GDP complex and EF-G without a nucleotide bound. It has not yet been possible to solve the complex EF-G*GTP. EF-G consists of 690 residues and it has 5 domains. The overall shape of EF-G has similarities with the ternary complex of EF-Tu. This is shown in figure 2.6 on the next page. Domains 1 and 2 in EF-G have structures similar to the structures of domains 1 and 2 in EF-Tu, when GTP is bound in EF-Tu. In EF-G*GDP, there is inserted a β sheet between the two domains and this stabilizes the interface between the two domains. Domains 3 to 5 have folds that include a small β sheet with helices on one side. Domain 4 contains an unusual left-handed $\beta - \alpha - \beta$ folding motif

and this domain is more elongated and sticks out from the rest of the protein. The folding shown in the domains 3 to 5 is also found in ribosomal proteins [11, 85]. The great resemblance of EF-G*GDP and the ternary complex, indicates that they bind in the same binding pocket on the ribosome. The binding pocket is probably formed by the EF-G*GTP complex binding to the ribosome to make it ready for the next ternary complex. Before the translation can occur, the EF-G*GTP complex must bind in a pocket of different form but the crystal structure of EF-G*GTP must be solved to determine the details of this binding [64].

Figure 2.6 EF-G and the ternary complex of EF-Tu

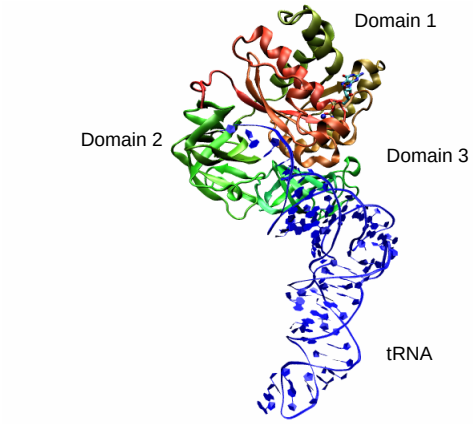

(a) Ternary complex of EF-Tu

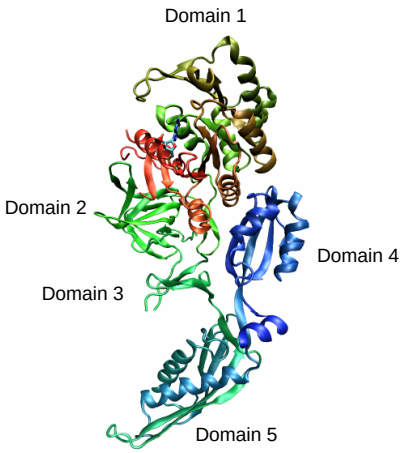

(b) EF-G

Structural resembles between the ternary complex and EF-G. (a) is from the crystal structure 1TTT [84] and (b) is from the crystal structure 1DAR [7].

2.4 Antibiotic Ligands

All antibiotics have the capacity to inhibit growth of microorganisms by changing their fundamental cellular metabolic processes. Many antibiotics used in animal food and in clinical medicine have an effect on the ribosome and its associated factors. For antimicrobial agents that disturb the protein bio-synthesis, the most important target is the ribosome, but EF-Tu is the second most important target [56]. There are four classes of antibiotics which act on EF-Tu and they all have one thing in common: They all increase the GTP affinity of EF-Tu. The remaining properties of EF-Tu are GDP affinity, aa-tRNA affinity, EF-Ts affinity, and GTPase activity. Besides the interest in the antibiotics as microbial agents, antibiotics also play an important role in the study of the intrinsic activity of EF-Tu, the ligands interaction with EF-Tu, and the visualization of the EF-Tu*GTP binding site on the protein [66]. The four classes of antibiotics are structurally unrelated and there are more than 30 compounds that have an effect on EF-Tu counting the analogs. The primary compounds in the four classes are kirromycin (figure 2.8 on the following page), enacyloxin IIa (figure 2.9 on page 15), pulvomycin (figure 2.12 on page 17), and GE2270 A (figure 2.14 on page 18). Kirromycin and enacyloxin IIa have similar properties and they function by inhibiting the release of EF-Tu*GDP from the ribosome by hindering the peptide bond formation and the recycling of the factor. This is depicted in the right-hand side of figure 2.7 on the following page. A similar figure is shown in [56]. The complex is kept in an EF-Tu*GTP-like state, regardless of which nucleotide is bound. Pulvomycin and GE2270 A also have similar properties and they function by preventing the formation of the ternary complex between EF-Tu*GTP and aa-tRNA [11, 56, 66]. This is depicted in the left-hand side of figure 2.7. A similar figure is shown in article[56].

2.4.1 Kirromycin and Enacyloxin IIa

Kirromycin (Kir) is part of an ever growing family of structurally related antimicrobial agents and Kir now has at least 15 analogs. It is also the most studied of the antibiotics [2, 31, 41, 115]. Figure 2.8 on the next page shows the structure of the compound. Kir and its analogs are produced by several actinomycetes, and antibiotics from the Kir family are known to interact with both EF-Tu*GTP and EF-Tu*GDP complexes. When Kir binds to EF-Tu there is a change in several of the known functional traits of the protein, some of which are the reduction in GDP and EF-Ts affinity and increased intrinsic and ribosome stimulated GTPase

Figure 2.7 Antibiotic effect on the elongation cycle

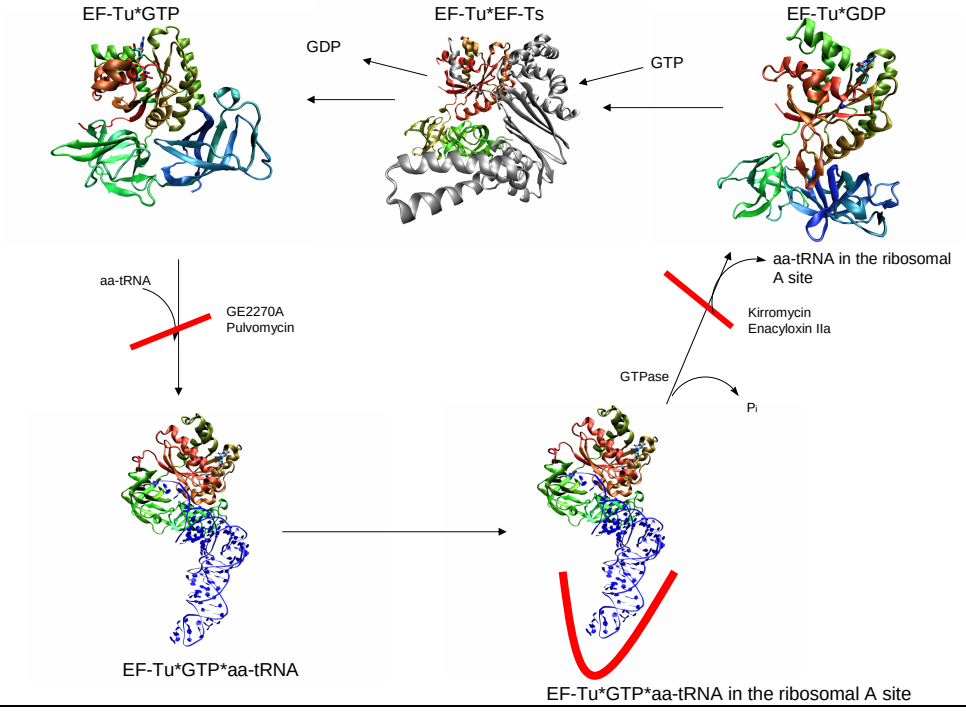

Figure 2.8 Kirromycin

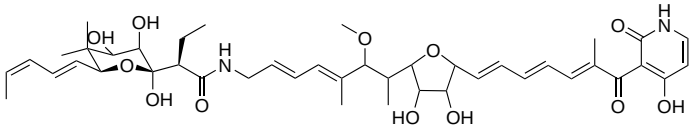

activity [56]. The most significant functional change applied by the binding of Kir has to do with the aa-tRNA affinity for EF-Tu. The complex Kir*EF-Tu*GTP shows reduced affinity for aa-tRNA whereas the complex Kir*EF-Tu*GDP*aa-tRNA forms a very stable quaternary complex. The consequence of this is that the EF-Tu*GDP complex which normally dissociates away from aa-tRNA and the ribosome after hydrolysis of GTP, cannot do this when Kir is bound. Therefore the Kir*EF-Tu*GDP*aa-tRNA complex is fixed to the ribosome and all ribosome activity is blocked [56, 85]. The conformations of EF-Tu in complex with Kir and either GTP or GDP, have similar structures and this is why the dissociation from the ribosome does not happen. Kir also has other activities [115]:

- stimulates the intrinsic GTPase activity of EF-Tu
- decreases the aa-tRNA binding affinity to EF-Tu*GTP complex
- inhibits EF-Ts binding
- increases the EF-Tu nucleotide exchange rate for GDP, while at the same time the affinity for GDP is unchanged
- increases GTP affinity for EF-Tu
- prevents the phosphorylation of EF-Tu

Figure 2.9 Enacyloxin IIa

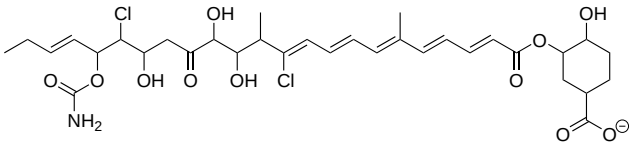

Enacyloxin IIa (Enx) is isolated from Frateuria species W-315 and is not an actinomycete like other antibiotics [56]; see figure 2.9 for the structure. Enx is active against both Gram-positive and Gram-negative microorganisms. Enx is believed to function by blocking the peptidyl-transfer of the P-site polypeptide-tRNA complex onto the adjacent A-site aa-tRNA. This is most likely achieved by locking the EF-Tu*GDP complex in a GTP-like conformation and thereby immobilizing the EF-Tu*GDP*aa-tRNA complex on the ribosome. This hypothesis is supported by the fact that Enx*EF-Tu*GDP has a higher affinity for aa-tRNA than the corresponding Kir complex [119]. Enx sensitivity is dominant in a mixed population of EF-Tu, probably because of obstruction of the trailing

polysomal ribosome. It can be argued that Enx and Kir belong to the same class because of the pleiotropic similarities of the binding to EF-Tu. However, this is not the case because of the obvious differences in structures, and because Enx inhibits the formation of a new peptide bond by blocking the C-terminal in the polypeptide chain placed in the P-site. This is also done by Kir, however, without blocking the release of EF-Tu*GDP. Since Enx also inhibits the incorporation of tRNA bound amino acid in lack of EF-Tu, in case of high concentrations of Mg^{2+}, it appears that Enx can directly affect the A-site. Compared to Kir, Enx only binds briefly to EF-Tu [56, 85, 119]. Figure 2.10 shows Kir and Enx in EF-Tu. The figure illustrates that the ligand binding site is not quite the same size when the two ligands are bound. The site is smaller when Enx is bound, compared to when Kir is bound. This is because the Kir ligand is bulkier than the Enx ligand.

Figure 2.10 Comparison of EF-Tu with kirromycin and enacyloxin IIa

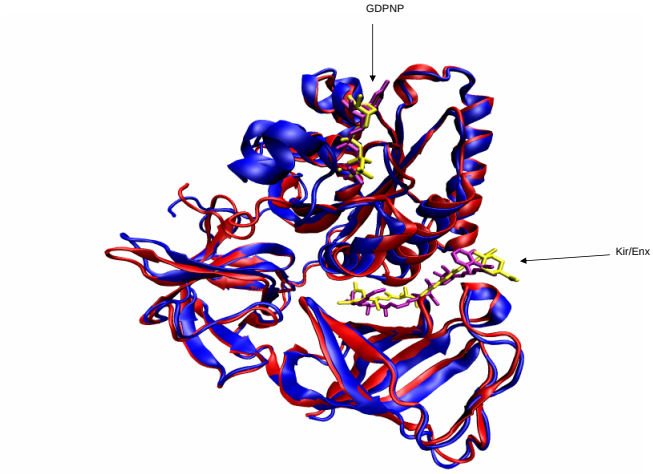

Red protein is with the ligand Enx from crystal structure 2BVN [89]; the ligand, GDPNP, and the magnesium ion are shown in yellow. Blue protein is with ligand Kir from crystal structure 1OB2 [89]; the ligand, GDPNP, and the magnesium ion are purple. Both structures are from E. coli.

The Enx ligand forms more hydrogen bonds than the Kir ligand and the hydrophobic interactions between the protein and the two ligands are also different. The hydrophobic tail of Enx is smaller than the one of Kir. Furthermore, it does not lie in the hydrophobic pocket as it is the case for the tail of Kir. The tail of Enx passes along outside the cavity [89]. Figure 2.11 on the facing page shows a comparison of EF-Tu*GTP*Kir and EF-Tu*GTP and it can be seen that domains 1 and 3 move further apart when Kir is bound. See [30, 89, 119] for further descriptions of both Kir and Enx bindings in EF-Tu.

Figure 2.11 EF-Tu*GTP*kirromycin versus EF-Tu*GTP

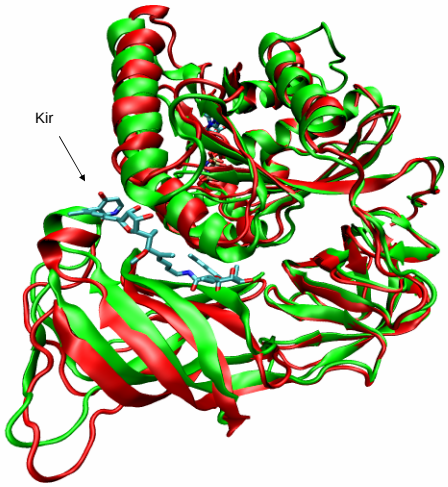

The protein in red is the structure with Kir bound (from E. coli crystal structure 1OB2 [89]) and the structure in green is when Kir is not bound (from Thermus Thermophilus crystal structure 1EXM [55]).

2.4.2 Pulvomycin and GE2270 A

Figure 2.12 Pulvomycin

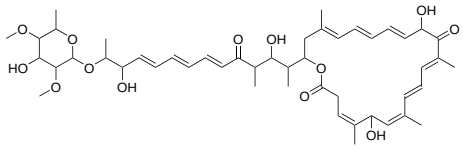

Pulvomycin (Pul) is produced from different forms of actinomycetes such as Streptomyces Netropsis and Streptomyces Mobaraense [56]. Figure 2.12 shows the structure of the compound. Pul binds to Escherichia coli (E. coli) EF-Tu with an affinity which is comparable to the one of Kir. The antibiotic Pul has an effect on the nucleotide affinity and stimulates the replacement of GDP for GTP, and it has an effect that is similar to the one of the stable translation factor EF-Ts. The stimulation of the GTPase activity is not as profound as the one induced by Kir, but the main inhibitory action of Pul seems to be the disturbance of the aa-tRNA binding to EF-Tu*GTP complex. This interferes with the formation of the ternary complex and the result of this is that EF-Tu does not deliver aa-tRNA to the ribosomal A-site and that the protein synthesis is interrupted [9].

Pul does not bind in the same place as Kir and Enx do. Pul binds between domains 1 and 2 and not between domains 1 and 3 as Kir does. This means that

Figure 2.13 Pulvomycin binding in protein

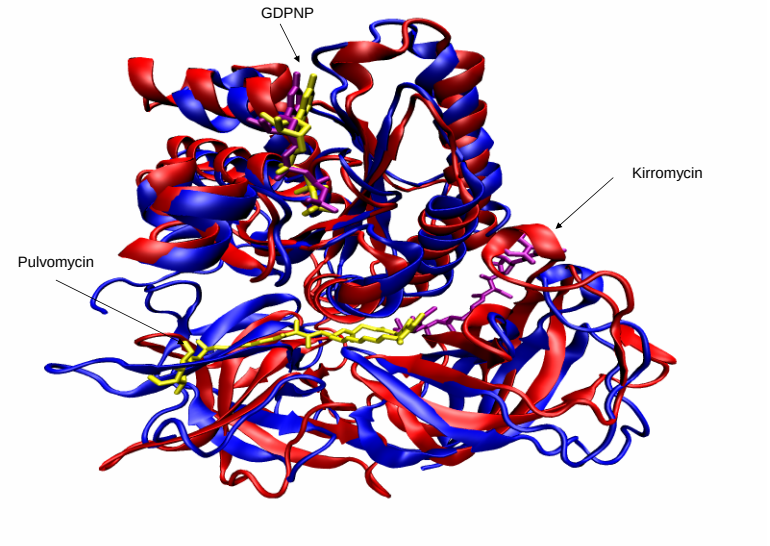

The protein with Pul is shown in red; Pul and GTP are shown in yellow (from Thermus thermophilus crystal structure 2C78 [88]). The protein with Kir is shown in blue; Kir and GTP are shown in purple (from E. coli crystal structure 1OB2 [89]) .

the conformations of the two protein structures are not quite the same, because domains 2 and 3 are placed differently in the two structures. The binding of Pul compared to the binding of Kir is shown in figure 2.13. See [56, 118] for further description of the effects of Pul and how these were investigated.

Figure 2.14 GE2270 A

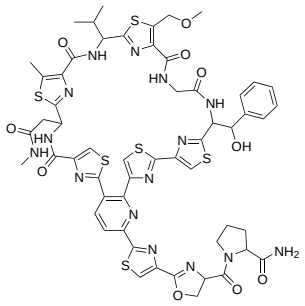

GE2270 A is structurally unrelated to Kir, Pul, and Enx as seen in figures 2.8, 2.9, 2.12, and 2.14. GE2270 A is produced by the actinomycete Planobispora Rosea and is a member of the cyclic thiazolol family, which also contains other EF-Tu specific inhibitors like amythiamycins isolated from Amycolatopsis species [56]. GE2270 A consists of a chain originating from 14 modified amino acids arranged in six tiazol rings, and one pyridine arranged in a cyclic structure with one side chain; see figure 2.14. GE2270 A has similarities with other

thiazolyl peptides and is found to be specially active against Gram-positive and anaerobic micro-organisms [10]. Like Pul, GE2270 A inhibits the protein synthesis by having an inhibitory effect on the formation of the EF-Tu*GTP*aa-tRNA ternary complex and consequently the binding of the ternary complex to the ribosome. GE2270 A can bind to both EF-Tu in complex with GTP and GDP, but the functional consequences will only manifest themselves when GE2270 A binds to the EF-Tu*GTP complex. GE2270 A produces a tight, abnormal complex which is characterised by slower dissociation when GTP is bound, and no change when GDP is bound. GE2270 A has a greater antibiotic effect than both Kir and Pul [10, 56].

Figure 2.15 Binding of GE2270 A compared to the binding of kirromycin

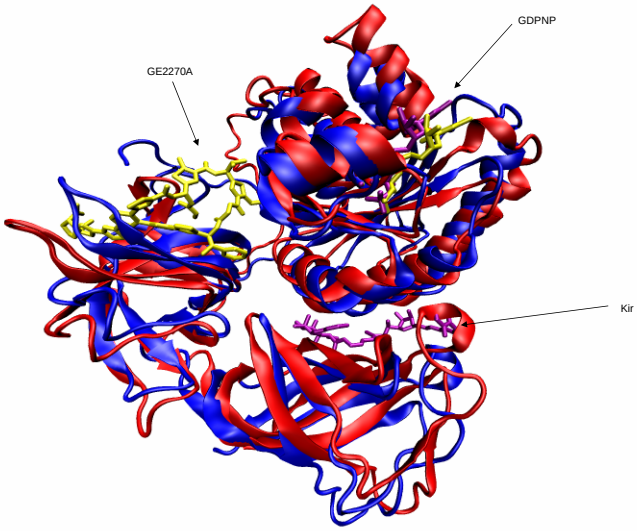

The protein with GE2270 A is shown in red; GE2270 A and GDPNP are shown in yellow from Thermus Thermophilus (crystal structure 2C77 [88]). The protein with Kir is shown in blue and Kir and GDPNP are shown in purple from E. coli (crystal structure 1OB2 [89]).

Figure 2.15 shows the binding site for GE2270 A and it is obvious that it is not the same as for Kir. The ligand binds in the same area as Pul and this is between domains 1 and 2. This means that the overall conformation of the protein is not quite the same for Kir and GE2270 A.

Chapter 3

Theory

Molecular mechanics (MM) is a method of computing the structure, energy, and dynamics of a molecule based on nuclear motions. Today, MM is performed by computer calculations, but it can also be done using simple models and hand calculations. MM approaches are widely used in the study of molecular structure refinement, molecular dynamics simulations, Monte Carlo simulations, and ligand docking studies. MM can be used to study small molecules as well as large biological systems [70]. Molecular mechanics stems from the concept of molecule binding and van der Waals forces. Electrons are not considered explicitly; it is assumed that they will find their optimal distribution when the positions of the nuclei are found. The Born-Oppenheimer approximation says that nuclei are much heavier than electrons and will therefore move much slower than the electrons and therefore the electrons will adjust to the movements of the nuclei [96]. Force fields used in MM ignore the electron motion and computes the energy of the system as a function of the nuclear positions. Another approach is quantum mechanics (QM) calculations where the electrons of the system are taken into consideration explicitly and, as a consequence, it is very time consuming. Calculations performed on large biological systems are therefore not feasible for QM calculations because of complex algorithms and the large number of atoms and thereby the large number of electrons. Therefore the MM approach is chosen for calculations on larger systems [70, 96]. This chapter focuses on the MM approaches applied in this thesis.

3.1 De Novo Design

> *De novo design is the design of bio-active compounds by incremental construction of a ligand model within a model of the receptor or enzyme active site, the structure of which is known from X-ray or NMR data [117].*

This method to design new compounds is a complementary approach to high-throughput screening (HTS). It is still a novel way of finding new leads for drug design, and the automated *de novo* design programs were only invented about 15 years ago [97]. Because the estimated number of drug-like molecules exceeds 10^{60}, it is not possible to use HTS alone, even though much progress has been made in this field [57]. Therefore, *de novo* design is used to explore the entire chemical space by examining the 3-dimensional structure of the target protein, and constructing novel active compounds based on the findings. Since the 1980s, many different *de novo* design programs have been developed including HSITE [38], LUDI [21, 22], LEGEND [83], SPROUT [46], GrowMol [20], PRO-LIGAND [33], and CONCERTS [91]. The programs use different approaches to finding new lead compounds; some combine individual atoms into new compounds while others combine larger fragments. Because of the differences in algorithms for the different programs, it is likely that different programs will find different lead compounds for the same system [57, 97]. One of the problems with *de novo* design is that the output structures can be difficult or impossible to synthesise and it can be very difficult to predict the binding affinity of the structures. Fortunately, new strategies are being developed to solve these problems. One promising way of doing this is by validating smaller substructures of the *de novo* design lead compounds using NMR, X-ray, and MS. Another possibility is to prioritise the output structures from *de novo* design based on how easy it is to synthesise them [57].

The focus for the following description of *de novo* design programs is on the programs that design small molecules; there are also attempts to develop programs that can design peptides [98] and other polymeric structures [108], but these are beyond the scope of this thesis. It is possible to design new structures from two different starting points; one is receptor-based and the other is ligand-based. The former is used when a crystal structure of the receptor is known. The latter is used when only a ligand structure is known. Receptor-based *de novo* design starts with determining a binding site. The binding site is then investigated for possible interaction sites, which can be of hydrophobic

or electrostatic nature, or hydrogen bond interactions [97]. One of the first programs on the market, HSITE [38], only considers hydrogen bond regions when examining the binding site. Later other programs, which consider hydrophobic interactions and more complex hydrogen bond regions were developed. Several *de novo* design programs implement grid-based approaches for the derivation of primary target constraints [97]. This means that a grid of points is generated for the binding site, and interaction site energies are generated by placing atoms or fragments on the grid. Some programs perform these calculations with the program GRID [48], while others have their own implementation of this algorithm. After placing the fragments or atoms in the binding site and generating new structures, the structures are evaluated to determine the best new molecule. Receptor-based scoring can be divided into three different types of scoring: Explicit force-fields method, empirical scoring functions, and knowledge-based scoring functions [97]. They all try to approximate the binding free energy. The first empirical scoring function used for *de novo* design was implemented in LUDI [21, 22], which is described in more detail in the following section. LUDI is the *de novo* design program of choice in this thesis work.

3.2 LUDI

LUDI is a *de novo* design program and is part of the Cerius^2 [5] package. The program can be used for drug discovery and structure-based design. The program Cerius^2 is developed by Accelrys [3], which has more than 20 years of experience in making computer software.

LUDI uses the fragment approach where molecule fragments are placed in the active site to make hydrogen bonds and hydrophobic interactions possible. The advantage of this approach is that it is fast and yields great variations in the produced compounds. LUDI works in three steps. It calculates interaction sites within the active site of the protein or from the active analogs. It searches libraries for fragments to fit in the interaction sites and it proposes a linking or alignment of the fragments. The interaction sites are generated from a set of rules that are based on statistical analysis of non-bonded contacts found in the literature [49, 50, 68, 80, 109, 112].

Interaction sites are positions in space which are not filled by the protein and where an atom from a functional group in a ligand can have a favourable interaction with the protein. The interaction sites are generated from the following interactions: H-bond donor, H-bond acceptor, lipophilic-aliphatic, and

lipophilic-aromatic. These four interactions are suitable for different interaction types. The rules used to generate the interaction sites are described in detail in [21, 22]. The next step is to fit the small molecules on the interaction sites by root mean square (RMS) super-positioning. The algorithm used is described in [60]. LUDI searches through a series of interaction sites to locate the most optimal for the fragment at hand, and finds from two to six possible interaction sites for the fragment. A fragment will be fitted if the RMS value is smaller than a user defined value (normally 0.2 - 0.6 Å), and if there is no van der Waal overlay between the receptor and the fragment [5, 23]. In addition to fitting fragments in interactions sites, LUDI can also propose an alignment with an existing ligand. LUDI can propose at most three link sites for the ligand; see figure 3.1, which is inspired from a figure in [5].

Figure 3.1 Fragment linking

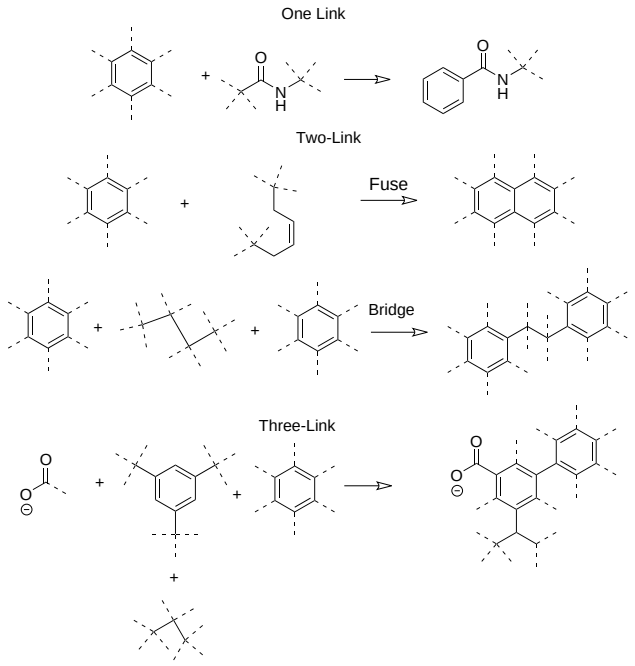

The doted lines show where linking is possible.

There are several different scoring functions implemented in LUDI. They are used for ranking and scoring the fragments during a *de novo* design run. LUDI implements four scoring functions for receptor mode scoring ($score_{1-4}$). These functions are used when a receptor structure is known. The $score_5$ function is the active analog mode scoring function and it is used when no receptor structure is known, but a ligand structure is known. The last scoring function is the link scoring function ($score_{\text{link}}$) and it is used when fragments are linked

together. The original scoring function is as follows:

$$score_1 = \left[\sum_{\text{h-bonds}} 100 f_1(\Delta R) f_2(\Delta\alpha) \right] + \frac{5}{3} A_{\text{lipo}}$$

The first term measures the number and quality of the hydrogen bonds between the receptor and the fragment, whereas the second term measures the hydrophobic contact area between the receptor and the fragment. ΔR is the deviation in the hydrogen bond length H$\cdots$O/N from an ideal length of 1.9 Å. $\Delta\alpha$ is the deviation in the hydrogen bond angle N/O-H$\cdots$O/N from an ideal angle of 180°. A_{lipo} is the area of the hydrophobic contact between the receptor and the ligand in Å^2. The functions $f_1(\Delta R)$ and $f_2(\Delta\alpha)$ are defined as follows [24]:

$$f_1(\Delta R) = \begin{cases} 0 & \Delta R \geq 0.6 \\ 1 - \frac{(\Delta R - 0.2)}{0.4} & 0.2 < \Delta R < 0.6 \\ 1 & \Delta R \leq 0.2 \end{cases}$$

$$f_2(\Delta\alpha) = \begin{cases} 0 & \Delta\alpha \geq 80° \\ 1 - \frac{(\Delta\alpha - 30)}{50} & 30° < \Delta\alpha < 80° \\ 1 & \Delta\alpha \leq 30° \end{cases}$$

The second scoring function gives a score which is correlated with the dissociations constant K_i for the ligand-receptor complex [24]:

$$score_2 = 100 \cdot log_{10} K_i$$

By looking at the relation between the Gibbs free energy binding, ΔG, and the dissociations constant with equilibrium the following equation is found:

$$\Delta G = -R \cdot T \cdot ln(K_i) \Leftrightarrow K_i = e^{-\frac{\Delta G}{R \cdot T}}$$

The LUDI score is calculated from the just mentioned equation when ΔG is expressed by an empirical function [24]:

$$\begin{aligned} \Delta G \;=\; & \Delta G_0 + \Delta G_{\text{hb}} \sum_{\text{h-bond}} f(\Delta R) f(\Delta\alpha) + \\ & \Delta G_{\text{ion}} \sum_{\text{ionic}} f(\Delta R) f(\Delta\alpha) + \Delta G_{\text{lipo}} A_{\text{lipo}} + \Delta G_{\text{rot}} N_{\text{R}} \end{aligned}$$

ΔG_0 is the contribution of the binding energy that is not directly dependent

on any specific interactions with the receptor, ΔG_{hb} is the contribution from an ideal hydrogen bond, and ΔG_{ion} is the contribution from an unperturbed ionic interaction. ΔG_{lipo} is the contribution from lipophilic interaction in the lipophilic contact area A_{lipo} between the receptor and the fragment. ΔG_{rot} describes the loss of binding energy due to constraining the internal degree of freedom in the ligand. N_{R} is the number of acyclic sp^3 - sp^3 and sp^3 - sp^2 binding [25]. The third scoring function, $score_3$, is like $score_2$ but takes the aromatic-aromatic interactions into account and is defined as follows:

$$\Delta G' = \Delta G + \Delta G_{\text{aro}} \sum_{\text{aro-aro interactions}} f(R)$$

In the new term, the angular dependence of aromatic-aromatic interaction is ignored and a simple distance cutoff is used:

$$f(R) = \begin{cases} 1 & R < 4.5 \\ 0 & R \geq 4.5 \end{cases}$$

The fourth scoring function ($score_4$) is equivalent to $score_3$ with $\Delta G_{\text{aro}} < 0$. When LUDI is run in the active analog mode, the following scoring function is used:

$$score_5 = 80 N_{\text{HB}} + \frac{5}{3} A_{\text{lipo}} + 100 \cdot (\frac{occ}{100})^2$$

where N_{HB} is the number of hydrogen bonds the fragment can make, A_{lipo} is the accessible hydrophobic area (Å^2) of the fragment and occ is the occupancy percentage of the hypothetical active site. When LUDI is run in link mode the link scoring function is used:

$$score_{\text{link}} = 200.0 - 3.0(r_{l1-f2} \cdot r_{l2-f1} \cdot \angle_{l1-l2-f2} \cdot \angle_{l2-l1-f1})$$

where $l1$ and $l2$ are the two ligand link atoms (see figure 3.2 on the next page) and $f1$ and $f2$ are the fragment link atoms that are being fitted on the ligand. r_{x-y} is the distance between the atoms x and y, and $\angle_{x-y-z}$ is the angle formed by the atoms x, y, z. A score of 200 indicates a perfect score, a score higher than 100 is a reasonable score and a score lower than 100 indicates a poor link. A score is reported for the link and another score is found for the overall score of the fragment.

Figure 3.2 Link sites

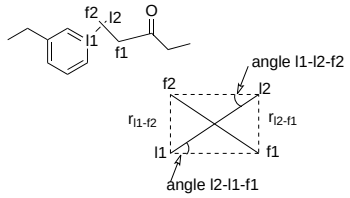

3.3 Molecular Docking

Molecular docking is the prediction of the structure of a receptor-ligand complex, where the receptor often is a protein or a protein oligomer and the ligand is either a small molecule or a protein. Molecular docking is used to propose new protein inhibitors and to understand the binding of known ligands in protein structures [12, 28, 79]. The first studies of protein-ligand complexes were performed in the early 1970s, when interactive molecular graphics programs were developed. The development of such programs allowed the combination of molecules, and the possibility to perform energy calculation on these to examine the different configurations that appeared complementary. In the early 1980s, the first docking algorithm was published. This was the DOCK algorithm [69, 79]. The development of docking programs allowed for an automatised search and more objective roads to examining the fit between two molecules. The first studies of protein-ligand complexes used a negative image of the receptor-sphere, which fills the pockets and grooves on the receptor surface. These spheres describe the potential interaction sites on the receptor. The first algorithms only handled rigid ligands and receptors and therefore only considered the six degrees of translational and rotational freedom. The interactions were evaluated by assessing overlap between atoms, and the potential for formation of hydrogen bonds.

Structure-based drug design is a fast growing area and many different docking programs and algorithms are found on the market today [13, 44, 67, 72, 78, 110, 113, 114, 116]. Most programs today allow ligand flexibility and some also allow some degree of protein flexibility [43, 105], both of which have been made possible by the development of faster computers. To every docking program there are two key parts: The search for configurational and conformational degrees of freedom and the scoring or evaluation function. The search algorithm traverses the potential energy landscape in great detail to find the global energy minimum. The greater the time span available, the greater the precision of the search algorithm can be. In rigid docking, this means that the algorithm exam-

ines different positions of the ligand in the active site of the receptor by means of translational and rotational degrees of freedom. Flexible ligand docking contributes with an exploration of torsional degrees of freedom for the ligand. Normally, the scoring function will assess both the steric complementarity between the ligand and receptor and also the ligand complementarity [12, 28, 79].

3.4 Glide

Glide is the docking program from Schrödinger. Schrödinger was founded in 1990 by Richard Friesner and William Goddard III. The initial product that they developed was Jaguar [99], but in 1998, Schrödinger acquired rights to the Macro Model technology which was developed by Clark Still. Glide is only one of many docking programs, but one of the better ones [54, 65]. Glide is a grid based docking program and the present version of the program is 4.0.

Glide [100] searches for favourable interactions between the ligand and the receptor. The ligand is usually a small molecule and the receptor is a larger molecule, typically a protein. The ligand has to be a single molecule whereas the receptor can be more than one molecule e.g. a protein with co-factors. Glide can be run in different modes; the ligand can be rigid or flexible. Glide performs a comprehensive and systematic search of the conformational, orientational, and positional space of the docked ligand [44]. To reduce computational cost, a dramatic reduction in search space appears in this search. This happens by an initial rough positioning and scoring phase. The search space reduction is followed by a minimization of the ligand in the receptor using a standard molecular mechanics energy function, in this case the OPLS-AA force field [59]. From this, the best candidates are chosen and are refined by a Monte Carlo sampling of pose conformations. The best poses are selected by use of a model energy function which combines empirical and force-field based terms [44].

Glide uses a series of hierarchical filters to search through possible locations of the ligand in the active site region of the receptor [44]. The shape and properties of the receptor are represented on a grid by different sets of fields which give progressively more precise scoring of the ligand pose. After generating the grid, a set of initial ligand conformations is produced. From this set an initial screening is performed over the whole phase space which is accessible for the ligand. This is done to find promising ligand poses [44]. The initial screening dramatically reduces the region for phase space. Starting from the poses that are selected from the initial screening, the ligand is minimized in the field of

the receptor by use of a standard MM energy function in conjugation with a distance-dependent dielectric model. The poses with the lowest energy are selected, and a Monte Carlo procedure is performed on these. The Monte Carlo procedure explores the nearby torsional minima.

Glide has implemented a modified and extended version of the ChemScore scoring function [40] to be able to predict the binding affinity and rank the ligands. This improved scoring function is known as the GlideScore. Glide uses a combination of GlideScore, ligand-receptor MM interaction energy, and ligand strain energy to choose the correct docked poses. They have discovered that this composite scoring function, called the E-model, is the best way to choose the correct pose; better than both the MM energy and the GlideScore alone. It is possible to scale down the van der Waals radii of selected protein and ligand atoms to make it possible to dock flexible ligands in rigid proteins [44]. The following function is the ChemScore scoring function which is similar to the scoring function used in LUDI [24]:

$$\begin{aligned}\Delta G_{\text{binding}} &= \Delta G_0 + \Delta G_{\text{h-bond}} \sum_{iI} g_1(\Delta r) g_2(\Delta\alpha) + \\ &\quad \Delta G_{\text{metal}} \sum_{aM} f(r_{aM}) + \Delta G_{\text{lipo}} \sum_{lL} f(r_{lL}) + \Delta G_{\text{rot}} H_{\text{rot}}\end{aligned}$$

The scoring function distributes general atom types to all ligand atoms and receptor atoms in contact with the ligand. The different atom types are lipophilic, hydrogen bond donor, hydrogen bond donor/acceptor, hydrogen bond acceptor, polar (non hydrogen bonding), and metal. The ΔGs are not known and are obtained by linear regression. The hydrogen bond term $\sum_{ij} g_1 g_2$ is calculated for all complementary possibilities of hydrogen bonds between the ligand atoms i and the receptor atoms I. The functions g_1 and g_2 are the same as used by Böhm [24]:

$$g_1(\Delta r) = \begin{cases} 1 & \Delta r \leq 0.25 \\ 1 - \frac{(\Delta r - 0.25)}{0.4} & 0.25 < \Delta r \leq 0.65 \\ 0 & \Delta r > 0.65 \end{cases}$$

$$g_2(\Delta\alpha) = \begin{cases} 1 & \Delta\alpha \leq 30^\circ \\ 1 - \frac{(\Delta\alpha - 30)}{50} & 30^\circ < \Delta\alpha \leq 80^\circ \\ 0 & \Delta\alpha > 80^\circ \end{cases}$$

The Δr parameter is the deviation in the hydrogen bond length $H \cdots O/N$ from an optimal length of 1.85 Å, and $\Delta\alpha$ is the deviation in the hydrogen bond angle $N/O - H \cdots O/N$ from the ideal angle of $180°$. The scoring function does not see any difference between an ionic and a non-ionic hydrogen bond. Not all water molecules are taken into account, but water molecules that are in contact with the receptor are. If there is more than one hydrogen bond between the receptor and the water, the water is seen as part of the protein. The metal term $\Sigma_{aM} f(r_{aM})$ is calculated for all acceptor/donor atoms a in the ligand and for any metal atoms M in the receptor. The function $f(r)$ is a simple contact term and r_{aM} is the distance between the ligand and the receptor atoms. The lipophilic term $\Sigma_{lL} f(r_{lL})$ is calculated for all lipophilic ligand atoms (l) and all lipophilic receptor atoms (L). The last term identifies frozen rotable bonds, where a rotable bond is defined by a sp^3- sp^3 and sp^3- sp^2 bond, but not by terminal CH_3, CF_3, NH_2, and NH_3 groups. Bonds are seen as frozen if atoms on both sides of the rotable bond are in contact with the receptor. The following function is used to estimate the flexibility punishment for molecules that contain constrained rotable bonds:

$$H_{\text{rot}} = 1 + \left(1 - \frac{1}{N_{\text{rot}}}\right) \sum_r \frac{P_{n1}(r) + P'_{n1}(r)}{2}$$

In the formula, N_{rot} is the number of frozen rotable bonds. The summarization is over the frozen rotable bonds, and $P_{n1}(r)$ and $P'_{n1}(r)$ are the percentage of non lipophilic heavy atoms on each side of the bond.

GlideScore is based on the ChemScore function, but it also includes a steric clash term and adds buried polar terms devised by Schrödinger to punish electrostatic mismatches [44]:

$$\begin{aligned}
\Delta G_{\text{binding}} \;=\; & C_{\text{lipo-lipo}} \sum f(r_{lr}) + \\
& C_{\text{hbond-neut-neut}} \sum g(\Delta r) h(\Delta\alpha) + \\
& C_{\text{hbond-neut-charged}} \sum g(\Delta r) h(\Delta\alpha) + \\
& C_{\text{hbond-charged-charged}} \sum g(\Delta r) h(\Delta\alpha) + \\
& C_{\text{max-metal-ion}} \sum f(r_{lm}) + C_{\text{rotb}} H_{\text{rotb}} + \\
& C_{\text{polar-phob}} V_{\text{polar-phob}} + C_{\text{coul}} E_{\text{coul}} + \\
& C_{\text{vdW}} E_{\text{vdW}} + \text{solvation terms}
\end{aligned}$$

The lipophilic-lipophilic term is defined as in ChemScore, but the hydrogen

bonding term is divided into three different weighted components, which are dependent on whether both the donor and acceptor are neutral, one is neutral and the other is charged, or both are charged. The last form is the least important. Metal-ligand interactions use the same functional form as in ChemScore, but vary in three principal ways. First, the term only considers interactions with anionic acceptor atoms, second it only counts the single best interaction when two or more metal ligations are found. The third difference is that the net charge of the metal ion is assessed in the apo protein structure. The second term added to the ChemScore is the Coulomb and van der Waals interaction energies between the ligand and receptor. The third component is the solvation model. The best docked structure for every ligand is chosen from the model energy score (E-model). Glide also gives a special constructed Coulomb and van der Waals interactions energy score, which is formulated to avoid overlap rewarding charge-charge interactions on the expense of charge-dipole and dipole-dipole interactions. Because of the hierarchical search method used, a very precise binding mode of ligands is found and the computer cost is minimized.

3.5 Induced Fit Docking

In a standard Glide docking, the receptor is held rigid and the ligand is free to move. This does not always give valid results because some proteins undergo side chain or backbone movement during ligand binding. These changes allow the protein to alter its binding site to make the binding of the ligand more optimal. The easiest way to improve docking is to reduce the van der Waals radii of the protein and ligand atoms, and to remove side chains of residues that are expected to be very flexible in ligand binding. This can make the ligand dock, but the problem is that this does not yield an ideal picture of the protein and ligand interactions. It is also possible to make an ensemble of protein structures and dock the ligand in this, or to perform a molecular dynamic (MD) study of the protein-ligand complex. None of these ways are perfect for predicting interactions between the protein and ligand, and therefore a new and improved way has been developed. Schrödinger's Induced Fit Docking protocol is a new program that combines Glide and the Refinement model in Prime [103] to induce adjustments in the receptor structure [105]. Prime is a combination of Comparative Modelling and Threading programs. Comparative Modelling consists of the complete protein structure prediction process from template identification to alignment, model building, and finally refinement. Refinement involves side-

chain prediction, loop prediction, and minimization. The Threading program consists of sequence alignment, model building and refinement [103]. In the Induced Fit Docking protocol from Schrödinger, only the Refinement model of Prime is used [101].

There are four steps in the induced fit docking (IFD) from Schrödinger and these are: Initial ligand sampling, receptor sampling, ligand re-sampling, and final scoring. The first step is where an initial softened-potential docking of the ligand in a rigid protein is performed to generate an ensemble of poses. Here the van der Waal potential is reduced with 50% for some atoms and very flexible or bulky side chains can be modified to alanine. The problem that can occur in this step is that it can be difficult to generate at least one pose of the receptor-ligand complex. The second step is sampling of the protein for every ligand pose that is generated in the first step; a maximum of 20 poses are generated for every ligand. Prime refinement is used here and if any side chains have been mutated in the first step they are mutated back in the second step. Furthermore, by default only residues within 5.0 Å of any of the ligand atoms are sampled. The rest are fixed during minimization. The program generates 20 new protein conformations for the initial 20 complexes and these are ranked by their Prime energies. The problem that can occur in the second step is predicting the low energy receptor conformation for the correct ligand, starting from the guess in the initial step. The third step is to re-dock the ligand in a low energy induced-fit structure from step two using a hard potential docking, the default setting. The problem in the third step is to generate the low energy ligand, when the low energy protein is found. The fourth step is to score the complexes by using the docking energy (GlideScore), the receptor stain, the solvation terms, and the Prime energy. The final ranking is found using:

$$\text{IFDScore} = \text{GlideScore} + 0.05 \cdot \text{PrimeEnergy}$$

If the score gap in the top ranking complexes is smaller than 0.2, the IFD should be run again for the top ranking receptor structures starting from the first round of IFD. It can be difficult for the program to rank the complexes in the right order [105]. Studies have shown that this program is found to be a promising way to find receptor-ligand interaction and get new compounds to dock in other receptors [105].

3.6 Force Fields

There are many different molecular modelling force fields today [29, 32, 53, 73]. They have all been developed since the 1980s and are modified regularly. Many of these force fields are off-springs of the same original force field developed in the early 1980s. They can all be interpreted as a model of intra- and intermolecular forces in the system. Energetic punishments are present if there are deviations in bond and angles from a reference value. The force fields also contain terms that describe the non-bonded interactions between atoms. The following formula shows the potential energy function which most force fields are based on:

$$V = E_{\text{bond-length}} + E_{\text{angle-bend}} + E_{\text{torsional}} + E_{\text{van-der-Waals}} + E_{\text{electrostatic}}$$

The potential energy function consists of bonded and non-bonded terms. The bonded terms are bond lengths, angle strains, and torsional potentials. The non-bonded terms are van der Waals interactions which model molecular repulsions at short intra-atomic separations and attractions at great distances and the electrostatic interactions, which represent the ionic interactions between charged or partly charged molecules [37, 70, 96]. The bond term $E_{\text{bond-length}}$ can be computed using a Morse term or by a harmonic potential. The Morse potential has the following formula:

$$v(l) = D_e \cdot (1 - e^{-a(l-l_0)})^2$$

Here D_e is the depth of the potential energy minimum and $a = \omega\sqrt{\frac{\mu}{2D_e}}$, where μ is the reduced mass and ω is the frequency of the bonds vibration. The frequency ω is related to the stretch constant k by $\omega = \sqrt{\frac{k}{\mu}}$ and l_0 is the reference value for the bond [70]. Reference values for different chemical bonds can be found using X-ray crystallographic structures or from QM calculations. The Morse potential is not used very often in molecular mechanic force fields because the method is not very cost efficient, and it is rare that bonds deviate significantly from their equilibrium value. In such calculations, the Morse potential describes a large range of behaviours for bonds from large stretches to small bond lengths. The most elementary approach for calculating bond stretching is using a harmonic potential which is based on Hooke's law. Here the energy variates with the

square of the displacement from the reference bonds length l_0:

$$v(l) = \frac{k}{2}(l - l_0)^2$$

The functional form of Hooke's law is a reasonable approximation for the shape of the potential energy curve at the bottom of the potential well, which is where distances correspond to bindings in ground-state molecules. Away from the equilibrium, Hooke's law is less accurate [15, 70, 96].

The second term in the potential energy function is the angle term $E_{\text{angle-bend}}$. The deviation of angles from their references value is often described by Hooke's law or the harmonic potential:

$$v(\theta) = \frac{k}{2}(\theta - \theta_0)^2$$

The contribution from every angle is characterised by a force constant and a reference equilibrium value. It takes less energy to distort an angle away from its equilibrium than to get a bond away from its equilibrium. Therefore, the energy added by the angle term is often smaller than the energy contribution from the bond term [15, 70, 96].

The last bonded term is the torsional term $E_{\text{torsional}}$. Not all molecular mechanics force fields use torsional potentials, because it can be trusted that non-bonding interactions between atoms in each end of every torsion give the desired energy profile [70]. Most force fields used for organic molecules have an explicit torsional potential with a contribution from every bonded quartet of atoms in the system. Existence of a barrier that hinders free rotation around a chemical bond is fundamental for the understanding of the structural properties of molecules and conformation analysis. QM calculations suggest that this rotational barrier originates from the hydrogen bonds at opposite ends of the molecule. The anti-bonding interaction is minimized when the conformation is staggered and is maximized when the conformation is eclipsed. Many force fields are used for modelling flexible molecules, where the greatest change in the conformation is caused by the rotation around bonds. To simulate this, it is essential that the force field represents the energy profile of these changes properly [70]. The torsional potential is almost always represented by a cosine series:

$$v(\omega) = \sum_{n=1}^{N} \frac{V_n}{2}[1 + \cos(n\omega - \gamma)]$$

where ω is the torsional angle. The parameter V_n gives qualitative indication of the relative barriers for rotation, and γ is the phase factor which determines where the rotation angle passes through its minimum value. The parameter N is the multiplicity. Its value gives the number of minimum points in the function during a 360° rotation around the bond. An example of this is the energy profile for a rotation around a single bond between two sp^3 carbon atoms. This is represented as $N = 3$ and $\gamma = 0^\circ$ and it gives a threefold rotational profile with minima at torsional angles $\pm 60^\circ$ and 180° and maxima at $\pm 120^\circ$ and 0°. A double bond between two sp^2 carbon atoms is represented as $N = 2$ and $\gamma = 180^\circ$ with minima at 0° and 180°. Another term can be added to the torsional term and this is the improper torsion and out-of-plane motions term. There are several ways of incorporating the out-of-plane term in force fields. One way is to treat the four atoms as an improper torsion angle, i.e. a torsional angle where the four atoms are disconnected in a 1-2-3-4 sequence. This means that the central atom 2 is bound to atoms 1, 3, and 4 as the angle between bond atoms 2-4 and the plane 1-2-3. A torsional potential in the following form can be used to keep the improper torsion angle of 0° or 180°:

$$v(\omega) = k(1 - cos(2\omega))$$

There are also other ways of incorporating the out-of-plane bending contribution. One way, which is a harmonic potential, is to include a calculation of the angle between the bond from the central atom and the plane defined by the central atom and the other two atoms. A value of 0° corresponds to the fact that all four atoms are coplanar:

$$v(\theta) = \frac{k}{2}\theta^2$$

Another method, which also is a harmonic potential, is to use a calculation of the height of the central atom over a plane defined by the three other atoms:

$$v(h) = \frac{k}{2}h^2$$

The method used most is the improper torsion because it is easy to incorporate in the ordinary torsion term, even though the two latter ones give a better calculation of the out-of-plane bend. It it not always necessary to incorporate the out-of-plane term, but it is commonly used in a united atom force field to maintain stereo-chemistry at chiral centers [70, 96].

It has been discovered that it can be a good idea to include cross terms in

force fields. Most cross terms are functions of two internal coordinates such as stretch-stretch, stretch-bend, and stretch-torsion, but cross terms which include more than two internal coordinates, such as bend-bend-torsion, are also used. An example of a cross term, is when an angle is decreased and there is also an adjacent bond stretch reduction interaction between atoms 1 and 3 [15, 70, 96]. Sometimes, a Urey-Bradley term is added to the potential energy function. This term takes the in-plane deformations and the separating symmetric and asymmetric bond stretching modes into account [15, 37, 70, 96].

The two last terms in the force field are the non-bonded terms: An electrostatic term and a van der Waals term. The electrostatic term, $E_{\text{electrostatic}}$, represents the ionic interactions between charged or partly charged molecules. Electrostatic elements attract electrons more than less electrostatic elements. This results in an uneven distribution of charge in a molecule. This charge distribution can be represented in a number of ways, where one common way is a distribution of fractional point charges throughout a molecule. These charges are designed to represent the electrostatic properties of a molecule. The electrostatic interaction between two molecules or between different parts of the same molecule is calculated as the sum of interactions between pairs of point charges by use of Coulomb's law [70, 96]:

$$v = \sum_{i=1}^{N_A} \sum_{j=1}^{N_B} \frac{q_i q_j}{4\pi\epsilon_0 r_{ij}}$$

where N_A and N_B are the number of point charges in the two molecules. The Coulomb's interactions decrease slowly when the distances increase. The partial potential energy, v, is positive if the particles have the same charge, and negative if the particles have opposite charge.

The last term is the van der Waals term, $E_{\text{van-der-Waals}}$, and the best known potential function for this is the so-called 6/12 Lennard-Jones function [70, 96]:

$$v(r) = 4\epsilon \left[\left(\frac{\sigma}{r}\right)^{12} - \left(\frac{\sigma}{r}\right)^{6} \right]$$

This formula consists of two parameters: σ which is the collision diameter and ϵ which is the well depth. The attractive term r^{-6} and repulsive term r^{-12} depend on the type of the two interacting atoms. The attractive term is determined from QM calculations and the repulsive term is often chosen from computational convince. Several formulations, where the standard r^{-12} term in the Lennard-Jones term is replaced by a more theoretical, but more realistic, exponential term have been suggested [70, 96]. One of these is the Buckingham potential described in

[15, 70, 96].

This concludes the general description of the potential energy function used in many force fields and the following formula shows the potential energy function in full:

$$
\begin{aligned}
V \;=\; & \sum_{\text{bonds}} \frac{k_i}{2}(l_i - l_{i,0})^2 + \sum_{\text{angles}} \frac{k_i}{2}(\theta_i - \theta_{i,0})^2 + \\
& \sum_{\text{torsion}} \sum_{n} \frac{V_n}{2}(1 + cos(n\omega - \gamma)) + \\
& \sum_{i=1}^{N} \sum_{j=i+1}^{N} \left(4\epsilon_{ij} \left[\left(\frac{\sigma_{ij}}{r_{ij}} \right)^{12} - \left(\frac{\sigma_{ij}}{r_{ij}} \right)^{6} \right] + \frac{q_i q_j}{4\pi\epsilon_0 r_{ij}} \right)
\end{aligned}
$$

A force field is the combination of an energy function and all the parameters used in the energy function. The potential energy function described here is common for CHARMM [73, 74], AMBER [29], GROMOS [32], OPLS [59], and others, but the force fields for the different programs have different parameters. For that reason, it is difficult to transfer parameters from one program to another. The development of parameters used in force fields is described in numerous articles [6, 59, 73, 74, 94].

Generally, parameters are found using QM calculations and bonded parameters can be found from fragments of other molecules. Historically, parameters were found using spectroscopy or other X-ray methods. The most important parameters in force fields are the non-bonded parameters. To determine these, partial atomic charges are needed. The different force fields use different approaches to find them. For biomolecular force fields, the most used method for finding partial atomic charges are QM electrostatic potential (ESP) and supramolecular approaches. CHARMM and OPLS uses HF/6-31G* supramolecular approaches, which calculates the interaction between model compound and water [73]. AMBER uses the restrained electrostatic potential (RESP) method, which fits a QM calculated electrostatic potential to a molecule surface by use of an atom-centered point charge model to find partial charges [36, 47].

VCharge [47] is a new and fast way of assigning partial atomic charges to molecules. It has been developed by VeraChem LLC and is used to assign partial charges to molecules before MD simulations are run. VCharge is an electronegativity equalization method where the electro-negativity of every atom depends on its atom number, hybridization, and binding environment within the molecule and where special constraints are added to prevent too much charge

from flowing off ionized groups [47].

3.7 Molecular Dynamics Simulations

The molecular dynamics (MD) method was introduced by Alder and Wainwright at the end of the 1950s [8]. They studied interactions between hard spheres, and this gave important insights into the behavior of simple liquids. The first protein simulations were performed by McCammon *et al.* in 1977 with a simulation of the bovine pancreatic trypsin inhibitor [75]. In the literature today, there are many studies of MD simulations on solvated proteins, protein-DNA complexes, and lipid systems, which look at different issues including thermodynamics of ligand binding and folding of small proteins. Molecular dynamics is used to estimate an equilibrium and the dynamic characteristics of complex systems which cannot be computed analytically. It is possible to obtain a static view of a biomolecule from X-ray crystallography, but this approach only gives an average frozen view of the complex system. Because of this, there is a long range of biological properties that remain unknown. By using MD, the missing biological information on the activity of the system can be estimated. Such properties include the geometry and energy of the molecule, local interaction velocities for conformational changes, enzyme or substrate binding, and free energy calculations [70, 96].

Each step in an MD simulation is based on Newtons second law:

$$F = m \cdot a = -\frac{dV}{dr} \tag{3.1}$$

where F is the force exerted on a particle, m is the mass, and a is the acceleration. The net force F is also given by the negative gradient of the potential energy V with respect to the position of the atom r [6]. Given the force on each atom, it is possible to determine the acceleration of each atom in the system. Integrations of equations for movement yield a path which describes positions, velocities, and accelerations of particles as a function of time. From this path, it is possible to determine an average of the properties. The method is deterministic and this means that when a position and a velocity of every atom is known, the state of the system can be predicted for any given time.

The most used algorithm for molecular dynamic simulations is the velocity Verlet method [6, 70, 96]. This method gives positions, velocities, and accelera-

tions at the same time without compromising the precision:

$$r(t+\delta t) = r(t) + \delta t v(t) + \frac{\delta t^2 a(t)}{2} \tag{3.2}$$

$$v(t+\delta t) = v(t) + \frac{\delta t[a(t) + a(t+\delta t)]}{2} \tag{3.3}$$

This method is implemented as a three step procedure. The acceleration for both the time step t and $t+\delta t$ are needed to calculate new velocities. In the first step, the positions at $t+\delta t$ are calculated according to 3.2 using the velocities and the accelerations at the time t. The velocities at time $t + \frac{\delta t}{2}$ are then calculated according to

$$v\left(t + \frac{\delta t}{2}\right) = v(t) + \frac{\delta t a(t)}{2} \tag{3.4}$$

The next step is to compute new forces from the current positions; this gives $a(t+\delta t)$. The final step is to determine the velocities at the time $t+\delta t$ using 3.5:

$$v(t+\delta t) = v\left(t + \frac{\delta t}{2}\right) + \frac{\delta t a(t+\delta t)}{2} \tag{3.5}$$

The starting position, $r(0)$, of the particle can be taken from experimental structures, such as X-ray structures of the protein. The initial distribution of velocities is normally determined from a random distribution corresponding to a preselected temperature [70]. Other algorithms have been developed for MD simulations and they are described in [6, 70, 96].

The most time-consuming part of computing the potential energy function, and therefore of the molecular dynamics simulation, is the non-bonded term in the force field. In principle, one should calculate every interaction between every non-bonding atom pair. This is not possible because the number of atom pairs increases with the square of the number of atoms (N^2). To make the calculations possible in a reasonable time span, a cut-off distance is introduced. This is used for the van der Waals interactions [106]. The cut-off distance is usually in the range 10-12 Å. For the electrostatic interactions, a simple cut-off distance is not used because of the importance of long-range electrostatic interactions. In the early years of MD simulations, the long-range electrostatic interactions were ignored because of the computational cost, but new ways of calculating them have been introduced. One method is the particle mesh Ewald algorithm (PME) [39], which is a fast numerical method to calculate the Ewald sum using a fast Fourier transformation. PME is based on periodic boundary conditions. The cost of PME is proportional to $N \cdot \log(N)$ and the time reduction is significant

even for small systems.

In MD simulations, there are other aspects to consider before a simulation can be run. Some of these are choice of ensemble, solvation of the system, selection of border conditions for the system, and how to control temperature and pressure [15, 70, 94, 96].

The software used for MD simulations in this thesis is the program NAMD [61, 82, 92]. This program was developed in the 1990s by Klaus Schulten's group at the Beckman Institute at the University of Illinois [82]. NAMD is a parallel molecular dynamics program designed for high-performance calculations on large biomolecular systems. The program scales to several hundreds of processors in high-end parallel platforms, but can also run on a single computer. NAMD works with AMBER, CHARM, and OPLS potential functions, parameters, and file formats. NAMD is a scripting program and to obtain graphical insights, the program VMD is available to visualise the results from a NAMD run [58].

Chapter 4

Methods

In this thesis, two conformations of the protein EF-Tu were used as starting structures for the study of EF-Tu and the binding of new lead compounds for antibiotic studies. The two conformations have different ligands bound and different resolutions. Atomic coordinates were supplied by professor Poul Nissen's group at the Department of Molecular Biology at the University of Aarhus, but they can also be found as entries 1OB2 [89] and 2BVN [89] in the Protein Data Bank [19]. Both structures are from Escherichia coli (E. coli) and 1OB2 has the ligand kirromycin bound and 2BVN has the ligand enacyloxin IIa bound. Furthermore, both structures have two co-factors bound to the protein on the opposite side of the ligand. These are the GTP-analog GDPNP and an Mg^{2+} ion, which coordinates to GDPNP and the protein. The structure of EF-Tu with PDB code 1OB2 also contains a tRNA. The crystal structures 1OB2 and 2BVN have resolutions of 3.35 Å and 2.30 Å, respectively. This is summarized in table 4.1.

Table 4.1: Conformations of EF-Tu

Structure	Crystal structure	Resolution	Co-factors	Ligand
K	1OB2	3.35 Å	GDPNP/Mg^{2+}/tRNA	Kirromycin
E	2BVN	2.30 Å	GDPNP/Mg^{2+}	Enacyloxin IIa

Three different programs have been used in this thesis. The *de novo* design program LUDI [21, 23] was used for the first part of the calculations. For the docking study the docking program Glide [100] was used and for the MD simulations the program NAMD [61] was used.

4.1 De Novo Design

For the *de novo* design, the program LUDI [21, 23], a part of the Cerius^2 package, version 4.10L was used. Structure K was used for the *de novo* ligand design and the structure contains the ligand Kir, the co-factors GDPNP and Mg^{2+}, and has a tRNA bound. Structure K was chosen over structure E because it was the most examined structure and the easiest to prepare for *de novo* design. The protein structure, and not the ligand, was used to design new compounds. The PDB structure was loaded into the program LUDI and the tRNA and water molecules were removed from the structure. The protein and ligand were looked at separately. Bond and atom types of the ligand and the co-factors were corrected and hydrogen atoms were added to the ligand before it was minimized. The *de novo* library was used as the fragment library. The first calculations were performed using the protein structure as basis for finding new lead structures and the calculations were performed using default settings. The default scoring function is $score_2$ described in section 3.2. The binding site was selected by using the co-crystallized ligand to find the center for building new fragments. The center for the starting position was also found by selecting known amino acids in the binding site. Both ways were tried but the results were almost identical. After the run, the fragments found were sorted according to how well the fragments scored. After choosing a fragment as the starting position, the calculations were run in link mode with a single link site and a specified growth direction using the link library. The calculations were performed multiple times and therefore several fragments were linked together and several fragments were chosen as starting fragments. The starting fragments and the linking of fragments were chosen based on the score of the fragments and on chemical intuition of how well they would bind to the receptor.

In LUDI, it is possible to select target atoms in the receptor which the fragments are required to interact with. The interactions can be of hydrogen bonding character. This was tried, but as it gave no results, no fragments were selected from these calculations.

4.2 Dockings

Glide docking calculations require several steps before the actual docking can be performed. Prior to the docking, a protein preparation and a grid calculation has to be performed.

4.2.1 Preparations

To prepare the protein, ligand, and co-factors for docking, the PDB file was downloaded and the structures were inspected superfluously to check if any elements needed modification. When the structures were loaded into Maestro [102], the program added colour codes to the protein if any residues were unknown. This is typically the case for the ligand and the co-factors. Structure K is a monomer and has a tRNA bound, but to reduce computation time, the tRNA was removed because it is not near the binding site and does not effect the binding of the ligands. Structure E is a dimer and therefore the structure was truncated to a monomer. The protein, ligand, water, and co-factors were handled separately. For the ligand and co-factor GDPNP, the bond and atom types where corrected and the formal charge was changed. Hydrogens were added to the ligand and co-factor. The Mg^{2+} ion was also checked and the atom type was corrected and bonds to GDPNP were removed. The water molecules were examined to decide if any of them were positioned in the active site and therefore could play a role in the docking of the ligand. For structure E, water molecule number 83 in the active site was kept for the first set of dockings, but the water molecule was later removed from the binding site. No water was kept in the protein structure K. The protein structures were both truncated, from structure K the tRNA was removed and structure E was truncated to a monomer, and all the hydrogens were removed from the protein. The protein preparation and refinement was performed to neutralize the amino acids beyond a 10 Å radius of the ligand. This distance is usually 10-20 Å and it is used to detect and correct hydrogen bond clashes in the protein structure. The refinement performed a series of restrained, partial minimizations until the average RMS deviation had reached a limit of 0.3 Å. This calculation was performed with the Schrödinger program Impact. After this, the protein, ligand, and cofactor were ready for grid calculations.

4.2.2 Calculations

The grid calculations were performed using Glide version 3.5 and 4.0 [44] and the default settings were used except for the size of the inner grid box. For the calculation on structure K, the default settings of 10x10x10 $Å^3$ was used for the inner grid box. For the calculations on structure E, different sizes of the inner grid box were tried. With the old version (Glide 3.5), the inner grid box size was 10x10x10 $Å^3$ or 30x30x30 $Å^3$ and for the new version (Glide 4.0) 10x10x10 $Å^3$ or

14x14x14 $Å^3$ was used. It it possible to setup the grids with constraints and this was done for the structure E. The constraints were of hydrophobic character and were used to get the hydrophobic tail of the ligands to dock in the hydrophobic pocket in the protein. The grid calculations took between 10 minutes and several hours depending on the size of the grid box.

Having the grids, it was possible to perform flexible dockings of ligands. In some of the dockings, the co-crystallized ligand was used as a reference ligand. It was necessary to change the settings for the number of atoms and the number of rotable bonds in the ligand, because some of the ligands were quite big. The number of atoms was set to 200 and the number of rotable bonds to 30. Furthermore, the number of conjugated gradient minimization steps was changed from 100 to 5000. For some of the dockings, the constraints made in the grid calculations were added. The dockings took from 30 seconds to several minutes per ligand.

After the dockings were completed, the Glide Pose Viewer was used to examine the results. The Glide Pose Viewer shows the number of hydrogen bonds, van der Waals interactions, and the scoring of the ligands: The GlideScore, the E-model and the energy. Low GlideScores and E-models indicate good docking results.

4.2.3 Induced Fit Docking

The protein preparations for an induced fit docking (IFD) [105] were done as for regular dockings. The IFDs on structures K and E were performed using default settings. For structure E, however, Arg373 was mutated to an alanine residue in the initial run to make more room in the binding site.

4.3 Molecular Dynamics Simulations

The GTP analog, GDPNP, was changed to GTP for more realistic simulation conditions. Coordinates for residues 1-8 and 41-44 in structure E were missing from the PDB file. These were obtained through structural superpositioning of structure K and structure E and copying of the missing residues from structure K to structure E. These residues were later put through special treatment during minimization of the system.

Coordinates for missing amino acid, side chains, and hydrogen atoms in the crystallographic structures were reconstructed with the *psfgen* structure builder module of VMD [61] and by use of the CHARMM27 force field [73]. The systems

were solvated in a pre-equilibrated water box using the solvate plug-in to VMD [58] and extended 10 Å beyond the protein using the TIP3 water model. This solvation resulted in the systems having the size 90x100x80 $Å^3$. All crystal water molecules were kept in the simulations.

4.3.1 Amino Acid Protonation States

Eleven histidine residues were found in the EF-Tu structure. None of these were near the binding site, so the protonation states of them were not important for the ligand binding. The protonation states of the residues were chosen based on their local surroundings. Therefore, ten were chosen to have δ protonation and these were residues 11, 19, 22, 75, 78, 84, 118, 301, 319, and 364. The last histidine residue (66) was chosen to have ϵ protonation, because of more favorable hydrogen bonding properties. The amino acids Asp, Lys, Arg, and Glu were modelled charged while the Tyr residues were modelled neutral.

4.3.2 Modelling Ligands and GTP

Force field parameters to model the ligands and GTP were extracted from the CHARMM27 force field [73] and supplemented by sugar parameters for the sugar ring in Kir. For GTP, the parameters for guanine and ATP were used [90]. The force field was supplemented by Accelrys-CHARMm parameters as included in Quanta 2000 [4]. Partial charges for the ligands were calculated using VCharge [47] by equalization of electro-negativity. This method has recently been shown to give charges very similar to those in the CHARMM force field [47]. Charges and added parameters are found in appendix A.

4.3.3 Minimization

The solvated systems were minimized with NAMD [61] using the Conjugate Gradient algorithm in two steps to remove steric strain introduced when adding hydrogen atoms, missing side chain atoms, and residues. During the first 10000 steps of minimization, only hydrogens, missing side chains, and residues were allowed to move while all hetero atoms were kept fixed. In the second round of the minimization, hetero atoms were restrained in a harmonic potential with a force constant of $0.5 \frac{\text{kcal}}{\text{mol} \cdot Å^2}$.

4.3.4 Simulations

The simulations in table 4.2 were performed using the CHARMM27 force field [73] with added parameters for the ligands and for GTP using a parallel version of the program NAMD version 2.6 [61]. The MD simulations were performed in the isothermal NPT ensemble, which means with constant pressure, temperature, number of atoms, and with periodic boundary conditions. The partial mesh Ewald method [39] was used for full employment of the electrostatic interactions while the van der Waals interactions were accounted for up to a cutoff distance of 12 Å and were gradually faced out using a switch function from 10 Å. To achieve constant temperature, Langevin dynamics with a damping constant of 0.1 ps^{-1} was included; the atmospheric pressure was obtained with the implementation of the Langevin piston method [42]. Table 4.2 shows the different simulation runs.

Table 4.2: Simulations

	Initial conformation	Ligand	To study
1	Structure K	No ligand	Conformational changes in the protein and changes in the binding site
2	Structure K	Kirromycin	Conformational changes in the protein and ligand. Does the ligand stay in place?
3	Structure E	No ligand	Conformational changes in the protein and changes in the binding site
4	Structure E	Enacyloxin IIa	Conformational charges in the protein and ligand. Does the ligand stay in place?
5	Structure K	UF3-1	Conformational charges in the protein and ligand. Does the ligand stay in place?
6	Structure K	R29	Conformational charges in the protein and ligand. Does the ligand stay in place?

4.3.5 Data Analysis

Analyses of the MD simulations were performed with VMD version 1.8.4 [58] and the included Tcl-scripting facilities. The figures were drawn in VMD and the root-mean-square-deviations (RMSD) of the protein C-α atoms in each simulation were computed with respect to the initial minimized structure of the protein. Distances and angles for the interactions between GTP and the protein and between the ligands and the protein were also computed with respect to the initial minimized structure. These are shown in appendix G on page 235.

Chapter 5

Results

This chapter describes the results obtained as part of the thesis work in a systematic order. The first section describes the results obtained from the *de novo* design study. The second section describes the different sets of dockings performed: Docking of Enx using different setups and programs, docking of Kir- and Enx derivatives and vinylamycin compounds, docking of hybrid molecules, and docking of *de novo* design molecules. The last section describes molecular dynamics simulations performed on the crystal structures with and without their co-crystallised ligands, and on structure K with a hybrid molecule and a *de novo* design molecule. As such, this chapter represents several months of computation time. The docking studies and the *de novo* design were performed on a single computer while the MD simulations were performed on a 32 processor cluster at the University of Odense [111]. The docking analysis was conducted by first looking visually at the results and determining if the ligand was placed in the critical part of the binding site. If the ligand was placed correctly, the G-scores were considered. I have not examined the hydrogen bonds for most of the molecules because of the great number of dockings performed. The critical part of the binding site is defined from the experimental determination of the critical part of the ligand Kir in article [31]. The critical part of Enx has not been determined experimentally, but I have defined the critical part of Enx by superimposing the two ligands, Kir and Enx, and choosing the same amount of Enx as the critical part of Kir. These definitions of the critical parts are shown in figure 5.1 on the next page.

Figure 5.1 Definition of critical part of binding site

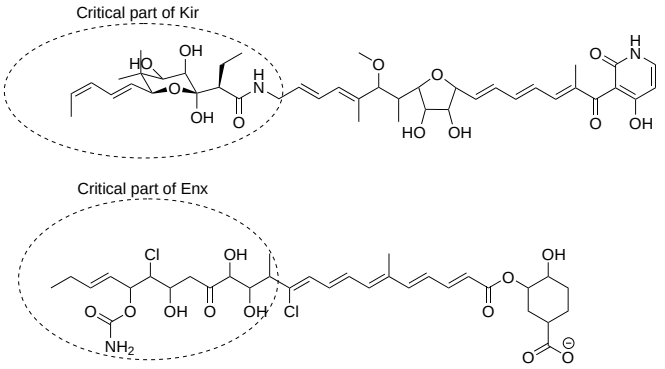

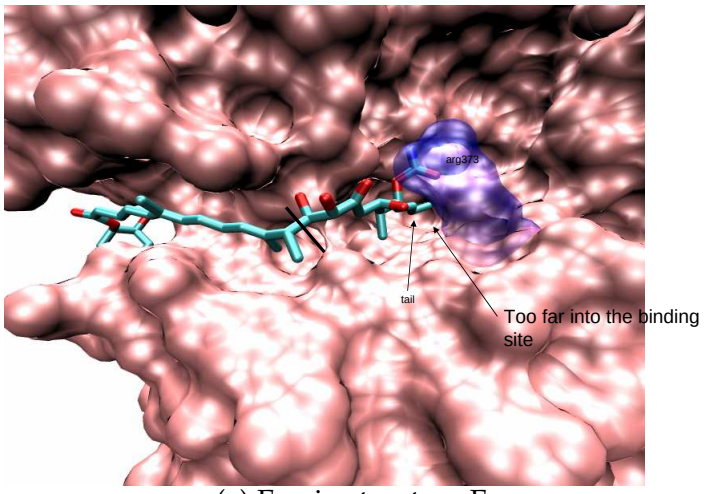

(a) Enx in structure E

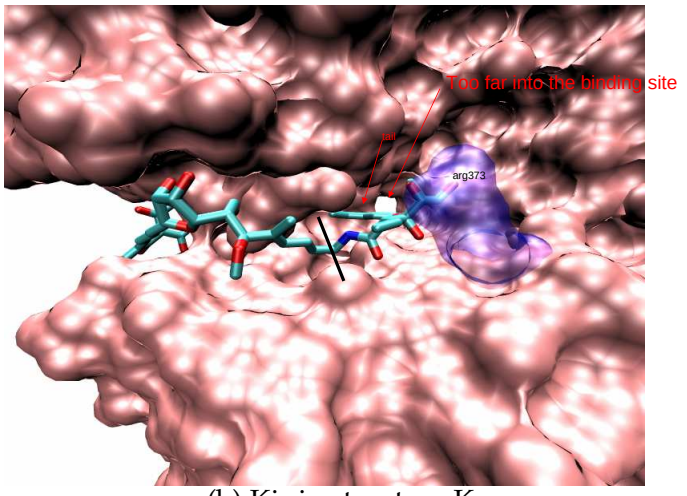

(b) Kir in structure K

The lines in the pictures above show where the critical part of the binding site starts. The part to the right of the line is the critical part.

5.1 De Novo Design

The result of the *de novo* design process was 57 new compounds. The structures of the compounds are shown in appendix D. The molecules were made from the protein structure K with the ligand Kir in the binding site. This protein structure was chosen because it is a monomer and for that reason it was the easiest to prepare for *de novo* design. Furthermore, it has the largest binding site of the two protein structures allowing greater flexibility of the ligands. The 57 new molecules were designed to fulfill Lipinski's rule of five [71]. Lipinski's rule of five is a set of criteria used for the design of orally active drugs. The rules are based on a distribution of calculated properties among several thousands drugs. The rule of five predicts that poor absorption or permeability is more likely for molecules when there are more than five hydrogen bond donors or ten hydrogen bond acceptors, and when the molecular weight is greater than 500 or the calculated $\log P$ ($C \cdot \log P$) is greater than 5, where P is the octanol-water partition coefficient [71].

Tables 5.1, 5.2 on the next page, and 5.3 on page 51 show the results for the rule of five criteria for the *de novo* design molecules. It can be seen that UB3-3 does not fulfill the rule of five because too many hydrogen bond donors are present; the ligand has six instead of five. H24-25 and H24-26 do not fulfill the rule of five because the calculated $\log P$ is higher than five for the two molecules. For H24-25 the value is 6.80 and for H24-26 the value is 5.65.

Table 5.1: CD7 and UB3 derivatives and HC6, HC5, and C18

Ligand	H-bond donors	H-bond acceptors	Molecular weight	$C \cdot \log P$
CD7-1	3	6	433.6	2.45
CD7-2	2	7	421.6	-0.43
CD7-3	1	6	391.5	0.66
CD7-4	3	6	433.3	2.45
CD7-5	3	3	293.4	3.04
CD7-6	4	4	278.3	-0.024
UB3-1	4	7	357.4	0.66
UB3-2	5	3	340.5	4.95
UB3-3	**6**	5	341.5	1.58
UB3-4	3	6	343.1	1.09
UB3-5	3	5	333.2	-2.85
HC6	2	2	268.2	4.17
HC5	3	3	293.4	4.35
C18	2	5	365.4	2.46

Table 5.2: H24 derivatives

Ligand	H-bond donors	H-bond acceptors	Molecular weight	$C \cdot \log P$
H24-1	5	6	373.5	0.86
H24-2	2	4	383.5	1.32
H24-3	2	4	279.4	0.96
H24-4	3	4	302.4	2.27
H24-5	3	4	302.4	2.27
H24-6	3	3	341.5	4.16
H24-7	2	3	384.4	4.74
H24-8	5	6	411.5	1.69
H24-9	3	4	354.5	3.48
H24-10	3	4	354.5	3.48
H24-11	2	5	341.5	2.84
H24-12	3	4	317.4	2.24
H24-13	2	2	208.3	2.08
H24-14	2	2	250.4	3.63
H24-15	3	3	251.4	1.45
H24-16	3	4	340.5	2.95
H24-17	3	4	316.4	2.65
H24-18	4	5	317.4	0.46
H24-19	4	4	267.4	0.11
H24-20	3	3	260.4	2.30
H24-21	5	4	280.4	0.087
H24-22	4	3	197.2	2.28
H24-23	4	4	281.4	-0.013
H24-24	3	3	280.4	2.18
H24-25	2	2	392.6	**6.80**
H24-26	3	3	265.6	**5.65**

Table 5.3: UF3 and H17 derivatives

Ligand	H-bond donors	H-bond acceptors	Molecular weight	$C \cdot \log P$
UF3-1	3	6	407.5	-0.87
UF3-2	3	3	262.3	1.76
UF3-3	4	5	429.6	4.69
UF3-4	4	5	379.6	2.43
UF3-5	3	6	321.4	-2.87
UF3-6	2	7	383.4	-2.97
UF3-7	5	8	362.6	-3.25
H17-1	4	7	348.7	-3.47
H17-2	2	5	265.3	-2.39
H17-3	2	5	291.3	-1.79
H17-4	2	5	263.3	-2.84
H17-5	1	5	309.4	1.70
H17-6	1	5	294.4	-1.52
H17-7	1	4	293.4	1.43
H17-8	1	4	308.4	4.21
H17-9	1	4	293.4	0.99
H17-10	1	3	292.4	3.99

The molecules were constructed using LUDI and then docked using Glide to see how well they would score. After docking in both proteins, some of the structures were imported into LUDI again and fragments were changed manually to make the molecules fit better in the binding site of both protein structures. Some of the structures were modified in several steps; this was achieved by creating the molecules, docking them using Glide, and then improving them manually by looking at the results. If a fragment showed good interactions with the protein, I tried attaching it to other fragments, thereby optimizing the structures by combining the results from LUDI with my chemical knowledge and the docking results.

5.2 Docking

The dockings performed in this thesis were performed using different versions of Glide. The first round of dockings were carried out with Glide version 3.5, but after these calculations were performed, a new version of Glide was released and therefore the calculations were carried out again with version 4.0 of Glide. The results will be described for the two different versions of Glide, but the weight will be on the results from Glide version 4.0. The two versions of Glide

will also be compared to examine the differences between them. I have performed different docking studies: Docking of *de novo* design molecules, docking of hybrid molecules, and re-docking of a study performed by PhD student Mette Lie, which contains the dockings of Enx and Kir derivatives and vinylamycin compounds.

To have a foundation for comparison for the rest of the dockings, the first dockings performed were of the co-crystallised ligands in their own proteins. The docking of Kir in its own protein, structure K, was performed without problems, but the docking of Enx gave some problems. Enx would not dock correctly and did not place itself as in the co-crystallised structure, so part of the work performed in this thesis was to try different approaches to get a co-crystallised ligand to dock in its own protein.

Figure 5.2 on the next page and table 5.4 show the results for docking Enx and Kir. The docking of Enx is only possible when hydrophobic constraints are added; otherwise the ligand docks on the surface of the protein structure E. When docking Enx in structure K, the ligand is placed with the wrong end in the critical part of the binding site. Docking of Kir is only possible in structure K. Without constraints, the ligand will not fit in the critical part of the binding site of structure E. With constraints, the wrong end of the ligand is placed in the binding site of structure E as shown in figure 5.2. Table 5.4 shows that Kir scores better then Enx when the ligands dock in their own sites. It can also be seen that Enx docks with better G-scores and E-models when no constraints are added. This may be because of better interactions between the ligand and protein. When comparing the two versions of Glide, it can be seen that ligands score better in version 3.5 than in version 4.0. Furthermore, figure 5.2 shows that only version 3.5 makes Enx dock correctly when using hydrophobic constraints. Version 3.5 shows better G-scores and E-models for docking in structure K. For both versions, docking without constraints gave better scores than docking with hydrophobic constraints.

Table 5.4: Results for docking in structure K and structure E

Ligand	Results	Structure K	Structure E, no constraints	Structure E, with constraints
Kirromycin, version 3.5	G-score/E-Model	-13.11/-216.03	-8.08/-104.36	-8.71/-128.48
Enacyloxin, version 3.5	G-score/E-Model	-9.33/-120.6	-11.22/-138.69	-9.47/-121.95
Kirromycin, version 4.0	G-score/E-Model	-13.2/-170.48	-7.82/-107.47	-6.77/-82.30
Enacyloxin, version 4.0	G-score/E-Model	-6.92/-99.08	-8.86/-116.98	-7.16/-84.32

Figure 5.2 Docking results for structure K and structure E

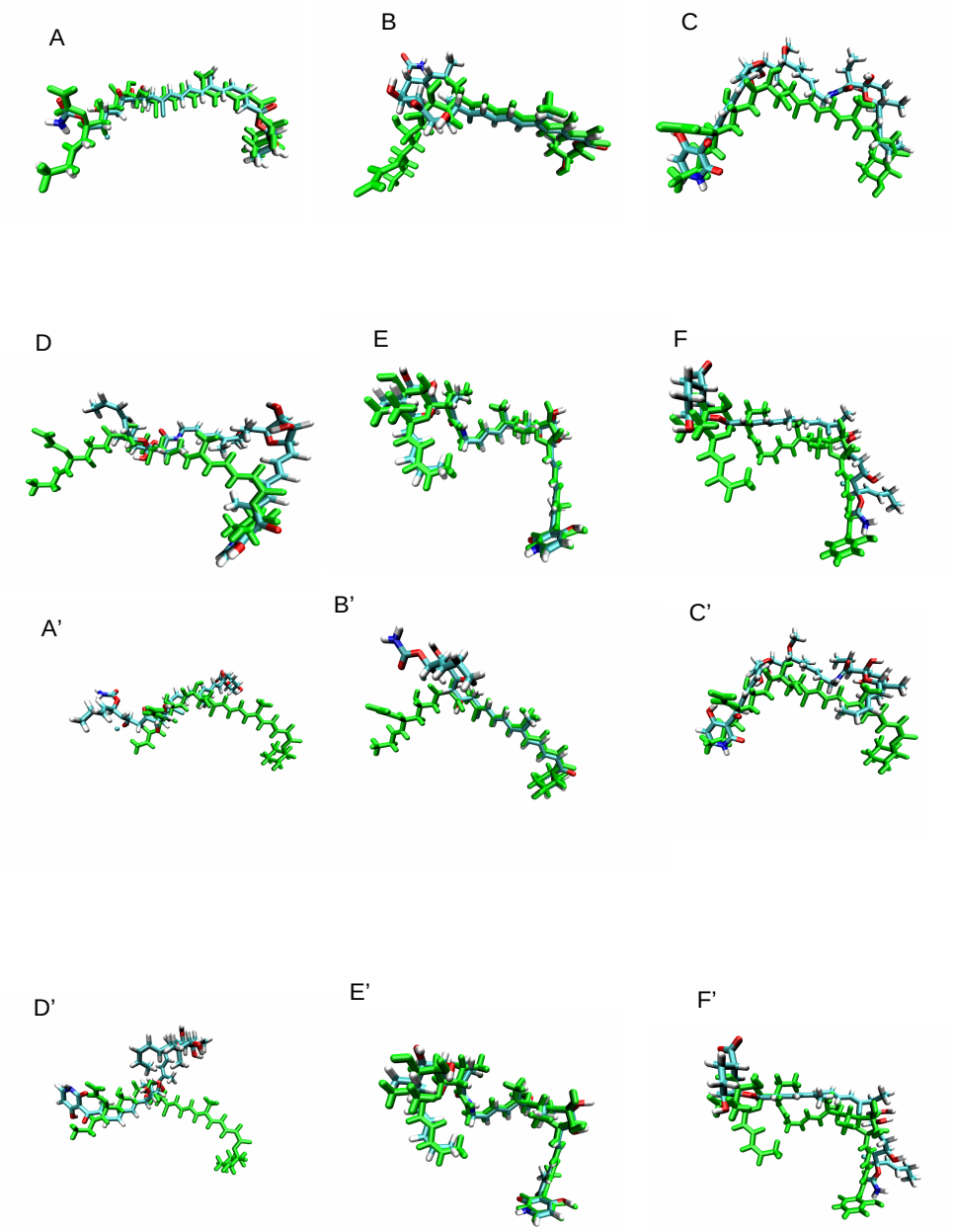

The figures show docking of Enx and Kir in structure E with and without hydrophobic constraints and docking in structure K. The figures without marks (A-F) are from version 3.5, whereas the figures with marks (A'-F') are from version 4.0. The A figures show Enx with constraints in structure E, the B figures show Enx with no constraints in structure E, the C figures show Kir with constraints in structure E, the D figures show Kir with no constraints in structure E, the E figures show Kir in structure K, and the F figures show Enx in structure K.

5.2.1 Docking of Enacyloxin IIa

The docking of Enx turned out to be a difficult challenge. I have tried to dock Enx in many different ways and with different settings and programs. I found that the only way I could get the co-crystallised ligand Enx to dock in its own protein was by using hydrophobic constraints. I have tried Glide docking with default settings, changing van der Waals radii, induced fit docking, and docking with constraints. I have also tried the programs LigandFit [113] and MolDock [110]. I have performed a dihedral drive and performed a conformational search on Enx to find the minimum of the ligand. These computations were performed to examine the structure of Enx and to find the global minimum of the structure. The global minimum was compared to the co-crystallised structure and differences were examined. The following sections give more details on the results of the individual experiments.

5.2.1.1 Glide with van der Waals Scaling

I have tried docking Enx in its protein, structure E, with softened potential by scaling of the van der Waal (vdW) radii. The settings used are shown in table 5.5 on the next page for the calculations on protein structure E and ligand Enx. The inner grid box had the default size (10x10x10 $Å^3$) or a grid size of 30x30x30 $Å^3$. Because of water molecules found in the binding site in the crystal structure the calculations were performed both with and without water. The water molecule chosen is number 83 and the molecule forms hydrogen bonds to amino acids Glu126(O), Val125(O), and to the NH_2 group in the carbamat of Enx.

The settings were chosen because PhD student Mette Lie has performed docking on Enx with Glide version 3.0 and chose the inner grid box size to be 30x30x30 $Å^3$. She estimated this was the correct way of performing the docking. The program would, in this way, have less influence on where the ligand was placed during docking. Water molecule number 83 in the binding site was also kept for the docking, and the results showed that Enx could not dock correctly when water molecule 83 was present. The two protein structures K and E were superimposed and the water molecule was added to structure K, and now it was possible to get Enx to dock in it. If water molecule 83 was not present in structure K, Mette Lie's results showed that Enx would flip and lie with the wrong end of the ligand in the critical part of the binding site.

In all my dockings, five poses were saved from each setup and examined to see if any of the dockings or poses could show the ligand in the active site as in

Table 5.5: Softened potential, scaling vdW radii

Docking number	Protein	Partial atomic charge	Ligand	Partial atomic charge
1	1.0	0.25	0.8	0.15
2	1.0	0.25	0.8	0.25
3	1.0	0.25	0.8	0.30
4	1.0	0.25	0.8	0.35
5	1.0	0.25	0.8	0.40
6	1.0	0.25	0.8	0.45
7	1.0	0.25	0.8	0.50
8	1.0	0.25	0.8	0.55
9	1.0	0.25	0.7	0.15
10	1.0	0.25	0.8	0.15 (XP)
11	0.9	0.25	0.8	0.15
12	0.9	0.25	0.8	0.25
13	0.9	0.25	0.7	0.15
14	0.8	0.25	0.8	0.15
15	0.8	0.25	0.8	0.25
16	0.8	0.25	0.7	0.15
17	0.7	0.25	0.8	0.15
18	0.7	0.25	0.8	0.25
19	0.7	0.25	0.7	0.15

19 different dockings were performed, with an inner grid box size of 30x30x30 $Å^3$ and Glide version 3.5. The calculations were performed in such a way that any atoms that have a partial atomic charge less than a predefined value (default 0.25 for the protein and 0.15 for the ligand) was given a van der Waal radius of 1.0 for the protein and 0.8 for the ligand as default. Columns two and four show the radius used in the different dockings. XP is a calculation performed with extra precision instead of standard precision (SP) which the rest of the dockings were performed with.

the crystal structure. Only a few poses show docking of Enx in a similar way but with a high G-score and usually also a high RMSD value. The G-scores are not shown in this thesis. The measured RMSD values for the docking of Enx are shown in the table 5.6.

Table 5.6: RMSD values from docking with scaling vdW radii

Docking number	10x10x10 Å^3 (no water)	10x10x10 Å^3 (with water)	30x30x30 Å^3 (no water)	30x30x30 Å^3 (with water)
1 (best/average)	34.40/35.37	5.11/5.93	4.61/4.71	5.01/5.27
2 (best/average)	34.40/35.57	5.20/6.37	4.63/4.72	4.88/4.99
3 (best/average)	34.40/35.37	5.20/6.37	4.63/4.72	4.88/4.99
4 (best/average)	32.21/35.32	5.09/6.08	4.60/4.68	5.10/5.29
5 (best/average)	32.21/35.32	5.09/6.08	4.60/4.68	5.10/5.29
6 (best/average)	34.12/35.05	5.58/7.11	4.61/4.75	4.91/5.23
7 (best/average)	34.12/35.05	5.24/6.58	4.57/4.68	1.96/4.39
8 (best/average)	34.30/35.45	5.24/6.58	4.57/4.68	1.96/4.39
9 (best/average)	34.12/35.02	4.94/5.19	4.39/4.66	3.13/5.21
10 (best/average)	34.29/34.95	5.37/5.87	4.59/4.63	11.30/12.00
11 (best/average)	33.73/36.87	33.73/36.87	4.63/4.74	3.98/4.98
12 (best/average)	33.73/36.87	34.84/36.46	4.63/4.74	3.98/4.72
13 (best/average)	37.05/40.84	34.26/36.43	4.57/4.9	4.34/6.26
14 (best/average)	34.68/36.95	34.28/35.9	4.55/4.74	5.11/8.86
15 (best/average)	34.68/37.26	34.28/35.65	4.55/4.76	5.11/8.86
16 (best/average)	34.06/37.18	34.37/37.86	4.24/4.73	4.51/9.78
17 (best/average)	34.60/37.11	35.68/37.09	4.19/4.50	7.13/9.57
18 (best/average)	34.60/37.11	35.02/36.65	4.19/4.63	4.18/7.89
19 (best/average)	33.77/38.30	8.04/31.27	4.52/4.76	4.93/12.22

Figure 5.3 on the next page shows two typical docking results: In A, Enx docks over Arg373 compared to the co-crystallised ligand and in B, Enx docks under Arg373, but does not place the hydrophobic tail in the hydrophobic pocket.

Table 5.6 with the RMSD values for the dockings and figure 5.3 show that it was not possible to dock Enx in its own site. Dockings 7 and 8 with the big grid and water give a RMSD value of 1.96 (shown in green) in table 5.6, but when looking at the structure figure (5.3 B), the hydrophobic tail of Enx is not in the right place. The dockings performed with the default grid showed a few poses were the critical part of the ligand was placed almost correctly, but they all have a RMSD value over 30 Å. They are coloured red in the table. Having performed these dockings, I can conclude that Glide version 3.5 is not capable of docking Enx in its own site and therefore I had to find alternative ways of getting Enx to dock in its protein. It is unclear why it is not possible to get Enx to dock in structure E with Glide version 3.5, when it is possible with an older

Figure 5.3 Typical dockings of Enx in structure E

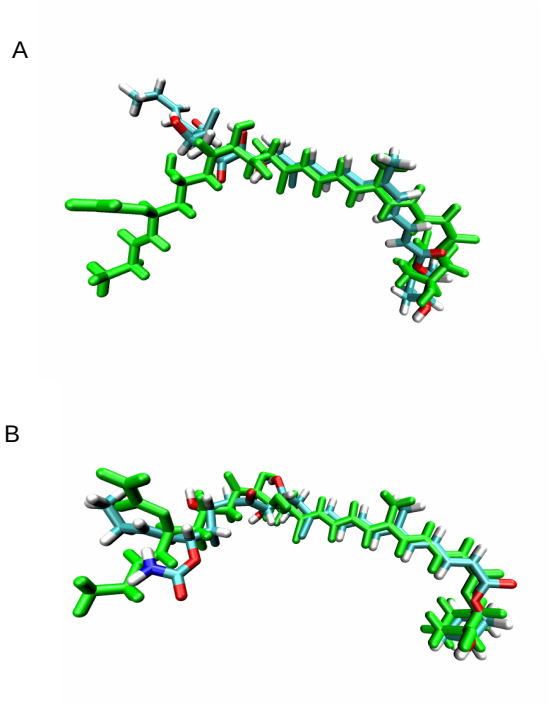

The figure shows Enx before and after docking. The co-crystallised structure is in green and the docked structure is in cyan.

version of Glide (version 3.0). There must be changes in the docking algorithm or other aspects of the docking. I have also performed docking in structure K, which is also an EF-Tu protein, but co-crystallised with Kir. It is possible to dock Kir in its own site, which is bigger than the binding site in structure E. Enx only docks correctly in this site when the water molecule from structure E is added to structure K. The results for these dockings are shown in section 5.2.2.

5.2.1.2 Docking of Enacyloxin IIa using MolDock and LigandFit

I have also tried the docking programs MolDock [110] and LigandFit [113] to get Enx to dock in its own protein structure. The results were that MolDock was not able to handle a molecule the size of Enx, so docking was not possible. With LigandFit, it was possible to dock Enx if the binding site was defined from the ligand instead of searching the protein structure for possible cavities, but then it was not possible to dock other molecules that are smaller than the co-crystallised ligand. If the binding site is found by searching the protein structure for possible cavities, it is possible to dock other ligands but not the co-crystallised ligand Enx. Using these two docking programs did not solve the problem of docking Enx in

structure E.

5.2.1.3 Dihedral Drive on Enacyloxin IIa

I have performed a dihedral drive on Enx to map out the potential energy for the dihedral angles. The process involves stepping through a set of specified dihedral angles. For each combination of the target dihedral angles, the angles are restrained while a minimization is performed. The angles chosen for the dihedral drive were the ones where the rotation occurs when a docking is performed. Figure 5.4 illustrates the distribution of the torsion angles in the molecule. The angles measured are the torsion angles between carbons 8-9-10-11 ($\omega 1$) and 9-10-11-12 ($\omega 2$); see figure 5.5 for the structure of Enx. In figure 5.4, the torsion angles are shown as angle 1 and angle 2; the former is $\omega 1$ and the latter is $\omega 2$.

Figure 5.4 Ramachandran plot of energy as function of torsion angles $\omega 1$ and $\omega 2$

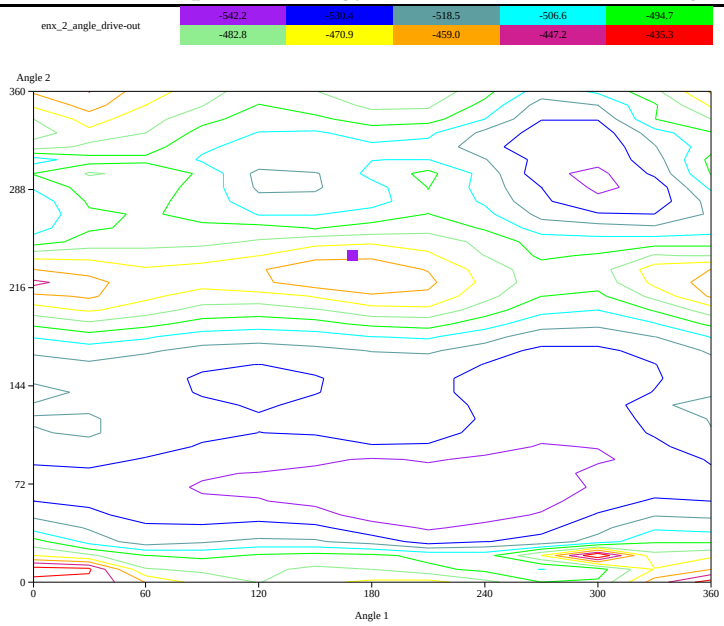

Figure 5.5 Structure of enacyloxin

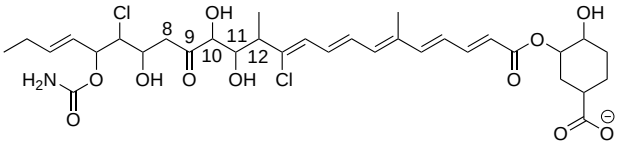

The plot shows one large minimum and a smaller minimum. The large has the torsion angle $\omega 1$ from 120 to 300°, while torsion angle $\omega 2$ is around 72°. The

smaller minimum is found where torsion angle $\omega 1$ is 300° and torsion angle $\omega 2$ is around 300°. For comparison, the torsion angle $\omega 1$ in the co-crystallised ligand is 176.2° and $\omega 2$ is 308.1°. These torsion angles were measured using Maestro [102]. Figure 5.4 shows that the co-crystallised structure is in a local minimum but not in any of the global minima. The ligand has a favorable conformation and this does not give an explanation to why Enx will not dock in its own site. The site is probably too small for the ligand to fit in or alternatively the scoring function prohibits the ligand from docking.

5.2.1.4 Induced Fit Docking of Enacyloxin IIa

In my search to find a way to dock Enx in structure E, I also tried to use Induced Fit Docking (IFD) [105]. This is a new type of docking algorithm that takes the protein flexibility into account and it was released from Schrödinger at the same time as Glide version 4.0. In an IFD calculation, side chain and some backbone flexibility around the ligand is allowed. The reason for using this was to see if the binding site is too tight for the ligand to enter. By letting the protein move, it may be possible to make room for the ligand to enter. I have performed three IFDs: Two with default settings, with and without water molecule number 83, and one where Arg373 was mutated to an Ala without water molecule number 83. The reason for doing this is that Arg373 lies over the entrance to the binding site and it may be in the way of Enx entering the binding site. I have used the default settings for the calculations with and without water and for the IFD with the mutation, this is the only changed setting. Unfortunately, this was not successful either, as it was not possible to get the co-crystallized ligand to dock in the ligand binding site. Pictures of this are shown in Appendix C.

The results for the dockings are still the same: Enx will not dock in the right place in the protein. Therefore, it was not a possibility to use IFD for the docking of Enx. The results of the dockings are shown in appendix C.

5.2.1.5 Docking with Constraints

Glide allows docking ligands with constraints, and I have tried this to see if this would make Enx fit in the binding site. I used hydrophobic constraints because the ligand has a hydrophobic tail that lies in a hydrophobic pocket. When performing a grid calculation, it is possible to add constraints and this was done for the docking in structure E. Glide finds all hydrophobic pockets in the protein and the one where the hydrophobic tail of Enx lies was chosen to be

used for further calculations. The adding of constraints means that part of the ligand is forced to dock in a given part of the protein. This made the ligand fit in the binding site. The ligand does not dock with as good a G-score as Kir does in its own protein, but it is acceptable. The results are shown in section 5.2.

5.2.2 Docking of Kir- and Enx Derivatives

This section describes the results obtained from the docking study started by PhD student Mette Lie and completed in this thesis. The dockings have been performed with three different versions of Glide. Mette Lie performed calculations using Glide version 3.0 and I have used versions 3.5 and 4.0. The dockings were performed in protein structures K and E to compare the binding of the ligands in the two proteins. The results are compared in groups of similar molecules and the different versions are compared. All the dockings have shown that the ligands dock better in structure K than in structure E, and there have been a lot of problems with the docking in structure E as described in subsection 5.2.1. Many of the ligands would not dock in the same way as the critical part of Enx when no constraints were used, but only when they were forced by the constraints.

The first set of ligands that were docked can be seen in figure 5.6 on the facing page and the results for this docking study are presented in tables 5.7 and 5.8 on the next page. This docking study was performed because it was discovered that vinylamycin had some of the same characteristics as Kir and Enx. The dockings in structure K show that the vinylamycin derivative R2 scores best in all three versions of Glide, and that the ligand was placed with the hydrophobic tail in the hydrophobic pocket in the protein. This means that the ligand is placed correctly according to the co-crystallised ligand Kir. The derivative R2 was initially drawn by mistake by PhD student Mette Lie when trying to draw vinylamycin. In versions 3.0 and 4.0, derivative R1 follows just after derivative R2 in score, but in version 3.5 derivative R1 is placed second last. For the dockings in structure E, only one structure was placed in the critical part of the binding site and this was derivative R1 when versions 3.5 and 4.0 with constraints was used. The rest of the structures are placed too far into the protein or on the surface of the protein.

The next docking study was performed on Kir and cutoffs of Kir; the structures are shown in figure 5.7 on page 62. The results for the cutoff study of Kir are shown in table 5.9 on page 63 and the dockings show that when docking in structure K, the results of docking of Kir, without cutoffs, are very similar for

Figure 5.6 Vinylamycin and derivatives

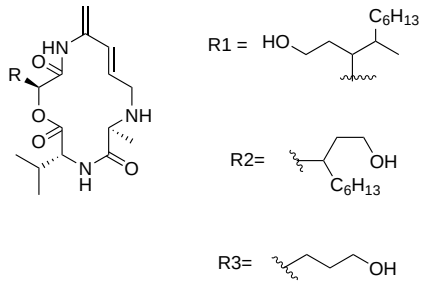

Table 5.7: Docking results for vinylamycin and derivatives in structure K

Ligand/Glide version	3.0	3.5	4.0
R1 Scores(G/E)	-6.39/-55.02	-4.98/-51.66	-6.73/-58.70
R2 Scores (G/E)	**-7.04/-68.57**	**-6.91/-69.15**	**-6.96/-69.74**
R3 Scores (G/E)	-6.78/-56.02	-6.32/-56.60	-5.25/-46.19
R=H Scores (G/E)	-6.13/-46.29	-4.97/-41.86	-4.38/-42.41

G/E indicates G-score/E-model. The numbers shown in bold indicate the top ranking ligand that is placed correctly.

Table 5.8: Docking results for vinylamycin and derivatives in structure E

LigandGlide version	3.0 water	3.0 no water	3.5*	3.5**	4.0*	4.0**
R1 Scores(G/E)	-4.48/-60.74	-6.04/-62.36	-6.02/-59.25	**-3.51/-36.42**	-4.93/-59.35	**-4.67/-43.81**
R2 Scores (G/E)	-5.22/-59.05	-6.09/-56.64	-5.38/-53.89	-4.5/-43.62	-4.40/-54.06	-4.78/-43.98
R3 Scores (G/E)	-4.81/-50.31	-6.59/-53.41	-4.72/-45.98	-/-	-3.96/-47.53	-/-
R=H Scores (G/E)	-5.48/-39.83	-5.13/-42.19	-5.37/-43.63	-/-	-4.45/-45.11	-/-

G/E indicates G-score/Emodel. * means docking with no constraints and ** means docking with constraints. The numbers shown in bold indicate the top ranking ligand that is placed correctly.

the three versions of Glide. The critical part of Kir has been found experimentally [31] and it is structure 7 in figure 5.7. When performing the dockings, this structure was found not to dock in the right place in the binding site, but when an extra C-atom was retained (the difference in structures 6 and 7 in figure 5.7), the ligand docked in the right place. This was found in all the docking using the different versions of Glide. Table 5.9 on the next page shows that when cutting parts off Kir, the G-score increases, but the ligands still bind even though not as strongly as Kir, as expected.

The dockings of Kir and cutoffs were also performed in structure E to examine the binding in this protein, and the results are shown in table 5.10 on the facing page. When docking with constraints, Kir is often placed in the binding site, but with the wrong end in the critical part. The G-scores for the dockings with constraints are higher than the dockings without. This could indicate that the scoring function is different or a punishment is added when using constraints, but I have not been able to find any documentation on this behavior. Table 5.10 also shows that the G-score increases with newer versions of Glide. When no constraints are added, the Kir and its cutoffs were not placed far enough into the binding site. The hydrophobic tail of Kir is greater than the one found on Enx and the protein structure E does not have room for the tail of Kir. This is probably the reason why Kir does not dock correctly. The amino acid Arg373, which is placed over the co-crystallised ligand in the crystal structure may also be in the way of Kir docking in the protein structure E.

Figure 5.7 Kirromycin and cutoffs

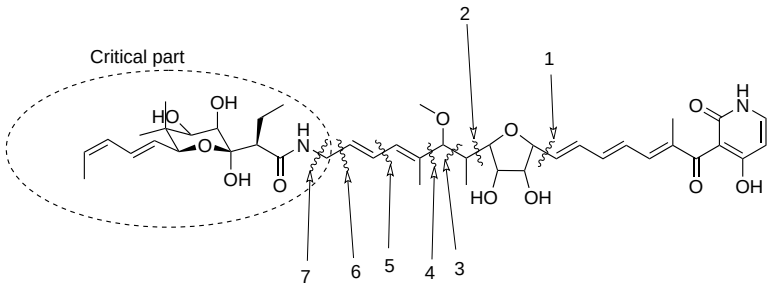

The numbers show where the molecule is cut to examine the effect of making the molecule smaller and shows the critical part of Kir. The numbers are used in the table showing the results for the dockings. The molecules is cut from the right.

Figure 5.8 on page 65 shows Enx and the cutoffs that were docked in structure K and structure E and the results are shown in tables 5.11 on page 65 and 5.12 on page 65. When docking Enx and cutoffs in structure K, the ligands were placed with the wrong end in the critical part or not far enough into

Table 5.9: Docking results for kirromycin and cutoffs in structure K

Ligand/Glide version	3.0	3.5	4.0
Kir scores (G/E)	**-13.14/-169.36**	**-13.11/-216.03**	**-13.20/-170.48**
1 scores (G/E)	-9.70/-102.88	-8.78/-104.11	-9.06/-104.65
2 scores (G/E)	-6.52/-72.92	-6.19/-64.59	-7.25/-72.51
3 scores (G/E)	-7.56/-77.93	-7.33/-65.17	-6.66/-65.35
4 scores (G/E)	-6.96/-69.87	-5.63/-58.92	-6.50/-59.05
5 scores (G/E)	-4.97/-52.66	-5.11/-52.31	-4.60/-49.01
6 scores (G/E)	-5.01/-47.53	-5.45/-46.95	-5.97/-46.94
7 scores (G/E)	-4.92/-46.46	-4.54/-45.15	-4.88/-46.37

G/E indicates G-score/E-model. The numbers shown in bold indicate the top ranking ligand that is placed correctly.

Table 5.10: Docking results for kirromycin and cutoffs in structure E

Ligand/Glide version	3.0, water	3.0, no water	3.5*	3.5**	4.0*	4.0**
Kir scores (G/E)	-9.48/-101.7	-10.7/-105.15	-8.08/-104.36	-8.71/-128.48	-7.82/-107.47	-6.77/-82.30
1 scores (G/E)	-6.71/-68.94	-6.14/-66.10	-5.81/-69.82	-6.27/-65.23	-4.82/-70.11	-4.74/-58.25
2 scores (G/E)	-6.91/66.94	-6.34/-66.20	-4.59/-57.57	-5.54/-57.47	-6.74/-64.77	-5.33/-47.23
3 scores (G/E)	-5.66/-60.64	-6.05/-70.25	-5.89/-58.44	-5.35/-56.63	-5.80/-56.29	-5.90/-54.23
4 scores (G/E)	-5.92/-52.58	-6.12/-58.2	-4.78/-51.53	-3.69/-38.02	-4.54/-51.72	-4.63/-41.82
5 scores (G/E)	-4.98/-51.27	-5.05/-51.90	-4.63/-48.69	-2.50/-17.72	-3.93/-48.50	-3.59/-30.22
6 scores (G/E)	-5.79/-45.73	-6.67/-47.95	-4.83/-39.11	-2.79/-14.83	-5.97/-42.72	-3.85/-29.14
7 scores (G/E)	-6.86/-45.26	-5.29/-47.63	-4.53/-41.07	-3.22/-16.55	-3.62/-40.64	-4.35/-26.31

G/E indicates G-score/E-model. * means docking with no constraints and ** means docking with constraints. No numbers are shown in bold, because no ligands dock correctly.

the binding site. Glide version 4.0 in particular placed the ligand away from the critical part of the binding site. This means that the binding site of structure K is not suitable or not able to make favorable interactions for the ligand Enx and its cutoffs.

When docking Enx and its cutoffs in structure E, I expected the dockings with constraints to show that Enx is able to dock in its own site. The results in table 5.12 on the facing page show that the G-scores for the dockings with constraints are higher than the dockings without, even though the dockings without constraints do not place the ligand or its cutoffs in the critical part of the binding site. The dockings with version 3.0 with water molecule number 83 show that the ligands were placed further into the binding site than the critical part of Enx in the crystal structure, but the ligands have the right end into the binding site. The same is true for the dockings with Glide version 3.0 without water, although some of the ligands docked with the wrong end into the binding site.

The results of the dockings using the two newer versions of Glide showed that for docking without constraints many of the ligands dock over Arg373 and therefore not in the binding site's critical part. Using Glide version 3.5, without water, cutoffs 3 and 5 docked in the correct place of the binding site and using Glide version 4.0 without water cutoff 5 docked in the right place. The dockings with constraints in Glide version 3.5 showed that all but cutoff 2 docked in the critical part of the binding site with the right end into the site; cutoff 2 docked with the wrong end into the binding site. For Glide version 4.0 with constraints, Enx and cutoff 1 docked too far into the binding site and did not have their hydrophobic tail in the hydrophobic pocket of the protein. The rest of the cutoff ligands of Enx docked correctly in the binding site. This means that Glide version 3.5 is able to dock Enx correctly when hydrophobic constraints are added, but the newer version 4.0 is not able to dock the entire ligand correctly. Only version 4.0 was able to dock the cutoffs correctly. The ligands do not dock with as good G-scores as the G-scores found when docking Kir and cutoffs in structure K.

The results for the dockings of derivatives of Kir are shown in tables 5.13 and 5.14 on page 67 and the structures are drawn in figure 5.9 on page 66. For the dockings in structure K, the results show that the newer versions of Glide improve the placing of the ligands in the critical part of the binding site. For version 4.0, only the ligand with R_{24} and R_1= OH did not have the hydrophobic tail in the hydrophobic pocket; the rest of the ligands were placed correctly. For version 3.5, six of the ten ligands were placed correctly, and for version 3.0 five

Figure 5.8 Enacyloxin and cutoffs

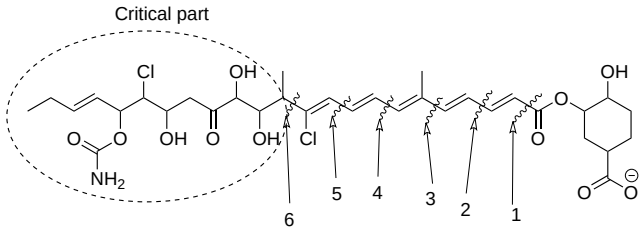

The numbers show where the molecule is cut to examine the effect of making the molecule smaller and shows the critical part of Enx, the numbers will be used in the table showing the results for the dockings. The molecules is cut from the right.

Table 5.11: Docking results for enacyloxin and cutoffs structure K

Ligand/Glide version	3.0	3.5	4.0
Enx Scores (G/E)	-7.45/-91.42	-9.33/-120.6	-6.92/-99.08
1 Scores (G/E)	-7.06/-71.23	-6.24/-66.19	-6.13/-63.37
2 Scores (G/E)	-6.62/-62.92	-7.05/-71.19	-6.09/-70.06
3 Scores (G/E)	-5.28/-56.55	-5.85/-61.84	-4.89/-59.65
4 Scores (G/E)	-5.34/-55.38	-5.58/-54.25	-5.03/-53.59
5 Scores (G/E)	-5.42/-58.19	-5.77/-50.11	-5.70/-61.21
6 Scores (G/E)	-6.64/-60.36	-7.35/-56.31	-4.38/-49.68

G/E indicates G-score/E-model. No numbers are shown in bold, because no ligands dock correctly.

Table 5.12: Docking results for enacyloxin and cutoffs in structure E

Ligand/Glide version	3.0, water	3.0, no water	3.5*	3.5**	4.0*	4.0**
Enx Scores (G/E)	-8.34/-110.6	**-8.7/-103.98**	-11.22/-138.69	**-9.47/-121-95**	-8.86/-116.98	**-7.16/-84.32**
1 Scores (G/E)	-6.92/-77.14	-6.5/-76.16	-6.26/-77.31	-7.2/-67.9	-5.93/-81.37	-4.11/-64.32
2 Scores (G/E)	-6.45/-79.6	-6.52/-77.3	-6.66/-59.77	-6.47/-57.8	-4.97/-61.18	-5.38/-59.66
3 Scores (G/E)	-6.23/-76.58	-6.76/-71.54	-5.12/-58.62	-5.38/-62.35	-4.97/-61.22	-5.21/-56.34
4 Scores (G/E)	-4.94/-61.01	-7.15/-70.03	-6.08/-55.36	-4.55/-52.81	-5.26/-60.47	-4.97/-49.24
5 Scores (G/E)	-6.99/-65.73	-8.09/-72.6	-4.45/-46.52	-4.48/-51.26	**-5.05/-54.35**	-5.00/-48.11
6 Scores (G/E)	-5.04/-59.62	-7.46/-63.78	-4.86/-50.23	-5.05/-53.54	-3.49/-43.43	-4.96/-50.82

G/E indicates G-score/E-model. * means docking with no constraints and ** means docking with constrains. The numbers shown in bold indicate the top ranking ligand that is placed correctly

of ten were placed correctly. The G-scores are very similar for the three dockings in structure K. Versions 3.0 and 4.0 both have R_{23} and R_1= OH as the ligand that docked best, whereas version 3.5 have R_{25} and R_1= OH as the best ligand. It is only for version 4.0 that the ligand with the best G-score is placed correctly; the two for the older versions did not have the hydrophobic tail in the hydrophobic pocket. Comparing the G-scores to the dockings for Kir, the derivatives of Kir do not score as well as Kir but almost as well or better than the cutoffs. From the dockings it seems as if the R-group should be R_{21}, R_{22}, or R_{23} for the best docking results and the R_1 group should be an OH group.

The docking study in the protein structure E show that the dockings performed with version 3.0 placed the ligand too far into the binding site and not over the critical part of the site. The docking studies, using versions 3.5 and 4.0, showed that when adding constraints the ligands were placed in the critical part, but without the constraints the ligands were not placed far enough into the binding site and therefore not in the critical part of the site. Version 3.5 of Glide with constraints give higher G-scores than version 3.0 but because it is the only version that will place the ligand in the critical part of the binding site, these are compared to the docking of Enx. The results for the docking showed that the Kir derivatives dock poorly in structure E.

Figure 5.9 Derivatives based on kirromycin

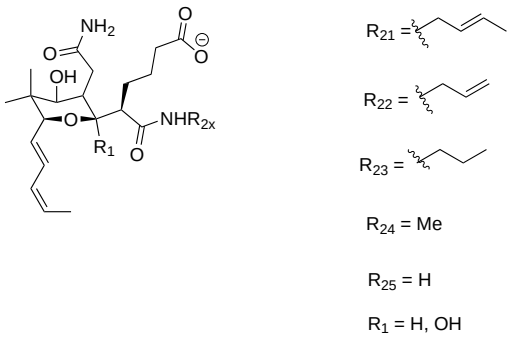

I have also docked derivatives of Enx, and the results for docking in structure K are shown in table 5.15 on page 68 and the structures of the ligands are shown in figure 5.10 on page 68. The results of the dockings show that most of the structures docked in the critical part of the binding site in structure K. There is a great variance in the G-scores, but the three versions are in good agreement on the scoring order of the best ligands. To get good results when docking in structure K, the number of carbons, n, should be three and R_1 should be an OH group. More of the Enx derivatives dock with a higher G-score than the

Table 5.13: Docking results for derivatives based on kirromycin in structure K

Ligand/Glide version	3.0	3.5	4.0
R_{21}, R_1 = OH (G/E)	-6.17/-82.93	-6.20/-79.60	-6.44/-76.85
R_{21}, R_1 = H (G/E)	-5.59/-75.3	-5.84/-76.33	-6.79/-72.61
R_{22}, R_1 = OH (G/E)	-6.8/-77.17	-5.79/-76.80	-6.2/-73.74
R_{22}, R_1 = H (G/E)	-5.72/-75.26	-5.55/-73.06	-6.17/-68.67
R_{23}, R_1 = OH (G/E)	**-6.83/-76.4**	-6.64/-76.38	**-6.81/-68.79**
R_{23}, R_1 = H (G/E)	-6.53/-71.64	-6.74/-75.37	-5.78/-61.99
R_{24}, R_1 = OH (G/E)	-6.29/-71.88	-5.74/-72.45	-5.91/-67.66
R_{24}, R_1 = H (G/E)	-5.56/-66.38	-6.38/-68.58	-5.86/-63.36
R_{25}, R_1 = OH (G/E)	-6.39/-68.88	**-6.98/-71.99**	-5.69/-68.77
R_{25}, R_1 = H (G/E)	-5.52/-64.85	-6.41/-68.90	-6.19/-63.05

G/E indicates G-score/E-model. The numbers shown in bold indicate the top ranking ligand that is placed correctly.

Table 5.14: Docking results for derivatives based on kirromycin in structure E

Ligand/Glide version	3.0 water	3.0 no water	3.5*	3.5**	4.0*	4.0**
R_{21}, R_1 = OH (G/E)	-5.07/-84.4	-6.09/-88.01	-6.21/-68.8	**-4.59/-56.23**	-3.89/-57.42	-4.42/-51.2
R_{21}, R_1 = H (G/E)	-5.79/-81.87	-5.6/-81.26	-4.66/-54.25	-4.49/-53.44	-4.4/-50.64	-4.75/-48.36
R_{22}, R_1 = OH (G/E)	-7.32/-84.27	-6.03/-82.46	-5.27/-68.02	-3.7/-27.63	-3.05/-40.88	-3.77/-41.01
R_{22}, R_1 = H (G/E)	-4.69/-69.45	-5.57/-78.00	-5.6/-63.52	-1.79/-23.57	-4.14/-56.79	-3.74/-37.99
R_{23}, R_1 = OH (G/E)	-6.35/-77.45	-5.3/-85.88	-5.36/-66.34	-/-	-4.13/-57.89	-2.88/-24.76
R_{23}, R_1 = H (G/E)	-4.82/-75.87	-5.54/-77.27	-4.96/-57.1	-2.29/-27.04	-5.36/-57.18	-3.72/-37.57
R_{24}, R_1 = OH (G/E)	-5.03/-78.84	-4.92/-78.94	-5/-60.02	-/-	-2.81/-60.08	-1.9/-17.32
R_{24}, R_1 = H (G/E)	-4.92/-75.45	-7.71/-78.69	-4.81/-56.57	-2.41/-25.35	-5.22/-53.39	-/-
R_{25}, R_1 = OH (G/E)	-6.15/-81.83	-5.31/-78.17	-5.41/-55.04	-3.58/-22.16	-4.98/-48.17	-/-
R_{25}, R_1 = H (G/E)	-5.51/-77.13	-5.7/-74.49	-4.95/-58.32	-3.31/-25.06	-4.91/-52.27	**-4.32/-30.41**

G/E indicates G-score/E-model. * means docking with no constraints and ** means docking with constraints The numbers shown in bold indicate the top ranking ligand that is placed correctly.

derivatives of Kir. The explanation for this is that the derivatives of Kir are structurally closer to Kir, which is the co-crystallised ligand for structure K. Both types of derivatives do not dock as well as Kir but some are better than the cutoffs of Kir.

Figure 5.10 Derivatives of enacyloxin IIa

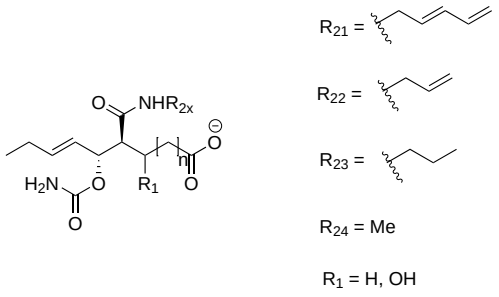

Table 5.15: Docking results for derivatives of enacyloxin IIa in structure K

Ligand/Glide version	3.0	3.5	4.0
R_{21}, R_1=OH, [1] (G/E)	-4.79/-64.59	-5.32/-60.63	-4.38/-53.4
R_{21}, R_1=H, [1] (G/E)	-5.37/-66.36	-3.18/-56.31	-4.14/-52.39
R_{21}, R_1=OH, [2] (G/E)	-5.42/-58.19	-4.60/-64.67	-5.38/-60.05
R_{21}, R_1=H, [2] (G/E)	-4.19/-62.89	-5.25/-64.29	-5.63/-59.69
R_{21}, R_1=OH, [3] (G/E)	-4.94/-73.4	**-6.14/-75.15**	**-6.73/-69.94**
R_{21}, R_1=H, [3] (G/E)	**-6.43/-71.87**	-4.49/-70.04	-5.79/-66.11
R_{22}, R_1=OH, [1] (G/E)	-1.76/-55.36	-1.29/-54.35	-2.49/-50.49
R_{22}, R_1=H, [1] (G/E)	-0.89/-54.66	-3.24/-60.04	-2.72/-55.73
R_{22}, R_1=OH, [2] (G/E)	-4.59/-61.88	-4.38/-61.95	-5.83/-58.07
R_{22}, R_1=H, [2] (G/E)	-3.14/-64.58	-1.61/-59.73	-1.87/-49.51
R_{22}, R_1=OH, [3] (G/E)	-5.89/-68.47	-5.95/-70.16	-6.41/-65.6
R_{22}, R_1=H, [3] (G/E)	-6.27/-70.56	-5.09/-65.37	-5.87/-60.6
R_{23}, R_1=OH, [1] (G/E)	-3.86/-54.82	-3.67/-53.08	-4.54/-48.3
R_{23}, R_1=H, [1] (G/E)	-1.52/-53.24	-1.26/-51.24	-2.5/-48.21
R_{23}, R_1=OH, [2] (G/E)	-4.80/-62.48	-4.61/-61.34	-5.78/-56.72
R_{23}, R_1=H, [2] (G/E)	-2.09/-59.11	-3.24/-60.04	-3.53/-54.89
R_{23}, R_1=OH, [3] (G/E)	-5.43/-63.03	-4.49/-43.29	-6.19/-63.87
R_{23}, R_1=H, [3] (G/E)	-5.15/-59.15	-5.28/-64.44	-4.84/-60.43
R_{24}, R_1=OH, [1] (G/E)	-2/-50.99	-1.78/-49.44	-3.03/-46.21
R_{24}, R_1=H, [1] (G/E)	-1.44/-48.71	-1.41/-48.39	-2.65/-44.98
R_{24}, R_1=OH, [2] (G/E)	-2.79/-57.56	-2.67/-57.91	-3.92/-53.08
R_{24}, R_1=H, [2] (G/E)	-2.17/-56.21	-1.93/-55.91	-3.33/-52
R_{24}, R_1=OH, [3] (G/E)	-4.97/-66.27	-6.02/-66.13	-6.64/-62.28
R_{24}, R_1=H, [3] (G/E)	-4.16/-63.07	-3.91/-32.22	-2.95/-57.14

G/E indicates G-score/E-model. The numbers shown in bold indicate the top ranking ligand that is placed correctly.

The results for docking in structure E are shown in table 5.16 on the next page. The dockings in structure E generally show that without constraints the ligands did not dock in the critical part of the binding site. The dockings for version 3.0 show that the ligands were placed too far into the binding site and only small parts of the ligands were in the critical part of binding site. The dockings for version 3.5 and 4.0 show that when no constraints were added, the ligands were placed in the wrong end of the binding site, but when constraints were added the ligands were placed in the critical part of the binding site. This indicates that the ligands have more possibilities for making favorable interactions in the wrong end of the binding site and only docked correctly when forced to by constraints. However, when looking at the G-scores for version 4.0, almost all ligands docked with constraints have a better G-score than the corresponding docking without constraints. This is not the case for version 3.5.

The last set of dockings were performed on annular structures based on Enx. The structures are shown in figure 5.11 and the results of the dockings are shown in tables 5.17 on page 71 and 5.18 on page 72. The results of docking in structure K show that version 4.0 is the best version for placing the ligands in the critical part of the binding site, but the G-scores are the worst of the three versions of Glide. Comparing the scores to the ones obtained from the dockings of Kir and cutoffs, the annular structures are not as good as the top ranking Kir cutoffs, but a few are better than the smallest cutoffs of Kir. The results show that the structure that binds best in structure K is structure 3 with an OH group as the R group. The number of carbon atoms, n, does not seem significant.

Figure 5.11 Annular structure based on enacyloxin IIa

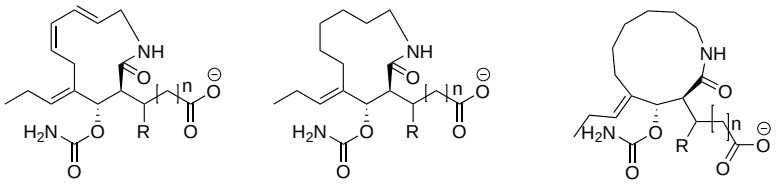

The results of docking in structure E, shown in table 5.18 on page 72, show that when no constraints are used, the ligands were placed too far into the binding site or in the part of the site that is before Arg373. Only when constraints were added, the ligands were placed in the critical part of the binding site of structure E. The G-scores are higher than the ones found for the cutoff study of Enx. As is the case for the dockings in structure K, structure 3 is the best.

Table 5.16: Docking results for derivatives of enacyloxin IIa in structure E

Ligand/Glide version	3.0 water	3.0 no water	3.5*	3.5**	4.0*	4.0**
R_{21}, R_1=OH, [1] (G/E)	-5.82/-76.22	-4.94/-71.28	-4.94/-63.94	**-4.06/-47.48**	-4.21/-55.01	**-5.3/-46.56**
R_{21}, R_1=H, [1] (G/E)	-5.97/-68.42	-5.72/-75.3	-4.41/-58.48	-6.15/-68.8	-3.56/-57.54	-3.92/-39.67
R_{21}, R_1=OH, [2] (G/E)	-6.69/-70.46	-6.67/-75.9	-5.25/-65.05	-2.81/-44.66	-4.53/-62.7	-4.12/-44.74
R_{21}, R_1=H, [2] (G/E)	-6.16/-61.18	-6.39/-71.05	-5.06/-64.3	-2.64/-44.96	-3.52/-54.23	-4.98/-47.19
R_{21}, R_1=OH, [3] (G/E)	-6.45/-72.35	-5.86/-68.2	-3.94/-47.9	-2.63/-42.14	-4.42/-62.07	-3.84/-41.13
R_{21}, R_1=H, [3] (G/E)	-7.09/-77.78	-7.04/-79.49	-4.38/-60.95	-3.69/-59.64	**-4.99/-45.33**	-4.31/-46.32
R_{22}, R_1=OH, [1] (G/E)	-2.51/-62.64	-3.07/-71.62	-0.72/-46.15	-1.67/-55.49	-1.05/-48.83	-1.76/-34.21
R_{22}, R_1=H, [1] (G/E)	-4.76/-71.1	-4.79/-71.09	-2.07/-58.72	0/-40.6	-0.29/-44.91	-1.28/-35.76
R_{22}, R_1=OH, [2] (G/E)	-6.13/-69.97	-6.47/-69.94	-3.28/-49.01	-2.77/-43.78	-2.99/-52.82	-4.17/-46.97
R_{22}, R_1=H, [2] (G/E)	-3.61/-64.07	-3.44/-64.31	-1.05/-61.06	-0.86/-47.38	-1.26/-39.08	-1.85/-44.16
R_{22}, R_1=OH, [3] (G/E)	**-5.6/-69.05**	-5.98/-70.22	-3.44/-49.67	-3.8/-48.19	-2.45/-54.83	-4.89/-54.83
R_{22}, R_1=H, [3] (G/E)	-7.2/-61.92	**-5.45/-61.52**	-3.91/-59.76	-3.43/-48.59	-3.89/-55.91	-4.37/-47.14
R_{23}, R_1=OH, [1] (G/E)	-6.81/-69.97	-5.57/-72.71	-4.47/-51.41	-3.79/-51.74	-3.63/-43.74	-3.89/-40.22
R_{23}, R_1=H, [1] (G/E)	-2.69/-64.43	-1.77/-52.11	-1.58/-47.39	-2.53/-36.8	-1.32/-45.22	-1.7/-36.2
R_{23}, R_1=OH, [2] (G/E)	-6.08/-65.65	-6.34/-67.16	-4.22/-52.09	-2.78/-42.23	-4.05/-43.51	-4.1/-44.42
R_{23}, R_1=H, [2] (G/E)	-3.97/-62.04	-4.06/-61.6	-2.96/-49.13	-1.31/-39.58	-0.09/-47.68	-1.97/-44.07
R_{23}, R_1=OH, [3] (G/E)	-6.27/-67.05	-6.11/-65.11	-4.13/-57.94	-3.14/-42.28	-4.51/-50.96	-5.24/-45.85
R_{23}, R_1=H, [3] (G/E)	-6/-66.63	-5.79/-63.72	-3.72/-49.86	-6.15/-66.63	-2.94/-43.76	-3.94/-40.9
R_{24}, R_1=OH, [1] (G/E)	-3.67/-51.33	-2.47/-53.27	-2.73/-54.42	-1.7/-47.95	-1.31/-40.16	-2.65/-38.79
R_{24}, R_1=H, [1] (G/E)	-4.29/-55.74	-4.75/-60.26	-2.39/-54.1	-1.58/-39.4	-2.01/-49.81	-2.42/-35.06
R_{24}, R_1=OH, [2] (G/E)	-5.01/-63.77	-5.9/-51.95	-1.76/-50.12	-1.13/-45	-2.74/-53.13	-3.51/-32.71
R_{24}, R_1=H, [2] (G/E)	-4.67/-59.46	-3.42/-55.24	-1.95/-52.78	-1.63/-45.89	-2.51/-40.24	-3.33/-41.22
R_{24}, R_1=OH, [3] (G/E)	-8.31/-64.68	-7.48/-64.69	-3.49/-52.77	-3.78/-49.03	-4.61/-48.96	-4.04/-45.31
R_{24}, R_1=H, [3] (G/E)	-4.93/-63.62	-4.17/-62.37	-0.45/-47.25	-1.55/-50.67	-1.48/-49.14	-2.98/-44.61

G/E indicates G-score/E-model. * means docking with no constraints and ** means docking with constrains. The numbers shown in bold indicate the top ranking ligand that is placed correctly. [n] indicates the number of carbons.

Table 5.17: Docking results for annular structure based on enacyloxin IIa in structure K

Ligand/Glide version	3.0	3.5	4.0
Structure 1, R=OH, [1] (G/E)	-5.85/-61.69	-6.32/-65.6	-4.82/-34.72
Structure 1, R=H, [1] (G/E)	-5.96/-61.8	-5.35/-49.08	-5.76/-43.78
Structure 1, R=OH, [2] (G/E)	-7.03/-69.44	-3.91/-32.22	-3.94/-31.17
Structure 1, R=H, [2] (G/E)	-5.82/-63.23	-2.99/-37.28	-3.12/-34.4
Structure 1, R=OH, [3] (G/E)	-5.29/-55.32	-4.49/-43.29	-4.44/-43.47
Structure 1, R=H, [3] (G/E)	-5.08/-54.43	-5.45/-49.89	-4.81/-52.27
Structure 2, R=OH, [1] (G/E)	-6.21/-65.47	-4.49/-43.29	-4.64/-38.43
Structure 2, R=H, [1] (G/E)	-5.92/-64.87	-5.46/-49.52	-5.54/-44.6
Structure 2, R=OH, [2] (G/E)	-5.73/-52.32	-4.15/-44.12	-4.67/-37.89
Structure 2, R=H, [2] (G/E)	-5.61/-55.83	-4.64/-48.72	-4.09/-43.92
Structure 2, R=OH, [3] (G/E)	-5.94/-51.72	-5.28/-52.41	-5.93/-47.83
Structure 2, R=H, [3] (G/E)	-4.35/-49.18	-5.1/-47.01	-5.86/-43.93
Structure 3, R=OH, [1] (G/E)	-6.24/-63.16	-4.98/-51.89	-6.02/-57.89
Structure 3, R=H, [1] (G/E)	-6.15/-63.48	-4.98/-52.56	-5.31/-48.59
Structure 3, R=OH, [2] (G/E)	**-6.68/-63.53**	-4.87/-53.19	**-6.05/-50.09**
Structure 3, R=H, [2] (G/E)	-6.63/-58.66	-5.24/-55.85	-5.52/-51.7
Structure 3, R=OH, [3] (G/E)	-5.67/-60.91	-5.84/-58.6	-5.99/-55.42
Structure 3, R=H, [3] (G/E)	-6.77/-63.63	**-5.97/-59.58**	-5.81/-55.14

G/E indicates G-score/E-model. The numbers shown in bold indicate the top ranking ligand that is placed correctly. [n] indicates the number of carbons.

Table 5.18: Docking results for annular structures based on enacyloxin IIa in structure E

Ligand/Version	3.0, water	3.0, no water	3.5*	3.5**	4.0*	4.0**
Structure 1, R=OH, [1] (G/E)	-5.85/-59.75	-5.85/-60.27	-4.38/-47.38	-/-	-4.22/-49.16	-3.72/-26.51
Structure 1, R=H, [1] (G/E)	-5.48/-39.83	-4.84/-52.09	-4.06/-43.87	-/-	-4.32/-39.2	-/-
Structure 1, R=OH, [2] (G/E)	-3.77/-44.91	-5.15/-51.56	-5.23/-42.03	-4.28/-32.47	-4.16/-53.98	-4.31/-30.6
Structure 1, R=H, [2] (G/E)	-3.94/-45.26	-6.09/-50.24	-4.29/-42.41	-4.17/-39.37	-4.87/-37.72	-5.19/-35.48
Structure 1, R=OH, [3] (G/E)	-4.9/-53.84	-4.71/-51.83	-5.54/-49.25	-4.11/-36.17	-4.97/-39.91	-3.46/-29.32
Structure 1, R=H, [3] (G/E)	-3.24/-50.88	-5.1/-56.77	-5.46/-46.87	-4.45/-39.24	-5.83/-42.93	-5.29/-36.33
Structure 2, R=OH, [1] (G/E)	-5.12/-52.56	-3.73/-47.18	-5.02/-53.16	-/-	-4.15/-27.99	-/-
Structure 2, R=H, [1] (G/E)	-5.06/-47.6	-3.69/-47.47	-4.31/-42.71	-/-	-4.53/-31.03	-/-
Structure 2, R=OH, [2] (G/E)	-4.77/-41.68	-7.25/-63.51	-5.02/-43.54	-4.76/-39.2	-3.81/-51.58	-4.79/-27.73
Structure 2, R=H, [2] (G/E)	-5.38/-49.21	-3.5/-45.38	-3.98/-42.73	-4.61/-41.56	-4.59/-37.44	-5.94/-39.67
Structure 2, R=OH, [3] (G/E)	-4.02/-47.65	-5.15/-55.08	-5.58/-52.81	-5.15/-46.91	-4.02/-49.21	-5.41/-39.92
Structure 2, R=H, [3] (G/E)	-4.22/-50.72	-4.03/-48.57	-5.08/-47.65	-4.5/-41.24	-4.11/-41.11	-5.34/-38.75
Structure 3, R=OH, [1] (G/E)	-5.72/-55.03	-5.62/-54.57	-3.6/-38.39	-3.34/-4.58	-4.04/-33.04	-/-
Structure 3, R=H, [1] (G/E)	-4.21/-45.26	-4.56/-45.29	-5.52/-47.8	-/-	-3.73/-34.63	-4.29/-34.68
Structure 3, R=OH, [2] (G/E)	-3.5/-42.59	-4.06/-43.76	-5.4/-37.9	-4.3/-30.28	-4.1/-35.64	-5.06/-29.69
Structure 3, R=H, [2] (G/E)	-4.9/-44.99	-5.93/-54.04	-4.32/-42.83	-4.57/-41.42	-4.97/-38.14	**-5.37/-35.51**
Structure 3, R=OH, [3] (G/E)	-4.9/-51.71	-4.28/-41.91	-3.6/-38.46	**-4.74/-42.45**	-3.16/-31.61	-5.17/-35.39
Structure 3, R=H, [3] (G/E)	-4.6/-46.33	-4.54/-46.66	-4.46/-44.13	-4.69/-43.56	-5.91/-43.43	-4.97/-34.9

G/E indicates G-score/E-model. * means docking with no constraints and ** means docking with constrains. The number in [] indicates how many carbons there are present in the [] in figure 5.11 The numbers shown in bold indicate the top ranking ligand that is placed correct. [] indicates what n is

5.2.3 Docking of Hybrid Molecules

This section describes the docking study of 1200 molecules, which I have designed in collaboration with Professor Troels Skydstrup's group at the Department of Chemistry at the University of Aarhus. The molecules have been tested to provide a starting point for a synthetic study and to narrow down the number of molecules to be synthesised and tested in the laboratories. I have docked the molecules using Glide versions 3.5 and 4.0 and in the two different protein structures: Structures K and E. This was done to compare the versions of Glide and to determine if the two protein structures would have different molecules that bind best. The structures of the molecules and the tables that contain the results are found in appendix E. The molecules were designed with Kir and Enx in mind and the two hydrophobic side chains were added to have similarities with the two co-crystallised ligands. Figure 5.12 on the following page shows the structures. The R_{2X} group was designed to resemble the tail of Kir or Enx or a combination of the two. The R_{3X} group was designed because Enx has a carbamat group and the OH group was chosen to see if the carbamat group had a significant influence on the binding of the ligands. The rest of the side chains and main structures were designed from free imagination to examine different aspects of the binding site in the two protein structures and to see if it was possible to find a lead compound for further testing.

The results will be discussed for the different dockings, and the different proteins and versions of Glide will be compared to find the best ligand for further calculations. The results show that the dockings in structure K compared to the dockings in structure E placed more molecules in the critical part of the binding site. The dockings without constraints only placed a few molecules correctly, whereas the dockings with constraints placed most of the molecules in the critical part of the binding site. The results show that when docking in structure K, the main structure should contain a lactam ring with an acid, because these molecules docked with the lowest G-scores and were placed in the critical part of the binding site. Many of the dockings show that the molecules were not placed with the R_{2X} group in the hydrophobic pocket as expected, and many had the R_{1X} group in the hydrophobic pocket. This is probably because both the side chains are hydrophobic and there is not a great difference in how big they are. When looking at the two side chains, the R_{1X} group should have R_{14} as the side chain and the R_{2X} group should be R_{23} or R_{24}. However, the choice of the R_{2X} group does not significantly affect how well the molecules dock.

For the docking studies in structure E without constraints, the results show

Figure 5.12 Structures of the designed ligands

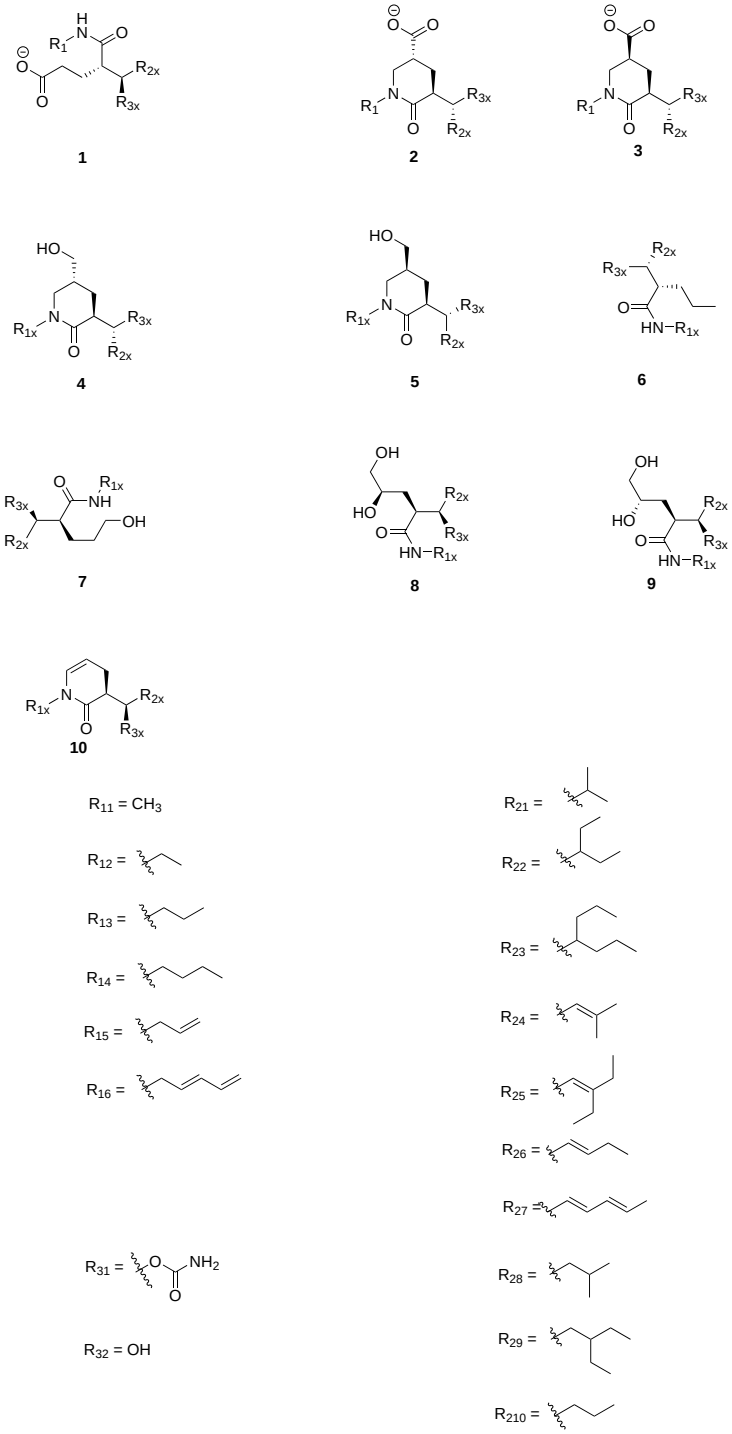

that the molecules that dock with the best G-scores all have the R_{1X} group in the hydrophobic pocket and none have the R_{2X} group in the pocket. This indicates that the pocket is not big enough for the R_{2X} group to fit. Not many of the molecules were placed in the critical part of the binding site so there are not that many molecules to base the conclusions on. Again, the lactam ring is important and the acid on the ring is the more favorable of the main structures. The R_{2X} group should be R_{27} or another side chain that is not too big and consequently does not take up too much room in the binding site.

For the dockings in structure E with constraints, the results show that the molecules that dock with the best G-scores are also here the ones with the lactam ring, and as before the R_{1X} group is in the hydrophobic pocket in the binding site. The R_{2X} group should be R_{27}, whereas R_{25} is the best group when using version 3.5. There is good agreement between docking in structure E with and without constraints for both versions of Glide. In the docking studies, the OH group is favored over the carbamat group, and this was not expected for the dockings in structure E, because the co-crystallised ligand Enx has the carbamat group.

Tables 5.19 to 5.24 show the results for the docking of the five best molecules that are placed in the binding site in the two versions of Glide and in the two protein structures. Overall, the five best docked molecules show the best G-scores in the dockings in structure E using version 4.0 of Glide without constraints. The second best dockings are in structure K also using version 4.0 of Glide. For none of the three sets of dockings do the same molecules dock among the five best when comparing the two versions of Glide. When looking at the five best docked ligands, it can be seen that the lactam ring is favored in all the dockings. In the dockings without constraints, the smaller R_{1X} and R_{2X} are favored, whereas in the dockings in structure K and structure E with constraints, the larger R_{1X} and R_{2X} are favored. The G-scores show that adding constraints give worse results compared to the dockings without constraints. The G-scores improve with version 4.0 of Glide, but the two versions of Glide do not agree on the structures with the best G-scores. When examining the results to see if R_{3X} should be an OH or a carbamat group, it is seen than when docking in structure K the two groups are equally good in both versions of Glide, but when docking in structure E using Glide version 4.0, the OH group is preferred.

Table 5.19: Top five docking results for structure K sorted by Glide version 3.5

Rank	Ligand	3.5	3.5*	3.5**	4.0	4.0*	4.0**
1	[3][R_{16}] [R_{28}] [R_{32}] (G/E)	**-6.5/-61.52!**	**-5.28/-61.21**	**-4.97/-43.55!**	-5.56/-45.34#	-4.8/-55.84	-5.49/-40.05!
2	[5][R_{14}] [R_{24}] [R_{31}] (G/E)	-6.13/-46.97!	-4.5/-40.65	-3.79/-40.15!	**-6.37/-54.61#**	-4.23/-38.47	-4.79/-34.3!
3	[5][R_{16}] [R_{26}] [R_{31}] (G/E)	-6.02/-57.74#	-3.45/-41.83	-3.4/-31.17#	-5.72/-56.42#	**-4.88/-44.02**	-4.96/-38.59#
4	[5][R_{13}] [R_{21}] [R_{31}] (G/E)	-6.01/-45.53#	-4.9/-40.48	-3.66/-34.22!	-6.26/-3.47#	-4.03/-37.15	-/-
5	[3][R_{15}] [R_{24}] [R_{32}] (G/E)	-6/-56.29!	-4.83/-54.8	-4.32/-50.32#	-6.18/-50.85!	-4.39/-51.65	**-5.92/-46.26#**

G/E indicates G-score/E-model. Without asterisk mean docking in structure K . In structure E, * means docking with no constraints and ** means docking with constrains. ! means that the ligand lies with R_2 in the hydrophobic pocket and # means that the ligand lies with R_1 in the hydrophobic pocket; [n] indicates which main structure is used. The numbers in bold are the top ranking structures.

Table 5.20: Top five docking results for structure E without constraints using Glide version 3.5*

Rank	Ligand	3.5	3.5*	3.5**	4.0	4.0*	4.0**
1	[3][R_{12}] [R_{210}] [R_{32}] (G/E)	-4.22/-33.04	**-5.8/-51.34#**	-5.12/-51.3#	-4.91/-28.09	-6.66/-46.35#	**-7.18/-46.45#**
2	[2][R_{11}] [R_{21}] [R_{32}] (G/E)	-4.51/-33.61	-5.75/-50.4#	-/-	-4.99/-29.5	**-6.69/-47.57#**	-5.65/-37.78#
3	[3][R_{12}] [R_{21}] [R_{31}] (G/E)	**-5.64/-55.91#**	-5.74/-53.97#	-4.97/-49.59#	-5.52/-32.35#	-4.85/-32.62#	-4.6/-36.62!
4	[7][R_{12}] [R_{210}] [R_{31}] (G/E)	-3.96/-40.62!	-5.56/-54.92#	-5.43/-54.21#	-4.86/-36.03!	-3.83/-43.07	-6.06/-49.52#
5	[2][R_{14}] [R_{22}] [R_{32}] (G/E)	-4.92/-46.4!	-5.51/-58.03!	**-5.49/-62.2#**	**-6.35/-42.4!**	-4.58/-50.58	-5.97/-48.85#

G/E indicates G-score/E-model. Without asterisk mean docking in structure K . In structure E, * means docking with no constraints and ** means docking with constrains. ! means that the ligand lies with R_2 in the hydrophobic pocket and # means that the ligand lies with R_1 in the hydrophobic pocket; [n] indicates which main structure is used. The numbers in bold are the top ranking structures.

Table 5.21: Top five docking results for structure E with constraints sorted by Glide version 3.5**

Rank	Ligand	3.5	3.5*	3.5**	4.0	4.0*	4.0**
1	[1][R_{15}] [R_{27}] [R_{31}] (G/E)	-4.96/-60.14!	-3.72/-59.83	**-6.48/-67.24#**	-5.37/-59.43#	-2.32/-57.88	-5.31/-49.94#
2	[3][R_{14}] [R_{29}] [R_{32}] (G/E)	-4.79/-53.97!	-3.54/-47.1	-6.4/-57.86!	-5.82/-47.9!	-3.77/-36.95	-4.39/-38.16#
3	[9][R_{14}] [R_{27}] [R_{31}] (G/E)	-4.9/-59.16#	**-5.38/-58.95**	-6.29/-62.09#	-5.39/-55.11#	**-7.17/-60.26#**	**-6.45/-54.41#**
4	[2][R_{13}] [R_{25}] [R_{31}] (G/E)	-4.47/-49.83!	-4.75/-51.12	-6.2/-60.16!	-5.19/-45.24!	-3.84/-50.65	-4.85/-40.05!
5	[2][R_{14}] [R_{23}] [R_{32}] (G/E)	**-5.46/-60.5!**	-4.1/-47.87	-6.15/-65.29#	**-6.15/-50.88!**	-4.14/-52.19	-5.3/-45.3#

G/E indicates G-score/E-model. Without asterisk mean docking in structure K . In structure E, * means docking with no constraints and ** means docking with constrains. ! means that the ligand lies with R_2 in the hydrophobic pocket and # means that the ligand lies with R_1 in the hydrophobic pocket; [n] indicates which main structure is used. The numbers in bold are the top ranking structures.

Table 5.22: Top five docking results for structure K sorted by Glide version 4.0

Rank	Ligand	3.5	3.5*	3.5**	4.0	4.0*	4.0**
1	[3][R_{12}] [R_{27}] [R_{32}] (G/E)	-5.39/-59.76!	**-5.23/-57.15**	**-5.45/-55.26#**	**-7.48/-50.59#**	**-6.61/-51.07#**	**-5.55/-46.41#**
2	[2][R_{16}] [R_{23}] [R_{32}] (G/E)	-5.59/-61.69!	-4.89/-62.44	-3.62/-42.87!	-7.03/-59.19!	-4.46/-58.54	-4.05/-32.34!
3	[9][R_{14}] [R_{21}] [R_{31}] (G/E)	-4.75/-43.86	-5.4/-49.42	-4.87/-43.82!	-7.02/-49.59#	-3.89/-49.23	-/-
4	[4][R_{12}] [R_{23}] [R_{32}] (G/E)	**-5.95/-43.16!**	-5.04/-41.43	-3.71/-34.72!	-7.01/-49.88#	-5.06/-42	-4.01/-32.39!
5	[5][R_{14}] [R_{28}] [R_{31}] (G/E)	-5.3/-46.28#	-5.05/-41.26	-3.82/-36.33#	-7/-58.78#	-5.33/-51.48	-3.86/-33.55!

G/E indicates G-score/E-model. Without asterisk mean docking in structure K . In structure E, * means docking with no constraints and ** means docking with constrains. ! means that the ligand lies with R_2 in the hydrophobic pocket and # means that the ligand lies with R_1 in the hydrophobic pocket; [n] indicates which main structure is used. The numbers in bold are the top ranking structures.

Table 5.23: Top five docking results for structure E without constraints sorted by Glide version 4.0*

Rank	Ligand	3.5	3.5*	3.5**	4.0	4.0*	4.0**
1	[2][R_{13}] [R_{22}] [R_{32}] (G/E)	**-5.51/-54.94!**	-4.94/-53.64	-5.41/-58.46#	-5.71/-46.25#	**-7.47/-56.88#**	-6.14/-46.6#
2	[2][R_{12}] [R_{22}] [R_{32}] (G/E)	-5.3/-45.04!	-4.16/-39.86	-5.44/-56.53#	-5.67/-44.08#	-7.39/-54.69#	-6.01/-44#
3	[2][R_{14}] [R_{25}] [R_{32}] (G/E)	-3.77/-43.44!	-3.77/-52.98	-5.27/-61.94#	-5.82/-43.33!	-7.35/-58.52#	-5.39/-45.29#
4	[2][R_{13}] [R_{28}] [R_{32}] (G/E)	-4.35/-35.35	-4.95/-52.67	-5.78/-54.44#	**-5.83/-39.62!**	-7.19/-53.69#	-5.88/-45.34#
5	[2][R_{14}] [R_{27}] [R_{31}] (G/E)	-4.9/-59.16#	**-5.38/-58.95**	**-6.29/-62.09#**	-5.39/-55.11#	-7.17/-60.26#	**-6.45/-54.41#**

G/E indicates G-score/E-model. Without asterisk mean docking in structure K . In structure E, * means docking with no constraints and ** means docking with constrains. ! means that the ligand lies with R_2 in the hydrophobic pocket and # means that the ligand lies with R_1 in the hydrophobic pocket; [n] indicates which main structure is used. The numbers in bold are the top ranking structures.

Table 5.24: Top five docking results for structure E with constraints sorted by Glide version 4.0**

Rank	Ligand	3.5	3.5*	3.5**	4.0	4.0*	4.0**
1	[3][R_{12}] [R_{210}] [R_{32}] (G/E)	-4.22/-33.04	**-5.8/-51.34#**	-5.12/-51.3#	-4.91/-28.09	**-6.66/-46.35#**	**-7.18/-46.45#**
2	[2][R_{14}] [R_{27}] [R_{32}] (G/E)	-4.32/-54.47#	-4.17/-53.76	**-5.82/-59.3#**	**-6.01/-48.51#**	-6.3/-51.18#	-7.01/-56.22#
3	[2][R_{14}] [R_{26}] [R_{32}] (G/E)	-4.4/-45.04!	-4.6/-54.81	-4.77/-56.77#	-5.11/-32.92!	-5.73/-46.54#	-6.97/-53.63#
4	[5][R_{11}] [R_{28}] [R_{32}] (G/E)	**-4.54/-39.42**	-5.68/-40.96	-2.96/-30.84!	-4.51/-37.18	-5.97/-39.75	-6.89/-41.84#
5	[2][R_{13}] [R_{24}] [R_{32}] (G/E)	-4.48/-36.34	-4.92/-53.02#	-5.11/-53.9#	-5.96/-34.8!	-4.75/-49.58	-6.76/-54.43#

G/E indicates G-score/E-model. Without asterisk mean docking in structure K . In structure E, * means docking with no constraints and ** means docking with constrains. ! means that the ligand lies with R_2 in the hydrophobic pocket and # means that the ligand lies with R_1 in the hydrophobic pocket; [n] indicates which main structure is used. The numbers in bold are the top ranking structures.

5.2.3.1 Induced Fit Dockings of Hybrid Molecules

I have performed induced fit docking (IFD) on the five best molecules found from docking in structure K using Glide version 4.0. The selected molecules are shown in figure 5.13.

Figure 5.13 Structures of the five best molecules from Glide version 4.0 docking

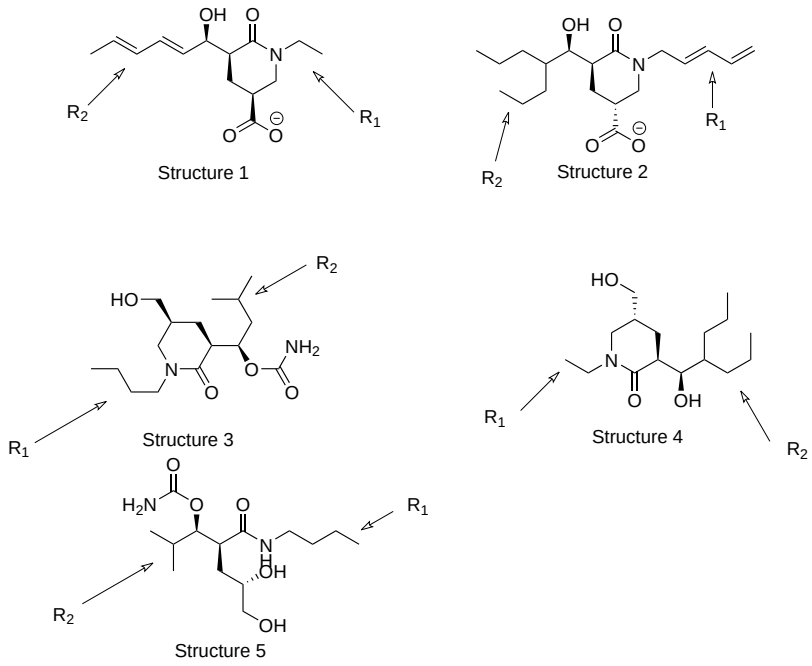

The results of the IFD were examined in the same way as the rest of the dockings performed. This includes visually inspecting where the molecules were placed in the binding site and examining with respect to which side chain (R_1 or R_2) was placed in the hydrophobic pocket. Here I also looked at the amino acid side chains to examine if it was possible to create the two hydrophobic pockets that are seen in the two protein structures and to find out which amino acid side chains had moved to make the binding site more favorable for the five molecules.

Four of the five molecules have a cyclic ring and I found in my earlier dockings that this ring is important for the scoring of the ligands. The fifth molecule has a carbon chain with two OH groups that might be hydrogen bond donors. Before the IFD, structures 1, 3, 4, and 5 were placed with R_1 in the hydrophobic pocket and structure 2 was placed with R_2 in the hydrophobic pocket. The purpose of the IFD was to investigate if it would make the ligands turn and place R_2 group in the hydrophobic pocket and if the molecules with the lactam ring

would still dock with the best scores after an IFD run. The full results for the IFD are shown in appendix F on page 229.

The IFD results showed that the molecules with the cyclic ring have more poses that dock in the right place in the binding site, but they do not have the best G-scores. Structure 4 is the molecule that has the most poses with the R_2 group placed in the hydrophobic pocket of structure K. This molecule was placed with the R_1 group in the hydrophobic pocket during Glide docking; see appendix E on page 185 for results. Structure 5, the molecule without the lactam ring, was placed with the R_1 group in the hydrophobic pocket when docking using Glide, and this was also the case for all poses with IFD. For structures 1, 2, and 3, some of the poses lie with the R_1 group in the hydrophobic pocket and others lie with the R_2 group in the pocket. Most of the poses are placed far into the binding site, because the molecules are small compared to the critical part of Kir and therefore not able to fill the critical part of the binding site. The structures move too far into the binding site and the site probably collapses because nothing is present to keep it open. The structures were all placed in one of three possible places in the binding site, two of which was in the critical part of the binding site with R_1 or R_2 in the hydrophobic pocket and the last possible place was outside the critical part. These results are very similar to the ones obtained from Glide docking when saving more poses. In the active site, many arginine residues were found and these move around a lot. In fact, they do not find the same positions in any of the poses, except for Arg333 which stays in place in most of the poses.

Structure 3 has the pose with the best G-score and the next best IFD-score and 10 out of 13 poses dock in the right place in the binding site. Only two poses lie with their hydrophobic arm in the right place and the rest lie in different ways. Structure 4 has the most poses that lie in the right place of the binding site, but they have the worst IFD-scores. With Glide docking, the molecule has the R_1 group in the hydrophobic pocket, but after IFD all but one pose have the R_2 group in the hydrophobic pocket. Structure 2 has 13 out of 18 poses that lie in the right place of the binding site; the ligand lies with the R_2 group in the hydrophobic pocket after Glide docking, but only 3 of the poses keep R_2 in the pocket after IFD. It is not possible for the protein to find a stable site for the ligand. Structure 1 has 5 out of 17 poses that lie with the R_2 group in the hydrophobic pocket after IFD; 3 of the poses do not lie in the right place in the binding site. Structure 5 has only five out of 13 poses that lie in the right place in the binding site. The rest lie over the middle of the binding site. However, the

best IFD-score is found for structure 5.

The results for the IFD show that the gaps in IFD-scores are close to or below the required 0.2 and therefore the dockings should be performed again with the results of the first round of IFD as the starting point [105]. This was not done because the knowledge of this was only received after the calculations were finished. I have not continued with IFD calculations because the results are very similar to Glide docking and it was not possible to find structures where the two hydrophobic pockets were found and occupied by the ligands.

5.2.4 Docking of De Novo Design Molecules

This section contains docking results for the *de novo* design molecules generated using LUDI. The dockings were performed to give a picture of how well the new molecules bind in the two proteins. I have docked the molecules in structure K and in structure E with and without hydrophobic constraints. The dockings show that some of the new molecules bind quite well and dock with a G-score that is comparable to the G-scores of Kir and Enx and their derivatives.

The structures for CD7 derivatives are shown in appendix D in figure D.1 on page 179 and the docking results are shown in table 5.25 on the next page. The dockings demonstrate that when no constraints were used, none of the ligands would bind in the critical part of the binding site. For that reason the focus will be on the results from docking in structure K and in structure E with constraints. The results also show that the dockings without constraints are the ones with the highest G-scores and this indicates that the ligands dock poorly in structure E when no constraints are used. CD7-2 is the ligand that docked with the best G-score in all the dockings, where it was placed in the critical part of the protein. So for these dockings, there is agreement between the two versions of Glide and the two protein structures.

The structures of UB3 derivatives are shown in appendix D in figure D.2 on page 180 and the results of the dockings are shown in table 5.26 on the next page. The dockings show that the UB3 derivatives did not dock well; UB3-5 would not dock in either structure K or structure E with any versions of Glide and UB3-2 would only dock in structure K using version 3.5 of Glide and only with a high G-score. UB3-1, UB3-3, and UB3-4 all docked fairly well in structure K with both versions of Glide, but none of the ligands docked well in structure E. Again it was seen that the ligands would only dock in the critical part of the binding site when constraints were added to the docking settings. For version 4.0 of Glide, UB3-1 docked best in the two proteins, but there is no agreement between the

Table 5.25: Results for CD7 derivatives

Ligand	3.5	3.5*	3.5**	4.0	4.0*	4.0**
CD7-1 (G/E)	-7.66/-84.7	-6.49/-69.7	-/-	-7.59/-81.88	-6.16/-62.94	-/-
CD7-2 (G/E)	**-7.74/-86.1**	-6.12/-77.69	**-8.24/-78.88**	**-8.53/-86.97**	-3.89/-76.04	**-7.01/-66.69**
CD7-3 (G/E)	-7.54/-90.84	-5.97/-80.03	-6.81/-63.78	-6.33/-90.92	-5.04/-82.66	-6.36/-69.37
CD7-4 (G/E)	-5.85/-61.02	-6.83/-65.22	-4.33/-48.07	-5.33/-45.69	-5.01/-53.89	-6.31/-54.81
CD7-5 (G/E)	-6.53/-58.09	-5.57/-45.05	-4.57/-37.5	-7.68/-57.18	-5.36/-44.62	-5.65/-38.49
CD7-6 (G/E)	-3,29/-44.09	-3.19/-47.15	-2.46/-46.79	-5.75/-56.5	-2.89/-51.07	-3.25/-34.19

G/E indicates G-score/E-model. The two dockings without asterisks are the dockings in structure K; the dockings with * are the dockings in structure E without constraints and the dockings with ** are the dockings in structure E with constraints. The numbers shown in bold indicate the top ranking ligand that is placed correctly.

two versions of Glide for either of the proteins.

Table 5.26: Results for UB3 derivatives

Ligand	3.5	3.5*	3.5**	4.0	4.0*	4.0**
UB3-1 (G/E)	-6.2/-74.48	-4.66/-61.87	-4.55/-47.67	**-7.88/-76.41**	-4.43/-61.33	**-4.75/-39.34**
UB3-2 (G/E)	-4.1/-47.23	-/-	-/-	-/-	-/-	-/-
UB3-3 (G/E)	**-6.58/-65.54**	-6.09/-50.47	-4.18/-24.8	-7.7/-68.31	-4.11/-48.69	-/-
UB3-4 (G/E)	-5.04/-61.21	-6.2/-60.39	**-5.32/-55.36**	-7.46/-86.45	-5.89/-56.86	-3/32.51
UB3-5 (G/E)	-/-	-/-	-/-	-/-	-/-	-/-

G/E indicates G-score/E-model. The two dockings without asterisks are the dockings in structure K; the dockings with * are the dockings in structure E without constraints and the dockings with ** are the dockings in structure E with constraints. The numbers shown in bold indicate the top ranking ligand that is placed correctly.

The structures of HC5, HC6, and C18 are shown in appendix D in figure D.3 on page 180 and the results of the dockings are shown in table 5.27 on the next page. The dockings show that the only way to get the ligands to dock in the critical part of the binding site is to use constraints, because none of the ligands were placed in the critical part of the binding site of either of the proteins. The two versions of Glide show the same results and there is agreement between the G-scores of the two versions and the way the ligands dock. The dockings in structure E with constraints show that ligand C18 docks with the best G-score in both versions of Glide.

The structures of the H24 derivatives are shown in appendix D in figures D.4 on page 181 and D.5 on page 182 and the results for the dockings are shown in table 5.28 on page 83. These dockings also show that when docking in structure E without constraints, only a few of the molecules would dock in the critical part of the binding site. The dockings in structure K both show that the ligand that binds best in this site is H24-1. Version 3.5 was able to place 12 ligands in the right place in the binding site, and version 4.0 was able to place 13 ligands

Table 5.27: Results for HC6, HC5, and C18

Ligand	3.5	3.5*	3.5**	4.0	4.0*	4.0**
HC6 (G/E)	-5.47/-37.72	-4.87/-35.92	-/-	-5.51/-32.97	-5.01/-35.74	-/-
HC5 (G/E)	-6.36/-54.76	-6.36/-50.25	-5.13/-42.28	-6.15/-53.55	-5.93/-50.71	-6.55/-45.18
C18 (G/E)	-4.52/-54.67	-4.92/-54.03	**-6.85/-65.14**	-4.36/-51.75	-4.95/-51.89	**-7.67/-60.01**

G/E indicates G-score/E-model. The two dockings without asterisks are the dockings in structure K; the dockings with * are the dockings in structure E without constraints and the dockings with ** are the dockings in structure E with constraints. The numbers shown in bold indicate the top ranking ligand that is placed correctly.

in the right place, but the two versions only agreed on six ligands that docked in the right place in the binding site. The two dockings without constraints did not give the same results: Both versions of Glide placed two ligands in the critical part of the binding site but it was not the same two ligands. Version 3.5 placed H24-1 and H24-25 in the critical part of the binding site and H24-1 had the best score. In version 4.0, the ligands placed in the critical part were H24-7 and H24-13, with H24-7 being the one with the best score. In the dockings with constraints, almost all the ligands were placed in the critical part of the binding site. Again there was no agreement between the structures that docked best in the two versions. In version 3.5, H24-8 docked best and in version 4.0, H24-18 docked best. The two structures do have similarities and in version 3.5, H24-18 docked as one of the better ones. The ligand that docks best in structure K is H24-1 for both versions of Glide. The result for the dockings with constraints, is that H24-8 docks best using version 3.5 and when using version 4.0, H24-18 docks best. The results for the docking of H24 derivatives showed that there is agreement between the two versions of Glide when docking in structure K, but not when docking in structure E. There is no agreement between the two protein structures either.

The structures for the docking of UF3 derivatives are depicted in appendix D in figure D.6 on page 183 and the results for the docking are shown in table 5.29 on page 84. The results show that the dockings in structure K give much better G-scores than the dockings in structure E and that the dockings without constraints were not able to place any ligands in the critical part of the binding site. For the dockings in structure K, the ligands with the highest G-scores are the ones that are not placed in the critical part of the binding site. This shows that it is more favorable to lie in the critical part of the binding site, and some of the ligands are not able to make enough favorable interactions in the critical part of the protein. The two versions of Glide both have UF3-1 as the ligand that has the best score for docking in structure K. The same result is shown when docking in

Table 5.28: Results for H24 derivatives

Ligand	3.5	3.5*	3.5**	4.0	4.0*	4.0**
H24-1 (G/E)	**-7.16/-64.39**	**-6.45/-73.54**	-5.73/-63.69	**-7.68/-71.21**	-6.36/-65.44	-5.58/-63.72
H24-2 (G/E)	-6.47/-74.57	-5.94/-69.49	-6.77/-76.77	-7.16/-68.84	-5.67/-66.71	-5.3/-62.96
H24-3 (G/E)	-3.84/-53.01	-6.6/-54.07	-4.53/-50.83	-6.41/-52.88	-5.62/-44.97	-5.85/-42.9
H24-4 (G/E)	-5.38/-50.84	-6.02/-53.74	-6.07/-56.89	-7.48/-57.06	-5.57/-52.34	-5.91/-48.65
H24-5 (G/E)	-5.71/-53.99	-5.37/-54.2	-5.66/-51.27	-4.98/-53.8	-5.56/-53.21	-5.77/-48.91
H24-6 (G/E)	-5.1/-49.31	-6.88/-59.58	-5.94/-52.86	-5.05/-50.02	-6.36/-53.89	-5.43/-48.68
H24-7 (G/E)	-5.03/-51.26	-5.53/-49.25	-5.27/-56.0	-4.9/-45.35	**-6.26/-50.4**	-5.22/-46.42
H24-8 (G/E)	-6.6/-71.6	-7.23/-73.28	**-6.81/-70.33**	-7.19/-71.78	-6.93/-73.55	-5.95/-66.3
H24-9 (G/E)	-6.37/-52.53	-6.2/-60.03	-4.71/-50.84	-6.74/-53.38	-5.37/-55.91	-4.13/-46.62
H24-10 (G/E)	-6.01/-56.74	-6.06/-58.25	-6.21/-58.5	-5.16/-51.84	-5.95/-55.87	-6.51/-56.42
H24-11 (G/E)	-5.18/-50.1	-6.39/-56.23	-5.07/-49.13	-5.65/-53.92	-6.17/-54.74	-6.07/-46.95
H24-12 (G/E)	-4.62/-48.14	-5.49/-53.53	-4.67/-48.42	-4.83/-53.04	-5.55/-58.32	-5.64/-45.64
H24-13 (G/E)	-4.54/-33.2	-5.41/-40.84	-4.53/-37.11	-4.81/-32.52	-5.26/-34.54	-5.9/-33.94
H24-14 (G/E)	-5.07/-40.29	-4.55/-43.96	-4/-38.08	-6.55/-41.54	-5.62/-41.62	-5.98/-38.01
H24-15 (G/E)	-4.45/-41.28	-5.16/-44.74	-4.93/-44.84	-5.43/-41.89	-5.58/-43.64	-5.08/-38.95
H24-16 (G/E)	-/-	-/-	-/-	-4.25/-58.77	-/-	-6.01/-55.47
H24-17 (G/E)	-6.11/-57.03	-6.08/-62.03	-6.09/-59.08	-5.07/-50.97	-6.01/-60.6	-5.94/-50.89
H24-18 (G/E)	-5.96/-63.24	-6.16/-60.7	-6.37/-65.08	-7.08/-59.32	-5.66/-59.22	**-6.99/-57.36**
H24-19 (G/E)	-3.45/-50.62	-3.97/-52.06	-3.93/-55.88	-4.06/-49.58	-2.91/-46.99	-3.85/-44.9
H24-20 (G/E)	-2.57/-44.87	-2.88/-48.51	-3.35/-51.71	-4.41/-48.54	-3.2/-47.59	-4.92/-52.24
H24-21 (G/E)	-2.35/-44.63	-4.03/-51.66	-3.82/-53.98	-4.18/-47.04	-3.79/-50	-4.85/-45.74
H24-22 (G/E)	-3.5/-50.62	-2.73/-48.75	-2.98/-48.12	-5.33/-52.98	-3.3/-46.06	-3.86/-46.14
H24-23 (G/E)	-2.95/-51.39	-3.65/-51.77	-3.56/-54.24	-4.38/-46.97	-3.53/-48.89	-3.97/-47.54
H24-24 (G/E)	-/-	-2.05/-49.74	-3.3/-52.05	-5.05/-53.27	-2.68/-48.57	-4.59/-50.08
H24-25 (G/E)	-5.81/-58.24	-6.16/-65.7	-6.14/-65.52	-5.56/-56.66	-6.51/-63.84	-6.55/-57.69
H24-26 (G/E)	-5.35/-57.27	-5.63/-61.26	-5.65/-53.96	-5.29/-61.38	-5.47/-60.38	-5.36/-47.48

G/E indicates G-score/E-model. The two dockings without asterisks are the dockings in structure K; the dockings with * are the dockings in structure E without constraints and the dockings with ** are the dockings in structure E with constraints. The numbers shown in bold indicate the top ranking ligand that is placed correctly.

structure E, but here the G-scores are higher and this is probably because it was only possible to dock the ligands with constraints where the ligands are forced to dock in a certain part of the binding site. There is substantial agreement between the two versions of Glide and also between the two protein structures, when looking at the dockings in structure E with constraints.

Table 5.29: Results for UF3 derivatives

Ligand	3.5	3.5*	3.5**	4.0	4.0*	4.0**
UF3-1 (G/E)	**-8.29/-93.84**	-6.52/-77.73	**-6.63/-68.17**	**-9/-90.97**	-4.7/-60.89	**-6.59/-62.89**
UF3-2 (G/E)	-6.34/-51.53	-5.74/-50.32	-4.81/-42.91	-6.12/-69.46	-4.75/-46.41	-6.12/-39.75
UF3-3 (G/E)	-8.03/-77.36	-5.86/-53.91	-6.48/-62.91	-6.04/-51.56	-5.6/-58.28	-5.93/-57.22
UF3-4 (G/E)	-6.35/-55.93	-5.54/-56.47	-5.59/-62.25	-6.8/-58.04	-5.29/-54.9	-4.28/-35.43
UF3-5 (G/E)	-7.19/-81.46	-4.94/-63.57	-6.06/-62.13	-8.19/-76.58	-5.37/-54.05	-5.35/-46.3
UF3-6 (G/E)	-5.34/-74.96	-6.38/-99.76	-2.01/-35.01	-5.02/-72.29	-4.7/-59.93	-3.56/-50.93
UF3-7 (G/E)	-4.12/-55.35	-4.94/-70.61	-5.15/-50.11	-8.15/-90.67	-3.65/-67.31	-4.66/-52.24

G/E indicates G-score/E-model. The two dockings without asterisks are the dockings in structure K; the dockings with * are the dockings in structure E without constraints and the dockings with ** are the dockings in structure E with constraints. The numbers shown in bold indicate the top ranking ligand that is placed correctly.

The structures of the H17 derivatives are depicted in appendix D in figure D.7 on page 184 and the results of the dockings are shown in table 5.30 on the facing page. The results show that none of the H17 derivatives dock very well. The best G-scores are higher than for most of the other dockings. For dockings in structure K, the ligand that docked best with both versions of Glide was H17-3. The newer version of Glide was better at docking the ligands correctly and gave a better G-score. The docking results for structure E without constraints show that none of the ligands were placed in the critical part of the binding site and the G-scores are not very good either. Docking with constraints in structure E show poor G-scores, but the ligands were placed in the critical part of the binding site. The two versions of Glide did not give the same results; version 3.5 docked H17-1 with the best G-score, while version 4.0 docked H17-5 with the best G-score. Again, this shows that the binding site of structure E is smaller than the one of structure K, and it explains why it was far more difficult to get ligands to dock correctly in structure E. There is no agreement between the two protein structures and the dockings in structure K are far better than the dockings in structure E.

In summary, the results of docking the *de novo* design molecules show that when docking in structure K the best ligand is UF3-1 and this ligand docked best in both versions of Glide. The dockings in structure E show that when docking without constraints it was only possible to get a few ligands to dock in the crit-

Table 5.30: Results for H17 derivatives

Ligand	3.5	3.5*	3.5**	4.0	4.0*	4.0**
H17-1 (G/E)	-3.97/-52.54	-5.39/-66.59	**-6.04/-63.24**	-4.92/-60.59	-4.51/-68.55	-3.48/-43.02
H17-2 (G/E)	-5.39/-72.33	-3.7/-57.77	-2.93/-57.48	-5.99/-69.75	-3.65/-53.21	-4.4/-47.93
H17-3 (G/E)	**-5.89/-75.99**	-3.96/-66.24	-3.79/-53.68	**-6.45/-72.05**	-4.13/-60.11	-3.63/-48.19
H17-4 (G/E)	-5.48/-71.83	-3.74/-57.17	-3.02/-39.2	-5.97/-67.95	-3.37/-50	-3.48/-46.18
H17-5 (G/E)	-5.67/-52.96	-5.28/-51.59	-4.46/-50.11	-5/-50.39	-4.02/-54.77	**-5.26/-45.6**
H17-6 (G/E)	-3.82/-58.21	-4.28/-58.4	-2.46/-58.09	-3.71/-48.33	-3.72/-52.91	-3.92/-49.64
H17-7 (G/E)	-3.36/-50.99	-4.32/-56.25	-3.24/-50.77	-2.66/-50.05	-5.05/-49.93	-3.94/-44.21
H17-8 (G/E)	-/-	-4.37/-45.15	-4.35/-46.7	-4.62/-45.63	-5.26/-52.59	-4.04/-39.56
H17-9 (G/E)	-/-	-2.17/-54.12	-2.8/-54.19	-3.81/-50.43	-2.99/-51.4	-3.63/-44.21
H17-10 (G/E)	-/-	-4.01/-54	-2.93/-44.41	-3.6/-48.86	-3.76/-53.79	-3.9/-46.97

G/E indicates G-score/E-model. The two dockings without asterisks are the dockings in structure K; the dockings with * are the dockings in structure E without constraints and the dockings with ** are the dockings in structure E with constraints. The numbers shown in bold indicate the top ranking ligand that is placed correctly.

ical part of the binding site and the ligands that docked correctly were H24-1 and H24-25 for version 3.5 and H24-7 and H24-13 for version 4.0. This shows that when only looking at the ligands that dock correctly there is no agreement between the two versions of Glide. In structure E the dockings with constraints demonstrated that ligand CD7-3 was the best for version 3.5 and C18 for version 4.0, but in version 3.5 C18 docked as the second best ligand. Overall, the best results were obtained when docking in structure K and the reason for this is probably that the ligands were designed from structure K.

5.3 Molecular Dynamics Study

I have performed several molecular dynamics simulations to examine the protein EF-Tu and to observe the conformational changes that occur during a 5 ns run. The overall protein structure, the binding of ligands, the binding site as well as the binding of GTP, and the GTP binding pocket were examined. The simulations were performed on a 32 processor cluster at the University in Odense [111]. Table 5.31 on the next page shows the simulations performed on the protein EF-Tu; snapshots were taken every 0.5 ps during the simulation.

Table 5.31: Simulations on EF-Tu

Initial conformation	Ligand	To study	Simulation number
Structure E	none	Binding site, GTP binding pocket	1
Structure E	Enx	Binding site, Enx conformation, GTP binding pocket	2
Structure K	none	Binding site, GTP binding pocket	3
Structure K	Kir	Binding site, Kir conformation, GTP binding pocket	4
Structure K	UF3-1	Binding site, UF3-1 conformation, GTP binding pocket	5
Structure K	R29	Binding site, R29 conformation, GTP binding pocket	6

The simulations were performed to examine the conformational changes that might occur in the protein EF-Tu, when a ligand is bound and when no ligand is bound. I have examined the results by calculating hydrogen bonds between the receptor and the ligand and hydrogen bonds between GTP and the receptor, because it is important to see if GTP stays in its bindings site. If GTP leaves its binding pocket, a large conformational changes will occur and the possible inhibitory effect of the two new molecules, R29 (see figure 5.21) and UF3-1 (see figure 5.22), will not be present. I have visually examined the size of the binding site to see if the site collapses when no ligand is bound and to see if the site changes when a smaller ligand is bound. Structure K was chosen as protein structure because this structure showed the best docking results and the dockings were performed without adding extra constraints to get the ligand to dock. The ligands in simulations 5 and 6 were chosen because of favorable G-scores and for simulation 6 the ligand was chosen because of the possibility for the R_2 group to fit in both hydrophobic pockets.

I have calculated the RMSD values for all the simulations to examine the overall stability of the protein during the 5 ns simulation. The RMSD values are calculated for the C-α atoms in the protein structure and figure 5.14 on the facing page shows the charts for the six simulations performed.

None of the simulations have great variations in the C-α movement during the 5 ns simulation. This means that even when no ligand is bound, the overall conformation of the protein is stable. The binding site does not collapse during the simulation. One explanation for this is that the water present in the binding site enters the empty binding site when the system is solvated before the simulation is run. The three charts in figure 5.14 show that for all the simulations the RMSD value is under 3 Å and this also supports the conclusion that no great conformationally changes occur in the protein. Some of the simulations have some spikes in the RMSD during the simulation, which could be changes in the overall conformation, but when examining the protein visually using VMD [58],

Figure 5.14 RMSD for the simulations

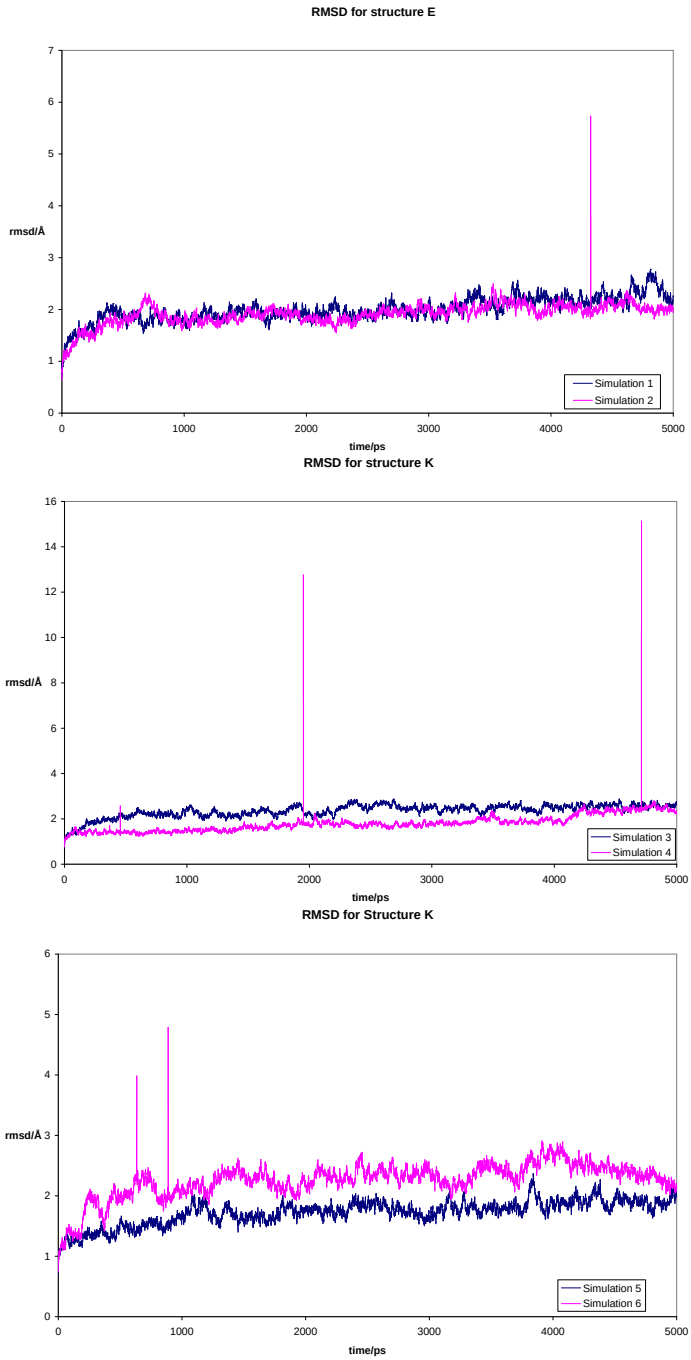

no conformational changes are seen.

5.3.1 GTP Binding

In the following section, the hydrogen bonds between GTP and the receptor for the 6 different simulations are described. A hydrogen bond is defined by a distance between hetero atoms of 3±0.5 Å and an angle of 180± 30° [17]. Electrostatic interactions are also possible between two charged atoms with a distance less than 4 Å, and here the angle is not important [14]. Figures 5.15 and 5.16 on the facing page, show the hydrogen bond donors and acceptors for the possible hydrogen bonds between GTP and the receptor in the different simulations.

Figure 5.15 GTP and its possible hydrogen bond donors and acceptors

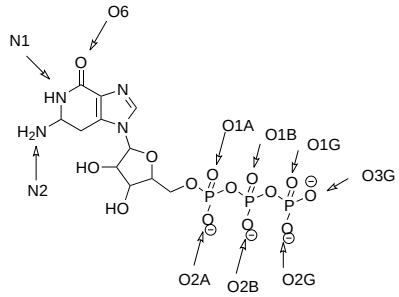

Table 5.32 on page 90 shows the hydrogen bonds between GTP and the receptor during the 5 ns MD simulation for the 6 different simulations. The table is based on measurements of distances and angles which are depicted in appendix G on page 235. From looking at the table, it is seen that many of the same hydrogen bonds are preserved during the simulation. Simulations 1 and 2 are the ones with the most hydrogen bonds preserved during the simulation. Simulation 1 has one more hydrogen bond preserved during the simulation than simulation 2; the bond is the one from the amino acid Asp21(N) to O2G in GTP. Simulations 3 and 4 have the same number of hydrogen bonds preserved during the 5 ns simulation. The bonds are almost the same, and the only variation is the hydrogen bond to O6 in GTP. In simulation 4, the bond is from Leu175(N) and in simulation 3 the bond is from Ala174(N). The difference between simulations 1 and 2 and simulations 3 and 4 are the hydrogen bonds Thr25N$-$H$\cdots$O2B and Gly23N$-$H$\cdots$O1B. They are present in simulations 1 and 2, but not in simulations 3 and 4. This is because the phosphate group in GTP in simulations 3 and 4 is further away from the amino acids Thr25 and Gly23 than they are in simulations 1 and 2. There are less hydrogen bonds in simulations 5 and 6; more hydrogen bonds are broken and formed and less are present during the

Figure 5.16 Amino acids present in hydrogen bonds between GTP and the receptor

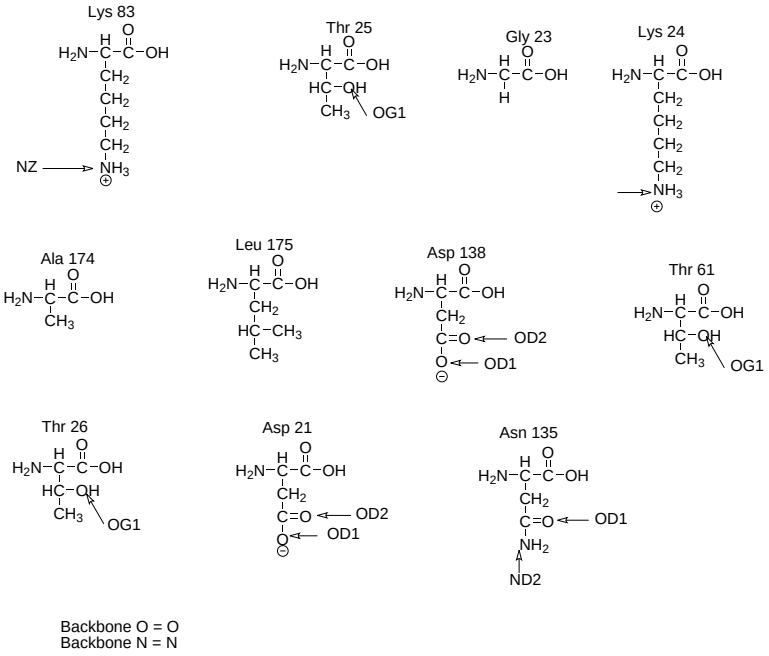

entire simulation. This may be because the docked ligands are much smaller than the co-crystallised ligands and therefore the binding site undergoes conformational changes which affect the GTP binding site. None of the GTP bindings sites go through large conformational changes, but small changes occur because the number of hydrogen bonds to water before and after the 5 ns simulations differs significantly.

Table 5.33 on the next page shows the hydrogen bonds to water before and after the 5 ns simulations. In all the simulations, water molecules move into the GTP binding site and form hydrogen bonds to GTP. This indicates that the binding site opens more for water to be able to enter the binding site. Structure E, simulations 1 and 2, is more open from the beginning of the simulations, because of the three hydrogen bonds between GTP and the water molecules present after the minimization.

5.3.2 Magnesium Complex

In the GTP binding site, there is a magnesium ion (Mg^{2+}) present and this ion coordinates to the GTP molecule and to the receptor. During some of the sim-

Table 5.32: Hydrogen bonds between the receptor and GTP

Hydrogen bond	Simulation 1	Simulation 2	Simulation 3	Simulation 4	Simulation 5	Simulation 6
83N — H · · · O2B	● — ○	● — ○	○ — ○	● — ○	● — ○	● — ○
25N — H · · · O2B	● — ●	● — ●	○ — ○	○ — ○	○ — ○	○ — ○
23N — H · · · O1B	● — ●	● — ●	○ — ●	○ — ●	○ — ○	● — ○
24N — H · · · O1B	● — ●	● — ●	● — ●	● — ●	● — ●	● — ●
174N — H · · · O6	○ — ○	○ — ○	● — ●	○ — ○	● — ○	● — ○
175N — H · · · O6	● — ●	● — ●	○ — ○	● — ●	○ — ●	○ — ●
135ND2 — H · · · N7	● — ●	● — ●	● — ●	● — ●	● — ●	● — ●
138OD1 · · · H — N1	● — ●	● — ●	● — ●	● — ●	● — ●	● — ●
138OD1 · · · H — N2	○ — ○	○ — ○	○ — ○	○ — ○	○ — ○	○ — ○
138OD2 · · · H — N1	○ — ○	○ — ○	○ — ○	○ — ○	○ — ○	○ — ○
138OD2 · · · H — N2	● — ●	● — ●	● — ●	● — ●	● — ●	● — ●
61OG1 — H · · · O1G	○ — ●	○ — ○	○ — ○	○ — ○	○ — ○	○ — ○
61OG1 — H · · · O2G	○ — ○	○ — ○	○ — ○	○ — ●	○ — ○	○ — ○
61OG1 — H · · · O3G	○ — ○	○ — ○	○ — ○	○ — ●	○ — ○	○ — ○
24NZ — H · · · O1G	○ — ○	○ — ○	● — ●	● — ●	● — ●	● — ●
24NZ — H · · · O2G	● — ●	● — ●	○ — ○	○ — ○	● — ○	○ — ○
24NZ — H · · · O3G	○ — ○	○ — ○	○ — ○	○ — ○	○ — ○	○ — ○
24NZ — H · · · O1B	● — ●	● — ●	○ — ○	○ — ○	○ — ○	○ — ○
24NZ — H · · · O2B	○ — ○	○ — ○	○ — ○	○ — ○	○ — ○	○ — ○
26N — H · · · O1A	● — ●	● — ●	● — ●	● — ●	● — ●	● — ●
26N — H · · · O2A	○ — ○	○ — ○	○ — ○	○ — ○	○ — ○	○ — ○
26OG1 — H · · · O1A	● — ●	● — ●	● — ●	● — ●	● — ●	● — ●
26OG1 — H · · · O2A	○ — ○	○ — ○	○ — ○	○ — ○	○ — ○	○ — ○
21N — H · · · O1G	○ — ○	○ — ○	○ — ○	○ — ○	○ — ○	○ — ○
21N — H · · · O2G	● — ●	○ — ○	● — ●	● — ●	○ — ○	● — ●
21N — H · · · O3G	○ — ○	○ — ○	○ — ○	○ — ○	○ — ○	○ — ○

● — ● hydrogen bond present during the entire 5 ns simulation. ○ — ○ no hydrogen bond present at any time during the 5 ns simulation. ● — ○ hydrogen bond present in the beginning of the simulation. ○ — ● hydrogen bond present at the end of the simulation. The amino acids are only shown by their number, but the amino acids can be seen in figure 5.16. The different atoms in the amino acids are N = backbone nitrogen, O = backbone oxygen, NZ = side chain NH_3^+, OD1= side chain OH, and ND2 = side chain NH_2. The atoms where the hydrogen bond ends are from GTP and these can be seen in figure 5.15.

Table 5.33: Hydrogen bonds between GTP and water

Hydrogen bonds	Simulation 1	Simulation 2	Simulation 3	Simulation 4	Simulation 5	Simulation 6
Before simulation	O3G, O3′, N3	O3G, O3′, N3	-	-	-	N2
After simulation	O2G, O3G, O2A, O2′, O3′, N3, O1	O1G, O2G, O3G, O2A, O2′,O3′,N3	O2G, O3G, O2A, O2′, O3′, N3	O2G, O3G, O2A, N2, N3, O2′, O3′	O1G, O2G, O3G, O1B, O2′, O3′, N2, N3	O2G, O3G, O1B, O2B, O2A, O2′, O3′

ulations, the coordination changes so water becomes part of the coordination. This is also an indication that the GTP binding site opens slightly so that water molecules can enter. The ionic interaction is octahedron and this means that six atoms coordinate to the Mg^{2+} ion. Table 5.34 shows the atoms that coordinate to the ion during the simulations. Table 5.34 is based on measurements between the atoms in the table and the Mg^{2+} ion and charts for these are shown in appendix H on page 273. I have measured distances between the Mg^{2+} ion and the atoms found in a radius of 3 Å of the ion.

Table 5.34: Mg^{2+} complex

Atom	Simulation 1	Simulation 2	Simulation 3	Simulation 4	Simulation 5	Simulation 6
Asp50(OD1)	○ − ○	○ − ○	● − ●	○ − ●	○ − ○	○ − ○
Asp50(OD2)	○ − ○	○ − ○	○ − ●	○ − ●	○ − ○	○ − ○
Thr61(OG1)	● − ○	○ − ○	○ − ○	● − ○	● − ○	● − ●
Thr25(OG1)	● − ●	● − ●	● − ●	● − ●	● − ●	● − ●
O1G	● − ●	● − ●	● − ●	● − ●	● − ●	● − ●
O2G	● − ●	● − ●	● − ●	● − ●	● − ●	● − ●
O3G	○ − ○	○ − ○	● − ●	● − ●	● − ●	● − ●
Water	● − ● x 2 and ○ − ●	● − ● x 3	○ − ○	○ − ○	○ − ●x 2	○ − ●

● − ● interaction present during the entire 5 ns simulation. ○ − ○ no interaction present at any time during the 5 ns simulation. ● − ○ interaction present in the beginning of the simulation. ○ − ● interaction present at the end of the simulation. x3 means that three water molecules coordinate to the Mg^{2+} ion and x2 means that two water molecules coordinate to the Mg^{2+} ion.

Table 5.34 shows that simulations 1 and 2 have six atoms that coordinate to the ion during the entire simulation, while the rest of simulations start out with 5 atoms that coordinate to the ion, and during the simulation, the last atom moves close enough to coordinate to the Mg^{2+} ion. In all the simulations, the ion has ionic interactions to O1G, O2G from GTP and Thr25(OG1), but in simulations 3 and 4 the ion does not have any interactions with water. This is because the binding site is too small for water to enter the site. In simulation 4, the coordination is to Asp50 and Thr61(OG1) instead, and in simulation 3 the coordination is to Asp50(OD1) and Asp50(OD2). In simulations 5 and 6, the GTP binding site opens more because there are water molecules that interact with the ion. Here Asp50 does not move close enough to the Mg^{2+} ion to interact with it.

5.3.3 Binding of Enacyloxin IIa in Structure E

Enx is the co-crystallised ligand for the protein structure E. The reason for examining structure E is to see if Enx stays in the binding site and to show that Enx inhibits the conformational changes that occur in EF-Tu during the elonga-

tion cycle. In the previous section, I have already shown that GTP stays in the binding site and this could indicate that Enx will also stay in its binding site. Figure 5.17 and figure 5.18 show the ligand Enx and the amino acids in the receptor and their possible hydrogen bond donors and acceptors.

Figure 5.17 Enacyloxin IIa and its hydrogen bond donors and acceptors

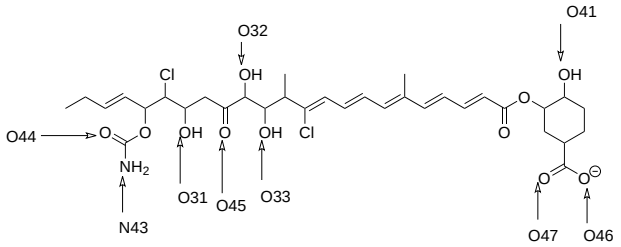

Figure 5.18 Amino acids

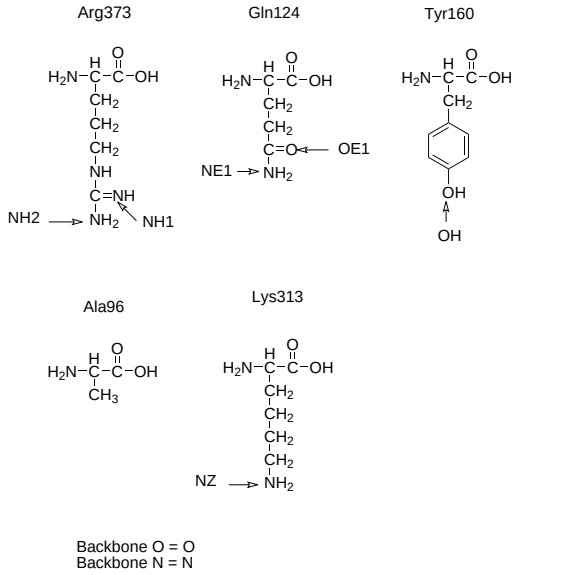

The simulation was studied visually using VMD by snapshots made for every 0.5 ps during the 5 ns simulation. Hydrogen bonds between Enx and the receptor were measured to study the stability of the binding site and to investigate if Enx stays in the binding site during the entire 5 ns simulation. The hydrogen bonds studied were taken from the article that describes the crystal structure of the ligand Enx bound in the protein structure E [89].

Table 5.35 shows the hydrogen bonds formed between the ligand Enx and the receptor during the simulation. In appendix G, the measured distances and angles can be found. In the article [89], the hydrogen bonds between Enx and the receptor in the crystal structure are described and, therefore, I have exam-

Table 5.35: Hydrogen bonds between structure E and Enx

Hydrogen bond	Found during simulation	Found in crystal structure [89]
123O · · · H − O33	○ − ○	+
123NH1 − H · · · O33	○ − ○	-
124O · · · H − O32	○ − ○	-
124O · · · H − O33	○ − ○	+
160OH − H · · · O41	● − ●	+
96O · · · H − N43	○ − ○	+
313NZ − H · · · O46	● − ●	-
313NZ − H · · · O47	● − ●	+
373NH1 − H · · · O31	○ − ○	-
373NH2 − H · · · O31	○ − ●	+
373NH1 − H · · · O44	● − ○	-
373NH2 − H · · · O44	○ − ●	-
373NH1 − H · · · O45	○ − ○	-
373NH2 − H · · · O45	● − ●	+

● − ● hydrogen bond present during the entire 5 ns simulation. ○ − ○ no hydrogen bond present at any time during the 5 ns simulation. ● − ○ hydrogen bond present in the beginning of the simulation. ○ − ● hydrogen bond present at the end of the simulation. + indicates that the bond is formed and - indicates that the bond is not formed

ined these. I have not been able to find all the hydrogen bonds described, but I have been able to find some others. The reason that I cannot find the same hydrogen bonds is probably that in the crystal structure no hydrogens are present, so the definition of hydrogen bonds must be based on the hetero atom distance. In the minimized structure, I measured the distance to be around 3 Å but the angle is less than 150° and therefore some of the bonds were not characterized as hydrogen bonds. Most of the hydrogen bonds were stable during the 5 ns simulation and when studying the protein-ligand interaction visually, it was seen that the ligand stayed in the binding site during the simulation. I also examined the number of water molecules in the binding site before and after the 5 ns simulation, and more ligand atoms bind to water after the simulation than before. This indicates that the binding site opens during the simulation, thus allowing more water to flow into the binding site. The reason Enx can form hydrogen bonds to water molecules is that the ligand lies on the surface of the protein and is exposed to the water surrounding the protein. The two ends of the ligand Enx have more contact to the water after the simulation than before the simulation, which means that the binding site becomes bigger and more water enters the binding site. Table 5.36 shows the hydrogen bonds formed between Enx and water before and after the 5 ns simulation.

Table 5.36: Hydrogen bonds between enacyloxin IIa and water

Hydrogen bond donor/acceptor	Before simulation	After simulation
O31	-	-
O32	+	-
O33	-	-
O41	-	+
O44	-	+
O45	+	+
O46	+	+
O47	-	+
N43	+	-

+ indicates that a hydrogen bond is formed and - indicates that a hydrogen bond is not formed.

5.3.4 Binding of Kirromycin in Structure K

This section describes simulation 4 which is the simulation of the crystal structure with the ligand Kir, and the hydrogen bonds formed between the receptor and the ligand Kir. I will also look at the hydrogen bonds formed to water before and after the simulation. The expected result is that Kir stays in the binding site and keeps its hydrogen bonds as described in article [89].

Kir is the co-crystallised ligand in the protein structure K. Kir is a known antibiotic and it works by blocking the protein EF-Tu, so the further protein synthesis is stopped. The reason for performing simulation 4 is to examine how Kir binds in the binding site and to show that no conformational changes occur in the protein when Kir is bound. I have already shown that GTP stays in its binding site and this is a good indication that the protein stays in the same conformation and that the ligand Kir stays in its binding site. Figures 5.19 and 5.20 on the facing page show Kir and the amino acids and the atoms that are possible hydrogen bond donors and acceptors.

Figure 5.19 Kirromycin and its hydrogen bond donors and acceptors

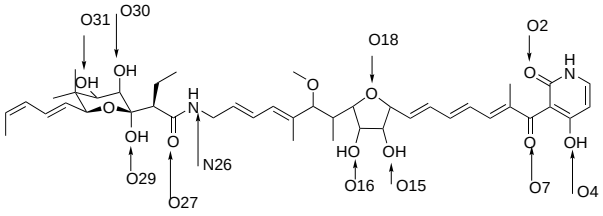

Table 5.37 on page 96 shows the hydrogen bonds found during the simulation and the hydrogen bonds found in the crystal structure. This shows that not all the hydrogen bonds found in the crystal structure are found during the sim-

Figure 5.20 Amino acids and their hydrogen bond donors and acceptors

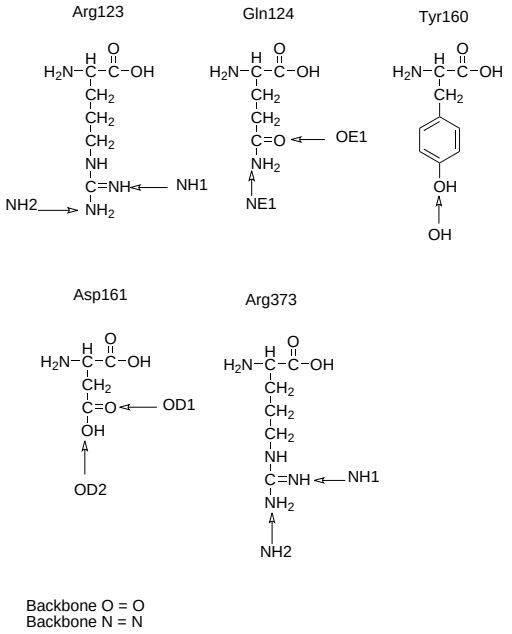

ulation. As it was the case for Enx in structure E, this may be because the crystal structure is without hydrogens and therefore the only basis for the hydrogen bonds is the hetero atomic distances. I have looked at both distances and angles and for that reason I have not found the same hydrogen bonds during my simulation. Only one hydrogen bond is present during the entire simulation, but this does not mean that Kir does not stay in the binding site. By inspecting the snapshots of the simulation visually it is seen that Kir stays in the binding site, but the amino acids move around the ligand. In particular, Arg373 moves during the simulation.

I have also examined the water molecules around the binding site to see if water enters the site and forms hydrogen bonds to Kir. Kir is placed on the surface of the protein and therefore some of the ligand is exposed to water during the whole simulation. Kir forms hydrogen bonds to water molecules and table 5.38 on the following page shows the atoms that form the hydrogen bonds. The ligand Kir lies in almost the same place before and after the 5 ns simulation and this also supports the hypothesis that the protein is stable and Kir stays in the binding site. Kir makes four hydrogen bonds to water before the simulation and only three after. This indicates that the binding site does not open more during the simulation and more water does not enter the binding site.

When comparing simulations 2 and 4, it is seen that simulation 2 has more

Table 5.37: Hydrogen bonds between kirromycin and structure K

Hydrogen bond	Found during simulation	Found in crystal structure [89]
123NH2 — H · · · O16	○ — ○	+
123NH1 — H · · · O16	○ — ○	+
124O · · · H — N26	● — ●	+
160O · · · H — O15	○ — ●	+
160OH — H · · · O4	○ — ●	+
161OD1 · · · H — O16	● — ○	-
161OD2 · · · H — O16	● — ○	-
373NH1 — H · · · O16	○ — ○	-
373NH2 — H · · · O16	○ — ○	-

● — ● hydrogen bond present during the entire 5 ns simulation. ○ — ○ no hydrogen bond present at any time during the 5 ns simulation. ● — ○ hydrogen bond present in the beginning of the simulation. ○ — ● hydrogen bond present at the end of the simulation. + indicates that a hydrogen bond is formed and - indicates that a hydrogen bond is not formed.

Table 5.38: Hydrogen bonds between Kir and water

Hydrogen bond donor/acceptor from Kir	Before simulation	After simulation
O4	+	-
O7	+	-
O15	-	-
O16	-	-
O18	-	-
O20	+	+
O27	-	+
O29	-	-
O30	-	-
O31	+	+
N26	-	-

+ indicates that the bond is formed and - indicates that the bond in not formed.

hydrogen bonds to amino acids and to water before and during the simulation than simulation 4 has. This seems to indicate that the binding site for Kir is more closed than the one for Enx and less water is able to enter the binding site.

5.3.5 Bindings of R29 and UF3-1 in Structure K

This section gives a review of simulations 5 and 6 with the hybrid molecule R29 and the *de novo* design molecule UF3-1; see figure 5.21 and figure 5.22. Both molecules were first docked in the structure K and selected from a range of hybrid and *de novo* design molecules; see sections 5.2.3 and 5.2.4. These particular ligands were selected because they docked with their side groups in the right directions, because the molecules have their hydrophobic groups in the hydrophobic pocket of the binding site. Furthermore, both ligands have G-scores lower than the critical part of Kir. They both had hydrogen bonds before the simulation was started and I have examined these to see if they are preserved throughout the simulations. I have also looked at snapshots to examine the molecules visually during the simulations.

Figure 5.21 Hybrid molecule R29 and the possible hydrogen bond donor and acceptors

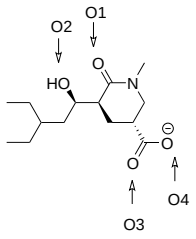

Figure 5.22 *De novo* design molecule UF3-1 and the possible hydrogen bond donors and acceptors

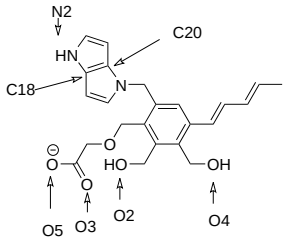

Simulations were performed on these molecules to investigate the stability of the protein with the molecules bound, and to see if the molecules stay in the binding site. The molecules are both much smaller than the co-crystallised

ligand, Kir, and therefore the binding site is not filled completely as when Kir is bound. The results for simulations 5 and 6 were examined separately and compared at the end of the section. Figure 5.23 shows the amino acids that are part of the hydrogen bonds formed to the two molecules, and figure 5.21 shows the possible hydrogen bond donors and acceptors for R29. The molecule R29 is the smallest of the two new molecules and does not fill the binding site. During the simulation, all hydrogen bonds to the receptor were broken and new ones were formed to the surrounding water. By inspecting snapshots of the simulation visually, it is seen that R29 moves further into the binding site and more hydrogen bonds are formed to water instead of the surrounding amino acids. The chart in figure 5.24 shows that the distances between hetero atoms quickly become greater than 3 Å which indicates that the hydrogen bonds are broken between R29 and the receptor.

Figure 5.23 Amino acids hydrogen bond donor and acceptors

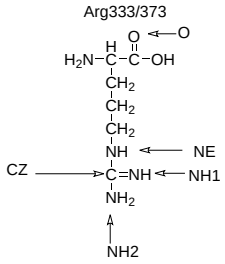

Figure 5.24 Hydrogen bond distances between R29 and structure K

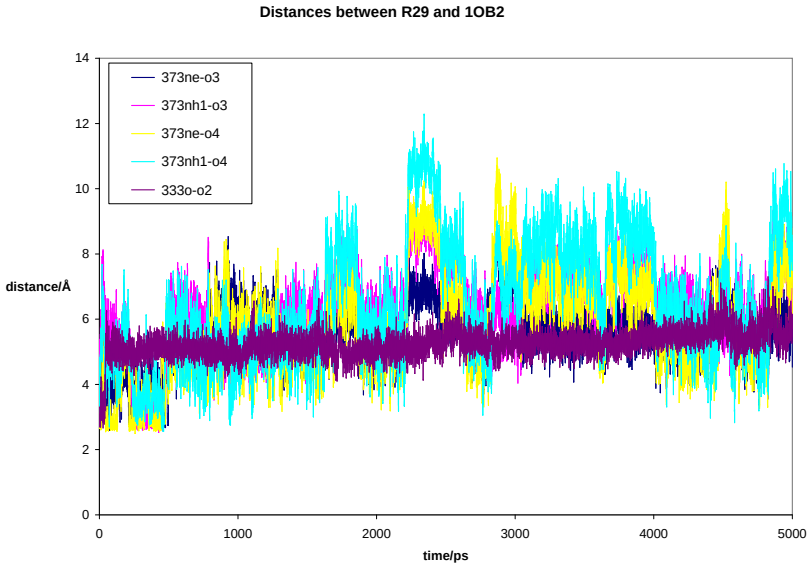

Table 5.39 on the next page shows the hydrogen bonds to water before and after the simulation, and here it is obvious that more water surrounds R29 after the simulation than before. This indicates that the binding site opens more and lets more water enter the binding site or that R29 moves towards the surface of the binding site, because nothing holds it in place. Visually studying the simulation reveals that the binding site closes more and the ligand moves towards the surface. After 5 ns of simulation, the amino acid Arg373 lies under the ring of the ligand R29. When trying to fit Kir in the binding site after the simulation it can be seen that there is no room for that big a ligand. The binding site closes when the ligand R29 is not placed in the binding site; see figure 5.26 on page 101. The hydrophobic side chains of R29 lie with one arm in the hydrophobic pocket for Kir and the other in the hydrophobic pocket for Enx. This is shown in figure 5.25. This means that the two hydrophobic pockets are created when the ligand R29 is present in the binding site during the 5 ns simulation. The ligand R29 is very small and it would be favorable to make a bigger ligand to keep more of the binding site open during the simulation. However, the GTP binding site stays open and GTP stays in place during the simulation, so the closing of the binding site does not affect the binding of GTP. There may occur a change in the GTP binding site if the simulation is continued.

Figure 5.25 Hydrophobic tail of R29

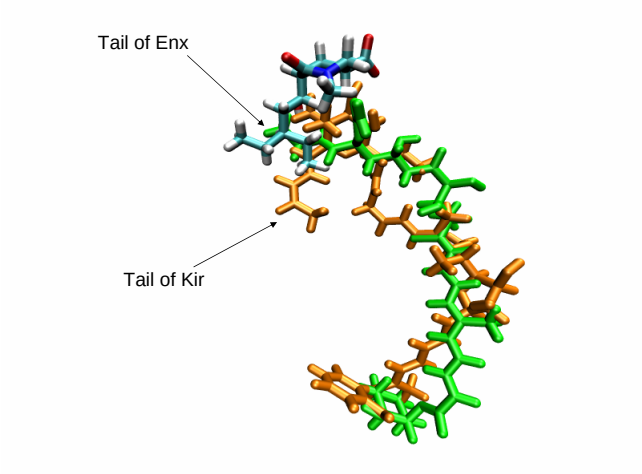

Simulation 6 shows that R29 stays in place, but also that the ligand becomes more exposed to water during the simulation and consequently none of the hydrogen bonds between the receptor and the ligand are preserved throughout the simulation. Again, this can be attributed to the relative small size of the ligand and it is probably why R29 does not keep its hydrogen bonds: The binding site

Table 5.39: Hydrogen bonds to water

Donor/acceptor R29	Before simulation	After simulation
O1	-	+
O2	-	-
O3	-	+
O4	+	+
Donor/acceptor UF3-1		
O2	-	-
O3	+	+
O4	-	+
O5	+	+
N2	+	-

+ indicates that the bond is formed and - indicates that the bond in not formed.

is too big and it is not possible for it to fold around the ligand and therefore the it starts to close. I conclude that this happens when R29 is bound and not when the binding site is empty because of the presence of a ligand that moves. When the binding site is filled with water the system is more stable because if one water moves another water molecule will take its place.

The *de novo* design molecule UF3-1 is bigger than R29 and has more hydrogen bond donors and acceptors. I have also studied this molecule visually during the simulation and I have measured the hydrogen bonds. Like R29 this molecule is also smaller than the co-crystallised ligand Kir. Figures 5.22 on page 97 and 5.23 on page 98 show the hydrogen bond donors and acceptors of the ligand and of the amino acids from the receptor that form hydrogen bonds to the ligand. During simulation 5, $\pi-$interactions between the ring system in UF3-1 and the Arg373 in the receptor were also observed, as seen in figure 5.27 on page 102. I have measured the distances between these to see if the $\pi-$interactions are found during the entire simulation [45].

The chart in figure 5.28 on page 102 shows that the π-interactions are found during the entire simulation and they play an essential part in holding the ligand in place in the binding site. UF3-1 also forms hydrogen bonds to water surrounding the protein and because the binding site is on the surface of the protein, the binding site is exposed to water. Table 5.39 shows the hydrogen bonds formed between UF3-1 and water and it is seen that the same number of hydrogen bonds are formed before and after the 5 ns simulation. The ligand UF3-1 stays in place during the simulation and the binding site stays open. The reason for this may be the stable hydrogen bonds between UF3-1 and the receptor and the $\pi-$interactions between the rings in UF3-1 and the amino acid

Figure 5.26 Binding site before and after simulation with R29

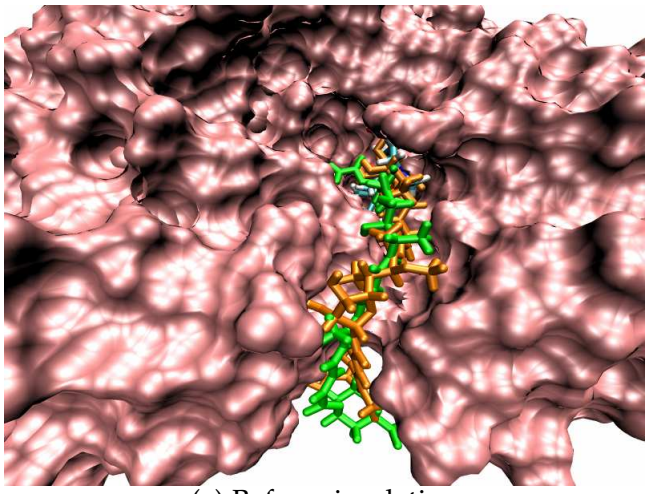

(a) Before simulation

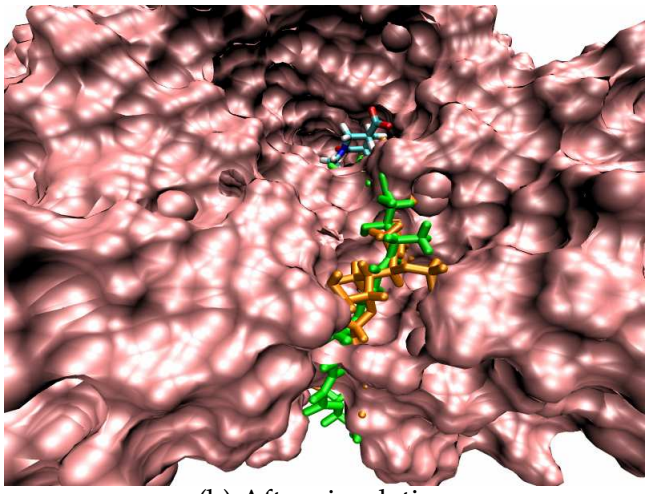

(b) After simulation

Kir is shown in orange, Enx is shown in green, and R29 is shown in cyan.

Figure 5.27 $\pi-$interactions between UF3-1 and Arg373

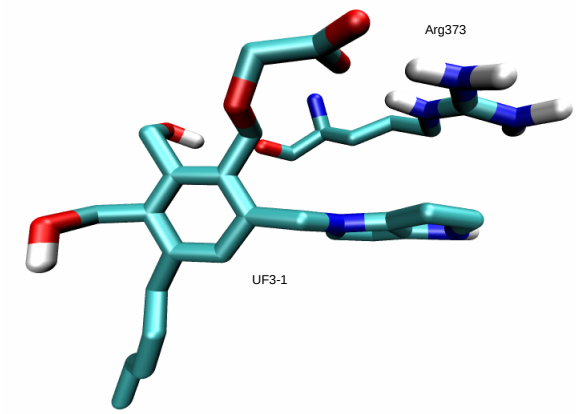

Figure 5.28 Distances between UF3-1 and Arg373

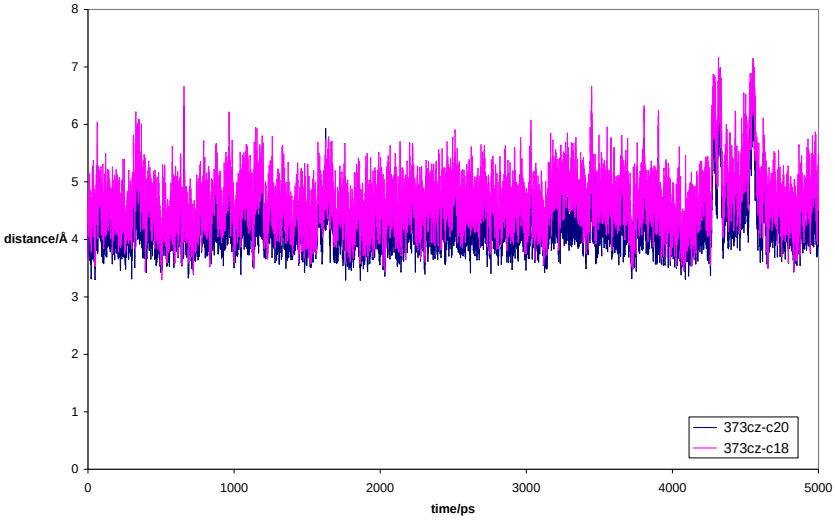

Arg373. This also keeps Arg373 from moving around as much as in the other simulations.

Table 5.40: Hydrogen bonds between UF3-1 and the receptor

Hydrogen bond	Found during simulation
373NE $-$ H $\cdots$ O3	$\bullet - \circ$
373NH1 $-$ H $\cdots$ O5	$\bullet - \bullet$
373O $\cdots$ H $-$ O2	$\bullet - \bullet$
333N $-$ H $\cdots$ O2	$\circ - \circ$
333O $\cdots$ H $-$ O4	$\bullet - \circ$
373NH1 $-$ H $\cdots$ O3	$\bullet - \bullet$
373NE $-$ H $\cdots$ O5	$\bullet - \bullet$

$\bullet - \bullet$ hydrogen bond present during the entire 5 ns simulation. $\circ - \circ$ no hydrogen bond present at any time during the 5 ns simulation. $\bullet - \circ$ hydrogen bond present in the beginning of the simulation. $\circ - \bullet$ hydrogen bond present at the end of the simulation.

The hydrogen bonds between UF3-1 and the receptor are shown in table 5.40. Four hydrogen bonds are preserved during the entire simulation, and two are found at the beginning of the simulation, but not at the end. This shows that UF3-1 is stable in the binding site during the 5 ns simulation. Because the $\pi-$ interactions are also preserved during the simulation, this means that UF3-1 is a promising lead compound for further study of antibacterial agents.

5.4 Cavity Calculations

I have performed calculations to examine the size and volume of the cavities in the protein structure before and after the MD simulations. I have tried several programs in my search to find one that could calculate the volume in an easy and consistent way. The programs tried were SCREEN [81], PASS [27], MolDock [110], and SiteMap [104]. None of the programs were able to find the volume of the cavity, partly because the cavity is on the surface of the protein and therefore exposed to water, and partly because some of the programs do not calculate the volume of cavities, but find site points instead.

SCREEN (Surface Cavity REcognition and EvaluatioN) is a new way of finding cavities on the surface of proteins and the program is described in [81]. According to the article, it should be possible to calculate cavity surface area, volume, diameter, number of residues, and number of atoms, but the program available for use is not yet capable of finding the volume of cavities. The program is freely accessible from the Internet [34]. From correspondences with one of the developers, I have been told that the further development of the program

will solve the problems with the calculations of the cavity volumes.

PASS is a simple computational tool, which uses geometry to characterise regions of buried volumes in proteins and to identify positions which may represent binding sites based on size, form, and burial extent of these volumes. The program searches the protein and fills cavities with layers of spheres where the first layer is calculated with the protein as substrate. Additional spheres are poured on top of the previously found sphere layers, but only spheres with low solvent exposure are retained. The problem with using PASS to calculate the binding site size in EF-Tu, is that the site is on the surface of the protein and therefore PASS is not able to find the whole binding site and calculate the size. Another problem I have found with the program is that the version available has not been upgraded since 1999 and is not possible to install on a new computer.

SiteMap is a cavity calculation program from Schrödinger and the program works by setting up a grid where the points are grouped into sets according to different criteria, which can be hydrophobic, hydrophilic, and donor acceptor sites. The problem with this program is also that the binding site is on the surface of the protein and SiteMap is not able to find the whole binding site without using the ligand. Unfortunately, when the ligand is used only the cavity around it is measured. It is not possible to use this approach, because when the smaller molecules are used it is not possible to measure the whole cavity size.

Part of the docking program MolDock is a function for detecting cavities. The function works by calculating a grid that detect changes in the surface of the protein, but the problem with this program is that the algorithm used for detecting the cavities is a stochastic algorithm and when performing the calculation several times, the size of the cavity changes. This can be resolved by performing the calculation several times and taking the average size of all the calculation. However, the MolDock cavity detection algorithm also has problems with surface-near cavities, and thus the program does not solve the problem with only detecting a part of the binding site.

Chapter 6

Conclusions

The objective of the work presented in this thesis was to design and test antibiotic compounds targeting the protein EF-Tu. The most promising compound is shown in figure 6.1. This molecule fulfills Lipinski's rule of five [71] and docks even better than cutoffs of both kirromycin and enacyloxin IIa. During a 5 ns molecular dynamics simulation, the molecule stayed in place and kept the binding site open during the entire 5 ns run. This shows that the lead compound is a possible new antibiotic with an inhibitory effect on EF-Tu.

Figure 6.1 Most promising antibiotic compound, UF3-1

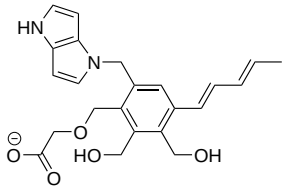

I have succeeded in designing 57 new molecules using the *de novo* design program LUDI. The molecules created in LUDI almost all fulfill Lipinski's rule of five, which is an important criteria for determining if the molecules are synthesizable and if the body will be able to absorb the molecules if they were to be approved as drugs.

Having designed the new molecules, I continued the experiments by conducting a docking study of the molecules and proteins. All the docking studies showed that it was easier to dock in the protein structure of EF-Tu, containing the ligand kirromycin, structure K, than in the protein structure of EF-Tu containing the ligand enacyloxin IIa, structure E, because here it was only possible to get the majority of the ligands to dock if hydrophobic constraints were added. As expected the docking study of cutoffs showed that the entire ligand docked

best followed by the cutoffs in decreasing size. Docking of the molecules designed based on the two co-crystallised ligands kirromycin and enacyloxin IIa, the hybrid molecules, gave a clear picture that a lactam ring was preferred for all dockings. The docking studies also showed that the best size or shape of the two side chains present in all the molecules could not be determined conclusively. The best of the docked hybrid molecules docked better than the critical part of Kir and Enx. Docking of *de novo* design molecules showed the ligand UF3-1 to be the best of all and the ligand also docked better than the cutoffs of Kir. UF3-1 is the ligand depicted in figure 6.1 on the preceding page. For all the dockings, the picture that evolved was that the smaller ligands would be placed too far into the binding site and they were probably not big enough to keep the binding site open. IFD calculations performed on the best five ligands from the docking study in structure K showed the same picture as the normal Glide dockings.

I experienced problems when docking the co-crystallised ligand Enx in the structure E X-ray structure. Many different approaches were tried and I finally found one that worked: Docking with hydrophobic constraints. This method forced the ligand to fit in the critical part of the binding site. Unfortunately, this approach was only successful when using Glide version 3.5; with the newer version 4.0 the ligand was placed too far into the binding site. There must have been made some modifications in the docking algorithm from version 3.5 to version 4.0, but because the docking algorithm is not publicly available I have not been able to determine the extent of any such modifications.

The performed MD simulations showed that the binding site is stable without ligands. This may be caused by water molecules entering the binding site when no ligand is bound. The co-crystallised ligands Kir and Enx stay in the binding site and keep most of their hydrogen bonds. The binding of GTP is stable in all the simulations, but more hydrogen bonds are broken when the smaller ligands are bound. This indicates that the smaller ligands are not as potent inhibitors of EF-Tu as the larger co-crystallised ligands. The magnesium ion coordination is found in all six simulations and kept throughout the simulation; this indicates a stable coordination of the Mg^{2+} ion and a stable environment around it. The simulations on the hybrid molecule R29 and the *de novo* design molecule UF3-1 showed that the bindings site closes when R29 is bound and the ligand is not capable of preserving the hydrogen bonds to the protein during the simulation. This means that the ligand is too small to keep the binding site open and over time a conformational change of the protein may occur. The ligand

UF3-1 keeps the binding site open and keeps hydrogen bonds to the protein. In this simulation, π-interactions are found to Arg373 which is placed over the binding site and this is also kept during the simulation. This means that UF3-1 stays in the binding site and keeps it open and may have an inhibitory effect on the protein.

6.1 Future Work

In this section, I will look at possible ways of continuing this project. It would be interesting to design new molecules using the ligands kirromycin and enacyloxin IIa as starting points in the *de novo* design program. It is also possible to start from the protein structure E, which has the better resolution of the two structure used in this thesis, to try to find more molecules that will dock well in the protein structure. Improving the *de novo* design molecules may give better dockings and thereby new lead compounds. Another project could be to continue the search for a docking program that could dock enacyloxin IIa without using constraints or at least get the ligand to dock using a newer version of Glide than 3.5. This could possibly give an indication to why the rest of the ligands are more difficult to dock in structure E than in structure K. The best hybrid molecules could be improved by making them a bit bigger to see if it will improve the docking score and also new MD simulations could be performed to see if the ligands will stay in the binding site and prevent the binding site from closing.

An interesting aspect that has yet to be investigated is whether or not enacyloxin IIa can find its place in structure E when it is placed over Arg373. To determine this, additional MD simulations are needed. It could also be interesting to perform an MD simulation on structure K and to keep the tRNA bound to examine the effects on this. The calculations would be more time consuming and may require longer simulation time.

Chapter 7

Estrogen Receptor

The purpose of this chapter is to briefly describe the work on the estrogen receptor (ER) that I have been involved in during my master's thesis work. We have recently submitted a paper titled "Conformational Dynamics of the Estrogen Receptor α: Molecular Dynamics Simulations of the Influence of Binding Site Structure on Protein Dynamics", and I will summarize the results. The entire paper is attached to this thesis and follows the bibliography.

7.1 System

The ER is part of the nuclear receptor (NR) transcription factor family, which consists of 48 different proteins [35]. NR proteins consist of three domains which are the C-terminal transactivating domain, the central DNA binding domain, and the N-terminal ligand binding domain (LBD), where the activation factor-2 is located [35]. The ER is involved in multiple biological processes in the human body and has very different effects [18, 26, 52, 76, 77]. From the structure determined of the ER, there are three conformations that are common for all the NRs: The apo, agonist, and antagonist conformations. The major difference in structure is the location of helix 12 [77, 107]. This is shown in figure 7.1 on the next page.

7.2 Setup

The purpose of the calculations performed on the ERα was to determine the protonation state of His524 positioned in the binding pocket and determine if His524 forms a hydrogen bond to Estradiol (E2). Furthermore, the effect of the

Figure 7.1 Three conformational states of ERα

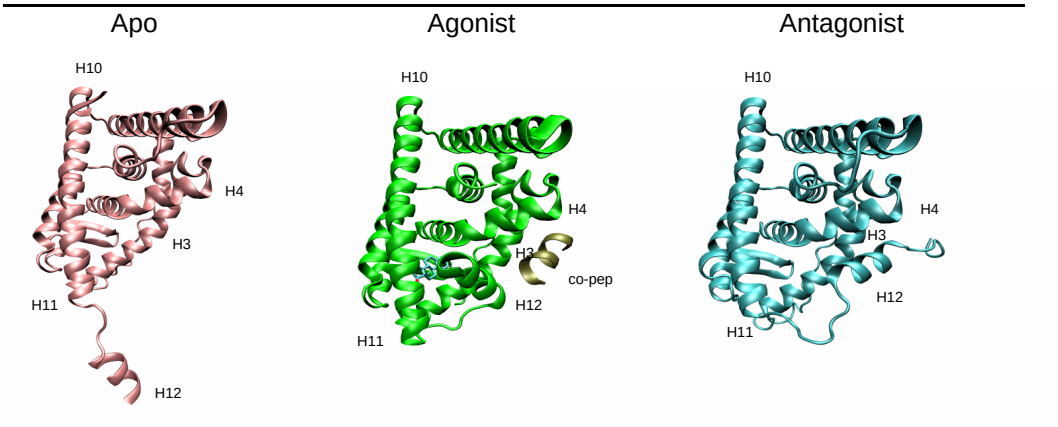

Estradiol is displayed in cyan and red in the LBD of the agonist structure. The helices (H) are numbered.

co-activator protein (co-pep) bound in a hydrophobic groove on the LBD core was examined. The co-pep is only found in the crystal structure of the agonist conformation. The conformational changes that happen in ERα from apo to agonist form was studied and the possibility to go from antagonist to agonist form was also examined. These different aspects to be examined yielded 10 different setups, which are shown in table 7.1 on the facing page. The different setups have been performed with three different protonation states; Nδ protonated (D), Nϵ protonated (E), and double protonated (P) I have performed simulations 7 to 10; simulations 7 and 8 were performed before my thesis work, simulations 9 and 10 were performed during my thesis work.

7.3 Results

Models 1 to 4 investigate the agonist conformation, the stability of the LBD, and the influence of co-pep on ERα. Models 5 to 10 were included to examine the conformational changes that may occur in the ER conformation when starting from an antagonist or apo structure and placing E2 in the LBD. Models 7 to 10 were included to study the hypothesis that the agonist conformation is produced from the apo form by binding of E2 and/or the co-pep followed by conformational changes. The hypothesis is described in [87, 107]. The results for the simulations are discussed in the manuscript; I will only discuss a few highlights here. The dynamics of H12 in models 7 to 10 are dependent on the protonation state of His524. A new stable conformation is found in model 7D, which is stable for the last 3 ns of the dynamics. This is shown in figure 7.2.

Table 7.1: Ten Models for MD simulations

	Initial conformation	Ligand	Co-activator peptide	To study
1	Agonist	E2	NALLRYLLD	E2 binding in biologically relevant form; evaluate His524 protonation
2	Agonist	E2	None	The influence on E2 binding in the absence of co-pep
3	Agonist	None	None	The stability of agonist confirmation of the protein without E2
4	Agonist	None	NALLRYLLD	The stability of agonist confirmation of the protein without E2 but in the presence of E2
5	Antagonist	E2	None	Antagonist conformation with E2
6[a]	Antagonist	E2	None	Antagonist conformation with E2 at higher temperature
7[b]	Apo	E2	None	The influence of co-pep on apo conformation with E2 bound
8	Apo	E2	NALLRYLLD	The influence of co-pep on apo conformation with E2 bound
9	Apo	None	None	The stability of the apo conformation, only protein
10[c]	Apo	None	NALLRYLLD	The stability of the apo conformation, including co-pep

All models were simulated for the three protonation states of His524. [a] models 6 are simulated at 600 K; [b] model 7E is simulated for 12 ns; [c] model 10P is simulated for 6 ns.

Figure 7.2 New stable conformation

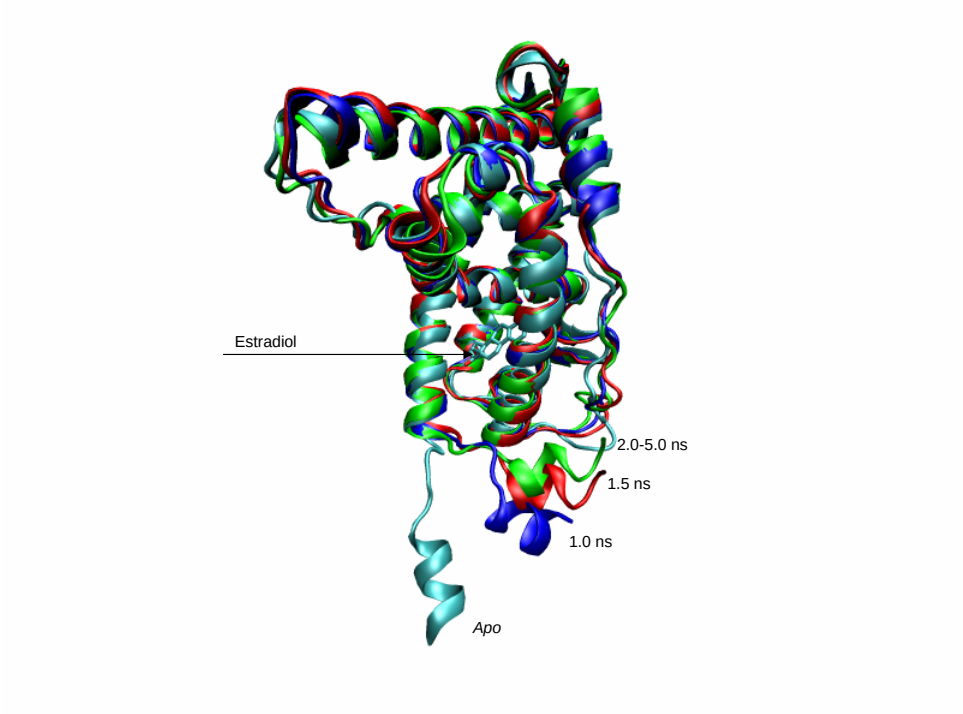

Apo conformation of ERα (cyan) and snapshots of simulation 7D after 1.0 ns (blue), 1.5 ns (red) and 2.0 ns (green).

The core conformation is the same as the one found in the crystal structure, but H12 is placed in a new position. In model 10P, we observed a dramatic change in the behavior of the binary complex. H12 travels towards the agonist position and after 6 ns, H12 is positioned in extension of its agonistic position. This is shown in figure 7.3 on the facing page.

Simulations on this are continued to examine if the agonist conformation will be found in future work. A new stable conformation was found and this conformation is tested by docking studies. The conformational changes that occur in ERα when a ligand binds in the binding site are still being investigated and will hopefully be determined in the near future.

Figure 7.3 Conformational change of the ERα

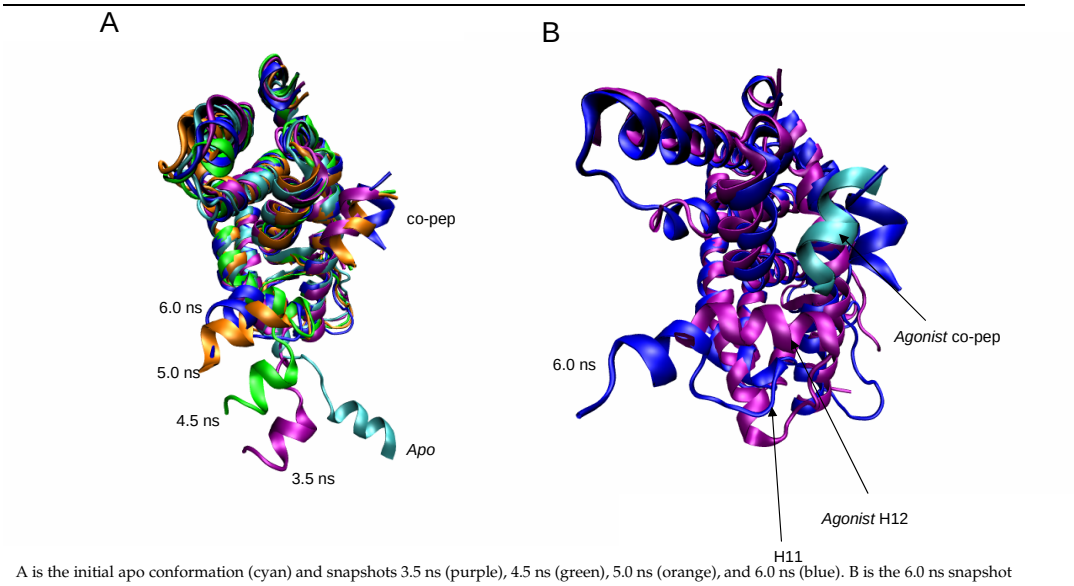

A is the initial apo conformation (cyan) and snapshots 3.5 ns (purple), 4.5 ns (green), 5.0 ns (orange), and 6.0 ns (blue). B is the 6.0 ns snapshot (blue) and the agonist conformation (purple with co-pep in cyan).

Appendix A

Charges and Parameters

A.1 Residues Topology of GTP

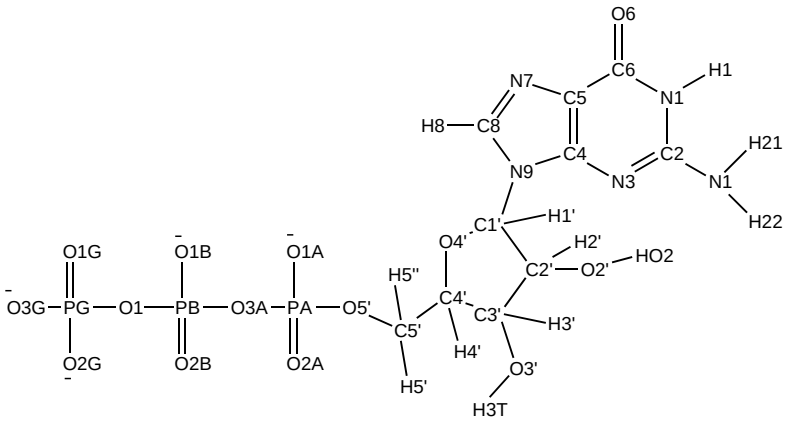

RESI GTP -4.00
GROUP
ATOM PG P2 1.100
ATOM O1G ON3 -0.900
ATOM O2G ON3 -0.900
ATOM O3G ON3 -0.900
ATOM O1 ON2 -0.805
ATOM PB P 1.500
ATOM O1B ON3 -0.820
ATOM O2B ON3 -0.820
GROUP
ATOM O3A ON2 -0.805
ATOM PA P 1.500

ATOM O1A ON3 -0.820
ATOM O2A ON3 -0.820
ATOM O5′ ON2 -0.570
ATOM C5′ CN8B -0.080
ATOM H5′ HN8 0.090
ATOM H5″ HN8 0.090
GROUP
ATOM C4′ CN7 0.160
ATOM H4′ HN7 0.090
ATOM O4′ ON6B -0.500
ATOM C1′ CN7B 0.160
ATOM H1′ HN7 0.090
GROUP
ATOM C3′ CN7 0.010
ATOM H3′ HN7 0.090
ATOM O3′ ON5 -0.570
ATOM H3T HN5 0.430
GROUP
ATOM C2′ CN7B 0.140
ATOM H2″ HN7 0.090
ATOM O2′ ON5 -0.660
ATOM H2′ HN5 0.430
GROUP
ATOM N9 NN2B -0.020
ATOM C8 CN4 0.250
ATOM N7 NN4 -0.600
ATOM C5 CN5G 0.000
ATOM C6 CN1 0.540
ATOM O6 ON1 -0.510
ATOM N1 NN2G -0.340
ATOM C2 CN2 0.750
ATOM N2 NN1 -0.680
ATOM N3 NN3G -0.740
ATOM C4 CN5 0.260
ATOM H8 HN3 0.160
ATOM H1 HN2 0.260
ATOM H21 HN1 0.320

ATOM H22 HN1 0.350
BOND PG O1G
BOND PG O2G
BOND PG O3G
BOND PG O1
GROUP
BOND O1 PB
BOND PB O1B
BOND PB O2B
BOND PB O3A
GROUP
BOND O3A PA
BOND PA O1A
BOND PA O2A
GROUP
BOND PA O5′
BOND O5′ C5′
BOND C5′ C4′
BOND C5′ H5′
BOND C5′ H5″
BOND C4′ O4′
BOND C4′ C3′
BOND C4′ H4′
BOND O4′ C1′
BOND C3′ O3′
BOND C3′ C2′
BOND C3′ H3′
BOND O3′ H3T
BOND C2′ O2′
BOND C2′ C1′
BOND C2′ H2″
BOND O2′ H2′
BOND C1′ N9
BOND C1′ H1′
GROUP
BOND N9 C8
BOND N9 C4

BOND C8 N7
BOND C8 H8
BOND N7 C5
BOND C5 C6
BOND C5 C4
BOND C6 O6
BOND C6 N1
BOND N1 C2
BOND N1 H1
BOND C2 N2
BOND C2 N3
BOND N2 H21
BOND N2 H22
BOND N3 C4
IMPH N6 C6 H61 H62
IMPH HC6 N1 C5 N6
IMPH C6 C5 N1 O6
IMPH C2 N1 N3 N2
IMPH N2 H21 H22 C2
IC O1G PG O1 PB 1.50 104.62 25.46 128.84 1.50
IC O2G PG O1 PB 1.46 109.91 139.29 128.84 1.50
IC O3G PG O1 PB 1.50 109.73 -88.44 128.84 1.50
IC PG O1 PB O1B 1.50 128.84 -142.55 111.52 1.50
IC PG O1 PB O2B 1.50 128.84 -16.27 111.49 1.51
IC PG O1 PB O3A 1.50 128.84 101.91 105.40 1.57
IC O1 PB O3A PA 1.50 105.40 -133.88 127.32 1.56
IC O1B PB O3A PA 1.50 106.81 107.39 127.32 1.56
IC O2B PB O3A PA 1.51 109.05 -14.07 127.32 1.56
IC PB O3A PA O1A 1.57 127.32 -62.98 110.83 1.50
IC PB O3A PA O2A 1.57 127.32 62.43 106.31 1.50
IC PB O3A PA O5′ 1.57 127.32 -179.21 101.05 1.59
IC O3A PA O5′ C5′ 1.56 101.05 50.86 123.44 1.45
IC O1A PA O5′ C5′ 1.50 109.71 -66.19 123.44 1.45
IC O2A PA O5′ C5′ 1.50 113.18 164.12 123.44 1.45
IC PA O5′ C5′ C4′ 1.59 123.44 165.39 110.80 1.53
IC PA O5′ C5′ H5′ 1.59 123.44 -74.60 109.49 1.09
IC PA O5′ C5′ H5″ 1.59 123.44 45.41 109.48 1.09

IC O5′ C5′ C4′ O4′ 1.45 110.80 -143.84 112.07 1.45
IC H5′ C5′ C4′ O4′ 1.09 108.80 95.74 112.07 1.45
IC H5″ C5′ C4′ O4′ 1.09 108.78 -23.45 112.07 1.45
IC O5′ C5′ C4′ C3′ 1.45 110.80 -25.36 117.92 1.53
IC O5′ C5′ C4′ H4′ 1.45 110.80 97.69 109.50 1.09
IC C5′ C4′ O4′ C1′ 1.53 112.07 102.30 109.48 1.42
IC C3′ C4′ O4′ C1′ 1.53 102.39 -25.02 109.48 1.42
IC H4′ C4′ O4′ C1′ 1.09 106.92 -137.71 109.48 1.42
IC C4′ O4′ C1′ C2′ 1.45 109.48 0.23 107.36 1.53
IC C4′ O4′ C1′ N9 1.45 109.48 -123.12 111.35 1.46
IC C4′ O4′ C1′ H1′ 1.45 109.48 123.56 109.49 1.09
IC O4′ C1′ C2′ C3′ 1.42 107.36 25.07 101.23 1.50
IC N9 C1′ C2′ C3′ 1.46 112.34 147.81 101.23 1.50
IC H1′ C1′ C2′ C3′ 1.09 113.25 -95.91 101.23 1.50
IC O4′ C1′ C2′ O2′ 1.42 107.36 152.37 113.67 1.41
IC O4′ C1′ C2′ H2″ 1.42 107.36 -88.95 105.33 1.09
IC O2′ C2′ C3′ C4′ 1.41 117.79 -163.72 101.92 1.53
IC C1′ C2′ C3′ C4′ 1.53 101.23 -39.15 101.92 1.53
IC H2″ C2′ C3′ C4′ 1.09 109.49 71.71 101.92 1.53
IC O2′ C2′ C3′ O3′ 1.41 117.79 -41.27 113.13 1.43
IC O2′ C2′ C3′ H3′ 1.41 117.79 80.37 109.47 1.09
IC O3′ C3′ C4′ C5′ 1.43 113.68 154.51 117.92 1.53
IC C2′ C3′ C4′ C5′ 1.50 101.92 -83.42 117.92 1.53
IC H3T C3′ C4′ C5′ 1.09 109.53 32.45 117.92 1.53
IC O3′ C3′ C4′ O4′ 1.43 113.68 -82.00 102.39 1.45
IC O3′ C3′ C4′ H4′ 1.43 113.68 30.37 107.33 1.09
IC C4′ C3′ O3′ H3T 1.53 113.68 179.98 109.48 0.96
IC C2′ C3′ O3′ H3T 1.50 113.13 64.36 109.48 0.96
IC H3′ C3′ O3′ H3T 1.09 108.90 -57.61 109.48 0.96
IC C3′ C2′ O2′ H2′ 1.50 117.79 -180.00 109.49 0.96
IC C1′ C2′ O2′ H2′ 1.53 113.67 61.88 109.49 0.96
IC H2″ C2′ O2′ H2′ 1.09 108.52 -54.95 109.49 0.96
IC O4′ C1′ N9 C8 1.42 111.35 80.08 127.34 1.38
IC C2′ C1′ N9 C8 1.53 112.34 -40.38 127.34 1.38
IC H1′ C1′ N9 C8 1.09 103.07 -162.63 127.34 1.38
IC O4′ C1′ N9 C4 1.42 111.35 -99.78 127.11 1.37
IC C1′ C8 ′N9 C4 1.46 127.34 179.89 105.54 1.37

IC C1′ N9 C8 N7 1.46 127.34 -179.93 113.97 1.30
IC C4 N9 C8 N7 1.37 105.54 -0.05 113.97 1.30
IC C1′ N9 C8 H8 1.46 127.34 0.06 120.00 1.08
IC N9 N7 ′C8 H8 1.38 113.97 -179.99 126.03 1.08
IC N9 C8 N7 C5 1.38 113.97 0.14 104.21 1.37
IC H8 C8 N7 C5 1.08 126.03 -179.85 104.21 1.37
IC C8 N7 C5 C6 1.30 104.21 -179.95 129.77 1.43
IC C8 N7 C5 C4 1.30 104.21 -0.18 111.21 1.39
IC N7 C6 ′C5 C4 1.37 129.77 -179.76 119.01 1.39
IC N7 C5 C6 O6 1.37 129.77 -0.30 126.85 1.23
IC C4 C5 C6 O6 1.39 119.01 179.94 126.85 1.23
IC N7 C5 C6 N1 1.37 129.77 179.87 112.97 1.43
IC C5 O6 ′C6 N1 1.43 126.85 179.82 120.18 1.43
IC C5 C6 N1 C2 1.43 112.97 -0.11 124.33 1.40
IC O6 C6 N1 C2 1.23 120.18 -179.95 124.33 1.40
IC C5 C6 N1 H1 1.43 112.97 179.86 120.01 1.01
IC C6 C2 ′N1 H1 1.43 124.33 -179.96 115.66 1.01
IC C6 N1 C2 N2 1.43 124.33 -179.93 116.88 1.34
IC H1 N1 C2 N2 1.01 115.66 0.10 116.88 1.34
IC C6 N1 C2 N3 1.43 124.33 0.08 122.64 1.37
IC N1 N2 ′C2 N3 1.40 116.88 179.99 120.48 1.37
IC N1 C2 N2 H22 1.40 116.88 0.01 120.03 1.01
IC N3 C2 N2 H22 1.37 120.48 179.99 120.03 1.01
IC N1 C2 N2 H21 1.40 116.88 -179.98 119.97 1.01
IC C2 H21 ′N2 H22 1.34 119.97 -179.99 120.00 1.01
IC N1 C2 N3 C4 1.40 122.64 -0.05 112.97 1.38
IC N2 C2 N3 C4 1.34 120.48 179.97 112.97 1.38
IC C2 N3 C4 N9 1.37 112.97 180.00 126.87 1.37
IC C2 N3 C4 C5 1.37 112.97 0.06 128.07 1.39
IC N9 C5 ′C4 N3 1.37 105.06 179.95 128.07 1.38
IC C5 C4 N9 C1′ 1.39 105.06 179.82 127.11 1.46
IC N3 C4 N9 C1′ 1.38 126.87 -0.12 127.11 1.46
IC C5 C4 N9 C8 1.39 105.06 -0.06 105.54 1.38
IC N9 C4 C5 N7 1.37 105.06 0.15 111.21 1.37
IC N3 C4 C5 N7 1.38 128.07 -179.90 111.21 1.37
IC N9 C4 C5 C6 1.37 105.06 179.96 119.01 1.43
END

A.2 Residue Topology of Kirromycin

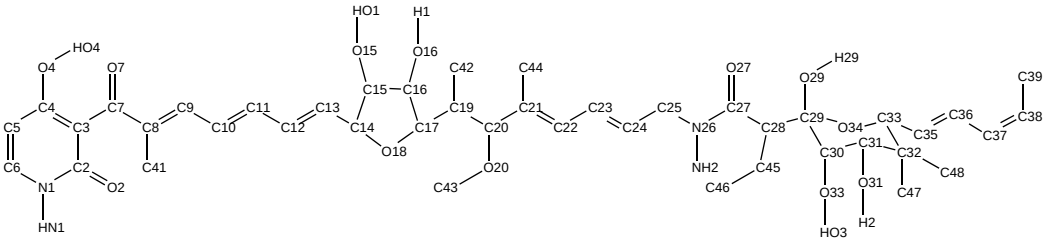

RESI KIR 0.000
GROUP
ATOM C2 CN1T 0.436909
ATOM C3 CA -0.008348
ATOM C4 CN1 0.199145
ATOM C5 CN3 -0.113555
ATOM C6 CN3 -0.067810
ATOM C7 C 0.397136
ATOM O4 OH1 -0.536616
ATOM O7 O -0.516273
ATOM N1 NN2 -0.290791
ATOM O2 ON1 -0.518096
ATOM H5 HN3 0.094889
ATOM H6 HN3 0.094114
ATOM HO4 H 0.383869
ATOM HN1 H 0.244447
GROUP
ATOM C8 CE1 0.008107
ATOM C9 CE1 -0.107584
ATOM C10 CE1 -0.104640
ATOM C11 CE1 -0.104640
ATOM C12 CE1 -0.104454
ATOM C13 CE1 -0.116363
ATOM C41 CT3 -0.257488
ATOM H9 HE1 0.094889
ATOM H10 HE1 0.094889
ATOM H11 HE1 0.094889
ATOM H12 HE1 0.094889

ATOM H13 HE1 0.095101
ATOM H411 HA 0.088207
ATOM H412 HA 0.088207
ATOM H413 HA 0.088207
GROUP
ATOM C14 CN7 0.123464
ATOM C15 CN7 0.115260
ATOM C16 CN7 0.115435
ATOM C17 CN7 0.117006
ATOM O15 ON5 -0.544113
ATOM O16 ON5 -0.544113
ATOM O18 ON6B -0.362697
ATOM H14 HN7 0.082745
ATOM H15 HN7 0.082956
ATOM H16 HN7 0.082956
ATOM H17 HN7 0.082956
ATOM HO1 HN5 0.384231
ATOM H1 HN5 0.384231
GROUP
ATOM C20 CT1 0.126063
ATOM C21 CE1 0.004729
ATOM C24 CE1 -0.111781
ATOM C19 CT1 -0.073534
ATOM C22 CE1 -0.107397
ATOM C23 CE1 -0.104454
ATOM C42 CT3 -0.261291
ATOM O20 ON6B -0.356065
ATOM C43 CT3 -0.071045
ATOM C44 CT3 -0.257313
ATOM H20 HA 0.082745
ATOM H24 HE1 0.095101
ATOM H19 HA 0.086131
ATOM H22 HE1 0.094889
ATOM H23 HE1 0.094889
ATOM H421 HA 0.088419
ATOM H422 HA 0.088419
ATOM H423 HA 0.088419

ATOM H431 HA 0.085245
ATOM H432 HA 0.085245
ATOM H433 HA 0.085245
ATOM H441 HA 0.088207
ATOM H442 HA 0.088207
ATOM H443 HA 0.088207
GROUP
ATOM C25 CT2 -0.024974
ATOM N26 NH1 -0.535352
ATOM C27 C 0.519500
ATOM O27 O -0.519838
ATOM C45 CT2 -0.159943
ATOM C46 CT3 -0.258812
ATOM C28 CT1 -0.083091
ATOM H251 HA 0.084757
ATOM H252 HA 0.084757
ATOM HN2 H 0.327484
ATOM H451 HA 0.087275
ATOM H452 HA 0.087275
ATOM H461 HA 0.088419
ATOM H462 HA 0.088419
ATOM H463 HA 0.088419
ATOM H28 HA 0.085919
GROUP
ATOM C29 CTS 0.407149
ATOM O29 OHS -0.551363
ATOM C30 CTS 0.107878
ATOM O30 OHS -0.544113
ATOM C31 CTS 0.118034
ATOM O31 OHS -0.544113
ATOM C32 CTS 0.027988
ATOM C47 CT3 -0.263770
ATOM C48 CT3 -0.263770
ATOM C33 CTS 0.126063
ATOM O34 OES -0.369946
ATOM HO2 HOS 0.384231
ATOM H30 HAS 0.082956

ATOM HO3 HOS 0.384231
ATOM H31 HAS 0.082956
ATOM H2 HOS 0.384231
ATOM H471 HA 0.088419
ATOM H472 HA 0.088419
ATOM H473 HA 0.088419
ATOM H481 HA 0.088419
ATOM H482 HA 0.088419
ATOM H483 HA 0.088419
ATOM H33 HAS 0.082746
GROUP
ATOM C35 CE1 -0.116363
ATOM C36 CE1 -0.104454
ATOM C37 CE1 -0.104454
ATOM C38 CE1 -0.105446
ATOM C39 CT3 -0.254834
ATOM H35 HE1 0.095101
ATOM H36 HE1 0.094889
ATOM H37 HE1 0.094889
ATOM H38 HE1 0.095101
ATOM H391 HA 0.088207
ATOM H392 HA 0.088207
ATOM H393 HA 0.088207
BOND C2 C3
BOND C2 N1
BOND C2 O2
BOND C3 C4
BOND C3 C7
BOND C4 C5
BOND C4 O4
BOND C5 C6
BOND C5 H5
BOND C6 N1
BOND C6 H6
BOND C7 C8
BOND C7 O7
BOND C8 C9

BOND C8 C41
BOND C20 C21
BOND C20 C19
BOND C20 O20
BOND C20 H20
BOND C21 C22
BOND C21 C44
BOND C24 C25
BOND C24 C23
BOND C24 H24
BOND C25 N26
BOND C25 H251
BOND C25 H252
BOND O4 HO4
BOND C9 C10
BOND C9 H9
BOND C10 C11
BOND C10 H10
BOND C11 C12
BOND C11 H11
BOND C12 C13
BOND C12 H12
BOND C13 C14
BOND C13 H13
BOND C14 C15
BOND C14 O18
BOND C14 H14
BOND C15 C16
BOND C15 O15
BOND C15 H15
BOND C16 C17
BOND C16 O16
BOND C16 H16
BOND C17 C19
BOND C17 O18
BOND C17 H17
BOND C19 C42

BOND C19 H19
BOND C22 C23
BOND C22 H22
BOND C23 H23
BOND O15 HO1
BOND N1 HN1
BOND C41 H411
BOND C41 H412
BOND C41 H413
BOND O16 H1
BOND C42 H421
BOND C42 H422
BOND C42 H423
BOND O20 C43
BOND C43 H431
BOND C43 H432
BOND C43 H433
BOND C44 H441
BOND C44 H442
BOND C44 H443
BOND N26 C27
BOND N26 HN2
BOND C27 O27
BOND C27 C28
BOND C45 C46
BOND C45 C28
BOND C45 H451
BOND C45 H452
BOND C46 H461
BOND C46 H462
BOND C46 H463
BOND C28 C29
BOND C28 H28
BOND C29 O29
BOND C29 C30
BOND C29 O34
BOND O29 HO2

BOND C30 O30
BOND C30 C31
BOND C30 H30
BOND O30 HO3
BOND C31 O31
BOND C31 C32
BOND C31 H31
BOND O31 H2
BOND C32 C47
BOND C32 C48
BOND C32 C33
BOND C47 H471
BOND C47 H472
BOND C47 H473
BOND C48 H481
BOND C48 H482
BOND C48 H483
BOND C33 O34
BOND C33 C35
BOND C33 H33
BOND C35 C36
BOND C35 H35
BOND C36 C37
BOND C36 H36
BOND C37 C38
BOND C37 H37
BOND C38 C39
BOND C38 H38
BOND C39 H391
BOND C39 H392
BOND C39 H393
IMPH C2 C3 N1 O2
IMPH C3 C2 C7 C4
IMPH C4 C5 O4 C3
IMPH C5 C4 H5 C6
IMPH C6 N1 H6 C5
IMPH C7 C3 C8 O7

IMPH C8 C7 C41 C9
IMPH C21 C20 C44 C22
IMPH C24 C25 H24 C23
IMPH C9 C10 H9 C8
IMPH C10 C9 H10 C11
IMPH C11 C12 H11 C10
IMPH C12 C11 H12 C13
IMPH C13 C14 H13 C12
IMPH C22 C23 H22 C21
IMPH C23 C22 H23 C24
IMPH N1 C2 C6 HN1
IMPH N26 C25 C27 HN2
IMPH C27 N26 C28 O27
IMPH C35 C33 H35 C36
IMPH C36 C37 H36 C35
IMPH C37 C36 H37 C38
IMPH C38 C39 H38 C37
IC N1 C2 C3 C4 1.38 119.81 0.04 118.00 1.45
IC O2 C2 C3 C4 1.27 119.99 -179.92 118.00 1.45
IC N1 C2 C3 C7 1.38 119.81 -179.97 121.16 1.50
IC C3 N1 *C2 O2 1.45 119.81 179.96 120.19 1.27
IC C2 C4 *C3 C7 1.45 118.00 -179.99 120.84 1.50
IC C2 C3 C4 C5 1.45 118.00 0.00 120.46 1.44
IC C7 C3 C4 C5 1.50 120.84 -179.99 120.46 1.44
IC C2 C3 C4 O4 1.45 118.00 -179.75 119.33 1.36
IC C3 C5 *C4 O4 1.45 120.46 179.75 120.20 1.36
IC C3 C4 C5 C6 1.45 120.46 0.00 118.19 1.44
IC O4 C4 C5 C6 1.36 120.20 179.75 118.19 1.44
IC C3 C4 C5 H5 1.45 120.46 -180.00 119.99 1.08
IC C4 C6 *C5 H5 1.44 118.19 -180.00 121.81 1.08
IC C4 C5 C6 N1 1.44 118.19 -0.06 120.67 1.37
IC H5 C5 C6 N1 1.08 121.81 179.94 120.67 1.37
IC C4 C5 C6 H6 1.44 118.19 179.94 119.97 1.08
IC C5 N1 *C6 H6 1.44 120.67 180.00 119.36 1.08
IC C5 C6 N1 C2 1.44 120.67 0.10 122.87 1.38
IC H6 C6 N1 C2 1.08 119.36 -179.90 122.87 1.38
IC C5 C6 N1 HN1 1.44 120.67 -179.90 117.12 1.01

IC C2 C6 *N1 HN1 1.38 122.87 -180.00 117.12 1.01
IC C6 N1 C2 C3 1.37 122.87 -0.09 119.81 1.45
IC HN1 N1 C2 C3 1.01 120.01 179.91 119.81 1.45
IC C6 N1 C2 O2 1.37 122.87 179.87 120.19 1.27
IC C3 C4 O4 HO4 1.45 119.33 -180.00 109.52 0.96
IC C5 C4 O4 HO4 1.44 120.20 0.25 109.52 0.96
IC C2 C3 C7 C8 1.45 121.16 114.91 122.78 1.53
IC C4 C3 C7 C8 1.45 120.84 -65.10 122.78 1.53
IC C2 C3 C7 O7 1.45 121.16 -64.95 116.91 1.23
IC C3 C8 *C7 O7 1.50 122.78 179.85 120.31 1.23
IC C3 C7 C8 C9 1.50 122.78 -0.09 119.49 1.40
IC O7 C7 C8 C9 1.23 120.31 179.76 119.49 1.40
IC C3 C7 C8 C41 1.50 122.78 -179.96 118.24 1.53
IC C7 C9 *C8 C41 1.53 119.49 179.86 122.26 1.53
IC C7 C8 C9 C10 1.53 119.49 -179.82 128.60 1.47
IC C41 C8 C9 C10 1.53 122.26 0.04 128.60 1.47
IC C7 C8 C9 H9 1.53 119.49 0.17 120.01 1.08
IC C8 C10 *C9 H9 1.40 128.60 -180.00 111.38 1.08
IC C8 C9 C10 C11 1.40 128.60 166.18 116.21 1.34
IC H9 C9 C10 C11 1.08 111.38 -13.81 116.21 1.34
IC C8 C9 C10 H10 1.40 128.60 -13.81 120.01 1.08
IC C9 C11 *C10 H10 1.47 116.21 179.99 123.78 1.08
IC C9 C10 C11 C12 1.47 116.21 -179.98 121.48 1.45
IC H10 C10 C11 C12 1.08 123.78 0.01 121.48 1.45
IC C9 C10 C11 H11 1.47 116.21 0.03 119.99 1.08
IC C10 C12 *C11 H11 1.34 121.48 179.99 118.53 1.08
IC C10 C11 C12 C13 1.34 121.48 179.70 118.61 1.34
IC H11 C11 C12 C13 1.08 118.53 -0.31 118.61 1.34
IC C10 C11 C12 H12 1.34 121.48 -0.30 119.99 1.08
IC C11 C13 *C12 H12 1.45 118.61 179.99 121.40 1.08
IC C11 C12 C13 C14 1.45 118.61 179.98 121.37 1.52
IC H12 C12 C13 C14 1.08 121.40 -0.03 121.37 1.52
IC C11 C12 C13 H13 1.45 118.61 -0.01 120.00 1.08
IC C12 C14 *C13 H13 1.34 121.37 179.99 118.63 1.08
IC C12 C13 C14 C15 1.34 121.37 -110.56 114.71 1.54
IC H13 C13 C14 C15 1.08 118.63 69.43 114.71 1.54
IC C12 C13 C14 O18 1.34 121.37 132.19 108.48 1.43

IC C12 C13 C14 H14 1.34 121.37 6.69 109.51 1.09
IC C13 C14 C15 C16 1.52 114.71 -148.23 98.84 1.52
IC O18 C14 C15 C16 1.43 105.19 -29.12 98.84 1.52
IC H14 C14 C15 C16 1.09 104.62 91.77 98.84 1.52
IC C13 C14 C15 O15 1.52 114.71 -34.37 110.76 1.44
IC C13 C14 C15 H15 1.52 114.71 97.88 109.51 1.09
IC C14 C15 C16 C17 1.54 98.84 18.34 104.40 1.57
IC O15 C15 C16 C17 1.44 108.62 -97.19 104.40 1.57
IC H15 C15 C16 C17 1.09 109.01 132.61 104.40 1.57
IC C14 C15 C16 O16 1.54 98.84 138.84 110.85 1.44
IC C14 C15 C16 H16 1.54 98.84 -102.14 109.49 1.09
IC C15 C16 C17 C19 1.52 104.40 119.88 115.18 1.61
IC O16 C16 C17 C19 1.44 111.78 0.00 115.18 1.61
IC H16 C16 C17 C19 1.09 112.34 -121.56 115.18 1.61
IC C15 C16 C17 O18 1.52 104.40 -0.72 108.96 1.21
IC C15 C16 C17 H17 1.52 104.40 -119.51 109.53 1.09
IC C16 C17 C19 C20 1.57 115.18 161.61 107.21 1.59
IC O18 C17 C19 C20 1.21 107.31 -76.89 107.21 1.59
IC H17 C17 C19 C20 1.09 106.98 39.62 107.21 1.59
IC C16 C17 C19 C42 1.57 115.18 -78.11 110.26 1.59
IC C16 C17 C19 H19 1.57 115.18 42.22 110.68 1.09
IC C17 C19 C20 C21 1.61 107.21 179.20 114.74 1.52
IC C42 C19 C20 C21 1.59 110.45 59.05 114.74 1.52
IC H19 C19 C20 C21 1.09 109.51 -60.67 114.74 1.52
IC C17 C19 C20 O20 1.61 107.21 -60.52 109.00 1.44
IC C17 C19 C20 H20 1.61 107.21 56.99 107.74 1.09
IC C19 C20 C21 C22 1.59 114.74 -117.72 117.04 1.37
IC O20 C20 C21 C22 1.44 107.26 121.05 117.04 1.37
IC H20 C20 C21 C22 1.09 109.49 3.53 117.04 1.37
IC C19 C20 C21 C44 1.59 114.74 62.36 120.25 1.53
IC C20 C22 *C21 C44 1.52 117.04 179.91 122.71 1.53
IC C20 C21 C22 C23 1.52 117.04 -179.82 124.13 1.45
IC C44 C21 C22 C23 1.53 122.71 0.09 124.13 1.45
IC C20 C21 C22 H22 1.52 117.04 0.17 120.00 1.08
IC C21 C23 *C22 H22 1.37 124.13 -179.99 115.87 1.08
IC C21 C22 C23 C24 1.37 124.13 179.91 119.28 1.34
IC H22 C22 C23 C24 1.08 115.87 -0.08 119.28 1.34

IC C21 C22 C23 H23 1.37 124.13 -0.11 120.70 1.08
IC C24 C22 *C23 H23 1.34 119.28 179.98 120.70 1.08
IC C22 C23 C24 C25 1.45 119.28 -179.42 122.06 1.52
IC H23 C23 C24 C25 1.08 120.03 0.60 122.06 1.52
IC C22 C23 C24 H24 1.45 119.28 0.58 120.00 1.08
IC C25 C23 *C24 H24 1.52 122.06 -180.00 120.00 1.08
IC C23 C24 C25 N26 1.34 122.06 -19.11 112.31 1.45
IC H24 C24 C25 N26 1.08 117.94 160.88 112.31 1.45
IC C23 C24 C25 H251 1.34 122.06 100.88 109.48 1.09
IC C23 C24 C25 H252 1.34 122.06 -139.12 109.51 1.09
IC C24 C25 N26 C27 1.52 112.31 120.96 122.90 1.42
IC H251 C25 N26 C27 1.09 108.02 0.13 122.90 1.42
IC H252 C25 N26 C27 1.09 108.02 -118.17 122.90 1.42
IC C24 C25 N26 HN2 1.52 112.31 -59.06 117.10 1.01
IC C25 C27 *N26 HN2 1.45 122.90 -179.98 120.00 1.01
IC C25 N26 C27 O27 1.45 122.90 -0.32 121.26 1.24
IC HN2 N26 C27 O27 1.01 120.00 179.69 121.26 1.24
IC C25 N26 C27 C28 1.45 122.90 -179.54 117.76 1.52
IC N26 O27 *C27 C28 1.42 121.26 179.19 120.98 1.52
IC N26 C27 C28 C45 1.42 117.76 125.66 112.75 1.60
IC O27 C27 C28 C45 1.24 120.98 -53.56 112.75 1.60
IC N26 C27 C28 C29 1.42 117.76 -110.74 110.12 1.62
IC N26 C27 C28 H28 1.42 117.76 2.06 109.51 1.09
IC C27 C28 C45 C46 1.52 112.75 -49.91 112.65 1.48
IC C29 C28 C45 C46 1.62 110.26 -173.44 112.65 1.48
IC H28 C28 C45 C46 1.09 110.60 73.08 112.65 1.48
IC C27 C28 C45 H451 1.52 112.75 -170.84 107.86 1.09
IC C27 C28 C45 H452 1.52 112.75 71.04 107.82 1.09
IC C28 C45 C46 H461 1.60 112.65 -180.00 109.50 1.09
IC H451 C45 C46 H461 1.09 109.48 -60.00 109.50 1.09
IC H452 C45 C46 H461 1.09 109.52 60.02 109.50 1.09
IC C28 C45 C46 H462 1.60 112.65 -60.02 109.52 1.09
IC C28 C45 C46 H463 1.60 112.65 60.00 109.48 1.09
IC C27 C28 C29 O29 1.52 110.12 -59.72 108.25 1.46
IC C45 C28 C29 O29 1.60 110.26 65.32 108.25 1.46
IC H28 C28 C29 O29 1.09 103.19 -176.54 108.25 1.46
IC C27 C28 C29 C30 1.52 110.12 -179.34 112.58 1.54

IC C27 C28 C29 O34 1.52 110.12 54.04 112.24 1.44
IC C28 C29 O29 HO2 1.62 108.25 179.98 109.50 0.96
IC C30 C29 O29 HO2 1.54 108.25 -57.72 109.50 0.96
IC O34 C29 O29 HO2 1.44 103.63 60.63 109.50 0.96
IC C28 C29 C30 O30 1.62 112.58 -57.67 110.77 1.16
IC O29 C29 C30 O30 1.46 108.25 -177.28 110.77 1.16
IC O34 C29 C30 O30 1.44 111.38 69.42 110.77 1.16
IC C28 C29 C30 C31 1.62 112.58 -178.22 106.37 1.54
IC C28 C29 C30 H30 1.62 112.58 62.90 109.50 1.09
IC C29 C30 O30 HO3 1.54 110.77 -179.99 109.51 0.96
IC C31 C30 O30 HO3 1.54 110.86 -62.15 109.51 0.96
IC H30 C30 O30 HO3 1.09 109.26 59.30 109.51 0.96
IC C29 C30 C31 O31 1.54 106.37 -179.93 111.92 1.41
IC O30 C30 C31 O31 1.16 110.86 59.58 111.92 1.41
IC H30 C30 C31 O31 1.09 110.05 -61.41 111.92 1.41
IC C29 C30 C31 C32 1.54 106.37 57.42 110.90 1.57
IC C29 C30 C31 H31 1.54 106.37 -57.26 109.50 1.09
IC C30 C31 O31 H2 1.54 111.92 -180.00 109.50 0.96
IC C32 C31 O31 H2 1.57 109.54 -56.58 109.50 0.96
IC H31 C31 O31 H2 1.09 110.33 57.81 109.50 0.96
IC C30 C31 C32 C47 1.54 110.90 65.04 112.17 1.55
IC O31 C31 C32 C47 1.41 109.54 -58.98 112.17 1.55
IC H31 C31 C32 C47 1.09 104.40 -177.13 112.17 1.55
IC C30 C31 C32 C48 1.54 110.90 -178.89 111.75 1.51
IC C30 C31 C32 C33 1.54 110.90 -56.53 105.26 1.54
IC C31 C32 C47 H473 1.57 112.17 60.01 109.49 1.09
IC C48 C32 C47 H473 1.51 103.78 -60.79 109.49 1.09
IC C33 C32 C47 H473 1.54 111.61 177.86 109.49 1.09
IC C31 C32 C47 H471 1.57 112.17 -179.99 109.48 1.09
IC C31 C32 C47 H472 1.57 112.17 -59.98 109.52 1.09
IC C31 C32 C48 H483 1.57 111.75 59.98 109.49 1.09
IC C47 C32 C48 H483 1.55 103.78 -178.95 109.49 1.09
IC C33 C32 C48 H483 1.54 112.46 -58.17 109.49 1.09
IC C31 C32 C48 H481 1.57 111.75 -179.99 109.52 1.09
IC C31 C32 C48 H482 1.57 111.75 -60.00 109.48 1.09
IC C31 C32 C33 O34 1.57 105.26 54.15 114.89 1.25
IC C47 C32 C33 O34 1.55 111.61 -67.77 114.89 1.25

IC C48 C32 C33 O34 1.51 112.46 176.06 114.89 1.25
IC C31 C32 C33 C35 1.57 105.26 177.62 113.65 1.52
IC C31 C32 C33 H33 1.57 105.26 -69.33 109.51 1.09
IC C32 C33 O34 C29 1.54 114.89 -55.40 119.88 1.44
IC C35 C33 O34 C29 1.52 106.83 177.57 119.88 1.44
IC H33 C33 O34 C29 1.09 109.34 68.17 119.88 1.44
IC C33 O34 C29 C28 1.25 119.88 -179.00 112.24 1.62
IC C33 O34 C29 O29 1.25 119.88 -62.43 103.63 1.46
IC C33 O34 C29 C30 1.25 119.88 53.73 111.38 1.54
IC C32 C33 C35 C36 1.54 113.65 -115.98 124.67 1.37
IC O34 C33 C35 C36 1.25 106.83 11.78 124.67 1.37
IC H33 C33 C35 C36 1.09 101.77 126.40 124.67 1.37
IC C32 C33 C35 H35 1.54 113.65 64.04 115.33 1.08
IC C33 C36 *C35 H35 1.52 124.67 179.98 120.00 1.08
IC C33 C35 C36 C37 1.52 124.67 179.29 121.50 1.41
IC H35 C35 C36 C37 1.08 120.00 -0.74 121.50 1.41
IC C33 C35 C36 H36 1.52 124.67 -0.71 120.00 1.08
IC C35 C37 *C36 H36 1.37 121.50 180.00 118.51 1.08
IC C35 C36 C37 C38 1.37 121.50 179.46 123.56 1.37
IC H36 C36 C37 C38 1.08 118.51 -0.55 123.56 1.37
IC C35 C36 C37 H37 1.37 121.50 -0.56 119.99 1.08
IC C36 C38 *C37 H37 1.41 123.56 -179.98 116.45 1.08
IC C36 C37 C38 C39 1.41 123.56 -0.31 124.49 1.53
IC H37 C37 C38 C39 1.08 116.45 179.71 124.49 1.53
IC C36 C37 C38 H38 1.41 123.56 179.69 119.99 1.08
IC C37 C39 *C38 H38 1.37 124.49 180.00 115.53 1.08
IC C37 C38 C39 H391 1.37 124.49 -179.99 109.49 1.09
IC H38 C38 C39 H391 1.08 115.53 0.01 109.49 1.09
IC C37 C38 C39 H392 1.37 124.49 -60.01 109.50 1.09
IC C37 C38 C39 H393 1.37 124.49 60.01 109.49 1.09
IC C20 C21 C44 H441 1.52 120.25 180.00 109.49 1.09
IC C22 C21 C44 H441 1.37 122.71 0.09 109.49 1.09
IC C20 C21 C44 H442 1.52 120.25 -60.00 109.49 1.09
IC C20 C21 C44 H443 1.52 120.25 60.00 109.47 1.09
IC C21 C20 O20 C43 1.52 107.26 -97.07 111.22 1.44
IC C19 C20 O20 C43 1.59 109.00 138.15 111.22 1.44
IC H20 C20 O20 C43 1.09 108.48 21.10 111.22 1.44

IC C20 O20 C43 H431 1.44 111.22 -179.99 109.53 1.09
IC C20 O20 C43 H432 1.44 111.22 -60.00 109.49 1.09
IC C20 O20 C43 H433 1.44 111.22 60.02 109.49 1.09
IC C20 C19 C42 H421 1.59 110.45 -179.99 109.48 1.09
IC C17 C19 C42 H421 1.61 110.26 61.71 109.48 1.09
IC H19 C19 C42 H421 1.09 108.72 -59.80 109.48 1.09
IC C20 C19 C42 H422 1.59 110.45 -60.01 109.48 1.09
IC C20 C19 C42 H423 1.59 110.45 60.00 109.51 1.09
IC C16 C17 O18 C14 1.57 108.96 -19.95 112.45 1.43
IC C19 C17 O18 C14 1.61 107.31 -145.28 112.45 1.43
IC H17 C17 O18 C14 1.09 108.70 99.35 112.45 1.43
IC C17 O18 C14 C13 1.21 112.45 156.20 108.48 1.52
IC C17 O18 C14 C15 1.21 112.45 33.01 105.19 1.54
IC C17 O18 C14 H14 1.21 112.45 -81.23 114.41 1.09
IC C15 C16 O16 H1 1.52 110.85 180.00 109.49 0.96
IC C17 C16 O16 H1 1.57 111.78 -63.98 109.49 0.96
IC H16 C16 O16 H1 1.09 107.97 60.07 109.49 0.96
IC C14 C15 O15 HO1 1.54 110.76 179.97 109.53 0.96
IC C16 C15 O15 HO1 1.52 108.62 -72.50 109.53 0.96
IC H15 C15 O15 HO1 1.09 118.32 52.39 109.53 0.96
IC C7 C8 C41 H411 1.53 118.24 180.00 109.49 1.09
IC C9 C8 C41 H411 1.40 122.26 0.14 109.49 1.09
IC C7 C8 C41 H412 1.53 118.24 -60.03 109.50 1.09
IC C7 C8 C41 H413 1.53 118.24 60.01 109.50 1.09
END

A.3 Residue Topology of Enacyloxin IIa

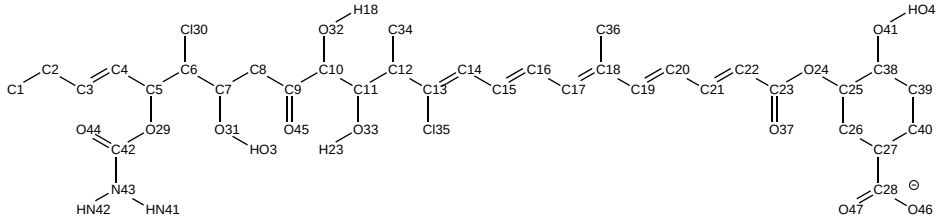

RESI ENX -1.000
GROUP
ATOM C1 CT3 -0.260374
ATOM C2 CT2 -0.154698
ATOM C3 CE1 -0.109680
ATOM C4 CE1 -0.117654
ATOM C5 CT1 0.125047
ATOM C6 CT1 -0.008967
ATOM C7 CT1 0.124575
ATOM C8 CT2 -0.172474
ATOM C9 CD 0.386260
ATOM C10 CT1 0.117843
ATOM C11 CT1 0.118777
ATOM C12 CT1 -0.067324
ATOM C13 CE1 0.067545
ATOM C14 CE1 -0.110683
ATOM C15 CE1 -0.106117
ATOM C16 CE1 -0.106117
ATOM C17 CE1 -0.109060
ATOM C18 CE1 0.014976
ATOM C19 CE1 -0.109060
ATOM C20 CE1 -0.106117
ATOM C21 CE1 -0.106117
ATOM C22 CE1 -0.119308
ATOM C23 CC 0.582669
ATOM O24 OS -0.35966
ATOM C25 CT1 0.117924
ATOM C26 CT2 -0.171366
ATOM C27 CT2 -0.072583
ATOM C28 CD 0.640164

ATOM O29 OS -0.362792
ATOM Cl30 CLAL -0.178291
ATOM O31 OH1 -0.545187
ATOM O32 OH1 -0.545597
ATOM O33 OH1 -0.545187
ATOM C34 CT3 -0.262853
ATOM Cl35 CLAL -0.163303
ATOM C36 CT3 -0.258874
ATOM O37 O -0.522867
ATOM C38 CT1 0.121606
ATOM C39 CT2 -0.168712
ATOM C40 CT2 -0.163809
ATOM O41 OH1 -0.545187
ATOM C42 C 0.709731
ATOM N43 NH2 -0.721557
ATOM O44 O -0.527007
ATOM O45 O -0.516602
ATOM O46 OC -0.634344
ATOM O47 OC -0.634344
ATOM H11 HA 0.087779
ATOM H12 HA 0.087779
ATOM H13 HA 0.087779
ATOM H21 HA 0.086423
ATOM H22 HA 0.086423
ATOM H3 HE1 0.094461
ATOM H4 HE1 0.094461
ATOM H5 HA 0.082105
ATOM H6 HA 0.084080
ATOM H7 HA 0.082317
ATOM H81 HA 0.086423
ATOM H82 HA 0.086423
ATOM H10 HA 0.082105
ATOM H1 HA 0.082317
ATOM H2 HA 0.085279
ATOM H14 HE1 0.094249
ATOM H15 HE1 0.094249
ATOM H16 HE1 0.094249

ATOM H17 HE1 0.094249
ATOM H19 HE1 0.094249
ATOM H20 HE1 0.094249
ATOM H8 HE1 0.094249
ATOM H9 HE1 0.094249
ATOM H25 HA 0.082317
ATOM H261 HA 0.086635
ATOM H262 HA 0.086635
ATOM H27 HA 0.085279
ATOM HO3 H 0.383223
ATOM H18 H 0.383223
ATOM H23 H 0.383223
ATOM H341 HA 0.087779
ATOM H342 HA 0.087779
ATOM H343 HA 0.087779
ATOM H361 HA 0.087568
ATOM H362 HA 0.087568
ATOM H363 HA 0.087568
ATOM H38 HA 0.083217
ATOM H391 HA 0.086635
ATOM H392 HA 0.086635
ATOM H401 HA 0.086635
ATOM H402 HA 0.086635
ATOM HO4 H 0.383223
ATOM HN41 H 0.329025
ATOM HN42 H 0.329025
BOND C1 C2
BOND C1 H11
BOND C1 H12
BOND C1 H13
BOND C2 C3
BOND C2 H21
BOND C2 H22
BOND C3 C4
BOND C3 H3
BOND C4 C5
BOND C4 H4

BOND C5 C6
BOND C5 O29
BOND C5 H5
BOND C6 C7
BOND C6 Cl30
BOND C6 H6
BOND C7 C8
BOND C7 O31
BOND C7 H7
BOND C8 C9
BOND C8 H81
BOND C8 H82
BOND C9 C10
BOND C9 O45
BOND C10 C11
BOND C10 O32
BOND C10 H10
BOND C11 C12
BOND C11 O33
BOND C11 H1
BOND C12 C13
BOND C12 C34
BOND C12 H2
BOND C13 C14
BOND C13 Cl35
BOND C14 C15
BOND C14 H14
BOND C15 C16
BOND C15 H15
BOND C16 C17
BOND C16 H16
BOND C17 C18
BOND C17 H17
BOND C18 C19
BOND C18 C36
BOND C19 C20
BOND C19 H19

BOND C20 C21
BOND C20 H20
BOND C21 C22
BOND C21 H8
BOND C22 C23
BOND C22 H9
BOND C23 O24
BOND C23 O37
BOND O24 C25
BOND C25 C26
BOND C25 C38
BOND C25 H25
BOND C26 C27
BOND C26 H261
BOND C26 H262
BOND C27 C28
BOND C27 C40
BOND C27 H27
BOND C28 O46
BOND C28 O47
BOND O29 C42
BOND O31 HO3
BOND O32 H18
BOND O33 H23
BOND C34 H341
BOND C34 H342
BOND C34 H343
BOND C36 H361
BOND C36 H362
BOND C36 H363
BOND C38 C39
BOND C38 O41
BOND C38 H38
BOND C39 C40
BOND C39 H391
BOND C39 H392
BOND C40 H401

BOND C40 H402
BOND O41 HO4
BOND C42 N43
BOND C42 O44
BOND N43 HN41
BOND N43 HN42
IMPH C3 C2 H3 C4
IMPH C4 C5 H4 C3
IMPH C9 C8 C10 O45
IMPH C13 C12 Cl35 C14
IMPH C14 C15 H14 C13
IMPH C15 C14 H15 C16
IMPH C16 C17 H16 C15
IMPH C17 C16 H17 C18
IMPH C18 C19 C36 C17
IMPH C19 C18 H19 C20
IMPH C20 C21 H20 C19
IMPH C21 C20 H8 C22
IMPH C22 C23 H9 C21
IMPH C23 C22 O24 O37
IMPH C28 O46 O47 C27
IMPH C42 N43 O44 O29
IMPH N43 HN41 HN42 C42
IC H11 C1 C2 C3 1.09 109.51 179.99 111.41 1.48
IC H12 C1 C2 C3 1.09 109.51 -60.03 111.41 1.48
IC H13 C1 C2 C3 1.09 109.50 60.01 111.41 1.48
IC H11 C1 C2 H21 1.09 109.51 -60.02 109.50 1.09
IC H11 C1 C2 H22 1.09 109.51 60.02 109.51 1.09
IC C1 C2 C3 C4 1.50 111.41 175.19 123.67 1.34
IC H21 C2 C3 C4 1.09 108.47 54.60 123.67 1.34
IC H22 C2 C3 C4 1.09 108.45 -64.21 123.67 1.34
IC C1 C2 C3 H3 1.50 111.41 -4.82 116.34 1.08
IC C2 C4 *C3 H3 1.48 123.67 -179.98 119.99 1.08
IC C2 C3 C4 C5 1.48 123.67 -179.31 122.82 1.51
IC H3 C3 C4 C5 1.08 119.99 0.70 122.82 1.51
IC C2 C3 C4 H4 1.48 123.67 0.68 120.01 1.08
IC C3 C5 *C4 H4 1.34 122.82 -179.99 117.17 1.08

IC C3 C4 C5 C6 1.34 122.82 -165.15 113.07 1.56
IC H4 C4 C5 C6 1.08 117.17 14.86 113.07 1.56
IC C3 C4 C5 O29 1.34 122.82 71.58 109.81 1.46
IC C3 C4 C5 H5 1.34 122.82 -41.90 109.50 1.09
IC C4 C5 C6 C7 1.51 113.07 -178.57 111.44 1.55
IC O29 C5 C6 C7 1.46 110.01 -55.41 111.44 1.55
IC H5 C5 C6 C7 1.09 110.16 58.54 111.44 1.55
IC C4 C5 C6 Cl30 1.51 113.07 57.52 109.44 1.76
IC C4 C5 C6 H6 1.51 113.07 -54.66 109.52 1.09
IC C5 C6 C7 C8 1.56 111.44 179.97 112.86 1.53
IC Cl30 C6 C7 C8 1.76 111.60 -57.35 112.86 1.53
IC H6 C6 C7 C8 1.09 111.55 57.22 112.86 1.53
IC C5 C6 C7 O31 1.56 111.44 -58.40 108.48 1.42
IC C5 C6 C7 H7 1.56 111.44 58.35 109.47 1.09
IC C6 C7 C8 C9 1.55 112.86 -171.25 113.71 1.51
IC O31 C7 C8 C9 1.42 109.58 67.74 113.71 1.51
IC H7 C7 C8 C9 1.09 109.03 -49.38 113.71 1.51
IC C6 C7 C8 H81 1.55 112.86 -51.25 109.53 1.09
IC C6 C7 C8 H82 1.55 112.86 68.76 109.49 1.09
IC C7 C8 C9 C10 1.53 113.71 -173.30 117.16 1.55
IC H81 C8 C9 C10 1.09 107.28 65.43 117.16 1.55
IC H82 C8 C9 C10 1.09 107.30 -52.08 117.16 1.55
IC C7 C8 C9 O45 1.53 113.71 6.38 122.70 1.24
IC C8 C10 *C9 O45 1.51 117.16 -179.69 120.14 1.24
IC C8 C9 C10 C11 1.51 117.16 -49.09 109.69 1.55
IC O45 C9 C10 C11 1.24 120.14 131.23 109.69 1.55
IC C8 C9 C10 O32 1.51 117.16 -171.18 111.75 1.43
IC C8 C9 C10 H10 1.51 117.16 73.00 109.50 1.09
IC C9 C10 C11 C12 1.55 109.69 172.28 114.12 1.55
IC O32 C10 C11 C12 1.43 109.86 -64.51 114.12 1.55
IC H10 C10 C11 C12 1.09 111.05 51.12 114.12 1.55
IC C9 C10 C11 O33 1.55 109.69 -64.47 105.60 1.43
IC C9 C10 C11 H1 1.55 109.69 49.00 109.52 1.09
IC C10 C11 C12 C13 1.55 114.12 178.78 109.74 1.51
IC O33 C11 C12 C13 1.43 111.85 58.98 109.74 1.51
IC H1 C11 C12 C13 1.09 109.60 -57.99 109.74 1.51
IC C10 C11 C12 C34 1.55 114.12 -59.42 111.47 1.54

IC C10 C11 C12 H2 1.55 114.12 56.99 109.48 1.09
IC C11 C12 C13 C14 1.55 109.74 -114.68 121.22 1.35
IC C34 C12 C13 C14 1.54 109.76 122.50 121.22 1.35
IC H2 C12 C13 C14 1.09 110.79 6.33 121.22 1.35
IC C11 C12 C13 Cl35 1.55 109.74 64.77 116.60 1.72
IC C12 C14 *C13 Cl35 1.51 121.22 -179.42 122.18 1.72
IC C12 C13 C14 C15 1.51 121.22 178.89 126.46 1.45
IC Cl35 C13 C14 C15 1.72 122.18 -0.53 126.46 1.45
IC C12 C13 C14 H14 1.51 121.22 -1.10 120.00 1.08
IC C13 C15 *C14 H14 1.35 126.46 179.99 113.54 1.08
IC C13 C14 C15 C16 1.35 126.46 179.49 122.27 1.35
IC H14 C14 C15 C16 1.08 113.54 -0.52 122.27 1.35
IC C13 C14 C15 H15 1.35 126.46 -0.52 120.01 1.08
IC C14 C16 *C15 H15 1.45 122.27 -179.99 117.72 1.08
IC C14 C15 C16 C17 1.45 122.27 178.29 121.62 1.44
IC H15 C15 C16 C17 1.08 117.72 -1.70 121.62 1.44
IC C14 C15 C16 H16 1.45 122.27 -1.69 119.99 1.08
IC C15 C17 *C16 H16 1.35 121.62 179.98 118.39 1.08
IC C15 C16 C17 C18 1.35 121.62 179.39 127.36 1.35
IC H16 C16 C17 C18 1.08 118.39 -0.63 127.36 1.35
IC C15 C16 C17 H17 1.35 121.62 -0.63 119.98 1.08
IC C16 C18 *C17 H17 1.44 127.36 -179.98 112.67 1.08
IC C16 C17 C18 C19 1.44 127.36 177.22 116.95 1.47
IC H17 C17 C18 C19 1.08 112.67 -2.76 116.95 1.47
IC C16 C17 C18 C36 1.44 127.36 -0.97 124.34 1.50
IC C17 C19 *C18 C36 1.35 116.95 178.30 118.68 1.50
IC C17 C18 C19 C20 1.35 116.95 177.07 126.70 1.35
IC C36 C18 C19 C20 1.50 118.68 -4.63 126.70 1.35
IC C17 C18 C19 H19 1.35 116.95 -2.92 119.99 1.08
IC C18 C20 *C19 H19 1.47 126.70 179.99 113.31 1.08
IC C18 C19 C20 C21 1.47 126.70 -164.72 122.19 1.44
IC H19 C19 C20 C21 1.08 113.31 15.27 122.19 1.44
IC C18 C19 C20 H20 1.47 126.70 15.32 120.01 1.08
IC C19 C21 *C20 H20 1.35 122.19 179.97 117.80 1.08
IC C19 C20 C21 C22 1.35 122.19 -178.83 122.72 1.35
IC H20 C20 C21 C22 1.08 117.80 1.14 122.72 1.35
IC C19 C20 C21 H8 1.35 122.19 1.19 120.02 1.08

IC C20 C22 *C21 H8 1.44 122.72 179.98 117.26 1.08
IC C20 C21 C22 C23 1.44 122.72 170.79 122.58 1.48
IC H8 C21 C22 C23 1.08 117.26 -9.22 122.58 1.48
IC C20 C21 C22 H9 1.44 122.72 -9.23 120.01 1.08
IC C21 C23 *C22 H9 1.35 122.58 -179.97 117.41 1.08
IC C21 C22 C23 O24 1.35 122.58 -3.19 113.04 1.40
IC H9 C22 C23 O24 1.08 117.41 176.84 113.04 1.40
IC C21 C22 C23 O37 1.35 122.58 176.71 127.69 1.24
IC C22 O24 *C23 O37 1.48 113.04 -179.91 119.26 1.24
IC C22 C23 O24 C25 1.48 113.04 179.84 120.68 1.46
IC O37 C23 O24 C25 1.24 119.26 -0.07 120.68 1.46
IC C23 O24 C25 C26 1.40 120.68 -81.46 107.78 1.55
IC C23 O24 C25 C38 1.40 120.68 158.67 111.30 1.55
IC C23 O24 C25 H25 1.40 120.68 38.42 109.52 1.09
IC O24 C25 C26 C27 1.46 107.78 -64.36 110.91 1.54
IC C38 C25 C26 C27 1.55 109.32 56.75 110.91 1.54
IC H25 C25 C26 C27 1.09 110.19 176.18 110.91 1.54
IC O24 C25 C26 H261 1.46 107.78 55.67 109.48 1.09
IC O24 C25 C26 H262 1.46 107.78 175.65 109.51 1.09
IC C25 C26 C27 C28 1.55 110.91 -179.67 110.79 1.51
IC H261 C26 C27 C28 1.09 108.76 59.87 110.79 1.51
IC H262 C26 C27 C28 1.09 108.72 -59.21 110.79 1.51
IC C25 C26 C27 C40 1.55 110.91 -56.89 111.10 1.55
IC C25 C26 C27 H27 1.55 110.91 57.55 109.50 1.09
IC C26 C27 C28 O46 1.54 110.79 89.93 129.71 1.24
IC C40 C27 C28 O46 1.55 110.14 -33.40 129.71 1.24
IC H27 C27 C28 O46 1.09 111.01 -148.17 129.71 1.24
IC C26 C27 C28 O47 1.54 110.79 -89.91 113.88 1.22
IC C27 O46 *C28 O47 1.51 129.71 179.84 116.41 1.22
IC C26 C27 C40 C39 1.54 111.10 56.09 111.35 1.54
IC C28 C27 C40 C39 1.51 110.14 179.25 111.35 1.54
IC H27 C27 C40 C39 1.09 104.11 -61.68 111.35 1.54
IC C26 C27 C40 H401 1.54 111.10 176.08 109.49 1.09
IC C26 C27 C40 H402 1.54 111.10 -63.90 109.48 1.09
IC C27 C40 C39 C38 1.55 111.35 -55.32 110.10 1.54
IC H401 C40 C39 C38 1.09 108.50 -175.88 110.10 1.54
IC H402 C40 C39 C38 1.09 108.51 65.24 110.10 1.54

IC C27 C40 C39 H391 1.55 111.35 -175.52 109.16 1.09
IC C27 C40 C39 H392 1.55 111.35 64.90 109.16 1.09
IC C40 C39 C38 C25 1.54 110.10 56.70 112.19 1.55
IC H391 C39 C38 C25 1.09 109.48 176.71 112.19 1.55
IC H392 C39 C38 C25 1.09 109.49 -63.32 112.19 1.55
IC C40 C39 C38 O41 1.54 110.10 -179.74 107.68 1.42
IC C40 C39 C38 H38 1.54 110.10 -64.74 109.00 1.09
IC C39 C38 C25 O24 1.54 112.19 61.65 111.30 1.46
IC O41 C38 C25 O24 1.42 111.91 -59.52 111.30 1.46
IC H38 C38 C25 O24 1.09 109.49 -177.20 111.30 1.46
IC C39 C38 C25 C26 1.54 112.19 -57.29 109.32 1.55
IC C39 C38 C25 H25 1.54 112.19 -177.63 108.73 1.09
IC C25 C38 O41 HO4 1.55 111.91 -180.00 109.51 0.96
IC C39 C38 O41 HO4 1.54 107.68 56.27 109.51 0.96
IC H38 C38 O41 HO4 1.09 106.37 -60.46 109.51 0.96
IC C17 C18 C36 H361 1.35 124.34 -179.99 109.49 1.09
IC C19 C18 C36 H361 1.47 118.68 1.84 109.49 1.09
IC C17 C18 C36 H362 1.35 124.34 -59.98 109.49 1.09
IC C17 C18 C36 H363 1.35 124.34 59.97 109.49 1.09
IC C11 C12 C34 H341 1.55 111.47 179.96 109.48 1.09
IC C13 C12 C34 H341 1.51 109.76 -58.25 109.48 1.09
IC H2 C12 C34 H341 1.09 105.55 61.19 109.48 1.09
IC C11 C12 C34 H342 1.55 111.47 -59.97 109.51 1.09
IC C11 C12 C34 H343 1.55 111.47 59.97 109.48 1.09
IC C10 C11 O33 H23 1.55 105.60 -179.98 109.47 0.96
IC C12 C11 O33 H23 1.55 111.85 -55.30 109.47 0.96
IC H1 C11 O33 H23 1.09 105.76 63.96 109.47 0.96
IC C9 C10 O32 H18 1.55 111.75 -179.97 109.50 0.96
IC C11 C10 O32 H18 1.55 109.86 58.03 109.50 0.96
IC H10 C10 O32 H18 1.09 104.93 -61.40 109.50 0.96
IC C6 C7 O31 HO3 1.55 108.48 -179.99 109.49 0.96
IC C8 C7 O31 HO3 1.53 109.58 -56.37 109.49 0.96
IC H7 C7 O31 HO3 1.09 107.26 61.85 109.49 0.96
IC C4 C5 O29 C42 1.51 109.81 -99.20 120.73 1.40
IC C6 C5 O29 C42 1.56 110.01 135.75 120.73 1.40
IC H5 C5 O29 C42 1.09 103.89 17.84 120.73 1.40
IC C5 O29 C42 N43 1.46 120.73 -176.49 111.84 1.37

```
IC C5 O29 C42 O44 1.46 120.73 4.19 121.98 1.26
IC O29 N43 *C42 O44 1.40 111.84 179.28 126.17 1.26
IC O29 C42 N43 HN41 1.40 111.84 -179.99 120.00 1.01
IC O44 C42 N43 HN41 1.26 126.17 -0.71 120.00 1.01
IC O29 C42 N43 HN42 1.40 111.84 -0.01 120.00 1.01
IC C42 HN41 *N43 HN42 1.37 120.00 -179.98 120.01 1.01
END
```

A.4 Residue Topology of UF3-1

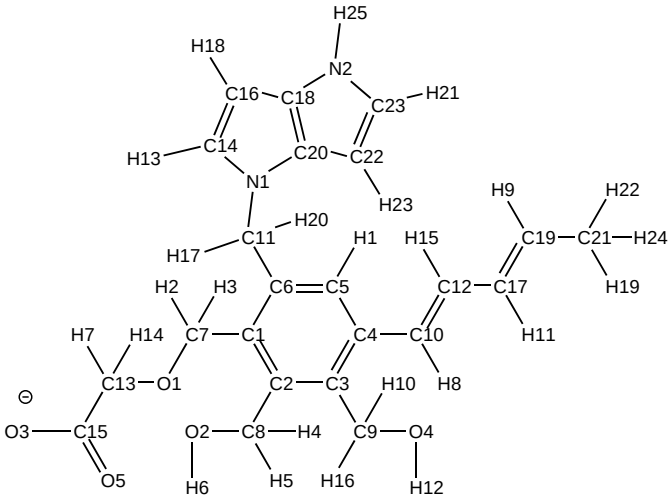

RESI UF3-1 -1.000
GROUP
ATOM C1 CA -0.029082
ATOM C2 CA -0.029082
ATOM C3 CA -0.029317
ATOM C4 CA -0.017190
ATOM C5 CA -0.127721
ATOM C6 CA -0.023488
ATOM C7 CT2 0.031329
ATOM C8 CT2 0.034836
ATOM C9 CT2 0.034836
ATOM C10 CE1 -0.109816
ATOM C11 CT2 -0.130839
ATOM O1 OS -0.365743
ATOM O2 OH1 -0.550475
ATOM C12 CE1 -0.116924
ATOM C13 CT2 0.006254
ATOM C15 CC 0.627546 !from glu
ATOM O3 OC -0.648738 !from glu
ATOM O5 OC -0.648738 !from glu
ATOM C17 CE1 -0.116461
ATOM C19 CE1 -0.117452
ATOM C21 CT3 -0.266106

ATOM O4 OH1 -0.550475
ATOM N1 NN2B -0.057809 ! from guanine
ATOM C14 CA -0.114057 ! from trp
ATOM C16 CA -0.125664 !from trp
ATOM C18 CPT 0.002032 !from trp
ATOM C20 CPT -0.001412 !from trp
ATOM C22 CA -0.125664 !from trp
ATOM C23 CA -0.110613 !from trp
ATOM N2 NY -0.192906 !from trp
ATOM H1 HA 0.100438
ATOM H2 HA 0.078388
ATOM H3 HA 0.078388
ATOM H4 HA 0.078388
ATOM H5 HA 0.078388
ATOM H6 H 0.376039
ATOM H7 HA 0.078687
ATOM H14 HA 0.078687
ATOM H19 HA 0.083005
ATOM H22 HA 0.083005
ATOM H24 HA 0.083005
ATOM H8 HE1 0.089388
ATOM H15 HE1 0.089687
ATOM H9 HE1 0.089899
ATOM H10 HA 0.078388
ATOM H16 HA 0.078388
ATOM H11 HE1 0.089687
ATOM H12 H 0.376039
ATOM H17 HA 0.080847
ATOM H20 HA 0.080847
ATOM H13 HP 0.100234 !from trp
ATOM H18 HP 0.100438 !from trp
ATOM H21 HP 0.100438 !from trp
ATOM H23 HP 0.100234 !from trp
ATOM H25 H 0.218008 !from trp
BOND C1 C2
BOND C1 C6
BOND C1 C7

BOND C2 C3
BOND C2 C8
BOND C3 C4
BOND C3 C9
BOND C4 C5
BOND C4 C10
BOND C5 C6
BOND C5 H1
BOND C6 C11
BOND C7 O1
BOND C7 H2
BOND C7 H3
BOND C8 O2
BOND C8 H4
BOND C8 H5
BOND C9 H10
BOND C9 O4
BOND C9 H16
BOND C10 C12
BOND C10 H8
BOND C11 N1
BOND C11 H17
BOND C11 H20
BOND O1 C13
BOND O2 H6
BOND C12 C17
BOND C12 H15
BOND C13 C15
BOND C13 H7
BOND C13 H14
BOND C15 O3
BOND C15 O5
BOND C17 C19
BOND C17 H11
BOND C19 C21
BOND C19 H9
BOND C21 H19

```
BOND C21 H22
BOND C21 H24
BOND O4 H12
BOND N1 C14
BOND N1 C20
BOND C14 C16
BOND C14 H13
BOND C16 C18
BOND C16 H18
BOND C18 C20
BOND C18 N2
BOND C20 C22
BOND C22 C23
BOND C22 H21
BOND C23 N2
BOND C23 H23
BOND N2 H25
IMPH C6 C1 C2 C3
IMPH C2 C1 C6 C5
IMPH C1 C2 C3 C4
IMPH C2 C3 C4 C5
IMPH C3 C4 C5 C6
IMPH C4 C5 C6 C1
IMPH C1 C2 C6 C7
IMPH C2 C1 C3 C8
IMPH C3 C2 C4 C9
IMPH C4 C3 C5 C10
IMPH C5 C4 C6 H1
IMPH C6 C1 C5 C11
IMPH C10 C4 H8 C12
IMPH C12 C17 H15 C10
IMPH C15 O3 O5 C13
IMPH C17 C12 H11 C19
IMPH C19 C21 H9 C17
IMPH N1 C14 C20 C11
IMPH C14 N1 H13 C16
IMPH C16 C18 H18 C14
```

IMPH C18 C16 N2 C20
IMPH C20 N1 C22 C18
IMPH C22 C20 H21 C23
IMPH C23 N2 H23 C22
IMPH N2 C18 C23 H25
IC C6 C1 C2 C3 1.42 119.35 -5.56 120.44 1.42
IC C7 C1 C2 C3 1.52 119.72 173.99 120.44 1.42
IC C6 C1 C2 C8 1.42 119.35 176.53 119.89 1.52
IC C2 C6 *C1 C7 1.43 119.35 -179.54 120.93 1.52
IC C1 C3 *C2 C8 1.43 120.44 177.92 119.64 1.52
IC C1 C2 C3 C4 1.43 120.44 5.71 119.22 1.41
IC C8 C2 C3 C4 1.52 119.64 -176.37 119.22 1.41
IC C1 C2 C3 C9 1.43 120.44 -173.55 120.60 1.51
IC C2 C4 *C3 C9 1.42 119.22 179.26 120.18 1.51
IC C2 C3 C4 C5 1.42 119.22 -2.41 119.61 1.40
IC C9 C3 C4 C5 1.51 120.18 176.85 119.61 1.40
IC C2 C3 C4 C10 1.42 119.22 175.32 121.88 1.47
IC C3 C5 *C4 C10 1.41 119.61 -177.81 118.47 1.47
IC C3 C4 C5 C6 1.41 119.61 -1.05 122.33 1.41
IC C10 C4 C5 C6 1.47 118.47 -178.87 122.33 1.41
IC C3 C4 C5 H1 1.41 119.61 178.99 118.71 1.09
IC C4 C6 *C5 H1 1.40 122.33 179.96 118.96 1.09
IC C4 C5 C6 C1 1.40 122.33 1.21 118.81 1.42
IC H1 C5 C6 C1 1.09 118.96 -178.83 118.81 1.42
IC C4 C5 C6 C11 1.40 122.33 -179.69 117.23 1.52
IC C1 C5 *C6 C11 1.42 118.81 179.10 117.23 1.52
IC C5 C6 C1 C2 1.41 118.81 2.09 119.35 1.43
IC C11 C6 C1 C2 1.52 123.96 -176.95 119.35 1.43
IC C5 C6 C1 C7 1.41 118.81 -177.45 120.93 1.52
IC C1 C6 C11 N1 1.42 123.96 -117.21 112.27 1.45
IC C5 C6 C11 N1 1.41 117.23 63.74 112.27 1.45
IC C1 C6 C11 H17 1.42 123.96 2.26 110.74 1.10
IC C1 C6 C11 H20 1.42 123.96 119.42 112.33 1.09
IC C6 C11 N1 C14 1.52 112.27 39.41 127.38 1.38
IC H17 C11 N1 C14 1.10 106.95 -82.25 127.38 1.38
IC H20 C11 N1 C14 1.09 109.08 164.58 127.38 1.38
IC C6 C11 N1 C20 1.52 112.27 -135.77 125.04 1.37

IC C11 C14 *N1 C20 1.45 127.38 175.87 107.44 1.37
IC C11 N1 C14 C16 1.45 127.38 -178.04 110.11 1.38
IC C20 N1 C14 C16 1.37 107.44 -2.17 110.11 1.38
IC C11 N1 C14 H13 1.45 127.38 2.25 120.43 1.09
IC N1 C16 *C14 H13 1.38 110.11 179.68 129.46 1.09
IC N1 C14 C16 C18 1.38 110.11 1.63 104.72 1.41
IC H13 C14 C16 C18 1.09 129.46 -178.69 104.72 1.41
IC N1 C14 C16 H18 1.38 110.11 -179.10 126.33 1.08
IC C14 C18 *C16 H18 1.38 104.72 -179.25 128.94 1.08
IC C14 C16 C18 C20 1.38 104.72 -0.48 109.44 1.36
IC H18 C16 C18 C20 1.08 128.94 -179.73 109.44 1.36
IC C14 C16 C18 N2 1.38 104.72 179.24 141.83 1.37
IC C16 C20 *C18 N2 1.41 109.44 -179.82 108.73 1.37
IC C16 C18 C20 N1 1.41 109.44 -0.82 108.25 1.37
IC N2 C18 C20 N1 1.37 108.73 179.36 108.25 1.37
IC C16 C18 C20 C22 1.41 109.44 179.10 108.72 1.42
IC N1 C18 *C20 C22 1.37 108.25 179.93 108.72 1.42
IC C18 C20 N1 C11 1.36 108.25 177.80 125.04 1.45
IC C22 C20 N1 C11 1.42 143.03 -2.09 125.04 1.45
IC C18 C20 N1 C14 1.36 108.25 1.82 107.44 1.38
IC N1 C20 C22 C23 1.37 143.03 -179.67 104.95 1.38
IC C18 C20 C22 C23 1.36 108.72 0.44 104.95 1.38
IC N1 C20 C22 H21 1.37 143.03 0.04 128.34 1.08
IC C20 C23 *C22 H21 1.42 104.95 -179.71 126.71 1.08
IC C20 C22 C23 N2 1.42 104.95 -0.01 109.87 1.37
IC H21 C22 C23 N2 1.08 126.71 -179.72 109.87 1.37
IC C20 C22 C23 H23 1.42 104.95 179.70 130.24 1.08
IC C22 N2 *C23 H23 1.38 109.87 -179.74 119.89 1.08
IC C22 C23 N2 C18 1.38 109.87 -0.42 107.73 1.37
IC H23 C23 N2 C18 1.08 119.89 179.84 107.73 1.37
IC C22 C23 N2 H25 1.38 109.87 179.76 128.61 1.01
IC C18 C23 *N2 H25 1.37 107.73 -179.82 128.61 1.01
IC C23 N2 C18 C16 1.37 107.73 -179.02 141.83 1.41
IC H25 N2 C18 C16 1.01 123.66 0.81 141.83 1.41
IC C23 N2 C18 C20 1.37 107.73 0.70 108.73 1.36
IC C3 C4 C10 C12 1.41 121.88 160.11 122.75 1.34
IC C5 C4 C10 C12 1.40 118.47 -22.13 122.75 1.34

IC C3 C4 C10 H8 1.41 121.88 -18.97 115.23 1.09
IC C4 C12 *C10 H8 1.47 122.75 179.02 122.01 1.09
IC C4 C10 C12 C17 1.47 122.75 -179.74 122.69 1.45
IC H8 C10 C12 C17 1.09 122.01 -0.72 122.69 1.45
IC C4 C10 C12 H15 1.47 122.75 -0.29 119.79 1.09
IC C10 C17 *C12 H15 1.34 122.69 -179.46 117.52 1.09
IC C10 C12 C17 C19 1.34 122.69 -16.50 122.80 1.34
IC H15 C12 C17 C19 1.09 117.52 164.05 122.80 1.34
IC C10 C12 C17 H11 1.34 122.69 163.46 117.21 1.09
IC C12 C19 *C17 H11 1.45 122.80 -179.95 119.99 1.09
IC C12 C17 C19 C21 1.45 122.80 179.95 123.75 1.49
IC H11 C17 C19 C21 1.09 119.99 -0.01 123.75 1.49
IC C12 C17 C19 H9 1.45 122.80 -0.02 120.18 1.09
IC C17 C21 *C19 H9 1.34 123.75 179.96 116.08 1.09
IC C17 C19 C21 H19 1.34 123.75 120.46 109.88 1.09
IC H9 C19 C21 H19 1.09 116.08 -59.57 109.88 1.09
IC C17 C19 C21 H22 1.34 123.75 -120.42 109.87 1.09
IC C17 C19 C21 H24 1.34 123.75 0.05 112.26 1.09
IC C2 C3 C9 O4 1.42 120.60 -102.18 109.70 1.42
IC C4 C3 C9 O4 1.41 120.18 78.57 109.70 1.42
IC C2 C3 C9 H10 1.42 120.60 137.15 111.96 1.09
IC C2 C3 C9 H16 1.42 120.60 19.27 111.43 1.09
IC C3 C9 O4 H12 1.51 109.70 140.00 106.04 0.97
IC H10 C9 O4 H12 1.09 108.62 -97.33 106.04 0.97
IC H16 C9 O4 H12 1.09 109.51 17.41 106.04 0.97
IC C1 C2 C8 O2 1.43 119.89 103.22 109.44 1.42
IC C3 C2 C8 O2 1.42 119.64 -74.71 109.44 1.42
IC C1 C2 C8 H4 1.43 119.89 -136.06 111.96 1.09
IC C1 C2 C8 H5 1.43 119.89 -18.46 112.37 1.09
IC C2 C8 O2 H6 1.52 109.44 -63.77 103.81 0.98
IC H4 C8 O2 H6 1.09 108.80 173.61 103.81 0.98
IC H5 C8 O2 H6 1.09 109.35 59.71 103.81 0.98
IC C2 C1 C7 O1 1.43 119.72 65.20 108.51 1.43
IC C6 C1 C7 O1 1.42 120.93 -115.26 108.51 1.43
IC C2 C1 C7 H2 1.43 119.72 -173.31 109.47 1.10
IC C2 C1 C7 H3 1.43 119.72 -53.48 111.41 1.09
IC C1 C7 O1 C13 1.52 108.51 176.15 111.66 1.45

```
IC H2 C7 O1 C13 1.10 111.17 55.71 111.66 1.45
IC H3 C7 O1 C13 1.09 107.92 -62.99 111.66 1.45
IC C7 O1 C13 C15 1.43 111.66 -58.27 113.13 1.55
IC C7 O1 C13 H7 1.43 111.66 62.23 106.90 1.10
IC C7 O1 C13 H14 1.43 111.66 178.04 109.03 1.10
IC O1 C13 C15 O3 1.45 113.13 110.14 114.75 1.27
IC H7 C13 C15 O3 1.10 109.41 -8.93 114.75 1.27
IC H14 C13 C15 O3 1.10 110.74 -127.11 114.75 1.27
IC O1 C13 C15 O5 1.45 113.13 -69.50 115.84 1.26
IC C13 O3 *C15 O5 1.55 114.75 179.58 129.40 1.26
END
```

A.5 Residue Topology of R29

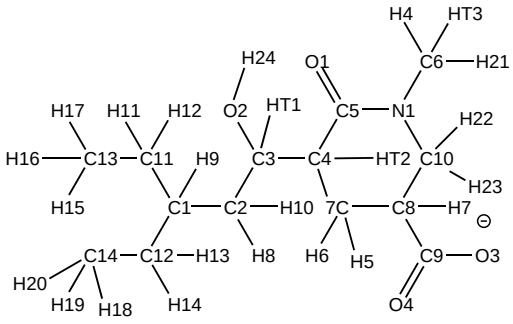

RESI R29 -1.00
GROUP
ATOM C1 CT1 -0.074867
ATOM C2 CT2 -0.183947
ATOM C3 CT1 0.113753
ATOM C4 CT1 -0.089676
ATOM C5 C 0.500356
ATOM N1 NT -0.361439
ATOM C6 CT3 -0.145646
ATOM O1 O -0.534922
ATOM O2 OH1 -0.555069
ATOM C7 CT2 -0.179219
ATOM C8 CT1 -0.088829
ATOM C9 CC 0.626576
ATOM O3 OC -0.652917
ATOM O4 OC -0.652917
ATOM HT1 HA 0.076430
ATOM HT2 HA 0.079392
ATOM H4 HA 0.079586
ATOM H21 HA 0.079586
ATOM H5 HA 0.080748
ATOM H6 HA 0.080748
ATOM C10 CT2 -0.049256
ATOM H7 HA 0.079392
ATOM H8 HA 0.080748
ATOM C11 CT2 -0.173911
ATOM H9 HA 0.079604

ATOM C12 CT2 -0.173911
ATOM H10 HA 0.080748
ATOM H11 HA 0.080748
ATOM C13 CT3 -0.272955
ATOM H12 HA 0.080748
ATOM H13 HA 0.080748
ATOM H14 HA 0.080748
ATOM C14 CT3 -0.272955
ATOM H15 HA 0.081892
ATOM H16 HA 0.081892
ATOM H17 HA 0.081892
ATOM H18 HA 0.081892
ATOM H19 HA 0.081892
ATOM H20 HA 0.081892
ATOM HT3 HA 0.079586
ATOM H22 HA 0.078442
ATOM H23 HA 0.078442
ATOM H24 H 0.373952
BOND C1 C2
BOND C1 C11
BOND C1 H9
BOND C1 C12
BOND C2 C3
BOND C2 H8
BOND C2 H10
BOND C3 C4
BOND C3 O2
BOND C3 HT1
BOND C4 C5
BOND C4 C7
BOND C4 HT2
BOND C5 N1
BOND C5 O1
BOND N1 C6
BOND N1 C10
BOND C6 HT3
BOND C6 H4

BOND C6 H21
BOND O2 H24
BOND C7 C8
BOND C7 H5
BOND C7 H6
BOND C8 C9
BOND C8 C10
BOND C8 H7
BOND C9 O3
BOND C9 O4
BOND C10 H22
BOND C10 H23
BOND C11 H11
BOND C11 C13
BOND C11 H12
BOND C12 H13
BOND C12 H14
BOND C12 C14
BOND C13 H15
BOND C13 H16
BOND C13 H17
BOND C14 H18
BOND C14 H19
BOND C14 H20
IMPH C5 C4 N1 O1
IMPH N1 C6 C10 C5
IMPH C9 O3 O4 C8
IC C11 C1 C2 C3 1.55 112.59 -65.21 113.90 1.54
IC H9 C1 C2 C3 1.10 106.23 49.09 113.90 1.54
IC C12 C1 C2 C3 1.54 114.47 164.17 113.90 1.54
IC C11 C1 C2 H8 1.55 112.59 55.47 107.73 1.10
IC C11 C1 C2 H10 1.55 112.59 170.37 109.58 1.09
IC C1 C2 C3 C4 1.55 113.90 -134.34 113.84 1.54
IC H8 C2 C3 C4 1.10 108.72 105.54 113.84 1.54
IC H10 C2 C3 C4 1.09 110.56 -10.44 113.84 1.54
IC C1 C2 C3 O2 1.55 113.90 103.06 107.64 1.44
IC C1 C2 C3 HT1 1.55 113.90 -11.05 108.97 1.10

IC C2 C3 C4 C5 1.54 113.84 68.03 110.38 1.53
IC O2 C3 C4 C5 1.44 110.32 -170.85 110.38 1.53
IC HT1 C3 C4 C5 1.10 110.08 -54.64 110.38 1.53
IC C2 C3 C4 C7 1.54 113.84 -171.50 114.33 1.54
IC C2 C3 C4 HT2 1.54 113.84 -48.56 108.28 1.10
IC C3 C4 C5 N1 1.54 110.38 173.98 114.18 1.39
IC C7 C4 C5 N1 1.54 106.83 49.12 114.18 1.39
IC HT2 C4 C5 N1 1.10 106.81 -68.52 114.18 1.39
IC C3 C4 C5 O1 1.54 110.38 -5.48 122.60 1.23
IC C4 N1 *C5 O1 1.53 114.18 179.46 123.22 1.23
IC C4 C5 N1 C6 1.53 114.18 177.18 121.35 1.45
IC O1 C5 N1 C6 1.23 123.22 -3.37 121.35 1.45
IC C4 C5 N1 C10 1.53 114.18 4.79 119.87 1.46
IC C5 C6 *N1 C10 1.39 121.35 172.50 118.35 1.46
IC C5 N1 C6 H21 1.39 121.35 128.31 108.84 1.09
IC C10 N1 C6 H21 1.46 118.35 -59.19 108.84 1.09
IC C5 N1 C6 HT3 1.39 121.35 7.93 111.74 1.09
IC C5 N1 C6 H4 1.39 121.35 -112.40 108.69 1.09
IC C5 N1 C10 C8 1.39 119.87 -48.08 111.87 1.53
IC C6 N1 C10 C8 1.45 118.35 139.30 111.87 1.53
IC C5 N1 C10 H22 1.39 119.87 -169.36 108.61 1.10
IC C5 N1 C10 H23 1.39 119.87 75.71 106.32 1.10
IC N1 C10 C8 C7 1.46 111.87 32.88 113.37 1.53
IC H22 C10 C8 C7 1.10 109.74 153.51 113.37 1.53
IC H23 C10 C8 C7 1.10 112.99 -87.07 113.37 1.53
IC N1 C10 C8 C9 1.46 111.87 157.50 101.32 1.53
IC N1 C10 C8 H7 1.46 111.87 -88.18 110.08 1.10
IC C9 C8 C7 C4 1.53 115.68 -96.91 111.62 1.54
IC C10 C8 C7 C4 1.53 113.37 19.52 111.62 1.54
IC H7 C8 C7 C4 1.10 107.98 141.76 111.62 1.54
IC C9 C8 C7 H5 1.53 115.68 28.07 110.66 1.09
IC C9 C8 C7 H6 1.53 115.68 143.48 107.74 1.10
IC C8 C7 C4 C3 1.53 111.62 177.22 114.33 1.54
IC H5 C7 C4 C3 1.09 111.64 52.79 114.33 1.54
IC H6 C7 C4 C3 1.10 108.98 -63.90 114.33 1.54
IC C8 C7 C4 C5 1.53 111.62 -60.36 106.83 1.53
IC C8 C7 C4 HT2 1.53 111.62 55.19 109.96 1.10

IC C7 C8 C9 O3 1.53 115.68 -159.05 115.99 1.26
IC C10 C8 C9 O3 1.53 101.32 77.92 115.99 1.26
IC H7 C8 C9 O3 1.10 108.17 -37.82 115.99 1.26
IC C7 C8 C9 O4 1.53 115.68 19.29 114.49 1.26
IC C8 O3 *C9 O4 1.53 115.99 -178.04 129.49 1.26
IC C2 C3 O2 H24 1.54 107.64 -62.58 105.34 0.98
IC C4 C3 O2 H24 1.54 110.32 172.68 105.34 0.98
IC HT1 C3 O2 H24 1.10 105.65 53.74 105.34 0.98
IC C2 C1 C11 H11 1.55 112.59 169.49 109.59 1.10
IC H9 C1 C11 H11 1.10 104.91 54.40 109.59 1.10
IC C12 C1 C11 H11 1.54 112.83 -59.06 109.59 1.10
IC C2 C1 C11 C13 1.55 112.59 -65.78 116.78 1.52
IC C2 C1 C11 H12 1.55 112.59 54.73 107.90 1.10
IC C1 C11 C13 H15 1.55 116.78 -175.85 109.75 1.10
IC H11 C11 C13 H15 1.10 109.16 -50.89 109.75 1.10
IC H12 C11 C13 H15 1.10 107.02 63.18 109.75 1.10
IC C1 C11 C13 H16 1.55 116.78 -56.02 112.56 1.09
IC C1 C11 C13 H17 1.55 116.78 65.73 111.36 1.09
IC C2 C1 C12 H13 1.55 114.47 61.87 108.63 1.10
IC C11 C1 C12 H13 1.55 112.83 -68.64 108.63 1.10
IC H9 C1 C12 H13 1.10 104.75 177.81 108.63 1.10
IC C2 C1 C12 H14 1.55 114.47 176.30 109.31 1.10
IC C2 C1 C12 C14 1.55 114.47 -60.28 116.34 1.52
IC C1 C12 C14 H18 1.54 116.34 -171.17 109.85 1.09
IC H13 C12 C14 H18 1.10 108.07 66.39 109.85 1.09
IC H14 C12 C14 H18 1.10 108.61 -47.38 109.85 1.09
IC C1 C12 C14 H19 1.54 116.34 -51.42 111.99 1.09
IC C1 C12 C14 H20 1.54 116.34 70.56 111.16 1.09
END

A.6 Force Field Parameters

A.6.1 Bonds Parameters

!GTP Parameters
!ON2 HN2 545.0 0.960 !same as ON5 HN5
!Kir Parameters
CA CN1T 302.0 1.403 !same as CN1 CN3T
CN1T NN2 340.0 1.389 !same as CN1 NN2U
C CA 250.0 1.49 !same as CP1 C
C CE1 250.0 1.49 !same as CT1 C
H NN2 474.0 1.01 !same as HN2 NN2U
CE1 CN7 222.5 1.512 !same as CN7 CN8B
CN7 CT1 222.5 1.512 !same as CN7 CN8B
CE1 CT1 365.0 1.5020 !same as CE1 CT2
CT1 ON6B 240.0 1.480 !same as CN7 ON6B
CT3 ON6B 390.0 1.407 !same as CT OE From Accelrys CHARMm
CT1 CTS 325.5297 1.5060 !same as CTS CTS
CT3 CTS 325.5297 1.5060 !same as CTS CTS
CE1 CTS 325.5297 1.5060 !same as CTS CTS
CA CN1 320.0 1.406 !same as CN2 CN3
CN1 OH1 334.3 1.411 !same as CA OH1
!Enx Parameters
CT1 OS 340.0 1.43 !same as CT3 OS
CLAL CT1 254.0 1.783 !same as CT XCL From Accelrys CHARMm
CD O 620.0 1.23 !same as C O
CE1 CLAL 232.0 1.71 !same as CUA1 XCL
C NH2 430.0 1.36 !same as NH2 CC
CC CE1 282.0 1.476 !same as C CUA1 From Accelrys CHARMm
CC OS 150.0 1.334 !same as OS CD
CD OC 525.0 1.26 !same as OC CC
C OS 150.0 1.334 !same as OS CD
!UF3-1 Parameters
CA CE1 230.0 1.49 !same as CT2 CA
CT2 OS 340.0 1.43 !same as OS CT3
CT2 NN2B 220.0 1.458 !same as CN7B NN2B
CA NN2B 302.0 1.375 !same as CN5 NN2B
CPT NN2B 300.0 1.378 !same as CN4 NN2B

!R29 Parameters
C NT 400.0 1.416 !same as C NT From Accelrys CHARMm
CT3 NT 340.0 1.458 !same as CT NT From Accelrys CHARMm
CT2 NT 340.0 1.458 !same as CT NT From Accelrys CHARMm

A.6.2 Angle Parameters

!GTP Parameters
!HN2 ON2 CN7 57.5 109.0 ! same as HN5 ON5 CN7B
!Kir Parameters
CN1T NN2 H 40.5 115.4 !same as CN1 NN2U HN2
CN1T NN2 CN3 50.0 124.1 !same as CN1 NN2 CN3
C CA CN1T 65.0 120.0 !same as C C C6R From Accelrys CHARMm
CA C O 86.0 127.0 !same as C6R C O From Accelrys CHARMm
CA C CE1 70.0 117.5 !same as C6R C CUA1 From Accelrys CHARMm
CA CN1T ON1 100.0 124.6 !same as CN3T CN1 ON1
CA CN1T NN2 120.0 123.6 !same as CN3T CN3 NN2B
CN3 NN2 H 30.0 120.0 !same as H N6R C6R From Accelrys CHARMm
C CE1 CT3 60.0 120.0 !same as C CUA1 CT From Accelrys CHARMm
C CE1 CE1 72.0 119.5 !same as C CUA1 CUA2 From Accelrys CHARMm
NN2 CN1T ON1 100.0 124.4 !same as NN2U CN1T ON1
CE1 CE1 CE1 55.0 122.7 !same as CUA1 CUA1 CUA2 From Accelrys CHARMm
CE1 C O 40.0 120.0 !same as CUA1 C O From Accelrys CHARMm
CE1 CE1 CN7 60.0 122.0 !same as CUA1 CUA1 C5R From Accelrys CHARMm
CE1 CN7 HN7 34.5 110.1 !same as HN7 CN7 CN8B
CE1 CN7 ON6B 90.0 108.2 !same as ON6B CN7 CN8B
CE1 CN7 CN7 45.0 110.0 !same as CN7 CN7 CN8B
CN7 ON6B CN7 110.0 115.0 !same as CN7 ON6B CN7B
CN7 CN7 CN7 60.0 100.0 !same as CN7B CN7 CN7
CN7 CE1 HE1 40.0 117.0 !same as C5R CUA1 HA From Accelrys CHARMm
CN7 CN7 CT1 45.0 110.0 !same as CN7 CN7 CN8B
CN7 CT1 HA 34.53 110.1 !same as CN7 CN8B HN8
CN7 CT1 CT3 70.0 109.47 !same as C5R CT CT From Accelrys CHARMm
CT1 ON6B CT3 58.0 112.4 !same as CT OE CT From Accelrys CHARMm
CN7 CT1 CT1 70.0 109.47 !same as C5R CT CT From Accelrys CHARMm
CT1 CE1 CT3 50.0 114.2 !same as CT CUA1 CT From Accelrys CHARMm
CE1 CE1 CT1 40.0 122.9 !same as CT CUA1 CUA1 From Accelrys CHARMm
CE1 CT1 HA 50.0 110.00 !same as HA CT CUA1 From Accelrys CHARMm

CE1 CT1 ON6B 60.0 109.47 !same as CUA1 CT OE From Accelrys CHARMm
CE1 CT1 CT1 45.0 112.90 !same as CT CT CUA1 From Accelrys CHARMm
CE1 CT2 NH1 70.0 113.5 !same as NH1 CT2 CT2
CT1 CT1 ON6B 57.0 110.0 !same as CT CT OE From Accelrys CHARMm
CT1 CN7 HN7 34.5 110.1 !same as HN7 CN7 CN8B
CT1 CN7 ON6B 90.0 108.2 !same as ON6B CN7 CN8B
HA CT3 ON6B 55.5 109.47 !same as HA CT OE From Accelrys CHARMm
HA CT1 ON6B 55.5 109.47 !same as HA CT OE From Accelrys CHARMm
C CT1 CTS 70.0 109.47 !same as C CT C6R From Accelrys CHARMm
CT2 CT1 CTS 70.0 116.6 !same as C6R CT CT From Accelrys CHARMm
CT1 CTS OES 169.0276 108.3759 !same as CTS CTS OES
CT1 CTS CTS 167.3535 110.6156 !same as CTS CTS CTS
CT1 CTS OHS 112.2085 107.6019 !same as CTS CTS OHS
CTS CT1 HA 42.9062 109.7502 !same as CTS CTS HAS
CT3 CTS CTS 167.3535 110.6156 !same as CTS CTS CTS
CE1 CTS CTS 90.0 120.0 !same as C6R C6R CUA1 From Accelrys CHARMm
CTS CT3 HA 42.9062 109.7502 !same as CTS CTS HAS
CT3 CTS CT3 58.35 112.70 !same as CT CT CT From Accelrys CHARMm
CTS CE1 HE1 40.0 117.0 !same as C6R CUA1 HA
CE1 CE1 CTS 50.0 118.0 !same as C6R CUA1 CUA1
CE1 CTS OES 169.0276 108.3759 !same as CTS CTS OES
CE1 CTS HAS 50.0 110.0 !same as CUA1 CT HA
CN1 CA CN1T 120.0 116.7 !same as CN1 CN3T CN3
CA CN1 OH1 45.2 120.0 !same as CA CA OH1
CA CN1 CN3 40.0 120.00 35.00 2.4162 !same as CA CA CA
CN1 OH1 H 65.0 108.0 !same as CA OH1 H
C CA CN1 70.0 120.0 !same as C C6R C6R
CN3 CN1 OH1 45.2 120.0 !same as CA CA OH1
!Enx Parameters
CE1 CT1 OS 50.0 109.47 !same as CUA1 CT OS From Accelrys CHARMm
C OS CT1 83.0 115.9 !same as C OS CT From Accelrys CHARMm
CLAL CT1 CT1 45.0 109.47 !same as CT CT XCL From Accelrys CHARMm
CT1 CE1 HE1 33.0 115.2 !same as CT CUA1 HA From Accelrys CHARMm
CT1 CT1 OS 80.0 109.47 !same as CT CT OS From Accelrys CHARMm
CT2 CD O 70.0 125.0 20.0 2.442 !same as OB CD CT2
CT1 CD CT2 58.0 117.0 !same as CT C CT From Accelrys CHARMm
CT2 CT1 OH1 75.7 110.1 !same as CT1 CT1 OH1

CD CT1 OH1 80.0 109.47 !same as C CT OT From Accelrys CHARMm
CD CT1 CT1 52.0 108.0 !same as CT1 CT2 CD
CT1 CD O 80.0 121.0 !same as O C CT1
CLAL CE1 CT1 60.0 112.0 !same as CT CUA1 XCL From Accelrys CHARMm
CE1 CT1 CT3 32.0 112.5 !same as CE1 CT2 CT3
CE1 CE1 CLAL 50.0 124.3 !same as CUA1 CUA1 XCL
HA CT1 OS 60.0 109.5 !same as OS CT2 HA
CT2 CT1 OS 80.0 109.47 !same as CT CT OS From Accelrys CHARMm
O C OS 90.0 125.9 160.0 2.25760 !same as OS CD OB
NH2 C OS 0.0 0.0 !same as NP CUA1 OE From Accelrys CHARMm
CLAL CT1 HA 46.0 107.47 !same as HA CT XCL
C NH2 H 50.0 120.0 !same as N NH2 CC
NH2 C O 98.0 125.1 !same as NP C O From Accelrys CHARMm
CC CE1 CE1 72.0 119.5 !same as C CUA1 CUA1 From Accelrys CHARMm
CE1 CC O 40.0 120.0 !same as CUA1 C O From Accelrys CHARMm
CE1 CC OS 40.0 120.0 !same as CUA1 C OS From Accelrys CHARMm
CC OS CT1 40.0 109.6 30.0 2.2651 !same as CT2 OS CD
CC CE1 HE1 28.0 119.5 !same as C CUA1 HA From Accelrys CHARMm
O CC OS 90.0 125.9 160.0 2.2576 !same as OB CD OS
CT2 CD OC 40.0 118.0 !same as OC CC CT2
OC CD OC 100.0 124.0 70.0 2.225 !same as OC CC OC
!UF3-1 Parameters
CA CT2 OS 80.0 109.47 !same as C6R CT OS From Accelrys CHARMm
CA CT2 OH1 80.0 109.47 !same as C6R CT OT From Accelrys CHARMm
CA CA CE1 90.0 120.0 !same as C6R C6R CUA1 From Accelrys CHARMm
CA CE1 HE1 40.0 117.0 !same as C6R CUA1 HA From Accelrys CHARMm
CA CE1 CE1 50.0 118.0 !same as C6R CUA1 CUA1 From Accelrys CHARMm
CA CT2 NN2B 70.0 111.6 !same as C6R CT N5R From Accelrys CHARMm
CT2 OS CT2 58.0 112.4 !same as CT OE CT From Accelrys CHARMm
CPT NN2B CT2 70.0 130.0 !same as CT N5R C5R From Accelrys CHARMm
CA NN2B CT2 70.0 130.0 !same as CT N5R C5R From Accelrys CHARMm
CC CT2 OS 80.0 109.47 !same as C CT OE From Accelrys CHARMm
CA CPT NN2B 100.0 104.6 !same as CN5G CN5 NN2B
CPT CPT NN2B 100.0 104.6 !same as CN5G CN5 NN2B
HP CA NN2B 32.0 125.0 25.0 2.177 !same as NY CA HP
CA CA NN2B 120.0 110.0 25.0 2.24 !same as NY CA CY
HA CT2 NN2B 37.5 109.47 !same as HA CT N5R From Accelrys CHARMm

CA NN2B CPT 110.0 108.0 !same as CA NY CPT
CA CA NY 120.0 110.0 25.0 2.24 !same as NY CA CY
!R29 Parameters
CT2 CT1 CT2 58.35 113.50 11.16 2.561 !same as CT1 CT2 CT1
CT1 C NT 55.0 123.6 !same as CT C NT From Accelrys CHARMm
C NT CT2 35.0 109.47 !same as C NT CT From Accelrys CHARMm
C NT CT3 35.0 109.47 !same as C NT CT From Accelrys CHARMm
HA CT2 NT 55.0 107.8 !same as HA CT NT From Accelrys CHARMm
CT1 CT2 NT 45.0 112.5 !same as CT CT NT From Accelrys CHARMm
HA CT3 NT 55.0 107.8 !same as HA CT NT From Accelrys CHARMm
NT C O 55.0 120.0 !same as NT C O From Accelrys CHARMm
CT2 NT CT3 35.0 110.5 !same as CT NT CT From Accelrys CHARMm
CC CT1 HA 33.0 109.5 30.0 2.163 !same as HA CT2 CC
!

A.6.3 Torsion Parameters

!Kir Parameters
CN7 CN7 ON2 HN2 0.3 3 0.00 !same as HN5 ON5 CN7B CN7
CN7 CN7 ON2 HN2 0.0 1 0.00 !same as HN5 ON5 CN7B CN7
HN7 CN7 ON2 HN2 0.0 3 0.00 !same as HN7 CN7B ON5 HN5
HN2 ON2 CN7 CN7B 0.3 3 0.00 !same as HN5 ON5 CN7B CN7
CN1T CA C CE1 0.5 2 180.0 !same as X C C6R X From Accelrys CHARMm
CN1T CA C O 0.5 2 180.0 !same as X C C6R X From Accelrys CHARMm
CA C CE1 CE1 0.9 2 180.0 !same as X C CUA1 X From Accelrys CHARMm
CA C CE1 CT3 0.9 2 180.0 !same as X C CUA1 X From Accelrys CHARMm
CA CN1T NN2 CN3 2.05 2 180.0 !same as X C6R N6R X From Accelrys CHARMm
CA CN1T NN2 H 4.8 2 180.0 !same as CN3T CN1 NN2U HN2
CN3 NN2 CN1T ON1 2.05 2 180.0 !same as X C6R N6R X From Accelrys CHARMm
C CE1 CT3 HA 1.2 3 180.0 !same as X CT CUA1 X From Accelrys CHARMm
C CA CN1T NN2 5.6 2 180.0 !same as NN2B CN1 CN3T CN9
C CA CN1T ON1 3.1 2 180.0 !same as X C6R C6R X
O C CE1 CE1 0.9 2 180.0 !same as X C CUA1 X
O C CE1 CT3 0.9 2 180.0 !same as X C CUA1 X
ON1 CN1T NN2 H 0.0 2 180.0 !same as ON1 CN1 NN2U HN2
CE1 CE1 CN7 CN7 0.7 2 180.0 !same as X CUA1 C5R X
CE1 CE1 CN7 ON6B 0.7 2 180.0 !same as X CUA1 C5R X
CE1 CE1 CN7 HN7 0.7 2 180.0 !same as X CUA1 C5R X

CE1 CN7 CN7 CN7 0.2 4 180.0 !same as CN7B CN7 CN7 CN8B
CE1 CN7 CN7 ON5 0.2 4 0.00 !same as ON5 CN7 CN7 CN8B
CE1 CN7 CN7 ON5 0.8 3 180.0 !same as ON5 CN7 CN7 CN8B
CE1 CN7 CN7 HN7 0.195 3 0.00 !same as HN7 CN7 CN7 CN8B
CE1 CN7 ON6B CN7 2.0 3 0.00 !same as CN7B ON6B CN7 CN8B
HE1 CE1 CN7 CN7 0.195 3 0.00 !same as HN8 CN8B CN7 CN7
HE1 CE1 CN7 ON6B 0.195 1 0.00 !same as HN8 CN8B CN7 ON6B
HE1 CE1 CN7 HN7 0.195 3 0.00 !same as HN8 CN8B CN7 HN7
CN7 ON6B CN7 CN7 0.0 6 180.0 !same as CN7 CN7 ON6B CN7B
CN7 ON6B CN7 CT1 2.0 3 0.00 !same as CN7B ON6B CN7 CN8B
CN7 ON6B CN7 HN7 0.0 3 0.00 !same as HN7 CN7B ON6B CN7
CN7 CN7 CN7 CN7 0.0 6 0.00 !same as CN7 CN7 CN7B CN7B
CN7 CN7 CN7 CT1 0.2 4 180.0 !same as CN7B CN7 CN7 CN8B
CN7 CN7 CN7 ON6B 0.4 6 0.00 !same as CN7 CN7B CN7B ON6B
CN7 CN7 CT1 CT1 0.01 6 0.00 !same as X CT C5R X From Accelrys CHARMm
CN7 CN7 CT1 CT3 0.01 6 0.00 !same as X CT C5R X From Accelrys CHARMm
CN7 CN7 CT1 HA 0.01 6 0.00 !same as X CT C5R X From Accelrys CHARMm
ON5 CN7 CN7 CT1 0.2 4 0.00 !same as ON2 CN7 CN7 CN8B
ON5 CN7 CN7 CT1 0.8 3 180.0 !same as ON2 CN7 CN7 CN8B
ON6B CN7 CT1 CT1 0.01 6 0.00 !same as X CT C5R X From Accelrys CHARMm
ON6B CN7 CT1 CT3 0.01 6 0.00 !same as X CT C5R X From Accelrys CHARMm
ON6B CN7 CT1 HA 0.195 1 0.00 !same as HN8 CN8B CN7 ON6B
HN7 CN7 CN7 CT1 0.195 3 0.00 !same as HN7 CN7 CN7 CN8B
HN7 CN7 CT1 CT1 0.01 6 0.00 !same as X CT C5R X From Accelrys CHARMm
HN7 CN7 CT1 CT3 0.01 6 0.00 !same as X CT C5R X From Accelrys CHARMm
HN7 CN7 CT1 HA 0.195 3 0.00 !same as HN7 CN7 CN8B HN8
CT1 ON6B CT3 HA 0.27 3 0.00 !same as X CT OE X From Accelrys CHARMm
CT1 CE1 CT3 HA 1.2 3 180.0 !same as X CT CUA1 X From Accelrys CHARMm
CE1 CT1 CT1 CT3 0.15 3 0.00 !same as X CT CT X From Accelrys CHARMm
CE1 CT1 ON6B CT3 0.27 3 0.00 !same as X CT OE X From Accelrys CHARMm
CE1 CT2 NH1 C 1.8 1 0.00 !same as CT2 CT2 NH1 C
CE1 CT2 NH1 H 0.0 1 0.00 !same as H NH1 CT2 CT2
CT1 CT1 CE1 CE1 0.12 1 0.00 !same as CT CT CUA1 CUA1 From Accelrys CHARMm
CT1 CT1 CE1 CE1 4.4 3 180.0 !same as CT CT CUA1 CUA1 From Accelrys CHARMm
CT1 CT1 CE1 CT3 1.2 3 180.0 !same as X CT CUA1 X From Accelrys CHARMm

CT1 CT1 ON6B CT3 0.82 1 0.00 !same as CT CT OE CT From Accelrys CHARMm
CT1 CT1 ON6B CT3 0.25 3 0.00 !same as CT CT OE CT From Accelrys CHARMm
CE1 CE1 CT1 ON6B 1.2 3 180.0 !same as X CT CUA1 X From Accelrys CHARMm
CE1 CE1 CT1 HA 1.2 3 180.0 !same as X CT CUA1 X From Accelrys CHARMm
CE1 CE1 CT2 NH1 0.0 1 0.00 !same as NH1 C CT2 CT2
CE1 CE1 CT2 HA 1.2 3 180.0 !same as X CT CUA1 X From Accelrys CHARMm
ON6B CT1 CE1 CT3 1.2 3 180.0 !same as X CT CUA1 X From Accelrys CHARMm
CT3 ON6B CT1 HA 0.27 3 0.00 !same as X CT OE X From Accelrys CHARMm
CT3 CE1 CT1 HA 1.2 3 180.0 !same as X CT CUA1 X From Accelrys CHARMm
HE1 CE1 CT2 NH1 1.2 3 180.0 !same as X CT CUA1 X From Accelrys CHARMm
NH1 C CT1 CTS 0.0 1 0.00 !same as NH1 C CT1 CT2
NH1 C CT1 HA 0.0 3 0.00 !same as NH1 C CT2 HA
C CT1 CTS OHS 0.01 6 0.00 !same as X CT C6R X From Accelrys CHARMm
C CT1 CTS CTS 0.01 6 0.00 !same as X CT C6R X From Accelrys CHARMm
C CT1 CTS OES 0.01 6 0.00 !same as X CT C6R X From Accelrys CHARMm
O C CT1 CTS 0.05 3 180.0 !same as X C CT X From Accelrys CHARMm
O C CT1 HA 0.05 3 180.0 !same as X C CT X From Accelrys CHARMm
CT2 CT1 CTS OHS 0.01 6 0.00 !same as X CT C6R X From Accelrys CHARMm
CT2 CT1 CTS CTS 0.01 6 0.00 !same as X CT C6R X From Accelrys CHARMm
CT2 CT1 CTS OES 0.01 6 0.00 !same as X CT C6R X From Accelrys CHARMm
CT1 CTS OHS HOS 1.0504 1 0.00 !same as CTS CTS OHS HOS
CT1 CTS OHS HOS 0.1336 2 0.00 !same as CTS CTS OHS HOS
CT1 CTS OHS HOS 0.3274 3 0.00 !same as CTS CTS OHS HOS
CT1 CTS CTS OHS -1.9139 1 0.00 !same as CTS CTS CTS OHS
CT1 CTS CTS OHS -1.9139 1 0.00 !same as CTS CTS CTS OHS
CT1 CTS CTS OHS -0.3739 2 0.00 !same as CTS CTS CTS OHS
CT1 CTS CTS OHS -0.0340 3 0.00 !same as CTS CTS CTS OHS
CT1 CTS CTS CTS -1.0683 1 0.00 !same as CTS CTS CTS CTS
CT1 CTS CTS CTS -0.5605 2 0.00 !same as CTS CTS CTS CTS
CT1 CTS CTS CTS 0.1955 3 0.00 !same as CTS CTS CTS CTS
CT1 CTS CTS HAS 0.0 1 0.00 !same as CTS CTS CTS HAS
CT1 CTS CTS HAS 0.0 2 0.00 !same as CTS CTS CTS HAS
CT1 CTS CTS HAS 0.1441 3 0.00 !same as CTS CTS CTS HAS
CT1 CTS OES CTS -0.8477 1 0.00 !same as CTS CTS OES CTS
CT1 CTS OES CTS -0.3018 2 0.00 !same as CTS CTS OES CTS
CT1 CTS OES CTS -0.3763 3 0.00 !same as CTS CTS OES CTS
HA CT1 CTS OHS 0.0 1 0.00 !same as HAS CTS CTS OHS

HA CT1 CTS OHS 0.0 2 0.00 !same as HAS CTS CTS OHS
HA CT1 CTS OHS 0.1472 3 0.00 !same as HAS CTS CTS OHS
HA CT1 CTS CTS 0.0 1 0.00 !same as HAS CTS CTS CTS
HA CT1 CTS CTS 0.0 2 0.00 !same as HAS CTS CTS CTS
HA CT1 CTS CTS 0.1441 3 0.00 !same as HAS CTS CTS CTS
HA CT1 CTS OES 0.0 1 0.00 !same as HAS CTS CTS OES
HA CT1 CTS OES 0.0 2 0.00 !same as HAS CTS CTS OES
HA CT1 CTS OES 0.1686 3 0.00 !same as HAS CTS CTS OES
CTS OES CTS CE1 -0.8477 1 0.00 !same as CTS OES CTS CTS
CTS OES CTS CE1 -0.3018 2 0.00 !same as CTS OES CTS CTS
CTS OES CTS CE1 0.3763 3 0.00 !same as CTS OES CTS CTS
CTS CTS CTS CT3 -1.0683 1 0.00 !same as CTS CTS CTS CTS
CTS CTS CTS CT3 -0.5605 2 0.00 !same as CTS CTS CTS CTS
CTS CTS CTS CT3 0.1955 3 0.00 !same as CTS CTS CTS CTS
CTS CTS CT3 HA 0.0 1 0.00 !same as CTS CTS CTS HAS
CTS CTS CT3 HA 0.0 2 0.00 !same as CTS CTS CTS HAS
CTS CTS CT3 HA 0.1441 3 0.00 !same as CTS CTS CTS HAS
CTS CTS CTS CE1 -1.0683 1 0.00 !same as CTS CTS CTS CTS
CTS CTS CTS CE1 -0.5605 2 0.00 !same as CTS CTS CTS CTS
CTS CTS CTS CE1 0.1955 3 0.00 !same as CTS CTS CTS CTS
OHS CTS CTS CT3 -1.9139 1 0.00 !same as OHS CTS CTS CTS
OHS CTS CTS CT3 -0.3739 2 0.00 !same as OHS CTS CTS CTS
OHS CTS CTS CT3 -0.0340 3 0.00 !same as OHS CTS CTS CTS
CTS CTS CE1 CE1 0.7 2 180.0 !same as X CUA1 C6R X From Accelrys CHARMm
CTS CTS CE1 HE1 0.7 2 180.0 !same as X CUA1 C6R X From Accelrys CHARMm
CT3 CTS CTS HAS 0.0 1 0.00 !same as CTS CTS CTS HAS
CT3 CTS CTS HAS 0.0 2 0.00 !same as CTS CTS CTS HAS
CT3 CTS CTS HAS 0.1441 3 0.00 !same as CTS CTS CTS HAS
CT3 CTS CT3 HA 0.01 6 0.00 !same as X CT C6R X From Accelrys CHARMm
CT3 CTS CTS OES -1.2007 1 0.00 !same as CTS CTS CTS OES
CT3 CTS CTS OES -0.3145 2 0.00 !same as CTS CTS CTS OES
CT3 CTS CTS OES -0.0618 3 0.00 !same as CTS CTS CTS OES
CT3 CTS CTS CE1 3.1 2 180.0 !same as X C6R C6R X From Accelrys CHARMm
OES CTS CE1 CE1 0.7 2 180.0 !same as X CUA1 C6R X From Accelrys CHARMm
OES CTS CE1 HE1 0.7 2 180.0 !same as X CUA1 C6R X From Accelrys CHARMm
HAS CTS CE1 CE1 0.7 2 180.0 !same as X CUA1 C6R X From Accelrys CHARMm
HAS CTS CE1 HE1 0.7 2 180.0 !same as X CUA1 C6R X From Accelrys CHARMm

CN1T CA CN1 CN3 0.2 2 180.0 !same as CA CA CA CA
CN1T CA CN1 OH1 3.1 2 180.0 !same as CA CA CA OH1
CA CN1 OH1 H 0.99 2 180.0 !same as H OH1 CA CA
CN1 CA CN1T NN2 1.8 2 180.0 !same as NN2U CN1 CN3T CN3
CN1 CA CN1T ON1 1.0 2 180.0 !same as X CN3T CN1 X From Accelrys CHARMm
CN1 CA C CE1 0.5 2 180.0 !same as X C C6R X From Accelrys CHARMm
CN1 CA C O 0.5 2 180.0 !same as X C C6R X From Accelrys CHARMm
CN3 CN1 CA C 3.1 2 180.0 !same as X C6R C6R X From Accelrys CHARMm
CN3 CN1 OH1 H 0.99 2 180.0 !same as CA CA OH1 H
C CA CN1 OH1 3.1 2 180.0 !same as CA CA CA OH1
!Enx Parameters
CT3 CT2 CE1 CE1 0.5 1 180.0 !same as CE2 CE1 CT2 CT3
CT3 CT2 CE1 CE1 1.3 3 180.0 !same as CE2 CE1 CT2 CT3
CE1 CE1 CT1 OS 1.2 3 180.0 !same as X CT CUA1 X From Accelrys CHARMm
CT1 OS C NH2 2.5 2 180.0 !same as X C OS X From Accelrys CHARMm
CT1 OS C O 2.5 2 180.0 !same as X C OS X From Accelrys CHARMm
CT1 CT1 CE1 CE1 0.5 1 180.0 !same as CE2 CE1 CT2 CT3
CT1 CT1 CE1 CE1 1.3 3 180.0 !same as CE2 CE1 CT2 CT3
CT1 CT1 CE1 HE1 0.12 3 0.0 !same as HE1 CE1 CT2 CT3
CT1 CT1 CE1 CLAL 0.05 0 0.0 !same as CT CT CT XCL
CE1 CE1 CT1 CT3 0.5 1 180.0 !same as CE2 CE1 CT2 CT3
CE1 CE1 CT1 CT3 1.3 3 180.0 !same as CE2 CE1 CT2 CT3
OS C NH2 H 2.6 2 180.0 !same as OS C NP H From Accelrys CHARMm
OS CT1 CE1 HE1 1.2 3 180.0 !same as X CT CUA1 X From Accelrys CHARMm
CT3 CT1 CE1 CLAL 0.05 0 0.0 !same as CT CT CT XCL From Accelrys CHARMm
CLAL CE1 CT1 HA 1.2 3 180.0 !same as X CT CUA1 X From Accelrys CHARMm
O C NH2 H 1.4 2 180.0 !same as O CC NH2 H
HE1 CE1 CT1 HA 0.0 3 0.0 !same as HE1 CE1 CT3 HA
CE1 CE1 CC OS 0.9 2 180.0 !same as X C CUA1 X From Accelrys CHARMm
CE1 CE1 CC O 1.5 1 0.0 !same as O C CUA1 CUA1 From Accelrys CHARMm
CE1 CC OS CT1 2.05 2 180.0 !same as X CD OS X
OS CC CE1 HE1 0.9 2 180.0 !same as X C CUA1 X From Accelrys CHARMm
CT1 OS CC O 2.05 2 180.0 !same as X CD OS X
O CC CE1 HE1 0.9 0 180.0 !same as X C CUA1 X From Accelrys CHARMm
!UF3-1 Parameters
CA CA CA CE1 3.1 2 180.0 !same as X C6R C6R X From Accelrys CHARMm
CA CA CE1 CE1 0.7 2 180.0 !same as X C6R CUA1 X From Accelrys CHARMm

CA CA CE1 HE1 0.7 2 180.0 !same as X C6R CUA1 X From Accelrys CHARMm
CA CT2 NN2B CA 0.15 6 180.0 !same as X CT N5R X From Accelrys CHARMm
CA CT2 NN2B CPT 0.15 6 180.0 !same as X CT N5R X From Accelrys CHARMm
CT2 CA CA CT2 3.1 2 180.0 !same as X C6R C6R X From Accelrys CHARMm
CT2 CA CA CE1 3.1 2 180.0 !same as X C6R C6R X From Accelrys CHARMm
CE1 CA CA HA 3.1 2 180.0 !same as X C6R C6R X From Accelrys CHARMm
CT2 NN2B CA CA 2.05 2 180.0 !same as X C5R N5R X From Accelrys CHARMm
CT2 NN2B CA HP 2.05 2 180.0 !same as X C5R N5R X From Accelrys CHARMm
CT2 NN2B CPT CPT 2.05 2 180.0 !same as X C5R N5R X From Accelrys CHARMm
CT2 NN2B CPT CA 2.05 2 180.0 !same as X C5R N5R X From Accelrys CHARMm
CT2 CA CA HA 3.1 2 180.0 !same as X C5R C5R X From Accelrys CHARMm
NN2B CPT CA CA 2.8 2 180.0 !same as NY CPT CA CA
NN2B CPT CA HP 3.0 2 180.0 !same as NY CPT CA HP
NN2B CA CA CPT 4.0 2 180.0 !same as NY CA CY CPT
NN2B CA CA HP 3.1 2 180.0 !same as X C5R C5R X From Accelrys CHARMm
CA NN2B CT2 HA 0.15 6 180.0 !same as X CT N5R X From Accelrys CHARMm
CA NN2B CPT CPT 5.0 2 180.0 !same as CPT CPT NY CA
CA NN2B CPT CA 3.0 2 180.0 !same as CA NY CPT CA
CA CA NN2B CPT 5.0 2 180.0 !same as CY CA NY CPT
CPT NY CA CA 5.0 2 180.0 !same as CY CA NY CPT
CPT CA CA NY 4.0 2 180.0 !same as NY CA CY CPT
CPT NN2B CT2 HA 0.15 6 180.0 !same as X CT N5R X From Accelrys CHARMm
CPT NN2B CA HP 2.05 20 180.0 !same as X N5R C5R X
CA CA NY H 0.8 2 180.0 !same as H NY CA CY
NY CA CA HP 3.1 2 180.0 !same as X C5R C5R X
!R29 Parameters
CT1 CT1 C NT 0.05 3 180.0 !same as X C CT X From Accelrys CHARMm
CT1 C NT CT3 0.16 2 0.0 !same as X C NT X From Accelrys CHARMm
CT1 C NT CT2 0.16 2 0.0 !same as X C NT X From Accelrys CHARMm
C NT CT3 HA 0.16 3 0.0 !same as X CT NT X From Accelrys CHARMm
C NT CT2 CT1 0.16 3 0.0 !same as X CT NT X From Accelrys CHARMm
C NT CT2 HA 0.16 3 0.0 !same as X CT NT X From Accelrys CHARMm
NT C CT1 CT2 0.05 3 180.0 !same as X C CT X From Accelrys CHARMm
NT C CT1 HA 0.05 3 180.0 !same as X C CT X From Accelrys CHARMm
CT3 NT C O 0.16 2 0.0 !same as X C NT X From Accelrys CHARMm
CT3 NT CT2 CT1 0.16 3 0.0 !same as X CT NT X From Accelrys CHARMm
CT3 NT CT2 HA 0.16 3 0.0 !same as X CT NT X From Accelrys CHARMm

O C NT CT2 0.16 2 0.0 !same as X C NT X From Accelrys CHARMm
HA CT3 NT CT2 0.16 3 0.0 !same as X CT NT X From Accelrys CHARMm

A.6.4 Improper Parameters

!Kir Parameters
CN3 CA HN3 CN3 15.0 0 0.0 !same as C6R X X C6R From Accelrys CHARMm
CN3 NN2 HN3 CN3 15.0 0 0.0 !same as C6R X X C6R From Accelrys CHARMm
NN2 CN1T CN3 H 35.0 0 0.0 !same as H X X N6R From Accelrys CHARMm
CE1 C CT3 CE1 150.0 0 0.0 !same as CUA1 X X CUA1 From Accelrys CHARMm
CE1 CE1 HE1 CE1 150.0 0 0.0 !same as CUA1 X X CUA1 From Accelrys CHARMm
CE1 CN7 HE1 CE1 150.0 0 0.0 !same as CUA1 X X CUA1 From Accelrys CHARMm
CE1 CT1 CT3 CE1 150.0 0 0.0 !same as CUA1 X X CUA1 From Accelrys CHARMm
CE1 CT2 HE1 CE1 150.0 0 0.0 !same as CUA1 X X CUA1 From Accelrys CHARMm
CE1 CTS HE1 CE1 150.0 0 0.0 !same as CUA1 X X CUA1 From Accelrys CHARMm
CE1 CT3 HE1 CE1 150.0 0 0.0 !same as CUA1 X X CUA1 From Accelrys CHARMm
CA CN1T C CN1 150.0 0 0.0 !same as CUA1 X X CUA1 From Accelrys CHARMm
CN1 CN3 OH1 CA 150.0 0 0.0 !same as CUA1 X X CUA1 From Accelrys CHARMm
CN3 CN1 HN3 CN3 150.0 0 0.0 !same as CUA1 X X CUA1 From Accelrys CHARMm
!Enx Parameters
CE1 CT1 HE1 CE1 150.0 0 0.0 !same as CUA1 X X CUA1 From Accelrys CHARMm
CD CT2 CT1 O 100.0 0 0.0 !same as OB X X CD
CE1 CT1 CLAL CE1 150.0 0 0.0 !same as CUA1 X X CUA1 From Accelrys CHARMm
CE1 CE1 CT3 CE1 0.0 0 0.0 !same as CUA1 X X CUA1 From Accelrys CHARMm
C NH2 O OS 40.0 0 0.0 !same as C X X OS From Accelrys CHARMm
NH2 H H C 60.0 0 0.0 !same as NP X X C
CE1 CC HE1 CE1 150.0 0 0.0 !same as CUA1 X X CUA1 From Accelrys CHARMm
CC CE1 OS O 147.0 0 0.0 !same as C X X O From Accelrys CHARMm
CD OC OC CT2 60.0 0 0.0 !same as C X X XT From Accelrys CHARMm
!UF3-1 Parameters
CA CA CA CA 15.0 0 0.0 !same as C6R X X C6R From Accelrys CHARMm
CA CA CA CT2 130.0 0 0.0 !same as C6R X X CT From Accelrys CHARMm
CA CA CA CE1 90.0 0 0.0 !same as C6R X X CUA1 From Accelrys CHARMm
CA CA CA HA 75.0 0 0.0 !same as C6R X X HA From Accelrys CHARMm
CE1 CA HE1 CE1 150.0 0 0.0 !same as CUA1 X X CUA1 From Accelrys CHARMm
NN2B CA CPT CT2 90.0 0 0.0 !same as CT X X N5R From Accelrys CHARMm
CA NN2B HP CA 130.0 0 0.0 !same as C5R X X C5R From Accelrys CHARMm
CA CPT HP CA 130.0 0 0.0 !same as C5R X X C5R From Accelrys CHARMm

CPT CA NY CPT 90.0 0 0.0 !same as CR55 X X CR55 From Accelrys CHARMm
CPT NN2B CA CPT 90.0 0 0.0 !same as CR55 X X CR55 From Accelrys CHARMm
CA NY HP CA 130.0 0 0.0 !same as C5R X X C5R From Accelrys CHARMm
NY CPT CA H 35.0 0 0.0 !same as H X X N5R From Accelrys CHARMm
!R29 Parameters
NT CT3 CT2 C 90.0 0 0.0 !same as C X X NT From Accelrys CHARMm

Appendix B

Docking with van der Waal Scaling

This appendix shows the whole table for the RMSD values for the dockings with van der Waal scaling.

Docking number	10x10x10 Å (no water)	10x10x10 Å (with water)	30x30x30 Å (no water)	30x30x30 Å (with water)
1	35.99	5.11	4.61	5.51
	35.35	7.81	4.63	5.51
	34.4	5.2	4.69	5.01
	35.36	5.23	4.89	5.20
	34.74	6.32	4.71	5.10
2	35.99	7.81	4.63	4.89
	35.35	5.2	4.66	4.88
	34.4	5.23	4.88	4.98
	35.36	6.23	4.70	5.07
	34.74	7.36	4.71	5.13
3	35.99	7.81	4.63	4.89
	35.35	5.20	4.66	4.88
	34.4	5.23	4.88	4.98
	35.36	6.23	4.70	5.07
	34.74	7.36	4.71	5.13
4	36.86	5.09	4.61	5.78
	34.55	6.26	4.60	5.10
	35.52	6.36	4.69	5.18
	36.55	7.35	4.81	5.22
	32.21	5.36	4.71	5.17

Docking number	10x10x10 Å (no water)	10x10x10 Å (with water)	30x30x30 Å (no water)	30x30x30 Å (with water)
5	36.86	5.09	4.61	5.78
	34.55	6.26	4.60	5.18
	35.52	6.36	4.69	5.10
	36.55	7.35	4.81	5.17
	32.21	5.36	4.71	5.22
6	36.03	7.03	4.61	4.91
	34.72	5.58	4.65	5.94
	34.12	7.62	4.75	4.97
	35.39	7.59	4.88	5.12
	34.97	7.72	4.84	5.21
7	36.03	5.24	4.57	5.17
	34.72	7.21	4.64	4.98
	34.12	6.28	4.76	4.89
	35.39	6.61	4.63	1.96
	34.97	7.54	4.78	4.96
8	36.76	5.24	4.57	5.17
	34.30	7.21	4.64	4.98
	35.23	6.28	4.76	4.89
	36.03	6.61	4.63	1.96
	34.95	7.54	4.78	4.96
9	35.49	5.09	4.39	3.13
	34.65	5.37	4.71	4.07
	34.12	5.33	4.62	7.46
	34.47	4.94	4.88	5.63
	36.39	5.24	4.68	5.75
10	34.45	6.37	4.59	11.30
	35.38	5.37	4.60	12.69
	34.43		4.71	
	35.2			
	34.29			
11	38.57	38.57	4.84	5.34
	37.9	37.9	4.64	5.09
	35.78	35.78	4.73	6.23
	33.73	33.73	4.63	3.98
	38.37	38.37	4.88	4.28

Docking number	10x10x10 Å (no water)	10x10x10 Å (with water)	30x30x30 Å (no water)	30x30x30 Å (with water)
12	38.57	36.4	4.84	5.09
	37.9	36.7	4.64	6.23
	35.78	38.58	4.73	4.20
	33.73	35.76	4.63	4.09
	38.37	34.84	4.88	3.98
13	38.59	38.33	5.68	4.55
	37.05	34.26	4.57	4.46
	42.87	35.67	4.85	4.95
	43.2	39.3	4.58	4.34
	42.48	34.6	4.82	12.98
14	36.33	38.27	4.80	5.39
	38.17	34.28	4.55	5.11
	38.4	35.28	4.74	7.72
	37.19	36.94	4.84	6.69
	34.68	34.73	4.78	19.39
15	39.91	34.28	4.87	5.39
	36.33	35.28	4.55	5.11
	38.17	36.94	4.74	7.72
	37.19	34.73	4.84	6.69
	34.68	37.03	4.78	19.39
16	38.36	35.39	4.9	17.17
	34.06	43.22	4.81	4.51
	35.54	37.93	4.57	17.09
	43.29	34.37	4.24	5.10
	34.65	38.37	5.12	5.02
17	34.6	38.4	4.68	12.59
	39.37	35.68	4.63	7.13
	37.89	37.26	4.19	8.03
	36.66	35.89	4.22	7.3
	37.05	38.2	4.78	12.82
18	34.6	35.02	4.74	7.13
	39.37	38.4	4.19	8.03
	37.89	35.68	4.22	7.3
	36.66	38.26	5.12	4.18
	37.05	35.89	4.87	12.82

Docking number	10x10x10 Å (no water)	10x10x10 Å (with water)	30x30x30 Å (no water)	30x30x30 Å (with water)
19	38.2	38.63	4.84	16.89
	43.08	37.83	4.67	16.77
	38.26	8.04	4.52	16.79
	33.77	38.58	4.80	5.71
	38.2	38.28	4.98	4.93

Appendix C

Induced Fit Docking

The tables C.1, C.2, and C.3 show the IFD results for Enx in structure E.

Table C.1: IFD mutation of Arg373, no water

Pose number	Prime Energy	Glide G-score	Glide E-model	IFDScore
1	-19497.52	-10.232040	-147.265587	-985.108040
2	-19505.880000	-8.932178	-120.317735	-984.226178
3	-19490.200000	-9.645669	-151.082480	-984.155669
4	-19499.350000	-9.103573	-122.737244	-984.071073
5	-19485.410000	-9.552113	-133.006091	-983.822613
6	-19493.970000	-9.119975	-156.803571	-983.818475
7	-19488.420000	-9.145840	-133.531186	-983.566840
8	-19492.330000	-8.812425	-106.015316	-983.428925
9	-19478.980000	-9.040419	-118.746193	-982.989419
10	-19487.900000	-8.572840	-130.725889	-982.967840
11	-19489.860000	-8.264346	-98.875616	-982.757346
12	-19492.000000	-7.915155	-146.933224	-982.515155
13	-19476.160000	-8.477997	-96.430844	-982.285997
14	-19476.480000	-8.424143	-120.520965	-982.248143
15	-19478.780000	-7.927595	-120.687336	-981.866595

The figures C.1, C.2, and C.3 show examples of Enx placement in the binding site after IFD. Figure C.1 shows a result of the docking where Arg373 is mutated, figure C.2 shows a result for docking without water molecule number 83 in the binding site, and figure C.3 shows a result for docking with water molecule number 83 in the binding site.

Table C.2: IFD with water

Pose number	Prime Energy	Glide G-score	Glide E-model	IFDScore
1	-16958.28	-10.068586	-141.159292	-857.982586
2	-16938.49	-11.017764,	-165.731538	-857.942264
3	-16956.51	-10.049999	-149.878786	-857.875499
4	-16964.17	-9.387546	-133.983922	-857.596046
5	-16957.18	-9.626612	-136.292248	-857.485612
6	-16946.46	-10.018273	-115.50883	-857.341273
7	-16937.54	-10.356976	-133.372021	-857.233976
8	-16956.54	-9.071312	-141.402292	-856.898312
9	-16957.43	-9.015709	-117.092684	-856.887209
10	-16943.7	-9.525893	-141.532119	-856.713393
11	-16945.42	-9.302294	-122.627105	-856.573294
12	-16951.38	-8.34996	-139.990341	-855.91896
13	-16938.48	-8.88511	-119.704263	-855.80911
14	-16958.86	-7.576134	-119.151122	-855.519134
15	-16948.5	-7.514092	-99.030353	-854.939092
16	-16935.09	-8.023803	-96.558311	-854.778303

Table C.3: IFD without water

Pose number	Prime Energy	Glide G-score	Glide E-model	IFDScore
1	-16938.110000	-11.319293	-168.227579	-858.224793
2	-16935.730000	-9.497460	-137.510061	-856.283960
3	-16944.840000	-8.524526	-123.710759	-855.766526
4	-16916.260000	-9.637229	-152.202178	-855.450229
5	-16921.800000	-9.338010	-152.466119	-855.428010
6	-16940.460000	-7.697967	-92.770128	-854.720967
7	-16927.190000	-8.173584	-152.269891	-854.533084
8	-16916.810000	-8.002329	-96.025064	-853.842829

Figure C.1 IFD mutation of Arg373

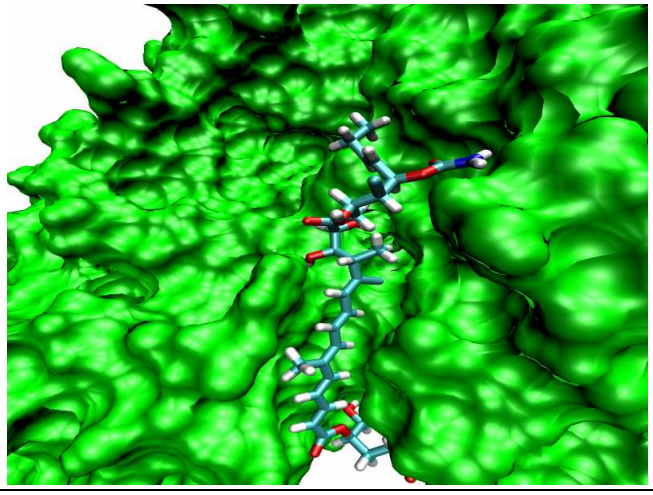

Figure C.2 IFD no water

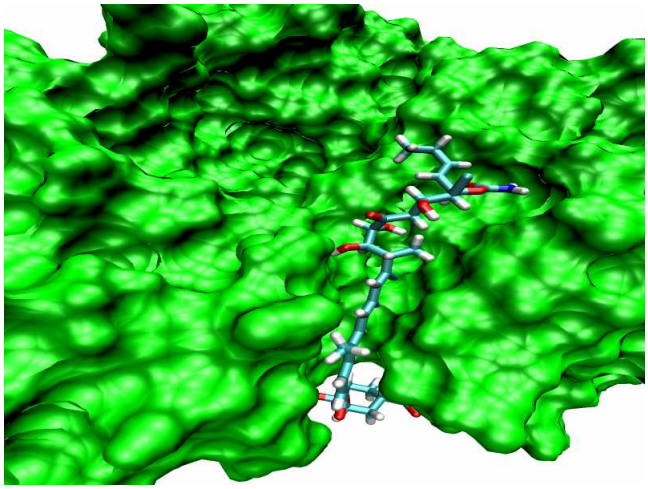

Figure C.3 IFD with water

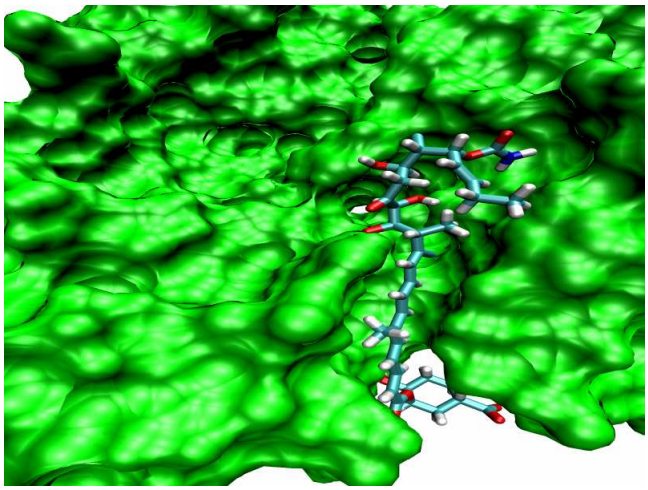

Appendix D

De Novo Design Structures

Figure D.1 Molecules with start fragment CD7

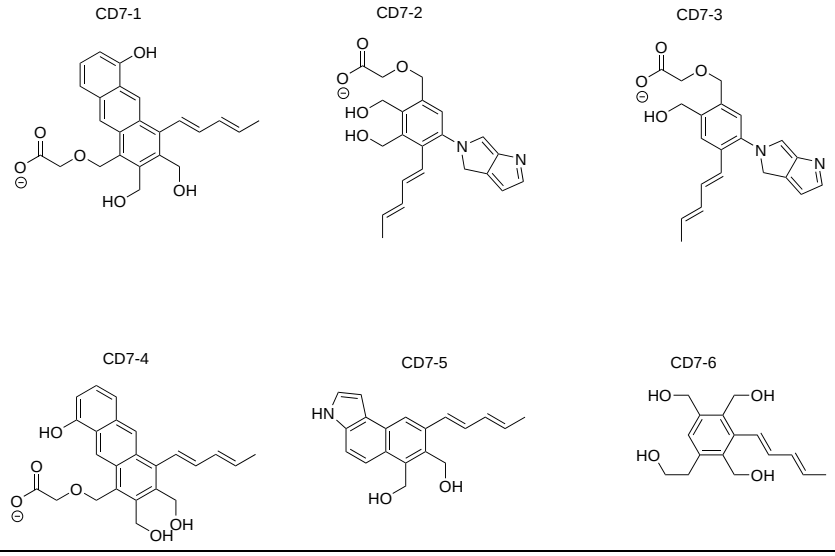

Figure D.2 Molecules with start fragment UB3

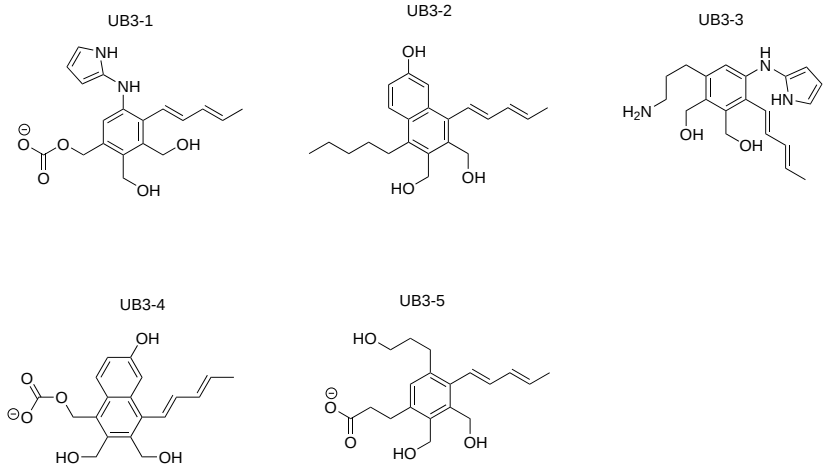

Figure D.3 Molecules with start fragment HC6, HC5 and C18

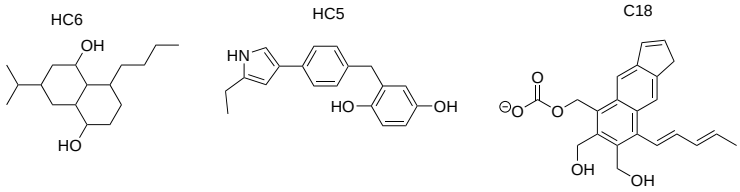

Figure D.4 Molecules with start fragment H24

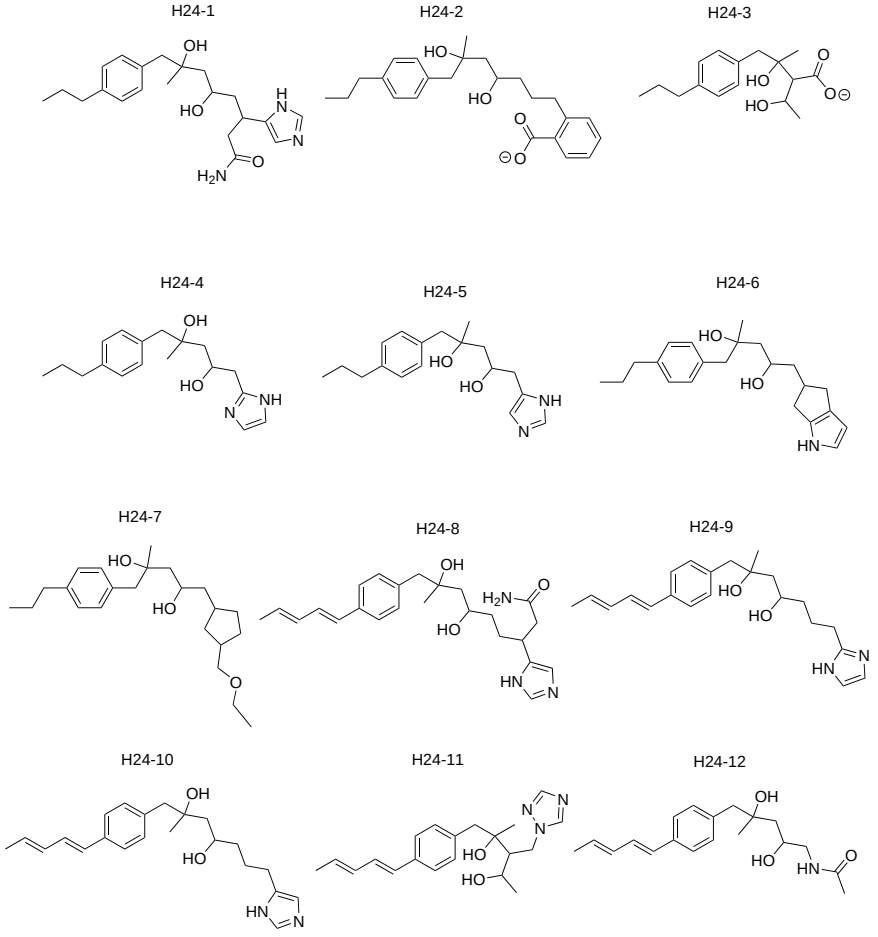

Figure D.5 Molecules with start fragment H24

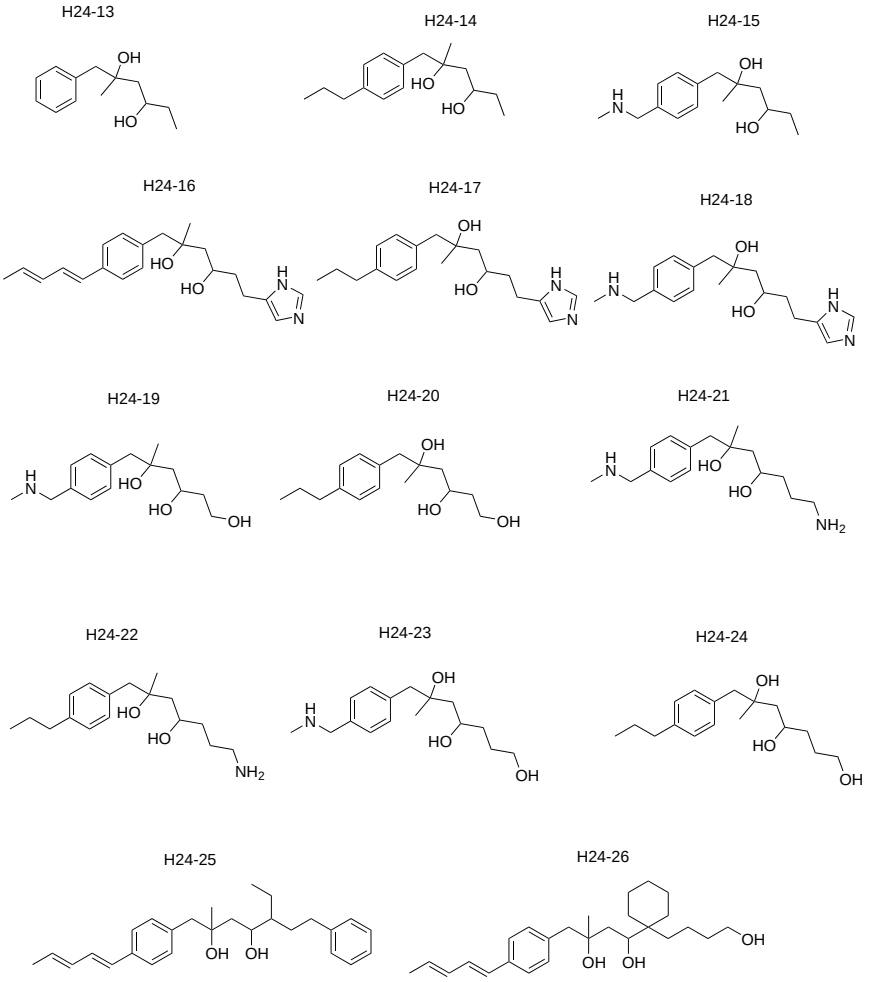

Figure D.6 Molecules with start fragment UF3

UF3-1

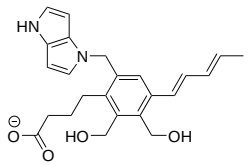

UF3-2

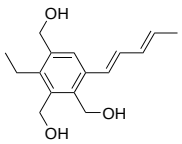

UF3-3

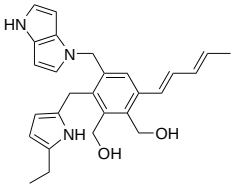

UF3-4

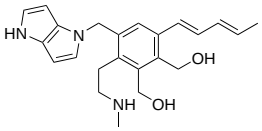

UF3-5

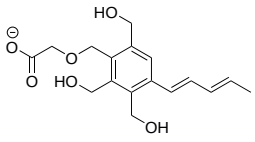

UF3-6

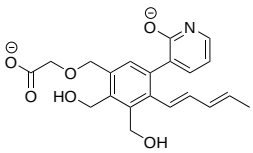

UF3-7

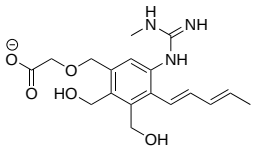

Figure D.7 Molecules with start fragment H17

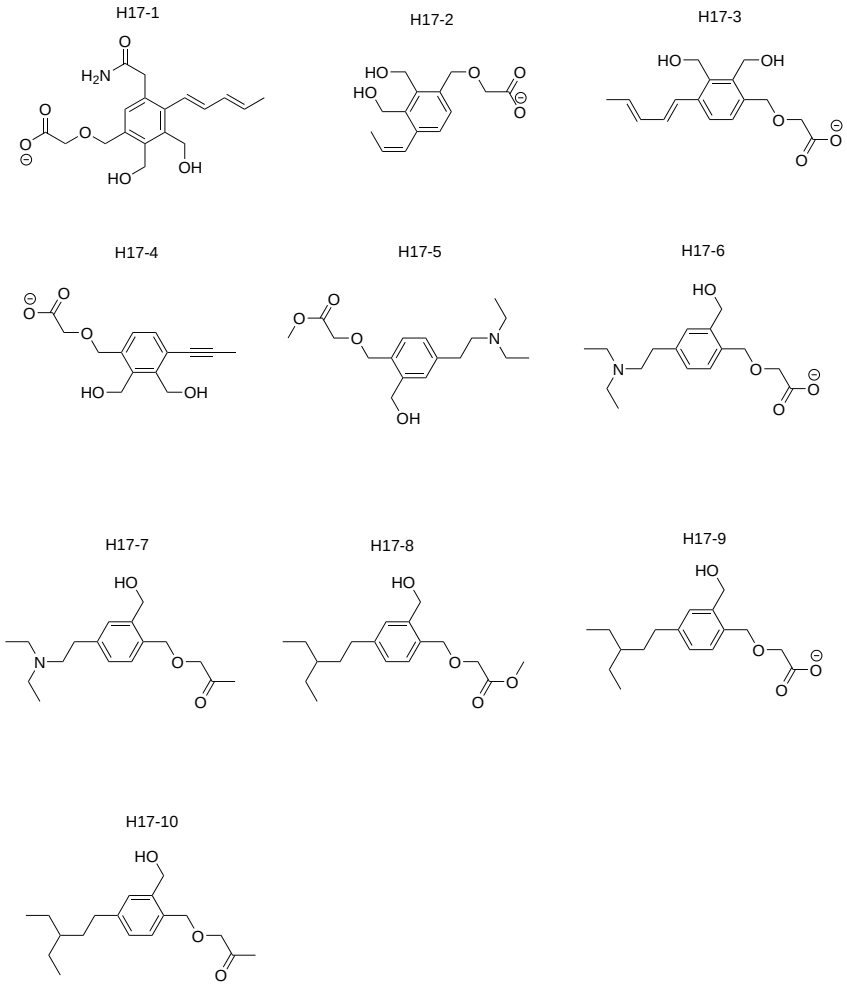

Appendix E

Results for Docking of Hybrid Molecules

Figure E.1 shows the main structure of the hybrid molecules and figure E.2 shows the side chains added to the main structures for making the 1200 new molecules. Section E.1 to section E.10 shows the docking results for the 1200 hybrid molecules.

Figure E.1 Main structures of hybrid molecules

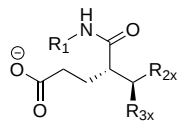

1

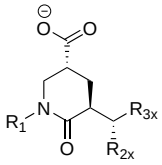

2

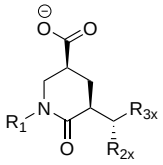

3

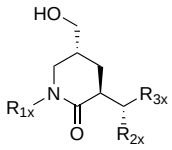

4

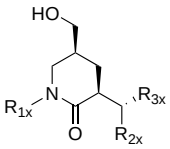

5

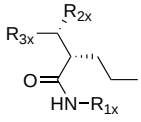

6

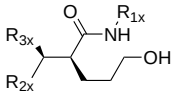

7

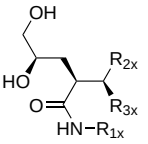

8

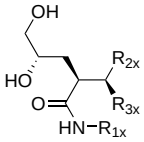

9

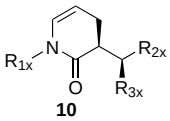

10

Figure E.2 Side chains

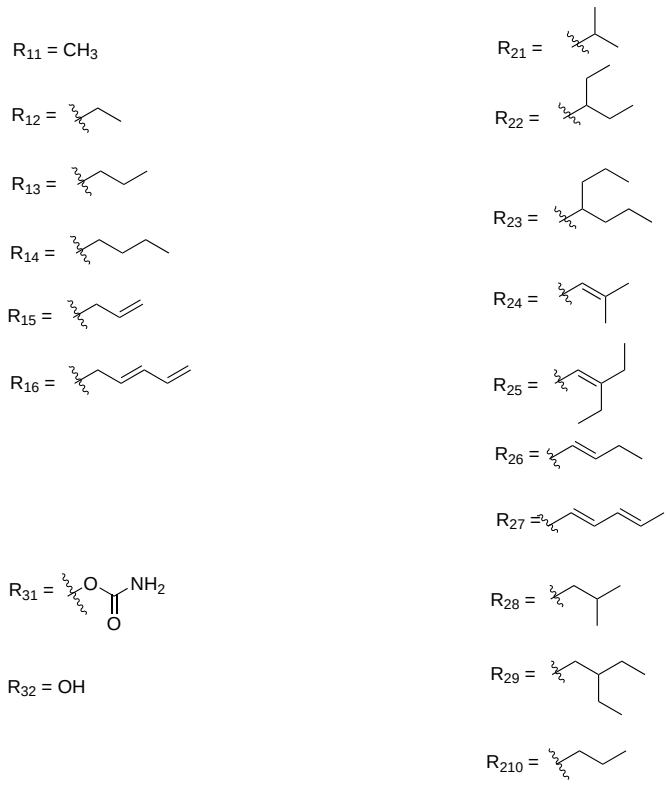

E.1 Main Structure 1

Ligand	3.5	3.5*	3.5**	4.0	4.0*	4.0**
$[R_{11}][R_{21}][R_{31}]$	-3.35/-40.88#	-3.89/-33.79	-2.54/-36.52#	-4.11/-33.04#	-3.85/-39.54	-3.73/-32.39#
$[R_{11}][R_{21}][R_{32}]$	-4.48/-34.4	-4.98/-44.51	-2.09/-30.69!	-3.74/-29.24	-3.72/-45.11	-3.59/-29.78#
$[R_{12}][R_{21}][R_{31}]$	-2.03/-35.36	-2.21/-52.19	-3.2/-54.12!	-1.53/-27.9	-1.83/-50.24	-3.06/-39.53!
$[R_{12}][R_{21}][R_{32}]$	-4.28/-48.77#	-4.18/-50.92	-4.43/-44.71!	-4.3/-38.77!	-4.07/-46.1	-4.16/-36.5!
$[R_{13}][R_{21}][R_{31}]$	-3.68/-50.47#	-3.12/-43.5	-0.76/-31.35!	-3.04/-49.17#	-2.77/-41.5	-2.45/-45.83#
$[R_{13}][R_{21}][R_{32}]$	-0.47/-34.88	-1.98/-51.85	-0.97/-42.68!	-1.84/-32.04#	-1.24/-48	-3.42/-42.15!
$[R_{14}][R_{21}][R_{31}]$	-5.04/56.7#	-2.98/-44.51	-2.87/-36.52#	-4.16/-53.47#	-4.04/-39.9	-4.29/-40.72#
$[R_{14}][R_{21}][R_{32}]$	-0.44/-37.54#	-2.42/-48.78	-2.83/-46.51!	-3/-48.02!	-1.73/-38.55#	-2.39/-39.76!
$[R_{15}][R_{21}][R_{31}]$	-1.6/-53.99#	-0.8/-42.37	-0.77/-34.75!	-2.68/-49.73#	-0.67/-47.99	-1.93/-37.08!
$[R_{15}][R_{21}][R_{32}]$	-3.17/-52.08#	-1.21/-52.5	-0.75/-45.96!	-1.26/-43.31#	-1.52/-54.13	-2.53/-43.19!
$[R_{16}][R_{21}][R_{31}]$	-5.41/-59.68#	-4.53/-56.73	-3.72/-49.15!	-4.79/-55.55#	-3.44/-47.78	-4.01/-39.29#
$[R_{16}][R_{21}][R_{32}]$	-3.61/-55.62#	-2.37/-61.64	-3.67/-53.15!	-3.42/-52.94#	-2.23/-56.46	-2.71/-44.59!
$[R_{11}][R_{22}][R_{31}]$	-2.62/-37.57!	-1.94/-32.17	-1.73/-37.47!	-3.33/-32.52!	-2.1/-32.12	-2.89/-37.3!
$[R_{11}][R_{22}][R_{32}]$	-4.42/-32.61	-2.82/-35.41	-2.56/-31.59!	-3.39/-26.27	-3.26/-26.71	-3.67/-36.39#
$[R_{12}][R_{22}][R_{31}]$	-4.74/-51.91!	-2.25/-35.63	-4.9/-44.65#	-3.79/-23.71!	-3.11/-31.56	-2.26/-38.24!
$[R_{12}][R_{22}][R_{32}]$	-2.71/-42.88#	-2.41/-28.11	-1.7/-40.14#	-3.55/-45.03!	-2.66/-31	-2.85/-42.14#
$[R_{13}][R_{22}][R_{31}]$	-4.11/-53.5#	-4.33/-58.59	-2.54/-21#	-3.94/-48.79#	-3.7/-34.8	-1.61/-35.4#
$[R_{13}][R_{22}][R_{32}]$	-2.72/-46.51!	-0.33/-33.15	-1.81/-42.71!	-1.74/-27.42!	-1.02/-34.52	-1.91/-36.99#
$[R_{14}][R_{22}][R_{31}]$	-4.41/-61.41#	-3.76/-44.07	-4.21/-40.59#	-4.99/-57.83#	-3.19/-37.2	-4.29/-42.53#
$[R_{14}][R_{22}][R_{32}]$	-1.81/-54.26!	-1.1/-44.73!	-0.94/-34.95!	-3.24/-48.33!	-1.64/-37.91#	-1.75/-43.51!
$[R_{15}][R_{22}][R_{31}]$	-3.09/-33.82	-3.71/-42.31	-2.91/-37.16#	-4.43/-53.86#	-2.67/-43.15	-0.69/-39.68!
$[R_{15}][R_{22}][R_{32}]$	-0.83/-46.58!	-0.09/-35.93	-3.36/-53.16!	-1.55/-33.74!	-0.62/-29.58	-1.65/-40.59#
$[R_{16}][R_{22}][R_{31}]$	-2.73/-40.69#	-3.71/-48.26	-3.84/-40.32#	-4.7/-53.56#	-3.69/-62.37	-4.19/-44.09!
$[R_{16}][R_{22}][R_{32}]$	-4.38/-58.95#	-2.55/-62.75	-3.71/-55.3!	-2.2/-47.58!	-2.56/-45.97!	-3.73/-49.22!
$[R_{11}][R_{23}][R_{31}]$	-2.54/-26.3	-3.05/-34.56	-3.69/-26.24!	-4.25/-40.64!	-3.03/-33.26	-2.44/-31.34!
$[R_{11}][R_{23}][R_{32}]$	-1.59/-41.39!	-0.69/-34.21	-1.28/-40.97!	-1.09/-16.19!	-1.52/-30.4	-4.36/-28.95#
$[R_{12}][R_{23}][R_{31}]$	-3.38/-44.69!	-3.21/-39.75	-3.56/-43.87!	-4.91/-52.63#	-3.93/-33.36#	-5.05/-41.05!
$[R_{12}][R_{23}][R_{32}]$	-1.21/-47.76!	-2.18/-34.92	-1.11/-43.08!	-1.89/-42.85!	-1.23/-34.7	-1.8/-30.12!
$[R_{13}][R_{23}][R_{31}]$	-4.24/-55.41!	-4.59/-50.43	-3.02/-37.84!	-5.47/-58.16!	-4.77/-42.4	-3.51/-30.28#
$[R_{13}][R_{23}][R_{32}]$	-4.06/-54.8	-2.66/-35.45	-1.92/-34.28!	-5.64/-52.34!	-4.15/-40.46	-3.1/-39.1#

Ligand	3.5	3.5*	3.5**	4.0	4.0*	4.0**
$[R_{14}][R_{23}][R_{31}]$	-4.44/-62.74#	-3.56/-45.71	-2.24/-37.03#	-5.25/-58.71!	-5/-45.01	-2.62/-27.67#
$[R_{14}][R_{23}][R_{32}]$	-5.38/-56.67!	-2.84/-48.84	-3.05/-39.64!	-5.6/-54.21!	-3.74/-43.99	-1.36/-33.14#
$[R_{15}][R_{23}][R_{31}]$	-3.36/-57.01!	-3.75/-56.18	-2.39/-31.05!	-3.78/-44.89!	-3.8/-42	-3.1/-28.64#
$[R_{15}][R_{23}][R_{32}]$	-2.2/-60.9#	-0.13/-44.22	0.04/-40.45!	-2.21/-48.57!	-1.51/-37.67	-0.94/-33.76#
$[R_{16}][R_{23}][R_{31}]$	-5.58/-65.3#	-3.3/-48.38	-3.66/-43.38!	-5.45/-63.11#	-2.95/-57.86	-3.86/-37.13#
$[R_{16}][R_{23}][R_{32}]$	-4.62/-62.84!	-6.04/-66.35	-4.42/-56.07!	-3.82/-47.06!	-4.03/-47.17	-3.16/-46.5!
$[R_{11}][R_{24}][R_{31}]$	-2.68/-55.87!	-2.7/-54.43	-1.9/-44.16!	-3.92/-51.13!	-1.87/-33.85	-/-
$[R_{11}][R_{24}][R_{32}]$	-4.24/-55.06#	-3.65/-38.21	-2.58/-36.57!	-5.24/-44.17#	-4.07/-30.14	-1.82/-35.77!
$[R_{12}][R_{24}][R_{31}]$	-2.68/-58.12!	-1.56/-49.63	-2.16/-45.36!	-3.78/-52.81!	-1.74/-50.05	-/-
$[R_{12}][R_{24}][R_{32}]$	-1.77/-36.73!	-1.18/-42.16	-1.6/-44.06#	-2.78/-44.53!	-2.28/-38.69	-3.2/-46.07#
$[R_{13}][R_{24}][R_{31}]$	-2.19/-57.34!	-2.13/-54.9	-1.49/-38.5#	-3.97/-54.72!	-1.37/-51.98	-/-
$[R_{13}][R_{24}][R_{32}]$	-1.01/-50.77#	-1.97/-53.83	-0.42/-43.42#	-2.56/-43.17#	-1.76/-39.62	-5.84/-43.86#
$[R_{14}][R_{24}][R_{31}]$	-4.68/-63.05!	-3.43/-48.4	-3.91/-43.43#	-5.66/-57.73!	-3.69/-55.69	-/-
$[R_{14}][R_{24}][R_{32}]$	-4.09/-67.75#	-1.93/-56.47	-3.35/-54.39!	-2.44/-42.35!	-1.69/-52.83	-3.45/-37.7!
$[R_{15}][R_{24}][R_{31}]$	-2.25/-61.04!	-2.04/-52.73	-0.92/-42.65!	-3.38/-56.39!	-0.93/-52	-/-
$[R_{15}][R_{24}][R_{32}]$	-0.82/-56.56#	-1.34/-55.14	-4.16/-68.18!	-1.87/-38.37#	-2.23/-46.64!	-1.19/-37.39!
$[R_{16}][R_{24}][R_{31}]$	-5.47/-62.5!	-4.31/-63.26	-2.87/-49.2#	-5.23/-57.89!	-3.69/-59.09	-/-
$[R_{16}][R_{24}][R_{32}]$	-3.84/-69.55#	-2.14/-62.42	-4.19/-61.87#	-1.57/-47.55!	-2.68/-46.45!	-4.55/-44.12!
$[R_{11}][R_{25}][R_{31}]$	-2.54/-58.03!	-0.82/-41.16	-0.97/-35.31!	-3.85/-54.01/!	-1.56/-25.19	-2.84/-39.01!
$[R_{11}][R_{25}][R_{32}]$	-2.71/-44.51!	-0.63/-39.17	-0.91/-40.02!	-2.6/-39.94!	-1.77/-35.2	-3.54/-34.96#
$[R_{12}][R_{25}][R_{31}]$	-4.61/-59.83!	-4.37/-58.82	-2.64/-38.12!	-5.95/-56.27!	4.3/-38.24#	-2.57/-39.92!
$[R_{12}][R_{25}][R_{32}]$	-1.37/-50.68!	-1.9/-38.99	-0.03/-38.01!	-2.42/-42.22!	-2.15/-39.01	-3.23/-39.57!
$[R_{13}][R_{25}][R_{31}]$	-4.52/-60.7!	-3.35/-53.3	-2.28/-39.74#	-4.7/-48.18!	-4.55/-49.19#	-2.56/-35.75#
$[R_{13}][R_{25}][R_{32}]$	-0.9/-48.91!	-1.98/-41.17	-3.21/-49.03#	-2.48/-45.61!	-0.45/-49.95	-2.36/-40.62!
$[R_{14}][R_{25}][R_{31}]$	-4.43/-64.08!	-3.95/-51.15	-4/-45.5#	-4.15/-50.36!	-4.68/-44.59#	-3/-39.9!
$[R_{14}][R_{25}][R_{32}]$	-0.73/-50.3!	-1.69/-57.42	-0.34/-43.24#	-2.84/-53.88#	-1.41/-54.24	-2.6/-39.85#
$[R_{15}][R_{25}][R_{31}]$	-4.61/-63.85!	-4.07/-56.99	-2.8/-41.29#	-5.98/-58.6!	-2.76/-52.01	-2.56/-41.92!
$[R_{15}][R_{25}][R_{32}]$	-1.34/-54.28!	0.54/-47.02	-2.56/-48.32#	0.29/-39.36!	0.15/-35.73	-2.01/-45.39!
$[R_{16}][R_{25}][R_{31}]$	-3.86/-61.42!	-4.69/-63.41	-4.54/-50.61!	-5.94/-61.32!	-5.18/-58.25#	-3.7/-43.12#
$[R_{16}][R_{25}][R_{32}]$	-5.3/-59.47!	-4.38/-64.25	-3.15/-49.91!	-5.92/-56.55!	-3.95/-58.71	-2.68/-46.71!

Ligand	3.5	3.5*	3.5**	4.0	4.0*	4.0**
[R_{11}] [R_{26}] [R_{31}]	-2.09/-54.82!	-1.28/-61.08	-1.12/-41.29!	-3.31/-50.35!	-3.44/-50.29#	-2.73/-50.24#
[R_{11}] [R_{26}] [R_{32}]	-2.47/-44.87#	-0.34/-40	-0.52/-40.45!	-1.96/-38.33#	-1.41/-46.98#	-2.63/-39.59#
[R_{12}] [R_{26}] [R_{31}]	-1.92/-55.67!	-1.8/-53.73	-1.04/-44#	-3.28/-51.96!	-2.87/-53.87#	-2.63/-52.32#
[R_{12}] [R_{26}] [R_{32}]	-0.19/-47.56!	-1.62/-54.42	-0.24/-42.08#	-3.26/-36.62!	-2.72/-45.42	-2.67/-42.94#
[R_{13}] [R_{26}] [R_{31}]	-1.4/-55.46!	-1.77/-60.02	-1.85/-61.33#	-2.42/-49.42#	-2.94/-56.53#	-2.78/-55.54#
[R_{13}] [R_{26}] [R_{32}]	-2.61/-54.27#	-1.08/-54.32	-0.9/-51.04#	-1.5/-41.09#	-0.97/-49.28	-2.6/-44.52#
[R_{14}] [R_{26}] [R_{31}]	-3.32/-54.27#	-4.13/-61.08#	-2.69/-47!	-4.27/-55.48#	-5.44/-55.75#	-5.38/-55.19#
[R_{14}] [R_{26}] [R_{32}]	-0.48/-49.15!	-0.88/-53.02	-0.57/-43.04#	-3.16/-53.01#	-1.28/-52.63	-2.01/-44.82#
[R_{15}] [R_{26}] [R_{31}]	-1.66/-59.39!	-3.24/-55.47#	-1.11/-47.82!	-2.89/-53.89!	-2.92/-54.99#	-1.94/-48.08#
[R_{15}] [R_{26}] [R_{32}]	-0.45/-42.17!	0.29/-41.45	-3.19/-53.39!	-0.55/-41.32!	-1.57/-53.86!	-1.59/-43.16!
[R_{16}] [R_{26}] [R_{31}]	-4.13/-61.35!	-4.33/-64.35	-2.68/-48.17!	-5.38/-57.41!	-3.61/-58.58	-3.56/-42.91#
[R_{16}] [R_{26}] [R_{32}]	-1.12/-56.43#	-1.9/-58.56	-3.98/-58.67!	-1.5/-52.52#	-1.06/-52.05	-2.09/-46!
[R_{11}] [R_{27}] [R_{31}]	-4.21/-59.72#	-2.46/-53.3	-0.47/-40.88!	-2.39/-50.19!	-1.63/-42.34	-3.67/-49.29#
[R_{11}] [R_{27}] [R_{32}]	-4.09/-57.75#	-1.79/-43.28	-1.18/-44.06!	-4.3/-53.72#	-1.81/-37.72	-2.86/-42.64#
[R_{12}] [R_{27}] [R_{31}]	-1.08/-59.02!	-2.04/-51.84#	-3.71/-45.72#	-2.96/-54.37!	-0.86/-44.17	-3.13/-51.66#
[R_{12}] [R_{27}] [R_{32}]	-1/-47.95#	-3.64/-46.17	-1.8/-52.1#	-3.07/-42.27#	-1.99/-37.67#	-2.53/-45.28#
[R_{13}] [R_{27}] [R_{31}]	-5.26/-59.67#	-4.08/-57.63	-5.07/-57.33#	-5.02/-54.36!	-2.21/-56.91	-6/-55.34#
[R_{13}] [R_{27}] [R_{32}]	-1.24/-50.81#	-1.5/-54.79	-4.03/-57.53#	-1.86/-45.96#	-3.8/-54.64#	-2.81/-46.5#
[R_{14}] [R_{27}] [R_{31}]	-5.05/-61.73#	-4.26/-59.81	-3.67/-51.99#	-5.92/-60.61!	-3.7/-56.18	-5.8/-53.21#
[R_{14}] [R_{27}] [R_{32}]	-3.67/-50.41!	-1.47/-54.46	-3.21/-55.5#	-3.03/-48.18#	-0.63/-43.59	-2.46/-43.89#
[R_{15}] [R_{27}] [R_{31}]	-4.96/-60.14!	-3.72/-59.83	-6.48/-67.24#	-5.37/-59.43#	-2.32/-57.88	-5.31/-49.94#
[R_{15}] [R_{27}] [R_{32}]	-2.59/-51.42#	-3.42/-61.25#	-3.67/-61.27#	-2.75/-58.17#	-3.29/-55.82	-2.35/-46.37#
[R_{16}] [R_{27}] [R_{31}]	-5.57/-63.86#	-4.28/-62.18	-3.02/-45.9#	-5.13/-61.59#	-3.96/-63.66	-3.48/-46.46#
[R_{16}] [R_{27}] [R_{32}]	-3.82/-69.01!	-1.85/-61.94	-0.25/-50.19#	-1.47/-49.29!	-1.7/-59.4	-1.89/-46.49!
[R_{11}] [R_{28}] [R_{31}]	-1.65/-30.91	-1.77/-37.31	-1.83/-43.44!	-1.57/-32.88!	-2.87/-38.09	-2.84/-38.54!
[R_{11}] [R_{28}] [R_{32}]	-3.87/-35.23#	-5.09/-48.11	-3.67/-39.6!	-5/-38.65#	-3.31/-38.81	-4.73/-39.28!
[R_{12}] [R_{28}] [R_{31}]	-1.73/-49.16!	-2.26/-59.3	-2.37/-55.56#	-3.73/49.88!	-1.45/-43.76	-2.35/-37.8!
[R_{12}] [R_{28}] [R_{32}]	-0.54/-45.61#	-1.45/-35.59	-1.23/-43.91!	-2.25/-40.2!	-1.63/-33.63	-1.46/-41.33!
[R_{13}] [R_{28}] [R_{31}]	-4.02/-55.14!	-3.34/-46.64	-2.08/-33.51!	-4.65/-43.96!	-2.92/-39.02	-4.2/-43.49!
[R_{13}] [R_{28}] [R_{32}]	-2.33/-44.58!	-1.17/-47.47!	-1.73/-52.88!	-2.11/-45.35#	-1.6/-48.53	-2.39/-41.61#

Ligand	3.5	3.5*	3.5**	4.0	4.0*	4.0**
$[R_{14}][R_{28}][R_{31}]$	-3.69/-49.37!	-3.74/-47.98	-3.65/-45.33#	-4.82/-54.84#	-5/-45.55	-3.74/-39.33
$[R_{14}][R_{28}][R_{32}]$	-3.27/-51.89#	-0.55/-48.7	-1.08/-47.73#	-1.88/-42.01!	-1.24/-51.3	-2.59/-43.89!
$[R_{15}][R_{28}][R_{31}]$	-1.56/-56.92#	-2.95/-43.53	-1.11/-42.58!	-2.7/-50.83!	-0.94/-38.55#	-2.55/-39.51!
$[R_{15}][R_{28}][R_{32}]$	-1.62/-56.04#	-2.33/-58.96	-0.64/-48.14!	-2.22/-52.1#	-3.84/-63.06!	-2.18/-45.37!
$[R_{16}][R_{28}][R_{31}]$	-5.42/-62.45#	-4.47/-60.4	-3.3/-43.9!	-5.57/-58.57!	-4.13/-43.16#	-4.57/-41.64!
$[R_{16}][R_{28}][R_{32}]$	-4.15/-58.45#	-4.79/-63.51	-4.72/-64.3!	-3.36/-58.99	-2.26/-57.98	-2.34/-48.95!
$[R_{11}][R_{29}][R_{31}]$	-3.05/-34.79!	-3.06/-45.14	-4.29/-51.41!	-4.97/-43.4!	-1.4/-35.05	-/-
$[R_{11}][R_{29}][R_{32}]$	-1.21/-44.45!	-2.82/-42.49	-1.79/-42.11!	-1.9/-30.46	-1.35/-36.4	-3.26/-35.38!
$[R_{12}][R_{29}][R_{31}]$	-4.2/-56.04!	-2.53/-36.94	-4.12/-47.99!	-4.73/-44.67!	-4.02/-41.79	-/-
$[R_{12}][R_{29}][R_{32}]$	-2.76/-44.75!	-0.43/-44.01	-1.81/-45.63!	-2.53/-43.3!	-1.9/-36.91	-3.23/-40.29!
$[R_{13}][R_{29}][R_{31}]$	-4.43/-59.21!	-4.62/-56.78!	-4.34/-54.36!	-5.18/-53.53!	-4.25/-40.51#	-/-
$[R_{13}][R_{29}][R_{32}]$	-2.08/-51.85!	-1.88/-53.42	-1.55/-42.51#	-2.97/-43.11!	-0.8/-50.64	-2.09/-39.8#
$[R_{14}][R_{29}][R_{31}]$	-3.97/-50.68!	-4.94/-53.14	-4.43/-49.94!	-5.59/-56.65!	-4.86/-45.63#	-/-
$[R_{14}][R_{29}][R_{32}]$	-3.37/-51.31!	-3.5/-52.76	-3.48/-49.05!	-5.75/-58.04!	-3.66/-50.65	-4.07/-39.16#
$[R_{15}][R_{29}][R_{31}]$	-3.58/-51.46!	-3.86/-46.24	-4.26/-41.39#	-5.44/-54.33!	-4.78/-44.72#	-/-
$[R_{15}][R_{29}][R_{32}]$	-1.33/-54.52	-0.12/-43.94	-2.88/-45.16!	-2.7/-45!	-0.31/-37.08	-0.34/-39.27#
$[R_{16}][R_{29}][R_{31}]$	-4.35/-57.62!	-3.84/-57.06	-3.16/-49.88#	-5.76/-55.2!	-3.17/-51.92	-/-
$[R_{16}][R_{29}][R_{32}]$	-4.37/-54.16!	-3.25/-47.62	-3.16/-43.25#	-6.08/-60.22#	-4.52/-45.06	-4.65/-40.56!
$[R_{11}][R_{210}][R_{31}]$	-3.44/-49.65#	-2.16/-50.66	-1.81/-43.1!	-3.4/-47.18!	-1.26/-49.45	-2.89/-37.3!
$[R_{11}][R_{210}][R_{32}]$	-4.18/-48.49	-3.74/-36.06	-3.28/-37.64!	-5.21/-43.9#	-3.15/-37.75	-3.67/-36.39#
$[R_{12}][R_{210}][R_{31}]$	-1.74/-54.15!	-1.7/-43.4#	-4.21/-56.11#	-3.03/-50.71!	-2.26/-51.28	-2.26/-38.24!
$[R_{12}][R_{210}][R_{32}]$	-1.33/-41.7#	-1.61/-37.42	-2.89/-48.35!	-2.72/-36.12#	-1.35/-44.43	-2.85/-42.14#
$[R_{13}][R_{210}][R_{31}]$	-3.11/-51.11!	-2.57/-42.26	-0.69/-37.96#	-3.26/-51.15!	-0.91/-50.85	-1.61/-35.4#
$[R_{13}][R_{210}][R_{32}]$	-3.04/-52.97#	-0.87/-45.04	-3.74/-53.49#	-2.14/-45.13!	-1.38/-46.91	-1.91/-39.66#
$[R_{14}][R_{210}][R_{31}]$	-5.01/-57.18#	-3.7/-41.23	-3/-41.09#	-4.39/-52.63#	-4.63/-38.47	-4.29/-42.53#
$[R_{14}][R_{210}][R_{32}]$	-1.79/-45.1!	-0.66/-42.47!	-0.8/-50.72!	-3.55/-52.83!	-0.54/-40.61	-1.75/-43.51!
$[R_{15}][R_{210}][R_{31}]$	-1.21/-56.3!	-0.75/-42.43	-0.47/-43.35!	-2.21/-52.93#	-3.38/-52.03!	-0.69/-39.68!
$[R_{15}][R_{210}][R_{32}]$	-3.21/-55.82#	-1.06/-55.49	-0.17/-49.33!	-1.13/-46.35#	0.98/-28.31	-1.65/-41.59#
$[R_{16}][R_{210}][R_{31}]$	-3.97/-61.36#	-3.05/-47.94	-3.36/-42.13!	-4.87/-56.77#	-2.74/-46.49	-4.19/-44.09!
$[R_{16}][R_{210}][R_{32}]$	-4/-62.21#	-1.73/-61.5	-1.36/-61.59!	-3.54/-58.14#	-1.54/-54.81	-3.73/-49.22!

E.2 Main Structure 2

Ligand	3.0	3.5*	3.5**	4.0	4.0*	4.0**
[R_{11}] [R_{21}] [R_{31}]	-5.42/-54.99#	-3.89/-38.65	-/-	-5.98/-50#	-6.73/-48.77#	-6/-39.15#
[R_{11}] [R_{21}] [R_{32}]	-4.51/-33.61	-5.75/-50.4#	-/-	-4.99/-29.5	-6.69/-47.57#	-5.65/-37.78#
[R_{12}] [R_{21}] [R_{31}]	-5.69/-57.88#	-3.94/-44.98	-5.51/-50.77#	-6.07/-53.05#	-4.38/-48.04	-4.76/-34.53#
[R_{12}] [R_{21}] [R_{32}]	-4.55/-34.28	-4.04/-35.38	-5.4/-52.7#	-5.88/-41.97#	-6.9/-50.37#	-6.67/-44.96#
[R_{13}] [R_{21}] [R_{31}]	-5.33/-129.22#	-4.96/-56.11	-4.66/-43.38#	-5.84/-54.54#	-4.34/-52.41	-5.42/-35.72!
[R_{13}] [R_{21}] [R_{32}]	-4.15/-33.09	-4.56/-49.34	-3/-19.95#	-5.36/-40.97#	-5.02/-48.05	-5.28/-34.78#
[R_{14}] [R_{21}] [R_{31}]	-5.38/-185.29#	-4.86/-56.81	-3.9/-44.51#	-6.06/-55.96#	-4.38/-53.39	-4.59/-34.55#
[R_{14}] [R_{21}] [R_{32}]	-5.3/-50#	-3.9/-45.73	-5.37/-51.07!	-6.09/-44.85!	-4.63/-45.41	-5.61/-38.32!
[R_{15}] [R_{21}] [R_{31}]	-5.14/-148.14	-4.87/-57.09	-4.74/-45.38!	-5.66/-54.81#	-4.35/-47.07	-3.77/-32.26#
[R_{15}] [R_{21}] [R_{32}]	-4.61/-42.23!	-4.93/-52.74	-4.94/-54.67#	-4.15/-30.83	-4.74/-49.28	-6.25/-50.77#
[R_{16}] [R_{21}] [R_{31}]	-5.33/-120.53#	-5.25/-132.59	-2.83/-38.74#	-5.97/-60.91#	-4.27/-56.63	-4.24/-31.39!
[R_{16}] [R_{21}] [R_{32}]	-5.34/-55.58#	-5.04/-58.25	-3.83/-43.6!	-4.9/-46.85#	-5.02/-54.43	-6.2/-46.52#
[R_{11}] [R_{22}] [R_{31}]	4.17/-34.66	-3.12/-38.2	-2.85/-31.17!	-5.69/-52.29#	-4.07/-45.41	-4.32/-27.03#
[R_{11}] [R_{22}] [R_{32}]	-5.32/-49.54!	-4.79/-50.42	-3.06/-29.03	-6.15/-36.96!	-5.15/-45.68	-5.76/-43.23#
[R_{12}] [R_{22}] [R_{31}]	-4.11/-52.73#	-3.44/-29.22	-4.12/-35.3#	-5.96/-47.78!	-3.41/-25.41	-4.31/-27.22!
[R_{12}] [R_{22}] [R_{32}]	-5.3/-45.04!	-4.16/-39.86	-5.44/-56.53#	-5.67/-44.08#	-7.39/-54.69#	-6.01/-44#
[R_{13}] [R_{22}] [R_{31}]	-4.53/-37.05#	-3.55/-36.43	-4.18/-37.48#	-5.89/-56.9#	-4.7/-32.28	-4.24/-32.85#
[R_{13}] [R_{22}] [R_{32}]	-5.51/-54.94!	-4.94/-53.64	-5.41/-58.46#	-5.71/-46.25#	-7.47/-56.88#	-6.14/-46.6#
[R_{14}] [R_{22}] [R_{31}]	-4.93/-62.34#	-4.78/-42.9	-2.39/-9.68#	-5.97/-58.26#	-3.42/-41.45	-3.49/-31.17
[R_{14}] [R_{22}] [R_{32}]	-4.92/-46.4!	-5.51/-58.03!	-5.49/-62.2#	-6.35/-42.4!	-4.58/-50.58	-5.97/-48.85#
[R_{15}] [R_{22}] [R_{31}]	-4.99/-41.46	-4.79/-59.26	-1.99/-10.78!	-5.41/-51.96#	-3.96/-55.82	-3.98/-30.09!
[R_{15}] [R_{22}] [R_{32}]	-5.18/-46.97!	-4.52/-53.67	-5.13/-58.82#	-6.14/-41.2!	-7.03/-56.7#	-5.45/-44.96#
[R_{16}] [R_{22}] [R_{31}]	-5.41/-78.31#	-5.27/-81.74	-/-	-5.93/-61.75#	-3.67/-40.77	-4.19/-25.79!
[R_{16}] [R_{22}] [R_{32}]	-5.4/-53.67#	-5.18/-60.71	-4.35/-37.79!	-6.25/-43.85!	-4.8/-56.36	-4.09/-30.68!
[R_{11}] [R_{23}] [R_{31}]	-5.07/-39.72#	-2.03/-120.32	-3.02/-30.31#	-4.74/-40.22!	-3.99/-36.56	-/-
[R_{11}] [R_{23}] [R_{32}]	-3.86/-33.24	-4.26/-50.8	-4.95/-56.42#	-5.82/-47.86!	-4.34/-33.6	-4.79/-43.21#
[R_{12}] [R_{23}] [R_{31}]	-5.34/-114.57#	-2.97/-33.32	-2.07/-14.68!	-5.36/-41.02!	-3.45/-28.1	-/-
[R_{12}] [R_{23}] [R_{32}]	-5.32/-49.54!	-4.52/-51.59	-3.5/-35.73!	-6.03/-48.55!	-4.38/-38.61	-5.83/-49.13#
[R_{13}] [R_{23}] [R_{31}]	-3.77/-56.77	-4.69/-76.74	-3.5/-31.01#	-5.55/-52.02!	-4.65/-42.06	-/-
[R_{13}] [R_{23}] [R_{32}]	-3.95/-32.94	-4.02/-45.69	-3.1/-37.35!	-6.45/-51.64!	-7.15/-60.08#	-5.69/-49.18#

Ligand	3.5	3.5*	3.5**	4.0	4.0*	4.0**
$[R_{14}]\,[R_{23}]\,[R_{31}]$	-/-	-4.72/-167.85	-2.65/-35.87!	-5.39/-51.71!	-3.51/-49.89	-/-
$[R_{14}]\,[R_{23}]\,[R_{32}]$	-5.46/-60.5!	-4.1/-47.87	-6.15/-65.29#	-6.15/-50.88!	-4.14/-52.19	-5.3/-45.3#
$[R_{15}]\,[R_{23}]\,[R_{31}]$	-4.53/-193.96#	-4.01/-47.09	-3.11/-32.7#	-5.24/-46.76!	-4.38/-40.83	-/-
$[R_{15}]\,[R_{23}]\,[R_{32}]$	-5.13/-51.67!	-3.84/-45.82	-5.04/-62#	-5.92/-48.32!	-4.62/-40.62	-5.63/-49.96#
$[R_{16}]\,[R_{23}]\,[R_{31}]$	-4.89/-162.5!	-5.23/-157.42	-2.31/-34.78#	-2.88/-40.36	-4/-61.66	-/-
$[R_{16}]\,[R_{23}]\,[R_{32}]$	-5.59/-61.69!	-4.89/-62.44	-3.62/-42.87!	-7.03/-59.19!	-4.46/-58.54	-4.05/-32.34!
$[R_{11}]\,[R_{24}]\,[R_{31}]$	-4.69/-47.13!	-3.64/-46.47	-2.9/-24.92#	-5.54/-40.21#	-4.12/-43	-5.36/-36.98#
$[R_{11}]\,[R_{24}]\,[R_{32}]$	-5.67/-50.33!	-4.45/-47.36	-5/-48.84#	-5.21/-42.28!	-6.02/-44.96#	-5.98/-45.22#
$[R_{12}]\,[R_{24}]\,[R_{31}]$	-4.84/-49.39!	-4.78/-52.73	-3.54/-41.27#	-5.78/-43.29!	-4.02/-43.38	-3.57/-27.4#
$[R_{12}]\,[R_{24}]\,[R_{32}]$	-4.64/-41.19!	-4.79/-50.47	-5.13/-51.85#	-6.15/-41.5!	-4.94/-45.07	-6.65/-49.17#
$[R_{13}]\,[R_{24}]\,[R_{31}]$	-4.73/-49.74!	-4.65/-52.86	-4.04/-30.19#	-5.7/-43.94!	-3.89/-45.01	-5.01/-35.94#
$[R_{13}]\,[R_{24}]\,[R_{32}]$	-4.48/-36.34	-4.92/-53.02#	-5.11/-53.9#	-5.96/-34.8!	-4.75/-49.58	-6.76/-54.43#
$[R_{14}]\,[R_{24}]\,[R_{31}]$	-4.72/-49.76!	-4.74/-55.47	-4.07/-32.6#	-5.09/-42!	-3.57/-44.37	-4.34/-28.62#
$[R_{14}]\,[R_{24}]\,[R_{32}]$	-4.2/-44.87!	-3.99/-52.76	-4.91/-53.53#	-6.23/-51.48!	-6.86/-51.59#	-6.19/-51.74#
$[R_{15}]\,[R_{24}]\,[R_{31}]$	-4.57/-51.89!	-4.63/-55.84	-3.27/-39.51#	-5/-46.8#	-4.47/-38.56	-4.64/-37.95#
$[R_{15}]\,[R_{24}]\,[R_{32}]$	-5.6/-54.04!	-4.63/-54.01	-4.71/-54.29#	-6.15/-49.35!	-4.48/-50.23	-6.11/-50.73#
$[R_{16}]\,[R_{24}]\,[R_{31}]$	-4.46/-53.92!	-4.96/-59.48	-3.04/-38.04#	-4.89/-46.51!	-4.13/-56.1	-4.2/-31.8!
$[R_{16}]\,[R_{24}]\,[R_{32}]$	-5.88/-60.13!	-5.09/-59.38	-5.55/-54.76!	-6.18/-55.64!	-4.82/-54.65	-5.4/-34.92!
$[R_{11}]\,[R_{25}]\,[R_{31}]$	-4.83/-50.7!	-3.51/-48.35	-2.68/-25.89#	-5.71/-43.76!	-3.76/-30.83	–3.16/-29.18!
$[R_{11}]\,[R_{25}]\,[R_{32}]$	-3.95/-41.48!	-3.97/-31.86	-5.72/-52.86#	-5.65/-38.08!	-4.11/-44.2	-5.6/-48.37#
$[R_{12}]\,[R_{25}]\,[R_{31}]$	-5.04/-54!	-4.61/-41.51	-4.08/-35.14!	-6.1/-48.04!	-3.73/-35.85	-4.06/-32.34#
$[R_{12}]\,[R_{25}]\,[R_{32}]$	-4.9/-48!	-4.06/-49.54	-5.2/-56.4#	-5.45/-41.79!	-4.57/-47.4	-5.19/-40.44#
$[R_{13}]\,[R_{25}]\,[R_{31}]$	-5.01/-54.35!	-4.55/-47.53	-5.66/-59.98#	-5.93/-47.86!	-3.54/-48.18	-4.46/-36.26#
$[R_{13}]\,[R_{25}]\,[R_{32}]$	-3.57/-36.41!	-3.96/-49.62	-5.14/-58.25#	-4.63/-34.31!	-4.06/-47.48	-6/-50.79#
$[R_{14}]\,[R_{25}]\,[R_{31}]$	-3.55/-45.85	-4.18/-51.11	-2.31/-31.67#	-5.99/-47.96!	-4.21/-33.71	-5.05/-40.67#
$[R_{14}]\,[R_{25}]\,[R_{32}]$	-3.77/-43.44!	-3.77/-52.98	-5.27/-61.94#	-5.82/-43.33!	-7.35/-58.52#	-5.39/-45.29#
$[R_{15}]\,[R_{25}]\,[R_{31}]$	-4.37/-48.99!	-4.63/-58.26	-2.71/-34.84#	-5.82/-48.18!	-4.51/-42.09	-2.68/-19.2#
$[R_{15}]\,[R_{25}]\,[R_{32}]$	-3.47/-57.02!	-2.62/-53.49	-3.28/-58.64#	-5.07/-51.67!	-2.66/-48.75	-4.18/-52.56#
$[R_{16}]\,[R_{25}]\,[R_{31}]$	-4.76/-57.68!	-5.02/-63.38	-4.02/-35.41#	-5.84/-53.63!	-3.94/-59.96	-3.46/-30.98#
$[R_{16}]\,[R_{25}]\,[R_{32}]$	-4.05/-52.6#	-4.91/-62.35	-5.35/-65.29#	-6.43/-57.84!	-4.35/-58.77	-4.08/-34.65!

Ligand	3.5	3.5*	3.5**	4.0	4.0*	4.0**
[R_{11}] [R_{26}] [R_{31}]	-4.5/-49.48!	-4.01/-42.56	-3.87/-50.97#	-5.49/-43.78!	-4.32/-38.89	-5.82/-50.2#
[R_{11}] [R_{26}] [R_{32}]	-1.97/-50.73#	-4.48/-50.67	-4.81/-50.3#	-6.71/-48.02#	-4.27/-34.12	-5.74/-46.2#
[R_{12}] [R_{26}] [R_{31}]	-4.67/-50.96!	-4.66/-56.22#	-4.85/-56.78#	-5.78/-46.99!	-6/-53.23#	-5.72/-47.25#
[R_{12}] [R_{26}] [R_{32}]	-3.92/-45.51	-4.69/-52.72	-5.07/-51.74#	-4.47/-34.75!	-4.64/-48.59	-6.19/-48.27#
[R_{13}] [R_{26}] [R_{31}]	-4.51/-50.76!	-3.97/-47.64	-4.75/-56.99#	-5.65/-47!	-6.29/-54.05#	-5.59/-46.04#
[R_{13}] [R_{26}] [R_{32}]	-5.16/-47.42!	-4.7/-54.39	-4.49/-54.21#	-5.84/-48.2#	-5.97/-50.45#	-5.99/-47.37#
[R_{14}] [R_{26}] [R_{31}]	-4.64/-57.64#	-4.61/-53.71	-4.87/-55.89#	-5.28/-55.74#	-6.54/-56.9#	-5.78/-49.34#
[R_{14}] [R_{26}] [R_{32}]	-4.4/-45.04!	-4.6/-54.81	-4.77/-56.77#	-5.11/-32.92!	-5.73/-46.54#	-6.97/-53.63#
[R_{15}] [R_{26}] [R_{31}]	-4.32/-52.14!	-4.71/-57.09	-4.16/-58.14#	-5.38/-47.19!	-3.73/-52.89	-6.2/-54.33#
[R_{15}] [R_{26}] [R_{32}]	-4.51/-55.35	-4.41/-54.85	-5.37/-54.19#	-5.88/-46.53!	-4.16/-51.88	-5.39/-49.67#
[R_{16}] [R_{26}] [R_{31}]	-4.73/-64.21!	-4.99/-62.44	-3.34/-41.96!	-5.31/-60.69#	-3.98/-55.72	-4.04/-34.5!
[R_{16}] [R_{26}] [R_{32}]	-/-	-3.49/-61.04	-4.83/-60.5#	-4.06/-51.2!	-3.02/-57.4	-3.92/-45.88#
[R_{11}] [R_{27}] [R_{31}]	-4.35/-50.05!	-4.94/-53.86	-4.94/-54#	-5.13/-52.77#	-6.25/-51.93#	-6.29/-51.67#
[R_{11}] [R_{27}] [R_{32}]	-5.3/-55.57!	-4.69/-52	-5.08/-52.99#	-5.95/-48.9#	-4.7/-43.93	-5.79/-47.08#
[R_{12}] [R_{27}] [R_{31}]	-4.32/-40.66!	-4.58/-53.87	-5.26/-58.11#	-5.99/-47.11!	-6.08/-50.39#	-6.06/-52.45#
[R_{12}] [R_{27}] [R_{32}]	-4.96/-56.23!	-4.37/-51.57	-4.8/-54.82#	-6.16/-51.38#	-6.9/-51.59#	-6.31/-50.45#
[R_{13}] [R_{27}] [R_{31}]	-4.87/-52.81!	-4.23/-52.44	-5.35/-57.97#	-5.86/-47.29!	-6.75/-56.6#	-5.61/-51.49#
[R_{13}] [R_{27}] [R_{32}]	-5.9/-57.27!	-4.75/-54.45	-4.83/-57.12#	-6.17/-53.94#	-4.38/-49.09	-5.83/-48.58#
[R_{14}] [R_{27}] [R_{31}]	-4.9/-59.16#	-5.38/-58.95	-6.29/-62.09#	-5.39/-55.11#	-7.17/-60.26#	-6.45/-54.41#
[R_{14}] [R_{27}] [R_{32}]	-4.32/-54.47#	-4.17/-53.76	-5.82/-59.3#	-6.01/-48.51#	-6.3/-51.18#	-7.01/-56.22#
[R_{15}] [R_{27}] [R_{31}]	-4.68/-53.21!	-5.2/-58.12	-5.16/-57.22#	-5.59/-47.99!	-6.66/-58.6#	-6.43/-55.82#
[R_{15}] [R_{27}] [R_{32}]	-3.69/-53.17#	-4.03/-53.55	-4.67/-56.8#	-5.36/-47.35#	-4.25/-50.62	-5.92/-51.95#
[R_{16}] [R_{27}] [R_{31}]	-4.75/-66.77#	-5.09/-62.42	-5.82/-65.98#	-5.1/-62.01#	-3.81/-56.72	-6.33/-58.9#
[R_{16}] [R_{27}] [R_{32}]	-4.42/-52.7!	-5.03/-60.98	-5.21/-62.18#	-5.68/-49.03!	-4.5/-60.26	-6.13/-51.97#
[R_{11}] [R_{28}] [R_{31}]	-4.39/-41.65!	-4.62/-51.28	-1.95/-13.5!	-4.74/-32.67!	-4.12/-42.32	-4.23/-29.71#
[R_{11}] [R_{28}] [R_{32}]	-5.4/-46.85!	-4.45/-48.07	-4.88/-50.8#	-6.17/-42.42!	-4.94/-44.1	-5.87/-44.42#
[R_{12}] [R_{28}] [R_{31}]	-4.49/-56.16#	-4.13/-41.73	-3.23/-32.98!	-5.68/-53.05#	-4.34/-33.41	-4.3/-31.24#
[R_{12}] [R_{28}] [R_{32}]	-4.46/-34.77	-5.17/-52.44	-5.76/-52.49#	-5.25/-36.72!	-4.65/-32.82	-6.27/-47.64#
[R_{13}] [R_{28}] [R_{31}]	-4.49/-49.19!	-3.91/-43.62	-3.01/-24.15#	-5.36/-40.07#	-4.56/-38.13	-4.3/-31.89#
[R_{13}] [R_{28}] [R_{32}]	-4.35/-35.35	-4.95/-52.67	-5.78/-54.44#	-5.83/-39.62!	-7.19/-53.69#	-5.88/-45.34#

Ligand	3.5	3.5*	3.5**	4.0	4.0*	4.0**
$[R_{14}][R_{28}][R_{31}]$	-4.72/-60.06#	-3.97/-45.96	-3.22/-37.13!	-5.1/-54.99#	-4.63/-40.46	-3.88/-32.46
$[R_{14}][R_{28}][R_{32}]$	-4.23/-36.63	-4.7/-52.83	-5.15/-57.93#	-4.5/-32.79	-7.14/-56.95#	-6.35/-51.57#
$[R_{15}][R_{28}][R_{31}]$	-3.61/-40.6!	-4.71/-56.45	-2.74/-26.91#	-4.88/-39.62#	-3.97/-53.26	-4.13/-32.3!
$[R_{15}][R_{28}][R_{32}]$	-4.11/-36.03	-4.78/-54.21	-5.06/-58.34#	-5.57/-41.28!	-6.67/-53.9#	-5.67/-50.1#
$[R_{16}][R_{28}][R_{31}]$	-5/-63.3!	-5.21/-62.57	-3.95/-38.02#	-4.95/-59.57#	-4.28/-59.09	-4.24/-34.69!
$[R_{16}][R_{28}][R_{32}]$	-5.02/-55.69!	-5.16/-60.06	-4.08/-35.62!	-4.78/-45.42#	-4.95/-54.4	-5.49/-36.66#
$[R_{11}][R_{29}][R_{31}]$	-4.69/-45.64!	-4.1/-42.2	-3.58/-39.88!	-5.24/-34.96!	-3.99/-35.76	-/-
$[R_{11}][R_{29}][R_{32}]$	-4.1/-45.6!	-3.96/-46.83	-4.18/-45.96#	-6.28/-43.88!	-4.18/-43.23	-5.85/-44.46#
$[R_{12}][R_{29}][R_{31}]$	-4.12/-36.58!	-3.72/-49.29	-3.4/-34.25!	-5.24/-35.25!	-4.94/-35.2!	-/-
$[R_{12}][R_{29}][R_{32}]$	-4.09/-36.72	-4.01/-47.24	-3.37/-39.45!	-3.96/-33.97	-4.68/-47.33	-5.9/-46.69#
$[R_{13}][R_{29}][R_{31}]$	-4.4/-41.44!	-3.38/-49.05	-3.47/-41.05!	-5.29/-41.07!	-3.1/-46.28	-/-
$[R_{13}][R_{29}][R_{32}]$	-4.54/-43.15	-3.92/-48.78	-5.16/-57.1#	-6/-44.95!	-4.25/-48.51	-4.46/-36.53#
$[R_{14}][R_{29}][R_{31}]$	-4.28/-42.3!	-4.24/-47.94	-3.77/-44.25	-4.9/-54.98#	-4.7/-43.39	-/-
$[R_{14}][R_{29}][R_{32}]$	-5.27/-56.52!	-3.65/-42.93	-4.85/-53.78	-5.62/-41.15!	-4.4/-52.83	-5.13/-45.24
$[R_{15}][R_{29}][R_{31}]$	-4.4/-47.79!	-4.12/-46.36	-3.61/-38.59!	-4.88/-40.38!	-4.37/-40.4	-/-
$[R_{15}][R_{29}][R_{32}]$	-5.3/-51.25!	-3.53/-42.41	-4.97/-58.73#	-5.48/-36.08!	-4.41/-38.81	-4.91/-42.55#
$[R_{16}][R_{29}][R_{31}]$	-4.65/-55.75!	-5.41/-66.95	-2.38/-36.11#	-5.08/-50.74!	-4.45/-64.52	-/-
$[R_{16}][R_{29}][R_{32}]$	-5.15/-58.2!	-4.86/-58.51	-3.13/-37.94!	-6.08/-50.51#	-4.61/-55.69	-4.39/-32.66#
$[R_{11}][R_{210}][R_{31}]$	-4.82/-35.7#	-6.54/-45.27	-2.87/-31.38!	-4.54/-34.89!	-3.94/-40.96	-4.66/-33.67!
$[R_{11}][R_{210}][R_{32}]$	-5.14/-50.05!	-4.46/-47.34	-4.91/-49.48#	-5.4/-39.34#	-4.96/-43.19	-6.25/-45.03#
$[R_{12}][R_{210}][R_{31}]$	-3.97/-32.93#	-3.86/-41	-3.25/-38.04#	-4.73/-42.74!	-4.41/-37.33	-4.55/-37.2#
$[R_{12}][R_{210}][R_{32}]$	-4.83/-36.05!	-4.55/-48.86	-5.14/-53.24#	-5.91/-38.16#	-7.12/-51.03#	-6.42/-47.58#
$[R_{13}][R_{210}][R_{31}]$	-5.14/-55.77#	-4.68/-54.31	-3.05/-29.58!	-5.7/-53.32#	-4.3/-38.6	-4.2/-33.85!
$[R_{13}][R_{210}][R_{32}]$	-4.06/-35.09	-4.84/-53.01	-5.14/-55.26#	-4.56/-31.14	-4.69/-48.02	-6.01/-45.76#
$[R_{14}][R_{210}][R_{31}]$	-5.15/-44.72#	-3.96/-41.49	-3.31/-39.36#	-5.37/-52.32#	-4.08/-51.31	-4.54/-33.04#
$[R_{14}][R_{210}][R_{32}]$	-5.18/-55.24!	-4.83/-52.25	-5.15/-58.86#	-4.83/-44.28#	-4.35/-43.3	-6.39/-51.23#
$[R_{15}][R_{210}][R_{31}]$	-5.45/-26.76#	-3.87/-43.02	-3.02/-39.04#	-4.56/-37.35#	-3.09/-41.44	-4.45/-38.16#
$[R_{15}][R_{210}][R_{32}]$	-4.44/-38.23!	-4.65/-53.49	-4.81/-55.72#	-6.03/-50.33!	-6.71/-53.37#	-6.54/-51.08#
$[R_{16}][R_{210}][R_{31}]$	-3.42/-45.5#	-4.81/-58.29	-2.68/-34.27#	-5.79/-57.07#	-4.26/-57.72	-4.33/-37.81!
$[R_{16}][R_{210}][R_{32}]$	-5.26/-53.42#	-4.99/-59.09	-5.84/-59.16!	-5.43/-47.06#	-4.91/-55.08	-5.36/-37.74!

E.3 Main Structure 3

Ligand	3.0	3.5*	3.5**	4.0	4.0*	4.0**
$[R_{11}][R_{21}][R_{31}]$	-3.11/-38.53	-3.89/-47.51	-3.95/-21.74!	-5.34/48.43#	-4.34/-52.83	-5.32/-38.74#
$[R_{11}][R_{21}][R_{32}]$	-4.4/-31.55	-3.84/-37.74	-5.79/-47.49!	-4.99/-27.37	-6.83/-45.87#	-6.65/-45.87#
$[R_{12}][R_{21}][R_{31}]$	-5.64/-55.91#	-5.74/-53.97#	-4.97/-49.59#	-5.52/-32.35#	-4.85/-32.62#	-4.6/-36.62!
$[R_{12}][R_{21}][R_{32}]$	-3.97/-40.15!	-5.16/-50.56#	-5.35/-51.83#	-5.46/-27.24	-5.11/-31.24	-6.13/-43.83#
$[R_{13}][R_{21}][R_{31}]$	-5.15/-52.32#	-4.29/-46.06	-3.11/-39.57!	-6.29/-51.4#	-4.3/-55.05	-5.75/-35.64#
$[R_{13}][R_{21}][R_{32}]$	-4.26/-33.32	-5.15/-54.57	-3.24/-29.4!	-5.85/-43.77#	-4.98/-50.62	-5.45/-35.52#
$[R_{14}][R_{21}][R_{31}]$	-4.75/-57.28#	-5.04/-58.36	-2.86/-31.14!	-5.21/-52.86#	-4.28/-55.33	-4.36/-32.45#
$[R_{14}][R_{21}][R_{32}]$	-5.51/-51.78#	-5.07/-52.21#	-5.14/-45.75!	-6.32/-46.71#	-6.64/-48.22#	-6.36/-46.3#
$[R_{15}][R_{21}][R_{31}]$	-4.75/-52.4#	-3.86/-41.22	-4.35/-46.14#	-5.07/-53.27#	-4.18/-37.35	-4.08/-37.32#
$[R_{15}][R_{21}][R_{32}]$	-5.22/-46.35!	-4.63/-48.41	-4.09/-41.83#	-5.81/-43.86#	-4.6/-48.01	-5.95/-44.34#
$[R_{16}][R_{21}][R_{31}]$	-4.81/-56.66#	-5.3/-64.95	-3.26/-36.76!	-4.65/-44.73!	-4.44/-61.77	-3.97/-32.04#
$[R_{16}][R_{21}][R_{32}]$	-5/-55.9#	-5.42/-58.29	-5.8/-56.55!	-5.81/-40.4!	-4.87/-52.54	-6.38/-48.55!
$[R_{11}][R_{22}][R_{31}]$	-4.6/-43.98!	-3.35/-38.6	-4.94/-46.17#	-5.63/-49.08#	-4.32/-37.6	-5.2/-39.58#
$[R_{11}][R_{22}][R_{32}]$	-5.2/-42.06!	-5.09/-51.46	-5.39/-54.45#	-5.38/-38!	-5.39/-48.08	-5.91/-41.33#
$[R_{12}][R_{22}][R_{31}]$	-3.5/-28.46	-4.55/-51#	-5.19/-55.49#	-4.21/-36.17#	-4.36/-30.87	-5.36/-45.54#
$[R_{12}][R_{22}][R_{32}]$	-4.9/-48.16!	-3.96/-41.88	-4.15/-31.63#	-4.59/-35.68!	-5.22/-45.75	-5.74/-39.88#
$[R_{13}][R_{22}][R_{31}]$	-4.66/-57.35#	-5.25/-58.7	-5.24/-40.56#	-5.17/-50.69#	-4.09/-57.22	-4.5/-38.11!
$[R_{13}][R_{22}][R_{32}]$	-4.98/-37.75	-5.24/-53.5#	-5.27/-53.82#	-6.47/-51.94!	-4.87/-49.25	-5.06/-38.08!
$[R_{14}][R_{22}][R_{31}]$	-4.89/-62.13#	-3.92/-48.29	-3.03/-28.15#	-6.05/-58.9#	-3.65/-39.08	-2.82/-27.39#
$[R_{14}][R_{22}][R_{32}]$	-5.71/-53.53#	-4.79/-53.65	-4.83/-51.72#	-5.19/-47.72!	-4.84/-49.41	-5.8/-42.53#
$[R_{15}][R_{22}][R_{31}]$	-4.92/-55.91#	-4.01/-44.14	-4.07/-40.71#	-5.48/-51.03#	-3.6/-33.91	-4.11/-35.25!
$[R_{15}][R_{22}][R_{32}]$	-4.81/-36.27	-5/-57.71#	-5.04/-57.83#	-5.71/-40.75!	-4.22/-50.11	-6.12/-45.83#
$[R_{16}][R_{22}][R_{31}]$	-4.16/-190.05!	-5.32/-67.1	-2.88/-31.83!	-4.91/-57.69#	-4.37/-64.77	-3.04/-28.57#
$[R_{16}][R_{22}][R_{32}]$	-4.67/-49!	-5.39/-62.78	-2.9/-29.95!	-6.52/-53.18!	-5.07/-58.3	-3.37/-28.62!
$[R_{11}][R_{23}][R_{31}]$	-3.42/-38.83!	-4.2/-45.7	-3.3/-40.72!	-5.31/-47.39!	-4.45/-40.81	-/-
$[R_{11}][R_{23}][R_{32}]$	-4.68/-48.27!	-3.45/-38.88	-3.96/-45#	-6.38/-50.68!	-4.35/-42.9	-5.2/-44.37#
$[R_{12}][R_{23}][R_{31}]$	-5.61/-159.54!	-4.14/-32.72	-2.98/-36.14!	-5.78/-44.11#	-4.29/-35.2	-/-
$[R_{12}][R_{23}][R_{32}]$	-5.5/-58.3!	-3.56/-40.63!	-5.14/-55.79#	-6.54/-52.24!	-4.8/-36.74!	-5.27/-40.22#
$[R_{13}][R_{23}][R_{31}]$	-4.93/-134.57!	-4.26/-49.88	-2.69/-24.89#	-5.1/-50.92!	-4.29/-44.17	-/-
$[R_{13}][R_{23}][R_{32}]$	-5.42/-59.19!	-3.94/-47.57	-3.69/-43.18!	-5.05/-46.04!	-5.32/-41.54!	-5.08/-42.65#

Ligand	3.5	3.5*	3.5**	4.0	4.0*	4.0**
$[R_{14}][R_{23}][R_{31}]$	-5.82/-60.34#	-3.95/-51.02	-3.45/-31.21#	-5.12/-53.15#	-4.28/-46.59	-/-
$[R_{14}][R_{23}][R_{32}]$	-4.75/-48.09!	-3.76/-47.65!	-3.79/-47.98!	-5.91/-55.13!	-4.15/-50.05	-5.35/-45.29#
$[R_{15}][R_{23}][R_{31}]$	-4.61/-58.17!	-3.56/-47.55	-3.23/-32.35#	-3.7/-39.7!	-4.21/-42.77	-/-
$[R_{15}][R_{23}][R_{32}]$	-5.14/-59.23!	-4.42/-54.1#	-4.76/-58.57#	-6.37/-55.15!	-5.24/-50.88#	-4.34/-35.47!
$[R_{16}][R_{23}][R_{31}]$	-4.01/-50.38!	-5.46/-71.22	-2.13/-33.49#	-5.19/-53.31#	-3.65/-59.09	-/-
$[R_{16}][R_{23}][R_{32}]$	-5.48/-63.26!	-4.64/-59.63	-3.33/-43.55!	-6.96/-58.07!	-4.7/-38.19	-4.44/-38.75!
$[R_{11}][R_{24}][R_{31}]$	-4.71/-48.14!	-4.32/-44.25	-3.35/-35.31!	-5.53/-43.06!	-3.61/-38.88	-5.44/-37.89!
$[R_{11}][R_{24}][R_{32}]$	-4.41/-35.96	-4.49/-39.43	-5.46/-48.04#	-5.43/-37.41#	-4.67/-30.39	-6.53/-41.52#
$[R_{12}][R_{24}][R_{31}]$	-4.95/-50.87!	-4.01/-42.92	-3.91/-44.17#	-5.85/-45.88!	-2.72/-39.29	-4.83/-35.33!
$[R_{12}][R_{24}][R_{32}]$	-4.64/-50.87#	-5.19/-52.56	-5.83/-50.49#	-6.17/-40.87#	-6.5/-46.86#	-5.97/-45.29#
$[R_{13}][R_{24}][R_{31}]$	-4.8/-54.21#	-4.74/-35.69	-4.47/-35.36#	-5.74/-45.71!	-3.71/-39.7	-4.33/-38.32!
$[R_{13}][R_{24}][R_{32}]$	-4.17/-37.18	-5.15/-55.44	-5.07/-51.15#	-6.98/-51.17#	-4.82/-51.76	-5.71/-43.51#
$[R_{14}][R_{24}][R_{31}]$	-4.93/-57.09#	-4.89/-59.08	-3.98/-47.27#	-6.22/-46.92!	-3.99/-55.66	-4.26/-38.76!
$[R_{14}][R_{24}][R_{32}]$	-5.24/-56.18!	-4.6/-53.01	-4.67/-47.01#	-6.21/-52.12!	-4.44/-49.33	-5.88/-45.31#
$[R_{15}][R_{24}][R_{31}]$	-4.5/-52.82#	-4.66/-58.56	-3.8/-48.9#	-5.01/-47.69#	-3.76/-43.84	-4.58/-41.18#
$[R_{15}][R_{24}][R_{32}]$	-6/-56.29!	-4.83/-54.8	-4.32/-50.32#	-6.18/-50.85!	-4.39/-51.65	-5.92/-46.26#
$[R_{16}][R_{24}][R_{31}]$	-5.41/-55.08!	-5.13/-65.3	-3.37/-37.22!	-4.95/-49.41!	-4.37/-63.12	-3.89/-35.72!
$[R_{16}][R_{24}][R_{32}]$	-4.35/-43.68#	-5.15/-59.71	-5.12/-53.72#	-6.22/-53.9!	-4.72/-55.93	-5.44/-43.05#
$[R_{11}][R_{25}][R_{31}]$	-4.82/-51.66!	-4.33/-51.16	-3.56/-36.8!	-5.83/-46.75!	-3.82/-37.02	-5.38/-44.74#
$[R_{11}][R_{25}][R_{32}]$	-4.24/-43.37!	-4.11/-47.52	-5.25/-50.63#	-5.37/-41.23#	-4.43/-43.24	-6.09/-46.17#
$[R_{12}][R_{25}][R_{31}]$	-5.15/-55.04!	-3.35/-47.31	-5.22/-40.08!	-6.12/-48.57!	-4.11/-37.57	-5/-35.98!
$[R_{12}][R_{25}][R_{32}]$	-4.4/-45.34!	-4.28/-49.41	-3.47/-40.6#	-5.44/-39.87!	-5.01/-45.11	-4.74/-38.23#
$[R_{13}][R_{25}][R_{31}]$	-5.05/-53.74!	-3.74/-47.96	-3.72/-47.86#	-5.79/-50.16!	-4.16/-42.7	-4.41/-40#
$[R_{13}][R_{25}][R_{32}]$	-4.27/-45.77!	-4.13/-48.85	-4.65/-53.22#	-6.18/-44.09!	-4.39/-44.94	-5.06/-38.91#
$[R_{14}][R_{25}][R_{31}]$	-5.12/-55.23!	-3.55/-47.42	-4.17/-48.72#	-3.96/-42.99	-3.67/-57.44	-4.75/-43.61#
$[R_{14}][R_{25}][R_{32}]$	-4.77/-52.19#	-4.15/-51.37	-4.52/-53.33#	-4.32/-34.92	-4.53/-49.14	-5.18/-40.38#
$[R_{15}][R_{25}][R_{31}]$	-4.57/-55.01!	-4.73/-61.36	-3.59/-49.25#	-6.05/-53.13#	-4.46/-44.33	-4.49/-43.27#
$[R_{15}][R_{25}][R_{32}]$	-3.26/-56.6!	-2.58/-52.28	-3.13/-53.79#	-4.24/-53.13!	-2.67/-48.06	-4/-44.94#
$[R_{16}][R_{25}][R_{31}]$	-4.55/-52.85!	-5.23/-68.63	-3.11/-41.32!	-5.95/-53.31!	-4.14/-66.08	-3.15/-33.38#
$[R_{16}][R_{25}][R_{32}]$	-3.68/-51.9#	-5.23/-63.08	-5.3/-59.76#	-6.01/-58.95!	-4.38/-58.18	-4.25/-37.8!

Ligand	3.5	3.5*	3.5**	4.0	4.0*	4.0**
[R_{11}] [R_{26}] [R_{31}]	-4.4/-47.3!	-4.5/-54.01	-4.51/-53.94#	-5.25/-42.54!	-3.62/-39.87	-5.75/-49.79#
[R_{11}] [R_{26}] [R_{32}]	-4.89/-53.67!	-4.94/-53.25	-4.54/-48.92#	-6.05/-48.44!	-5.57/-41.85#	-5.53/-42.26#
[R_{12}] [R_{26}] [R_{31}]	-4.64/-50.06!	-4.43/-55.55	-5.5/-58.05#	-5.54/-45.51!	-4.16/-55.43	-5.97/-52.53#
[R_{12}] [R_{26}] [R_{32}]	-4.95/-49.38!	-4.81/-52.93	-5.62/-53.66#	-5.55/-44.89#	-4.77/-49.43	-6.01/-47.18#
[R_{13}] [R_{26}] [R_{31}]	-4.56/-50.12!	-4.68/-58.65	-4.41/-56.21#	-5.4/-45.99!	-6.71/-50#	-5.8/-51.78#
[R_{13}] [R_{26}] [R_{32}]	-5.4/-54.16#	-4.84/-55.77	-4.77/-52.89#	-5.55/-46.22#	-4.73/-52.6	-5.82/-47.74#
[R_{14}] [R_{26}] [R_{31}]	-4.22/-53.73#	-4.75/-60.6	-4.66/-57.74#	-5.15/-51.48#	-4/-57.61	-6.02/-51.31#
[R_{14}] [R_{26}] [R_{32}]	-4.41/-43.82!	-4.65/-52.69	-4.39/-49.21#	-6.52/-51.27#	-4.4/-52.44	-6.1/-45.9#
[R_{15}] [R_{26}] [R_{31}]	-5.34/-59.93#	-4.58/-60.38	-4.52/-58.33#	-4.67/-49.79#	-3.8/-58.33	-5.69/-54.41#
[R_{15}] [R_{26}] [R_{32}]	-4.69/-55.85#	-4.25/-52.28!	-4.29/-52.39#	-5.68/-51.59#	-5.84/-47.83#	-5.93/-48.24#
[R_{16}] [R_{26}] [R_{31}]	-5.29/-60.78#	-5/-66.65	-1.96/-31.36#	-4.91/-54.72#	-4.15/-64.08	-4.34/-39.56#
[R_{16}] [R_{26}] [R_{32}]	-2.61/-47.02!	-3.75/-60.65	-4.39/-59.12!	-3.36/-43.26!	-2.98/-55.83	-4.49/-48.23#
[R_{11}] [R_{27}] [R_{31}]	-4.71/-58.34!	-4.52/-55.83	-4.45/-55.58#	-5.85/-55.09#	-4.19/-40.66	-5.84/-50.81#
[R_{11}] [R_{27}] [R_{32}]	-4.75/-47.64#	-4.57/-51.09	-4.26/-48.12#	-5.04/-45.41#	-6.45/-48.34#	-6.19/-46.98#
[R_{12}] [R_{27}] [R_{31}]	-4.3/-56.99#	-5.07/-59.84#	-5.11/-59.87#	-4.57/-43.31!	-6.81/-54.73#	-6.4/-54.27#
[R_{12}] [R_{27}] [R_{32}]	-5.39/-59.76!	-5.23/-57.15	-5.45/-55.26#	-7.48/-50.59#	-6.61/-51.07#	-5.55/-46.41#
[R_{13}] [R_{27}] [R_{31}]	-3.92/-59.76!	-5.18/-60.84#	-5.09/-60.87#	-5.28/-53.05#	-6.22/-54.86#	-6.19/-54.58#
[R_{13}] [R_{27}] [R_{32}]	-5.46/-49.54!	-5.15/-58.14	-5.11/-56.66#	-6.36/-55.69!	-5.03/-53.86	-5.35/-46.57#
[R_{14}] [R_{27}] [R_{31}]	-4.5/-60.07#	-5.15/-60.99#	-5.17/-61.02#	-5.32/-56.38#	-6.38/-56.05#	-6.27/-55.08#
[R_{14}] [R_{27}] [R_{32}]	-5.37/-62.61!	-4.2/-52.52	-4.72/-52.79#	-6.52/-58.58!	-4.1/-51.2	-6.17/-47.41#
[R_{15}] [R_{27}] [R_{31}]	-5.9/-52.08!	-4.96/-61.26#	-4.94/-62.24#	-5.28/-45.71!	-6.16/-56.64#	-6.14/-56.47#
[R_{15}] [R_{27}] [R_{32}]	-4.03/-51.57#	-4.85/-56.78	-4.92/-57.9#	-6.01/-56.24!	-6.22/-51.53#	-6.37/-49.22#
[R_{16}] [R_{27}] [R_{31}]	-4.51/-55.71#	-5.12/-66.44	-5.74/-59.8#	-5.53/-56.2#	-4.05/-52.04	-5.06/-45.87#
[R_{16}] [R_{27}] [R_{32}]	-5.35/-67.19!	-5.14/-64.04	-5.6/-58.95#	-5.12/-43.35!	-4.75/-58.05	-5.34/-46.81#
[R_{11}] [R_{28}] [R_{31}]	-4.36/-44.67!	-4.84/-57.34	-3.32/-40.81!	-5.02/-38.7!	-4.12/-54.98	-4.64/-38.09!
[R_{11}] [R_{28}] [R_{32}]	-4.06/-31.46	-4.84/-51.25	-3.5/-34.94!	-6.28/-39.97#	-4.19/-35.76	-5.34/-39.21#
[R_{12}] [R_{28}] [R_{31}]	-4.61/-47.91!	-4.33/-45.61	-3.64/-42.98!	-5.4/-43.06!	-2.6/-42.63	-5.07/-41.5!
[R_{12}] [R_{28}] [R_{32}]	-4.24/-33.03	-4.1/-47.07	-5.03/-49.94#	-6.19/-42.34!	-4.43/-34.16	-5.93/-44.4#
[R_{13}] [R_{28}] [R_{31}]	-5.38/-42.27!	-4.13/-47.55	-3.68/-36.09#	-5.33/-50.58#	-4.69/-41.46	-4.54/-35.71#
[R_{13}] [R_{28}] [R_{32}]	-4.34/-45.59!	-4.95/-55.04	-4.95/-51.86#	-4.9/-29.79	-4.68/-50.9	-5.19/-38.87#

Ligand	3.5	3.5*	3.5**	4.0	4.0*	4.0**
$[R_{14}][R_{28}][R_{31}]$	-5.54/-61.34#	-4.25/-40.29	-4.22/-46.68#	-5.41/-56.64#	-4.99/-44.07#	-4.72/-42.84!
$[R_{14}][R_{28}][R_{32}]$	-4.82/-43.83#	-4.74/-51.8	-4.07/-49.69#	-5.49/-47.57#	-4.66/-51.62#	-5.43/-41.83#
$[R_{15}][R_{28}][R_{31}]$	-4.86/-55.22#	-3.86/-47.11	-4.34/-50.42#	-5.59/-51.26#	-4/-40.88	-4.55/-40.06!
$[R_{15}][R_{28}][R_{32}]$	-4.99/-48.49#	-4.77/-55.05	-4.73/-53.8#	-5.47/-40.74!	-5.74/-48.74	-5.99/-47.05#
$[R_{16}][R_{28}][R_{31}]$	-4.91/-32.12#	-5.31/-39.49	-3.75/-37.42#	-5.13/-50.98#	-4.39/-67.38	-3.09/-35.42!
$[R_{16}][R_{28}][R_{32}]$	-6.5/-61.52!	-5.28/-61.21	-4.97/-43.55!	-5.56/-45.34#	-4.8/-55.84	-5.49/-40.05!
$[R_{11}][R_{29}][R_{31}]$	-4.64/-41.82!	-3.85/-45.06	-3.52/-37.34#	-5.29/-36.75!	-4.59/-40.95	-/-
$[R_{11}][R_{29}][R_{32}]$	-3.65/-38.76!	-3.99/-40.11	-3.75/-40.26!	-6.71/-51.1!	-3.59/-34.56	-5.14/-36.31!
$[R_{12}][R_{29}][R_{31}]$	-4.75/-48.03!	-3.13/-44.76	-3.93/-38.09!	-5.43/-44.2!	-2.84/-37.62	-/-
$[R_{12}][R_{29}][R_{32}]$	-4.26/-43.16!	-3.79/-43.06	-3.7/-42.65!	-6.13/-46.61#	-4.15/-42.84	-6.18/-41.75#
$[R_{13}][R_{29}][R_{31}]$	-4.48/-46.75!	-4.15/-50.31	-3.67/-41.39#	-5.14/-34.49!	-4.82/-44.83	-/-
$[R_{13}][R_{29}][R_{32}]$	-5.01/-53.41!	-4.03/-47.12	-3.64/-44.07!	-5.45/-42.07!	-4.75/-51.25	-4.86/-40.06!
$[R_{14}][R_{29}][R_{31}]$	-4.91/-32.02!	-4.19/-45.59	-3.97/-48.6#	-6/-58.29#	-4.26/-40.03	-/-
$[R_{14}][R_{29}][R_{32}]$	-4.79/-53.97!	-3.54/-47.1	-6.4/-57.86!	-5.82/-47.9!	-3.77/-36.95	-4.39/-38.16#
$[R_{15}][R_{29}][R_{31}]$	-4.22/-48.34!	-4.03/-49.3	-3.75/-40.67#	-4.85/-42.47!	-4.71/-44.75	-/-
$[R_{15}][R_{29}][R_{32}]$	-4.72/-50.59!	-4.54/-50.43	-5.21/-60.85#	-6.64/-52.86!	-4.82/-50.04	-6.29/-50.84#
$[R_{16}][R_{29}][R_{31}]$	-4.85/-51.74#	-5.48/-73.39	-4.17/-48.12!	-5.22/-56.91#	-4.3/-71.21	-/-
$[R_{16}][R_{29}][R_{32}]$	-4.08/-49.95!	-5.36/-62.22	-3.56/-50.28!	-6.18/-43.1!	-4.51/-55.37	-4.09/-38.72!
$[R_{11}][R_{210}][R_{31}]$	-3.87/-39.14!	-4.67/-56.11	-4.06/-37.5#	-5.32/-44.41#	-4.14/-52.5	-5.58/-45.95#
$[R_{11}][R_{210}][R_{32}]$	-5.27/-52.97!	-4.94/-50.25	-4.89/-48.06#	-6.38/-48.05!	-4.68/-45.92	-6.34/-43.91#
$[R_{12}][R_{210}][R_{31}]$	-3.96/-40.62!	-5.56/-54.92#	-5.43/-54.21#	-4.86/-36.03!	-3.83/-43.07	-6.06/-49.52#
$[R_{12}][R_{210}][R_{32}]$	-4.22/-33.04	-5.8/-51.34#	-5.12/-51.3#	-4.91/-28.09	-6.66/-46.35#	-7.18/-46.45#
$[R_{13}][R_{210}][R_{31}]$	-5.25/-56.36#	-4.68/-56.75	-3.62/-39.84#	-5.7/-51.44#	-4.18/-56.62	-4.88/-38.16#
$[R_{13}][R_{210}][R_{32}]$	-5.23/-49.49#	-5.01/-55.13	-4.69/-50.13#	-6.55/-52.3!	-4.96/-51.38	-6.03/-43.09#
$[R_{14}][R_{210}][R_{31}]$	-5.34/-58.57#	-4.36/-51.25	-3.88/-48.3#	-5.83/-53.25#	-3.88/-48.74	-4.59/-39.8#
$[R_{14}][R_{210}][R_{32}]$	-5.36/-58.66!	-4.77/-50.8#	-4.26/-43.32#	-6.56/-54.56!	-6.02/-46.37#	-6.02/-46.37#
$[R_{15}][R_{210}][R_{31}]$	-4.46/-51.45#	-4.67/-60.03	-4.57/-55.63#	-5.46/-51.26#	-3.98/-44.57	-6.37/-54.69#
$[R_{15}][R_{210}][R_{32}]$	-5.13/-57.89!	-6.67/-54.3	-4.54/-51.89#	-6.19/-52.99!	-4.64/-51.25	-5.53/-46.41#
$[R_{16}][R_{210}][R_{31}]$	-4.6/-55.39#	-5.07/-65.24	-3.53/-38.32!	-6/-53.14#	-4.17/-62.85	-4.02/-34.61!
$[R_{16}][R_{210}][R_{32}]$	-4.59/-50.56!	-4.95/-58.62	-3.91/-46.54!	-6.32/-56.49!	-4.73/-54.95	-4.82/-36.79!

E.4 Main Structure 4

Ligand	3.0	3.5*	3.5**	4.0	4.0*	4.0**
$[R_{11}][R_{21}][R_{31}]$	-5.28/-43.15	-5.1/-40.71	-5.13/-34.41!	-5.39/-46.88	-4.31/-36.81	-/-
$[R_{11}][R_{21}][R_{32}]$	-4.94/-35.51	-4.68/-30.43	-4.34/-28.64!	-6.6/-36.83#	-5.83/-31.8	-6.73/-35.31#
$[R_{12}][R_{21}][R_{31}]$	-5.33/-44.6	-4.1/-30.84	-3.7/-28.15!	-3.29/-30.44	-4.78/-33.81	-/-
$[R_{12}][R_{21}][R_{32}]$	-4.95/-29.4#	-5.21/-37.59	-3.65/-23.73!	-6.91/-36.38#	-5.08/-35.39	-5.01/-26.11#
$[R_{13}][R_{21}][R_{31}]$	-5.86/-46.7#	-5.01/-39.09	-5.19/-36.4!	-5.82/-47.45#	-4.49/-35.52	-/-
$[R_{13}][R_{21}][R_{32}]$	-5.52/-39.66	-4.78/-37.13	-5.67/-37.35!	-6.78/-41.08#	-5.55/-37.17	-5.25/-27.86!
$[R_{14}][R_{21}][R_{31}]$	-4.2/-32.86	-4.74/-38.49	-5.27/-40.96!	-4.03/-33.11	-5.01/-38.96	-/-
$[R_{14}][R_{21}][R_{32}]$	-5.31/-42.02	-5.24/-40.84	-5.33/-39.84!	-4.98/-42.06	-4.7/-37.89	-6.44/-34.91!
$[R_{15}][R_{21}][R_{31}]$	-5.16/-42.84	-4.09/-33.57	-5.05/-38.87!	-5.64/-46.64#	-4.51/-39.37	-/-
$[R_{15}][R_{21}][R_{32}]$	-5.28/-42.18	-4.95/-40.07	-5.24/-41.54!	-5.21/-40.62	-4.76/-38.6	-5.7/-32.63!
$[R_{16}][R_{21}][R_{31}]$	-5.86/-50.39	-4.48/-38.81	-5.27/-45.57!	-4.21/-45.41	-4.83/-40.29	-/-
$[R_{16}][R_{21}][R_{32}]$	-5.04/-43.51	-4.78/-41.38	-5.15/-42.74!	-4.68/-42.57	-4.51/-39.87	-6.2/-36.24!
$[R_{11}][R_{22}][R_{31}]$	-6.23/-39.35	-4.8/-39.33	-3.27/-24.85!	-6.34/-46.41#	-3.68/-38.73	-/-
$[R_{11}][R_{22}][R_{32}]$	-5.64/-41.89	-5.26/-39.21	-2.7/-20.91!	-4.86/-39.21	-5.2/-38.02	-4.48/-30.48#
$[R_{12}][R_{22}][R_{31}]$	-5.4/-49.5#	-4.91/-35.82	-4.53/-43.24#	-3.87/-37.92	-4.45/-37.31	-/-
$[R_{12}][R_{22}][R_{32}]$	-4.64/-34.69	-5.41/-41.12	-2.89/-20.06#	-6.64/-42.33#	-5.29/-39.06	-4.7/-26.55!
$[R_{13}][R_{22}][R_{31}]$	-5.54/-49.57	-5.08/-40.91	-4.46/-41.49!	-5.29/-50.06	-4.86/-39.22	-/-
$[R_{13}][R_{22}][R_{32}]$	-5.73/-40.91	-4.43/-38.7	-4.14/-36.55!	-3.48/-35.43	-5.12/-40.51	-5.47/-36.1!
$[R_{14}][R_{22}][R_{31}]$	-5.52/-48.63#	-5.06/-42.93	-4.67/-28.77#	-6.48/-55.95#	-4.96/-43.84	-/-
$[R_{14}][R_{22}][R_{32}]$	-5.58/-46.52	-5.04/-43.15	-4.6/-23.67#	-4.97/-46.22	-4.96/-41.7	-4.15/-26.73#
$[R_{15}][R_{22}][R_{31}]$	-5.47/-49.43	-4.57/-39.42	-2.47/-21.64!	-5.08/-49.28	-4.12/-41.85	-/-
$[R_{15}][R_{22}][R_{32}]$	-5.45/-49.09	-5.13/-42.97	-3.9/-35.19!	-4.9/-45.46	-4.81/-41.92	-4.4/-30.58!
$[R_{16}][R_{22}][R_{31}]$	-4.68/-46.27!	-4.69/-42.54	-3.91/-37.09!	-3.96/-40.46	-4.2/-40.6	-/-
$[R_{16}][R_{22}][R_{32}]$	-3.78/-46.01	-2.95/-39.26	-3.04/-40.15!	-3.38/-45.54	-3.06/-40.05	-2.74/-33.96#
$[R_{11}][R_{23}][R_{31}]$	-4.82/-41.18#	-5.21/-41.47	-3.51/-32.74!	-5.58/-41.61!	-5.56/-43.18	-/-
$[R_{11}][R_{23}][R_{32}]$	-4.86/-38.66!	-4.19/-36.62	-4.06/-31.54!	-5.71/-36.07!	-5.25/-37.65	-4.28/-31.87!
$[R_{12}][R_{23}][R_{31}]$	-4.07/-34.83	-4.62/-38.59	-4.59/-43.57!	-6.05/-52.7#	-4.31/-40.26	-/-
$[R_{12}][R_{23}][R_{32}]$	-5.95/-43.16!	-5.04/-41.43	-3.71/-34.72!	-7.01/-49.88#	-5.06/-42	-4.01/-32.39!
$[R_{13}][R_{23}][R_{31}]$	-5.61/-55.42#	-5.16/-45.7	-4.59/-45.44!	-4.81/-37.18#	-3.85/-43.6	-/-
$[R_{13}][R_{23}][R_{32}]$	-3.88/-43.41	-3.8/-44.47	-2.54/-36.84!	-3.97/-45.88	-3.74/-43.81	-3.36/-34.28!

Ligand	3.5	3.5*	3.5**	4.0	4.0*	4.0**
$[R_{14}][R_{23}][R_{31}]$	-5.36/-47.24	-5.33/-51.89	-4.69/-37.86#	-5.75/-45.19#	-4.41/-48.84	-/-
$[R_{14}][R_{23}][R_{32}]$	-5.65/-45.69	-5.29/-46.63	-4.59/-39.46!	-5.42/-46.51	-4.89/-45.12	-4.21/-31.48!
$[R_{15}][R_{23}][R_{31}]$	-5.74/-51.86	-4.08/-39.15	-2.15/-10.38!	-5.05/-51.63	-4.15/-38.33	-/-
$[R_{15}][R_{23}][R_{32}]$	-3.45/-45.46	-3.54/-46.45	-1.48/-27.3!	-3.44/-44.49	-3.54/-46.33	-2.49/-31.23!
$[R_{16}][R_{23}][R_{31}]$	-5.85/-57.38!	-4.96/-40.78	-2.91/-23.91!	-6.65/-55.46#	-4.45/-40.35	-/-
$[R_{16}][R_{23}][R_{32}]$	-5.37/-47.67	-5.17/-47.75	-3.4/-28.44!	-5/-47.62	-4.76/-46.86	-3.37/-27.85!
$[R_{11}][R_{24}][R_{31}]$	-5.41/-42.53#	-3.97/-34.95	-4.04/-34.58!	-6.25/-42.62!	-4.46/-38.51	-5.1/-33.03!
$[R_{11}][R_{24}][R_{32}]$	-5.14/-39.31	-5.1/-39.67	-4.97/-33.94#	-5.18/-40	-5.39/-37	-5.78/-35.39#
$[R_{12}][R_{24}][R_{31}]$	-4.73/-30.6!	-3.86/-29.76	-4.34/-36.83!	-6.4/-43.5!	-4.84/-33.83	-5.34/-35.69!
$[R_{12}][R_{24}][R_{32}]$	-5.4/-39.98	-5.23/-38.69	-5.27/-45.32#	-5.26/-39.76	-5.31/-37.77	-5.85/-38.02#
$[R_{13}][R_{24}][R_{31}]$	-5.36/-48.77	-4.68/-36.72	-4.47/-37.76!	-6.29/-41.65#	-4.41/-36.55	-3.94/-26.75!
$[R_{13}][R_{24}][R_{32}]$	-5.36/-41.11	-5.26/-41.23	-2.76/-19.65!	-5.02/-41.03	-5.29/-38.57	-5.37/-28.21#
$[R_{14}][R_{24}][R_{31}]$	-5.39/-50.66	-3.94/-33.49	-3.87/-34.34#	-5.67/-56.06	-4.77/-35	-5.04/-37.78!
$[R_{14}][R_{24}][R_{32}]$	-5.27/-43.24	-4.09/-36.26	-2.67/-23.69#	-5.79/-42.79	-5.5/-40.19	-4.87/-29.36#
$[R_{15}][R_{24}][R_{31}]$	-3.68/-42.29#	-2.29/-36.27	-2.36/-38.41!	-3.05/-42.98	-2.04/-40.42	-2.89/-35.26!
$[R_{15}][R_{24}][R_{32}]$	-5.15/-41.37	-4.91/-42.2	-4.39/-35.91#	-4.75/-42.18	-4.95/-39.9	-6.1/-36.55#
$[R_{16}][R_{24}][R_{31}]$	-5.72/-62.74	-4.17/-41.09	-4.09/-33.32!	-5.21/-46.04#	-4.43/-42.19	-3.93/-30.98!
$[R_{16}][R_{24}][R_{32}]$	-3.42/-46.47	-3.32/-44.62	-2.4/-32.76!	-2.97/-45.03	-3.4/-43.33	-3.63/-36.48#
$[R_{11}][R_{25}][R_{31}]$	-4.16/-44.91#	-2.8/-36.34	-2.67/-31.61!	-3.83/-40.41!	-3.92/-41.29	-2.98/-34.66!
$[R_{11}][R_{25}][R_{32}]$	-4.1/-34.35	-4.68/-38.88	-3.29/-31.14!	-4.74/-41.97	-4.96/-36.69	-5.78/-35.3#
$[R_{12}][R_{25}][R_{31}]$	-4.65/-36.61	-4.51/-38.15	-4.33/-39.1!	-5.46/-37.03!	-4.62/-39.32	-4.7/-34.36!
$[R_{12}][R_{25}][R_{32}]$	-5.29/-42.64	-4.92/-40.1	-3.31/-32.34!	-4.86/-40.93	-4.9/-37.7	-3.66/-22.77!
$[R_{13}][R_{25}][R_{31}]$	-5.26/-46.64!	-4.57/-40.09	-4.02/-36.3#	-4.66/-42.01!	-3.86/-38.86	-4.89/-33.74!
$[R_{13}][R_{25}][R_{32}]$	-3.74/-44.34	-3.44/-41.95	-1.6/-34.99!	-3.75/-43.38	-3.35/-38.62	-3.14/-28.41#
$[R_{14}][R_{25}][R_{31}]$	-6.21/55.53	-4.22/-39.44	-2.52/-25.94#	-5.38/-56.08	-4.02/-43.81	-3.8/-32.12!
$[R_{14}][R_{25}][R_{32}]$	-3.48/-47.84	-3.28/-43.23	-2.21/-37.74!	-3.83/-46.8	-2.93/-40.85	-2.37/-26.71!
$[R_{15}][R_{25}][R_{31}]$	-3.77/-38.91	-4.53/-38.87	-3.84/-39.66!	-4.66/-42.7!	-4.31/-40.11	-3.86/-33.2!
$[R_{15}][R_{25}][R_{32}]$	-3.19/-44.86	-2.72/-41.15	-1.38/-34.41!	-2.34/-44.41	-2.76/-38.03	-2.33/-33.69!
$[R_{16}][R_{25}][R_{31}]$	-4.94/-49.3#	-4.28/-39.18	-4.51/-27.84#	-5.21/-47.19#	-4.39/-43.81	-4.52/-32.56#
$[R_{16}][R_{25}][R_{32}]$	-5.05/-45.46	-4.75/-45.28	-3.66/-40.52!	-4.6/-49.27	-4.56/-43.03	-5.41/-38.42#

Ligand	3.5	3.5*	3.5**	4.0	4.0*	4.0**
$[R_{11}][R_{26}][R_{31}]$	-4.94/-45.46#	-4.21/-37.34	-3.55/-29.89!	-5.1/-44.99	-3.4/-34.19	-4.24/-28.99#
$[R_{11}][R_{26}][R_{32}]$	-4.6/-38.17	-4.58/-35.66	-5.88/-43.84#	-3.74/-12.87!	-4.37/-33.55	-6.52/-35.98#
$[R_{12}][R_{26}][R_{31}]$	-5.34/-47.83#	-4.32/-39.94	-3.62/-31.86!	-5.85/-40.61!	-4.83/-40.41	-4.69/-34.43#
$[R_{12}][R_{26}][R_{32}]$	-4.64/-39.12	-4.53/-36.4	-4.24/-37.04#	-4.78/-36.92	-5.37/-32.69	-4.19/-27.3!
$[R_{13}][R_{26}][R_{31}]$	-4.36/-46.16	-2.96/-41.52	-2.43/-31.79#	-4.84/-45.86#	-3.07/-35.17	-2.56/-28.81!
$[R_{13}][R_{26}][R_{32}]$	-4.8/-38.51	-4.39/-37.03	-5.51/-33.21#	-6.57/-39.27#	-5.21/-37.1	-3.28/-24.61#
$[R_{14}][R_{26}][R_{31}]$	-5.09/-38.7!	-3.72/-40.36	-3.01/-25.3#	-6.19/-42.8!	-5.32/-47.7	-3.88/-29.33#
$[R_{14}][R_{26}][R_{32}]$	-2.65/-41.19	-1.68/-30.47	-2.39/-30.79#	-3.66/-43.43	-2.22/-37.2	-3.43/-30.2#
$[R_{15}][R_{26}][R_{31}]$	-4.15/-56.19	-4.25/-52.28	-3.01/-45.92#	-3.69/-41.19!	-2.66/-41.93	-2.14/-33.11#
$[R_{15}][R_{26}][R_{32}]$	-2.69/-40.75	-1.62/-38.46	-2.68/-40.65!	-2.5/-41.81	-2.2/-37.6	-3.49/-37.85!
$[R_{16}][R_{26}][R_{31}]$	-4.22/-45.95#	-4.22/-42.2	-4.36/-42.53!	-5.06/-47.14#	-4.13/-42.18	-3.1/-28.05#
$[R_{16}][R_{26}][R_{32}]$	-2.35/-44.39	-2.43/-38.56	-3.13/-42.8!	-2.39/-44.39	-3.21/-41.57	-3.86/-43.91#
$[R_{11}][R_{27}][R_{31}]$	-5.71/-50.79	-4.58/-42.23	-4.4/-37.47#	-3.6/-35.7	-4.83/-38.61	-4.38/-36.22!
$[R_{11}][R_{27}][R_{32}]$	-4.91/-37.28#	-4.83/-37.89	-5.98/-44.72#	-5.58/-30.87!	-5.1/-39.59	-6.04/-36.91#
$[R_{12}][R_{27}][R_{31}]$	-5.96/-49.2#	-4.73/-73.06	-4.23/-40.68!	-6.2/-50.37#	-4.76/-43.44	-4.89/-37.21!
$[R_{12}][R_{27}][R_{32}]$	-5.71/-44.68	-4.94/-38.5	-3.61/-30.93!	-3.29/-33.91	-5.4/-40.26	-4.49/-32.06#
$[R_{13}][R_{27}][R_{31}]$	-5.87/-49.78	-4.6/-43.77	-3.99/-36.37#	-6.01/-53.1	-4.92/-45.1	-4.19/-32.64!
$[R_{13}][R_{27}][R_{32}]$	-5.45/-45.3	-4.73/-40.92	-3.43/-25.71#	-4.34/-30.76	-4.35/-35.88	-4.42/-31.76!
$[R_{14}][R_{27}][R_{31}]$	-5.81/-51.96#	-5.05/-41.16	-3.22/-26.77#	-6.01/-49.67#	-4.61/-42.64	-3.56/-33.74#
$[R_{14}][R_{27}][R_{32}]$	-2.88/-43.96	-3.52/-45.5	-2.27/-32.07#	-3.38/-44.27	-2.42/-37.59	-2.16/-30.87!
$[R_{15}][R_{27}][R_{31}]$	-5.63/-52.17	-4.51/-44.4	-3.83/-40.82!	-5.02/-50.37	-4.81/-45.72	-4.91/-39.76!
$[R_{15}][R_{27}][R_{32}]$	-2.55/-42.33	-2.8/-39.68	-2.36/-37.93#	-3.37/-41.42	-2.29/-37.04	-3.36/-32.53#
$[R_{16}][R_{27}][R_{31}]$	-5.1/-49.74#	-5.37/-50.51	-3.41/-35.12!	-6.9/-55.72!	-4.5/-44.25	-4.1/-37.73!
$[R_{16}][R_{27}][R_{32}]$	-2.88/-45.89	-2.91/-42.75	-1.05/-28.79!	-3.04/-45.7	-2.74/-42.23	-2.07/-31.63!
$[R_{11}][R_{28}][R_{31}]$	-5.07/-44.47#	-4.36/-33.55	-3.62/-21.35!	-4.84/-43.08	-4.83/-35.73	-5.41/-35.01!
$[R_{11}][R_{28}][R_{32}]$	-4.67/-36.92	-5.05/-37.44	-3.48/-30.15!	-4.83/-38.83	-5.23/-35.47	-4.04/-26.64#
$[R_{12}][R_{28}][R_{31}]$	-4.54/-32.32	-4.5/-33.21	-2.79/-3.5!	-5.17/-32.21!	-4.48/-33.81	-5.61/-39.39!
$[R_{12}][R_{28}][R_{32}]$	-4.64/-32.87!	-5.29/-38.74	-5.35/-44.87#	-6.06/-32.93!	-5.37/-36.71	-5.49/-38.08#
$[R_{13}][R_{28}][R_{31}]$	-5.29/-48.14	-5.03/-37.36	-4.37/-35.8#	-5.27/-33.61#	-3.89/-36.56	-4.9/-29.56#
$[R_{13}][R_{28}][R_{32}]$	-4.84/-39.83	-5.16/-39.55	-3.77/-32.95!	-5.7/-42.26	-5.09/-37.08	-4.74/-28.02#

Ligand	3.5	3.5*	3.5**	4.0	4.0*	4.0**
$[R_{14}][R_{28}][R_{31}]$	-5.16/-41.59	-4.7/-41.68	-4.01/-20.08#	-4.97/-49.5	-4.64/-36.04	-3.39/-20.13!
$[R_{14}][R_{28}][R_{32}]$	-5.73/-42.91#	-5.05/-41.26	-4.99/-37.4!	-4.82/-41.04	-5.01/-39.81	-3.85/-29.41#
$[R_{15}][R_{28}][R_{31}]$	-4.02/-49.69	-2.82/-39.05	-2.59/-36.37#	-4.45/-46.66#	-2.55/-39.94	-2.72/-33.89!
$[R_{15}][R_{28}][R_{32}]$	-5.08/-42.85	-4.92/-41.51	-5.17/-39.17#	-4.56/-42.54	-4.79/-38.98	-5.54/-37.28#
$[R_{16}][R_{28}][R_{31}]$	-5.26/-50.15	-4/-38.39	-5.68/-40.28!	-567/-47.41#	-4.17/-38.83	-3.56/-54.52#
$[R_{16}][R_{28}][R_{32}]$	-3.28/-42.71	-3/-41.28	-2.97/-38.21!	-3.06/-43.98	-2.83/-41.82	-1.97/-29.56#
$[R_{11}][R_{29}][R_{31}]$	-4.44/-39.35	-3.78/-35.59	-3.53/-28.57!	-5.59/-53.36	-4.69/-43.19	-/-
$[R_{11}][R_{29}][R_{32}]$	-4.47/-38.33	-5.24/-41.19	-3.65/-34.68!	-4.49/-39.18	-4.95/-37.11	-6.23/-35.17#
$[R_{12}][R_{29}][R_{31}]$	-6.3/-52.95	-3.96/-37.41	-3.39/-30.31!	-5.09/-43.99	-4.51/-35.7	-/-
$[R_{12}][R_{29}][R_{32}]$	-4.77/-38.04	-5.47/-41.31	-3.68/-30.8!	-4.9/-30.59#	-5.28/-36.03	-4.78/-35.13!
$[R_{13}][R_{29}][R_{31}]$	-5.85/-52.31	-5.05/-35.4	-4.78/-43.73!	-5.72/-51.02	-4.75/-38.92	-/-
$[R_{13}][R_{29}][R_{32}]$	-5.04/-43.56	-5.35/-43.64	-4.02/-35.51!	-6.83/-42.36#	-4.92/-39.25	-5.04/-33.39!
$[R_{14}][R_{29}][R_{31}]$	-4.91/-44.76	-4.19/-43.14	-2.72/-21.98!	-6.01/-54.85	-3.75/-40.58	-/-
$[R_{14}][R_{29}][R_{32}]$	-4.06/-47.75	-3.98/-45.86	-1.8/-30.07!	-3.7/-47.88	-3.25/-39.5	-2.32/-30.18!
$[R_{15}][R_{29}][R_{31}]$	-5.21/-46.13	-4.09/-41.3	-2.92/-25.18!	-5.66/-43.55#	-4.29/-40.1	-/-
$[R_{15}][R_{29}][R_{32}]$	-3.66/-43.77	-3.75/-45.67	-2.37/-40.55#	-3.67/-42.81	-3.83/-44.32	-3.6/-36.2#
$[R_{16}][R_{29}][R_{31}]$	-5.3/-48.89#	-4.52/-42.49	-3.38/-25.59#	-4.16/-49.56	-4.37/-44.34	-/-
$[R_{16}][R_{29}][R_{32}]$	-5.38/-46.01	-5.29/-45.53	-3.1/-29.91!	-5.02/-46.16	-5.26/-45.35	-4.71/-31.64#
$[R_{11}][R_{210}][R_{31}]$	-5.86/-46.19	-4.34/-34.63	-3.79/-34.99!	-6.31/-46.02#	-4.57/-35.89	-4.35/-29.88!
$[R_{11}][R_{210}][R_{32}]$	-4.59/-37.33	-4.67/-35.57	-5.87/-40.85#	-4.66/-37.16	-4.91/-33.66	-6.62/-35.46#
$[R_{12}][R_{210}][R_{31}]$	-5.89/-50.77	-4.69/-37.92	-3.11/-25.85!	-4.63/-28.53!	-4.3/-37.61	-5.02/-37.34!
$[R_{12}][R_{210}][R_{32}]$	-4.99/-37.86	-4.97/-36.44	-3.96/-31.08!	-5.4/-37.02	-4.78/-34.82	-5.18/-29.08!
$[R_{13}][R_{210}][R_{31}]$	-5.57/-45.9#	-3.85/-35.63	-3.84/-39.01!	-6.73/-45.42#	-4.49/-36.74	-5.25/-33.05#
$[R_{13}][R_{210}][R_{32}]$	-4.2/-34.91	-4.72/-37.17	-3.41/-31.46!	-4.74/-41.36	-4.7/-35.72	-5.22/-28.57#
$[R_{14}][R_{210}][R_{31}]$	-5.89/-48.71#	-4.17/-35.72	-4.18/-35.77#	-6.1/-49.47#	-4.41/-38.05	-4.79/-37.06!
$[R_{14}][R_{210}][R_{32}]$	-4.13/-38.77	-4.68/-39.28	-4.28/-32.03#	-6.65/-42.04#	-4.46/-37.78	-5.89/-39.28#
$[R_{15}][R_{210}][R_{31}]$	-3.59/-44.72	-3.3/-37.24	-2.21/-34.29#	-3.26/-43.26	-2.64/-36.65	-3.32/-34.54#
$[R_{15}][R_{210}][R_{32}]$	-4.32/-38.27	-4.54/-38.99	-5.33/-47.5!	-5.38/-39.64	-4.52/-37.15	-5.47/-34.7!
$[R_{16}][R_{210}][R_{31}]$	-5.61/-48.68#	-4.25/-43.14	-5.37/-51.8!	-5.58/-57.17	-3.84/-40.3	-4.75/-39.49!
$[R_{16}][R_{210}][R_{32}]$	-2.41/-40.39	-2.61/-39.57	-3.94/-48.66!	-3.02/-45.21	-2.56/-39.3	-4.61/-39.09!

E.5 Main Structure 5

Ligand	3.0	3.5*	3.5**	4.0	4.0*	4.0**
$[R_{11}][R_{21}][R_{31}]$	-4.95/-41.52	-4.66/-38.37	-3.24/-30.23!	-4.3/-41.69	-4.93/-37.1	-/-
$[R_{11}][R_{21}][R_{32}]$	-5.47/-38.65	-5.91/-40.83	-5.11/-33.45!	-4.27/-38.97	-5.92/-39.26	-5.52/-33.59#
$[R_{12}][R_{21}][R_{31}]$	-5.2/-43.4	-4.66/-37.68	-4.05/-35.94!	-4.45/-42.9	-4.75/-36.93	-/-
$[R_{12}][R_{21}][R_{32}]$	-4.86/-26.75#	-6.2/-39.44	-3.61/-23.94!	-4.23/-26.37	-5.94/-38.94	-6.05/-30.7#
$[R_{13}][R_{21}][R_{31}]$	-6.01/-45.53#	-4.9/-40.48	-3.66/-34.22!	-6.26/-3.47#	-4.03/-37.15	-/-
$[R_{13}][R_{21}][R_{32}]$	-5.79/-45.51#	-6.05/-43.22	-3.62/-32.57#	-5.46/-40.23	-6.24/-42.87	-4.59/-26.07!
$[R_{14}][R_{21}][R_{31}]$	-5.67/-47.62#	-4.4/-39.33	-3.85/-28.78#	-4.72/-45.57	-4.87/-41.57	-/-
$[R_{14}][R_{21}][R_{32}]$	-4.5/-40.26	-5.77/-42.36	-4.58/-35.34#	-6.31/-36.28#	-5.88/-41.93	-5.46/-27.53#
$[R_{15}][R_{21}][R_{31}]$	-4.8/-44.58	-5.04/-36.62	-2.4/-25.61!	-4.3/-45.29	-4.51/-39.12	-/-
$[R_{15}][R_{21}][R_{32}]$	-4.85/-42.69	-5.71/-44	-5.24/-45.85!	-4.45/-43.7	-5.78/-43.3	-5.35/-29.41!
$[R_{16}][R_{21}][R_{31}]$	-5.18/-48.52	-5.05/-43.66	-4.51/-33.04!	-4.67/-48.46	-3.63/-43.48	-/-
$[R_{16}][R_{21}][R_{32}]$	-5.01/-46.17	-5.74/-46.33	-5.63/-43.68!	-4.43/-40.32	-5.76/-45.82	-5.46/-32.65
$[R_{11}][R_{22}][R_{31}]$	-5.33/-36.57	-4.82/-38.4	-4.07/-36.42!	-3.57/-27.36	-5.4/-40.22	-/-
$[R_{11}][R_{22}][R_{32}]$	-5.28/-38.86	-5.81/-43.28	-3.75/-33.51!	-5.21/-39.47	-5.82/-42.08	-4.93/-32.08!
$[R_{12}][R_{22}][R_{31}]$	-4.86/-41.13#	-4.61/-38.06	-3.65/-35.91!	-3.67/-33.33	-4.34/-35.41	-/-
$[R_{12}][R_{22}][R_{32}]$	-5.01/-29.97!	-5.95/-42.05	-2.87/-23.98!	-4.56/-35.25	-4.38/-33.48	-5.71/-31.75#
$[R_{13}][R_{22}][R_{31}]$	-5.47/-50.53	-4.36/-39.07	-3.76/-36.08!	-5.36/-51.94	-4.26/-39.06	-/-
$[R_{13}][R_{22}][R_{32}]$	-5.7/-43.76	-6.36/-44.19	-3.63/-36.36!	-5.32/-38.67	-5.85/-44.62	-5.42/-36.17!
$[R_{14}][R_{22}][R_{31}]$	-5.03/-49.4	-4.61/-41.12	-5.3/-40.93!	-4.63/-50.68	-4.48/-41.39	-/-
$[R_{14}][R_{22}][R_{32}]$	-5.48/-44.78	-5.52/-41.62	-5.36/-47.97#	-4.88/-49	-5.73/-46.15	-5.64/-34.19#
$[R_{15}][R_{22}][R_{31}]$	-4.94/-44.39	-5.16/-41.89	-3.67/-37.96!	-4.88/-47.07	-4.89/-41.13	-/-
$[R_{15}][R_{22}][R_{32}]$	-5.19/-43.6	-5.71/-46.74	-5.42/-42.13#	-4.56/-45.42	-5.79/-46.97	-3.84/-30.93!
$[R_{16}][R_{22}][R_{31}]$	-5.4/-52.63	-4.75/-44.82	-2.61/-29.7#	-4.71/-52.26	-4.5/-43.72	-/-
$[R_{16}][R_{22}][R_{32}]$	-3.93/-48.67	-3.86/-46.59	-3.41/-36.22!	-2.78/-45.87	-3.3/-47.16	-2.08/-31.55#
$[R_{11}][R_{23}][R_{31}]$	-4.64/-37.94	-5.75/-40.57	-2.78/-16.38!	-4.96/-43.19!	-3.43/-35.09	-/-
$[R_{11}][R_{23}][R_{32}]$	-4.98/-37.25!	-4.61/-41.17	-4.04/-34.19!	-5.85/-39.56#	-4.22/-37.6	-4.84/-30.6!
$[R_{12}][R_{23}][R_{31}]$	-4.44/-39.28	-4.56/-33.52	-4.07/-42.02!	-6.03/-35.47#	-3.94/-34.46	-/-
$[R_{12}][R_{23}][R_{32}]$	-3.4/-34.59#	-3.37/-32.63	-3.75/-37.19!	-4.51/-52.56	-4.49/-39.96	-4.91/-33.77!
$[R_{13}][R_{23}][R_{31}]$	-4.42/-39.54	-5.74/-49.16	-3.71/-36.71!	-4.51/-52.56	-4.9/-44.5	-/-
$[R_{13}][R_{23}][R_{32}]$	-3.27/-46.19	-3.18/-42.6	-2.34/-39.5!	-4.35/-48.62	-4.13/-42.44	-3.21/-33.49!

Ligand	3.5	3.5*	3.5**	4.0	4.0*	4.0**
$[R_{14}][R_{23}][R_{31}]$	-5.45/-54.51	-5.37/-48.97	-2.99/-26.71#	-6.89/-56.96#	-4.33/-38.44	-/-
$[R_{14}][R_{23}][R_{32}]$	-5.84/-49.68	-4.41/-36.9	-3.72/-41.37!	-6.05/-47.38#	-4.48/-43.83	-5.39/-38.76#
$[R_{15}][R_{23}][R_{31}]$	-5.26/-42.46	-3.39/-35.45	-4.23/-43.66!	-5.08/-53.73	-3.57/-38.57	-/-
$[R_{15}][R_{23}][R_{32}]$	-3.66/-46.8	-3.76/-46.16	-3.55/-40.6#	-3.26/-42.27	-2.6/-37.21	-4.03/-36.63#
$[R_{16}][R_{23}][R_{31}]$	-5.46/-55.15	-6.03/-57.06	-4.06/-42.35!	-6.15/-52.47!	-4.07/-50.63	-/-
$[R_{16}][R_{23}][R_{32}]$	-4.79/-46.35	-4.79/-40.22	-3.51/-36.73!	-6.13/-43.91!	-4.03/-41.47	-4.6/-33.93#
$[R_{11}][R_{24}][R_{31}]$	-5.64/-47.92	-5.5/-43.14	-4.19/-37.75#	-6.71/-41.8!	-4.72/-40.69	-5.3/-36.84!
$[R_{11}][R_{24}][R_{32}]$	-5.08/-38.03	-4.79/-36.67	-6.05/-47.26#	-6.95/-42.55#	-5.55/-36.35	-6.36/-37.88#
$[R_{12}][R_{24}][R_{31}]$	-4.57/-36.86!	-5.4/-45.13	-5.16/-39.06#	-6/-37.52!	-5.02/-44.39	-5.23/-37.83!
$[R_{12}][R_{24}][R_{32}]$	-5.38/-38.16	-5.2/-39.16	-3.36/-32.99!	-6.4/-39.12!	-4.93/-40.34	-6.2/-35.73#
$[R_{13}][R_{24}][R_{31}]$	-5.59/-47.55	-5.18/-44.37	-4.09/-38.39!	-5.46/-54.68	-5.57/-45.05	-5.59/-42.26!
$[R_{13}][R_{24}][R_{32}]$	-5.15/-40.95	-5.61/-37.28	-2.91/-25.94#	-5.1/-41.97	-4.79/-36.71	-4.64/-31.84#
$[R_{14}][R_{24}][R_{31}]$	-6.13/-46.97!	-4.5/-40.65	-3.79/-40.15!	-6.37/-54.61#	-4.23/-38.47	-4.79/-34.3!
$[R_{14}][R_{24}][R_{32}]$	-5.51/-43.53	-5.16/-43.2	-3.87/-12.98#	-5.72/-43.66!	-5.64/-38.88	-4.61/-33.01#
$[R_{15}][R_{24}][R_{31}]$	-4.68/-58.28	-3.52/-44.95	-2.24/-37.43!	-3.66/-50.03	-3.92/-45.96	-3.03/-33.85!
$[R_{15}][R_{24}][R_{32}]$	-5.34/-41.72	-5.6/-41.95	-4.27/-43.12#	-5.28/-41.49	-5.34/-42.32	-3.88/-29.47#
$[R_{16}][R_{24}][R_{31}]$	-5.19/-48.04#	-5.71/-51.2	-4.61/-33.11#	-5.96/-48.95#	-4.48/-41.34	-5.09/-39.66#
$[R_{16}][R_{24}][R_{32}]$	-3.52/-47.71	-4.05/-45.84	-3.06/-39.12#	-3.54/-43.91	-3.46/-39.62	-2.1/-33.31!
$[R_{11}][R_{25}][R_{31}]$	-3.12/-40.86	-3.59/-44.37	-2.44/-35.93!	-5.25/-44.57!	-3.1/-45.21	-3.89/-38.51!
$[R_{11}][R_{25}][R_{32}]$	-5.08/-38.06	-5.26/-42.63	-3.22/-33.39!	-5.18/-35.9	-5.23/-40.8	-6.72/-45.77#
$[R_{12}][R_{25}][R_{31}]$	-5.12/-44.35!	-5.04/-43.36	-4.16/-36.05!	-6.14/-39.39!	-4.56/-44.65	-5.69/-39.81!
$[R_{12}][R_{25}][R_{32}]$	-4.83/-39.75	-5.31/-39.71	-2.89/-25.96!	-3.5/-34.15	-5.13/-38.64	-6.1/-33.14#
$[R_{13}][R_{25}][R_{31}]$	-6.31/-59.68	-4.41/-37.97	-3.96/-35.58#	-3.29/-45.96	-5.04/-44.71!	-5.33/-38.69#
$[R_{13}][R_{25}][R_{32}]$	-3.87/-48.85	-3.89/-45.06	-1.83/-38.52!	-3.9/-44.13	-2.98/-40.37	-2.6/-28.16!
$[R_{14}][R_{25}][R_{31}]$	-5.96/-57.83	-4.05/-38.17	-5.27/-40.55#	-5.28/-56.86	-2.8/-43.81	-5.08/-42.13#
$[R_{14}][R_{25}][R_{32}]$	-3.79/-50.02	-2.52/-41.01	-2.85/-39.54#	-3.2/-49.12	-2.83/-42.09	-2.76/-34.09#
$[R_{15}][R_{25}][R_{31}]$	-6.11/-58.74	-3.07/-32.76	-4.66/-35.51#	-5.54/-56.41	-3.68/-34.17	-4.66/-43.82!
$[R_{15}][R_{25}][R_{32}]$	-3.42/-49.74	-3.26/-43.57	-1.71/-35.83#	-2.92/-48.79	-3.1/-44.26	-2.62/-34.37#
$[R_{16}][R_{25}][R_{31}]$	-6.17/-61.06	-5.85/-54.85	-5.16/-37.47#	-4.54/-54.84	-4.46/-57.13	-5.33/-42.85#
$[R_{16}][R_{25}][R_{32}]$	-5.2/-51.96	-3.32/-37.35	-4.55/-39.92#	-3.33/-45.33	-4.63/-49.93	-4.53/-35.43#

Ligand	3.5	3.5*	3.5**	4.0	4.0*	4.0**
$[R_{11}][R_{26}][R_{31}]$	-4.29/-28.89	-4.22/-34.09	-3.66/-37.88#	-4.56/-34.15	-4.72/-33.42	-4.08/-35.47!
$[R_{11}][R_{26}][R_{32}]$	-5.13/-39.78	-5.23/-39.76	-3.1/-30.27!	-6.37/-42.39#	-5.5/-38.12	-4.83/-32.22!
$[R_{12}][R_{26}][R_{31}]$	-5.5/-48.44	-3.13/-33.26	-4.18/-40.25#	-4.81/-47.58	-4.89/-38.43	-4.68/-37.48!
$[R_{12}][R_{26}][R_{32}]$	-5.5/-41.64	-5.6/-41.19	-4.43/-41.03#	-5.25/-42.06	-5.58/-39.72	-4.3/-27.71!
$[R_{13}][R_{26}][R_{31}]$	-4.67/-45.37!	-3.86/-45.93	-2.48/-38.33!	-4.83/-45.35#	-2.48/-45.73	-2.72/-35.91!
$[R_{13}][R_{26}][R_{32}]$	-5.36/-43.11	-5.38/-43.7	-4.63/-41.77#	-4.81/-43.8	-4.66/-42.05	-4.08/-26.51#
$[R_{14}][R_{26}][R_{31}]$	-5.22/-45.75#	-5.09/-45.68	-3.48/-32.93#	-6.61/-58.28#	-4.18/-48.34	-5.36/-39.2#
$[R_{14}][R_{26}][R_{32}]$	-3.73/-45.1	-3.34/-43.87	-2.49/-37.51#	-4.07/-37.56!	-3.38/-42.39	-2.57/-33.15#
$[R_{15}][R_{26}][R_{31}]$	-4.07/-56.27	-1.84/-40.39	-3.37/-37.33#	-1.46/-44.72	-2.18/-38.79	-2.92/-39.98#
$[R_{15}][R_{26}][R_{32}]$	-2.92/-41.56	-3.39/-44.01	-2.23/-42.43#	-4.38/-46.1#	-3.55/-43.24	-3.63/-32.4#
$[R_{16}][R_{26}][R_{31}]$	-6.02/-57.74#	-3.45/-41.83	-3.4/-31.17#	-5.72/-56.42#	-4.88/-44.02	-4.96/-38.59#
$[R_{16}][R_{26}][R_{32}]$	-3.72/-46.74#	-3.47/-46.36	-3.11/-44.39!	-2.03/-45.05	-4.26/-40.5!	-3.28/-40.19
$[R_{11}][R_{27}][R_{31}]$	-4.48/-36.88#	-5.36/-45.93	-4.45/-40.76!	-5.65/-50.49	-5.54/-43.55	-5.99/-44.56#
$[R_{11}][R_{27}][R_{32}]$	-4.55/-37.68!	-5.08/-40.98#	-5.77/-44.93#	-6.83/-37.63!	-5.49/-39.91	-6.1/-38.17#
$[R_{12}][R_{27}][R_{31}]$	-5.41/-41.86#	-5.31/-43.58	-4.66/-43.43!	-6.34/-43.47#	-5.47/-44.28	-5.81/-43.82#
$[R_{12}][R_{27}][R_{32}]$	-4.39/-32.98!	-5.46/-39.73	-4.06/-39.8#	-6.18/-36.96!	-5.42/-39.44	-6.31/-36.32#
$[R_{13}][R_{27}][R_{31}]$	-5.57/-53.12	-5.32/-48	-5.61/-51.5#	-6/-55.31	-5.35/-42.89	-5.47/-39.91#
$[R_{13}][R_{27}][R_{32}]$	-4.41/-39.61	-4.28/-40.68	-4.32/-42.82#	-3.68/-27.79	-5.75/-40.01	-5.95/-35.73#
$[R_{14}][R_{27}][R_{31}]$	-6.27/-61.3	-4.09/-44.74	-4.22/-45.19!	-4.43/-52.23	-4.51/-44.5	-4.68/-40.48!
$[R_{14}][R_{27}][R_{32}]$	-4.12/-47.13	-3.77/-44.94	-3.88/-44.16#	-4.28/-47.58	-3.87/-43.5	-3.17/-37.05#
$[R_{15}][R_{27}][R_{31}]$	-5.77/-54.16	-3.78/-42.9	-5.39/-51.46#	-4.79/-52.52	-4.47/-44.84	-5.41/-45.51#
$[R_{15}][R_{27}][R_{32}]$	-3.4/-44.32	-3.47/-44.6	-2.67/-43.01#	-3.53/-44.43	-3.32/-41.56	-3.98/-40.86#
$[R_{16}][R_{27}][R_{31}]$	-6.34/-64.19	-5.41/-51.78	-3.26/-34.34!	-5.54/-61.89	-3.86/-46.76	-5.28/-39.19#
$[R_{16}][R_{27}][R_{32}]$	-2.41/-43.84	-3.59/-48.52	-2.39/-45.64#	-2.76/-48.12	-1.92/-40.4	-3.18/-37.15#
$[R_{11}][R_{28}][R_{31}]$	-4.41/-36.02!	-5.53/-45.77	-3.2/-29.64!	-6.41/-49.72#	-5.18/-46.36	-4.48/-34.72!
$[R_{11}][R_{28}][R_{32}]$	-4.54/-39.42	-5.68/-40.96	-2.96/-30.84!	-4.51/-37.18	-5.97/-39.75	-6.89/-41.84#
$[R_{12}][R_{28}][R_{31}]$	-4.74/-37.52!	-5.82/-47.68	-4.34/-39.82!	-5.77/-38.1!	-5.02/-46.59	-4.85/-37.46!
$[R_{12}][R_{28}][R_{32}]$	-4.76/-33.57#	-5.99/-42.46	-4.44/-34.31#	-4.78/-34.11	-5.19/-33.86	-4.51/-32.62!
$[R_{13}][R_{28}][R_{31}]$	-5.19/-39.2#	-5.51/-47.78	-3.93/-40.77!	-5.74/-40.62#	-4.8/-43.88	-5.2/-40.38!
$[R_{13}][R_{28}][R_{32}]$	-5.56/-43.99	-5.89/-44.53	-3.56/-35.28!	-4.58/-43.26	-6.04/-44.36	-4.38/-28.16#

Ligand	3.5	3.5*	3.5**	4.0	4.0*	4.0**
[R_{14}] [R_{28}] [R_{31}]	-5.3/-46.28#	-5.05/-41.26	-3.82/-36.33#	-7/-58.78#	-5.33/-51.48	-3.86/-33.55!
[R_{14}] [R_{28}] [R_{32}]	-4.49/-37.97	-5.26/-46.41	-3.46/-36.36!	-4.94/-42.04	-5.93/-45.51	-4.56/-25.6#
[R_{15}] [R_{28}] [R_{31}]	-4.24/-49.57	-4.02/-48.57	-3.15/-40.29#	-3.18/-41.16	-3.99/-52.52	-3.22/-40.32!
[R_{15}] [R_{28}] [R_{32}]	-5.18/-43.57	-5.59/-45.55	-4.4/-38.25#	-3.76/-37.16	-5.79/-44.47	-5.52/-29.53!
[R_{16}] [R_{28}] [R_{31}]	-4.7/-47.85#	-5.55/-52.14	-3.07/-36.54!	-6/-50.9#	-4.89/-49.26	-3.74/-37.06!
[R_{16}] [R_{28}] [R_{32}]	-3.6/-43.33	-4.19/-47.78	-3.06/-40.49!	-3.42/-45.7	-3.14/-45.15	-4.09/-37.85!
[R_{11}] [R_{29}] [R_{31}]	-5.38/-41.25	-4.54/-38.87	-3.65/-37.13!	-4.44/-41.84	-5.01/-40.6	-/-
[R_{11}] [R_{29}] [R_{32}]	-4.59/-42.48	-5.26/-37.78	-3.31/-35.81!	-3.28/-31.6	-5.47/-37.33	-5.42/-33.2!
[R_{12}] [R_{29}] [R_{31}]	-5.96/-51.08	-5.78/-46.62	-4.31/-44.16!	-4.97/-40.98	-3.92/-26.06	-/-
[R_{12}] [R_{29}] [R_{32}]	-5.32/-36.05	-5.47/-40.25	-4.24/-38.16!	-4.82/-36.09	-5.83/-41.6	-4.78/-35.75!
[R_{13}] [R_{29}] [R_{31}]	-4.97/-36.31!	-5.04/-40.99	-4.36/-46.44!	-4.8/-37.78	-4.47/-46.6	-/-
[R_{13}] [R_{29}] [R_{32}]	-5.31/-44.93	-5.69/-43.89	-3.5/-36.1!	-5.69/-43.41	-5.67/-43.72	-4.69/-36.82!
[R_{14}] [R_{29}] [R_{31}]	-4.99/-47.08	-4.68/-37.96	-2.99/-27.19#	-4.3/-40.72	-4.26/-37.05	-/-
[R_{14}] [R_{29}] [R_{32}]	-4.2/-47.17	-4.27/-43.91	-2.64/-40.61!	-5.27/-51.3#	-4.11/-43.13	-3.51/-38.43!
[R_{15}] [R_{29}] [R_{31}]	-6.06/-45.15	-3.99/-37.99	-3.52/-29.42!	-4.97/-44.71	-4.32/-54.15	-/-
[R_{15}] [R_{29}] [R_{32}]	-3.45/-44.98	-3.98/-44.32	-2.7/-35.8!	-4.74/-48.11#	-3.8/-43.67	-3.03/-31.47!
[R_{16}] [R_{29}] [R_{31}]	-5.26/-53.44	-4.62/-43	-4.48/-24.76!	-6.54/-54.99#	-4.51/-49.21	-/-
[R_{16}] [R_{29}] [R_{32}]	-5.55/-49.9	-5.81/-47.96	-4.16/-43.99!	-5.11/-47.91	-4.26/-37.09	-4.08/-35.75
[R_{11}] [R_{210}] [R_{31}]	-4.7/-38.49	-4.53/-38.3	-2.77/-30.97!	-4.76/-35.71!	-5.54/-44.95	-4.39/-35.07!
[R_{11}] [R_{210}] [R_{32}]	-4.18/-35.46	-5.41/-39.28	-4.52/-31.52!	-5.09/-36.62	-4.82/-34.97	-5.85/-30.73#
[R_{12}] [R_{210}] [R_{31}]	-4.59/-35.54#	-5.09/-42.08	-3.07/-32.05!	-4.82/-44.85	-5.52/-43.73	-5.27/-37.12!
[R_{12}] [R_{210}] [R_{32}]	-4.91/-35.79	-5.62/-39.03	-4.18/-37.97!	-5.06/-36.63	-5.8/-39.26	-5.87/-33.77#
[R_{13}] [R_{210}] [R_{31}]	-5.36/-43.7	-4.07/-33.96	-3.91/-34.31!	-4.06/-45.03	-4.81/-37.7	-4.31/-36.77!
[R_{13}] [R_{210}] [R_{32}]	-5.33/-42.76	-5.52/-42.67	-4.75/-41.98#	-5.38/-40.62	-5.79/-42.75	-4.66/-29.26!
[R_{14}] [R_{210}] [R_{31}]	-5.27/-47.9#	-3.98/-39.75#	-5.57/-43.87#	-6.96/-48.17#	-4.01/-38.45	-4.51/-40.34!
[R_{14}] [R_{210}] [R_{32}]	-5.54/-48.29#	-5.71/-38.88	-3.37/-20.89#	-5.99/-35.84#	-5.73/-43.54	-5.4/-20.91#
[R_{15}] [R_{210}] [R_{31}]	-3.37/-43.89	-2.79/-40.7	-2.12/-39.67#	-2.94/-47.59	-3.03/-41.32	-2.71/-38.04!
[R_{15}] [R_{210}] [R_{32}]	-4.02/-42.25	-5.31/-43.67	-3.78/-32.64#	-4.13/-43.18	-5.57/-43.74	-5.76/-39.76#
[R_{16}] [R_{210}] [R_{31}]	-5.1/-50.19	-5.7/-51.18	-5.19/-42.84!	-4.6/-51.35	-4.71/-53.81	-3.64/-37.18!
[R_{16}] [R_{210}] [R_{32}]	-2.71/-40.04	-3.76/-45.99	-3/-35.01#	-4.01/-42.02#	-3.85/-45.48	-3.2/-33.28!

E.6 Main Structure 6

Ligand	3.0	3.5*	3.5**	4.0	4.0*	4.0**
$[R_{11}][R_{21}][R_{31}]$	-3.73/-31.89	-4.43/-33.1	-3.66/-32.58#	-4.83/-31.15	-3.85/-35.89	-/-
$[R_{11}][R_{21}][R_{32}]$	-3.12/-25.34	-3.3/-27.38	-2.74/-24.42!	-3.99/-27.63	-3.8/-31.05	-4.46/-27.11#
$[R_{12}][R_{21}][R_{31}]$	-4.3/-30.38	-3.75/-37.52	-3.82/-37.99!	-4.02/-31.6	-3.18/-28.23	-/-
$[R_{12}][R_{21}][R_{32}]$	-3.34/-27.5	-3.24/-28.11	-2.77/-27.8!	-/-	-3.57/-30.05	-4.42/-26.08#
$[R_{13}][R_{21}][R_{31}]$	-2.7/-36.3	-2.48/-35.75	-1.8/-38.51!	-2.47/-35.1	-1.6/-37.96	-/-
$[R_{13}][R_{21}][R_{32}]$	-2.76/-29.23	-3.4/-37.93	-2.42/-18.97!	-2.82/-26.87	-3.39/-30.45	-4.05/-29.27#
$[R_{14}][R_{21}][R_{31}]$	-2.52/-34.66	-2.16/-36.49	-2.05/-41.81!	-2.34/-42.66	-1.78/-40.26	-/-
$[R_{14}][R_{21}][R_{32}]$	-2.55/-29.14	-3.56/-37.59	-2.73/-35.85!	-0.78/-24.4	-1.17/-29.6	-1.52/-29.43!
$[R_{15}][R_{21}][R_{31}]$	-1.96/-34.48	-1.38/-40.47	-1.21/-38.71!	-0.86/-31.47	-2.62/-41.46!	-/-
$[R_{15}][R_{21}][R_{32}]$	-0.48/-26.44	-0.3/-29.87	0.23/-31.71!	-0.4/-28.65	-0.54/-28.81	-1.3/-28.85#
$[R_{16}][R_{21}][R_{31}]$	-2.6/-43.84	-1.61/-41.3	-0.82/-36.32!	-1.78/-37.38	-0.65/-37.78	-/-
$[R_{16}][R_{21}][R_{32}]$	-1.11/-34.97#	-1.09/-39.04	-0.57/-38.08#	-1.19/-29.64!	-0.86/-37.94	-1.22/-30.76#
$[R_{11}][R_{22}][R_{31}]$	-3.08/-7.24#	-4.08/-35.66	-3.03/-19.12#	-4.46/-15.77!	-3.97/-34.23	-/-
$[R_{11}][R_{22}][R_{32}]$	-4.43/-31.97	-2.87/-25.04	-/-	-5.85/-35.21!	-3.17/-29.86	-4.44/-25.5!
$[R_{12}][R_{22}][R_{31}]$	-0.9/-23.74	-2.11/-37.85	-/-	-1.6/-24.53	-1.72/-29.76	-/-
$[R_{12}][R_{22}][R_{32}]$	-4.15/-32.65	-3.64/-27.29	-3.05/-33.41!	-5/-32.11!	-3.32/-29.49	-4.41/-27.92#
$[R_{13}][R_{22}][R_{31}]$	-3.06/-42.03	-1.96/-37.44	-0.76/-14.09#	–2.29/-42.6	-1.84/-36.09	-/-
$[R_{13}][R_{22}][R_{32}]$	-1.68/-31.78#	-1.84/-37.08	-1.37/-34.9!	-3.04/-33.73!	-0.84/-22.33	-1.74/-26.75!
$[R_{14}][R_{22}][R_{31}]$	-3.88/-39.09	-3.92/-36.1	-4.44/-46.14!	-3.83/-39.64	-4.34/-34.76	-/-
$[R_{14}][R_{22}][R_{32}]$	-1.38/-35.06	-0.55/-33.79	-1.08/-35.22!	-0.52/-34.42	-1.72/-31.94	-2.27/-33.59!
$[R_{15}][R_{22}][R_{31}]$	-2.48/-43.4	-1.35/-34.28	-2.35/-48.23!	-1.77/-42.62	-0.93/-34.55	-/-
$[R_{15}][R_{22}][R_{32}]$	-0.43/-33.21!	0.3/-25.18	-0.79/-37.62!	-2.05/-34.09!	-0.14/-30.77	-1.82/-27.77!
$[R_{16}][R_{22}][R_{31}]$	-4.72/-44.55!	-4.3/-44.84	-4.21/-48.28!	-4.08/-45.34#	-4.02/-45.7	-/-
$[R_{16}][R_{22}][R_{32}]$	-1.32/-35.76#	-0.6/-37.32	-0.53/-34.42!	-2.63/-35.94#	-1.1/-42.36	-0.4/-27.4#
$[R_{11}][R_{23}][R_{31}]$	-2.92/-33.96	-1.68/-33.62	-1.39/-28.69!	-0.31/-21.2	-2.72/-37.9	-/-
$[R_{11}][R_{23}][R_{32}]$	-1.88/-32.95!	-2.53/-39.82	-0.59/-30.91#	-3.02/-32.54!	-1.97/-34.43	-2.41/-32.73!
$[R_{12}][R_{23}][R_{31}]$	-/-	-3.57/-40.75	-2.51/-19.39!	-/-	-2.82/-38.28	-/-
$[R_{12}][R_{23}][R_{32}]$	-1.2/-25.63!	-2.41/-38.92	-1.33/-34.91!	-4.27/-36.36!	-1.04/-31.21	-2.26/-30.16!
$[R_{13}][R_{23}][R_{31}]$	-3.88/-35.62	-3.88/-40.94	-4.35/-44.93!	-2.63/-22.94	-2.47/-37.54	-/-
$[R_{13}][R_{23}][R_{32}]$	-1.48/-34.56!	-0.36/-34.04	-1.17/-36.54!	-3.14/-37.96	-0.51/-35.52	-1.64/-33.8!

Ligand	3.5	3.5*	3.5**	4.0	4.0*	4.0**
[R_{14}] [R_{23}] [R_{31}]	-4.5/-47.73!	-3.86/-35.41	-3.5/-37.76#	-3.41/-39.39	-3.38/-38.17	-/-
[R_{14}] [R_{23}] [R_{32}]	-0.34/-33.16	-0.63/-36.96	-1.27/-40.67!	-2.82/-36.78!	-0.93/-41.62	-2.25/-32.82!
[R_{15}] [R_{23}] [R_{31}]	-4.39/-43.41	-3.76/-43.1	-2.26/-17.01!	-2.59/-28.39	-3.49/-42.8	-/-
[R_{15}] [R_{23}] [R_{32}]	-0.81/-36.07!	-0.82/-42.11	-0.48/-41.57!	0.15/-32.03	-0.96/-40.55	-1.29/-33.13!
[R_{16}] [R_{23}] [R_{31}]	-4.39/-46.7#	-4.09/-41.84	-4.21/-37.2#	-5.34/-47.55!	-4.02/-43.53	-/-
[R_{16}] [R_{23}] [R_{32}]	-1.21/-34.51!	-1.62/-47.1	-0.85/-43.87!	-3.25/-40.69!	-0.78/-43.49	-2.46/-35.29!
[R_{11}] [R_{24}] [R_{31}]	-3.85/-24.17!	-4.13/-34.61	-2.87/-27.44#	-4.84/-31.41!	-3.58/-36.37	-/-
[R_{11}] [R_{24}] [R_{32}]	-3.38/-26.62	-2/-39.74	-3.41/-29.16#	-4.33/-26.85!	-4.16/-32.59	-3.46/-25.89#
[R_{12}] [R_{24}] [R_{31}]	-2.43/-40.77!	-1.25/-37.76	-2.05/-41.35!	-3.5/-41.31!	-1.86/-36.13	-/-
[R_{12}] [R_{24}] [R_{32}]	-3.39/-31.68!	-3.97/-35.69	-3.14/-29.22#	-2.84/-31.29	-2.81/-31.06	-4.67/-28.15#
[R_{13}] [R_{24}] [R_{31}]	-2.38/-43.94!	-1.55/-37.26	-0.59/-30.77#	-3.36/-42.83!	-1.21/-37.59	-/-
[R_{13}] [R_{24}] [R_{32}]	-0.81/-32.03#	-1.61/-36.7	-0.73/-33.23!	-2.04/-32.65#	-1.33/-34.38	-1.97/-30.8!
[R_{14}] [R_{24}] [R_{31}]	-2.49/-43.13	-1.49/-39.76	-2.56/-35.44#	-1.83/-42.42	-1.27/-39.66	-/-
[R_{14}] [R_{24}] [R_{32}]	-0.64/-32.41#	-1.48/-38.79	-1.29/-37.31#	-2.08/-35.68#	-1.22/-37.07	-1.06/-30.83#
[R_{15}] [R_{24}] [R_{31}]	-1.35/-40.43#	-1.51/-37.8	-1.53/-44.69!	-2.57/-41.2!	-3.08/-48.5	-/-
[R_{15}] [R_{24}] [R_{32}]	-0.63/-31.53	-0.55/-37.38	-1.15/-41.78!	-0.25/-32.41	-1.47/-35.37	-1.03/-32.15!
[R_{16}] [R_{24}] [R_{31}]	-2.03/-42.15!	-1.55/-44.17	-4.61/-33.11#	-2.94/-46.19!	-1.03/-41.96	-/-
[R_{16}] [R_{24}] [R_{32}]	-0.84/-35.79#	-1.34/-40.32	-3.06/-39.12#	-1.47/-36.34#	-1.73/-38.59	-1.29/-33.54#
[R_{11}] [R_{25}] [R_{31}]	-1.94/-36.68!	-1.43/-33.23	-1.58/-40.21!	-2.77/-33.82!	-1.78/-40.61	-/-
[R_{11}] [R_{25}] [R_{32}]	-0.83/-31.73!	-1.78/-37.51	-0.87/-36.65!	-1.62/-31.66#	-1.21/-34.59	-2.49/-36.1!
[R_{12}] [R_{25}] [R_{31}]	-1.95/-37.91!	-1.08/-36.65	-0.48/-27.85!	-2.68/-39.22!	-0.41/-36.68	-/-
[R_{12}] [R_{25}] [R_{32}]	-0.61/-32.38!	-1.42/-36.51	-0.33/-30.8#	-1.24/-23.3#	-1.4/-37.25	-1.91/-35.66!
[R_{13}] [R_{25}] [R_{31}]	-1.84/-36.98!	-1.6/-37.28	-2.04/-48.86!	-3.39/-44.23!	-0.71/-37.68	-/-
[R_{13}] [R_{25}] [R_{32}]	-1.08/-32.42!	-1.49/-39.82	-0.82/-38.01!	-1.5/-35.76!	-2.27/-37.86!	-2.08/-32.52!
[R_{14}] [R_{25}] [R_{31}]	-4.44/-43.22#	-4.14/-40.28	-4.12/-49.34!	-5.83/-43.71!	-2.83/-42.75	-/-
[R_{14}] [R_{25}] [R_{32}]	-1.58/-40.22	-0.8/-40.28	-0.88/-40.82!	-2.78/-40.27#	-1.15/-41.07	-2.21/-38.59!
[R_{15}] [R_{25}] [R_{31}]	-1.86/-46.4!	-0.96/-40.16	-1.57/-49.36!	-3.06/-42.64!	-3.27/-52.49!	-/-
[R_{15}] [R_{25}] [R_{32}]	-0.14/-37.55	-0.88/-40.72	-0.26/-39.64!	-1.82/-36.9!	-1.33/-39.7!	-1.27/-37.92!
[R_{16}] [R_{25}] [R_{31}]	-4.12/-49.32#	-3.84/-42.49	-4.32/-52.81!	-5.21/-44.5!	-5.87/-55.47!	-/-
[R_{16}] [R_{25}] [R_{32}]	0.02/-31.04!	-0.91/-44.26	-0.5/-45.14!	-2.08/-38.91!	-2.07/-42.96!	1.99/-41.87!

Ligand	3.5	3.5*	3.5**	4.0	4.0*	4.0**
$[R_{11}][R_{26}][R_{31}]$	-2.54/-40.96	-2.24/-39.14	-1.16/-36.6!	-1.59/-36.22	-2.29/-38.77	-/-
$[R_{11}][R_{26}][R_{32}]$	-3.11/-26.59	-3.52/-33.57	-2.61/-27.86!	-3.47/-25.83!	-3.5/-31.56	-4.04/-27.96#
$[R_{12}][R_{26}][R_{31}]$	-1.59/-35.52	-2.02/-40.84	-0.88/-35.43!	-1.62/-36.21!	-2.04/-40.19	-/-
$[R_{12}][R_{26}][R_{32}]$	-0.93/-35.44#	-0.86/-34.49	-0.69/-33.33#	-2.07/-31.5!	-0.18/-32.89	-1.56/-28.25#
$[R_{13}][R_{26}][R_{31}]$	-2.31/-43.92	-1.84/-40.12	-1.07/-40.61#	-1.93/-43.61	-1.35/-10.68	-/-
$[R_{13}][R_{26}][R_{32}]$	-1.18/-34.81!	-0.81/-35.34	-0.01/-30.71#	-2.82/-36.17#	0.07/-33.7	-0.41/-23.23#
$[R_{14}][R_{26}][R_{31}]$	-1.64/-43.64#	-1.88/-42.05	-1.42/-36.42#	-2.55/-42#	-1.65/-10.59	-/-
$[R_{14}][R_{26}][R_{32}]$	-/-	-0.6/-39.61	-0.01/-35.34#	-3.29/-36.95!	-0.39/-40	-0.24/-29.13
$[R_{15}][R_{26}][R_{31}]$	-1.71/-43.52	-1.02/-42.29	-0.7/-43.1!	-1.34/-32.42	-0.37/-38.47	-/-
$[R_{15}][R_{26}][R_{32}]$	-0.37/-34.83!	0.39/-37.8	1.46/-29.61!	-1.41/-35.65#	0.34/-34.9	-0.66/-28.88#
$[R_{16}][R_{26}][R_{31}]$	-0.52/-37.76#	-1.35/-43.78	-0.22/-38.3#	-1.73/-46.44	-2.76/-41.87	-/-
$[R_{16}][R_{26}][R_{32}]$	-0.09/-39.25#	0.69/-39.3	0.6/-33.14!	-1.19/-38.04#	-0.14/-42.66	-0.65/-36.49#
$[R_{11}][R_{27}][R_{31}]$	-2.39/-36.12	-1.61/-35.26	-1.51/-36.69#	-2.89/-39.04!	-2.02/-37.73	-1.5/-29.74!
$[R_{11}][R_{27}][R_{32}]$	-4.33/-32.82!	-3.81/-33.8	-2.25/-31.11#	-4.43/-27.63!	-3.61/-33.3	-3.65/-24.46#
$[R_{12}][R_{27}][R_{31}]$	-1.17/-32.92	-1.73/-38.15	-0.91/-29.14#	-1.96/-34.78	-1.98/-41.05	-1.55/-31.3#
$[R_{12}][R_{27}][R_{32}]$	-0.23/-15.16	-0.89/-32.36	0.05/-25.91#	-1.63/-27.35!	-0.23/-32.42	-1.67/-26.21#
$[R_{13}][R_{27}][R_{31}]$	-1.74/-40.45!	-1.6/-40.17	-0.82/-36.52!	-2.64/-38.29#	-0.82/-37.88	-1.63/-34.55#
$[R_{13}][R_{27}][R_{32}]$	-1.63/-39.31	-1.33/-35.97	-0.73/-34.61#	-2.13/-33.19!	-0.65/-33.56	-0.83/-27.26!
$[R_{14}][R_{27}][R_{31}]$	-2.14/-46.82!	-1.6/-41.71	-2.54/-36.67#	-2.94/-43.57#	-2.35/-40.53	-2.29/-38.43#
$[R_{14}][R_{27}][R_{32}]$	-3.85/-40.38!	-0.92/-37.51	-0.19/-34.23!	-2.7/-39.91!	-0.33/-35.68	-1.53/-29.91#
$[R_{15}][R_{27}][R_{31}]$	-0.83/-36.19	-0.99/-40.79	-0.86/-42.44!	-2.86/-44.52!	-1.01/-41.43	-1.61/-35.09!
$[R_{15}][R_{27}][R_{32}]$	-3.23/-36.83!	-0.66/-38.44	0.34/-32.99!	-2.74/-36.93!	-0.39/-35.2	-0.08/-29.4!
$[R_{16}][R_{27}][R_{31}]$	-3.94/-43.77#	-3.16/-42.92	-3.86/-46.52#	-4.69/-46.11#	-3.08/-45.21	-4.3/-41.55!
$[R_{16}][R_{27}][R_{32}]$	-1.58/-40.41!	-1.22/-40.62	-0.07/-38.57#	-2.24/-39.19!	-0.6/-43.88	-1.2/-33.99#
$[R_{11}][R_{28}][R_{31}]$	-3.66/-28.28	-3.45/-34.62	-3.61/-34.95!	-4.88/-33.3!	-3.15/-32.25	-5.44/-39.99!
$[R_{11}][R_{28}][R_{32}]$	-3.68/-26.3	-3.55/-33.6	-2.91/-25.72!	-3.34/-26.82	-4/-31	-3.85/-23.3#
$[R_{12}][R_{28}][R_{31}]$	-2.01/-34.83!	-2.29/-35.41	-0.96/-28.45!	-3/-34.19!	-1.43/-31.89	-3.1/-37.46!
$[R_{12}][R_{28}][R_{32}]$	-3.59/-3.04	-3.92/-33.62	-3.28/-32.76!	-4.67/-29.38#	-3.8/-32.61	-4.33/-32.01!
$[R_{13}][R_{28}][R_{31}]$	-2.37/-37.9	-1.14/-35.29	-0.85/-33.21!	-2.25/-35.39	-0.97/-36.8	-2.89/-41.08!
$[R_{13}][R_{28}][R_{32}]$	-0.53/-29.93#	-0.36/-36.81	-1/-34.35!	-2.51/-32.39!	-1.12/-34.72	-1.91/-28.09!

Ligand	3.5	3.5*	3.5**	4.0	4.0*	4.0**
$[R_{14}][R_{28}][R_{31}]$	-2.14/-40.71!	-1.52/-37.45	-1.45/-37.21#	-2.5/-34.42!	-1.4/-41.05	-3.01/-42.05!
$[R_{14}][R_{28}][R_{32}]$	-1.29/-33.13#	-1.09/-40.6	-0.51/-34.84!	-1.3/-31.21	-1.17/-35.46	-1.53/-31.78!
$[R_{15}][R_{28}][R_{31}]$	-2.16/-42.3	-1.01/-37.65	-0.66/-31.77!	-5.56/-42.27#	-0.59/-37.6	-2.58/-43.06!
$[R_{15}][R_{28}][R_{32}]$	0.21/-31.38	0.94/-32.35	-0.24/-36.76!	-0.19/-34.66	-0.55/-34.75	-0.95/-32.59!
$[R_{16}][R_{28}][R_{31}]$	-2.27/-43.43	-2.51/-45.91	-1.78/-46.6!	-1.8/-45.12	-2.04/-46.53	-2.97/-45.26!
$[R_{16}][R_{28}][R_{32}]$	-1.24/-38.73#	-1.05/-36.43	-0.2/-35.09#	-2.43/-33.84#	-0.91/-36.55	-0.87/-33.27#
$[R_{11}][R_{29}][R_{31}]$	-1.17/-36.07	-2.18/-35.12	-0.46/-14.53!	-1.91/-34.33	-2.72/-40.74	-/-
$[R_{11}][R_{29}][R_{32}]$	-4.65/-31.61!	-3.18/-32.84	-3.66/-38.21!	-6.05/-30.94!	-3.48/-31.58	-4.93/-28.58!
$[R_{12}][R_{29}][R_{31}]$	-2.1/-31.47	-2.52/-40.67	-1.95/-36.74!	-1.04/-30.25	-2.17/-35.75	-/-
$[R_{12}][R_{29}][R_{32}]$	-1.41/-31.23!	-2.3/-37.8	-2.16/-34.51!	-1.61/-35.5	-2.07/-35.32	-2.66/-29.73!
$[R_{13}][R_{29}][R_{31}]$	-4.33/-35.31!	-3.9/-35.67	-3.95/-42.5!	-5.1/-37.73!	-3.67/-39.85	-/-
$[R_{13}][R_{29}][R_{32}]$	-1.15/-34.6!	-1.92/-38.69	-0.71/-31.72!	-2.99/-36.77!	-1.82/-37.19	-1.91/-29.03!
$[R_{14}][R_{29}][R_{31}]$	-4.19/-32.2	-5.17/-38.77	-3.14/-37.15#	-5.34/-42.47!	-3.96/-37.21	-/-
$[R_{14}][R_{29}][R_{32}]$	-2.09/-39.98#	-1.44/-41.16	-0.93/-34.18!	-1.13/-31.43	-1.6/-38.97	-0.83/-27.71#
$[R_{15}][R_{29}][R_{31}]$	-1.74/-38.89#	-1.84/-38.28	-2.05/-47.97!	-2.2/-33.41!	-1.84/-40.02	-/-
$[R_{15}][R_{29}][R_{32}]$	-0.8/-37.21	-1.32/-39.01	-0.85/-42.11!	-0.51/-37.64	-0.84/-35.32	-2.34/-37.53!
$[R_{16}][R_{29}][R_{31}]$	-4.62/-40.86#	-3.96/-41.29	-4.22/-43.06!	-4.23/-37	–3.71/-46.05	-/-
$[R_{16}][R_{29}][R_{32}]$	-0.71/-30.09#	-1.99/-43.29	-1.5/-29.65!	-1.48/-35.43#	-1.2/-39.95	-1.85/-33.68!
$[R_{11}][R_{210}][R_{31}]$	-2.37/-22.32	-3.63/-33.38	-3.79/-38.85!	-3.88/-28.84	-4.02/-34.47	-4.57/-32.36!
$[R_{11}][R_{210}][R_{32}]$	-2.32/-26.23	-3.08/-32.91	-2.88/-28.98!	-2.74/-26.2	-3.53/-32.18	-3.8/-25.49#
$[R_{12}][R_{210}][R_{31}]$	-2.18/-34.12	-1.55/-35.01	-0.78/-32.92!	-1.15/-30.88	-1.63/-35	-1.76/-28.62!
$[R_{12}][R_{210}][R_{32}]$	-3.65/-28.08#	-2.98/-33.34	-2.47/-29.47!	-2.79/-24	-3.15/-32.2	-3.9/-25.37!
$[R_{13}][R_{210}][R_{31}]$	-1.81/-33.03	-1.12/-38.55	-1.57/-37.31#	-2.14/-33.86#	-0.8/-38.3	-3.03/-42.99!
$[R_{13}][R_{210}][R_{32}]$	-1.14/-35.55#	-0.84/-36.84	1.11/-18.16#	-2.95/-35.7#	-1.6/-32.65	-0.85/-22.66!
$[R_{14}][R_{210}][R_{31}]$	-2.04/-40.72	-1/-35.97	-1.14/-38.08#	-2.69/-39#	-1.06/-37.78	-2.04/-37.05!
$[R_{14}][R_{210}][R_{32}]$	-0.28/-30.14	-0.58/-38.06	0.21/-32.71#	-2.28/-34.08#	-1.24/-38.89	-1.44/-24.16#
$[R_{15}][R_{210}][R_{31}]$	-1.34/-39.95#	-1.18/-38.56	-0.78/-41.45!	-2.43/-38.44#	-0.28/-37.45	-1.85/-38.72!
$[R_{15}][R_{210}][R_{32}]$	-0.1/-33.36#	-0.49/-40.28	1.08/-32.81!	-1.18/-33.72#	0.12/-33.54	-0.98/-30.56!
$[R_{16}][R_{210}][R_{31}]$	-2.08/-43.21	-1.79/-46.44	-1.11/-43.65!	-1.45/-38.8	-1.46/-44.34	-2.25/-38.62!
$[R_{16}][R_{210}][R_{32}]$	-0.51/-29.59#	-0.43/-36.25	0.44/-33.94#	-1.21/-32.32#	-1.02/-40.81	0.39/-27.14#

E.7 Main Structure 7

Ligand	3.0	3.5*	3.5**	4.0	4.0*	4.0**
$[R_{11}][R_{21}][R_{31}]$	-0.88/-32.83	-2.16/-35.82	-1.98/-36.75!	-1.41/-33.28	-1.05/-37.37	-/-
$[R_{11}][R_{21}][R_{32}]$	-3.96/-35.57	-3.68/-37.12	-3.05/-30.97!	-3.55/-34.93	-2.75/-31.66	-4.26/-28.96!
$[R_{12}][R_{21}][R_{31}]$	-2.28/-40.35	-1.64/-39.91	-1.92/-40.88!	-0.99/-31.88	-2.15/-39.78!	-/-
$[R_{12}][R_{21}][R_{32}]$	-1.82/-40.57	-1.42/-37.27	-0.25/-31.15!	-1.9/-41.97	-1.29/-33.53	-0.8/-29.74#
$[R_{13}][R_{21}][R_{31}]$	-2.28/-41.44	-1.49/-41.21	-0.61/-37.45!	-1.57/-41.08	-1.76/-42.66	-/-
$[R_{13}][R_{21}][R_{32}]$	-1.14/-38.36	-0.2/-34.78	-0.18/-34.72!	-0.45/-38.78	-0.73/-35	-1.21/-31.55!
$[R_{14}][R_{21}][R_{31}]$	-2.4/-44.8	-2.04/-40.06	-1.28/-37.35!	-2.67/-37.16#	-1.66/-40.18	-/-
$[R_{14}][R_{21}][R_{32}]$	-1/-42.45	-0.7/-41.79	-0.83/-37.7!	-2.84/-40.04#	-1.02/-42.59	-0.62/-30.28!
$[R_{15}][R_{21}][R_{31}]$	-2.02/-43.59#	-1.2/-38.32	-1.13/-42.29!	-1.65/-34.7#	-1.35/-35.18	-/-
$[R_{15}][R_{21}][R_{32}]$	-0.41/-34.28#	0.03/-39.94	0.3/-34.92!	-2.01/-40.19#	-0.2/-36.75!	-0.18/-34.01!
$[R_{16}][R_{21}][R_{31}]$	-2.66/-50.24	-1.03/-42.3	-2.56/-50.11!	-2.06/-49.65	-1.47/-51.91	-/-
$[R_{16}][R_{21}][R_{32}]$	-1/-42.95	-0.15/-45.09	0.03/-38.76#	-0.3/-41.13	-1.08/-39.39	-1.34/-35.97!
$[R_{11}][R_{22}][R_{31}]$	-2.24/-36.25!	-2.72/-41.29	-2.48/-45.54!	-3.12/-35.61!	-2.05/-39.68	-/-
$[R_{11}][R_{22}][R_{32}]$	-1.64/-31.47	-1.28/-34.95	-1.1/-37.54!	-1.38/-35.8	-0.58/-33.71	-2.22/-32.68!
$[R_{12}][R_{22}][R_{31}]$	-2.88/-42.76	-1.92/-34.19	-2.49/-46.18!	-1.18/-34.57	-1.33/-36.84	-/-
$[R_{12}][R_{22}][R_{32}]$	-1.76/-35.79	-0.39/-32.99	0/-25.82!	-1.16/-39.87	-0.3/-34.27	-2/-32.55!
$[R_{13}][R_{22}][R_{31}]$	-4.48/-42.46	-3.69/-37.63	-4.38/-46.64!	-3.69/-42.87	-3.28/-42.21	-/-
$[R_{13}][R_{22}][R_{32}]$	-2.23/-42.21	-0.97/-36.62	-0.24/-38.2!	-0.62/-38.08	-0.93/-29.8	-1.46/-31.7!
$[R_{14}][R_{22}][R_{31}]$	-4.74/-47.45	-4.11/-39.13	-2.38/-30.89!	-6.67/-36.82	-4.84/-39.74	-/-
$[R_{14}][R_{22}][R_{32}]$	-1.28/-41.15#	-2.39/-43.61	-0.01/-32.5!	-2.72/-40.37#	-1.23/-51.54	-0.97/-33.87!
$[R_{15}][R_{22}][R_{31}]$	-4.08/-43.45	-3.48/-39.38	-4.28/-50.18!	-5.4/-48.65#	-2.99/-44.6	-/-
$[R_{15}][R_{22}][R_{32}]$	-0.97/-42.92	0.59/-25.63	-2.34/-51.12!	-0.4/-52.15	-1.84/-41.64	-0.76/-38.34!
$[R_{16}][R_{22}][R_{31}]$	-5.07/-50.03	-5.14/-54.1	-4.54/-50.73!	-4.32/-47.8	-3.74/-46.26	-/-
$[R_{16}][R_{22}][R_{32}]$	-4.63/-47.9	-1.08/-44.53	-0.71/-44.74!	-1.23/-43.68	-1.02/-44.15	-0.85/-32.74!
$[R_{11}][R_{23}][R_{31}]$	-4.02/-40.24!	-3.32/-39.74	-4.37/-42.71!	-4.07/-26.2!	-3.45/-39.69	-/-
$[R_{11}][R_{23}][R_{32}]$	-0.77/-36.13!	-1.57/-42.03	-0.69/-38.35!	-2.48/-40.1!	-2.15/-36.63	-1.68/-34.96!
$[R_{12}][R_{23}][R_{31}]$	-2.22/-29.99	-4.4/-40.92	-4.54/-49.6!	-3.79/-31.45!	-3.84/-38.83	-/-
$[R_{12}][R_{23}][R_{32}]$	-1.45/-39.35!	-0.84/-30.44	-1.05/-40.82!	-2.97/-42.5!	-1.14/-40.23	-1.61/-33.86!
$[R_{13}][R_{23}][R_{31}]$	-4.4/-40.71	-5.69/-42.78	-4.79/-49.03!	-3.22/-35.74	-3.66/-39.15	-/-
$[R_{13}][R_{23}][R_{32}]$	-2.63/-48.96!	-1.89/-42.7	0.88/-21.77!	-3.61/-46.31!	-1.31/-43.9	-1.14/-33.94

Ligand	3.5	3.5*	3.5**	4.0	4.0*	4.0**
$[R_{14}]\,[R_{23}]\,[R_{31}]$	-5.42/-56.01#	-3.61/-41	-3.5/-37.76#	-6.2/-56.93#	-3.75/-44.87	-/-
$[R_{14}]\,[R_{23}]\,[R_{32}]$	-4.66/-39.94!	-5.03/-50.25	-1.27/-40.67!	-6.22/-48.34!	-3/-33.72	-3.12/-32.81#
$[R_{15}]\,[R_{23}]\,[R_{31}]$	-4.46/-45.51	-3.82/-45.7	-1.56/-29.57#	-5.64/-49.38#	-3.08/-44.15	-/-
$[R_{15}]\,[R_{23}]\,[R_{32}]$	-2.21/-48.91!	0.48/-32.98	-0.07/-42.25!	-2.56/-44.03#	0.39/-35.31	-0.3/-30.91!
$[R_{16}]\,[R_{23}]\,[R_{31}]$	-5.63/-60.09#	-3.49/-45.41	-4.04/-41.54!	-3.48/-49.51	-2.88/-43.55	-/-
$[R_{16}]\,[R_{23}]\,[R_{32}]$	-5.15/-51.31!	-3.79/-45.46	-3.5/-46.99!	-5.36/-41.62!	-3.16/-41.43	-3.97/-41.71!
$[R_{11}]\,[R_{24}]\,[R_{31}]$	-2.14/-40.23	-2/-39.74	-1.63/-39.37!	-2.91/-38.82!	-0.93/-39.58	-3.18/-41.8!
$[R_{11}]\,[R_{24}]\,[R_{32}]$	-1.29/-36.08	-1.38/-37.91	-0.2/-34.5!	-0.97/-37.41	-0.57/-38.65	-2.01/-32.23!
$[R_{12}]\,[R_{24}]\,[R_{31}]$	-0.88/-32.31!	-1.06/-42.36	-1.36/-42.56!	-3.16/-44.63!	-0.68/-41	-2.72/-42.37!
$[R_{12}]\,[R_{24}]\,[R_{32}]$	-0.9/-33.05!	-1.57/-41.46	-0.18/-36.68!	-0.64/-35.49	-0.14/-36.63	-1.19/-31.74!
$[R_{13}]\,[R_{24}]\,[R_{31}]$	-1.64/-44.18!	-1.19/-42.4	-0.87/-37.52!	-3.67/-46.92!	-1.08/-42.58	-1.77/-36.36!
$[R_{13}]\,[R_{24}]\,[R_{32}]$	-1.07/-42.59!	-1.44/-42.54	-1.26/-42.03!	-2.31/-39.03!	-0.79/-40.46	-0.85/-32.85!
$[R_{14}]\,[R_{24}]\,[R_{31}]$	-4.65/-48.01#	-3.76/-46.07	-5.19/-49.61!	-5.03/-48.38#	-3.54/-44.63	-4.24/-37.44#
$[R_{14}]\,[R_{24}]\,[R_{32}]$	-1.02/-40.45	-1.39/-40.01	-1.05/-40.96#	-2.96/-43.89!	-1.79/-42.87	-0.61/-34.78!
$[R_{15}]\,[R_{24}]\,[R_{31}]$	-1.58/-43.29#	-1.02/-44.15	-0.3/-41.09!	2.56/-43.24#	-0.73/-44.31	-2.79/-48.67!
$[R_{15}]\,[R_{24}]\,[R_{32}]$	-0.96/-43.38	-0.73/-42.91	-0.51/-35.4!	-1.98/-40.87#	-0.44/-41.13	-1.66/-36.3!
$[R_{16}]\,[R_{24}]\,[R_{31}]$	-4.79/-54.09#	-4.7/-50.04	-3.04/-41.8!	-5.46/-51.53#	-3.9/-50.5	-3.91/-40.42!
$[R_{16}]\,[R_{24}]\,[R_{32}]$	-1.37/-45.72	-1.64/-51.42	-0.65/-40.88!	-1.12/-47.4	-0.82/-44.18	-0.77/-33.96!
$[R_{11}]\,[R_{25}]\,[R_{31}]$	-2.79/-47.81!	-1.02/-38.15	-1.68/-46.73!	-2.77/-46.69!	-1.46/-39.93	-2.61/-38.88!
$[R_{11}]\,[R_{25}]\,[R_{32}]$	-1.16/-41.22	-1.71/-43.3	-0.27/-38.83!	-1.81/37.55#	-0.7/-35.7	-0.71/-35.62!
$[R_{12}]\,[R_{25}]\,[R_{31}]$	-4.75/-46.55!	-3.84/-40.26	-3.88/-47.06!	-5.25/-44.08!	-2.76/-41.97	-4.85/-42.34!
$[R_{12}]\,[R_{25}]\,[R_{32}]$	-0.68/-40.09!	-1.32/-40.72	-0.18/-39.31!	-1.87/-40.21#	-1.39/-34.68	-1.85/-35.73!
$[R_{13}]\,[R_{25}]\,[R_{31}]$	-5.01/-48.5!	-4.15/-45.13	-4.15/-49.38!	-5.12/-41.15!	-3.21/-42.57	-4.12/-41.15!
$[R_{13}]\,[R_{25}]\,[R_{32}]$	-0.8/-41.91!	-1.33/-45.86	-0.28/-41.84!	-0.04/-38	-1.55/-13.13	-0.43/-36.95!
$[R_{14}]\,[R_{25}]\,[R_{31}]$	-4.43/-51.32#	-3.75/-46.48	-2.86/-37.76#	-5.17/-46.76!	-3.44/-46.28	-4.71/-46.56!
$[R_{14}]\,[R_{25}]\,[R_{32}]$	-0.98/-43.69	-1.72/-48.07	-1.06/-42.03#	-0.6/-40.87	-1.34/-46.25	-1.24/-38.73!
$[R_{15}]\,[R_{25}]\,[R_{31}]$	-5.73/-60.31!	-3.61/-45.77	-2.48/-34.65!	-6.38/-53.48!	-2.67/-44.45	-5.1/-44.56!
$[R_{15}]\,[R_{25}]\,[R_{32}]$	-0.23/-44.3!	1.31/-41	0.49/-42.18!	-1.49/-43.94!	0.33/-42.79	-0.96/-36.52!
$[R_{16}]\,[R_{25}]\,[R_{31}]$	-5.69/-54.73!	-4.23/-49.34	-4.92/-48.7!	-5.48/-53.76#	-3.47/-49.79	-4.43/-44.59!
$[R_{16}]\,[R_{25}]\,[R_{32}]$	-1.07/-44.34	-1.66/-49.27	-0.51/-47.99!	-2.92/-47.85!	-0.7/-48.29	-1.27/-40.45!

Ligand	3.5	3.5*	3.5**	4.0	4.0*	4.0**
$[R_{11}][R_{26}][R_{31}]$	-1.75/-40.94!	-1.8/-42.54	-1.9/-42.51#	-2.56/-43.91!	-1.91/-38.97	-2.02/-41.56#
$[R_{11}][R_{26}][R_{32}]$	-0.55/-40.86	-0.79/-38.32	0.82/-34.83!	-1.64/-32.31#	-0.86/-31.03	-2.27/-37.38!
$[R_{12}][R_{26}][R_{31}]$	-1.38/-42.66#	-1.7/-43.75	-0.55/-41.5!	-1.13/-45.89	-2.18/-44.71#	-1.74/-41.32#
$[R_{12}][R_{26}][R_{32}]$	-1.27/-45.52	-0.2/-40.27	-0.94/-41.61#	-0.13/-39.38	0.04/-41.91	-2.09/-38.29!
$[R_{13}][R_{26}][R_{31}]$	0.16/-38.8	-1.38/-49.57	-0.28/-42.28!	-3.09/-47.6!	-2.34/-47.29#	-2.09/-44.59#
$[R_{13}][R_{26}][R_{32}]$	-0.71/-44.20	-0.84/-41.2	-0.78/-43.89#	-1.21/-36.67!	0.01/-42.69	-0.24/-35.36!
$[R_{14}][R_{26}][R_{31}]$	-4.58/-47.4#	-3.93/-42.69	-3.62/-40.39#	-3.4/-39.85	-5.75/-48.91#	-4.6/-44.03#
$[R_{14}][R_{26}][R_{32}]$	-0.63/-44.3	0.33/-41.19	0.35/-41.03!	-1.88/-51.92	-0.42/-38.89	-0.71/-33.51#
$[R_{15}][R_{26}][R_{31}]$	-1.81/-49.91!	-0.09/-42.22	-1.16/-47.92#	-2.19/-43.52#	-0.51/-43.28	-1.07/-40.61#
$[R_{15}][R_{26}][R_{32}]$	-0.7/-48.81	0.47/-42.05	-0.15/-42.73#	-2.59/-39.86!	0.8/-43.49	-0.72/-38.69!
$[R_{16}][R_{26}][R_{31}]$	-4.5/-47.75	-3.99/-48.12	-3.48/-48.47!	-3.91/-47.99	-3.16/-46.99	-4.85/-46.95#
$[R_{16}][R_{26}][R_{32}]$	-1.68/-54.11	-1.17/-52.79	-0.41/-45.95!	0.11/-44.95	-0.66/-53.52	-1.17/-40.97#
$[R_{11}][R_{27}][R_{31}]$	-2.34/-43.15#	-1.62/-41.34	-1.87/-41.53!	-2.45/-45.62!	-1.84/-42.53	-2.42/-39.39#
$[R_{11}][R_{27}][R_{32}]$	-4.04/-38.1!	-1.03/-40.17	0.03/-37.89!	-3.39/-37.96!	-1.36/-35.56	-1.57/-34.43!
$[R_{12}][R_{27}][R_{31}]$	-2.19/-48.11	-1.65/-44.47	-1.61/-39.14!	-2.93/-47.36!	-2.58/-43.38	-2.34/-41.61!
$[R_{12}][R_{27}][R_{32}]$	-1.51/-37.41!	-0.74/-39.73	-0.83/-42.29#	-2.53/-39.37!	-0.73/-38.46	-1.24/-34.94#
$[R_{13}][R_{27}][R_{31}]$	-2.39/-48.95	-1.41/-42.92	-2.16/-49.01!	-2.01/-48.85!	-1.46/-45.82	-2.75/-44.59#
$[R_{13}][R_{27}][R_{32}]$	-1.55/-44.18	-0.96/-43.4	0.04/-43.37!	-2.96/-40.52!	-0.44/-37.58	-1.33/-38.07#
$[R_{14}][R_{27}][R_{31}]$	-5.01/-55.57	-3.97/-46.83	-4.24/-48.26#	-4.37/-55.23	-2.83/-46.26	-4.75/-41.27#
$[R_{14}][R_{27}][R_{32}]$	-1.06/-46.44	-1/.48.45	-0.39/-40.31#	-4.2/-45.63!	-0.77/-46.79	-0.8/-33.11!
$[R_{15}][R_{27}][R_{31}]$	-1.72/-46.29!	-0.92/-46.79	-0.92/-41.3#	-2.36/-45.06!	-0.29/-43.99	-1.13/-43.92!
$[R_{15}][R_{27}][R_{32}]$	-0.23/-43.25	0.42/-39.11	-0.08/-39.12#	-2.51/-42.63!	0.35/-36.15	-0.64/-39.09#
$[R_{16}][R_{27}][R_{31}]$	-1.9/-54.4#	-4.16/-50.63	-2.7/-40.17#	-4.27/-49.54#	-3.81/-51.98	-4.38/-45.25!
$[R_{16}][R_{27}][R_{32}]$	-1.66/-48.01!	-1.64/-52.24	-0.04/-49.34!	-1.59/-45.27!	0.73/-48.45	-0.41/-38.16!
$[R_{11}][R_{28}][R_{31}]$	-1.46/-38.23!	-2.01/-38.21	-2.1/-44.12!	-2.48/-38.8!	-1.27/-38.31	-2.58/-36.85!
$[R_{11}][R_{28}][R_{32}]$	-1.1/-34.51	-1.65/-40.12	-1.4/-39.2!	-1.1/-32.35	-1.4/-33.72	-1.99/-32.65!
$[R_{12}][R_{28}][R_{31}]$	-2.19/-43.46	-1.66/-39.74	-1.82/-44.14!	-2.15/-38.89!	-2.12/-44.81	-2.43/-42.52!
$[R_{12}][R_{28}][R_{32}]$	-1.56/-39.64	-1.02/-39.47	-1.38/-34.6!	-1.41/-29.86#	-0.5/-37.59	-1.59/-35.49!
$[R_{13}][R_{28}][R_{31}]$	-1.64/-45.49	-1.53/-44.03	-1.7/-44.5!	-1.33/-44.9	-3.2/-46.77	-3.08/-42.87!
$[R_{13}][R_{28}][R_{32}]$	-0.99/-43.31	-1.24/-38.98	-0.35/-38.95!	-0.7/-40.49	-1.11/-38.6	-1.17/-35.62!

Ligand	3.5	3.5*	3.5**	4.0	4.0*	4.0**
$[R_{14}][R_{28}][R_{31}]$	-4.79/-51.27	-3.78/-39.25	-3.97/-45.45!	-5.65/-50.36#	-3.83/-39.06	-4.57/-41.12!
$[R_{14}][R_{28}][R_{32}]$	-1.63/-43.78	-1.65/-43.69	-0.23/-38.78!	-1.63/-36.7#	-0.67/-44.46	-0.79/-31.13!
$[R_{15}][R_{28}][R_{31}]$	-2.09/-50.68	-0.72/-42.23	-1.39/-48.16!	-1.73/-49.6	-0.62/-42.09	-2.27/-47.45!
$[R_{15}][R_{28}][R_{32}]$	-0.21/-40.28	-0.19/-41.52	0.22/-38.87!	0.34/-39.35	-1.18/-42.88	-0.73/-32.94#
$[R_{16}][R_{28}][R_{31}]$	-4.93/-53.99#	-3.44/-45.64	-4.32/-50.85!	-4.28/-52.15	-3.6/-47.25	-5.46/-47.17!
$[R_{16}][R_{28}][R_{32}]$	-1.34/-46.88	-1.88/-52.73	-1.32/-46.27!	-0.7/-44.1	-0.85/-44.7	-0.93/-43.01!
$[R_{11}][R_{29}][R_{31}]$	-2.56/-38.92	-1.77/-35.02	-2.09/-45.26!	-3.45/-51.64	-3.13/-13.52!	-/-
$[R_{11}][R_{29}][R_{32}]$	-2.17/-40.04!	-0.94/-37.5	-0.54/-38.99!	-1.12/-38.68	-0.42/-35.44	-1.3/-36.3!
$[R_{12}][R_{29}][R_{31}]$	-4.2/-34.39	-3.73/-39.48	-3.67/-47!	-4.38/-36.73!	-2.88/-40.77	-/-
$[R_{12}][R_{29}][R_{32}]$	-1.59/-39.87	-2.17/-43.34	-1.09/-41.28!	-1.73/-41.38	-1.67/-36.86	-2.35/-36.46!
$[R_{13}][R_{29}][R_{31}]$	-4.38/-44.89!	-4.34/-41.1	-3.7/-48.8!	-4.64/-42.83!	-3.23/-42.65	-/-
$[R_{13}][R_{29}][R_{32}]$	-0.75/-35.8	-0.54/-43.57!	-0.49/-42.39!	-2.37/-46.7	-0.1/-37.26	-1.39/-34.39!
$[R_{14}][R_{29}][R_{31}]$	-5.09/-50.83#	-3.91/-46.95	-4.55/-52.45!	-4.03/-41.04	-5.04/-49.32	-/-
$[R_{14}][R_{29}][R_{32}]$	-2.12/-47.34#	-1.33/-38.5	-0.26/-40.7!	-1.3/-43.66	-0.65/-39.25	-1.33/-37.81!
$[R_{15}][R_{29}][R_{31}]$	-3.08/-34.05!	-4.32/-49.82!	-4.74/-52.69!	-4.63/-39.8!	-3.3/-42.41	-/-
$[R_{15}][R_{29}][R_{32}]$	-0.89/-41.02	-0.57/-42.9	-1.68/-40.92!	-0.67/-42.28#	-1.06/-10.54	-2.25/-39.31!
$[R_{16}][R_{29}][R_{31}]$	-4.86/-47.15#	-4.68/-50.71	-4.78/-53.84!	-5.17/-47.07#	-4.76/-50.21	-/-
$[R_{16}][R_{29}][R_{32}]$	-2.09/-48.56#	-2/-47.6	-1.01/-45.97!	-1.42/-49.3	-0.42/-39.77	-0.43/-36.38
$[R_{11}][R_{210}][R_{31}]$	-1.91/-37.49	-1.35/-36.17	-1.44/-42.36!	-2.11/-34.55!	-0.42/-32.76	-2.9/-41.1!
$[R_{11}][R_{210}][R_{32}]$	0.15/-29.06	-0.29/-35.82	-1.19/-40.46!	-0.83/-31.48	-0.62/-34.77	-1.05/-29.52!
$[R_{12}][R_{210}][R_{31}]$	-0.79/-36.09#	0.98/-41.01	-0.56/-30.24#	-0.58/-34.57	-0.79/-41.45	-2.4/-38.65!
$[R_{12}][R_{210}][R_{32}]$	0.25/-27.87	-0.21/-38.99	-1.11/-42.84!	-2.86/-41.77#	-0.18/-40.19	-0.78/-31.25#
$[R_{13}][R_{210}][R_{31}]$	-1.47/-36.15	-0.89/-42.71	-1.53/-38.96#	-3.07/-46.85#	-0.65/-41.68	-1.89/-39.11!
$[R_{13}][R_{210}][R_{32}]$	-1.15/-40.09#	-1/-43.74	0.42/-36.45#	-1.69/-31.08#	-0.44/-48.3	-0.91/-34.18#
$[R_{14}][R_{210}][R_{31}]$	-2.04/-46.73#	-1/-45.13	-1.14/-44.12!	-2.69/-45.24#	-0.94/-43.44	-2.48/-43.89!
$[R_{14}][R_{210}][R_{32}]$	0.1/-30.32	-0.45/-40.4	-0.35/-38.3#	-1.87/-35.51#	-1.21/-38.26	-2/-36.71#
$[R_{15}][R_{210}][R_{31}]$	-1.37/-47.44	-1.84/-44.6	-0.71/-47.34!	-1.48/-48.6	-1.37/-43.55	-1.6/-42.29!
$[R_{15}][R_{210}][R_{32}]$	-0.28/-38.84!	-0.24/-43.23	-0.81/-42.38!	-1.15/-36.93#	-0.32/-42.8	-0.42/-31.24!
$[R_{16}][R_{210}][R_{31}]$	-1.54/-46.73#	-1.92/-49.41	-2.09/-49.31!	-2.43/-50.21#	-1.49/-43.75	-1.9/-42.11!
$[R_{16}][R_{210}][R_{32}]$	-0.54/-42.32	-1.22/-51.15	-0.55/-47.27!	-1.86/-46.43#	-1.21/-45.68	-1.98/-39.21!

E.8 Main Structure 8

Ligand	3.0	3.5*	3.5**	4.0	4.0*	4.0**
$[R_{11}][R_{21}][R_{31}]$	-3.28/-44.03	-2.91/-37.04	-1.93/-36.75!	-1.19/-33.92	-1.66/-36.55	-/-
$[R_{11}][R_{21}][R_{32}]$	-4.86/-40.94	-3.94/-35.73	-3.75/-34.59!	-3.9/-40.55	-2.81/-26.81	-4.52/-31.74!
$[R_{12}][R_{21}][R_{31}]$	-3.04/-50.22	-2.67/-40.4	-2.71/-43.75!	-0.79/-38.16	-1.37/-39.6	-/-
$[R_{12}][R_{21}][R_{32}]$	-1.99/-42.07	-1.97/-39.1	-1.51/-35.45!	-1.21/-41.09	-1.96/-39.16	-2.27/-30.81#
$[R_{13}][R_{21}][R_{31}]$	1.73/-36.01	-2.33/-44.15	-3.02/-46.81!	-1.75/-40.9	-2.8/-48.78	-/-
$[R_{13}][R_{21}][R_{32}]$	-2.35/-44.12	-2.54/-47.98	-1.35/-40.13#	-2.57/-46.91	-1.65/-54.32	-3.3/-35.46#
$[R_{14}][R_{21}][R_{31}]$	-6.92/-53.7	-4.58/-44.68	-1.61/-14.9#	-4.87/-55.51	-3.82/-43.76	-/-
$[R_{14}][R_{21}][R_{32}]$	-0.77/-33.22	-1.92/-39.35	-1.43/-40.62#	-1.76/-36.21	-0.93/-36.25	-2.66/-37.86#
$[R_{15}][R_{21}][R_{31}]$	-5.5/-55.43	-1.35/-41.39	-1.56/-43.93!	-3.19/-55.09	-1.7/-42.09	-/-
$[R_{15}][R_{21}][R_{32}]$	-1.94/-45.32	-0.65/-43.28	-0.75/-35.7!	-0.85/-44.4	-1.19/-42.17	-0.89/-38.26#
$[R_{16}][R_{21}][R_{31}]$	-5.72/-54.79#	-5.9/-52.68	-4.71/-42.56#	-5.42/-41.86#	-4.97/-45.31	-/-
$[R_{16}][R_{21}][R_{32}]$	-1.75/-45.27#	-0.81/-39.32	-2.51/-41.13#	-1.19/-42.25	-0.32/-39.85	-2.01/-37.2!
$[R_{11}][R_{22}][R_{31}]$	-2.98/-41.91	-2.21/-38.51	-2.58/-44.96!	-1.73/-38.59	-2.41/-45.41	-/-
$[R_{11}][R_{22}][R_{32}]$	-3/-51.73	-2.74/-38.78	-1.16/-17.74!	-2.37/-50.31	-2.74/-35.48	-3.96/-36.13!
$[R_{12}][R_{22}][R_{31}]$	-7.24/-48.2	-3.72/-37.3	-/-	-3.6/-41.54	-2.48/-33.3	-/-
$[R_{12}][R_{22}][R_{32}]$	-2.71/-46.97	-2.7/-46.26	-0.4/-1584!	-2.29/-47.79	-2.1/-37.89	-2.11/-36.13!
$[R_{13}][R_{22}][R_{31}]$	-3.57/-35.71	-3.05/-41.24	-2.86/-31.63#	-3.93/-43.09	-3.23/-35.95	-/-
$[R_{13}][R_{22}][R_{32}]$	-2.23/-46.47	-2.8/-40	-0.57/-27.84!	-1.58/-41.68	-1.64/-35.95	-0.28/-20.97!
$[R_{14}][R_{22}][R_{31}]$	-4.75/-45.47	-3.52/-37.3	-4.2/-39.85#	-4.06/-40.6#	-1.83/-39.63	-/-
$[R_{14}][R_{22}][R_{32}]$	-1.88/-47.29	-1.99/-43.89	-2.52/-46.81#	-2.1/-48.82	-2.23/-45.28	-1.75/-34.23!
$[R_{15}][R_{22}][R_{31}]$	-3.43/-30.92!	-3.91/-29.56	-4.51/-49.89!	-1.79/-29.7	-2.48/-36.56	-/-
$[R_{15}][R_{22}][R_{32}]$	-2.51/-47.27	-0.67/-37.81	0.37/-22.43!	-1.57/-46.68	-0.92/-38.89	-1.38/-32.06!
$[R_{16}][R_{22}][R_{31}]$	-5.49/-56.33	-6.07/-55.58	-4.59/-53.35!	-5.14/-52.88#	-4.48/-51.43	-/-
$[R_{16}][R_{22}][R_{32}]$	-1.19/-36.59	-0.61/-40.29#	-1.45/-47.73!	-0.32/-37.52	-0.93/-36.79	-2.38/-36.3!
$[R_{11}][R_{23}][R_{31}]$	-2.72/-19.11	-4.73/-40.99	-5.28/-50.02!	-2.16/-27.14	-3.62/-44.04	-/-
$[R_{11}][R_{23}][R_{32}]$	-1.68/-37.96	-2.35/-41.17	-0.81/-29.84!	-4.04/-43.85!	-2.04/-38.11	-3.12/-40.16!
$[R_{12}][R_{23}][R_{31}]$	-4.72/-47.04	-4.87/-50.96	-2.68/-19.71!	-4.47/-40.6!	-3.98/-40.7	-/-
$[R_{12}][R_{23}][R_{32}]$	-2.11/-38.85	-1.81/-37.88	0.25/-26.11!	-1.75/-29.5!	-2.03/-43.33	-2.77/-35.85!
$[R_{13}][R_{23}][R_{31}]$	-3.32/-30.22#	-3.56/-34.92	-2.55/-21.13!	-5.16/-55.04	-3.67/-45.61	-/-
$[R_{13}][R_{23}][R_{32}]$	-4.35/-44.12#	-3.87/-39.81	-4.25/-42.71#	-5.27/-39.54	-3.91/-40.29	-5.22/-36.51!

Ligand	3.5	3.5*	3.5**	4.0	4.0*	4.0**
$[R_{14}][R_{23}][R_{31}]$	-4.77/-50.52#	-5.03/-48.82!	-3.31/-42.23#	-4.3/-45.97#	-4.96/-47.4	-/-
$[R_{14}][R_{23}][R_{32}]$	-4.91/-48.82!	-4.11/-45.56!	-3.45/-43.98#	-6.3/-48.94!	-4.37/-45.21!	-4.04/-41.26#
$[R_{15}][R_{23}][R_{31}]$	-4.09/-50.9	-5.05/-46.83	-2.51/-32.81#	-2.18/-29.99	-4.27/-50.99	-/-
$[R_{15}][R_{23}][R_{32}]$	-4.54/-42.24!	-2.86/-34.68	-4/-43.11!	-5.27/-44.79!	-3.14/-44.57	-3.78/-25.96!
$[R_{16}][R_{23}][R_{31}]$	-3.53/-37.34!	-3.71/-46.68	-4.21/-44.26#	-4.17/-51.79	-3.45/-51.98	-/-
$[R_{16}][R_{23}][R_{32}]$	-4.68/-46.83	-2.5/-37.5	-4.23/-48.85!	-5.04/-43.98!	-4.3/-50.77	-3.23/-38.35#
$[R_{11}][R_{24}][R_{31}]$	-2.9/-44.7!	-1.21/-38.37	-2.64/-49.84!	-3.38/-42.8!	-2.94/-40.02!	-2.82/-41.68!
$[R_{11}][R_{24}][R_{32}]$	-2.02/-40.34	-2.13/-39.08	-2.42/-37.62!	-1.56/-42.86	-2.59/-37.81	-2.52/-35.22!
$[R_{12}][R_{24}][R_{31}]$	-3.04/-46.89	-2.42/-41.62	-2.91/-46.85!	-3.54/-45.43#	-3.86/-49.63!	-3.56/-47.09!
$[R_{12}][R_{24}][R_{32}]$	-1.94/-41.73	-2.65/-42.35	-0.42/-33.07!	-0.92/-42.48	-2.16/-39.41	-2.19/-35.02!
$[R_{13}][R_{24}][R_{31}]$	-4.21/-45.49!	-4.85/-50.86	-2.86/-28.74#	-5.84/-50.28!	-3.26/-51.6	-3.46/-35.02#
$[R_{13}][R_{24}][R_{32}]$	-1.11/-45.1	-1.82/-41.09	-1.21/-42.22#	-0.69/-35.08	-0.8/-48.03	-2.63/-36.85#
$[R_{14}][R_{24}][R_{31}]$	-3.76/-41.23#	-5.09/-49.63	-2.88/-37.72#	-5.28/-49.09!	-3.59/-49.24	-4.17/-39.65#
$[R_{14}][R_{24}][R_{32}]$	-2.23/-49.89	-1.78/-43.34	-1.75/-45.44#	-2.09/-51.54	-1.73/-43.4	-2/-39.34#
$[R_{15}][R_{24}][R_{31}]$	-3.98/-47.03!	-4.4/-44.79	-3.91/-39.32!	-5.9/-51.66!	-3.22/-51.47	-2.14/-41.16!
$[R_{15}][R_{24}][R_{32}]$	-1.95/-47.21	-1.67/-41.85	-0.1/-34.28!	-0.44/-43.34	-0.46/-40.68	-2.04/-37.69#
$[R_{16}][R_{24}][R_{31}]$	-5.92/-55.23!	-5/-53.77	-3.17/-39.57#	-6.4/-59.54#	-4.48/-50.79	-3.61/-39.41#
$[R_{16}][R_{24}][R_{32}]$	-1.64/-45.51	-1.46/-48.71	-1.48/-45.3#	-3.64/-48.06#	-1.65/-44.89	-1.34/-40.23#
$[R_{11}][R_{25}][R_{31}]$	-4.22/-43.6!	-3.66/-37.75	-4.99/-49.69!	-6.95/-52.12!	-4.41/-43.73	-4.96/-45.07!
$[R_{11}][R_{25}][R_{32}]$	-1.64/-44.6	-1.52/-39.29	-2.36/-42.47!	-2.45/-36.82!	-1.12/-39.81	-2.88/-42.13!
$[R_{12}][R_{25}][R_{31}]$	-5.37/-54.17!	-3.87/-42.68	-5.22/-50.36!	-6.48/-54.57!	-5.95/-53.59!	-5.03/-45.25!
$[R_{12}][R_{25}][R_{32}]$	-1.97/-43.94!	-2.07/-41.91	0.28/-32.83!	-2.02/-35.62#	-2.14/-42.95	-2.45/-38.37!
$[R_{13}][R_{25}][R_{31}]$	-4.62/-49.14!	-5.32/-54.71#	-3.57/-30.27#	-6.44/-55.57!	-4.89/-47.46!	-4.15/-37.16!
$[R_{13}][R_{25}][R_{32}]$	-1.74/-49.88	-1.58/-47.26	-1.04/-39.21#	-1.2/-48.36	-2.46/-47.07	-0.66/-35.21!
$[R_{14}][R_{25}][R_{31}]$	-5.28/-51.69!	-4.79/-49.96	-3.35/-39.75#	-3.08/-40.79	-5.1/-46.77!	-4.2/-42.66!
$[R_{14}][R_{25}][R_{32}]$	-4.85/-49.86	-4.58/-46.07	-3.04/-35.96#	-3.18/-40.26	-4.05/-39.48	-3.79/-36.85!
$[R_{15}][R_{25}][R_{31}]$	-5.01/-57.78!	-4.75/-50.75	-5.03/-52.55!	-5.2/-49.01!	-5/-48.5!	-4.6/-43.11!
$[R_{15}][R_{25}][R_{32}]$	-1.04/-46.17	-0.93/-43.59	-0.93/-33.08!	0.31/-39.45	-1.18/-39.37	-1.65/-40.73!
$[R_{16}][R_{25}][R_{31}]$	-5.08/-51.37!	-3.93/-48.41	-4.22/-44.96#	-3.59/-50.11	-3.42/-47.02	-5.07/-45.99#
$[R_{16}][R_{25}][R_{32}]$	-5.05/-52.18!	-3.74/-46.95	-4.31/-48.59#	-3.34/-53.59	-4.41/-52.15	-4.82/-45.5#

Ligand	3.5	3.5*	3.5**	4.0	4.0*	4.0**
$[R_{11}][R_{26}][R_{31}]$	-3.34/-53.83	-1.69/-44	-2.08/-43.11!	-2.96/-55.91	-2.32/-44.37	-2.05/-40.16#
$[R_{11}][R_{26}][R_{32}]$	-0.93/-39.65	-0.76/-36.94	-0.91/-45.79!	-3.03/-39.28	-0.4/-35.38	-2.72/-41.49!
$[R_{12}][R_{26}][R_{31}]$	-1.78/-44.27	-2.66/-44.78	-2.27/-44.45!	-0.91/-39.81#	-0.79/-47.92	-2.52/-41.61#
$[R_{12}][R_{26}][R_{32}]$	-1.27/-41.91	-1.21/-43.11	0.29/-32.98!	-1.3/-47.14	-1.73/-37.82	-1.74/-30.99!
$[R_{13}][R_{26}][R_{31}]$	-4.93/-47.53	-5.03/-48.06	-3.99/-37.99#	-4.62/-49.17	-3.84/-43.06	-4.82/-44.51#
$[R_{13}][R_{26}][R_{32}]$	-1.47/-46.88	-1.84/-41.48	0.53/-31.67!	-1.01/-47.14	-1.5/-44.61	-0.5/-33.97!
$[R_{14}][R_{26}][R_{31}]$	-5.34/-50.53	-4.19/-42.91	-3.13/-37.17!	-5.61/-52.64#	-4.22/-48.12	-4.28/-41.88#
$[R_{14}][R_{26}][R_{32}]$	-0.92/-42.3	-0.64/-41.73	-1.05/-43.71#	-1.01/-50.18	-0.68/-46.86	-1.23/-37.7#
$[R_{15}][R_{26}][R_{31}]$	-5.13/-54.96	-4.49/-50.92	-3.2/-44.83!	-5.07/-57.6	-3.32/-53.62	-5.21/-43.94!
$[R_{15}][R_{26}][R_{32}]$	-0.82/-47.75	-0.61/-46.24	-1.09/-45.02#	-0.32/-49.16	-0.41/-46.06	-1.36/-39.89!
$[R_{16}][R_{26}][R_{31}]$	-5.57/-60.38	-5.81/-58.55	-4.35/-52.09!	-5.53/62.15	-5.05/-55.17	-4.22/-47.87!
$[R_{16}][R_{26}][R_{32}]$	-2.4/-57.14	-2.06/-50.03	-1.18/-46.76!	-2.61/-55	-0.42/-54.57	-0.61/-39.65!
$[R_{11}][R_{27}][R_{31}]$	-2.99/-47.24	-2.14/-43.01	-1.65/-41.52!	-4.12/-50.17!	-2.97/-49.83	-2.89/-39.17!
$[R_{11}][R_{27}][R_{32}]$	-4.47/-40.8!	-2.14/-42.43	-1.87/-44.08!	-4.5/-40.32!	-1.86/-35.03	-1.96/-34.52!
$[R_{12}][R_{27}][R_{31}]$	-4.74/-42.09!	-4.26/-45.02	-3.53/-41.36#	-5.68/-51.34!	-4.48/-47.36	-5.1/-41.22!
$[R_{12}][R_{27}][R_{32}]$	-2.93/-49.76	-2.53/-45.92	-1.76/-40.79!	-1.48/-40.85!	-1.86/-44.56	-2.22/-36.28!
$[R_{13}][R_{27}][R_{31}]$	-4.62/-46.36	-4.39/-49.11	-4/-38.06#	-4.77/-49.13	-4.42/-46.93	-4.24/-40.6!
$[R_{13}][R_{27}][R_{32}]$	-2.38/-51.6	-2.63/-48.12	-1.57/-45.24#	-1.94/-51.63	-2.54/-47.72	-2.15/-38.36#
$[R_{14}][R_{27}][R_{31}]$	-4.93/-47.15#	-5.85/-55.86	-5.18/-45.35#	-5.46/-48.93#	-4.66/-48.97	-4.98/-43.32#
$[R_{14}][R_{27}][R_{32}]$	-2.79/-54.92	-2.32/-49.35	-0.56/-45.41#	-4.93/-55.56#	-1.82/-43.69	-1.5/-42.33#
$[R_{15}][R_{27}][R_{31}]$	-5.3/-53.5	-5.28/-53.68	-2.56/-36.61!	-4.65/-49.21!	-3.08/-50.7	-5.04/-45.39#
$[R_{15}][R_{27}][R_{32}]$	-1.73/-51.53	-0.39/-40.42	-1.03/-47.11#	-2.21/-52.47	-1.75/-46.84	-0.89/-36.81!
$[R_{16}][R_{27}][R_{31}]$	-5.15/-52.86#	-4.61/-53.92	-4.11/-41.92#	-5.32/-57.79#	-4.62/-54.14	-4.52/-43.01#
$[R_{16}][R_{27}][R_{32}]$	-2.8/-77.89	-2.47/-57.38	-1.13/-44.35!	-3/-56.23	-0.57/-59.55	-2.31/-41.23!
$[R_{11}][R_{28}][R_{31}]$	-2.1/-39.63	-1.94/-33.74	-2.77/-41.97!	-3.67/-54.42	-2.86/-40.78!	-3.26/-45.85!
$[R_{11}][R_{28}][R_{32}]$	-1.86/-36.66	-2.53/-40.5	-1.83/-44.81!	-1.15/-35.25	-2.72/-37.38!	-3.03/-38.35!
$[R_{12}][R_{28}][R_{31}]$	-2.42/-38.65!	-1.89/-40.4	-2.97/-46.1!	-2.18/-33.78	-3.75/-45.25!	-3.46/-45.79!
$[R_{12}][R_{28}][R_{32}]$	-2.49/-48.7	-1.77/-46.01	-1.72/-46.27!	-1.71/-41.82	-3.76/-41.03#	-2.84/-37.71!
$[R_{13}][R_{28}][R_{31}]$	-4.12/-39.17#	-4.56/-46.2	-5.05/-50.32!	-3.12/-46.25	-3.96/-51.51	-6.01/-42.17!
$[R_{13}][R_{28}][R_{32}]$	-2.02/-41.82	-1.92/-40.15	-1.25/-37.98#	-0.97/-37.39	-2.5/-34.95	-1.23/-36.4!

Ligand	3.5	3.5*	3.5**	4.0	4.0*	4.0**
$[R_{14}][R_{28}][R_{31}]$	-4.58/-38.92#	-4.33/-48.35	-4.89/-50.63!	-5.67/-46.16#	-3.38/-47.7	-5.21/-42.49!
$[R_{14}][R_{28}][R_{32}]$	-2.56/-48.52	-2.25/-42.28	-1.98/-45.28#	-2.34/-50.13	-1.21/-45.35	-0.87/-31.23#
$[R_{15}][R_{28}][R_{31}]$	-5.43/-57.03	-4.04/-46.89	-4.6/-48.95!	-5.32/-58.21	-4.2/-45.52	-5.02/-47.1!
$[R_{15}][R_{28}][R_{32}]$	-0.94/-44.74	-1.07/-41.95	-1.07/-41.96!	-0.86/-48.87	-0.95/-37.54	-1.46/-40.13!
$[R_{16}][R_{28}][R_{31}]$	-5.78/-61.33	-5.67/-57.52	-5.11/-54.69!	-5.77/-63.06	-5.36/-55.14	-5.41/-47.72!
$[R_{16}][R_{28}][R_{32}]$	-2.58/-51.66	-0.83/-41.13	-1.28/-44.16!	-1.73/-47.29	-1.51/-44.58	-2.01/-39.86#
$[R_{11}][R_{29}][R_{31}]$	-4.48/-37.36	-4.86/-43.24	-3.67/-32.59!	-2.66/-33.61	-3.24/-35.59	-/-
$[R_{11}][R_{29}][R_{32}]$	-1.99/-43.84	-2/-34.78	-0.89/-35.28!	-3.28/-41.06!	-2.69/-36.89	-3.03/-36.47!
$[R_{12}][R_{29}][R_{31}]$	-4.02/-35.29!	-4.69/-41.97	-4.16/-35.65!	-4.74/-36.08!	-3.85/-42.63	-/-
$[R_{12}][R_{29}][R_{32}]$	-0.24/-30.12	-2.84/-42.96	-1.61/-43.14!	-0.81/-41.99	-3.13/-46.68	-3.17/-41.95!
$[R_{13}][R_{29}][R_{31}]$	-5.79/-53.36#	-5.23/-48.05	-3.58/-27.87#	-5.2/-43.99!	-4.44/-49.06	-/-
$[R_{13}][R_{29}][R_{32}]$	-2.85/-49.65	-2.73/-45.15	-1.09/-40.95!	-2.52/-48.91	-0.82/-42.31	-2.5/-37.71!
$[R_{14}][R_{29}][R_{31}]$	-4.21/-45.53	-5.07/-48.29	-5.1/-43.13#	-3.06/-48.53	-4.72/-44.19#	-/-
$[R_{14}][R_{29}][R_{32}]$	-5.38/-52.53	-5.28/-50.45	-3.1/-36.57!	-4.23/-49.26	-4.2/-59.67	-3.97/-37.83!
$[R_{15}][R_{29}][R_{31}]$	-4.02/-37.99	-4.46/-46.95	-5.03/-52.53!	-4.9/-40.74!	-5.06/-54.16	-/-
$[R_{15}][R_{29}][R_{32}]$	-1.72/-49.66	-1.15/-44.93	-2.35/-43.79!	-1.26/-43.1	-2.11/-44.6!	-2.6/-39.4!
$[R_{16}][R_{29}][R_{31}]$	-4.26/-43.29	-4.56/-52.09	-4.88/-47.55!	-3.73/-54.82	-3.49/-47.17	-/-
$[R_{16}][R_{29}][R_{32}]$	-6.1/-55.51	-5.17/-57.5	-2.6/-33.37#	-5.51/-47.94!	-5.31/-51.17	-4.71/-36.15!
$[R_{11}][R_{210}][R_{31}]$	-3.91/-39.96	-2.75/-45.79	-2.39/-44.61!	-2.55/-48.8	-3.71/-46.1!	-3.87/-44.74!
$[R_{11}][R_{210}][R_{32}]$	-0.97/-38.16	-1.16/-41.66	-0.99/-34.48!	-1.3/-39.46	-1.48/-37.09	-1.77/-31.99!
$[R_{12}][R_{210}][R_{31}]$	-2.37/-50.09	-2.77/-45.71	-2.36/-46.94!	-3.16/-51.85	-1.56/-48.87	-3.66/-46.02!
$[R_{12}][R_{210}][R_{32}]$	-2.04/-45.2	-1.13/-40.02	0.59/-27.34!	-3.14/-40.08#	-2.03/-37.81	-1.3/-36.55!
$[R_{13}][R_{210}][R_{31}]$	-3.11/-44.36#	-2.59/-45.46	-1.92/-43.59#	-3.8/-42.9#	-1.8/-46.69	-2.59/-37.92!
$[R_{13}][R_{210}][R_{32}]$	-1.63/-45.6	-0.92/-40.51	-0.76/-37.21#	-3.27/-43.38#	-1.14/-54.67	-2.36/-40.42#
$[R_{14}][R_{210}][R_{31}]$	-5.32/-55.28	-4.82/-46.75	-4.02/-44.6#	-5.59/-44.72#	-3.28/-46	-3.42/-26.06#
$[R_{14}][R_{210}][R_{32}]$	-1.93/-44.99	-1.7/-43.29	-1.78/-45.04#	-2.62/-38.61#	-1.74/-45.71	-1.56/-36.35#
$[R_{15}][R_{210}][R_{31}]$	-1.52/-41.84	-1.68/-46.57	-1.97/-41.09!	-0.89/-44.55	-0.2/-48.4	-2.9/-46.98!
$[R_{15}][R_{210}][R_{32}]$	-1.01/-48.84	-0.64/-43.94	0.1/-40.26!	-0.53/-44.59	0.01/-42.8	0.44/-34.32!
$[R_{16}][R_{210}][R_{31}]$	-4.26/-50.3	-5.8/-56.79	-5.24/-47.71!	-4.9/-52.82	-4.19/-52.86	-5.22/-42.52!
$[R_{16}][R_{210}][R_{32}]$	-1/-45.4#	-2.2/-52.82	-1.07/-49.1#	-2.83/-47.59!	-2.15/-50.42	-0.43/-36.75#

E.9 Main Structure 9

Ligand	3.0	3.5*	3.5**	4.0	4.0*	4.0**
$[R_{11}][R_{21}][R_{31}]$	-3.14/-43.94	-2.53/-39.63	-2.9/-42.26!	-1.71/-38.98	-1.42/-32.96	-/-
$[R_{11}][R_{21}][R_{32}]$	-4.72/-44.65	-4.4/-33.84	-2.93/-27.07!	-4.53/-44.38	-3.95/-46.62	-5.14/-33.05!
$[R_{12}][R_{21}][R_{31}]$	-2.1/-38.31	-3.29/-45.46	-2.97/-41.48!	-1.88/-41.1	-2.49/-41.79	-/-
$[R_{12}][R_{21}][R_{32}]$	-2.3/-41.15	-2.64/-36.5	-0.03/-20.4!	-2.12/-45.09	-2.08/-32.76	-1.73/-33.01!
$[R_{13}][R_{21}][R_{31}]$	-2.26/-39.57	-2.68/-45.13	-0.24/-23.35!	-2.04/-44.01	-1.16/-32.88	-/-
$[R_{13}][R_{21}][R_{32}]$	-2.33/-45.32	-2.01/-41.42	-1.91/-45.19#	-2.22/-44.82	-1.01/-37.39	-2.88/-38.38#
$[R_{14}][R_{21}][R_{31}]$	-4.75/-43.86	-5.4/-49.42	-4.87/-43.82!	-7.02/-49.59#	-3.89/-49.23	-/-
$[R_{14}][R_{21}][R_{32}]$	-1.49/-39.4	-2.19/-39.09	-1.2/-40.6#	-0.4/-32.93	-1.27/-39.16	-2.09/-33.94!
$[R_{15}][R_{21}][R_{31}]$	-1.72/-38.25	-1.71/-44.25	-0.83/-18.64#	-2.03/-49.4	-2.04/-46.05	-/-
$[R_{15}][R_{21}][R_{32}]$	-2.06/-46.26	-1.34/-35.27	-1.29/-37.54#	-0.66/-38.22	-1.56/-42.84	-0.96/-38.05#
$[R_{16}][R_{21}][R_{31}]$	-4.87/-45.78	-4.44/-50.99	-5.23/-49.53!	-4.39/-51.62	-4.5/-51.53	-/-
$[R_{16}][R_{21}][R_{32}]$	-1.26/-45.19	-1.38/-43.27	-1.89/-44.84#	-2.9/-52.19	-1.35/-41.39	-1.52/-34.35!
$[R_{11}][R_{22}][R_{31}]$	-1.74/-19.05!	-2.76/-35.77	-0.94/-14.1!	-3.14/-28.85!	-3.09/-39.14	-/-
$[R_{11}][R_{22}][R_{32}]$	-3.4/-43.37	-2.38/-38.31	-2.22/-41.79!	-2.01/-37.81	-1.19/-27.89	-0.58/-15.16!
$[R_{12}][R_{22}][R_{31}]$	-5.4/-44.7	-4.63/-40.23	-3.05/-29.14!	-4.28/-48.56	-4.17/-47.78	-/-
$[R_{12}][R_{22}][R_{32}]$	-1.05/-21.57	-2.58/-36.1	-0.48/-16.29!	-0.14/-9.37	-1.5/-42.21	-2.15/-32.17#
$[R_{13}][R_{22}][R_{31}]$	-4.51/-38#	-3.88/-38.09	-4.55/-41.8!	-4.46/-49.65	-2.9/-35.85	-/-
$[R_{13}][R_{22}][R_{32}]$	-1.11/-36.97	-1.35/-40.68	-2.04/-44.87#	-2.68/-48.35	-1.36/-29.85	-1.83/-34.46!
$[R_{14}][R_{22}][R_{31}]$	-6.05/-57.67	-4.33/-43.73	-2/-30.25#	-3.55/-36.41#	-2.94/-36.04	-/-
$[R_{14}][R_{22}][R_{32}]$	-1.73/-42.91	-1.97/-37.51	-0.02/-29.07#	-2.7/-42.74#	-1.94/-39.45	-1.87/-38.54#
$[R_{15}][R_{22}][R_{31}]$	-4.31/-45.51	-4.75/-53.59	-2.42/-32.36#	-6.65/-45.27#	-2.91/-37.2	-/-
$[R_{15}][R_{22}][R_{32}]$	-4.31/-45.51	-4.75/-53.59	-2.42/-32.36#	-6.65/-45.27#	-2.91/-37.2	-/-
$[R_{16}][R_{22}][R_{31}]$	-4.32/-51.42	-4.37/-42.74	-4.95/-50.83!	-5.46/-57.42	–4.35/-42.16	-/-
$[R_{16}][R_{22}][R_{32}]$	-3.06/-53.77	-1.32/-46.83	-0.39/-27.13!	0.21/-39.02	-2.4/-46.79	-1.25/-34.68#
$[R_{11}][R_{23}][R_{31}]$	-4.86/-47.82	-3.74/-31.41	-3.96/-36.18!	-5.01/-41.03!	-4.22/-43.39	-/-
$[R_{11}][R_{23}][R_{32}]$	-2.52/-44.52	-1.26/-36.48	-2.06/-39.97!	-2.29/-42.8	-2.35/-40.65	-1.82/-36.99!
$[R_{12}][R_{23}][R_{31}]$	-4.88/-48.85!	-3.93/-47.71	-4.38/-43.35!	-3.14/-11.13!	-3.43/-45.03	-/-
$[R_{12}][R_{23}][R_{32}]$	-1.42/-18.83!	-2.52/-49.17	-1.89/-45.39!	-2.46/-34.35!	-1.7/-19.11	-2.33/-37.96!
$[R_{13}][R_{23}][R_{31}]$	-3.83/-36.25!	-3.47/-41.36	-2.35/-27.46#	-4.28/-42.7!	-4.55/-54.61	-/-
$[R_{13}][R_{23}][R_{32}]$	-5.21/-50.27	-4.06/-37.66	-3.76/-42.27!	-4.09/-39.54!	-5.05/-48.4!	-5.27/-40.34#

Ligand	3.5	3.5*	3.5**	4.0	4.0*	4.0**
[R_{14}] [R_{23}] [R_{31}]	-3.36/-43.9#	-4.4/-45.29	-3.01/-35.18#	-3.31/-36.85#	-3.47/-43.07	-/-
[R_{14}] [R_{23}] [R_{32}]	-4.96/-57.01	-2.85/-38.64	-2.76/-31.12#	-3.23/-45.86	-3.99/-50.48	-3.76/-37.04
[R_{15}] [R_{23}] [R_{31}]	-4.08/-42.35	-3.76/-42.56	-1.61/-28.24#	-2.96/-38.5	-3.96/-49.33	-/-
[R_{15}] [R_{23}] [R_{32}]	-4.37/-40.09!	-3.46/-40.94	-2.87/-40.29#	-3.15/-33.38!	-3.65/-50.67	-4.53/-41.98!
[R_{16}] [R_{23}] [R_{31}]	-5.27/-55.83	-4.71/-52.45	-4.6/-46.23#	-3.23/-51.26	-6.01/-57.01!	-/-
[R_{16}] [R_{23}] [R_{32}]	-5.5/-46.32!	-4.33/-52.22	-4.53/-55.68!	-6.18/-47.49!	-3.85/-52.13	-3.58/-37.64#
[R_{11}] [R_{24}] [R_{31}]	-3.05/-44.83	-2.65/-45.66	-2.46/-41.14!	-2.9/-41.04!	-2.38/-48.07	-3.54/-43.53!
[R_{11}] [R_{24}] [R_{32}]	-1.77/-37.76	-2.27/-37.15	-1.18/-38.61!	-2.49/-48.02	-1.42/-43.8	-3.6/-39.32!
[R_{12}] [R_{24}] [R_{31}]	-2.94/-46.33	-2.29/-44.34	-2.04/-40.94!	-1.82/-42.84	-1.37/-45.09	-3.28/-42.5!
[R_{12}] [R_{24}] [R_{32}]	-2.94/-46.33	-2.29/-44.34	-2.04/-40.94!	-1.82/-42.84	-1.37/-45.09	-3.28/-42.5!
[R_{13}] [R_{24}] [R_{31}]	-4.22/-45.87!	-5.17/-55.69	-3.43/-31.39!	-5.68/-49.28!	-3.93/-47.11	-5.37/-39.63!
[R_{13}] [R_{24}] [R_{32}]	-2.28/-40.46	-2.01/-38.94	-0.9/-33.33!	-1.66/-41.5	-2.16/-38.65	-1.72/-35.79!
[R_{14}] [R_{24}] [R_{31}]	-4.81/-48.72#	-5.07/-47.62	-4.3/-39.55#	-6.05/-55.25#	-4.1/-51.53	-5.34/-39.6#
[R_{14}] [R_{24}] [R_{32}]	-3.43/-48.77	-1.44/-39.84	-1.24/-46.54!	-2.13/-51.58	-0.96/-44.52	-2.58/-42.62!
[R_{15}] [R_{24}] [R_{31}]	-5.38/-54.25#	-4.51/-51.65	-3.76/-44.21!	-3.68/-51.97#	-2.93/-51.64	-4.68/-42.1!
[R_{15}] [R_{24}] [R_{32}]	-2.22/-47.02	-0.99/-44.8	-0.43/-44!	-6.17/-59.09#	-0.47/-48.17	-1.14/-37.01!
[R_{16}] [R_{24}] [R_{31}]	-5.79/-60.61#	-4.64/-53.87	-3.68/-41.44#	-4.59/-58.49#	-4.12/-53.17	-5.69/-47.88!
[R_{16}] [R_{24}] [R_{32}]	-3.41/-58.8#	-1.73/-51.65	-1.44/-43.63!	-4.59/-58.49#	-1.6/-48.79	-2.23/-38.87!
[R_{11}] [R_{25}] [R_{31}]	-4.54/-46.11!	-4.82/-45.76	-4.43/-43.69!	-4.74/-42.24!	-4.58/-45.37	-5.01/-44.68!
[R_{11}] [R_{25}] [R_{32}]	-1.97/-33.89!	-0.84/-37.49	-2.34/-41.48!	-3.31/-45.75!	-0.8/-42.63	-2.95/-40.37!
[R_{12}] [R_{25}] [R_{31}]	-4.86/-47.73!	-4.28/-48.61	-5.96/-56.07!	-6.26/-56.41!	-5.58/-53.52!	-5.65/-49.49!
[R_{12}] [R_{25}] [R_{32}]	-2.24/-47.92!	-1.03/-43.79	-2.29/-43.75!	-3.52/-48.63#	-1.28/-44.32	-2.47/-40.06!
[R_{13}] [R_{25}] [R_{31}]	-4.47/-49.83!	-4.75/-51.12	-6.2/-60.16!	-5.19/-45.24!	-3.84/-50.65	-4.85/-40.05!
[R_{13}] [R_{25}] [R_{32}]	-2.34/-43.8!	-1.85/-43.74	-0.68/-42.54!	-3.51/-51.29#	-2.02/-45.22	-2.16/-42.08!
[R_{14}] [R_{25}] [R_{31}]	-5.51/-51.49#	-4.39/-48.48	-4.45/-41.48#	-6.53/-59.68!	-3.04/-46.07	-4.93/-46.86!
[R_{14}] [R_{25}] [R_{32}]	-5.07/-54.02	-4.61/-45.39	-3.81/-40.68!	-6.09/-47.78!	-3.79/-59.43	-3.56/-34.42!
[R_{15}] [R_{25}] [R_{31}]	-5.15/-55.38!	-4.64/-49.72	-2.27/-28.2!	-5.36/-50.62!	-3.41/-50.35	-5.05/-44.29!
[R_{15}] [R_{25}] [R_{32}]	-1.66/-47.43!	-0.56/-44.14	-0.63/-44.94!	-1.04/-44.79	-1.29/-40.05	-1.81/-36!
[R_{16}] [R_{25}] [R_{31}]	-5.74/-60.82#	-4.99/-56.76	-3.65/-43.29#	-5.84/-60.25#	-4.07/-55.13	-4.5/-44.06#
[R_{16}] [R_{25}] [R_{32}]	-5.44/-56.38	-4.34/-52.63	-4.95/-44.7#	-4.32/-53.67	-4.19/-68.39	-4.56/-44.41!

Ligand	3.5	3.5*	3.5**	4.0	4.0*	4.0**
[R_{11}] [R_{26}] [R_{31}]	-2.56/-45.43#	-1.95/-44.52	-2.29/-47!	-3.16/-45.85!	-2.54/-41.89!	-2.72/-41.9#
[R_{11}] [R_{26}] [R_{32}]	-1.65/-48.37#	-1.31/-41.25	-0.66/-39.25!	-1.73/-43.28	0.07/-36.29	-1.45/-36.81!
[R_{12}] [R_{26}] [R_{31}]	-2.63/-48.8	-1.95/-47.19	-1.84/-44.34!	-1.97/-46.38	-3.25/-46.64	-3.06/-46.22#
[R_{12}] [R_{26}] [R_{32}]	-1.61/-46.89	-0.22/-41.49	0.57/-33.52!	-2.53/-45.51#	-1.43/-40.19	-1.29/-39.8!
[R_{13}] [R_{26}] [R_{31}]	-4.94/-40.7#	-5.78/-47.88	-4.84/-51.9#	-4.81/-45.27	-5.11/-48.09!	-4.23/-40.09#
[R_{13}] [R_{26}] [R_{32}]	-2.27/-49.82	-0.52/-44.21	-0.4/-40.99!	-0.68/-42.5	-1.66/-39.29	-1.19/-41.32!
[R_{14}] [R_{26}] [R_{31}]	-4.18/-43.27	-4.71/-48.79	-3.12/-40.65#	-3.31/-40.6	-4.47/-48.2	-5.05/-41.77#
[R_{14}] [R_{26}] [R_{32}]	-0.52/-42.97	-1.14/-45.53	-1.68/-47.87!	-1.04/-49.27	-0.66/-47.71	-0.91/-34.4!
[R_{15}] [R_{26}] [R_{31}]	-3.89/-46.51	-4.57/-48.34	-3.09/-38.13!	-5.38/-47.82#	-4.33/-48.66	-4.23/-43.6#
[R_{15}] [R_{26}] [R_{32}]	-0.88/-49.05	-0.23/-40.81	-0.02/-45.91!	-0.94/-46.68	0.2/-44.24	-0.46/-39.62!
[R_{16}] [R_{26}] [R_{31}]	-4.41/-50.17#	-4.97/-56.87	-4.38/-43.73#	-4.25/-51.37	-5.28/-56.36	-4.84/-40.2#
[R_{16}] [R_{26}] [R_{32}]	-1.89/-55.49	-1.35/-53.31	-1.37/-44.95!	-2.28/-55.73	-1.5/-50.08!	-1.49/-40.37!
[R_{11}] [R_{27}] [R_{31}]	-2.48/-42.04	-2.97/-50.96	-2.45/-44.29!	-3.13/-44!	-2.21/-46.28	-3.28/-46.09!
[R_{11}] [R_{27}] [R_{32}]	-1.64/–43.56	-2.18/-45.13	-1.25/-44.19!	-1.83/-43.65	0.09/-43.68	-2.66/-38.94!
[R_{12}] [R_{27}] [R_{31}]	-5.11/-43.98	-4.81/-53.43	-4.7/-50.26#	-5.76/-51.61#	-4.25/-59.24	-5.53/-45.39!
[R_{12}] [R_{27}] [R_{32}]	-2.21/-42.11!	-0.66/-42.5	-1.08/-45.65!	-1.65/-45.16	0.32/-45.08	-2.49/-46.01!
[R_{13}] [R_{27}] [R_{31}]	-5.45/-53.2#	-4.46/-51.1	-4.96/-53.07#	-5.61/-58.3	-3.96/-51.75	-5.59/-45.63#
[R_{13}] [R_{27}] [R_{32}]	-4.52/-43.89!	-0.61/-43.32!	-1.16/-41.66#	-1.36/-44.56	0.42/-46.52	-2.96/-40.11!
[R_{14}] [R_{27}] [R_{31}]	-4.71/-50.45!	-4.68/-54.96	-5.04/-53.83#	-6.54/-55.09!	-4.14/-54.81	-5.16/-40.65#
[R_{14}] [R_{27}] [R_{32}]	-1.97/-48.16	-2.27/-48.13	-1.16/-40.72#	-1.64/-49.18	0.38/-48.14	-2.29/-38.13!
[R_{15}] [R_{27}] [R_{31}]	-4.46/-53.06	-4.99/-53.21	-4.46/-52.49#	-4.28/-53.48	-3.79/-52.52	-5.05/-46.49#
[R_{15}] [R_{27}] [R_{32}]	-0.65/-45.6	-1.47/-48.17	-0.93/-45.71!	-0.69/-45.17	1.13/-46.31	-1.79/-39.4#
[R_{16}] [R_{27}] [R_{31}]	-5.4/-56.39!	-5.24/-58.45	-4.1/-39.22#	-3.77/-55.03	-4.05/-56.44	-5.08/-49.98#
[R_{16}] [R_{27}] [R_{32}]	-1.9/-48.84	-1.74/-50.96	-1.25/-54.76!	-2.36/-50.69	-1.86/-53.63	-1.48/-45.15!
[R_{11}] [R_{28}] [R_{31}]	-1.78/-37.25	-2.04/-42.68	-3.1/-46.91!	-2.64/-47.16	-1.84/-42.61	-3.31/-42.03!
[R_{11}] [R_{28}] [R_{32}]	-2.27/-35.78	-2.31/-44.65	-1.41/-39.67!	-2.41/-40.72	-3.4/-38.56!	-3.65/-40.1!
[R_{12}] [R_{28}] [R_{31}]	-4.07/-48.96	-2.33/-46.3	-2.13/-47.47!	-3.47/-48.05	-2.31/-41.21	-2.99/-42.16!
[R_{12}] [R_{28}] [R_{32}]	-1.08/-33.88	-1.98/-37.05	-1.02/-33.58!	-1.68/-44.92	-1.14/-43.8	-2.8/-36.8!
[R_{13}] [R_{28}] [R_{31}]	-5.59/-56.06	-4.68/-51.48	-3.81/-37.34!	-3.53/-47.49	-4.99/-55.06	-5.27/-46.8!
[R_{13}] [R_{28}] [R_{32}]	-2.17/-47.31	-2.1/-48.13	-1.3/-45.19#	-3.07/-43.77#	-1.51/-45.04	-1.6/-38.08!

Ligand	3.5	3.5*	3.5**	4.0	4.0*	4.0**
[R_{14}] [R_{28}] [R_{31}]	-5.36/-51.33#	-5.02/-53.29	-4.23/-51.56!	-6.61/-53.57#	-4.06/-50.31	-5.18/-41.48!
[R_{14}] [R_{28}] [R_{32}]	-0.58/-32.98	-2.87/-54.61	-1.73/-44.9#	-2.9/-44.84#	-1.47/-41.34	-2.23/-40.34#
[R_{15}] [R_{28}] [R_{31}]	-5.66/-57.42	-4.2/-49.92	-4.4/-50.27!	-5.3/-56.65	-4.96/-48.63	-4.9/-49.18!
[R_{15}] [R_{28}] [R_{32}]	-1.86/-48.46	-0.72/-43.97	0.83/-33.07!	-1.41/-44.08	-1.06/-38.82	-1.34/-40.83!
[R_{16}] [R_{28}] [R_{31}]	-4.63/-54.18	-4.62/-52.87	-3.75/-38.12!	-4.2/-54.78	-4.53/-51.3	-4.22/-42.99!
[R_{16}] [R_{28}] [R_{32}]	-1.19/-48.19	-2.17/-49.39	-0.96/-37.84!	-1.79/-46.37	-1.21/-46.65	-1.6/-40.48!
[R_{11}] [R_{29}] [R_{31}]	-3.98/-41.19	-4.51/-46.58	-4.77/-47.19!	-4.59/-37.13!	-3.96/-37.36	-/-
[R_{11}] [R_{29}] [R_{32}]	-2.92/-48.09!	-1.88/-42.25	-1.69/-41.76!	-2.66/-36.93!	-2.05/-41.77	-2.61/-35.37!
[R_{12}] [R_{29}] [R_{31}]	-3.84/-41.1	-4.74/-41.48	-4.58/-52.02!	-4.14/-39.65	-4.48/-49.93	-/-
[R_{12}] [R_{29}] [R_{32}]	-2.72/-49.37	-1.3/-37.17	-1.72/-45.91!	-2.51/-31.98!	-2.68/-45.44	-2.16/-39.38!
[R_{13}] [R_{29}] [R_{31}]	-4.83/-45.45	-4.62/-48.92	-5.68/-53.19!	-3.81/-41.09	-4.05/-49.24	-/-
[R_{13}] [R_{29}] [R_{32}]	-2.53/-48.58	-1.54/-47.7	-1.14/-38.84!	-1.79/-44.92	-0.41/-41.51	-1.82/-37.42!
[R_{14}] [R_{29}] [R_{31}]	-5.84/-56.62#	-5.61/-54.66	-5.46/-43.93#	-5.35/-54.29#	-4.71/-51.65	-/-
[R_{14}] [R_{29}] [R_{32}]	-4.93/-52.43	-2.56/-32.86	-4.55/-49.16!	-3.86/-55.58	-3.38/-39.1	-4.53/-41.71#
[R_{15}] [R_{29}] [R_{31}]	-5.47/-56.24	-4.96/-50.73	-5.61/-54.45!	-5.26/-56.09	-4.29/-51	-/-
[R_{15}] [R_{29}] [R_{32}]	-0.87/-41.11!	-2.62/-46.5	-2.15/-40.51!	-1.92/-34!	-2.18/-49.98	-2.01/-45.05!
[R_{16}] [R_{29}] [R_{31}]	-4.44/-49.5	-5.22/-56.86	-5.48/-63.5!	-5.71/-57.17!	-4.94/-55.17	-/-
[R_{16}] [R_{29}] [R_{32}]	-5.55/-57.39	-4.46/-56.16	-4.41/-56.24!	-4.54/-55.2	-4.63/-49.08	-5.16/-51.89!
[R_{11}] [R_{210}] [R_{31}]	-4.13/-41.42	-4.59/-36.73	-2.12/-39.94!	-1.38/-42.18	-1.78/-42.73	-2.06/-36.15!
[R_{11}] [R_{210}] [R_{32}]	-2.45/-38.88	-4.72/-33.17	-1.54/-41.59!	-1.66/-43.7	-0.65/-34.21	-2.94/-39.33!
[R_{12}] [R_{210}] [R_{31}]	-1.7/-38.81	-3.06/-47.64	-1.62/-44.81!	-2.58/-51.74	-3.76/-45.36!	-1.99/-39.17!
[R_{12}] [R_{210}] [R_{32}]	-2.02/-40.92	-1.58/-40.67	-1.44/-42.44!	0.08/-24.45	-1.03/-44.76	-1.44/-32.02!
[R_{13}] [R_{210}] [R_{31}]	-3.16/-51.6	-2.32/-50.24	-0.92/-37.17!	-4.82/-54.17#	-2.73/-52.97	-2.56/-39.85!
[R_{13}] [R_{210}] [R_{32}]	-1.68/-40.89#	-0.39/-39.15	-0.52/-40.74!	-1.1/-42.8	-0.8/-45.97	-1.23/-37.78!
[R_{14}] [R_{210}] [R_{31}]	-5.54/-53.31#	-4.43/-50.91	-3.34/-40.26#	-6.23/-50.79#	-3.9/-48.57	-4.17/-38.51!
[R_{14}] [R_{210}] [R_{32}]	-1.93/-45.76	-0.94/-42.07	0.59/-31.13#	-2.6/-38.02#	-0.86/-40.48	-1.15/-28.49#
[R_{15}] [R_{210}] [R_{31}]	-1.97/-47.47#	-1.45/-44.35	-1.9/-48.8!	-3.4/-48.26#	-2.06/-51.44	-1.93/-42.54!
[R_{15}] [R_{210}] [R_{32}]	-0.87/-41.11!	-1.59/-56.54	-0.24/-36.07#	-2.65/-45.22#	-0.28/-50.9	-1.23/-37.39#
[R_{16}] [R_{210}] [R_{31}]	-5.33/-57.45	-4.79/-50.09	-4.15/-49.77#	-5.28/-58.02	-4.26/-52.61	-4.65/-49.56!
[R_{16}] [R_{210}] [R_{32}]	-0.58/-45.17	-2.5/-49.6	-1.25/-50.33!	-1.33/-47.65	-0.83/-46.27	-2.3/-41.82#

E.10 Main Structure 10

Ligand	3.0	3.5*	3.5**	4.0	4.0*	4.0**
$[R_{11}][R_{21}][R_{31}]$	-3.88/-31.47	-4.52/-36.15	-3.36/-30.62!	-3.81/-31.11	-5.48/-32.62	-/-
$[R_{11}][R_{21}][R_{32}]$	-4.08/-29.72	-5.39/-34.74	-4.4/-26.31#	-4.08/-29.4	-5.76/-33.79	-6.33/-30.76#
$[R_{12}][R_{21}][R_{31}]$	-4.19/-34.27	-4.88/-38.22	-3.44/-30.43!	-5.92/-34.65#	-5.13/-36.41	-/-
$[R_{12}][R_{21}][R_{32}]$	-4.2/-31.96	-5.65/-36.27	-3.24/-23.15#	-4.09/-31.47	-6.2/-34.48	-5.82/-28.43#
$[R_{13}][R_{21}][R_{31}]$	-5.17/-36.35#	-4.36/-37.97	-4.34/-37.33#	-5.91/-36.31#	-5.04/-40.57	-/-
$[R_{13}][R_{21}][R_{32}]$	-5.4/-35.61#	-5.41/-36.18	-3.11/-23.52#	-6.77/-35.08#	-5.94/-34.78	-5.52/-30.3#
$[R_{14}][R_{21}][R_{31}]$	-4.99/-40.24#	-4.09/-39.51	-4.86/-36.44#	-4.21/-37.39	-4.72/-38.85	-/-
$[R_{14}][R_{21}][R_{32}]$	-4.14/-31.65	-5.19/-37.5	-3.44/-26.15#	-3.56/-33.6	-5.65/-35.97	-6.25/-33.84#
$[R_{15}][R_{21}][R_{31}]$	-4.68/-36.33	-4.71/-37.43	-4.69/-39.89!	-5.69/-36.85#	-4.61/-37.81	-/-
$[R_{15}][R_{21}][R_{32}]$	-4.03/-30.25#	-4.94/-36.99	-3.29/-29.19!	-3.42/-32.4	-5.47/-35.46	-5.55/-30.85#
$[R_{16}][R_{21}][R_{31}]$	-5.02/-41.08	-4.6/-40.54	-4.81/-39.4!	-4.63/-40.12	-4.81/-40.39	-/-
$[R_{16}][R_{21}][R_{32}]$	-3.48/-35.84	-4.88/-39.04	-3.1/-27.52#	-3.96/-35.19	-5.32/-36.98	-5.02/-31.74#
$[R_{11}][R_{22}][R_{31}]$	-4.8/-32.62	-4.79/-38.21	-5.25/-44.59#	-4.24/-32.81	-4.47/-38.1	-/-
$[R_{11}][R_{22}][R_{32}]$	-4.8/-32.2	-4.79/-38.21	-5.25/-44.59#	-4.24/-32.81	-4.47/-38.1	-/-
$[R_{12}][R_{22}][R_{31}]$	-4.6/-43.98	-4.54/-35.58	-4.45/-39.19#	-5.55/-31.98#	-4.43/-36.48	-/-
$[R_{12}][R_{22}][R_{32}]$	-4.06/-33.98	-5.47/-37.49	-3.29/-16.19#	-5.03/-32.02	-5.8/-36.97	-6.44/-33.93#
$[R_{13}][R_{22}][R_{31}]$	-4.55/-34.61#	-4.43/-35.76	-5.67/-48.45#	-6.41/-42.49#	-5.38/-38.74	-/-
$[R_{13}][R_{22}][R_{32}]$	-3.9/-36.08	-4.59/-37.25	-4.74/-36.61#	-4.02/-36.06	-5.24/-35.5	-4.01/-27.59#
$[R_{14}][R_{22}][R_{31}]$	-4.79/-35.27	-4.72/-40.12	-3.71/-39.98!	-4.99/-36.3#	-5/-43.24	-/-
$[R_{14}][R_{22}][R_{32}]$	-4.12/-38.67	-4.46/-38.25	-4.87/-38.39#	-4.65/-37.03	-5.32/-38.18	-6.2/-36.66#
$[R_{15}][R_{22}][R_{31}]$	-4.73/-36.61	-4.52/-41.02	-5.02/-39.06#	-5.95/-39.3#	-4.45/-40.2	-/-
$[R_{15}][R_{22}][R_{32}]$	-3.61/-36.35	-4.97/-39.14	-3.18/-30.6!	-5.19/-33.86#	-5.05/-38.37	-5.8/-36.58#
$[R_{16}][R_{22}][R_{31}]$	-3.84/-39.89	-4.2/-39.13	-3.68/-39.19!	-5.34/-40.98#	-3.89/-41.51	-/-
$[R_{16}][R_{22}][R_{32}]$	-4.78/-39.53	-5.05/-41.97	-2.59/-29.55!	-5.69/-35.13!	-5.08/-39.75	-3.93/-29.63#
$[R_{11}][R_{23}][R_{31}]$	-4.21/-36.95	-4.45/-36.95	-3.19/-26.37!	-5.61/-36.22#	-4.38/-37.43	-/-
$[R_{11}][R_{23}][R_{32}]$	-4.79/-34.3!	-4.27/-37.63	-3.22/-31.72!	-3.66/-35.49	-4.41/-36.95	-4.4/-29.18!
$[R_{12}][R_{23}][R_{31}]$	-4.45/-38.9	-4.65/-39.96	-3.74/-41.35!	-5.11/-39.06!	-4.88/-41.24	-/-
$[R_{12}][R_{23}][R_{32}]$	-5.11/-38.29!	-4.72/-40.09	-3.37/-33.24!	-5.92/-36.06!	-4.64/-38.22	-4.78/-30.97!
$[R_{13}][R_{23}][R_{31}]$	-4.44/-35.02	-4.59/-40.92	-3.09/-34.08#	-6.43/-44.15#	-4.41/-41.53	-/-
$[R_{13}][R_{23}][R_{32}]$	-3.57/-35.45	-4.53/-36.66	-4.85/-41.04#	-5/-36.6!	-4.28/-35.52	-4.62/-30!

Ligand	3.5	3.5*	3.5**	4.0	4.0*	4.0**
$[R_{14}]\,[R_{23}]\,[R_{31}]$	-4.67/-39.84	-4.05/-40.05	-3.54/-34.9#	-3.76/-39.99	-3.95/-40.78	-/-
$[R_{14}]\,[R_{23}]\,[R_{32}]$	-2.98/-38.14!	-2.91/-42.33	-1.51/-34.89!	-1.61/-39.62	-2.64/-40.29	-3.14/-33.96!
$[R_{15}]\,[R_{23}]\,[R_{31}]$	-4.67/-38.18	-3.61/-38.12	-3.57/-42.24!	-3.77/-39.63	-4.42/-42.43	-/-
$[R_{15}]\,[R_{23}]\,[R_{32}]$	-1.81/-37.78	-2.45/-40.35	-1.42/-35.59!	-1.29/-38.35	-2.45/-38.43	-2.57/-36.02!
$[R_{16}]\,[R_{23}]\,[R_{31}]$	-5.06/-44.71	-4.42/-43.55	-3.56/-35.31!	-5.38/-46.81!	-4.66/-43.65	-/-
$[R_{16}]\,[R_{23}]\,[R_{32}]$	-1.7/-37.55	-2.73/-42.16	-1.38/-35.52!	-4.14/-38.42!	-2.4/-42.04	-2.81/-36.3#
$[R_{11}]\,[R_{24}]\,[R_{31}]$	-4.57/-36.77	-4.95/-40.35	-4.47/-36.48!	-5.36/-33.66!	-4.91/-39.31	-5.15/-35.71!
$[R_{11}]\,[R_{24}]\,[R_{32}]$	-3.95/-32.03	-4.83/-32.15	-4.52/-34.65#	-4.41/-30.8	-5.21/-32.85	-6.15/-29.92#
$[R_{12}]\,[R_{24}]\,[R_{31}]$	-4.46/-32.8!	-5.31/-41.33	-4.79/-37.52#	-5.94/-37.28#	-5.07/-39.72	-/-
$[R_{12}]\,[R_{24}]\,[R_{32}]$	-4.46/-32.8!	-5.31/-41.33	-4.79/-37.52#	-5.94/-37.28#	-5.07/-39.72	-/-
$[R_{13}]\,[R_{24}]\,[R_{31}]$	-4.84/-43.52	-4.99/-39.72	-3.09/-32.94#	-5.91/-40.53#	-4.8/-40.58	-4.11/-33.21#
$[R_{13}]\,[R_{24}]\,[R_{32}]$	-4.68/-32.58	-4.15/-35.25	-3.91/-31.95!	-4.21/-33.54	-5.11/-35.06	-4.33/-29.77!
$[R_{14}]\,[R_{24}]\,[R_{31}]$	-4.74/-32.12#	-4.89/-41.83	-3.06/-35.09#	-5.86/-38.76#	-5.65/-42.26	-4.54/-34.28#
$[R_{14}]\,[R_{24}]\,[R_{32}]$	-4.38/-34.6#	-4.92/-36.66	-3.73/-34.1#	-5.34/-30.47#	-5.1/-36.66	-4.32/-29.93#
$[R_{15}]\,[R_{24}]\,[R_{31}]$	-4.6/-38.22#	-4.7/-40.29	-2.58/-30.25!	-5.54/-38.31#	-4.4/-38.52	-4.86/-35.61#
$[R_{15}]\,[R_{24}]\,[R_{32}]$	-3.83/-38.22#	-4.75/-38.41	-4.37/-34.56#	-5.51/-30.83#	-5.03/-37.04	-5.32/-34.29!
$[R_{16}]\,[R_{24}]\,[R_{31}]$	-2.85/-39.48	-3.09/-41.2	-2.31/-41.14!	-2.85/-42.88	-2.66/-42.24	-2.3/-37.17!
$[R_{16}]\,[R_{24}]\,[R_{32}]$	-3.9/-38.35	-4.68/-39.33	-3.85/-29.09!	-4.45/-37.16	-4.98/-38.14	-5.02/-34.22#
$[R_{11}]\,[R_{25}]\,[R_{31}]$	-4.57/-40.23	-4.68/-40.49	-4.37/-39.62!	-4.83/-32.62!	-4.71/-39.53	-5.1/-35.19!
$[R_{11}]\,[R_{25}]\,[R_{32}]$	-3.03/-25.72	-3.91/-33.03	-2.71/-26.91!	-6.08/-34.29!	-4.62/-32.97	-4.33/-31.35!
$[R_{12}]\,[R_{25}]\,[R_{31}]$	-4.89/-36.74#	-4.25/-38.63	-3.42/-33.26#	-5.79/-42.81!	-4.47/-35.29	-5.13/-32.01#
$[R_{12}]\,[R_{25}]\,[R_{32}]$	-4.02/-30.09#	-3.89/-36.66	-3.19/-28.72#	-3.68/-34.84	-4.87/-34.19	-4.14/-29.09#
$[R_{13}]\,[R_{25}]\,[R_{31}]$	-3.67/-45#	-2.88/-40.7	-1.89/-35.77#	-4.16/-40.44#	-3.17/-41.59	-3.38/-34.62#
$[R_{13}]\,[R_{25}]\,[R_{32}]$	-3.44/-32.87	-4.27/-36.49	-3.2/-31.72#	-4.89/-26.94!	-4.64/-35.85	-4.17/-30.73#
$[R_{14}]\,[R_{25}]\,[R_{31}]$	-4.7/-42.38	-4.13/-38.45	-3.49/-37.76#	-5.88/-42.69#	-4.61/-43.15	-4.56/-40.8!
$[R_{14}]\,[R_{25}]\,[R_{32}]$	-2.4/-34.68	-2.25/-38.88	-1.31/-34.14#	-2.15/-34.59	-2.99/-37.17	-2.82/-32.77#
$[R_{15}]\,[R_{25}]\,[R_{31}]$	-3.19/-42.7#	-2.97/-40.9	-2.06/-30.5#	-4.02/-42.7#	-2.68/-42.03	-2.64/-39.94!
$[R_{15}]\,[R_{25}]\,[R_{32}]$	-2.12/-32.27	-2.53/-38.52	-0.72/-30.66#	-3.44/-34.86#	-2.33/-36.1	-1.6/-30.32#
$[R_{16}]\,[R_{25}]\,[R_{31}]$	-5.58/-43.56	-4.4/-42.84	-4.95/-44.7#	-5.13/-45.21#	-4.46/-44.63	-4.69/-40.72!
$[R_{16}]\,[R_{25}]\,[R_{32}]$	-1.67/-37.9	-2.52/-40.41	-2.39/-42.46#	-1.47/-34.76	-2.52/-38.99	-2.35/-34.41#

Ligand	3.5	3.5*	3.5**	4.0	4.0*	4.0**
$[R_{11}][R_{26}][R_{31}]$	-3.73/-33.29	-4.64/-39.43	-4.08/-34.34#	-4.05/-34.28	-4.71/-38.11	-5.83/-36.55#
$[R_{11}][R_{26}][R_{32}]$	-3.63/-33.77	-3.58/-32.74	-3.8/-28.61#	-3.45/-33.43	-5.07/-31.24	-5.4/-32.31#
$[R_{12}][R_{26}][R_{31}]$	-4.35/-31.67!	-4.59/-38.79	-4.36/-35.56#	-5.06/-33.96#	-5.12/-39.45	-5.16/-34.47#
$[R_{12}][R_{26}][R_{32}]$	-4.27/-33.15!	-4.78/-34.43	-4.46/-64.61#	-4.82/-29.73!	-5.19/-32.27	-5.67/-33.13#
$[R_{13}][R_{26}][R_{31}]$	-3.98/-39.35	-4.46/-39.68	-4.26/-38.5#	-4.98/-29.66#	-4.59/-40.38	-5.53/-37.97#
$[R_{13}][R_{26}][R_{32}]$	-3.29/-30.27	-4.54/-33.78	-2.84/-31.34#	-4.16/-33.53	-4.78/-31.32	-5.17/-33.59#
$[R_{14}][R_{26}][R_{31}]$	-2.9/-40.85	-2.93/-41.51	-3.33/-40.11#	-2.83/-40.47	-3.26/-41.96	-2.73/-34.37!
$[R_{14}][R_{26}][R_{32}]$	-4.09/-31.34#	-4.29/-35.7	-4.17/-36.54#	-4.79/-33.41#	-4.82/-34.4	-3.58/-27.06#
$[R_{15}][R_{26}][R_{31}]$	-3.16/-46.78	-2.79/-42.28	-2.16/-38.66#	-2.42/-39.48	-2.93/-41.85	-2.98/-35.95#
$[R_{15}][R_{26}][R_{32}]$	-3.1/-36.9	-4.16/-36.87	-3.38/-36.15#	-4.93/-31.29#	-4.66/-34.69	-4.79/-29.71#
$[R_{16}][R_{26}][R_{31}]$	-2.45/-43.4#	-1.42/-35.87	-2.77/-3802#	-2.56/-45.41#	-2.99/-46.97	-3.48/-39.79#
$[R_{16}][R_{26}][R_{32}]$	-1.33/-38.41	-2.34/-39.22	-2.21/-30.93!	-1.19/-37.63	-2.98/-36.32	-3.41/-36.3#
$[R_{11}][R_{27}][R_{31}]$	-4.95/-44.59	-4.8/-38.9	-4.26/-33.55#	-5.4/-30.72#	-4.19/-40.37	-4.77/-34.48#
$[R_{11}][R_{27}][R_{32}]$	-3.39/-23.22!	-4.26/-34.34	-4.49/-33.23#	-3.99/-26.45	-4.91/-31.51	-5.38/-31.26#
$[R_{12}][R_{27}][R_{31}]$	-4.19/-39.24#	-4.92/-40.87	-4.46/-38.92#	-4.56/-41.76	-4.63/-38.8	-5.38/-38.99#
$[R_{12}][R_{27}][R_{32}]$	-4.55/-31.92!	-4.3/-35.9	-3.18/-28.65#	-5.97/-32.59!	-5.17/-33.39	-5.71/-32.54#
$[R_{13}][R_{27}][R_{31}]$	-4.73/-41.42#	-4.87/-41.5	-3.86/-34.18#	-3.74/-36.08	-4.63/-40.36	-4.62/-37.09#
$[R_{13}][R_{27}][R_{32}]$	-4.33/-34.41!	-3.97/-37.96	-4.48/-35.93#	-5.7/-34.22!	-4.83/-32.78	-4.08/-29.99#
$[R_{14}][R_{27}][R_{31}]$	-3.3-73/-49.34	-3.33/-39.58	-1.85/-40.1#	-3.46/-49.41	-2.98/-41.28	-4.18/-41.44#
$[R_{14}][R_{27}][R_{32}]$	-3.3/-23.9	-4.08/-39.96	-3.15/-33.23#	-3.66/-24.69	-4.33/-37.06	-4.66/-31.24!
$[R_{15}][R_{27}][R_{31}]$	-2.95/-44.27	-2.29/-42.84	-2.83/-40.37#	-2.91/-46.73	-2.48/-38.4	-3.7/-40.5#
$[R_{15}][R_{27}][R_{32}]$	-3.31/-24.07#	-3.94/-38.08	-3.99/-35.33#	-5.58/-32.75!	-4.4/-36.63	-4.87/-32.85#
$[R_{16}][R_{27}][R_{31}]$	-5.53/-53.69	-4.04/-38.77	-5.17/-46.35#	-4.81/-50.58	-4.24/-46.75	-5.59/-45.43#
$[R_{16}][R_{27}][R_{32}]$	-2.36/-36.77!	-2.26/-40.32	-0.91/-32.97!	-3.75/-37.43!	-2.9/-37.87	-2.51/-33.22!
$[R_{11}][R_{28}][R_{31}]$	-4.7/-33.13	-5/-42.34	-3.87/-32.02#	-4.38/-32.21	-5.1/-38.76	-6.05/-38.61#
$[R_{11}][R_{28}][R_{32}]$	-3.68/-30.57	-5.01/-35.98	-3.14/-26.11!	-3.88/-32.05	-5.59/-34.74	-5.86/-33.05#
$[R_{12}][R_{28}][R_{31}]$	-4.43/-33.26#	-4.91/-40.8	-4.26/-33.02#	-4.73/-34.58	-5.33/-42.59	-4.81/-34.12#
$[R_{12}][R_{28}][R_{32}]$	-4.47/-28.51	-5.3/-36.91	-4.72/-37.84#	-5.58/-29.53#	-5.85/-36.05	-5.05/-29.47#
$[R_{13}][R_{28}][R_{31}]$	-4.5/-37.43	-5.07/-43.7	-4.11/-30.09#	-5.73/-37.58#	-4.63/-39.66	-5.08/-33.08#
$[R_{13}][R_{28}][R_{32}]$	-3.57/-35.13	-4.2/-36.59	-4.63/-34.01#	-4.11/-31.03	-5.6/-36.1	-4.26/-27.51#

Ligand	3.5	3.5*	3.5**	4.0	4.0*	4.0**
[R_{14}] [R_{28}] [R_{31}]	-4.44/-40.37#	-4.7/-42.59	-4.33/-37.93#	-5.85/-46.12#	-4.93/-44.61	-4.6/-35.67!
[R_{14}] [R_{28}] [R_{32}]	-3.9/-33.8	-4.95/-39.24	-4.52/-42#	-4.73/-34.34	-5.25/-38.89	-5.39/-28.07#
[R_{15}] [R_{28}] [R_{31}]	-4.72/-38.34#	-4.79/-44.41	-3.22/-36.88#	-5.92/-38.83#	-5.01/-44.29	-4.25/-35.16!
[R_{15}] [R_{28}] [R_{32}]	-3.91/-30.32!	-4.76/-39.27	-4.3/-35.45#	-5.48/-31.21!	-5.24/-37.85	-5.42/-34.46#
[R_{16}] [R_{28}] [R_{31}]	-3.14/-43.39#	-3.58/-45.94	-2.84/-39.61#	-3.55/-40.85	-3.46/-44.43	-2.43/-38.24!
[R_{16}] [R_{28}] [R_{32}]	-4.27/-36.15#	-4.75/-41.22	-3.42/-28.74!	-4.75/-32.98#	-5.2/-40.1	-5/-33.18!
[R_{11}] [R_{29}] [R_{31}]	-4.77/-32.11	-4.84/-41.47	-4.75/-39.76#	-4.45/-33.22	-4.58/-38.73	-/-
[R_{11}] [R_{29}] [R_{32}]	-3.94/-35.78	-5.07/-37.81	-3.29/-30.83!	-4.02/-35.43	-5.21/-35.66	-5.11/-29.35!
[R_{12}] [R_{29}] [R_{31}]	-4.75/-35.83	-3.73/-36.62	-3.6/-32.55!	-5.15/-33.8#	-4.15/-37.44	-/-
[R_{12}] [R_{29}] [R_{32}]	-4.23/-37.41	-5.02/-35.56	-3.44/-32.02!	-3.79/-35.11	-5.02/-36.27	-5.27/-32.6#
[R_{13}] [R_{29}] [R_{31}]	-5.45/-43.07	-4.48/-37.18	-3.99/-39.53!	-6.14/-42.96#	-4.59/-41.85	-/-
[R_{13}] [R_{29}] [R_{32}]	-4.14/-36.58	-4.37/-40.1	-3.26/-28.11!	-3.79/-36.78	-4.91/-38.44	-4.87/-30.29!
[R_{14}] [R_{29}] [R_{31}]	-5.32/-37.95	-4.24/-44.18	-4.08/-34.19#	-5.96/-41.18#	-4.34/-39.82	-/-
[R_{14}] [R_{29}] [R_{32}]	-3.93/-36.89	-4.44/-40.96	-2.64/-20.49#	-3.83/-37.02	-5.09/-39.71	-5.27/-33.91#
[R_{15}] [R_{29}] [R_{31}]	-3/-36.73	-3.6/-45.76	-2.03/-36.91!	-4.52/-42.1#	-3.09/-43.34	-/-
[R_{15}] [R_{29}] [R_{32}]	-3.43/-36.27	-4.79/-40.03	-3.5/-35.23!	-3.44/37.54	-5.01/-38.82	-3.69/-29.8!
[R_{16}] [R_{29}] [R_{31}]	-3.94/-35.19	-5.08/-44.65	-3.48/-41.5!	-5.19/-46.98	-4.73/-45.46	-/-
[R_{16}] [R_{29}] [R_{32}]	-1.97/-39.98	-3.26/-41.85	-1.8/-30.55#	-2.49/-42	-2.99/-37.96	-3.02/-34.55#
[R_{11}] [R_{210}] [R_{31}]	-4.87/-30.14	-4.59/-36.73	-4.78/-37.99#	-5.46/-32.62#	-5.02/-38.23	-6.1/-36.59#
[R_{11}] [R_{210}] [R_{32}]	-3.34/-27.79	-4.72/-33.17	-4.69/-34.6#	-4.72/-27.79	-5.25/-32.75	-4.96/-28.92#
[R_{12}] [R_{210}] [R_{31}]	-3.76/-31.86	-4.06/-38.52	-3.71/-27.89#	-5.71/-32.29#	-4.95/-37.9	-4.14/-31.77!
[R_{12}] [R_{210}] [R_{32}]	-3.87/-33.27	-5.07/-35.25	-4.39/-65.69#	-4.06/-30.44	-5.55/-32.6	-5.34/-29.49#
[R_{13}] [R_{210}] [R_{31}]	-4.25/-31.16	-4.66/-38.78	-3.92/-35.42#	-5.52/-38.91#	-5.06/-41.54	-4.28/-32.68!
[R_{13}] [R_{210}] [R_{32}]	-4.2/-32.14#	-4.85/-35.51	-3.29/-26.24!	-5.14/-32.62#	-5.47/-34.8	-4.25/-27.88#
[R_{14}] [R_{210}] [R_{31}]	-4.17/-35.68#	-3.77/-38.58	-3.09/-34.81!	-5.22/-39.68#	-4.62/-40.52	-5.14/-34.71#
[R_{14}] [R_{210}] [R_{32}]	-4.19/-31.89#	-4.78/-36.94	-4.46/-34.31#	-4.76/-32.06#	-5.22/-36.37	-5.57/-32.9#
[R_{15}] [R_{210}] [R_{31}]	-4.21/-31.26#	-4.11/-36.62	-2.87/-37.15!	-5.29/-37.76#	-4.85/-40.71	-5.36/-36.96#
[R_{15}] [R_{210}] [R_{32}]	-3.67/-31.28#	-4.44/-36.87	-4.52/-37.13#	-3.2/-33.79	-4.96/-35.78	-5.16/-31.16#
[R_{16}] [R_{210}] [R_{31}]	-2.46/-41.24	-2.8/-39.92	-1.54/-40.4!	-3.48/-41.22#	-3.25/-42.84	-2.51/-38.34!
[R_{16}] [R_{210}] [R_{32}]	-3.27/-36.45	-4.46/-38.6	-3.41/-28.21#	-4.4/-35.24	-5/-37.38	-3.78/-31.18!

Appendix F

Induced Fit Docking of Hybrid Molecules

F.1 Structure 1

Pose	G-score	E-Model	IFDScore	Prime Energy
1	-7.356798	-57.507488	-1003.968798	-19932.24
2	-7.400721	-56.226255	-1003.724721	-19926.48
3	-6.565571	-53.760102	-1003.647571	-19941.64
4	-6.36176	-50.131004	-1003.56626	-19944.09
5	-6.367153	-52.115828	-1003.369653	-19940.05
6	-6.763068	-51.480423	-1003.241068	-19929.56
7	-6.470786	-42.870695	-1002.952786	-19929.64
8	-6.312844	-40.785583	-1002.820344	-19930.15
9	-6.195155	-41.482442	-1002.504655	-19926.19
10	-5.908154	-52.815342	-1002.473154	-19931.3
11	-5.739588	-36.572285	-1002.462088	-19934.45
12	-5.582279	-59.298945	-1002.450279	-19937.36
13	-5.486455	-43.693262	-1002.383955	-19937.95
14	-5.901444	-41.913847	-1001.836944	-19918.71
Pose not correct				
1	-5.882371	-45.384471	-1002.949871	-19941.35
2	-5.580902	-43.494409	-1002.610902	-19940.6
3	-5.665499	-38.423439	-1002.075999	-19928.21

F.2 Structure 2

Pose	G-score	E-Model	IFDScore	Prime Energy
1	-7.392859	-75.731734	-1004.741859	-19946.98
2	-6.482742	-53.087634	-1004.576742	-19961.88
3	-6.9639	-56.316693	-1004.2759	-19946.24
4	-6.588715	-62.871576	-1003.989715	-19948.02
5	-6.253259	-61.268216	-1003.872259	-19952.38
6	-6.251765	-56.871776	-1003.629265	-19947.55
7	-6.368369	-54.564701	-1003.213369	-19936.9
8	-5.851761	-49.117454	-1003.201261	-19946.99
9	-6.375351	-49.114308	-1003.061851	-19933.73
10	-5.638389	-53.519565	-1002.619389	-19939.62
11	-4.772581	-52.676651	-1002.443581	-19953.42
12	-5.618103	-48.571302	-1002.321103	-19934.06
13	-5.065874	-47.359993	-1002.004874	-19938.78
Pose not correct				
1	-6.514081	-49.082092	-1004.668081	-19963.08
2	-5.365838	-39.722342	-1002.851338	-19949.71
3	-4.54052	-36.917831	-1001.60402	-19941.27
4	-4.671975	-43.555799	-1001.383475	-19934.23
5	-4.406137	-49.436574	-1001.293137	-19937.74

F.3 Structure 3

Pose	G-score	E-Model	IFDScore	Prime Energy
1	-8.686991	-68.608851	-1006.301991	-19952.3
2	-7.362093	-64.397092	-1005.229593	-19957.35
3	-7.337493	-68.340318	-1004.983493	-19952.92
4	-7.099272	-65.468595	-1004.712272	-19952.26
5	-6.768437	-54.710101	-1004.421437	-19953.06
6	-6.441278	-58.350381	-1003.952778	-19950.23
7	-6.099694	-55.743017	-1003.582194	-19949.65
8	-5.152989	-42.304015	-1003.442489	-19965.79
9	-5.271212	-50.773415	-1002.817712	-19950.93
10	-4.401648	-39.140276	-1001.734648	-19946.66
Pose not correct				
1	-4.414453	-51.797319	-1001.800453	-19947.72
2	-3.529055	-49.528314	-1001.131055	-19952.04
3	-3.901021	-51.89637	-1000.880521	-19939.59

F.4 Structure 4

Pose	G-score	E-Model	IFDScore	Prime Energy
1	-7.349717	-50.262687	-1000.288717	-19858.78
2	-7.793032	-50.207027	-1000.192532	-19847.99
3	-7.914877	-55.295709	-1000.190377	-19845.51
4	-7.882577	-51.026912	-1000.000077	-19842.35
5	-7.964657	-54.657842	-999.988657	-19840.48
6	-7.338055	-55.223613	-999.971555	-19852.67
7	-7.692753	-47.856583	-999.724753	-19840.64
8	-7.248639	-49.734568	-999.584139	-19846.71
9	-7.879123	-52.819611	-999.524623	-19832.91
10	-6.986226	-49.015004	-999.375726	-19847.79
11	-6.68529	-44.548255	-999.22679	-19850.83
12	-7.089516	-51.056781	-998.925016	-19836.71
13	-6.837909	-44.730197	-998.762409	-19838.49
14	-5.777987	-36.202846	-998.748487	-19859.41
15	-6.7641	-49.11776	-998.3461	-19831.64
Pose not correct				
1	-4.922603	-40.229409	-997.669103	-19854.93
2	4.606873	-47.255439	-997.333373	-19854.53
3	-4.464392	-45.234693	-996.491892	-19840.55

F.5 Structure 5

Pose	G-score	E-Model	IFDScore	Prime Energy
1	-8.394204	-61.020834	-1006.426704	-19960.65
2	-6.945836	-47.223452	-1004.271336	-19946.51
3	-7.360299	-56.046379	-1004.262799	-19938.05
4	-6.601061	-48.359082	-1003.757061	-19943.12
5	-5.855323	-42.318537	-1003.208323	-19947.06
Pose not correct				
1	-5.760699	-39.395029	-1003.353699	-19951.86
2	-5.444567	-46.505807	-1003.136567	-19953.84
3	-5.089044	-41.552555	-1002.167044	-19941.56
4	-5.029984	-43.715425	-1002.140984	-19942.22
5	-5.342751	-52.582972	-1002.029251	-19933.73
6	-4.890429	-49.765291	-1001.552929	-19933.25
7	-4.636933	-38.434379	-1001.227933	-19931.82
8	-3.665179	-33.067778	-1000.288679	-19932.47

Appendix G

Hydrogen Bonds in MD Simulations

G.1 Hydrogen Bonds to GTP

This section shows charts for all the hydrogen bond distances and angles measured in the six different simulations, between GTP and the receptor. 1OB2 [89] is structure K and 2BVN [89] is structure E.

G.1.1 Simulation 1

G.1.1.1 Distances

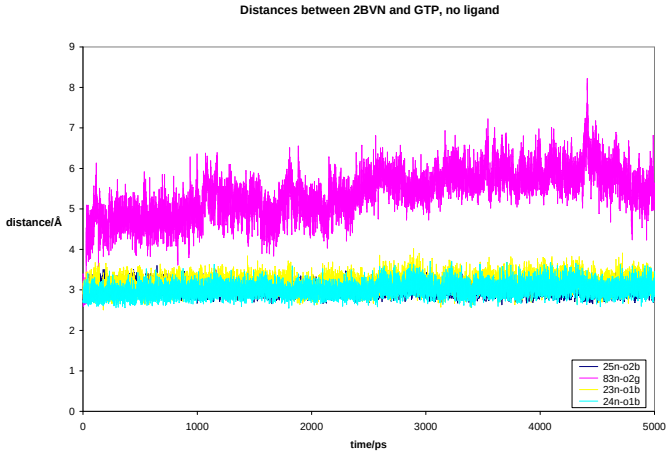

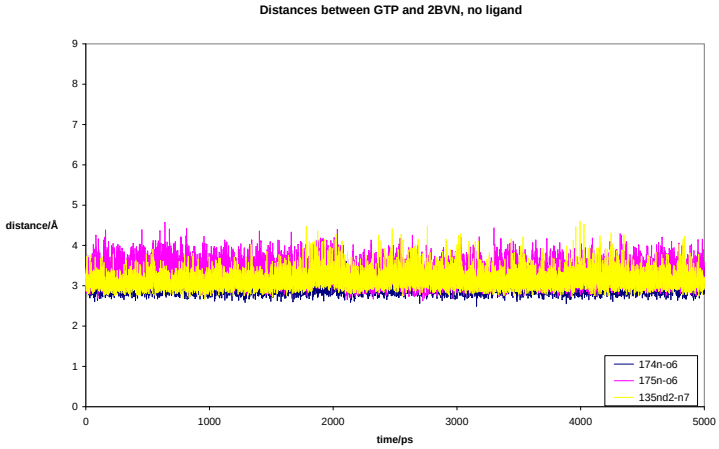
Distances between GTP and 2BVN, no ligand
distance/Å
time/ps
174n-o6
175n-o6
135nd2-n7

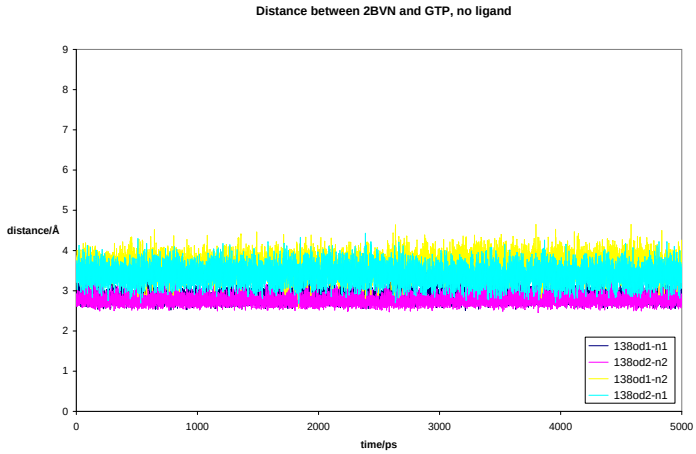
Distance between 2BVN and GTP, no ligand
distance/Å
time/ps
138od1-n1
138od2-n2
138od1-n2
138od2-n1

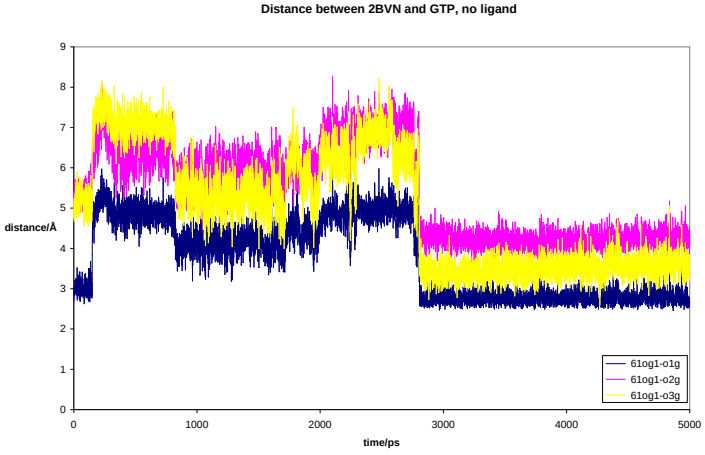
Distance between 2BVN and GTP, no ligand
distance/Å
time/ps
61og1-o1g
61og1-o2g
61og1-o3g

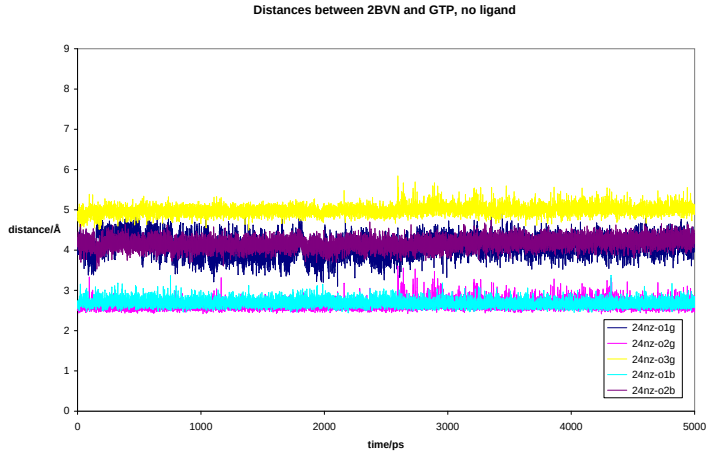
Distances between 2BVN and GTP, no ligand
distance/Å
time/ps
24nz-o1g
24nz-o2g
24nz-o3g
24nz-o1b
24nz-o2b

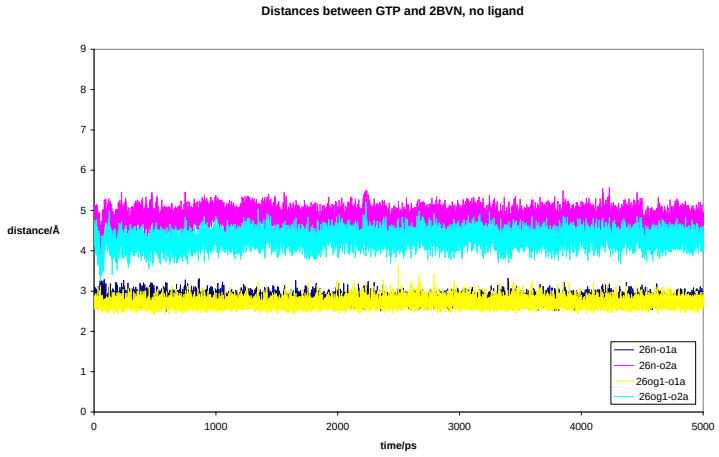
Distances between GTP and 2BVN, no ligand
distance/Å
time/ps
26n-o1a
26n-o2a
26og1-o1a
26og1-o2a

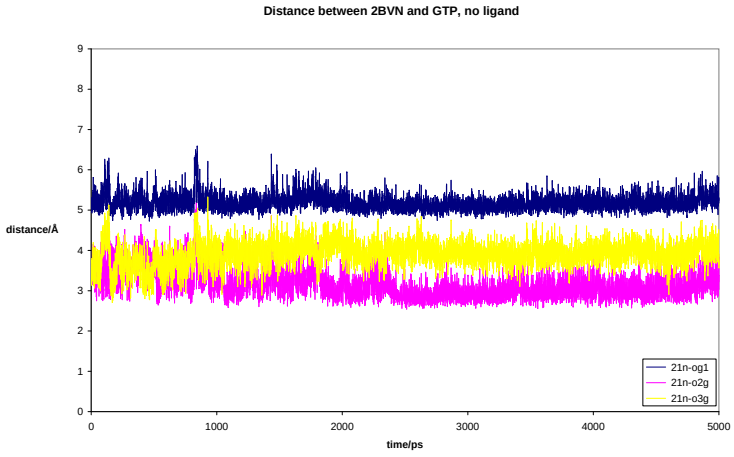
Distance between 2BVN and GTP, no ligand
distance/Å
time/ps
21n-og1
21n-o2g
21n-o3g

G.1.1.2 Angles

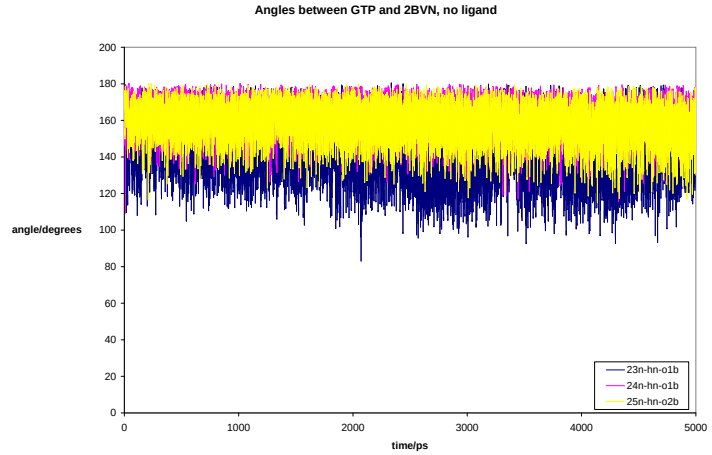
Angles between GTP and 2BVN, no ligand
angle/degrees
time/ps
23n-hn-o1b
24n-hn-o1b
25n-hn-o2b

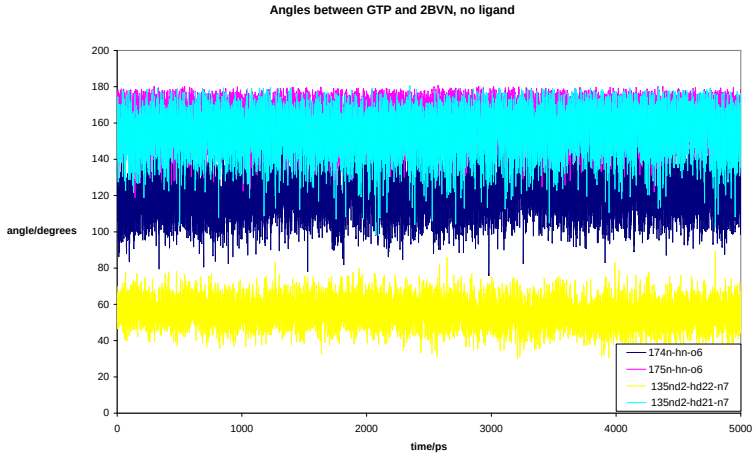
Angles between GTP and 2BVN, no ligand
angle/degrees
time/ps
174n-hn-o6
175n-hn-o6
135nd2-hd22-n7
135nd2-hd21-n7

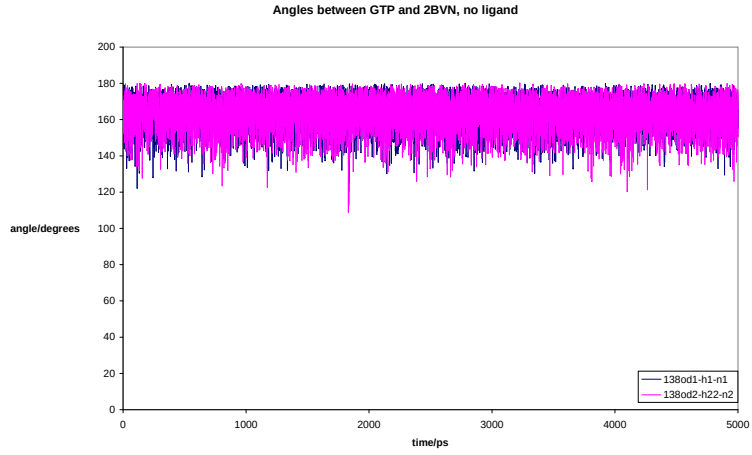
Angles between GTP and 2BVN, no ligand
angle/degrees
time/ps
138od1-h1-n1
138od2-h22-n2

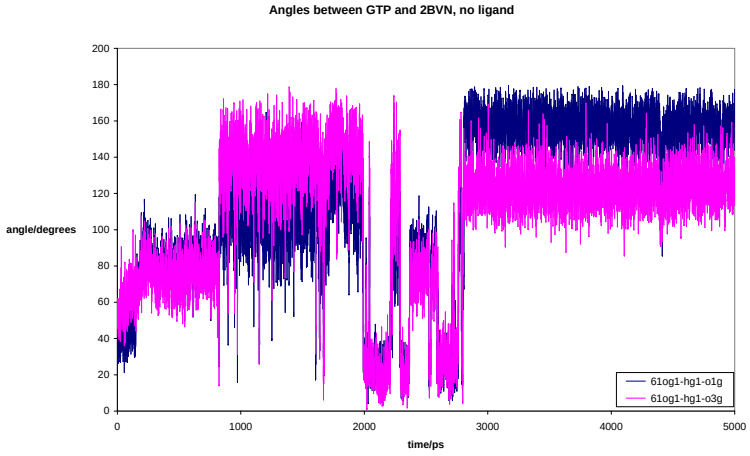
Angles between GTP and 2BVN, no ligand
angle/degrees
time/ps
61og1-hg1-o1g
61og1-hg1-o3g

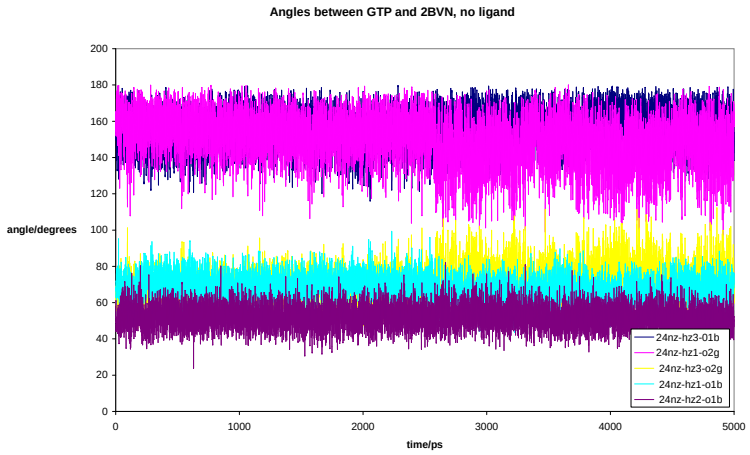
Angles between GTP and 2BVN, no ligand
angle/degrees
time/ps
24nz-hz3-01b
24nz-hz1-o2g
24nz-hz3-o2g
24nz-hz1-o1b
24nz-hz2-o1b

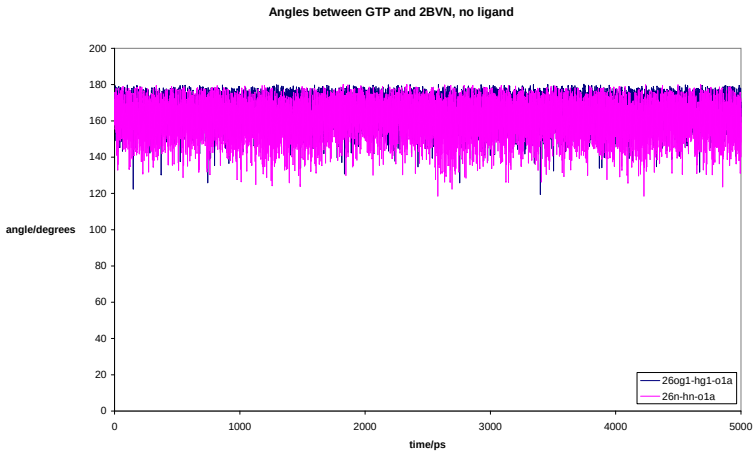
Angles between GTP and 2BVN, no ligand
angle/degrees
time/ps
26og1-hg1-o1a
26n-hn-o1a

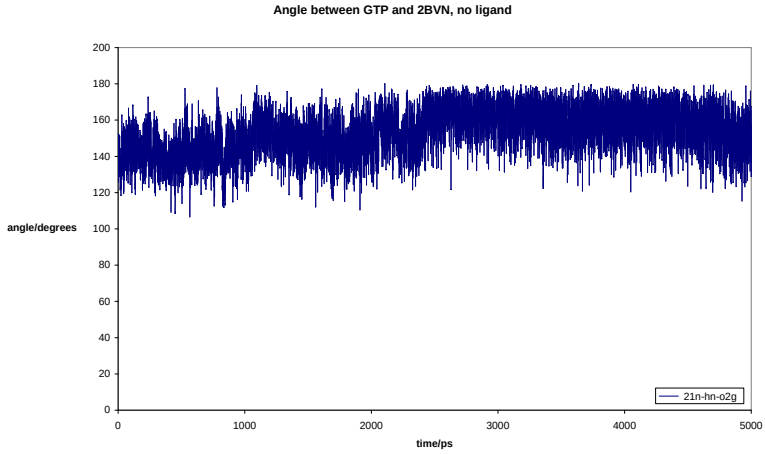

G.1.2 Simulation 2

G.1.2.1 Distances

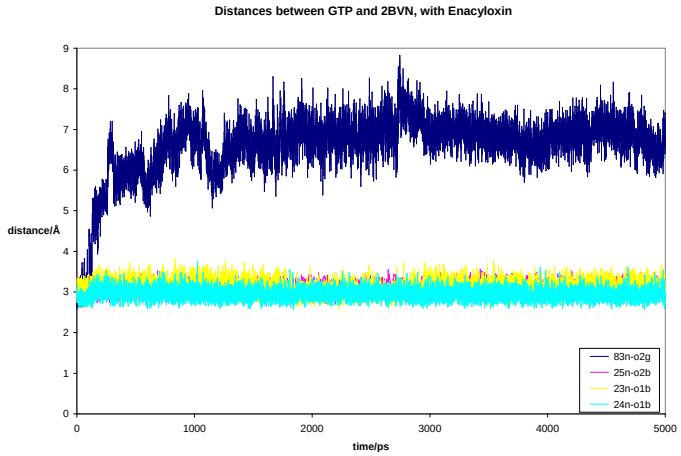

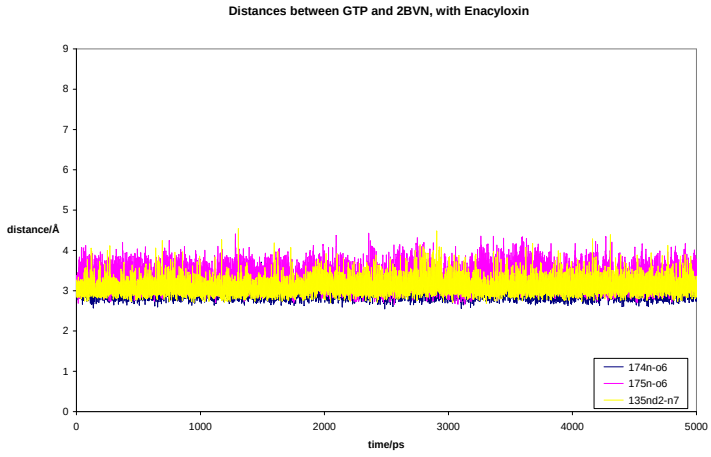

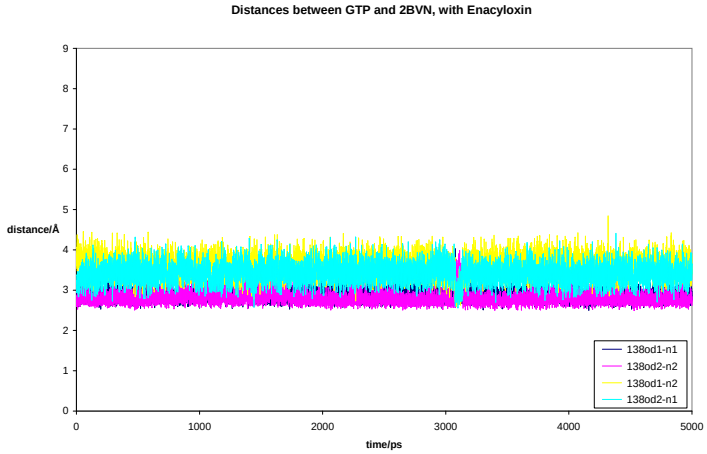
Distances between GTP and 2BVN, with Enacyloxin
distance/Å
time/ps
138od1-n1
138od2-n2
138od1-n2
138od2-n1

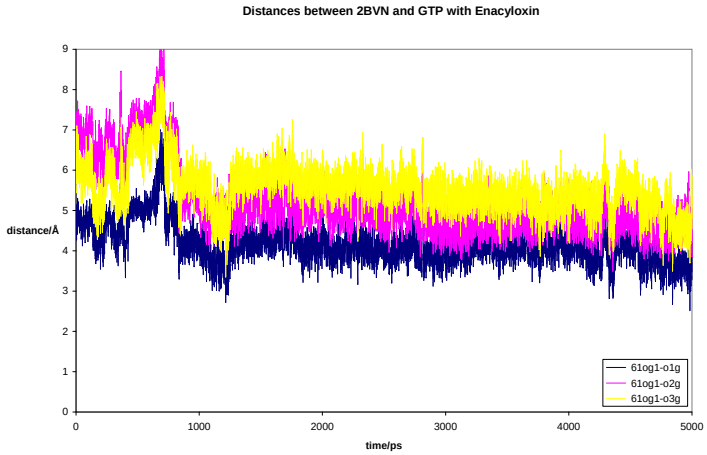
Distances between 2BVN and GTP with Enacyloxin
distance/Å
time/ps
61og1-o1g
61og1-o2g
61og1-o3g

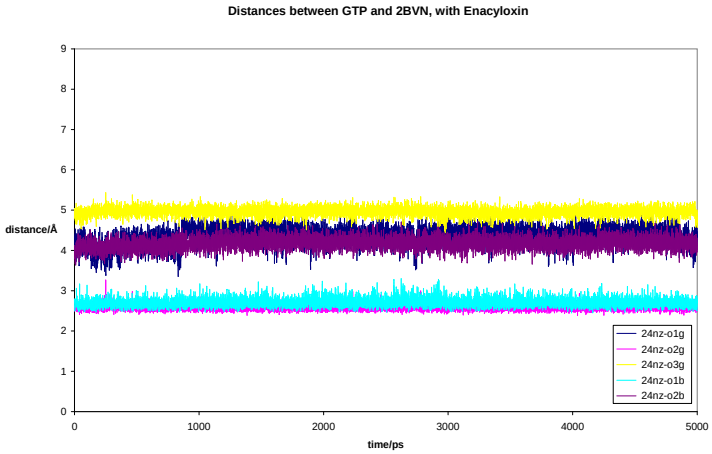
Distances between GTP and 2BVN, with Enacyloxin
distance/Å
time/ps
24nz-o1g
24nz-o2g
24nz-o3g
24nz-o1b
24nz-o2b

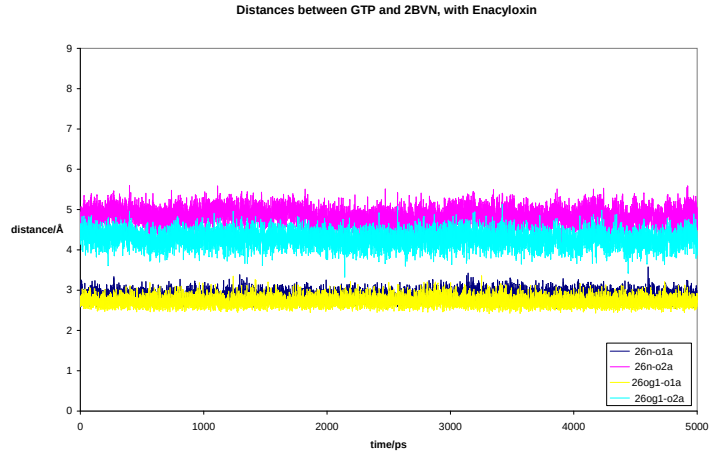
Distances between GTP and 2BVN, with Enacyloxin
distance/Å
time/ps
26n-o1a
26n-o2a
26og1-o1a
26og1-o2a

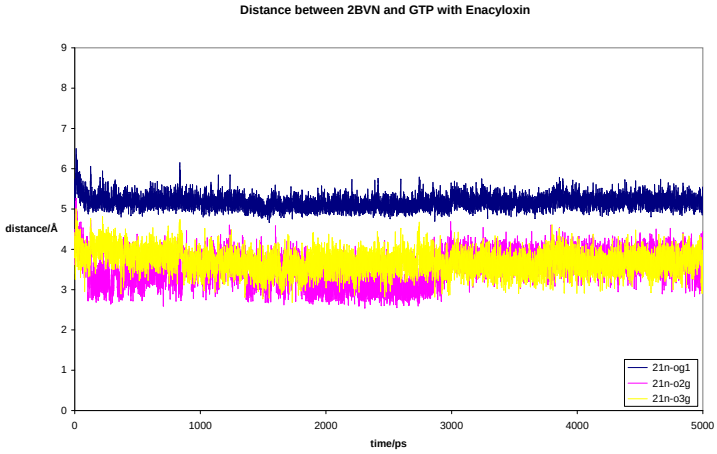
Distance between 2BVN and GTP with Enacyloxin
distance/Å
time/ps
21n-og1
21n-o2g
21n-o3g

G.1.2.2 Angles

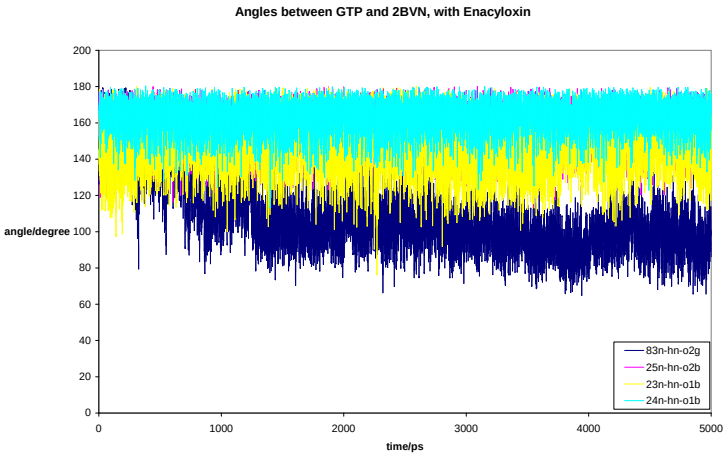
Angles between GTP and 2BVN, with Enacyloxin
angle/degree
time/ps
83n-hn-o2g
25n-hn-o2b
23n-hn-o1b
24n-hn-o1b

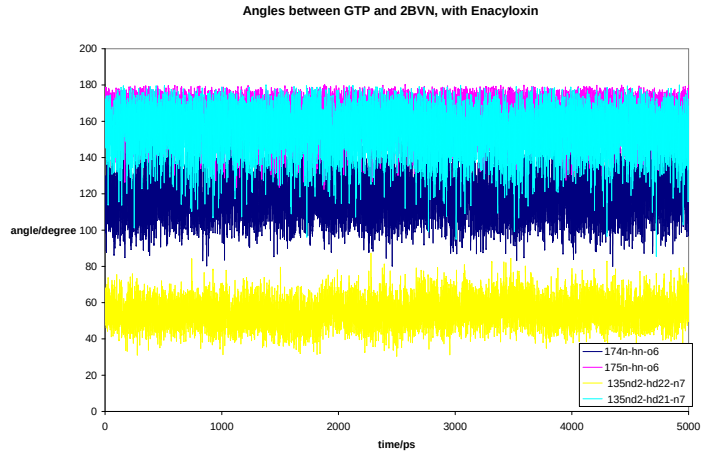
Angles between GTP and 2BVN, with Enacyloxin
angle/degree
time/ps
174n-hn-o6
175n-hn-o6
135nd2-hd22-n7
135nd2-hd21-n7

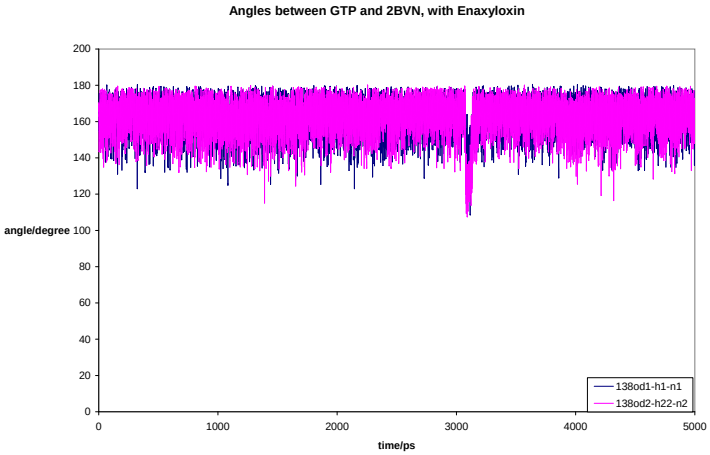
Angles between GTP and 2BVN, with Enaxyloxin
angle/degree
time/ps
138od1-h1-n1
138od2-h22-n2

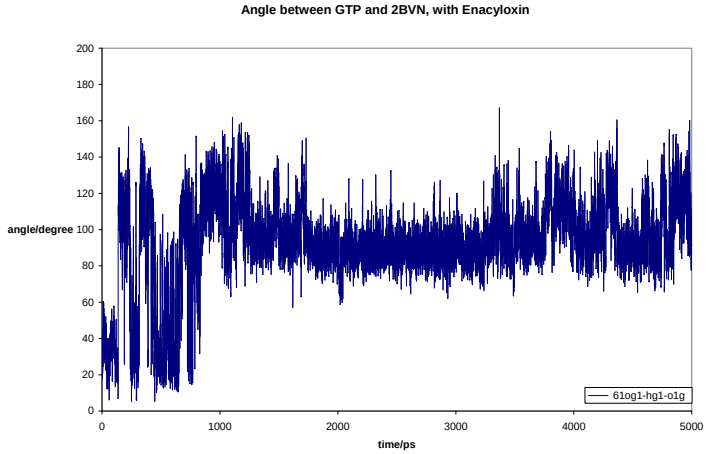
Angle between GTP and 2BVN, with Enacyloxin
angle/degree
time/ps
61og1-hg1-o1g

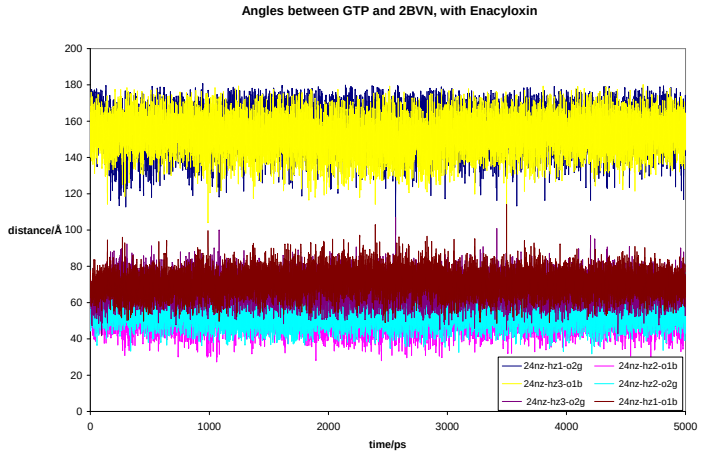

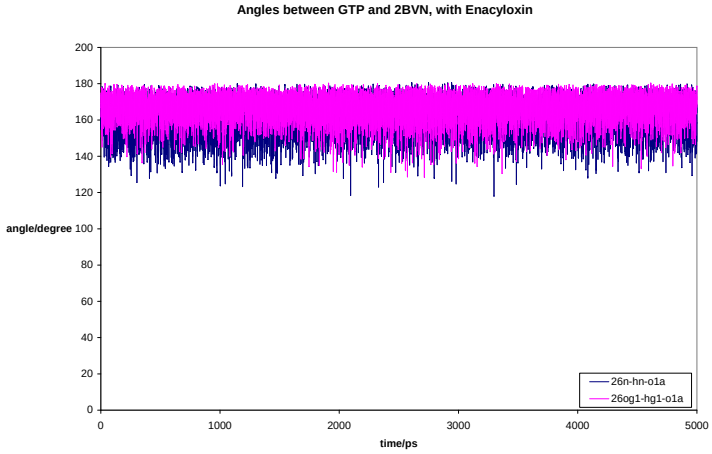

G.1.3 Simulation 3

G.1.3.1 Distances

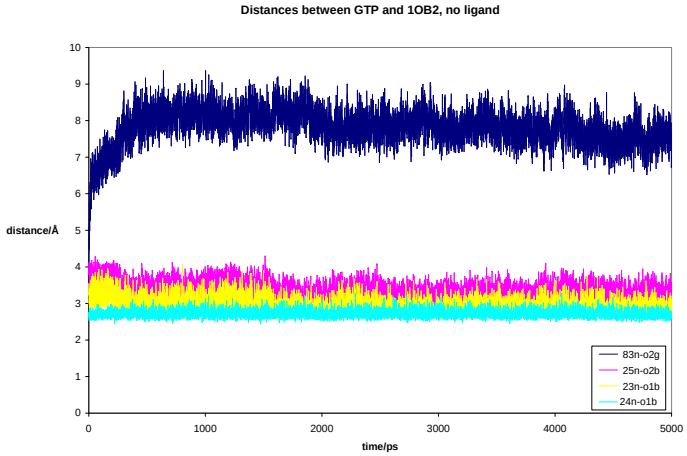

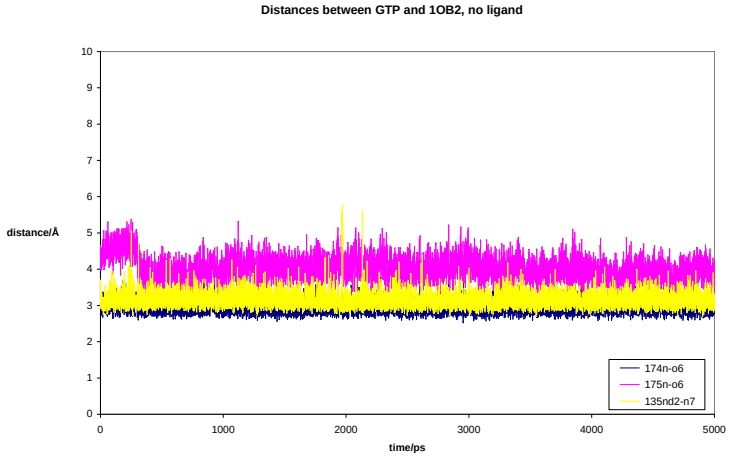
Distances between GTP and 1OB2, no ligand
distance/Å
time/ps
174n-o6
175n-o6
135nd2-n7

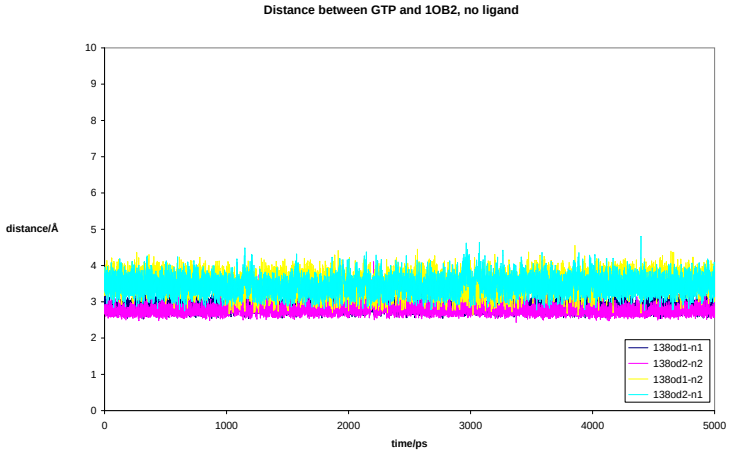
Distance between GTP and 1OB2, no ligand
distance/Å
time/ps
138od1-n1
138od2-n2
138od1-n2
138od2-n1

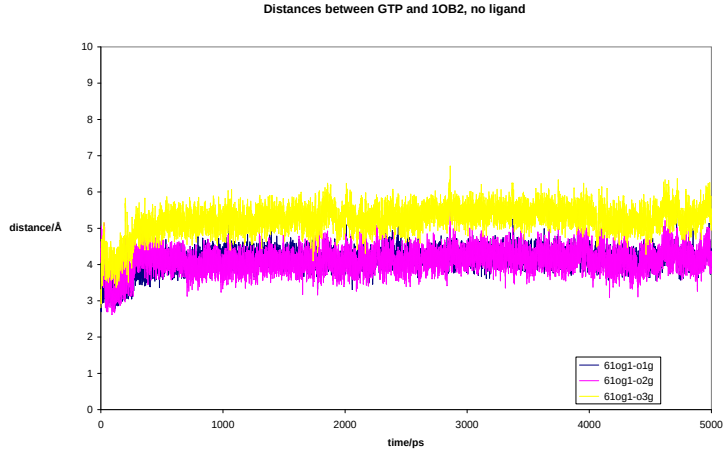
Distances between GTP and 1OB2, no ligand
distance/Å
time/ps
61og1-o1g
61og1-o2g
61og1-o3g

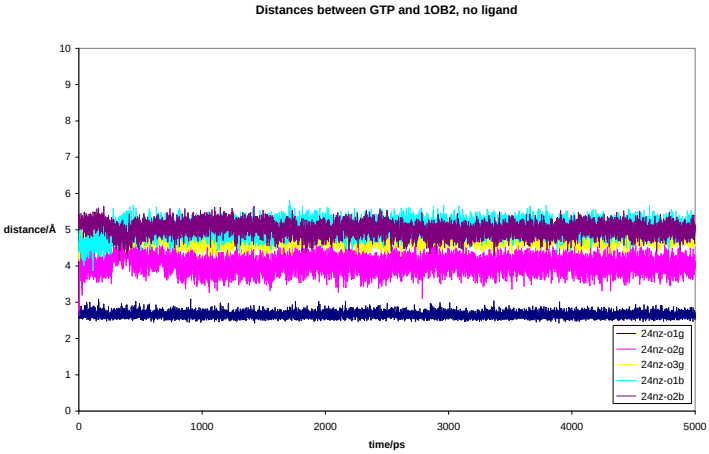
Distances between GTP and 1OB2, no ligand
distance/Å
time/ps
24nz-o1g
24nz-o2g
24nz-o3g
24nz-o1b
24nz-o2b

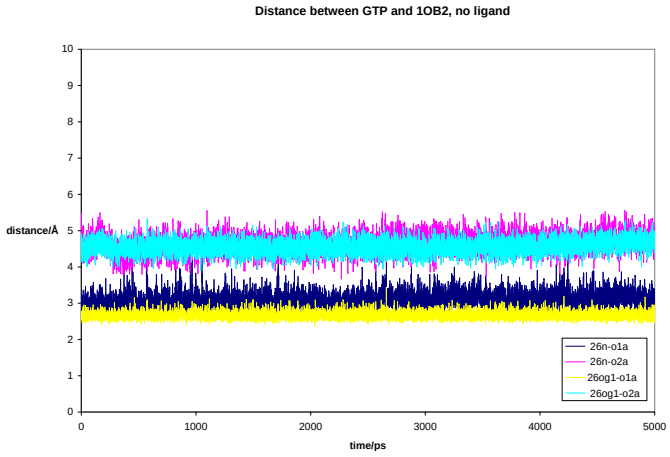
Distance between GTP and 1OB2, no ligand
distance/Å
time/ps
26n-o1a
26n-o2a
26og1-o1a
26og1-o2a

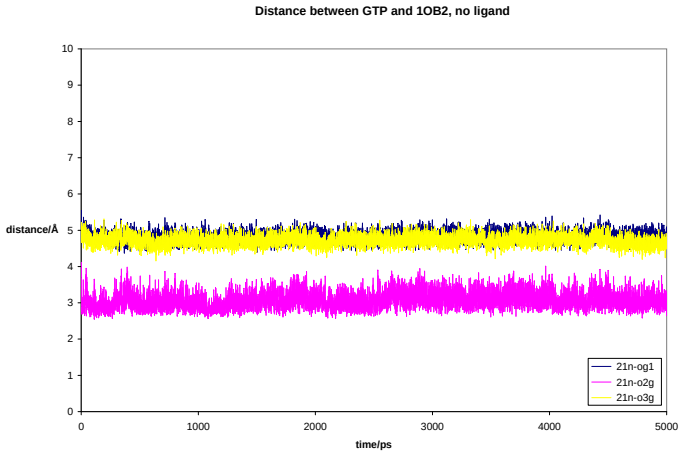
Distance between GTP and 1OB2, no ligand
distance/Å
time/ps
21n-og1
21n-o2g
21n-o3g

G.1.3.2 Angles


Angles between GTP and 1OB2, no ligand
angle/degree
time/ps
25n-hn-o2b
23n-hn-o1b
24n-hn-o1b

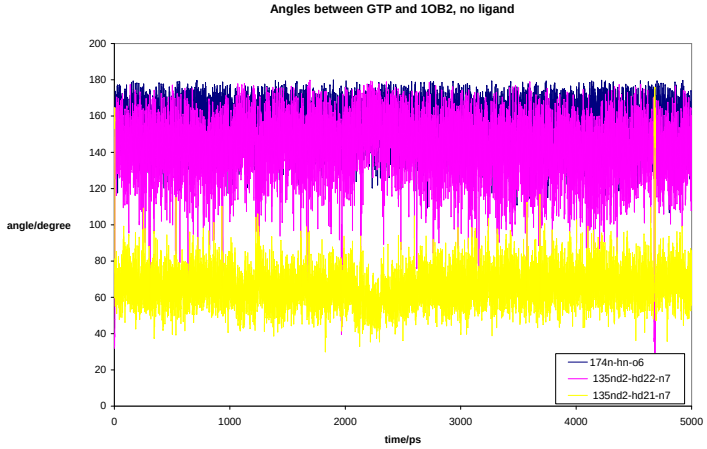
Angles between GTP and 1OB2, no ligand
angle/degree
time/ps
174n-hn-o6
135nd2-hd22-n7
135nd2-hd21-n7

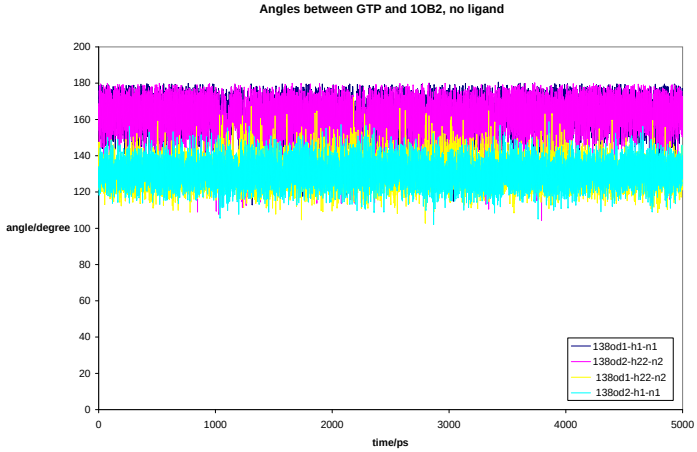
Angles between GTP and 1OB2, no ligand
angle/degree
time/ps
138od1-h1-n1
138od2-h22-n2
138od1-h22-n2
138od2-h1-n1

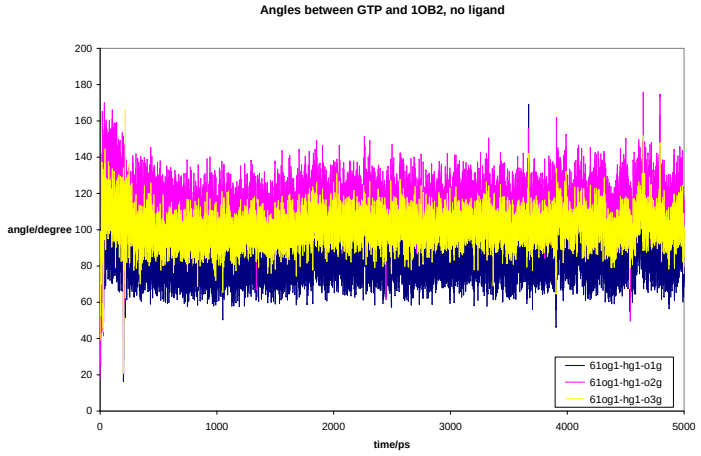
Angles between GTP and 1OB2, no ligand
angle/degree
time/ps
61og1-hg1-o1g
61og1-hg1-o2g
61og1-hg1-o3g

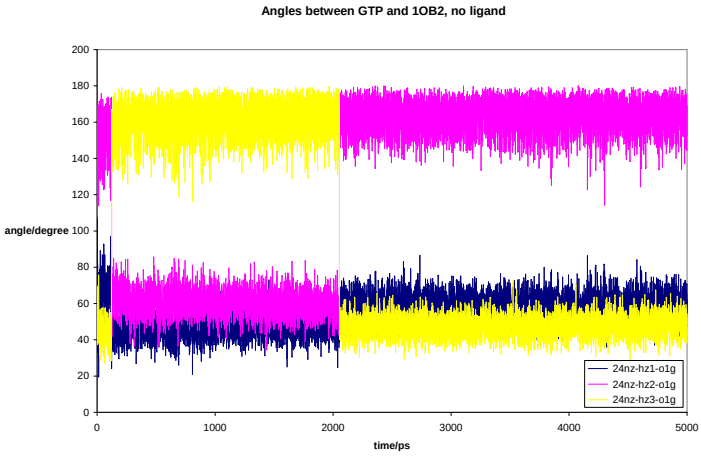
Angles between GTP and 1OB2, no ligand
angle/degree
time/ps
24nz-hz1-o1g
24nz-hz2-o1g
24nz-hz3-o1g

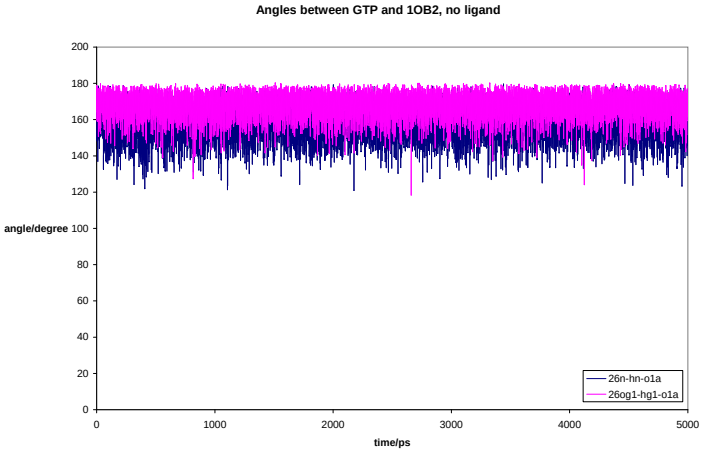
Angles between GTP and 1OB2, no ligand
angle/degree
time/ps
26n-hn-o1a
26og1-hg1-o1a

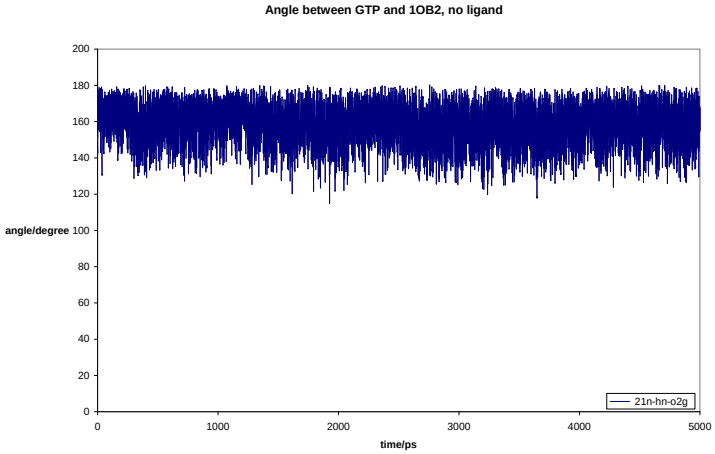

G.1.4 Simulation 4

G.1.4.1 Distances

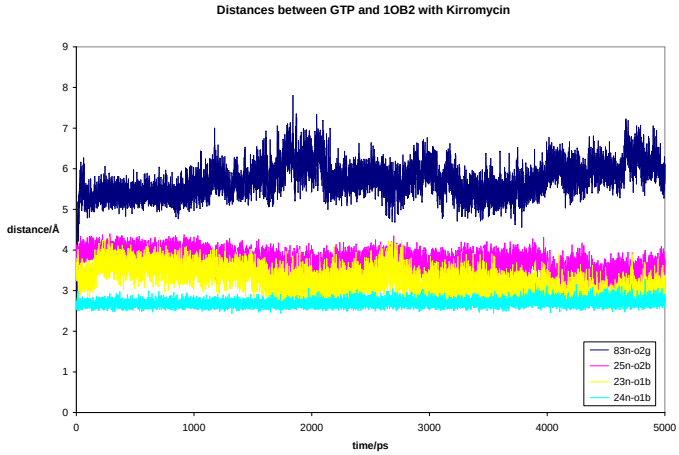

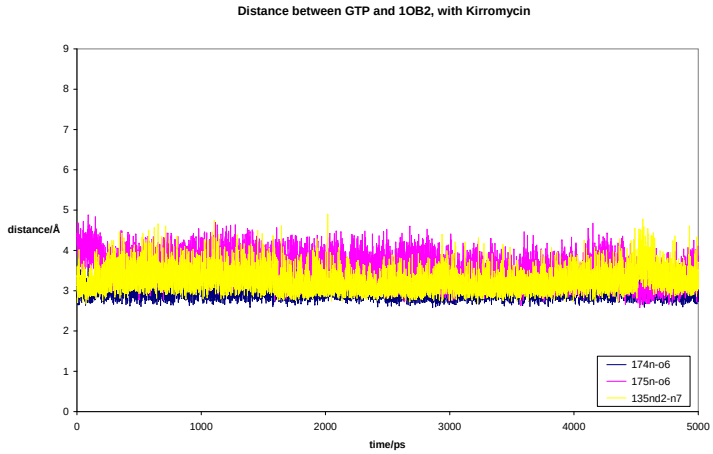

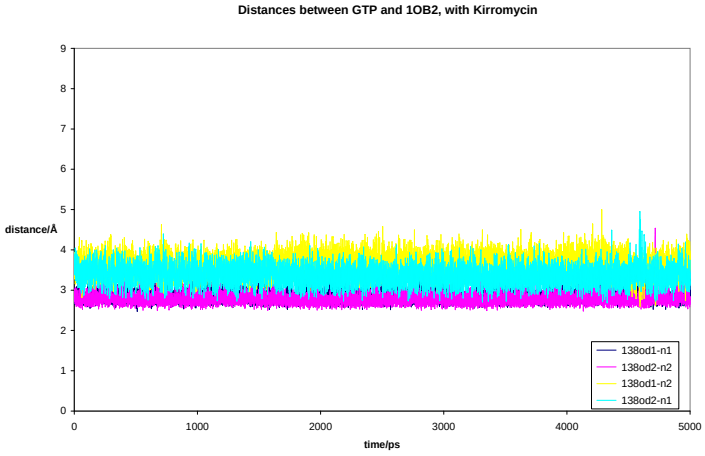
Distances between GTP and 1OB2, with Kirromycin
distance/Å
time/ps
138od1-n1
138od2-n2
138od1-n2
138od2-n1

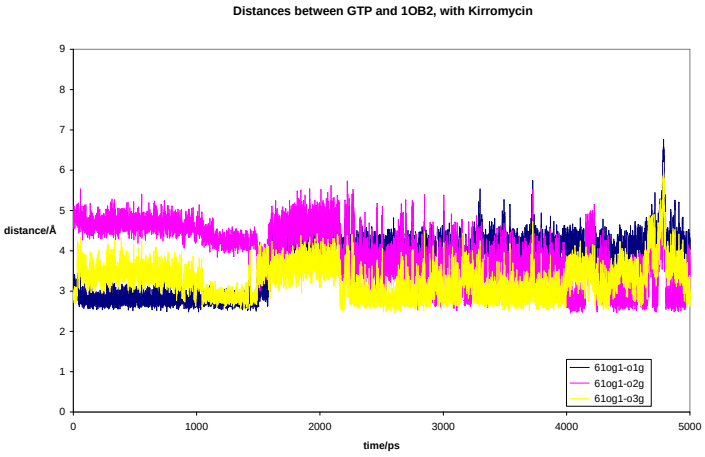
Distances between GTP and 1OB2, with Kirromycin
distance/Å
time/ps
61og1-o1g
61og1-o2g
61og1-o3g

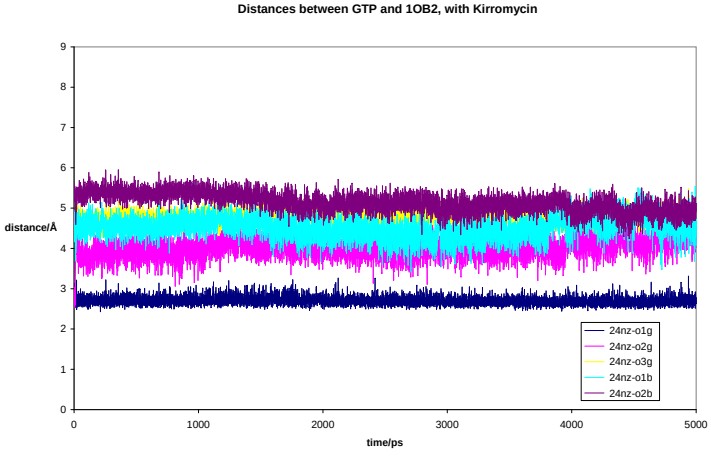
Distances between GTP and 1OB2, with Kirromycin
distance/Å
time/ps
24nz-o1g
24nz-o2g
24nz-o3g
24nz-o1b
24nz-o2b

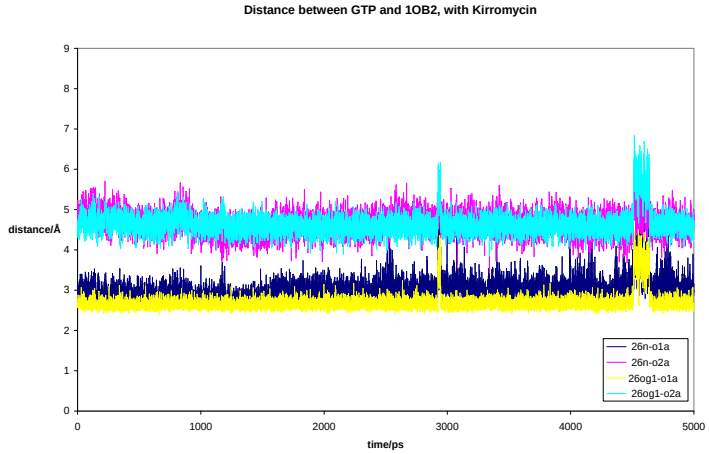
Distance between GTP and 1OB2, with Kirromycin
distance/Å
time/ps
26n-o1a
26n-o2a
26og1-o1a
26og1-o2a

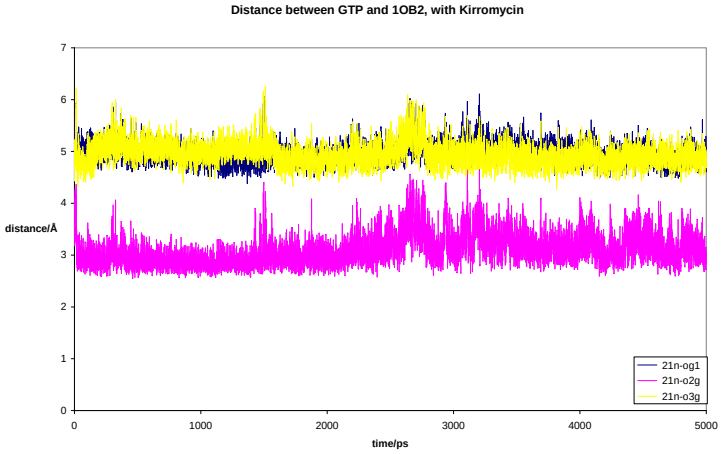
Distance between GTP and 1OB2, with Kirromycin
distance/Å
time/ps
21n-og1
21n-o2g
21n-o3g

G.1.4.2 Angles

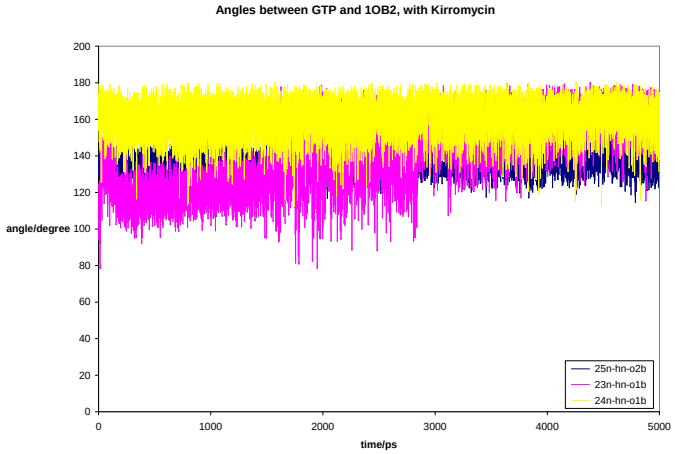
Angles between GTP and 1OB2, with Kirromycin
angle/degree
time/ps
25n-hn-o2b
23n-hn-o1b
24n-hn-o1b

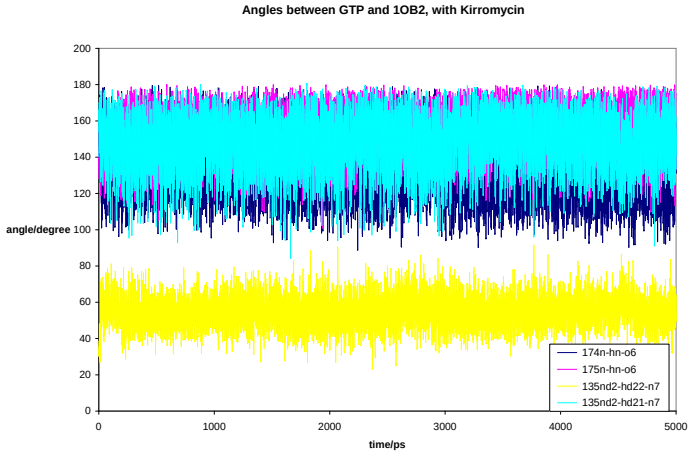
Angles between GTP and 1OB2, with Kirromycin
angle/degree
time/ps
174n-hn-o6
175n-hn-o6
135nd2-hd22-n7
135nd2-hd21-n7

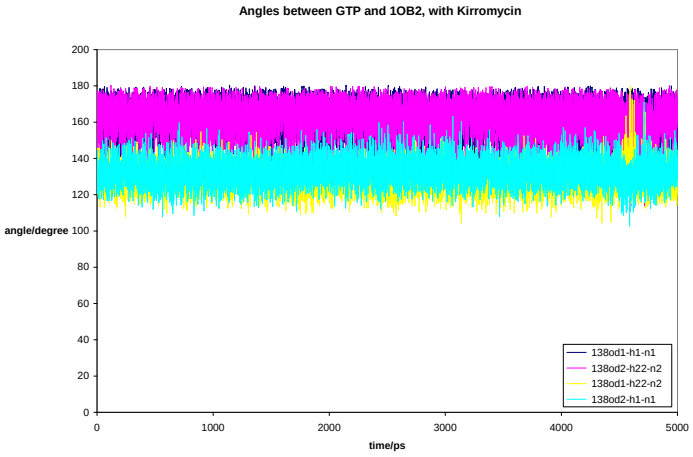
Angles between GTP and 1OB2, with Kirromycin
angle/degree
time/ps
138od1-h1-n1
138od2-h22-n2
138od1-h22-n2
138od2-h1-n1

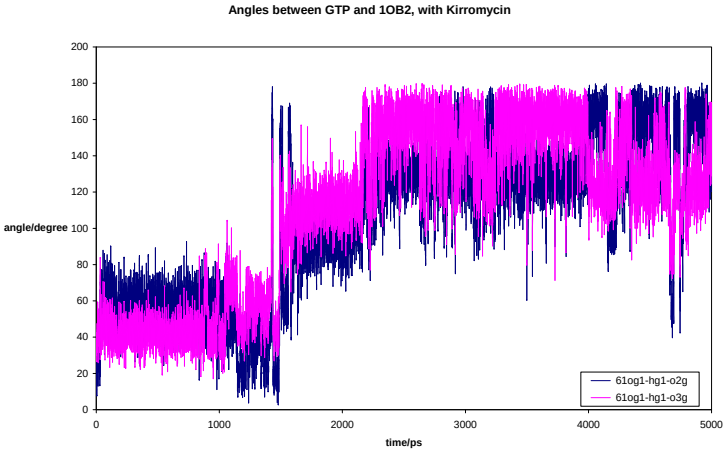
Angles between GTP and 1OB2, with Kirromycin
angle/degree
time/ps
61og1-hg1-o2g
61og1-hg1-o3g

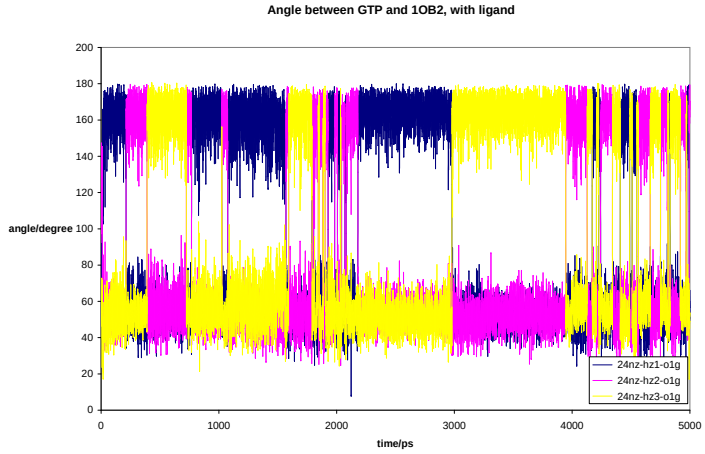
Angle between GTP and 1OB2, with ligand
angle/degree
time/ps
24nz-hz1-o1g
24nz-hz2-o1g
24nz-hz3-o1g

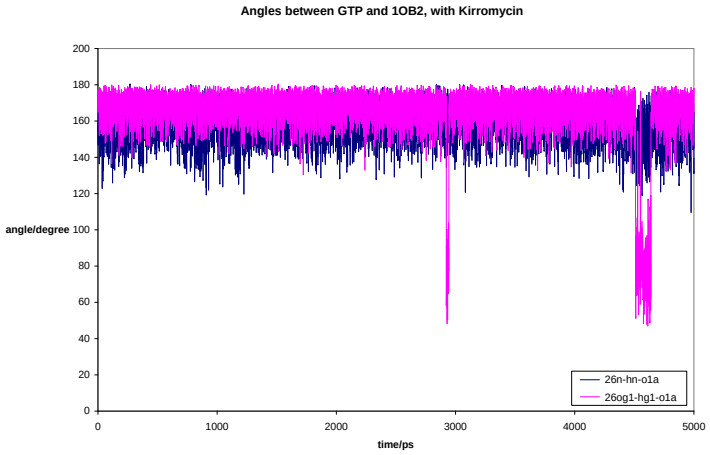
Angles between GTP and 1OB2, with Kirromycin
angle/degree
time/ps
26n-hn-o1a
26og1-hg1-o1a

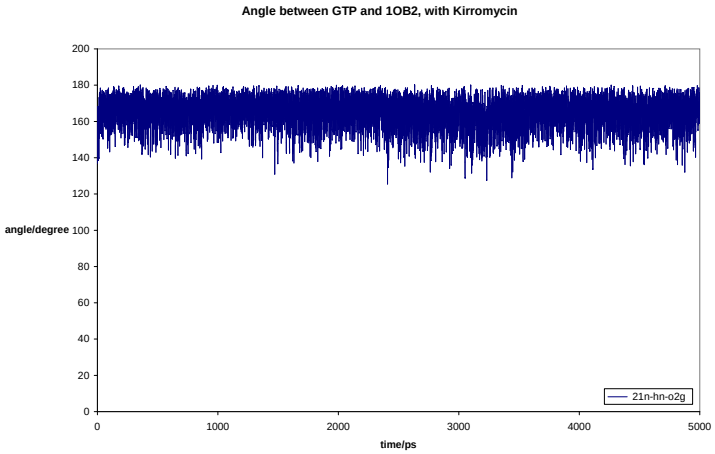
Angle between GTP and 1OB2, with Kirromycin
angle/degree
time/ps
21n-hn-o2g

G.1.5 Simulation 5

G.1.5.1 Distances

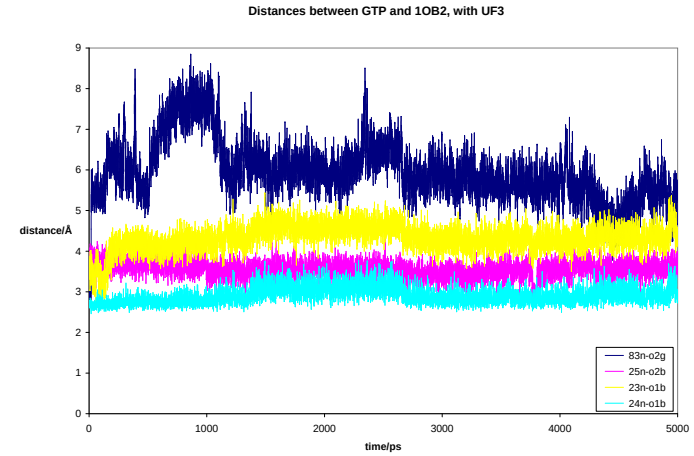

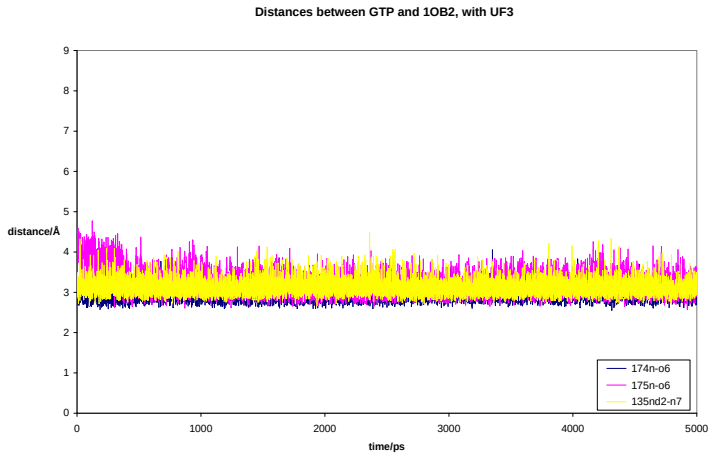

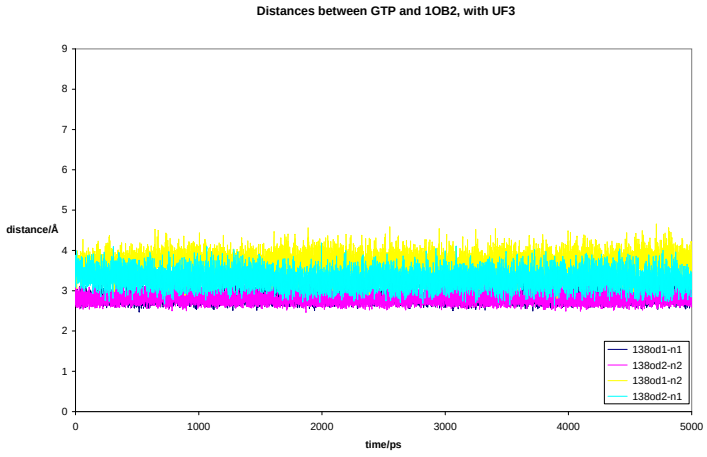

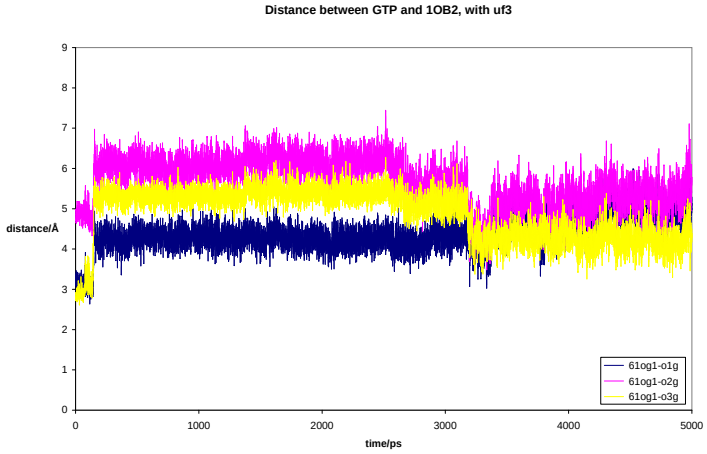
Distance between GTP and 1OB2, with uf3
distance/Å
time/ps
61og1-o1g
61og1-o2g
61og1-o3g

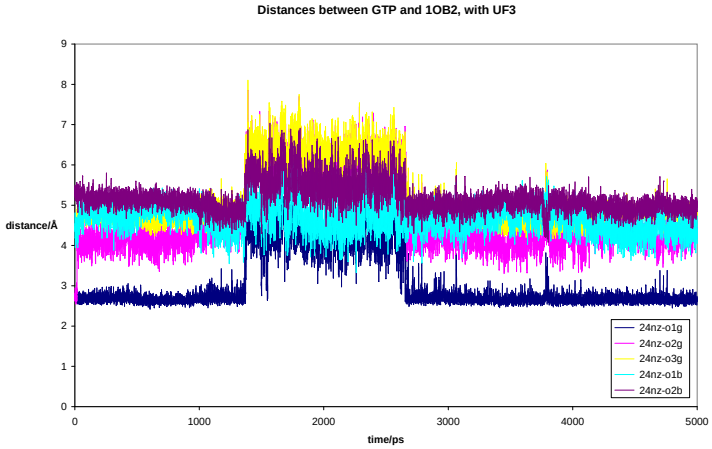
Distances between GTP and 1OB2, with UF3
distance/Å
time/ps
24nz-o1g
24nz-o2g
24nz-o3g
24nz-o1b
24nz-o2b

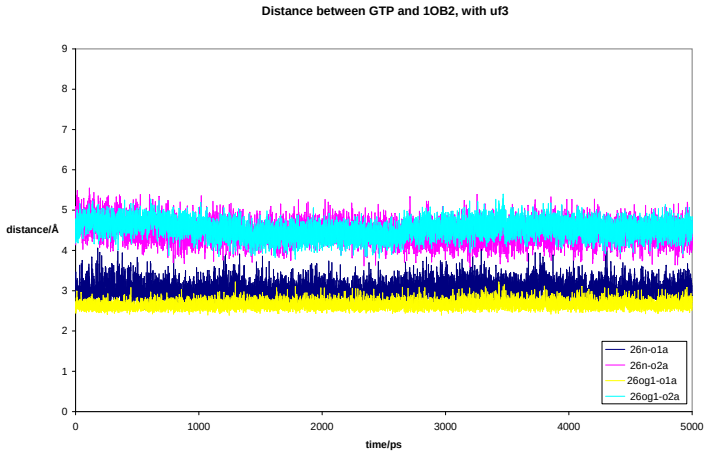
Distance between GTP and 1OB2, with uf3
distance/Å
time/ps
26n-o1a
26n-o2a
26og1-o1a
26og1-o2a

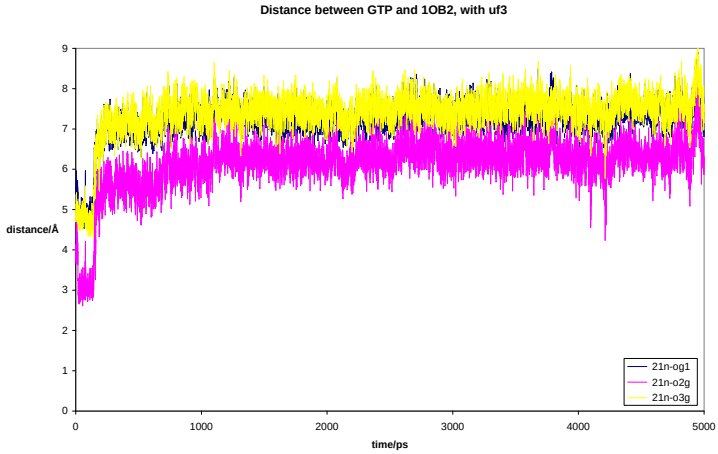
Distance between GTP and 1OB2, with uf3
distance/Å
time/ps
21n-og1
21n-o2g
21n-o3g

G.1.5.2 Angles

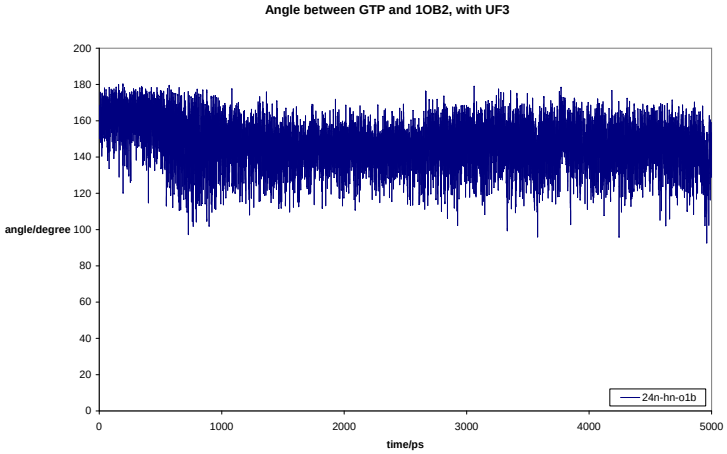
Angle between GTP and 1OB2, with UF3
angle/degree
time/ps
24n-hn-o1b

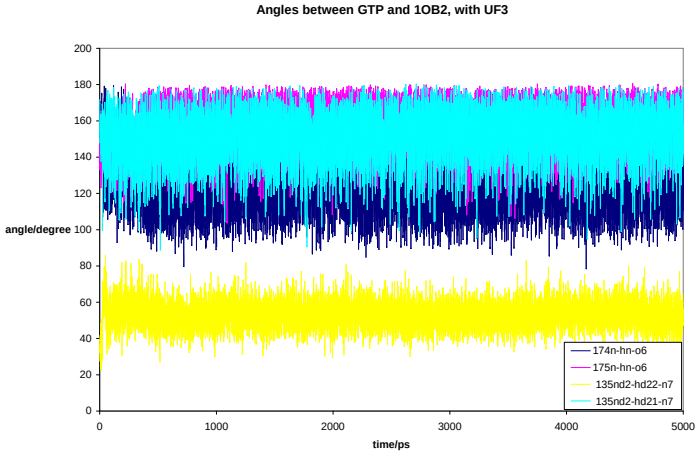
Angles between GTP and 1OB2, with UF3
angle/degree
time/ps
174n-hn-o6
175n-hn-o6
135nd2-hd22-n7
135nd2-hd21-n7

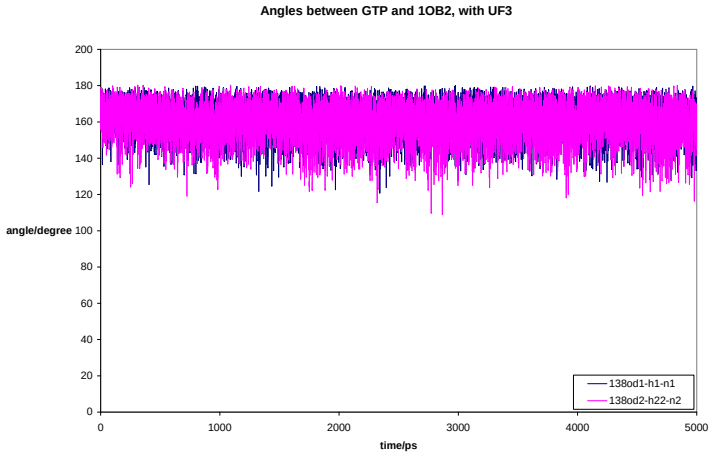
Angles between GTP and 1OB2, with UF3
angle/degree
time/ps
138od1-h1-n1
138od2-h22-n2

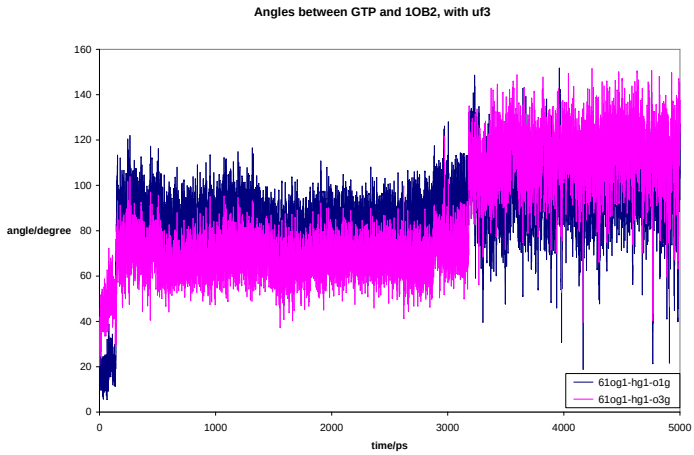
Angles between GTP and 1OB2, with uf3
angle/degree
time/ps
61og1-hg1-o1g
61og1-hg1-o3g

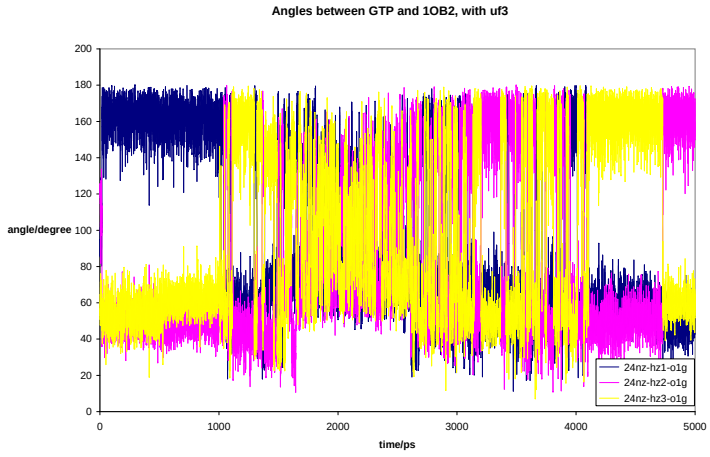
Angles between GTP and 1OB2, with uf3
angle/degree
time/ps
24nz-hz1-o1g
24nz-hz2-o1g
24nz-hz3-o1g

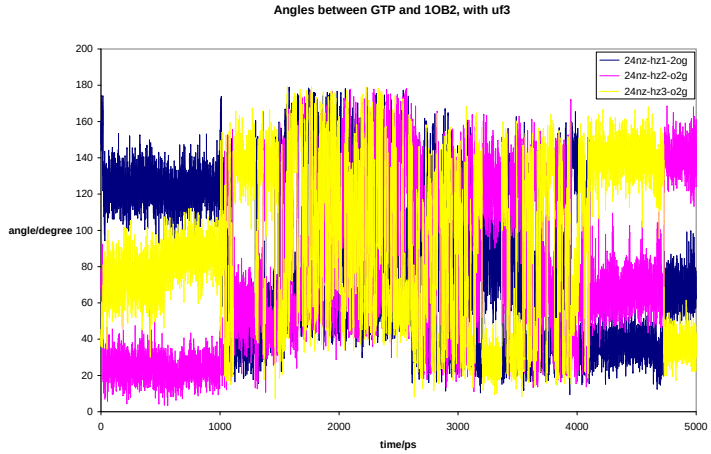

G.1.6 Simulation 6

G.1.6.1 Distances

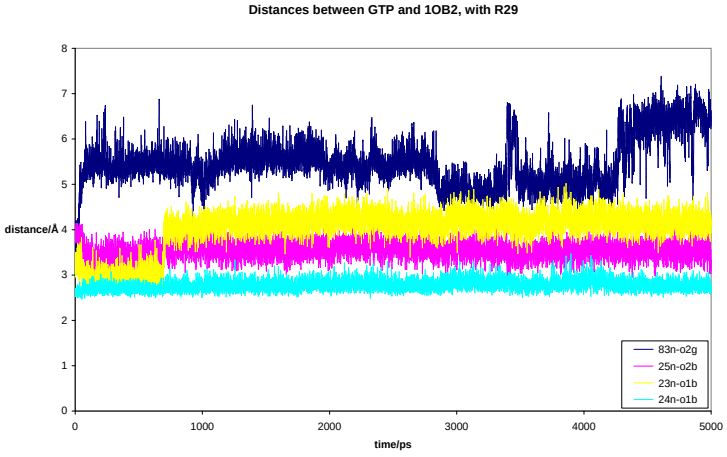

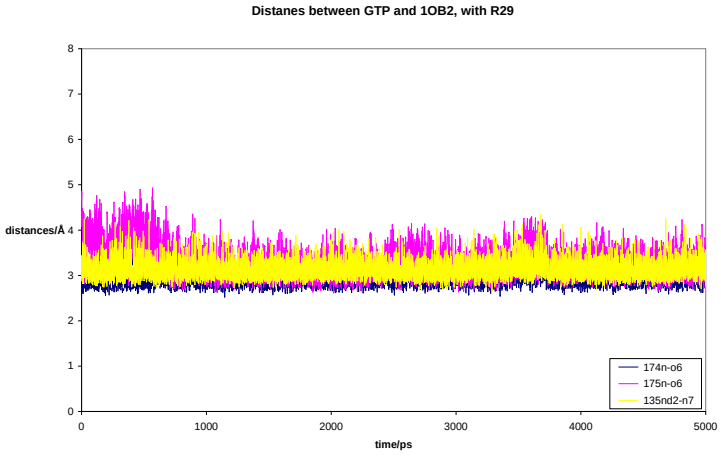
Distanes between GTP and 1OB2, with R29
distances/Å
time/ps
174n-o6
175n-o6
135nd2-n7

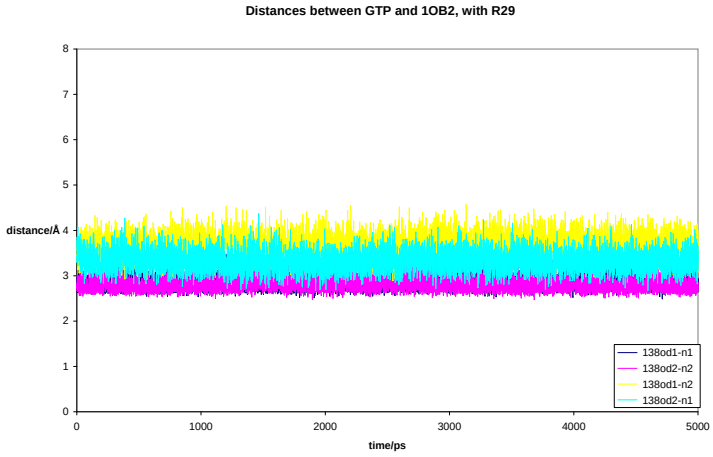
Distances between GTP and 1OB2, with R29
distance/Å
time/ps
138od1-n1
138od2-n2
138od1-n2
138od2-n1

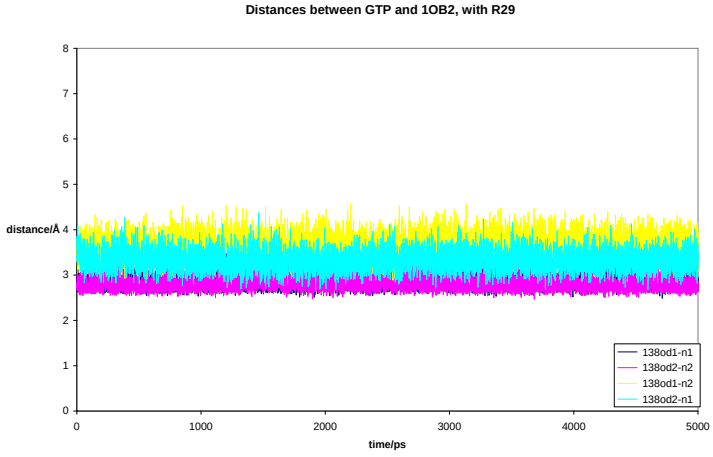
Distances between GTP and 1OB2, with R29
distance/Å
time/ps
138od1-n1
138od2-n2
138od1-n2
138od2-n1

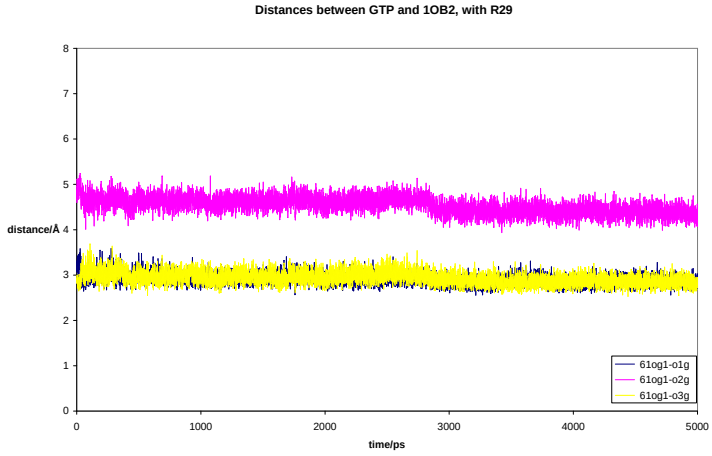
Distances between GTP and 1OB2, with R29
distance/Å
time/ps
61og1-o1g
61og1-o2g
61og1-o3g

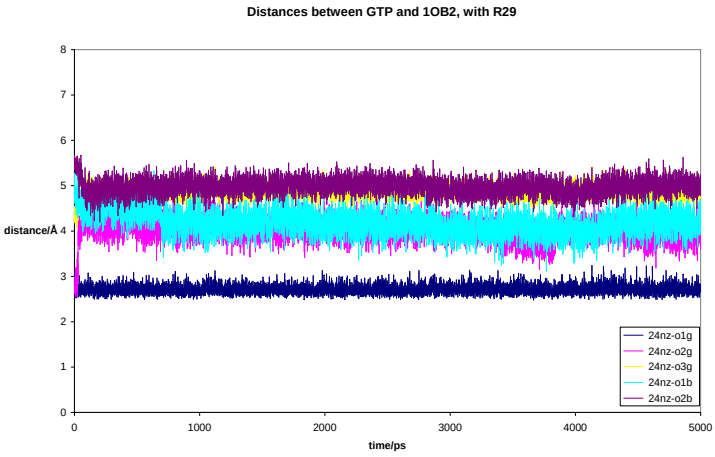
Distances between GTP and 1OB2, with R29
distance/Å
time/ps
24nz-o1g
24nz-o2g
24nz-o3g
24nz-o1b
24nz-o2b

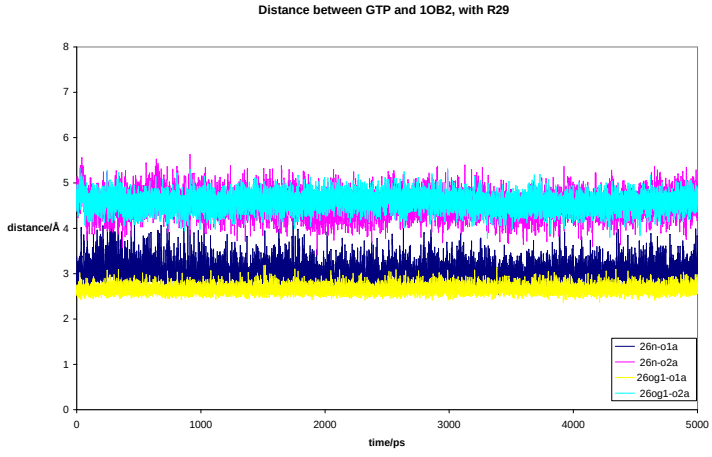
Distance between GTP and 1OB2, with R29
distance/Å
time/ps
26n-o1a
26n-o2a
26og1-o1a
26og1-o2a

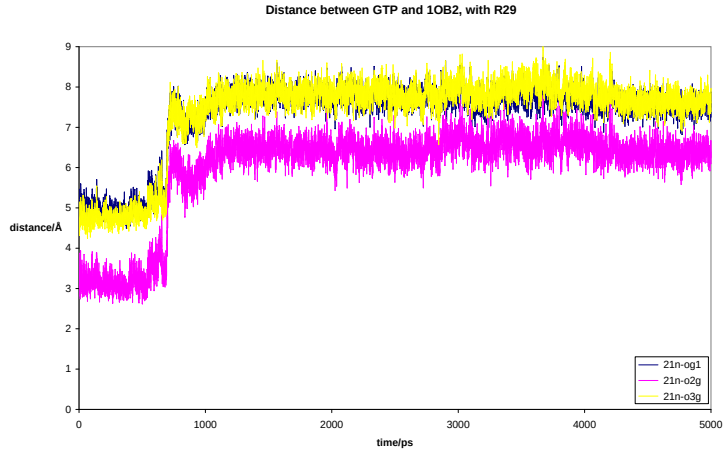
Distance between GTP and 1OB2, with R29
distance/Å
time/ps
21n-og1
21n-o2g
21n-o3g

G.1.6.2 Angles

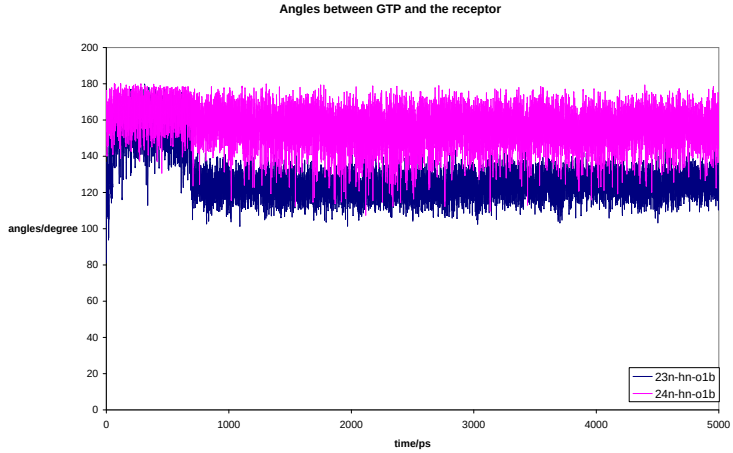
Angles between GTP and the receptor
angles/degree
time/ps
23n-hn-o1b
24n-hn-o1b

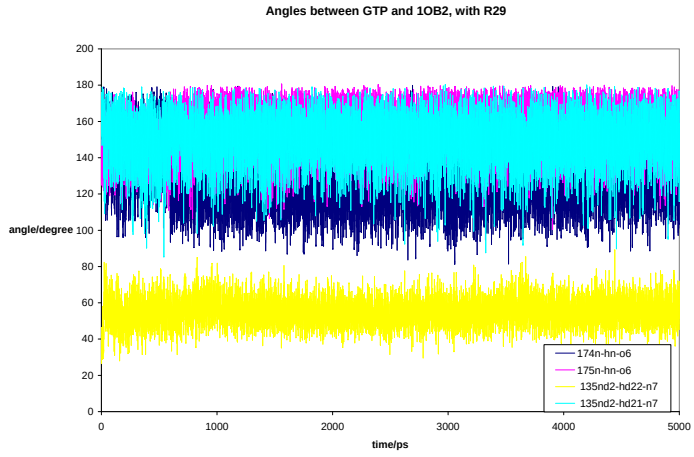
Angles between GTP and 1OB2, with R29
angle/degree
time/ps
174n-hn-o6
175n-hn-o6
135nd2-hd22-n7
135nd2-hd21-n7

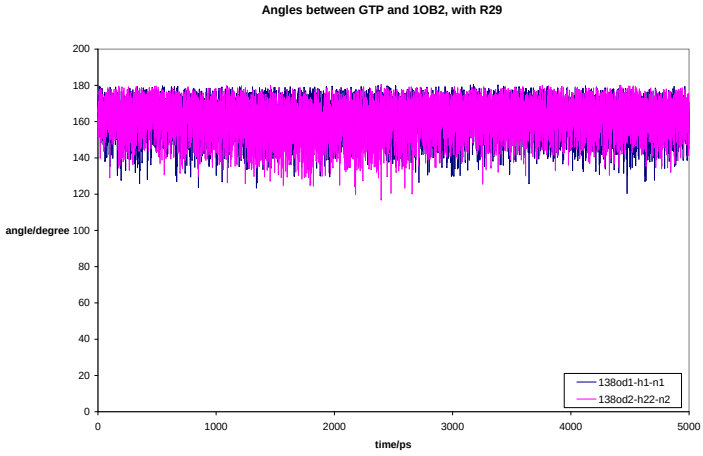
Angles between GTP and 1OB2, with R29
angle/degree
time/ps
138od1-h1-n1
138od2-h22-n2

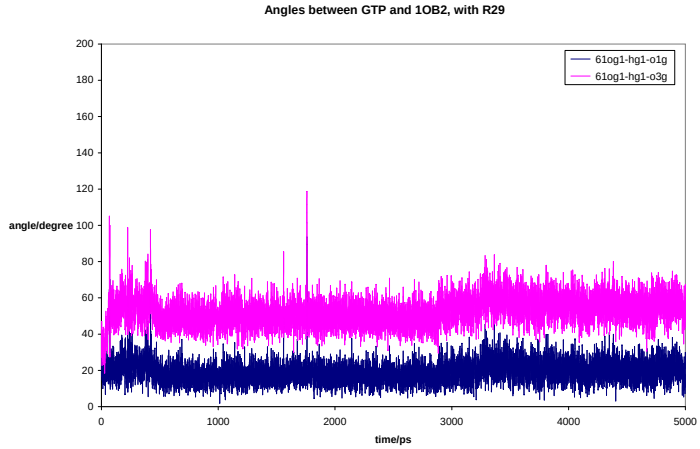
Angles between GTP and 1OB2, with R29
angle/degree
time/ps
61og1-hg1-o1g
61og1-hg1-o3g

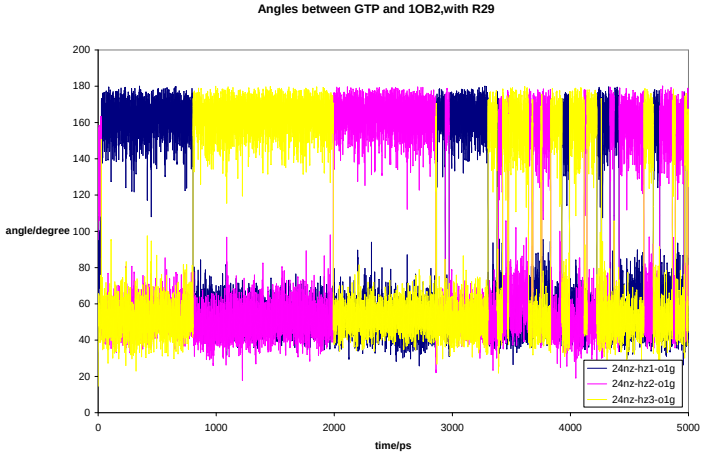
Angles between GTP and 1OB2,with R29
angle/degree
time/ps
24nz-hz1-o1g
24nz-hz2-o1g
24nz-hz3-o1g

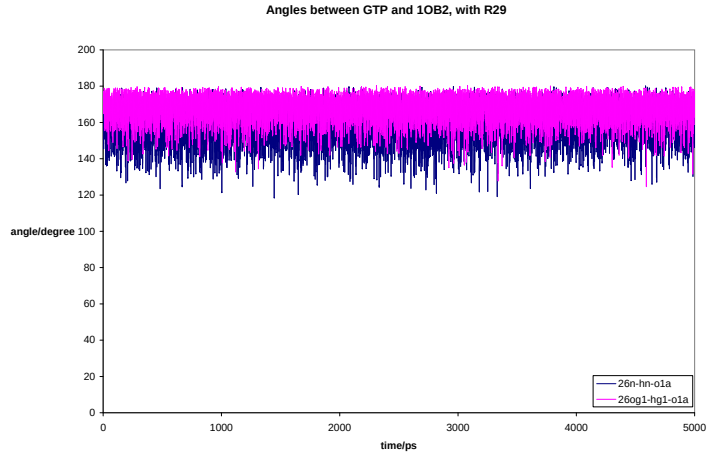

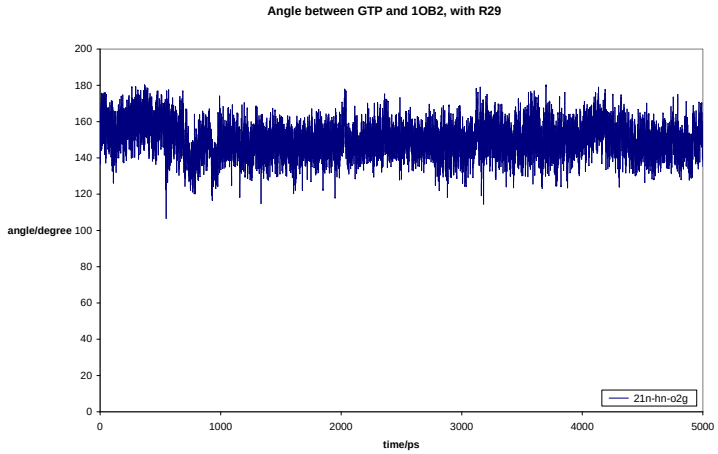

G.2 Hydrogen Bonds to Enacyloxin

This section shows the hydrogen bond distances and angles measured between Enx and the structure E.

G.2.1 Distances

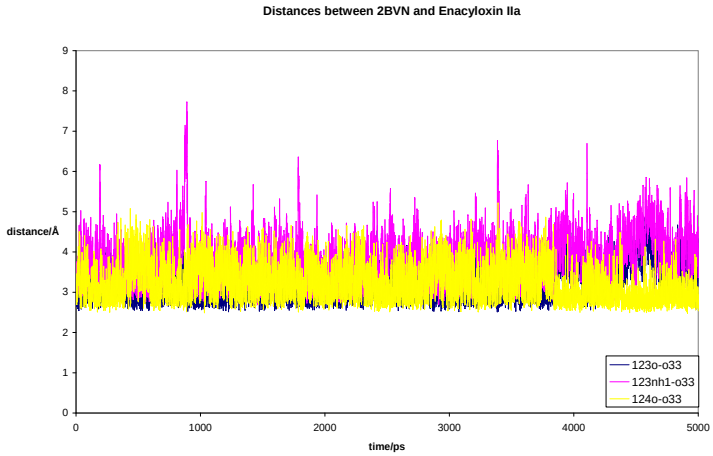

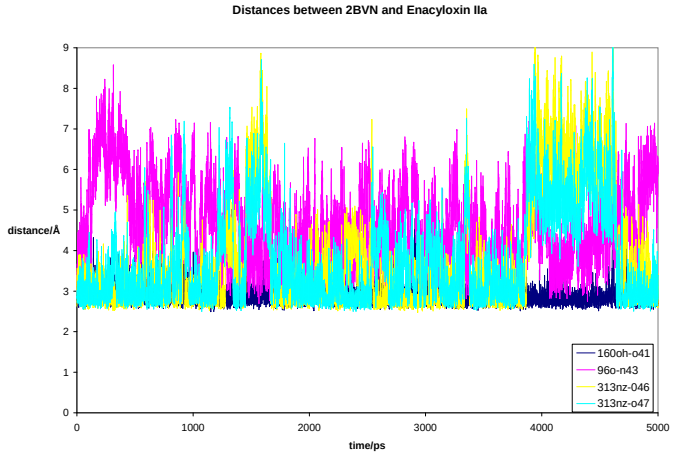

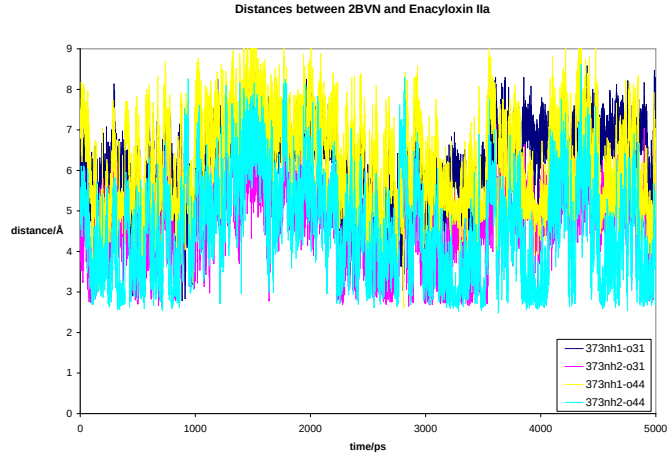

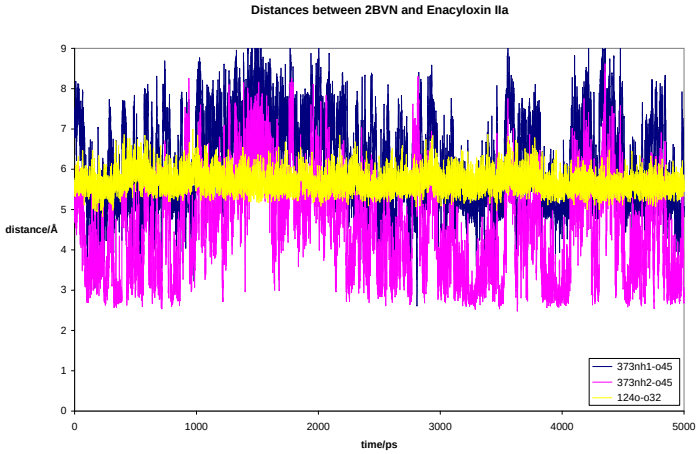
Distances between 2BVN and Enacyloxin IIa
distance/Å
time/ps
373nh1-o45
373nh2-o45
124o-o32

G.2.2 Angles

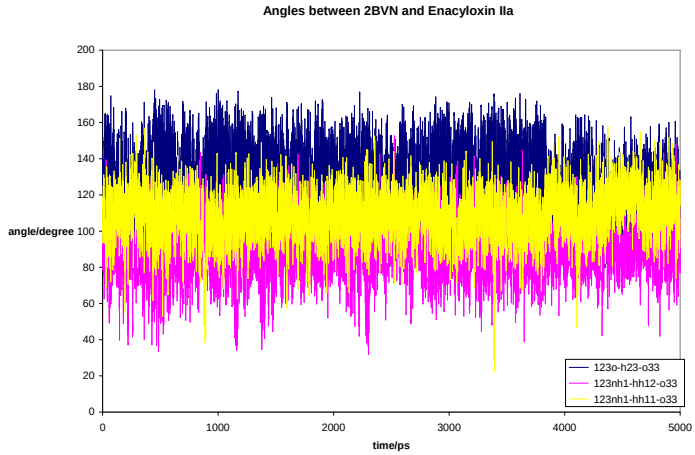
Angles between 2BVN and Enacyloxin IIa
angle/degree
time/ps
123o-h23-o33
123nh1-hh12-o33
123nh1-hh11-o33

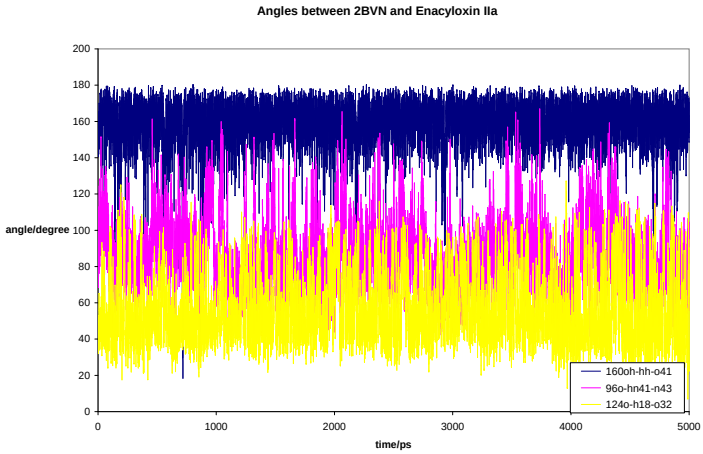
Angles between 2BVN and Enacyloxin IIa
angle/degree
time/ps
160oh-hh-o41
96o-hn41-n43
124o-h18-o32

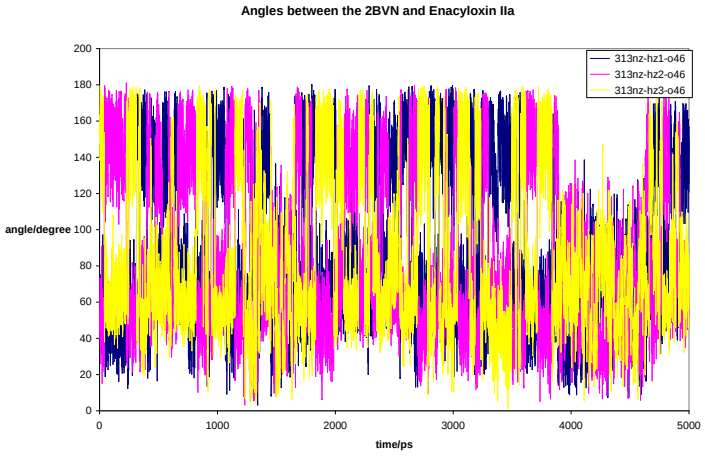
Angles between the 2BVN and Enacyloxin IIa
313nz-hz1-o46
313nz-hz2-o46
313nz-hz3-o46
angle/degree
time/ps

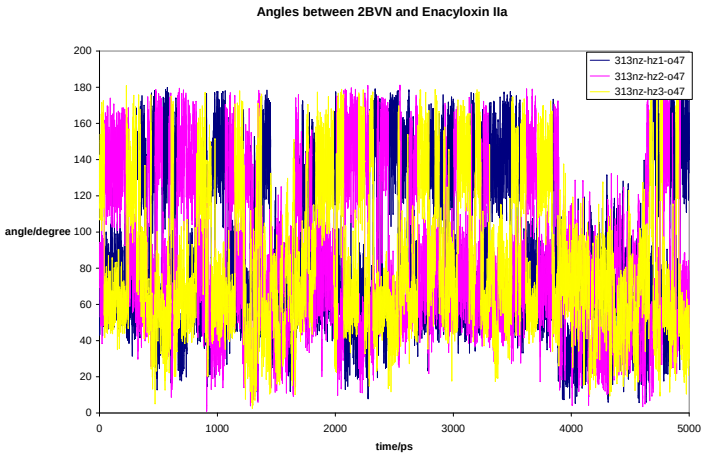
Angles between 2BVN and Enacyloxin IIa
313nz-hz1-o47
313nz-hz2-o47
313nz-hz3-o47
angle/degree
time/ps

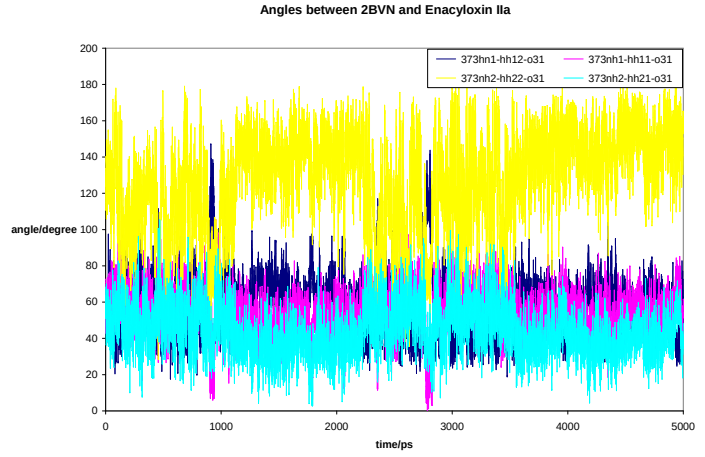
Angles between 2BVN and Enacyloxin IIa
373hn1-hh12-o31
373nh1-hh11-o31
373nh2-hh22-o31
373nh2-hh21-o31
angle/degree
time/ps

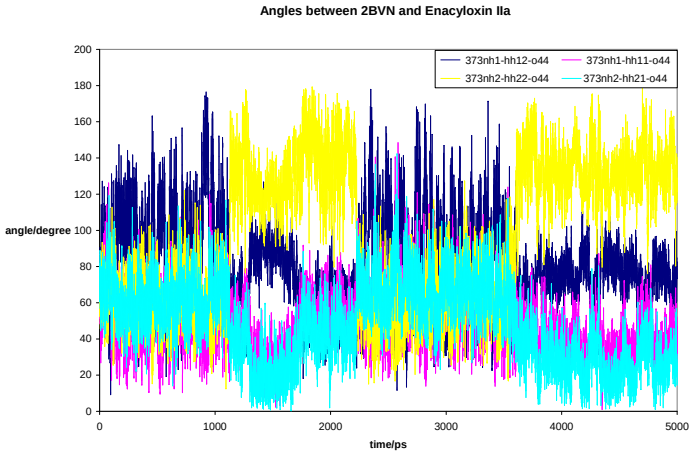

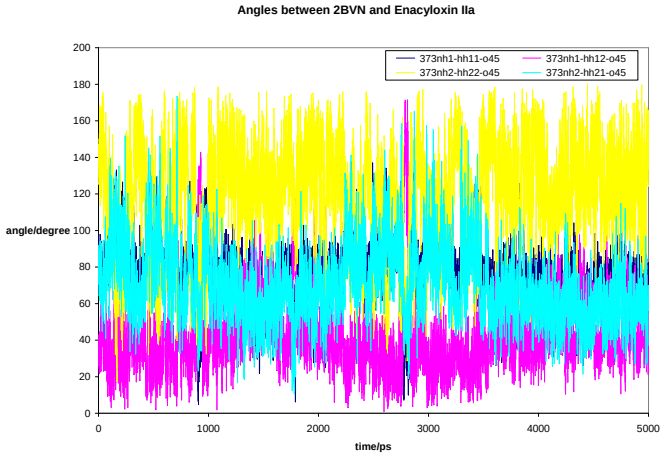

G.3 Hydrogen Bonds to Kirromycin

This section shows the hydrogen bond distances and angles measured between Kir and structure K.

G.3.1 Distances

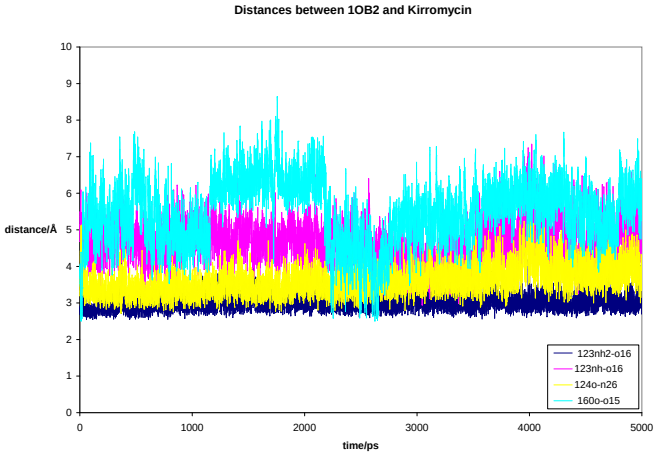

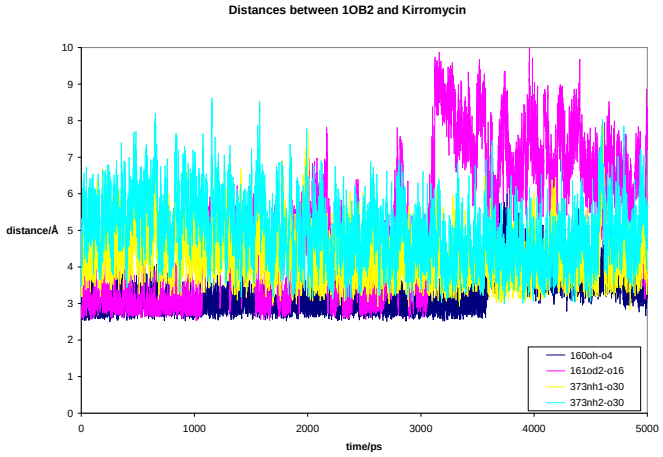

G.3.2 Angles

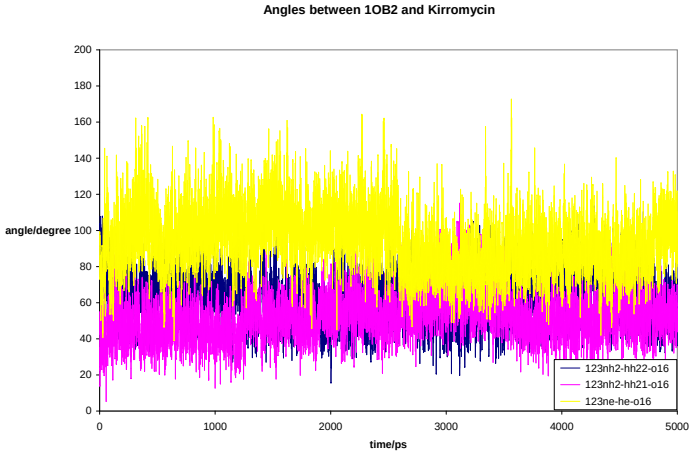

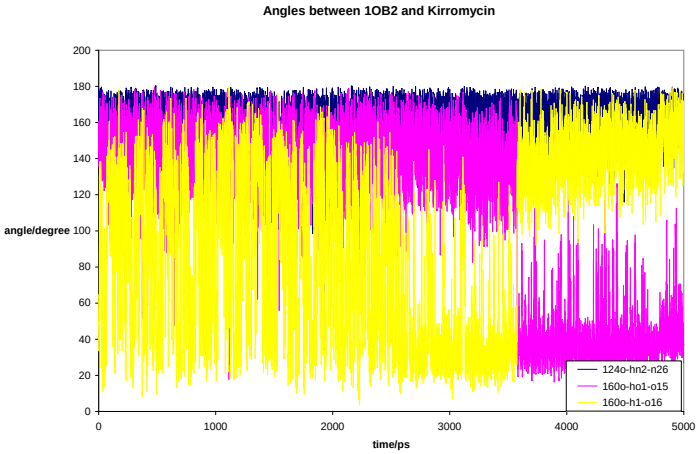
Angles between 1OB2 and Kirromycin
angle/degree
time/ps
124o-hn2-n26
160o-ho1-o15
160o-h1-o16

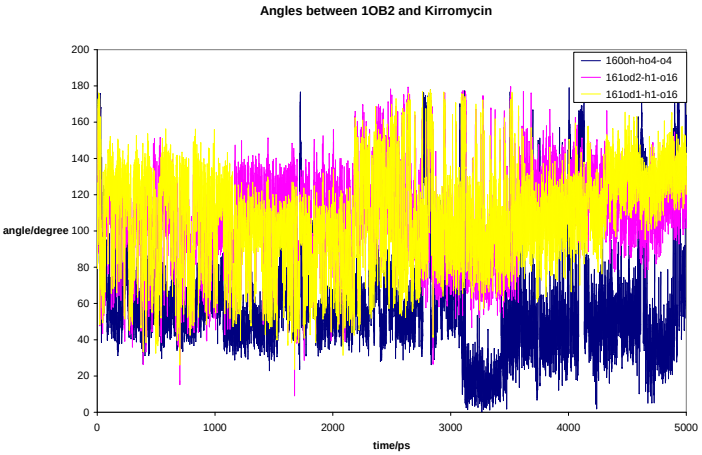
Angles between 1OB2 and Kirromycin
angle/degree
time/ps
160oh-ho4-o4
161od2-h1-o16
161od1-h1-o16

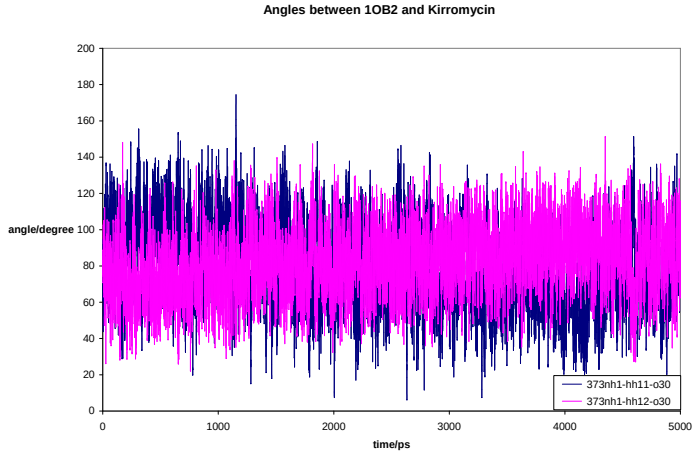
Angles between 1OB2 and Kirromycin
angle/degree
time/ps
373nh1-hh11-o30
373nh1-hh12-o30

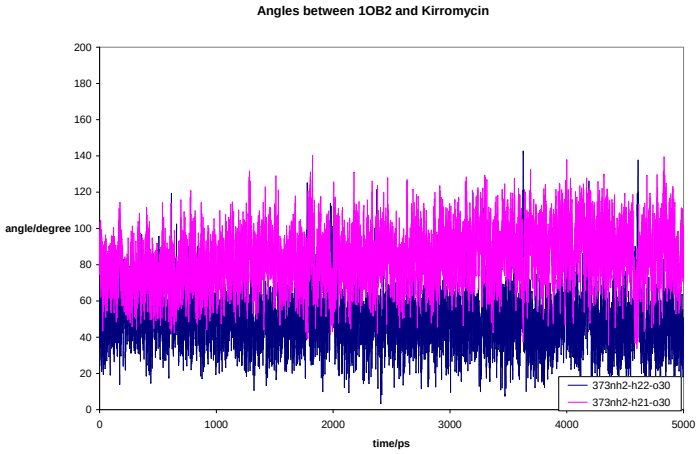

G.4 Hydrogen Bonds to UF3-1

This section shows the hydrogen bond distances and angles measured between UF3-1 and structure K.

G.4.1 Distances

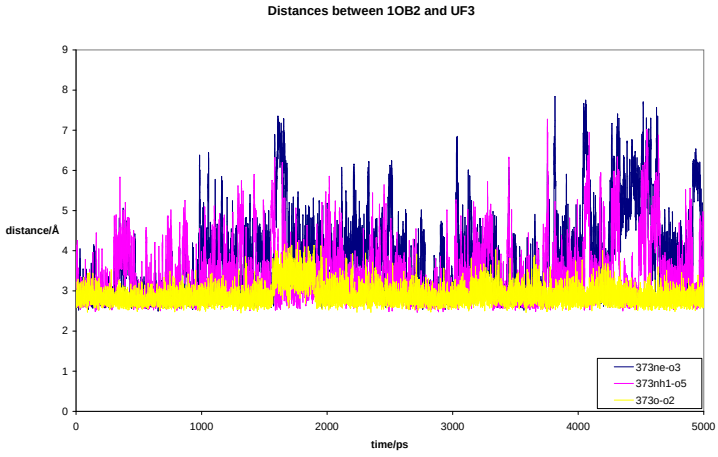

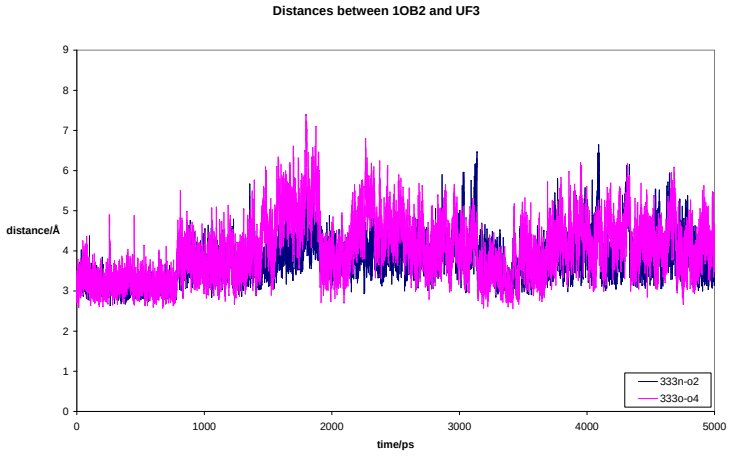
Distances between 1OB2 and UF3
distance/Å
time/ps
333n-o2
333o-o4

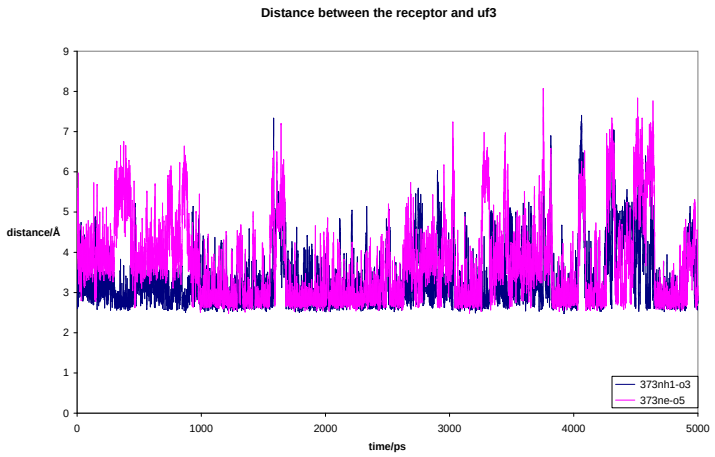
Distance between the receptor and uf3
distance/Å
time/ps
373nh1-o3
373ne-o5

G.4.2 Angles

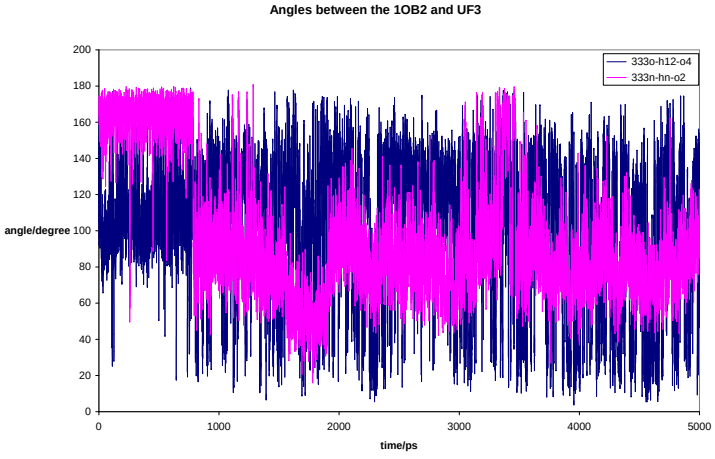
Angles between the 1OB2 and UF3
angle/degree
time/ps
333o-h12-o4
333n-hn-o2

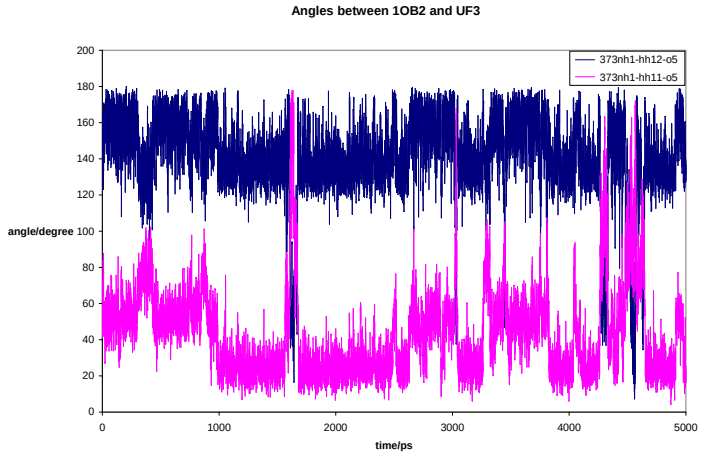
Angles between 1OB2 and UF3
373nh1-hh12-o5
373nh1-hh11-o5
angle/degree
time/ps
0
20
40
60
80
100
120
140
160
180
200
0
1000
2000
3000
4000
5000

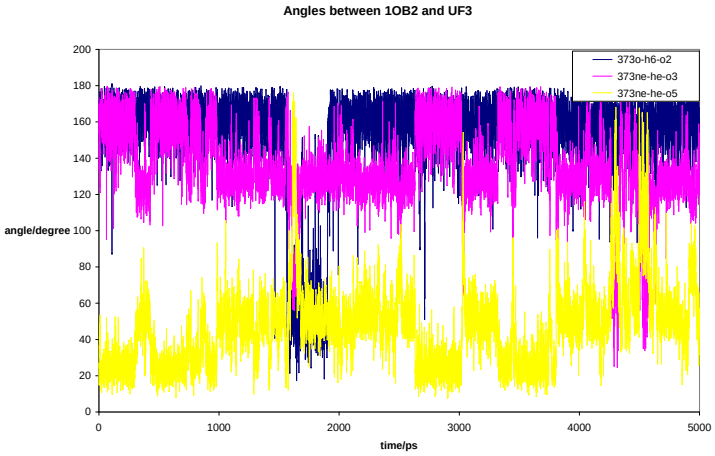
Angles between 1OB2 and UF3
373o-h6-o2
373ne-he-o3
373ne-he-o5
angle/degree
time/ps
0
20
40
60
80
100
120
140
160
180
200
0
1000
2000
3000
4000
5000

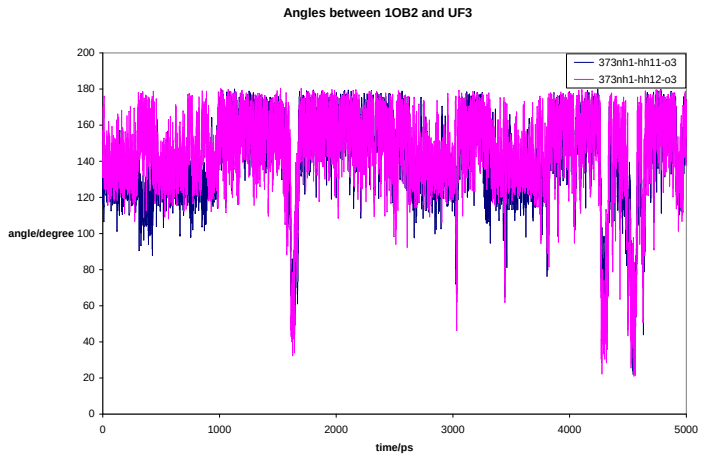
Angles between 1OB2 and UF3
373nh1-hh11-o3
373nh1-hh12-o3
angle/degree
time/ps
0
20
40
60
80
100
120
140
160
180
200
0
1000
2000
3000
4000
5000

Appendix H

Charts for Magnesium Coordination

The following charts show the coordination to the Mg^{2+} ion found in the GTP binding pocket. For the coordination to be present the distance should be around 2 Å.

H.1 Simulation 1

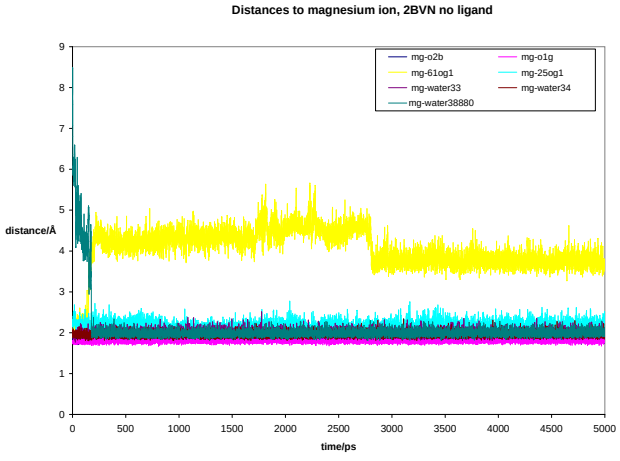

H.2 Simulation 2

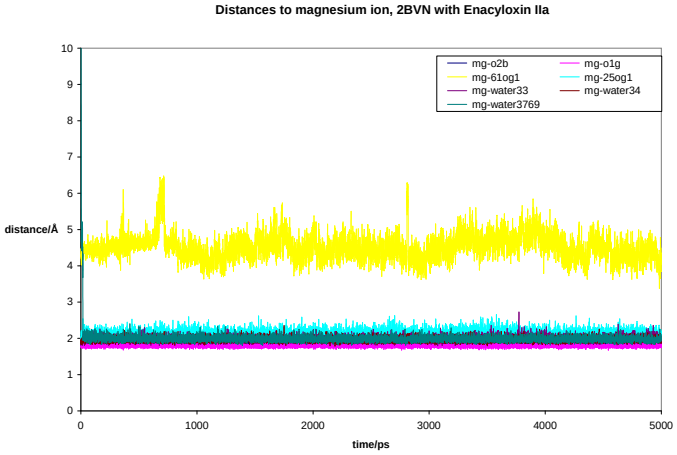

H.3 Simulation 3

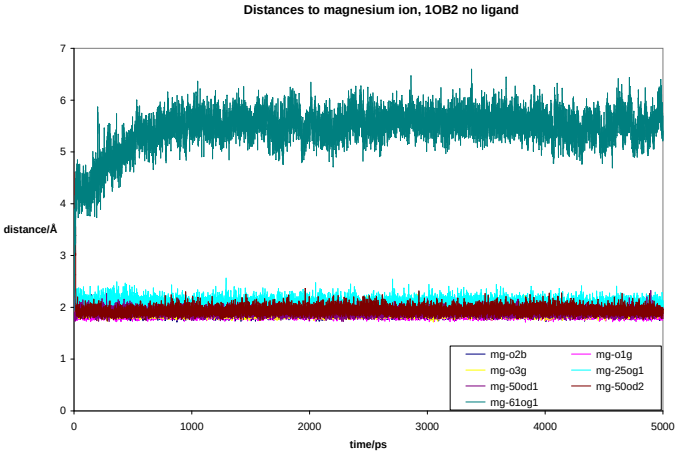

H.4 Simulation 4

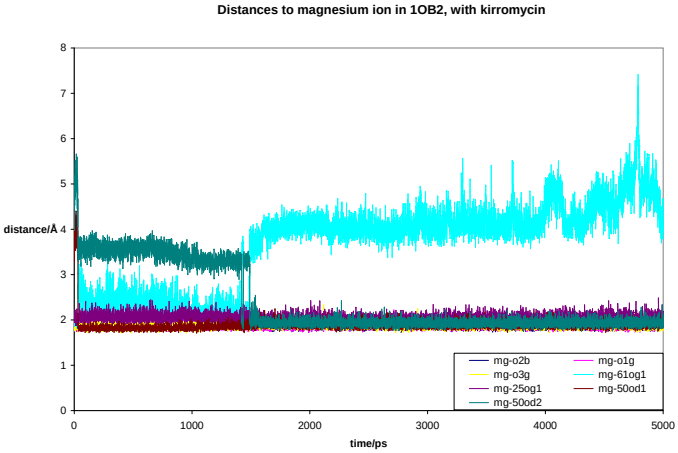

H.5 Simulation 5

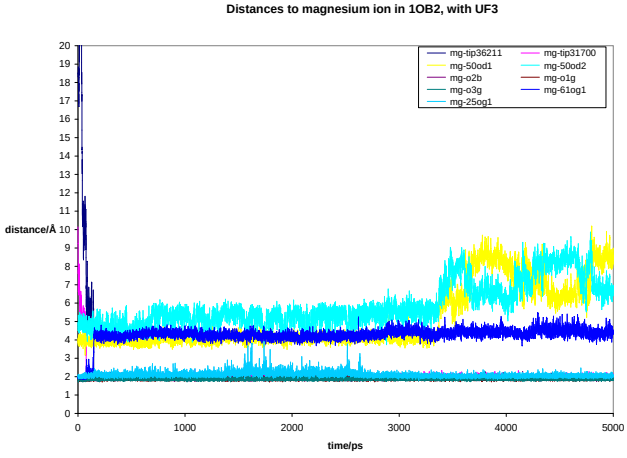

H.6 Simulation 6

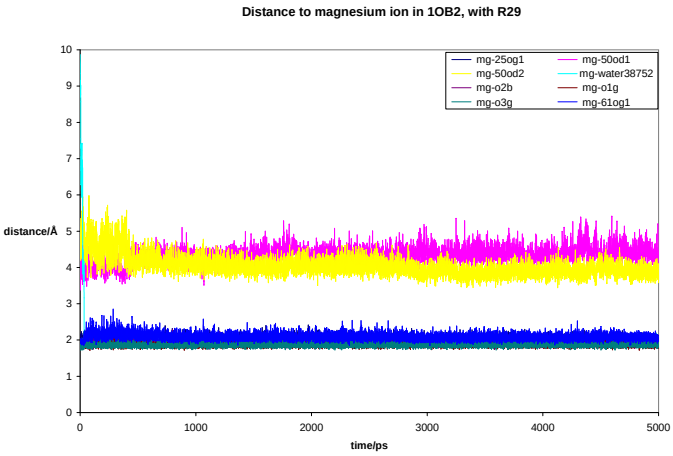

Bibliography

[1] Kenton Abel and Frances Jurnak. A complex profile of protein elongation: translating chemical energy into molecular movement. *Structure*, 4:229–238, 1996.

[2] Jan Pieter Abrahams, Mark J. van Raaij, Günther Ott, Barend Kraal, and Leendert Bosch. Kirromycin Drastically Reduces the Affinity of Escherichia coli Elongation Factor Tu for Aminoacyl-tRNA. *Biochemistry*, 30:6705–6710, 1991.

[3] Accelrys Software, Inc. Accelrys company web page on the internet. `http://www.accelrys.com/`.

[4] Accelrys Software, Inc. *Quanta2000*. San Diego: Accelrys Software, Inc., 2000.

[5] Accelrys Software, Inc. *Cerius^2, Release 4.10*. San Diego: Accelrys Software, Inc., 2005.

[6] Stewart A. Adcock and J. Andrew McCammon. Molecular Dynamics: Survey of Methods for Simulating the Activity of Proteins. *Chemical Reviews*, 106:1589–1615, 2006.

[7] Salam Al-Karadaghi, Arnthor Ævarsson, Maria Garber, Julia Zheltonosova, and Anders Liljas. The structure of elongation factor G in complex wiht GDP: conformational flexibility and nucleotide exchange. *Structure*, 4:555–565, 1996.

[8] B. J. Alder and T. E. Wainwright. Phase Transition for a Hard Sphere System. *Journal of Chemical Physics*, 27:1208–1209, 1957.

[9] Pieter H. Anborgh, Sumio Okamura, and Andrea Parmeggiani. Effects of the Antibiotic Pulvomycin on the Elongation Factor Tu-Dependent Reac-

tions. Comparison with Other Antibiotics. *Biochemistry*, 43:15550–15556, 2004.

[10] Pieter H. Anborgh and Andrea Parmeggiani. New antibiotic that acts specially on the GTP-bound form of elongation factor Tu. *The EMBO Journal*, 10:779–784, 1991.

[11] Gregers R. Andersen, Poul Nissen, and Jens Nyborg. Elongation factors in protein biosynthesis. *Trends in Biochemical Sciences*, 28:434–441, 2003.

[12] Amy C. Anderson. The Process of Structure-Based Drug Design. *Chemistry and Biology*, 10:787–797, 2003.

[13] Jay L. Banks, Hege S. Beard, Yixiang Cao, Art E. Cho, Wolfgang Damm, Ramy Farid, Anthony K. Felts, Thomas A. Halgreen, Daniel T. Mainz, Jon R. Maple, Robert Murphy, Dean M. Philipp, Matthew P. Repasky, Linda Y. Zhang, Bruce J. Berne, Richard A. Friesner, Emilio Gallicchio, and Ronald M. Levy. Interated Modeling Program, Applied Chemical Theory (IMPACT). *Journal of Computational Chemistry*, 26:1752–1780, 2005.

[14] D. J. Barlow and J. M. Thornton. Ion-pairs in Proteins. *Journal of Molecular Biology*, 168:867–885, 1983.

[15] Oren M. Becker, Alexander D. MacKerell, Jr., Benoît Roux, and Masakatsu Watanabe. *Computational Biochemistry and Biophysics*. Marcel Dekker Inc., New York, 2001.

[16] Harald Berchtold, Ludmila Reshetnikova, Christian O. A. Reiser, Norbert K. Schirmer, Mathias Sprinzi, and Rolf Hilgenfeld. Crystal structure of active elongation factor Tu reveals major domain rearrangements. *Nature*, 365:126–132, 1993.

[17] Jeremy M. Berg, John L. Tymoczko, and Lubert Stryer. *Biochemistry*. W. H. Freeman and Company, New York, fifth edition, 2001.

[18] Anders Berkenstam and Jan-Åke Gustafsson. Nuclear receptors and their relevance to diseases related to lipid metabolism. *Current Opinion in Pharmacology*, 5:171–176, 2005.

[19] Helen M. Berman, John Westbrook, Zukang Feng, Gary Gilliland, T. N. Bhat, Helge Weissing, Ilya N. Shindyalov, and Philip E. Bourne. The Protein Data Bank. *Nucleic Acids Research*, 28:235–242, 2000.

[20] Regine S. Bohacek and Colin McMartin. Multiple Highly Diverse Structures Complementary to Enzyme Binding Sites: Results of Extensive Application of a de Novo Design Method Incorporating Combinatorial Growth. *Journal of the American Chemical Society*, 116:5560–5571, 1994.

[21] Hans-Joachim Böhm. LUDI: Rule-based automatic design of new substituents for enzyme inhibitor leads. *Journal of Computer-Aided Molecular Design*, 6:593–606, 1992.

[22] Hans-Joachim Böhm. The computer program LUDI: A new method for the de novo design of enzyme inhibitors. *Journal of Computer-Aided Molecular Design*, 6:61–78, 1992.

[23] Hans-Joachim Böhm. On the use of LUDI to search the Fine Chemicals Directory for ligands of proteins of known three-dimensional structure. *Journal of Computer-Aided Molecular Design*, 8:623–632, 1994.

[24] Hans-Joachim Böhm. The development of a simple empirical scoring function to estimate the binding constant for a protein-ligand complex of known three-dimensional structure. *Journal of Computer-Aided Molecular Design*, 8:243–256, 1994.

[25] Hans-Joachim Böhm. Prediction of binding constants of protein ligands: A fast method for the prioritization of hits obtained from de novo design or 3D database search programs. *Journal of Computer-Aided Molecular Design*, 12:309–323, 1998.

[26] William Bourguet, Pierre Germain, and Hinrich Gronemeyer. Nuclear receptor ligand-binding domains: three-dimensional structures, molecular interactions and pharmacological implications. *Trends in Pharmacological Sciences*, 21:381–388, 2000.

[27] G. Patrick Brady Jr. and Pieter F. W. Stouten. Fast prediction and visualization of protein binding pockets with PASS. *Journal of Computer-Aided Molecular Design*, 14:383–401, 2000.

[28] Natasja Brooijimans and Irwin D. Kuntz. Molecular Recognition and Docking Algorithms. *Annual Review of Biophysics and Biomolecular Structure*, 32:335–373, 2003.

[29] David A. Case, Thomas E. Cheatham, III, Tom Darden, Holger Gohlke, Ray Luo, Kenneth M. Merz, Jr., Alexey Onufriev, Carlos Simmerling, Bing

Wang, and Robert J. Woods. The Amber Biomolecular Simulation Programs. *Journal of Computational Chemistry*, 26:1668–1688, 2005.

[30] Rengül Cetin, Ivo M. Krab, Pieter H. Anborgh, Robbert H. Cool, Toshihiko Watanabe, Takeyoshi Sugieyama, Kazuo Izaki, and Andrea Parmeggiani. Enacyloxin IIa, an inhibitor of protein biosynthesis that acts on elongation factor Tu and the ribosome. *The EMBO journal*, 15:2604–2611, 1996.

[31] Gianni Chinali. Identification of the Part of Kirromycin Structure that Acts on Elongation Factor Tu. *Federation of European Biochemical Societies*, 131:94–98, 1981.

[32] Markus Christen, Philippe H. Hünberger, Dirk Bakowies, Riccardo Baron, Roland Bürgi, Daan P. Geerke, Tim N. Heinz, Mika A. Kastenholz, Vincent Kräutler, Chris Oostenbrink, Christine Peter, Daniel Trzesniak, and Wilfred F. van Gunsteren. The GROMOS Software for Biomolecular Simulation: GROMOS05. *Journal of Computational Chemistry*, 26:1719–1751, 2005.

[33] David E. Clark, David Frenkel, Stephen A. Levy, Jin Li, Christopher W. Murray, Barry Robson, Bohdan Waszkowycz, and David R. Westhead. PRO-LIGAND: An approach to de novo molecular design. 1. Application to the design of organic molecules. *Journal of Computer-Aided Molecular Design*, 9:13–32, 1995.

[34] Columbia University. SCREEN: Surface Cavity REcognition and EvaluatioN. `http://interface.bioc.columbia.edu/screen/`.

[35] Nuclear Receptors Nomeclature Committee. A Unified Nomenclature System of the Nuclear Receptor Superfamily. *Cell*, 97:161–163, 1999.

[36] Wendy D. Cornell, Piotr Cieplak, Christopher I. Bayly, and Peter A. Kollman. Application of RESP Charges to Calculate Conformational Energies, Hydrogen Bond Energies, and Free Energies of Solvation. *Journal of the American Society*, 115:9620–9631, 1993.

[37] Christopher J. Cramer. *Essentials of Computational Chemistry. Theories and Models*. John Wiley & Sons, second edition, 2005.

[38] D. J. Danziger and P. M. Dean. Automated Site-Directed Drug Design: A General Algorithm for Knowledge Acquisition about Hydrogen-Bonding

Regions at Protein Surfaces. *Proceedings of the Royal Society of London. Series B, Biological Sciences*, 236:101–113, 1989.

[39] Tom Darden, Darrin York, and Lee Pedersen. Particle mesh Ewald: An N·log(N) method for Ewald sums in large systems. *Journal of Chemical Physics*, 98:10089–10092, 1993.

[40] Matthew D. Eldridge, Christopher W. Murray, Timothy R. Auton, Gaia V. Paolini, and Roger P. Mee. Emperical scoring functions: I. The development of a fast emperical scoring function to estimate the binding affinity of ligands in receptor complexes. *Journal of Computer-Aided Molecular Design*, 11:425–445, 1997.

[41] Ottavio Fasano, Wolfgang Bruns, Jean-Bernard Crechet, Gernot Sander, and Andrea Parmeggiani. Modification of Elongation-Factor-Tu Guanine-Nucleotide Interaction by Kirromycin. A Comparison with the Effect of Aminoacyl-tRNA and Elongation Factor Ts. *European Journal of Biochemistry*, 89:557–567, 1978.

[42] Scott E. Feller, Yuhong Zang, Richard W. Pastor, and Bernard R. Brooks. Constant Pressure Molecular Dynamics Simulation: The Langevin Piston Method. *Journal of Chemical Physics*, 103:4613–4621, 1995.

[43] Anna Maria Ferrari, Binqing Q. Wei, Luca Costantino, and Brian K. Shoichet. Soft Docking and Multiple Receptor Conformations in Virtual Screening. *Journal of Medicinal Chemistry*, 47:5076–5084, 2004.

[44] Richard A. Friesner, Jay L. Banks, Robert B. Murphy, Thomas A. Halgren, Jasna J. Klicic, Daniel T. Mainz, Matthew P. Repasky, Eric H. Knoll, Mee Shelley, Jason K. Perry, David E. Shaw, Perry Francis, and Peter S. Shenkin. Glide: A New Approach for Rapid, Accurate Docking and Scoring. 1. Method and Assessment of Docking Accuracy. *Journal of Medical Chemistry*, 47:1739–1749, 2004.

[45] Justin P. Gallivan and Dennis A. Dougherty. Cation-π interactions in structural biology. *Proceedings of the National Academy of Sciences*, 96:9459–9464, 1999.

[46] Valerie Gillet, A. Peter Johnson, Pauline Mata, Sandor Sike, and Philip Williams. SPROUT: A program for structure generation. *Journal of Computer-Aided Molecular Design*, 7:127–153, 1993.

[47] Michael K. Gilson, Hillary S. R. Gilson, and Michael J. Potter. Fast Assignment of Accurate Partial Atomic Charges: An Electronegativity Equalization Method that Accounts for Alternate Resonance Forms. *Journal of Chemical Information and Computer Sciences*, 43:1982–1997, 2003.

[48] P. J. Goodford. A Computational Procedure for Determining Energetically Favorable Binding Sites on Biologically Important Macromolecules. *Journal of Medicinal Chemistry*, 28:849–857, 1985.

[49] Carl Henrik Görbitz. Hydrogen-Bond Distances and Angles in the Structures of Amino Acids and Peptides. *Acta Crystallographica Section B*, B45:390–395, 1989.

[50] Carl Henrik Görbitz and Margaret C. Etter. Hydrogen Bonds to Carboxylate Groups. Syn/Anti Distributions and Steric Effects. *Journal of the American Chemical Society*, 114:627–631, 1992.

[51] Andrew G. Gridge, Louise L. Major, Alhad A. Mahagaonkar, Elizabeth S. Poole, Leif A. Isaksson, and Warren P. Tate. Comparison of characteristics and function of translation termination signals between and within prokaryotic and eukaryotic organisms. *Nucleic Acids Research*, 34:1959–1973, 2006.

[52] Hinrich Gronemeyer, Jan-Åke Gustafsson, and Vincent Laudet. Principles for Modulation of the Nuclear Receptor Superfamily. *Nature Review Drug Discovery*, 3:950–964, 2004.

[53] Thomas A. Halgren. MMFF VII. Characterization of MMFF94, MMFF94s, and Other Widely Available Force Fields for Conformational Energies and for Intermolecular-Interaction Energies and Geometries. *Journal of Computational Chemistry*, 20:730–748, 1999.

[54] Thomas A. Halgren, Robert B. Murphy, Richard A. Friesner, Hege S. Beard, Leah L. Frye, W. Thomas Pollard, and Jay L. Banks. Glide: A New Approach for Rapid, Accurate Docking and Scoring. 2. Enrichment Factors in Database Screening. *Journal of Medicinal Chemistry*, 47:1750–1759, 2004.

[55] R. Hilgenfeld, J. R. Mesters, and T. Hogg. Insights into the GTPase Mechanism of EF-Tu from Structural Studies. *The Ribosome: Structure, Function, Antibiotics, and Cellular Interactions*, 28:347–357, 2000.

[56] T. Hogg, J. R. Mesters, and R. Hilgenfeld. Inhibitory Mechanisms of Antibiotics Targeting Elongation Factor Tu. *Current Protein and Peptide Science*, 3:121–131, 2002.

[57] Teruki Honma. Recent advances in de novo design strategy for practical lead identification. *Medicinal Research Reviews*, 23:606–632, 2003.

[58] William Humphrey, Andrew Dalke, and Klaus Schulten. VMD: Visual Molecular Dynamics. *Journal of Molecular Graphics*, 14:33–38, 1996.

[59] William L. Jorgensen, David S. Maxwell, and Julian Tirado-Rives. Development and Testing of the OPLS All-Atom Force Field on Conformational Energetics and Properties of Organic Liquids. *Journal of the American Chemical Society*, 118:11225–11236, 1996.

[60] W. Kabsch. A discussion of the solution for the best rotation to relate two sets of vectors. *Acta Crystallographia*, A34:827–828, 1978.

[61] Laxmikant Kalé, Robert Skeel, Milind Bhandarkar, Robert Brunner, Attila Gursoy, Neal Krawetz, James Phillips, Aritomo Shinozaki, Krishnan Varadarajan, and Klaus Schulten. NAMD2: Greater Scalabitity for Parallel Molecular Dynamics. *Journal of Computational Physics*, 151:283–312, 1999.

[62] Takemasa Kawashima, Carmen Berthet-Colominas, Michael Wulff, Stephen Cusack, and Reuben Leberman. The structure of the Escherichia coli EF-Tu·EF-Ts complex at 2.5 Å resolution. *Nature*, 379:511–518, 1996.

[63] Morten Kjeldgaard and Jens Nyborg. Refined Structure of Elongation Factor EF-Tu from Escherichia coli. *Journal of Molecular Biologi*, 223:721–742, 1992.

[64] Morten Kjeldgaard, Jens Nyborg, and Brian F. C. Clark. The GTP binding motif: variations on a theme. *The Federation of American Societies for Experimental Biology*, 10:1347–1368, 1996.

[65] Maria Kontoyianni, Laura M. McClellan, and Glenn S. Sokol. Evaluation of Docking Performance: Comparative Data on Docking Algorithms. *Journal of Medicinal Chemistry*, 47:558–565, 2004.

[66] Ivo M. Krab and Andrea Parmeggiani. EF-Tu, a GTPase odyssey. *Biochimeca et Biophysica Acta*, 1443:1–22, 1998.

[67] Bernd Kramer, Matthias Rarey, and Thomas Lengauer. Evaluation of the FlexX Incremental Construction Algorithm for Protein-Ligand Docking. *PROTEINS: Structure, Function, and Genetics*, 37:228–241, 1999.

[68] J. Kroon and J. A. Kanters. O-H$\cdots$O Hydrogen Bonds in Molecular Crystals. A Statistical and Quantum-Chemical Analysis. *Journal of Molecular Structure*, 24:109–129, 1975.

[69] Irwin D. Kuntz, Jeffrey M. Blaney, Stuart J. Oatley, Robert Landgridge, and Thomas E. Ferrin. A Geometric Approach to Macromolecule-Ligand Interactions. *Journal of Molecular Biology*, 161:269–288, 1982.

[70] Andrew R. Leach. *Molecular Modeling: Principles and Applications*. PEARSON, Prentice Hall, second edition.

[71] Christopher A. Lipinski, Franco Lombardo, Beryl W. Dominy, and Paul J. Feeney. Experimental and computational approaches to estimate solubility and permeability in drug discovery and development settings. *Advanced Drug Delivery Reviews*, 23:3–25, 1997.

[72] Brock A. Luty, Zelda R. Wasserman, Pieter F. W. Stouten, and C. Nicholas Hodge. A Molecular Mechanics / Grid Method for Evaluation of Ligand-Receptor Interactions. *Journal of Computational Chemistry*, 16:454–464, 1995.

[73] A. D. MacKerell, Jr., D. Bashford, M. Bellott, R. L. Dunbrack, Jr., J. D. Evanseck, M. J. Field, S. Fischer, J. Gao, H. Gou, S. Ha, D. Joseph-McCarthy, L. Kuchnir, K. Kuczera, F. T. K. Lau, C. Mattos, S. Michnick, T. Ngo, D. T. Nguyen, B. Prodhom, W. E. Reiher, III, B. Roux, M. Schlenkrich, J. C. Smith, R. Stote, J. Straub, M. Watanabe, J. Wiòrkiewicz-Kuczera, D. Yin, and M. Karplus. All-Atom Emperical Potential for Molecular Modeling and Dynamics Studies of Proteins. *Journal of Physical Chemistry B*, 102:3586–3616, 1998.

[74] Alexander D. MacKerell, Jr. Emperical Force Fields for Biological Macromolecules: Overview and Issues. *Jornal of Computational Chemistry*, 25:1584–1604, 2004.

[75] J. Andrew McCammon, Bruce R. Gelin, and Martin Karplus. Dynamics of Folded Proteins. *Nature*, 267:585–590, 1977.

[76] John T. Moore, Jon L. Collins, and Kenneth H. Pearce. The Nuclear Receptor Superfamily and Drug Discovery. *ChemMedChem*, 1:504–523, 2006.

[77] Dino Moras and Hinrich Gronemeyer. The nuclear receptor ligand-binding domain: structure and function. *Current Opinion in Cell Biology*, 10:384–391, 1998.

[78] Garrett M. Morris, David S. Goodsell, Robert S. Halliday, Ruth Huey, William E. Hart, Richard K. Belew, and Arthur J. Olson. Automated Docking Using a Lamarckian Genetic Algorithm and an Empirical Binding Free Energy Function. *Journal of Computational Chemistry*, 19:1639–1662, 1998.

[79] Ingo Muegge and Matthias Rarey. Small Molecule Docking and Scoring. *Reviews in Computational Chemistry*, 17:1–60, 2001.

[80] Peter Murray-Rust and Jenny P. Glusker. Directional Hydrogen Bonding to sp^2- and sp^3-Hybridized Oxygen Atoms and Its Relevance to Ligand-Macromolecule Interactions. *Journal of the American Chemical Society*, 106:1018–1025, 1984.

[81] Murad Nayal and Barry Honig. On the Nature of Cavities on Protein Surfaces: Application to the Identification of Drug-Binding Sites. *PROTEINS: Structure, Function, and Bioinformatics*, 63:892–906, 2006.

[82] Mark Nelson, William Humphrey, Attila Gursoy, Andrew Dalke, Laxmikant Kalé, Robert D. Skeel, and Klaus Schulten. NAMD – a Parallel, Object-Oriented Molecular Dynamics Program. *International Journal of Supercomputer Applications and High Performance Computing*, 10:251–268, 1996.

[83] Yoshihiko Nishibata and Akiko Itai. Automatic Creation of Drug Candidate Structures Based on Receptor Structure. Starting Point for Artificial Lead Generation. *Tetrahedron*, 47:8985–8990, 1991.

[84] Poul Nissen, Morten Kjeldgaard, Søren Thirup, Galina Polekhina, Ludmila Reshetnikova, Brian F. C. Clark, and Jens Nyborg. Crystal Structure of the Ternary Complex of Phe-$tRNA^{Phe}$, EF-Tu, and a GTP Analog. *Science*, 270:1464–1472, 1995.

[85] Poul Nissen and Jens Nyborg. EF-G and EF-Tu Structures and Translation Elongation in Bacteria. *Encyclopedia of Biological Chemistry*, 2:1–5, 2004.

[86] Poul Nissen, Søren Thirup, Morten Kjeldgaard, and Jens Nyborg. The crystal structure of Cys-$tRNA^{Cys}$-EF-Tu-GDPNP reveals general and spe-

cific features in the ternary complex and in tRNA. *Structure*, 7:143–156, 1999.

[87] Anthony W. Norman, Mathew T. Mizwicki, and Derek P. G. Norman. Steriod-hormone rapid actions, membrane receptors and a conformational ensemble model. *Nature Review Drug Discovery*, 3:27–41, 2004.

[88] Andrea Parmeggiani, Ivo M. Krab, Sumio Okamura, Rikke C. Nielsen, Jens Nyborg, and Poul Nissen. Structural Basis of the Action of Pulvomycin and GE2270 A on Elongation Factor Tu. *Biochemistry*, 45:6846–6857, 2006.

[89] Andrea Parmeggiani, Ivo M. Krab, Toshihiko Watanabe, Rikke C. Nielsen, Caroline Dahlberg, Jens Nyborg, and Poul Nissen. Enacyloxin IIa Pinpoints a Binding Pocket of Elongation Factor Tu for Development of Novel Antibiotics. *The Journal of Biological Chemistry*, 281:2893–2900, 2006.

[90] Joseph J. Pavelites, Jiali Gao, Paul A. Bash, and Alexander D. Mackerell, Jr. A Molecular Mechanics Force Field for NAD+, NADH and the Pyrophosphate Groups of Nucleotides. *Journal of Computational Chemistry*, 18:221–239, 1997.

[91] David A. Pearlman and Mark A. Murcko. CONCERTS: Dynamic Connection of Fragments as an Approach to de Novo Ligand Design. *Journal of Medicinal Chemistry*, 39:1651–1663, 1996.

[92] James C. Phillips, Rosemary Braun, Wei Wang, James Gumbart, Emad Tajkhorshid, Elizabeth Villa, Christophe Chipot, Robert D. Skeel, Laxmikant Kalé, and Klaus Schulten. Scalable Molecular Dynamics with NAMD. *Journal of Computational Chemistry*, 26:1781–1802, 2005.

[93] Galina Polekhina, Søren Thirup, Morten Kjeldgaard, Poul Nissen, Corinna Lippmann, and Jens Nyborg. Helix unwinding in the effector region of elongation factor EF-Tu-GDP. *Structure*, 4:1141–1151, 1996.

[94] Jay W. Ponder and David A. Case. Force Fields for Protein Simulations. *Advances in Protein Chemistry*, 66:27–85, 2003.

[95] V. Ramakrishnan. Ribosome Structure and the Mechanism of Translation. *Cell*, 108:557–572, 2002.

[96] Tamar Schlick. *Molecular Modeling and Simulation*. Springer-Verlag, New York.

[97] Gisbert Schneider and Uli Fechner. Computer-based de novo design of drug-like molecules. *Nature Rewiews*, 4:649–663, 2005.

[98] Gisbert Schneider, Wieland Schrödl, Gerd Wallukat, Johannes Müller, Eberhard Nissen, Wolfgang Rönspeck, Paul Wrede, and Rudolf Kunze. Peptide design by artificial neural networks and computer-based evolutionary search. *Proceedings of the National Academy of Sciences of the United States of America*, 95:12179–12184, 1998.

[99] Schrödinger, LLC. *Jaguar*. New York, NY.

[100] Schrödinger, LLC. *Glide version 4.0*. New York, NY, 2005.

[101] Schrödinger, LLC. *Induced Fit Docking protocol; Glide version 4.0*. New York, NY, 2005.

[102] Schrödinger, LLC. *Maestro version 7.5*. New York, NY, 2005.

[103] Schrödinger, LLC. *Prime version 1.5*. New York, NY, 2005.

[104] Schrödinger, LLC. *SiteMap version 2.0*. New York, NY, 2005.

[105] Woody Sherman, Tyler Day, Matthew P. Jacobson, Richard Friesner, and Ramy Farid. Novel Procedure for Modeling Ligand/Receptor Induced Fit Effects. *Journal of Medicinal Chemistry*, 49:534–553, 2006.

[106] Peter J. Steinbach and Bernard R. Brooks. New Spherical-Cutoff Methods for Long-Range Forces in Macromolecular Simulation. *Journal of Computational Chemistry*, 15:667–683, 1994.

[107] Anke C. U. Steinmetz, Jean-Paul Renaurd, and Dino Moras. Binding of Ligands and Activation of Transcription by Nuclear Receptors. *Annual Review of Biophysics and Biomolecular Structure*, 30:329–359, 2001.

[108] Anatha Sundaram and Venkat Venkatasubramanian. Parametric Sensitivity and Search-Space Characterization Studies of Genetic Algorithms for Computer-Aided Polymer Design. *Journal of Chemical Information and Computer Sciences*, 38:1177–1191, 1998.

[109] Robin Taylor and Olga Kennard. Hydrogen-Bond Geometry in Organic Crystals. *Account of Chemical Research*, 17:320–326, 1984.

[110] René Thomsen and Mikael H. Christensen. MolDock: A New Technique for High-Accuracy Molecular Docking. *Journal of Medicinal Chemistry*, 2006.

[111] University of Southern Denmark (SDU). The SDU Supercluster. `http://www.dcsc.sdu.dk/`.

[112] Angelo Vendani and Jack D. Dunitz. Lone-Pair Directionality in Hydrogen Bond Potential Functions for Molecular Mechanics Calculations: The Inihibition of Human Carbonic Anhydrase II by Sulfonamides. *Journal of the American Chemical Society*, 107:7653–7658, 1985.

[113] C. M. Venkatachalam, X. Jiang, T. Oldfield, and M. Waldman. LigandFit: a novel method for the shape-directed rapid docking of ligands to protein active sites. *Journal of Molecular Graphics and Modelling*, 21:289–307, 2003.

[114] Marcel L. Verdonk, Jason C. Cole, Michael J. Hartshorn, Christopher W. Murray, and Richard D. Taylor. Improved Protein-Ligand Docking Using GOLD. *PROTEINS: Structure, Function, and Genetics*, 52:609–623, 2003.

[115] Lutz Vogeley, Gottfried J. Palm, Jeroen R. Mesters, and Rolf Hilgenfeld. Conformational Changes of Elongation Factor Tu (EF-Tu) Induced by Antibiotic Binding. *The Journal of Biological Chemistry*, 276:17149–17155, 2001.

[116] Binqing Q. Wei, Larry H. Weaver, Anna M. Ferrari, Brian W. Matthews, and Brian K. Shoichet. Testing a Flexibe-receptor Docking Algorithm in a Model Binding Site. *Journal of Molecular Biology*, 337:1161–1182, 2004.

[117] C. G. Wermuth, C. R. Gannelin, P. Lindberg, and L. A. Mitscher. Glossary of terms used in medicinal chemistry. *Pure and Applied Chemistry*, 70:1129–1143, 1998.

[118] Heinz Wolf, Dagmar Assmann, and Eckhard Fischer. Pulvomycin, an inhibitor of protein biosynthesis preventing ternary complex formation between elongation factor Tu, GTP and aminoacyl-tRNA. *Proceedings of the National Academy of Sciences of the United States of America*, 75:5324–5328, 1978.

[119] Anne-Marie Zuurmond, Lian N. Olsthoorn-Tieleman, J. Martien de Graaf, Andrea Parmeggiani, and Barend Kraal. Mutant EF-Tu Species Reveal Novel Features of the Enacyloxin IIa Inhibition Mechanism on the Ribosome. *Journal of Molecular Biology*, 294:627–637, 1999.

Conformational Dynamics of the Estrogen Receptor α: Molecular Dynamics Simulations of the Influence of Binding Site Structure on Protein Dynamics. †

† This work was supported by the Danish Natural Science Foundation, the Carlsberg Foundation and the Danish Research Foundation as well as the Interdisciplinary Nanoscience Centre, *i*NANO.

*Leyla Celik,[‡] Julie Davey Dalsgaard Lund,[§] Birgit Schiøtt[‡§]**

[‡]Interdisciplinary Nanoscience Centre (*i*NANO) and the [§]Centre for Insoluble Protein Structures (*in*SPIN), Department of Chemistry, University of Aarhus, DK-8000 Aarhus C, Denmark

*To whom correspondence should be addressed. E-mail: birgit@chem.au.dk, fax: +45 8619 6199, phone: +45 8942 3953.

RECEIVED DATE (to be automatically inserted after your manuscript is accepted if required according to the journal that you are submitting your paper to)

TITLE RUNNING HEAD: *MD Simulations of ERα*

[1]Abbreviations: ER, Estrogen Receptor; hER, human ER; NR, Nuclear Receptor; LBD, Ligand Binding Domain; RAR, retinoic acid receptor; E2, estradiol; copep, co-activator peptide with sequence NAL***LRYLL***D; AF-2, activation function-2; RMSD, root mean square deviation; MD, molecular dynamics; OHT, orto-hydroxytamoxifen; RAL, raloxifen; H, helix; DDE, dichorodiphenyldichloroethylene; DDT, dichlorodiphenyltrichloroethane; PPAR, Peroxisome Proliferator-Activated Receptor; TR, Thyroid Receptor

Abstract: We present 158 ns of unrestrained all-atom molecular dynamics simulations of the human estrogen receptor α (ERα) sampling the conformational changes upon binding of estradiol. The pivotal role of His524 in maintaining the protein structure in the biologically active *agonist* conformation is elucidated. His524 must be protonated on the ε-nitrogen to form a conserved hydrogen bond to the ligand in the active complex. Helices 3 and 11 are held together by a hydrogen bonding network from His524 to Glu339 *via* Glu419 and Lys531, arresting the ligand in the binding pocket and creating the "mouse trap" binding site for helix 12 (H12). The simulations reveal how His524 serves as a communication point between these two events. When the natural ligand is bound His524 is positioned correctly for the hydrogen bond network to be established. H12 is then positioned correctly for interaction with the co-activator peptide leading to the biologically active complex. The conformational dynamics of ERα is further investigated from simulations of *antagonist* and *apo* conformations of the protein. These simulations suggest a likely sequence of events for the transition from the inactive *apo* structure to the transcriptionally active conformation of ERα. Stable conformations are identified where H12 is placed neither in the "mouse trap" nor in the co-activator binding groove, which is the case for antagonist structures of ERα. Finally, the influence of such conformations on the biological function of ER is discussed in relation to the interaction with selective estrogen receptor modulators and endocrine disrupting compounds.

The Estrogen Receptor (ER)[1] is a member of the Nuclear Receptor (NR) superfamily (*1, 2*). These proteins are ligand activated transcription factors involved in a number of biological processes such as homeostasis, lipid metabolism, embryonic development and cell death (*1, 3-7*). Upon dysfunction of NRs, diseases and malfunctions such as obesity, diabetes, infertility and cancer may develop (*4, 5, 8*). The NR family consists of 48 different proteins (*2, 9*), each consisting of three domains (*10*). These are the C-terminal transactivation domain, the central DNA binding domain and the N-terminal ligand binding domain (LBD) where the activation function-2 (AF-2) is positioned. The overall architecture of the LBD is conserved among NRs (*11*), however the selective ligand interaction is entirely due to this domain. Various isoforms of LBDs, all with their own particular ligand specificity, may be found in different tissues and thus provide opportunities for specific medicinal targeting of these. Apart from ligand binding, the LBD domain is involved in receptor dimerization and is additionally crucial for binding of cofactors that are important for correct transcriptional interaction (*3*). Upon activation of the ER a major conformational change takes place where the C-terminal helix, helix 12 (H12), is re-positioned to either cap the ligand binding site, in what has been termed the "mouse trap" (*7*), as for the *agonist* structures, or to reside in the so-called "charge clamp" site (*12*) in the *antagonist* structure. When H12 is positioned in the *agonist* position a co-activator peptide (copep), with a common LxxLL motif (*13*), is bound. These copeps are important for ERα activity since the homo-dimerization of ERα is induced upon coordination (*14*) allowing the transcription to take place. When an antagonist ligand binds in the ligand binding cavity, on the other hand, H12 occupies the surface area where the copep should bind, thus preventing dimerization and transcription from occuring. In this conformation ER instead recruits co-repressor peptides (*15*).

No three dimensional structure has yet been obtained of an entire NR with all domains intact. However, sepearate 3D structures of the DNA binding domain (*16-18*) and the ligand binding domain (*3*) of several human NRs have been solved during the last decade. They reveal that all NR LBDs share an overall common fold that primarily consists of α-helices. The first X-ray structure of the α isoform of

the human ER LBD was solved in 1997 (*19*). Since then, more than 20 different three dimensional protein structures have been solved of the α isoform of the hER LBD. Upon comparison of all three dimensional structures of the LBD of NRs it becomes obvious that (at least) three different structural conformations are found, as displayed in Figure 1 for hERα; an *apo* conformation (*20*) where H12 is extending away from the core of the LBD, an *agonist* conformation (*21*), which becomes the transcriptional active conformation of the protein upon binding of co-activators, and finally an *antagonist* conformation with H12 resting in the co-activator binding pocket (*22*). The *agonist* conformation of NRs always has the same tertiary structure and is often captured with a copep, while several *apo* and *antagonist* conformations are found (*23, 24*). All conformations share a certain similarity of the binding site region composed of amino acids from helices 3, 4, 6, 8 and 11. Three residues are particularly important for ligand binding in ERα, namely Glu353, Arg394 and His524. These are the only amino acids in the binding site with side-chains capable of forming hydrogen bonds to the ligands. Aside from these three residues, the ERα binding site is mostly hydrophobic and is thus appropriate for binding the endogenous steroid ligand, estradiol (E2), Scheme 1. For the larger antagonistic ligands like raloxifen (RAL) and 4-hydroxy-ortotamoxifen (OHT), Asp351 in H3 is well positioned to hydrogen bond to the side-chain of the ligand.

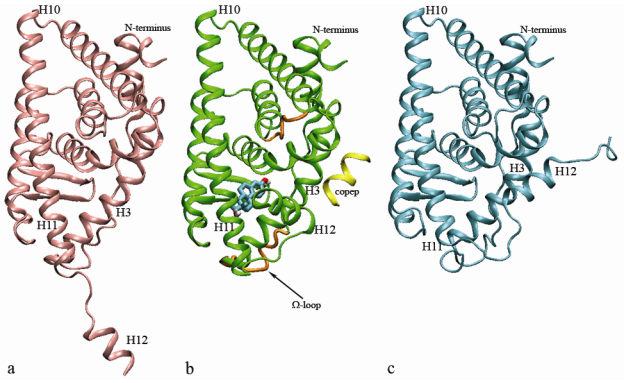

Figure 1: a) Backbone of *apo*- (pink) (*20*), b) *agonist*- (green) with the co-crystallized copep (yellow) and missing loops (orange) included (*21*) and c) *antagonist*- (cyan) (*22*) conformations of hERα, aligned by structure. E2 is shown as liquorice in cyan (C) and red (O). Important helices are labelled.

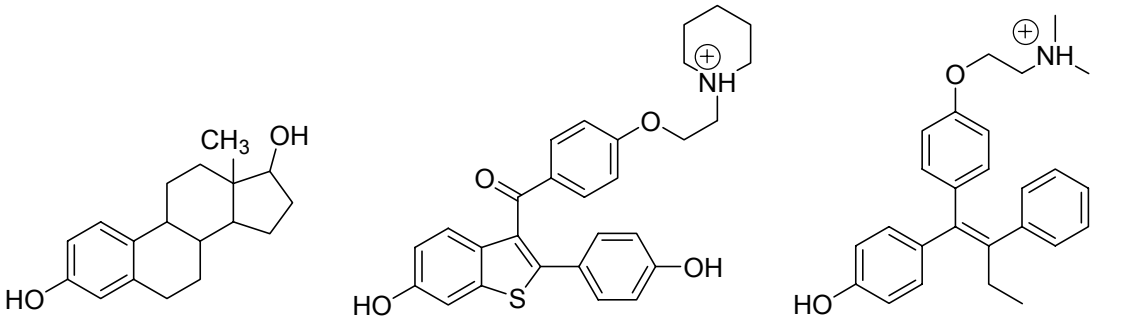

Estradiol, E2 Raloxifen, RAL 4-Hydroxy-tamoxifen, OHT

Scheme 1. Molecular structures of selected ERα ligands.

The major differences between the three conformational states of the ERα LBD are the position of H12, which confer the specific activity, the lengths of H11 and H12 as well as the separation of the N-terminal of H3 and the C-terminal of H11 along with the position of the Ω-loop (*25*). In the *apo* conformation H12 is extended away from the protein and is assumed to be fully solvated in the monomer. In the crystal structure used to model the *apo*-conformation, H12 is interacting with the other monomer of a LBD dimer. However, it serves as a model of an *apo*-conformation of ERα, as it very much resembles known apo structures of other NRs (*12, 20, 26, 27*). H12 is closed over the binding site in the *agonist* conformation, being held in place by what has been termed a "mouse trap" (*27*) thereby assisting in creating a co-activator binding groove between H3, H4 and H12. In the *antagonist* conformation H12 occupies a part of the co-activator binding groove and thus inhibits binding of the copep and as a consequence of that, dimerization and transcription activation are prevailed explaining the antagonism of these ligands.

In 1964, Belleau introduced the concept of macromolecular perturbation theory (*28*) accounting for the unique conformational adaptability of enzymes when interacting with various ligands and he extended the idea to include receptors also. Very recently this concept of a conformational ensemble as a necessity to account for the properties of macromolecules has gained much renewed interest in the study of *eg*. protein folding and function (*29*) as well as for enzyme catalysis (*30-33*). As the different

structures became available for the various NRs, it became evident that a large conformational change must accompany the biological function of this class of proteins, and the concept of a "canonical structure" of the LBD was born (*11*). This model was further developed for ERα by Moras and co-workers (*34*) who proposed a "dynamic model where H12 occupies two more or less favourable states". They termed this a "flip-flop" mechanism for positioning of H12 (*6*) where the equilibrium between ERα conformations with the two positions of H12 (*agonist* or *antagonist*) can be perturbed by point mutations or by the presence of various other compounds, as *eg*. co-factors (*34*). The two possible positions of H12 are guided by specific interactions with the remaining parts of the protein, the "mouse trap" (*11*) when H12 is resting in the agonist position and as the "charge clamp" (*12*) when it resides in the co-activator groove as for the antagonist structures. This "charge clamp" is slightly different than when acting on the copep, which is partially held tight by interaction with a residue within H12, namely Glu542. Instead His373 in the N-terminal of H4 interacts with Tyr537 in H12 in the *antagonist* structure (*22*). Moras and co-workers presented a proposal for the sequence of events during activation of ERα (*23*) where ligand binding to the *apo* conformation precedes any conformational changes of the protein. The opposite sequence of events was recently presented by Norman *et al*. (*35*); in their receptor ensemble model a rapid dynamic equilibrium between the three ERα conformations exists. They suggest that each receptor conformer preferentially can bind different ligands – meaning that ligand binding and any selectivity is determined by the conformation of the protein. No effort was presented in any of these papers to account for the binding of copep, as to whether it precedes ligand binding and the conformational changes or not.

The sequence of events, ligand binding, conformational change and cofactor binding, accompanying ERα activation has not yet been fully established. Much discussion, however, is currently ongoing in the literature with respect to allosteric control of ERα – how is the information regarding the type of ligand bound in the ligand binding cavity communicated to the transcriptional machinery of ERα (*7, 36-39*)? Is it imperative that the specific ligand bound to the protein is somehow connected to the

recruitment of cofactors or *vice versa*. However, the means of the actual coupling is still poorly understood (*37*). It has become evident that amino acid residues also distant from the ligand binding cavity are involved in an allosteric network that links the functional surface of NRs to the presence of a ligand in the ligand binding cavity (*36, 37, 39*).

Rapidly increasing scientific evidence suggests that a variety of chemicals released to the environment are xenoestrogens. Termed endocrine disrupting compounds (EDCs) (*40*), they can interfere with hormonally regulated biological processes, as in the transcription mediated by ER (*41-47*). EDCs comes from many different sources such as natural products, various pesticides, pharmaceuticals and other industrial compounds (*41, 46*). Recent research has focused on developing analytical techniques for identifying any endocrine action of an environmental sample (*40*) or to predict eventual risks from computer studies (*48*). It has been shown that some pesticides give rise to an agonistic behaviour of ER, others leads to antagonistic responses (*49, 50*), whereas some, including DDE (a metabolite of the pesticide DDT), recognizes neither co-activators nor co-regulators related to these classical responses, rather they adjoin different regulator peptides (*51*). This finding was interpreted as these compounds can induce yet another conformation of ER with different surface properties and thus interfering in the transcriptional process in a different manner, further supporting the ideas of a ligand sensitive conformational equilibrium between the different conformations of ERα (*52*) and indicating that (weak) binding of EDCs may be sufficient to disturb the position of this very delicate conformational equilibrium of ER. Very little detailed information on how all these events are controlled at the molecular level are available, and the dynamic parts of the protein machinery are not fully understood.

Even though the atomic structure of ERα has been known since 1997 (*19*) very little effort has been assigned to modelling the conformational changes that are so evident from a simple inspection of the static structures. The sequence in which these events occur for ER has, to the best of our knowledge, neither been targeted through dynamic studies (*eg*. NMR) nor by computer simulations. For the retinoic acid receptor (RAR) a simulation of the *agonist* to *apo* conformational change has been published

suggesting that the ligand dissociation is connected with minor conformational changes of H12 (*53*). From simulations of RAR and the thyroid receptor (TR) three ligand binding/unbinding pathways have been observed (*53-56*). These four studies revealed that the identified pathway depends on the set-up of the simulation, on the actual NR and on whether mutations are present in the starting structure as well as the structure of the ligand. Nonetheless, some overlap between the proposed pathways was found. It is obvious that the sequence of events and the actual pathways may not be directly transferable between different NRs. Importantly; none of these simulations included the copep in the set-up, which may obstruct some of the observed escape routes. However, the results are very promising in showing how MD simulations can help in disentangling reaction sequences and reveal the dynamics of larger conformational changes of proteins. In recent years MD simulation has proved to be a valuable tool for studying the dynamic behaviour of macromolecular systems (*57-60*), and the method is complementary to static X-ray diffraction methods. Especially for elucidation of the dynamic pathways of biological transport mechanisms (*61-65*) and conformational changes (*29, 66, 67*) MD techniques has recently been very successful in providing additional knowledge of such complicated biochemical reactions.

In this paper we present the results of a total of 158 ns unrestrained all-atom MD simulations of the hERα LBD. The focus will first be on describing the binding of the endogenous ligand, E2, with respect to the preferred tautomer of His524 in the *agonist* conformation of hERα and the influence of the copep on this binding. To the best of our knowledge, this is the first time that the copep has been included in simulations of a NR. Then, the conformational changes of the LBD will be examined from several long time MD simulations of the *apo* and the *agonist* conformations with and without ligand and copep present. The putative switching, or "flip-flop" mechanism (*6, 23, 34, 51, 52*) of H12 between either covering the ligand binding pocket, as caught in the "mouse trap", or resting in the co-regulator binding groove is also examined by MD simulations of the *antagonist* conformation. From the simulations, we propose a likely sequence of the events, ligand binding, copep binding and conformational changes of H12, required for formation of a transcriptional active complex and we will discuss the proposed

agonist to *antagonist* conformational changes. We present a likely allosteric mechanism for linking the two focal points for hERα activation, namely ligand binding and positioning of H12, and we also present results that shed light on the pivotal role of His524 for ligand binding and activation of hERα.

Materials and Methods

The *apo* and *agonist* conformations of hERα LBD with co-crystallized E2 and the *antagonist* conformation with co-crystallized OHT were chosen as the starting protein structures. Atomic coordinates were taken from the Protein Data Bank (*68*), entries 1A52 as a model for the *apo*-conformation (*20*), 1GWR (*agonist*) (*21*) and 3ERT (*antagonist*) (*22),* respectively. The proteins contain 238 (*apo*), 243 (*agonist*) and 246 (*antagonist*) amino acid residues in the modeled monomer, all starting from Leu306. The co-crystallized copep, sequence NAL***LRYLL***D in the *agonist* structure, 1GWR, was used in the simulations of the *apo* conformation with a copep present. The residues are numbered 1-9. The termini were modeled as charged.

Coordinates for backbone atoms in two loops, between H2 and H3 and between H8 and H9, were missing in the *agonist* conformation. These were modelled by including coordinates for residues 331-339 and 461-465 from pdb-code 1A52 into the *agonist* protein structure. These residues later underwent special treatment during minimization of the system. Several residues in the three conformations were solved to multiple positions in the X-ray structure and their treatment is included in the Supporting Information. Coordinates for missing amino acid side chains and hydrogen atoms were reconstructed with the psfgen structure builder module of NAMD (*69*) and by use of the CHARMM27 force field (*70*). The system was solvated in a pre-equilibrated water box using the solvate plug-in in VMD and extending 10 Å beyond the protein. The TIP3P water model was used (*71*). This solvation resulted in systems with overall sizes of approximately 80 x 100 x 60 $Å^3$ (*apo*), 80 x 80 x 60 $Å^3$ (*agonist*) and 80 x 80 x 80 $Å^3$ (*antagonist*) and contained approximately 40,000 (*apo* and *antagonist*) and 30,000 (*agonist*) atoms. All crystal water molecules were kept in the simulations.

Amino Acid Protonation States. There are 13 histidine residues in the hERα LBD. One of these,

His524, is positioned in the binding pocket and hydrogen bonds the ligand; and is thus important for appropriate ligand binding. In all X-ray *agonist* structures of the hERα LBD His524(Nδ) is pointing towards E2(O17) (see Scheme 2 for numbering of atoms) indicating a preferred binding mode. However, since hydrogen atom positions can normally not be determined by X-ray crystallography there is no direct evidence of the protonation state of His524. It is therefore not straight forward to decide whether His524 or the ligand acts as the hydrogen bond donor respectively acceptor, since both can act as such depending on the His524 protonation state and the orientation of the E2 hydroxyl-group. To study this issue, simulations were set up with all three tautomers of His524 for each of the models studied. Other histidine residues were modelled according to their local environment (see the Supporting Information for details) while all Arg, Lys, Asp and Glu residues were modelled charged and tyrosines neutral. By changing the protonation state of His356 in H4, which is distant from the binding site and surface exposed, at the same time as that of His524, the system is kept neutral in all set-ups.

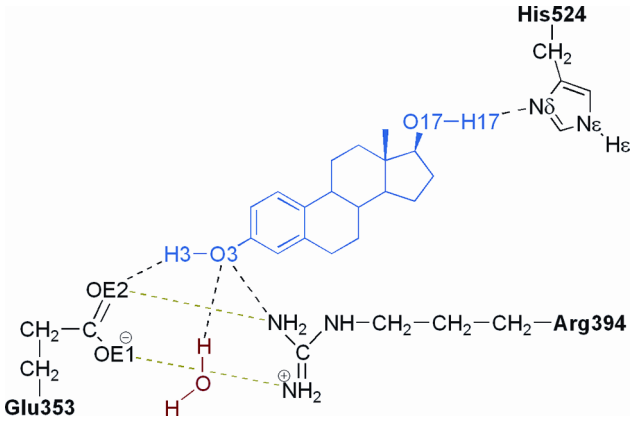

Scheme 2. Coordinaton of E2 in the ligand binding cavity. Important atoms in E2 (in blue) and the surrounding residues are labeled. His524 is drawn as the ε-tautomer, in the δ-tautomer the proton would be located on Nδ (denoted Hδ) while the histidinium ion includes both hydrogen atoms and a delocalized positive charge. A crystallized water molecule (in red) in the binding site interacts with E2.

Modelling Estradiol. Force field parameters to model estradiol were extracted from the CHARMM27 force field (*70*) and supplemented by parameters from a very recent simulation including cholesterol for the steroid skeleton (*72*) as well as Accelrys-CHARMm parameters as included in Quanta 2000 (*73*).

Partial charges for E2 were calculated with VCharge (*74*) by equalization of electronegativity. This method has recently been shown to give charges very similar to those in the CHARMM force field (*74*). Partial charges and added parameters for force constants and van der Waals terms are tabulated in the Supporting Information. The initial structure of E2 was extracted from the pdb file of the *agonist* structure (*21*) and used in all the *agonist* and *antagonist* simulations. Since E2 is not naturally found in the *antagonist* conformation it was manually positioned with the steroid A-ring on top of the phenol-ring of the co-crystallized OHT positioning the E2(O3)-hydroxyl group to hydrogen bond with Glu353 and Arg394. In the *apo* simulations the co-crystallised E2 from pdb-code 1A52 (*20*) was used.

Minimization. The solvated systems were minimized with NAMD (*69*) using the Conjugate Gradient algorithm twice for 2500 minimization iterations to remove steric strain introduced when adding hydrogen atoms and missing sidechain atoms. During the initial 2500 minimization steps, only hydrogens were allowed to move while all heteroatoms were kept fixed. In the second set of minimization, heteroatoms were restrained in a harmonic potential with a force constant of 0.5 kcal/(mol·Å^2). All atoms in the two loops that originally were missing coordinates in the *agonist* pdb-structure were allowed to move freely during both sets of minimizations.

Molecular Dynamics Simulations. All simulations were performed using the CHARMM27 force field (*70*) with the added parameters for E2 by use of the MD program NAMD 2.5 (*69*) on 32 processors. The MD simulations were performed in the NPT ensemble with periodic boundary conditions. For full employment of electrostatics, the particle mesh Ewald method (*75*) was used while Van der Waals interactions were accounted for to a cut-off distance of 12 Å and gradually dampened by use of a switching function from 10 Å. Langevin dynamics with a damping constant of 0.1 ps^{-1} was included to achieve constant temperature while the atmospheric pressure was realized with the Langevin piston method implemented in NAMD (*76*). A total of 10 different set-ups, models **1-10**, of the system were investigated, see Table 1 for details. Three simulations were run for each model to account for the three possible tautomers of His524, labelled *eg*. for model **1** as **1D**, **1E** and **1P**, for δ-protonation, ε-

protonation and positive histidinium, respectively, resulting in a total of 30 simulations. All simulations were carried out for at least 5 ns using 1 fs time step, structures for analysis were saved every 500 fs.

Table 1. The Ten hERα Models with Information About the Initial Conformation of the Protein, the Presence of E2 and a Co-Activator Peptide. The Purpose of Studying Each Model is Listed

	Initial conformation	Ligand	Co-activator peptide	To study
1	*Agonist*	E2	NAL***LRYLL***D	E2 binding in biologically relevant form; evaluate His524 protonation
2	*Agonist*	E2	None	The influence on E2 binding in the absence of copep
3	*Agonist*	None	None	The stability of *agonist* conformation of the protein without E2.
4	*Agonist*	None	NAL***LRYLL***D	The stability of *agonist* conformation without E2 but in the presence of copep.
5	*Antagonist*	E2	None	*Antagonist* conformation with E2.
6[a]	*Antagonist*	E2	None	*Antagonist* conformation with E2 at higher temperature.
7[b]	*Apo*	E2	None	Stability of the *apo* conformation with E2 bound.
8	*Apo*	E2	NAL***LRYLL***D	The influence of copep on *apo* conformation with E2 bound.
9	*Apo*	None	None	The stability of the *apo* conformation, only protein.
10[c]	*Apo*	None	NAL***LRYLL***D	The stability of the *apo* conformation, including copep.

[a] Models **6** are simulated at 400 K; [b] Model **7E** is simulated for 12 ns; [c] Model **10P** is simulated for 6 ns.

Data Analysis. Analyses of the computed trajectories were performed with VMD 1.8.3 (*77*) and the

included Tcl-scripting facility. All molecular figures were drawn in VMD. The root-mean-square-deviation (RMSD) of protein Cα atoms in each simulation was calculated with respect to the initial minimized structure. To measure the length of H11, backbone N···O distances from residues n to (n+4) are measured. If this distance is less than 3.5 Å the (n+4) residue is supposed to be included in H11. This is slightly longer than a normal hydrogen bond distance of approximately 3 Å (*78*) and is included to allow for "breathing" in the helix.

Results and Discussion.

We first set up systems to study the hERα *agonist* conformation with bound E2. Models **1** and **2** investigate the stability of this conformation and the influence of the copep on the binding of the natural ligand. Model **1** represents the functional biological form of the receptor; it can therefore be used to imply whether the applied protocol for modelling is reliable. Model **2** examines the binding of E2 in the absence of copep, whereas model **3** was included to evaluate the stability of un-liganded hERα in the *agonist* conformation. The influence of the bound copep is studied in models **1** and **4** for the *agonist* conformation where simulations with copep are done in the presence or absence of E2, respectively. Furthermore we set up simulations that were likely to result in conformational changes; the intention being to construct some of the protein-ligand complexes proposed to be involved in the mechanism of the structural transition from the transcriptionally inactive *apo* form to the active *agonist* form with ligand and copep bound (*23*). Models **5**-**10** are constructed to evaluate exactly such conformational changes. The two first sets, models **5** and **6**, investigate the dynamics of the *antagonist* form when it is bound to E2 at different temperatures. With this set-up one may then expect to observe a conformational change from the *antagonist* form to either the *apo* or *agonist* conformation. Such a mechanism has been proposed by Moras and co-workers (*11, 23*) and Shiau *et al*. (*52*) and has been further interpreted as a "switching mechanism of H12 between capping the ligand binding cavity and the co-regulator binding groove", (*51*) very similar to the "flip-flop" mechanism which stated that the two binding sites of H12 have very similar binding energies (*34*). The four next models, **7**-**10**, are simulations of the *apo*

conformation and are included in the study to test the hypothesis that the biological active form of hERα is produced from the *apo* form by binding of E2 and/or copep followed by the conformational changes (*23*) or the *vice-versa* (*35*). In models **8** and **10** the influence of a copep is further studied for the *apo* conformation of the protein and models **3**, **4**, **9** and **10** were included to observe the stability of the ligand binding site of hERα and to evaluate whether the binding cavity of hERα collapses without a bound ligand, similar to what has been described for the retinoid-X receptor α (*24*). It was recently shown that some EDCs recognize another conformation of hERα (*51*), thus it was of great interest to us to test if such (quasi) stable conformations could be identified from the MD simulations.

Conformational stability of simulations. For all simulations, the calculated RMSD for all Cα atoms reaches a stable value after approximately 1 ns. The *agonist* models **1-4** reaches a value of ~1.8-2.0 Å, the *antagonist* models are more dynamic and have RMSD values between 2 and 4 Å and the *apo* models show even more movement levelling out at 2-5 Å, see Figure 2. Initially this may indicate unstable simulations of the *antagonist* and *apo* models but since these calculations were set up to investigate conformational changes of especially H12 it is not surprising to get such rather high RMSDs. Therefore, another set of RMSD curves were calculated including only Cα atoms in residues 306 to 527, these curves are displayed in Figure 3 for *antagonist* and *apo* models. In this way, the last coil of H11, the loop H11-H12 and H12 itself are not included in the RMSD calculation and thus only the stability of the LBD core of hERα is calculated. Using this scheme, simulations of models **5** and **7-10** gave RMSD values of approximately 1.8-2.0 Å, similar to what is found for the whole protein in the *agonist* conformation. The RMSD value for model **6,** which was run at the higher temperature of 400 K, is logically somewhat higher and levels out at 2.5-3.0 Å.

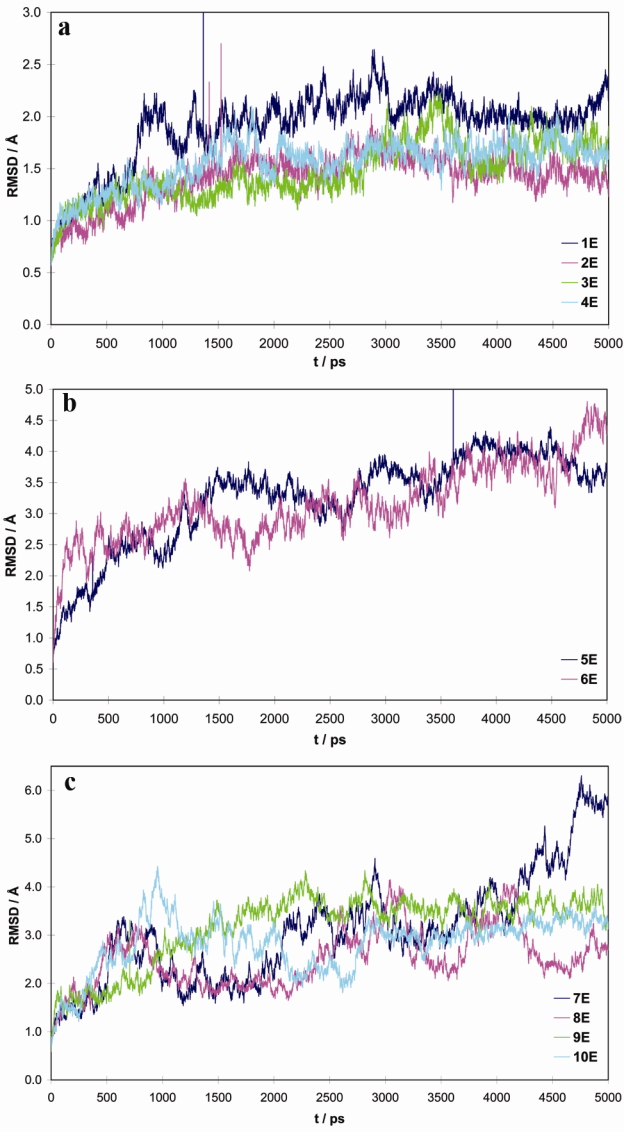

Figure 2: RMSD of Cα atoms of the hERα LBD throughout simulations for: a) *agonist* models **1-4**, b) *antagonist* models **5-6** and c) *apo* models **7-10**, all with His524 protonated on Nε. Data for Nδ and histidinium protonation of His524 can be found in the Supporting Information.

These results show that the dynamics are mostly associated with the H11-H12 region for the simulations of *antagonist* and *apo* models. The RMSD of the *agonist* model **1-4** did not change when excluding the C-terminal residues, showing that all *agonist* simulations are carried out on stable structures, also in the absence of ligand E2 and/or the copep. It can thus be concluded, that equilibrated systems are obtained after approximately 1 ns in all models.

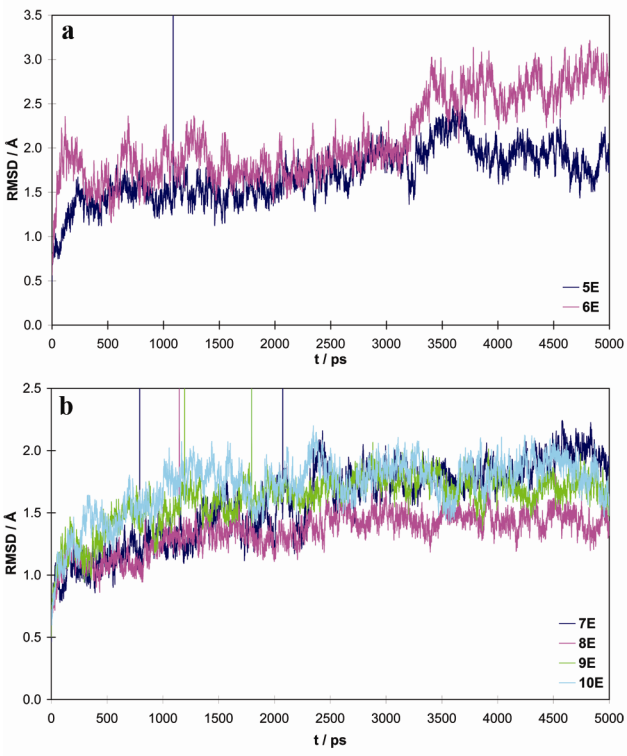

Figure 3: RMSD for hERα Cα atoms in the LBD core during simulations for a) *antagonist* models **5-6** and b) *apo* models **7-10**. All figures have His524 in the ε-protonated tautomer. Plots with the two other tautomers are found in the Supporting Information.

Hydrogen Bonds to Glu353 and Arg394. X-ray structures of hERα indicate the presence of hydrogen bonds between E2(O3) (see Scheme 2 for numbering of atoms) and the side chains of two residues, namely Glu353 and Arg394 in the binding site. In the X-ray structures a water molecule is similarly responsible for yet another stabilizing hydrogen bond between E2 and the protein. During the extent of all the present simulations a hydrogen bond can be identified to one of the carboxylic oxygen atoms of Glu353, most often to Glu353(OE2), that is positioned closest to E2 in the *agonist* and *apo* X-ray structures. A rotation of the sidechain is possible and results in hydrogen bonding the Glu353(OE1) instead. A direct hydrogen bond to Arg394, on the other hand, is not present in the simulations evidenced from average distances between E2(O3) and the two terminal nitrogen atoms of Arg394 of more than 4.2 Å. Rather, the Arg394 sidechain moves slightly to form two ionic hydrogen bonds to Glu353. In NRs with a keto-functionality on the A-ring of the steroid ligand, Glu353 is replaced by a

glutamine residue thereby favoring hydrogen bonds from both residues to the ligand while the hERα system is stabilized by the interactions of the formal charges at residues Glu353 and Arg394. In Figure 4, the resulting hydrogen bond network between E2(O3), Glu353, Arg394, His524 and a binding site water molecule is displayed.

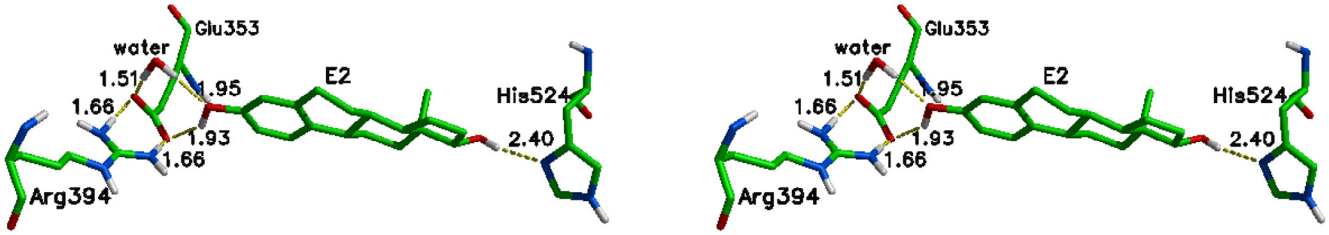

Figure 4: Stereo view of E2 in the binding site of hERα (snapshot of model **1E** at 1.5 ns) with Glu353, Arg394 and His524. A structural water molecule is present that further links E2 and Glu353. Average distances between interacting heteroatoms are listed in Ångstrøm.

Agonist conformation. The binding of E2 in the biologically active transcription complex of hERα with a bound copep is studied in model **1**. Three simulations were carried out to elucidate the likely protonation state of His524, models **1D**, **1E** and **1P** respectively. Based on X-ray structures (*19, 21, 22, 34, 79, 80*), it is believed that there is a hydrogen bond between His524(Nδ) and E2(O17). However, with X-ray diffraction techniques it is normally not possible to refine the hydrogen atom positions in protein crystals; therefore all three possibilities are explored in this study. Recently, we have shown that MD simulation is a suitable tool for assigning the protonation state of important residues in protein···ligand complexes (*81, 82*). Similar methodology is applied here focusing on identifying the tautomer of His524 that gives rise to the most stable hydrogen bonding pattern.

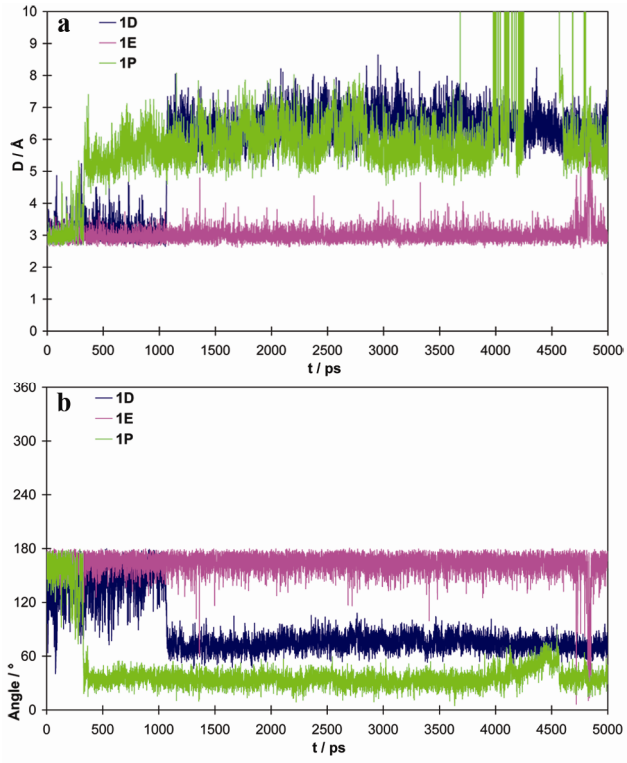

Figure 5. a) Hydrogen bond distance E2(O17)···His524(Nδ) in models **1D**, **1E**, and **1P** and b) the corresponding E2(O17)···H···His524(Nδ) angles. For **1D** H = Hδ, for **1E** and **1P** H = H17

In Figure 5 plots of the distance between His524(Nδ) and E2(O17) and the corresponding hydrogen bond angle are displayed for the three simulations of model **1**. It is apparent that only model **1E,** with the ε-protonated His524, has the hydrogen bond between E2(O17) and His524(Nδ) conserved throughout the simulation. This means that estradiol is the hydrogen bond donor and His524 is the hydrogen bond acceptor. Also the angle for the hydrogen bond is stable, with an average of 163° ± 12°. Neither δ-protonation nor the histidinium tautomer of His524 is able to retain the conserved hydrogen bond throughout the simulation. These two tautomers of His524 rotate after approximately 1 ns so the histidine ring system becomes almost perpendicular to the E2 D-ring with E2(O17)···His524(Nδ) and E2(O17)···His524(Nε) distances of 6-8 Å, too long for a hydrogen bond to form.

From the X-ray experiments it is suggested that His524 is placed in a rather shallow potential on the energy surface, as it occupies only one position and has normal B-factors. The average dihedral angles for the side chain of this amino acid is experimentally found to be a *gauche* conformation for χ1 (C-Cα-

Cβ-Cγ), measuring 45-60°, and a –*gauche* conformation for χ2 (Cα-Cβ-Cγ-Nδ) between -70° and -90°. The distribution in the two dihedral angles as a function of time is depicted in Figure 6 for the MD simulations of models **1**. Again, it is obvious from the curves, that only an ε-protonated His524 gives a dihedral angle distribution that is in accordance with the experimentally observed numbers, hence the simulations of models **1** support that His524 is ε-protonated and functions as a hydrogen bond acceptor whereas the ligand is the hydrogen bond donor.

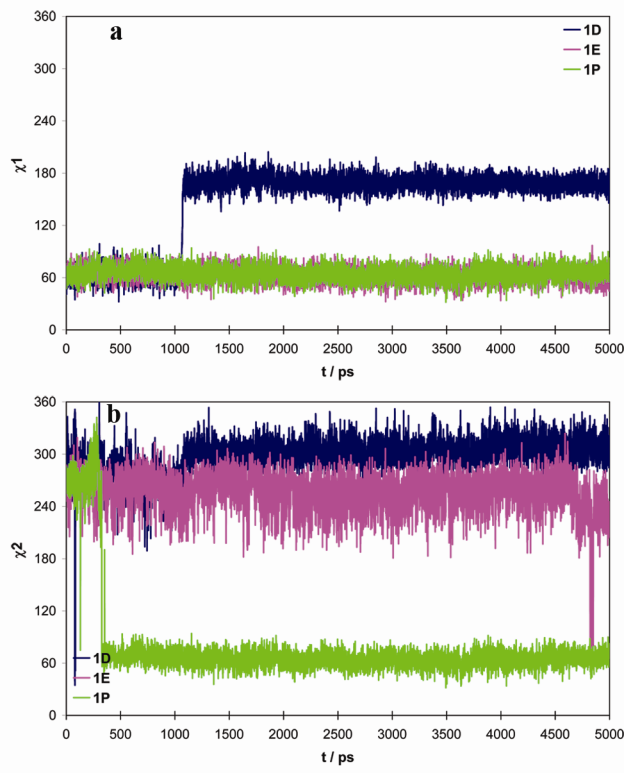

Figure 6. Variation in the dihedral angles of the sidechain of His524 in simulation **1E** (magenta), **1D** (blue) and **1P** (green), a) χ_1 and b) χ_2.

During the three simulations of model **1,** H1, which has been proposed to function as a lid of the ligand binding cavity, is held in the agonist position by the "mouse trap" mechanism. H12 is positioned in the groove between H3, H4 and H11, and is mainly held tight by hydrophobic interactions. The binding of the copep is also stable in all model **1** simulations. The copep is positioned in a shallow hydrophobic groove between H3, H4 and H12 and held in place by the so-called "charge clamp" made from Lys362 in H3 and Glu542 in H12 (*3, 19*). The former is coordinated through the 3 hydrogen atoms

at Lys362(NZ) forming hydrogen bonds with Leu7(O), Tyr6(O) and Asp9(OD2) of the copep in a nice tetrahedral manner whereas Glu542 interacts with Ala2(NH) and Leu3(NH). The LxxLL motif of the copep is made up by Leu4 to Leu8. These findings suggests that, on this time-scale, the finer details in the ligand binding cavity, as expressed in the three set-ups of model **1**, do not influence surface properties as judged by the binding of H12 and copep.

Based on a triple Cys → Ser mutation study of ERα, Moras *et al*. (*34*) proposed that the biologically active *agonist* conformation is partly stabilized by the presence of a conserved hydrogen bonding network "zipping" H3 and H11 together, originating at the His524 side-chain in the ligand binding pocket and terminating at Lys531 in the C-terminal of H11 and Glu339 in the N-terminal of H3 *via* Glu419. We have analyzed the presence of such a network with respect to the selection of tautomer for His524. The computed frequencies for formation of the hydrogen bonds involved in the "zipper" are listed in the Supporting Information. In model **1E** this hydrogen bonding network is indeed present throughout the simulation (Figure 7) whereas it is formed much less frequently in **1D** and **1P**. In conclusion, model **1E** must be a reliable set-up for the biological active structure of hERα, as all experimental data available are nicely reproduced in this model, and we conclude that the present MD simulation protocol represents an appropriate method for studying this system.

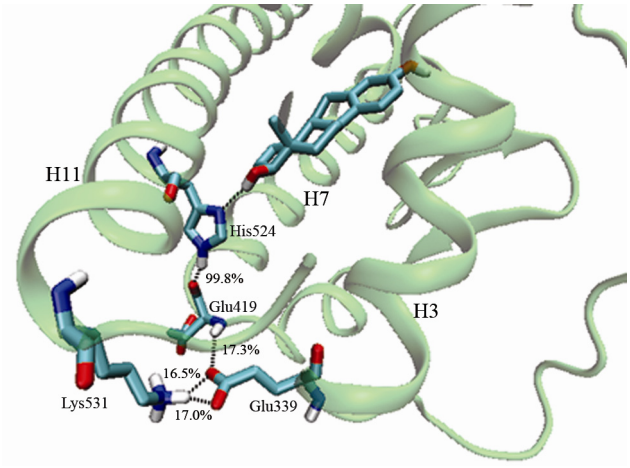

Figure 7. Snapshot of model **1E** at 1.5 ns showing the binding of E2 along with the residues in the hydrogen bond zipper. Numbers are included for presence of each hydrogen bond during the trajectory.

We next moved to study the *agonist* complex, where E2 is bound and H12 is capping the ligand binding site**,** but without the copep, models **2**. These simulations will reveal the influence of a copep on the stability and dynamic properties of the system upon comparison with models **1**. Focusing first on the interaction of E2(O17) with His524, the three simulations, **2D**, **2E** and **2P**, reveal that the hydrogen bond E2(O17)···His524(Nδ) can be maintained for both of the neutral tautomers of His524. The curves are shown in Figure 8 for the E2(O17)···His524(Nδ) distance and the corresponding bond angle.

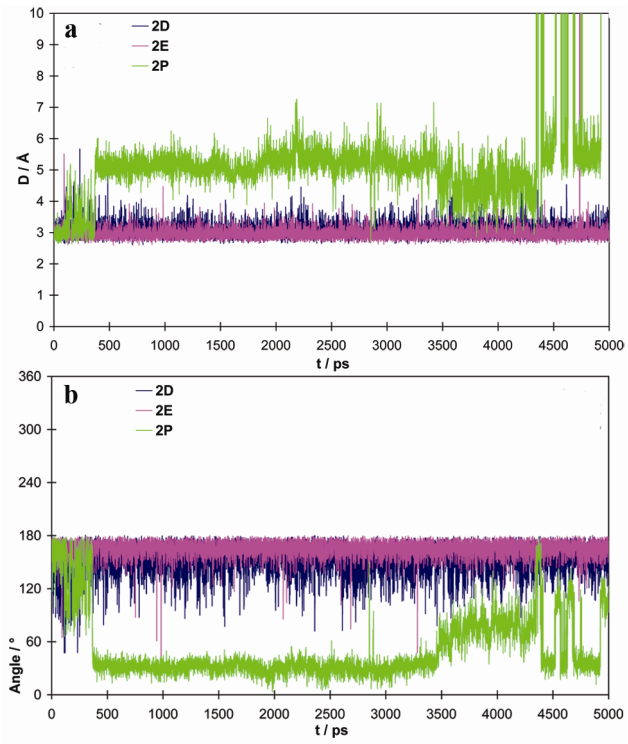

Figure 8. Time dependence of a) hydrogen bond distance E2(O17)···His524(Nδ) in models **2D**, **2E**, and **2P**; b) the corresponding E2(O17)···H···His524(Nδ) angle. For **2D** H = Hδ, for **2E** and **2P** H = H17.

Without the copep bound to the complex, more flexibility in the protonation of His524 seems to be possible since both model **2D** and **2E** show a conserved hydrogen bond from E2(O17) to His524(Nδ) throughout the simulation. In model **2E** the distance E2(O17)···His524(Nδ) is 2.96 ± 0.17 Å and the angle E2(O17)···H···His524(Nδ) is 165.1° ± 8.9°. The same geometric properties for model **2D** are 3.08 ± 0.23 Å and 153.4° ± 16.5°, respectively. Again, a protonated His524 is not suitable for conserving this hydrogen bond, as the residue rotates. In model **2D** a rotation around the E2(O17) hydroxyl bond has

taken place, so E2 is now the hydrogen bond acceptor and His(Nδ) is the hydrogen bond donor. An additional long hydrogen bond, 3.69 ± 0.44 Å, between E2(O17) and Gly521(O) were found to further stabilize this model. This is similar to what has been proposed for binding of E2 in ERβ (*52*). With respect to the hydrogen bonding network originating at His524 it is conserved in model **2E** with numbers of hydrogen bonds present very similar or slightly larger than found for **1E**. In model **2D,** on the other hand, only the distance from His524(Nε) to Glu419(O) remains below the limiting 4.0 Å, with an average of 3.87 ± 0.75 Å. This must be a very unfavourable situation due to the lack of an intermediate hydrogen atom, and we thus expect model **2D** to be unlikely on this basis. The rest of the hydrogen bonds are lost very early in the simulation of model **2D**. However, no further conformational consequence of this "un-zipping" of H3 and H11 can be detected, as the length of H11 is conserved, and terminates at Asn532 in all set-ups (Computed frequencies for the α-helical length of H11 are listed in the Supporting Information). This suggests that once H12 is placed in the "mouse trap" position, it is firmly bound and even the un-zipping of H3 and H11 does not influence the binding of H12 on this time scale.

The simulated trajectories of models **3** and **4**, both without E2, reveal that the protein is stable on a nanosecond timescale in the *agonist* fold with neither copep nor the ligand bound (models **3**) as well as in a set-up including copep but without ligand (models **4**). In model **4D** the length of H11 is slightly shortened indicating that the presence of the copep can induce some changes in the finer details of the conformation. This effect is not seen for other tautomers of His524, nor in any set-up in model **3**. Since the ligand binding cavity is empty in models **3** and **4**, His524 is not anchored to the ligand. In these simulations rotation of His524 is observed changing from -*gauche* for χ_2, which is found in *agonist* protein crystal structures. Instead both χ_1 and χ_2 are in the +*gauche* conformation. After ~1.5 ns of simulation in model **4D** both χ_1 and χ_2 dihedral angles shifts to the –*gauche* conformation still unlike the experimentally observed conformations. This is additionally revealed in the computed number of possible interactions between His524 and Glu419(O) where it is evident that His524 is flexible in the

absence of copep, models **3**. Inclusion of a copep in the simulations of model **4E** and **4P** result in a completely locked orientation of His524. Accompanying this freezing out of any rotation of His524 is the observation that the hydrogen bonding network is re-established, zipping H3 and H11 together in model **4E** only, showing how the presence of a copep is communicated to the ligand binding cavity through the conservation of this hydrogen bonding network and arresting His524 in an orientation set up for interaction with E2 once it is present in the ligand binding cavity.

Antagonist Conformation. In model **5** and **6** we examine the dynamical behaviour of a mismatched complex between an *antagonist* conformation of the protein, with H12 resting in the co-activator binding groove, and an agonist ligand, E2, in the ligand binding cavity. According to the "flip-flop" mechanism this situation should lead to a rearranged structure. Therefore, by running MD simulations on this unfavourable complex the idea was to stimulate the conformational changes to proceed. As for the *agonist* models discussed above, the first structural feature to look for is the presence of a hydrogen bond from E2(O17) to His524. The hydrogen bond was not found for extended periods of time in any of the three examined tautomers of models **5** and **6** during the 5 ns simulations. Another possibility would be a hydrogen bond to His524(Nε), but further analysis revealed this distance to be constantly larger than 5 Å for all models thus precluding this hydrogen bond to form.

In *antagonist* protein structures (*22, 34, 83, 84*) His524 is rotated compared to the *agonist* structure which explains the lack of formation of this hydrogen bond. We speculate that as a consequence of the rotation of His524 an unleashing of the hydrogen bond network zipping H3 and H11 together is taking place. Indeed, the simulations reveal that in neither of the set-ups, is the network starting to form and Glu339 and Lys531 are positioned to far away from each other to interact. This set of simulations therefore indicates that a direct equilibrium between the *agonist* and *antagonist* conformations may not be so likely. The very dynamic appearance of the binding site is not due to a simple continuous rotation of the His524 side chain as both χ_1 and χ_2 are alternating stable in either +*gauche*, -*gauche* or *anti* conformations. The dynamic behaviour is also due to movements of the backbone of H11 and the

ligand. Upon heating to 400 K, models **6**, the protein is more dynamic. Specifically, in model **6P** it is noted that H12 is slightly released from the co-activator binding groove. At the same time the small kink between H10 and H11 becomes more pronounced, and the two helices becomes almost perpendicular to one another. As a consequence, His524, which is located in the N-terminus of H11 near the kink, becomes surface exposed. These features will be further studied for mechanistic relevance.

Apo Conformation: We next set up models to study the dynamic behaviour of the *apo*-conformation of hERα. The influence of binding of E2 and copep is studied systematically in the four models, **7-10**, in order to obtain more information about the reaction sequence for binding of E2, copep and the conformational changes observed of hERα. The binary *apo* complex with E2 bound, models **7**, reveal that the dynamic behaviour of H12 is dependent of the chosen tautomer of His524. A new stable conformation is found in model **7D** that is stable for the last 3 ns of the dynamics. In this alternative structure the hydrogen bond between His524(Nδ) and E2(O17) reforms after approximately 2.0 ns. It was present in the very beginning of the simulation, but when H12 started to move after approximately 0.5 ns, the hydrogen bond broke and did not reform before the stable alternative position of H12 was re-established, Figure 9.

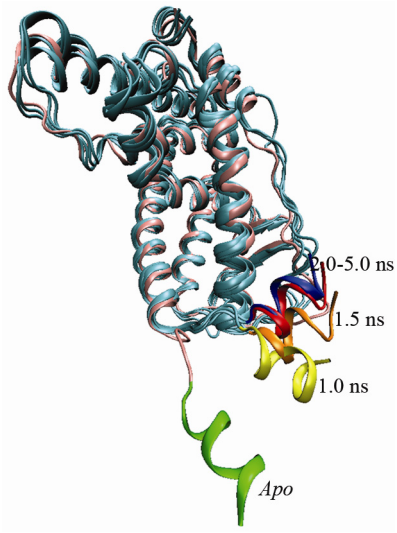

Figure 9. Overlay of snapshots of the conformational dynamics of model **7D**. The X-ray structure (1A52) is shown in pink with H12 in green. For the snapshots the core of the protein is depicted in cyan

while H12 is yellow after 1 ns, orange after 1.5 ns, red after 2.0 ns and blue after 5.0 ns.

Figure 10a shows the distance between E2(O17) and His524(Nδ) as a function of simulation time for models **7**. By following the dihedral angles of His524 in model **7D** it is found that the hydrogen bond breaks due to a rotation of χ_2 from a *–gauche* conformation to a *+gauche* conformation which changes back to *–gauche* as the hydrogen bond reforms (Figure 10b). Due to a lack of a hydrogen atom on His524(Nε) the hydrogen bond network from His524 to Glu339 can not be fully formed throughout the **7D** simulation but there are conserved hydrogen bonds between Lys531(NZ) and both carboxyl oxygens on Glu339 serving to keep H3 and H11 tied together. In accordance with this, it is found that H11 is not unwinding in this new alternative conformation. The binding of H12 to the core of the hERα LBD in the alternative conformation is firm based on the long stability of the conformation and on computed RMSD values between snapshots taken between 2 and 5 ns of approximately 1.2 Å.

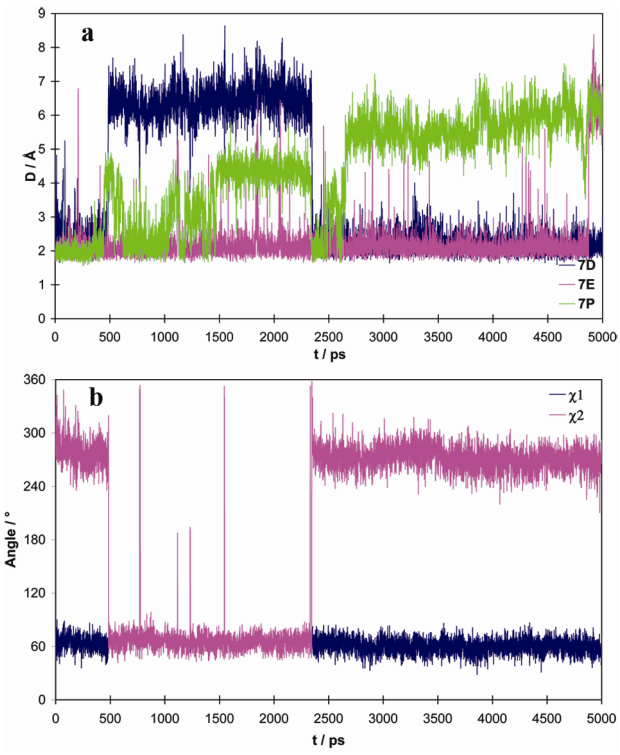

Figure 10. Time dependence of a) the distance between E2(O17) and His524(Nδ) and b) χ_1 and χ_2 in model **7D.**

In model **7E** H12 is solvent exposed during the first nanoseconds of the simulations. After 5.0 ns

snapshots indicate that H12 may be moving towards the "charge clamp" position in the co-activator binding site. Due to the possibility of a conformational change towards the *antagonist* conformation, the **7E** simulation was continued to 12 ns. However, instead of approaching the *antagonist* conformation further, the orientation of H12 once again shifted. The N-terminal of H12 is kept relatively at the same point in space while the C-terminal moves. This leads to a position after 7.5-8.0 ns which resemble the *agonist* structure. The E2(O17)···His524(Nδ) hydrogen bond is disrupted after around 4.8 ns of dynamics but is reformed for brief periods later in the simulation (6.8-7.4 ns and 11-12 ns). After approximately 9 ns the otherwise conserved hydrogen bond to Glu353 disappears and H12 is again fully flexible.

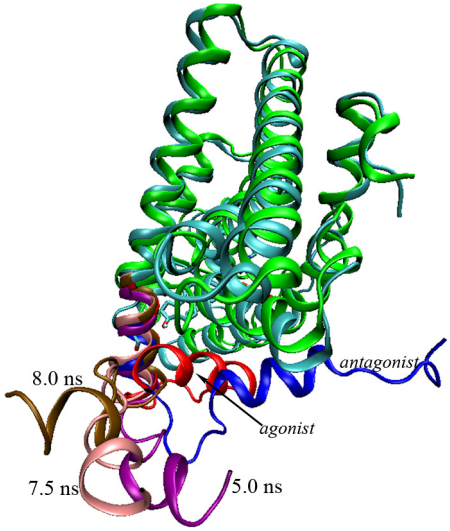

Figure 11. Snapshots from the simulation of model **7E** at 5.0 ns (H11-H12 in purple), 7.5 ns (H11-H12 in pink) and 8.0 ns (residues 306 to 520 in cyan and H11-H12 in brown). Also included is *agonist* (H11-H12 in red) and *antagonist* (residues 306 to 520 in green and H11-H12 in blue) X-ray structures with pdb-codes 1GWR (*21*) and 3ERT (*22*) respectively.

The dynamic consequences of modelling His524 as the charged histidinium in the *apo*-conformation, model **7P**, leads to a situation where H12 is not able to bind to the core of hERα LBD. It is persistently found in a conformation mostly resembling the *apo* form as solvent exposed. It moves in a seemingly random way, as a "dog wagging its tail". The effects on the dynamic properties of the binary *apo*-

hERα·E2 complex upon binding of a copep are studied in model **8**. A stable conformation of hERα cannot be identified from the trajectories for any of the three His524 tautomers. All give rise to a random dynamic behavior, like in model **7P**. This observation suggests that conformational change towards the active complex requires that copep and E2 can not both bind to the *apo* conformation of hERα prior to changing the conformation of the protein.

Finally, the dynamics of *apo*-hERα is studied in the absence of a ligand in the binding site, models **9** and **10.** Very interestingly, these simulations reveal a semi-stable conformation as well as new mechanistic aspects of the activation mechanism. In model **9E** a new conformation is found for about 1 ns during the simulation, this conformation is then reformed during the final ns. Further studies are in progress for this model. In model **10P,** with a copep bound to the *apo*-conformation of hERα, dramatic changes in the behavior of the binary complex is observed. H12 is very dynamic and travels towards the *agonist* position. After 6.0 ns H12 is positioned in extension of its agonistic position in the "mouse trap". Snapshots of this conformational change are included in Figure 12a and the end-point of **10P** is overlaid the *agonist* structure in Figure 12b.

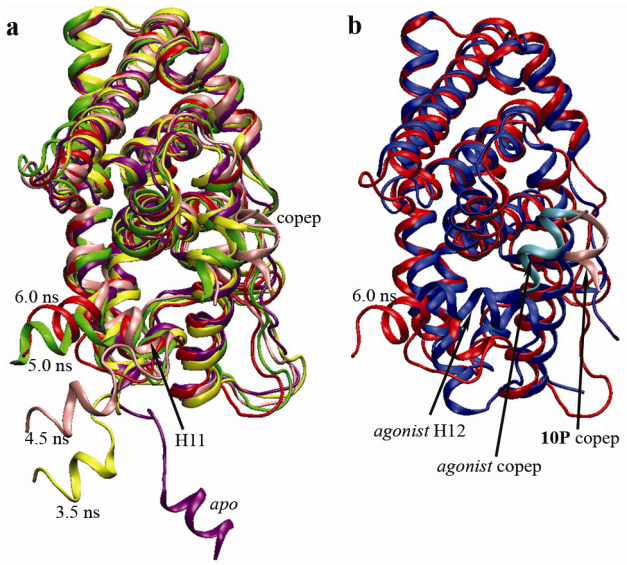

Figure 12. a) Trajectory of model **10P** including the initial conformation (magenta) and snapshots taken at 3.5 ns (yellow), 4.5 ns (pink), 5.0 ns (green) and 6.0 ns (red). b) The 6.0 ns snapshot (red) superpositioned with the *agonist* X-ray structure (blue). The copep is shown in cyan for the *agonist*

structure and in pink in **10P**. H12 is approaching the agonist position after 6 ns while the copep is tilted out of the site to possibly allow for H12 to be positioned.

It is furthermore seen that His524 becomes surface exposed during the dynamics of H12 due to a kink between H10 and H11, hindering the formation of the hydrogen bond zipper. This can be observed by counting how many snapshots preserve the hydrogen bonds in the zipper (see Supporting Information). An increase in these accumulated numbers can not be traced after the first nanosecond of the simulation. During the conformational change H11 is partially unwinding and during the last nanosecond of the simulation the copep, which is only held in place by half of the "charge clamp" (Lys362), is tilted out to allow for H12 to enter and form the complete co-activator binding site. The two other tautomers of His524, models **10D** and **10E,** do not lead to stable conformations of hERα. The behavior observed in **10P**, contrary to the other *apo* models, leads us to conclude that the shift from *apo* to *agonist* conformation may happen before a ligand is bound, but with a copep coordinated. It is possible that the copep can serve to pull H12 in place.

Conclusions and Perspectives.

In this paper we present exhaustive, 158 ns, non-restrained all-atom molecular dynamics simulation of the hERα LBD to elucidate the binding of the natural ligand E2 and to gain further insight in the dramatic conformational changes governing this protein from its inactive structure to the biologically active form. From the simulations it is concluded that E2 binding in the active form of hERα is favored with an ε-protonated His524, model **1**. This tautomer is able to maintain a conserved hydrogen bond from His524 to the substrate and also to keep a hydrogen bond network from His524 to Glu339 (H3) *via* Glu419 and Lys531 (H11) throughout the simulation. By conserving this network, H3 and H11 are kept in close contact, presumably preventing the ligand from escaping the ligand binding cavity. Furthermore, this network secures that H12 is positioned in the "mouse trap", as it can not reach the other favorable (*antagonist*) position on the hERα surface when H11 is not allowed to unwind. The

positioning of H12 then sets up the "charge clamp" that binds a co-activator peptide with a LxxLL-motif leading to the transcriptionally active tertiary complex. From simulations of *agonist* hERα (model **2**) it is proposed, that once the ligand is positioned correctly, the overall structure of the binary *agonist* hERα complex is stable. Once H12 is positioned in the agonist position in the "mouse trap" it does not move away again no matter if the copep stays bound or not. A similar simulation at an elevated temperature could further elucidate the most flexible parts of this complex. It is thus possible that if agonistic *holo*-hERα·E2 is found in the cell, co-activator proteins can diffuse and associate with this binary complex. We speculate that if other small molecules are present in the cellular environment they may be capable of binding in the co-activator binding cleft between H3, H4 and H12, thereby interfering with the transcriptional machinery at this stage of the cycle by inhibiting co-activator binding. Some inhibitors of ER activity have indeed been designed to bind in this site (*85, 86*). Ongoing research in our group will investigate the possibility for EDCs to bind in this cavity as well as to the alternative ligand binding cavity (*35, 87*). Simulations of models **3** and **4** of hERα in the agonist conformation without E2, revealed stable proteins on the examined timescale. Specifically, H12 is stable and stays tightly bound to the core of hERα, no signs of a conformational change towards an *apo* or *antagonist* structure could be detected.

The observation that the hydrogen bond network between E2, His524, Glu419, Lys531 and Glu339 is not intact in the *antagonist* simulations strongly indicates that His524 must serve a pivotal role in maintaining the local environment between H3 and H11. We suggest that hERα is working by having such a communication link between the presence of an agonist ligand and the overall fold of the protein, providing a possible mechanism for the observed allosteric activation within the ligand binding domain of ER. The former is signalled by the presence of a hydrogen bond from the ligand to His524, serving to keep this residue in position, whereas the latter is signalled by the position of H12. When a hydrogen bond from the ligand to His524 is present, H12 can only rest in the "mouse trap" because His524 is holding in place the hydrogen bond network, serving as the spring to the "mouse trap", which prevents

H3 and H11 from un-zipping and thereby from providing more flexibility to the positioning of H12. If the bound ligand is not capable of hydrogen bonding to His524, the conserved hydrogen bond network can be disrupted which then leads to the flexibility observed in the positioning of H12 and to the opening of the binding cavity allowing for more easy exchange of ligands. Another way to interrupt the hydrogen bonding network is to remove the Nε proton on His524. Without this atom His524 and Glu419 will be repelled and consequently the network is disrupted. A His524Ala mutation of ERα in the interaction with various EDCs points in the same direction (*51*), as the differential response seen for ERα wild type was eliminated by this site mutation pointing towards His524 having an essential role in the overall conformational dynamic picture of the protein. Model **4** revealed that the presence of a copep in the "charge clamp" can be communicated to the ligand binding cavity by zipping the hydrogen bond network only if His524 is found in the ε-tautomer.

Three of the most dynamic models studied were the *antagonist* conformation at 400K, the *apo* conformation with E2 in the binding site and the *apo* conformation with an empty binding site but including the copep, models **6P**, **7E** and **10P,** respectively. The end structures from simulations **6P** and **10P** and **7E** at 8.0 ns are highly similar. RMSD for all Cα-atoms equals less than 3 Å between the two latter structures. Low RMSDs, below 2.7 Å, are also calculated between model **6P** and models **10P** and **7E,** respectively, when H12 is excluded. **6P** and **10P** both have His524 modelled as a histidinium ion while **7E** includes the Nε tautomer of the residue. In both histidinium set-ups we observe the formation of a kink between H10 and H11 as well as a partial release of the component (copep or H12) bound in the "charge clamp". A close-up view of the final structures from the two simulations along with the *agonist* X-ray structure is depicted in Figure **13**. Although the two conformations are, of course, not entirely identical the similarities are easily seen. The C-terminal H12 of **6P** and the copep in **10P** are both partially held in place by hydrogen bonds to Glu362 while the N-terminals show more flexibility. For the **6P** simulation, it seems the displacement of H12 serves to pull H11 into the kinked position. Due to this conformational change, His524 is now positioned outside of the binding site and it is surface

exposed, hereby opening an entrance to the binding site between H3 and H11. Interestingly, a similar conformation of His524 is observed in **10P** which was initiated from the *apo*-conformation of the protein. Here the kink between H10 and H11 is observed without H12 positioned to pull; instead it appears to be the reverse, now H11 is positioned to drag H12 into the "mouse trap" forming the *agonist* conformation. Remarkably, **6P** and **10P** are the only stable set-ups identified with His524 modelled as a histidinium, strongly indicating this will only happen when this residue is solvent exposed. Since the kink between H10 and H11 is also only observed in **6P** and **10P** we anticipate that these two features must be highly correlated. In Figure 13b a close up view of **7E** along with **10P** and the agonist structure is depicted. It is clear that **7E** (8.0 ns) and **10P** (6.0 ns) are highly similar with respect to the conformation of H11 and H12.

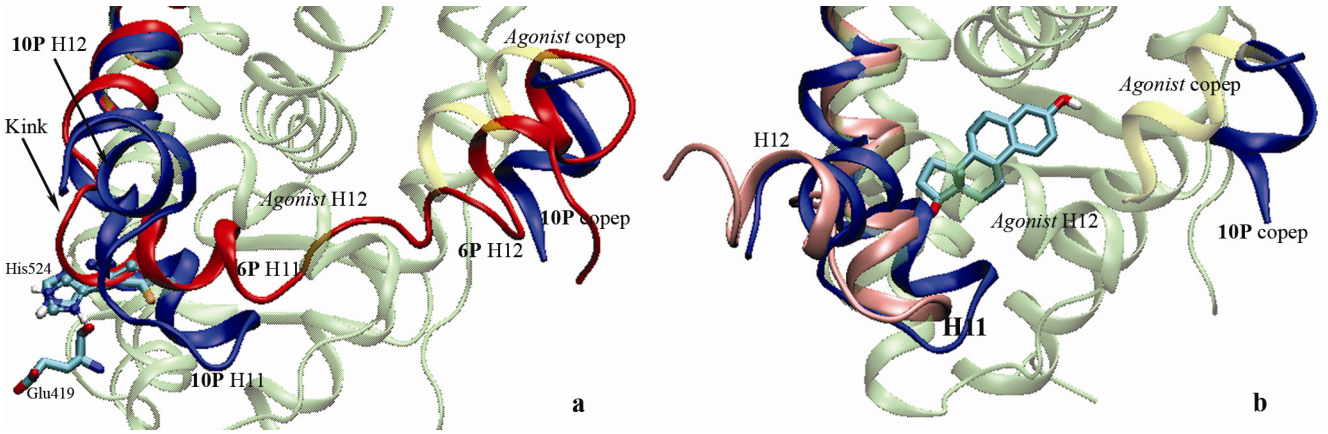

Figure 13. Overlay of the *agonist* X-ray structure (transparent green, copep transparent yellow) (21) with snapshots from a) **6P** (5 ns; red) and **10P** (6 ns; blue). His524 from **6P** and **10P** is depicted as well as Glu419 from **10P**; b) **7E** (8.0ns; pink) and **10P** (6 ns; blue).

The overall results of the simulations form the basis of a more detailed picture of the dynamic equilibrium of hERα where two pathways seem possible, Scheme 3. We suggest that the initial association of the copep to *apo*-hERα, upper part of Scheme 3, stimulates the movement of H12 towards the *agonist* position without closing the entrance to the ligand binding cavity between H3 and H11. This happens most likely with a surface exposed positive charged His524 as in model **10P**. Once

H12 is in or near the *agonist* position in the "mouse trap" we suggest that His524 becomes deprotonated at Nδ either by the solvent or by a neighbouring acidic residue, *eg*. Glu419. It is possible that E2 enters first and then, by forming a hydrogen bond from E2(O17) to His524(Nδ), pulls His524 inside the cavity thereby closing the entrance. Further simulations will shed more light on these proposed reaction sequences, by examining how the protein can discriminate between the E2 A and D rings to orient E2 correctly before entering the binding cavity. Also we plan to examine if E2(O3) is being guided into the binding cavity by specific interactions. New appropriate set-ups of the protein with wisely selected protonation states of central residues are needed and in progress in our group.

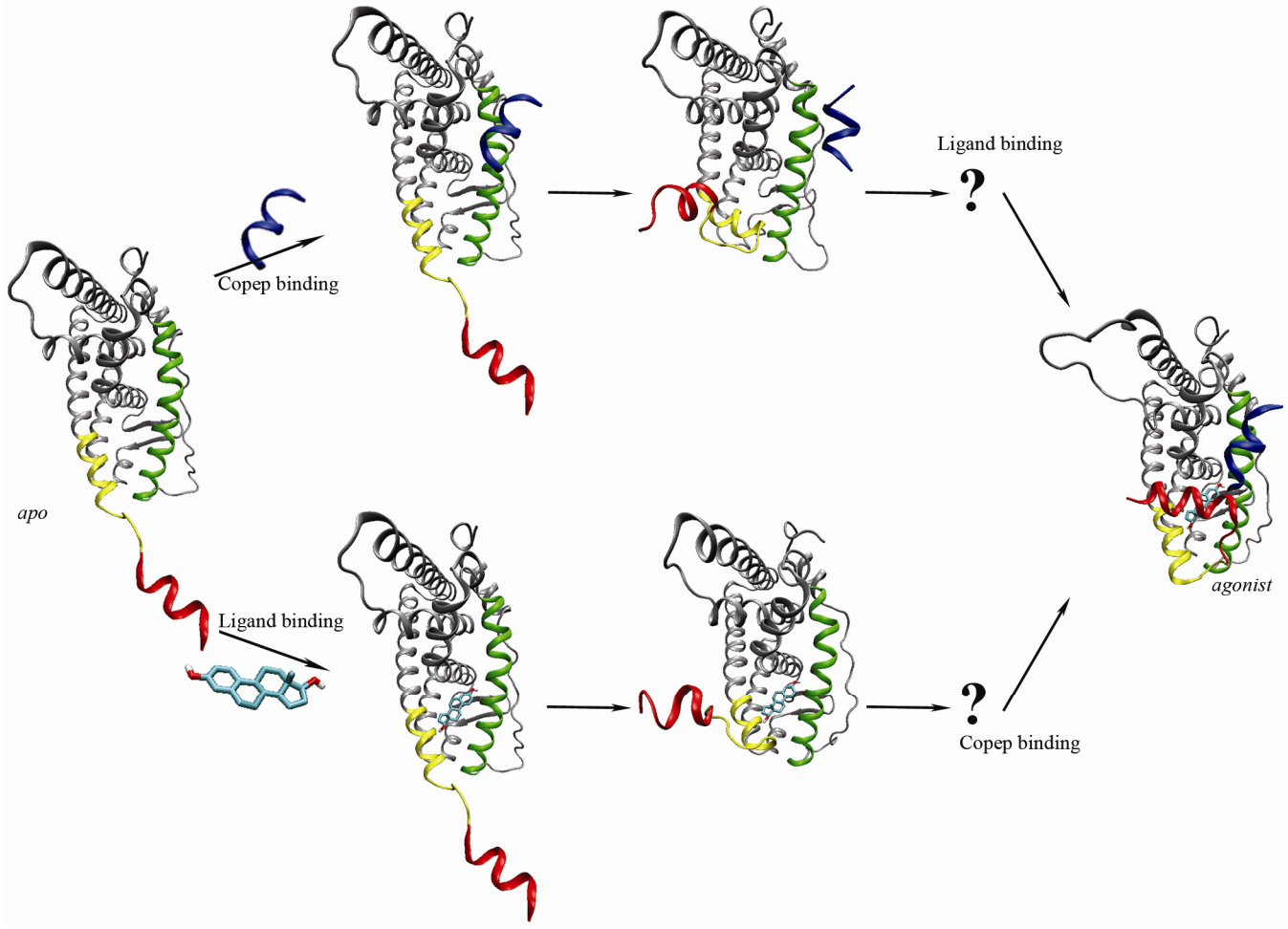

Scheme 3. The two possible pathways for activation of hERα. The pathway depends on whether copep or ligand is bound first to the *apo* protein and there may be a common intermediate before reaching the *agonist* conformation. The two question marks are included to account for other, yet,

undiscovered structures.

The other possible pathway involves an initial binding of E2 to the *apo* conformation of hERα with an ε-tautomer of His524, lower part of Scheme 3. After 7.5-8.0 ns of simulation a conformational change towards the agonist position of H12 is observed. The latter path, though stable on this time scale may not be as likely, because we expect that a charged His524 when solvent exposed is more feasible. Further calculations are underway to estimate the energetics associated with the conformational changes. It will be of utmost importance if experimental evidence for the activation of ER can be established with respect to the sequential binding of the two factors, E2 and copep. From the simulations we predict a two-step activation where addition of the co-activator peptide is likely to precede binding of E2, and furthermore that binding of the first of these factors will result in the conformational change before the other co-factor binds.

Moras, Karplus and co-workers have suggested, from multi ligand copy MD simulations (*53*), that the ligand enters the binding site from the "main entrance" closed by H12 in the *agonist* conformation. If the same mechanism is found for ER, it will be necessary to "un-zip" H3 and H11. Our simulations suggest that, if the copep binds prior to the ligand, His524 can not be present as the Nε tautomer when ligand recognition is taking place, as the entrance to the binding cavity is closed in model **4E**. It can, however proceed if the recognition is taking place in a structure similar to **10P**, followed by a deprotonation of His524, maybe by nearby residues in the hydrogen bond zipper, Glu419 or Lys531, also giving rise to a zipping of the hydrogen bonding network. Other pathways has also been studied for RAR and TR (*53-56*), studies are proceeding in our group to assess these with respect to our data.

The simulations of the *antagonist* and *agonist* structures did not show any signs of an easy conformational change between the two protein conformations in either direction on this time scale, even for miss-matched protein···ligand complexes. We think, that a change from an *agonist* to *antagonist* fold, or *vice versa*, is not happening directly, rather it probably proceeds *via* an open *apo*

conformation of the hERα. A set of new quasi stable conformations of hERα, models **7D** and **9E**, were identified from the simulations. They are stable for several nanoseconds, which should be enough to be recognized by *eg*. EDCs or SERMs thereby disturbing this very delicate conformational equilibrium of ERα. Continuing efforts in our group will look further in to this issue.

Acknowledgement. Computations were made possible through allocations of computer time at the PC-Cluster *Horseshoe* at the University of Southern Denmark under the Danish Center for Scientific Computing.

Supporting Information Available. A list with the assignments of the protonation states of histidine residues is provided (S1). Also included are residue topology descriptions (S2) and added force constants to model estradiol (S3). Figures illustrating the RMSD of C_α-atoms for HSD and HSP tautomers of His524 are included (S4-S5). Tables with frequencies for hydrogen bond formation in relation to the zipper and helix 11 are included (S6-S7). Complete citation for reference on CHARMM (*70*) is listed. This material is available free of charge via the Internet at http://pubs.acs.org.

REFERENCES.

1. Germain, P.; Altucci, L.; Bourguet, W.; Rochette-Egly, C.; Gronemeyer, H. (2003) Nuclear receptor superfamily: Principles of signaling, *Pure Appl. Chem. 75,* 1619-1664.

2. Nuclear Receptors Nomenclature Committee (1999) A Unified Nomenclature System for the Nuclear Receptor Superfamily, *Cell 97,* 161-163.

3. Gronemeyer, H.; Gustafsson, J. A.; Laudet, V. (2004) Principles for modulation of the nuclear receptor superfamily, *Nature Rev. Drug Disc. 3,* 950-964.

4. Moore, J. T.; Collins, J. L.; Pearce, K. H. (2006) The Nuclear Receptor Superfamily and Drug Discovery, *ChemMedChem 1,* 504-523.

5. Berkenstam, A.; Gustafsson, J. A. (2005) Nuclear receptors and their relevance to diseases related to lipid metabolism, *Curr. Opin. Pharm. 5,* 171-176.

6. Moras, D.; Gronemeyer, H. (1998) The nuclear receptor ligand-binding domain: structure and function, *Curr. Op. Cell Biol. 10,* 384-391.

7. Bourguet, W.; Germain, P.; Gronemeyer, H. (2000) Nuclear receptor ligand-binding domains: three-dimensional structures, molecular interactions and pharmacological implications, *Trends Pharmacol. Sci. 21,* 381-388.

8. Nilsson, S.; Gustafsson, J. A. (2002) Biological Role of Estrogen and Estrogen Receptors, *Crit. Rev. Biochem. Mol. Biol. 37,* 1-28.

9. Maglich, J. M.; Sluder, A.; Guan, X.; Shi, Y.; McKee, D. D.; Carrick, K.; Kamdar, K.; Wilson, T. M.; Moore, J. T. (2001) Comparison of complete nuclear receptor sets from the human, *Caenorhabditis elegans* and *Drosopila* genomes, *Genome 2,* 00029.1-00029.7.

10. Wrange, Ö; Gustafsson, J. A. (1978) Separation of the Hormone- and DNA-binding Sites of the Hepatic Glucocorticoid Receptor by Means of Proteolysis, *J. Biol. Chem. 253,* 856-865.

11. Wurtz, J. M.; Bourguet, W.; Renaud, J. P.; Vivat, V.; Chambon, P.; Moras, D.; Gronemeyer, H. (1996) A canonical structure for the ligand-binding domain of nuclear receptors, *Nat. Struct. Biol. 3,* 87-94.

12. Nolte, R. T.; Wisely, G. B.; Westin, S.; Cobbs, J. E.; Lambert, M. H.; Kurokawa, R.; Rosenfeld, M. G.; Willson, T. M.; Glass, C. K.; Milburn, M. V. (1998) Ligand binding and co-activator assembly of the peroxisome proliferator-activated receptor-γ, *Nature 395,* 137-143.

13. Heery, D. M.; Kalkhoven, E.; Hoare, S.; Parker, M. G. (1997) A signature motif in transcriptional co-activators mediates binding to nuclear receptors, *Nature 387,* 733-736.

14. Berg, J. M.; Tymoczko, J. L.; Stryer, L. (2001) *Transcriptional activation and repression are mediated by protein-protein interactions* In *Biochemistry* 5th ed., pp 879-883, W.H. Freeman and Company, New York.

15. Baniahmad, A. (2005) Nuclear hormone receptor co-repressors, *J. Steroid Biochem. Mol. Biol. 93,* 89-97.

16. Schwabe, J. W. R.; Chapman, L.; Finch, J. T.; Rhodes, D.; Neuhaus, D. (1993) DNA recognition by the oestrogen receptor: from solution to the crystal, *Structure 1,* 187-204.

17. Schwabe, J. W. R.; Chapman, L.; Fincd, J. T.; Rhodes, D. (1993) The Crystal Structure of the Estrogen Receptor DNA-Binding Domain Bound to DNA: How Receptors Discriminate between Their Response Elements, *Cell 75,* 567-578.

18. Gearhart, M. D.; Holmbeck, S. M. A.; Evans, R. M.; Dyson, H. J.; Wright, P. E. (2003) Monomeric Complex of Human Orphan Estrogen Related Receptor-2 with DNA: A Pseudo-dimer Interface Mediates Extended Half-site Recognition, *J. Mol. Biol. 327,* 819-832.

19. Brozozowski, A. M.; Pike, A. C. W.; Dauter, Z.; Hubbard, R. E.; Bonn, T.; Engström, O.; Öhman, L.; Greene, G. L.; Gustafsson, J. A.; Carlquist, M. (1997) Molecular basis of agonism and antagonism in the oestrogen receptor, *Nature 389,* 753-757.

20. Tanenbaum, D. M.; Wang, Y.; Williams, S. P.; Sigler, P. B. (1998) Crystallographic comparison of the estrogen and progesterone receptor's ligand binding domains, *Proc. Natl. Acad. Sci. 95,* 5998-6003.

21. Wärnmark, A.; Treuter, E.; Gustafsson, J. A.; Hubbard, R. E.; Brozozowski, A. M.; Pike, A. C. W. (2002) Interaction of Transcriptional Intermediary Factor 2 Nuclear Receptor Box Peptides with the Coactivator Binding Site of Estrogen Receptor α, *J. Biol. Chem. 277,* 21862-21868.

22. Shiau, A. K.; Barstad, D.; Loria, P. M.; Cheng, L.; Kushner, P. J.; Agard, D. A.; Greene, G. L. (1998) The structural Basis of Estrogen Receptor/Coactivator Recognition and the Antagonism of This Interaction by Tamoxifen, *Cell 95,* 927-937.

23. Steinmetz, A. C. U.; Renaud, J.; Moras, D. (2001) Binding of Ligands and Activation of Transcription by Nuclear Receptors, *Annu. Rev. Biophys. Biomol. Struct. 30,* 329-359.

24. Egea, P. F.; Klaholz, B. P.; Moras, D. (2000) Ligand-protein interactions in nuclear receptors of hormones, *FEBS Letters 476,* 62-67.

25. Egner, U.; Heinrich, N.; Ruff, M.; Gangloff, M.; Mueller-Fahrnow, A.; Wurtz, J. M. (2001) Different Ligands-Different Receptor Conformations: Modeling of the hERalpha LBD in Complex with Agonists and Antagonists, *Med. Res. Rev. 21,* 523-539.

26. Bourguet, W.; Ruff, M.; Chambon, P.; Gronemeyer, H.; Moras, D. (1995) Crystal structure of the ligand binding/domain of the human nuclear receptor RXRα, *Nature 375,* 377-382.

27. Renaud, J. P.; Rochel, N.; Ruff, M.; Vivat, V.; Chambon, P.; Gronemeyer, H.; Moras, D. (1995) Crystal structure of the RAR-gamma ligand-binding domain bound to all-*trans* retinoic acid, *Nature 378,* 681-689.

28. Belleau, B. (1964) Molecular Theory of Drug Action Based on Induced Conformational Perturbations of Receptors, *J. Med. Chem. 7,* 776-784.

29. Lindorff-Larsen, K.; Best, R. B.; DePristo, M. A.; Dobson, C. M.; Vendruscolo, M. (2005) Simultaneous determination of protein structure and dynamics, *Nature 433,* 128-132.

30. Estabrook, R. A.; Luo, J.; Purdy, M. M.; Sharma, V.; Weakliem, P.; Bruice, T. C.; Reich, N. O. (2005) Statistical coevolution analysis and molecular dynamics: Identification of amino acid pairs essential for catalysis, *Proc. Natl. Acad. Sci. 102,* 994-999.

31. Agarwal, P. K. (2005) Role of Protein Dynamics in Reaction Rate Enhancement by Enzymes, *J. Am. Chem. Soc. 127,* 15248-15256.

32. Schiøtt, B. (2004) Possible Involvement of Collective Domain Movement in the Catalytic Reaction of Soluble Epoxide Hydrolase, *Int. J. Quantum Chem. 99,* 61-69.

33. Eisenmesser, E. Z.; Bosco, D. A.; Akke, M.; Kern, D. (2002) Enzyme Dynamics During Catalysis, *Science 295,* 1520-1523.

34. Gangloff, M.; Ruff, M.; Eiler, S.; Duclaud, S.; Wurtz, J. M.; Moras, D. (2001) Crystal Structure of a Mutant hERα Ligand-Binding Domain Reveals Key Structural Features for the Mechanism of Partial Agonism, *J. Biol. Chem. 276,* 15059-15065.

35. Norman, A. W.; Mizwicki, M. T.; Norman, D. P. G. (2004) Steroid-hormone rapid actions, membrane receptors and a conformational ensemble model, *Nature Rev. Drug Disc. 3,* 27-41.

36. Shulman, A. I.; Larson, C.; Mangelsdorf, D. J.; Ranganathan, R. (2004) Structural Determinants of Allosteric Ligand Activation in RXR Heterodimers, *Cell 116,* 417-429.

37. Nettles, K. W.; Sun, J.; Radek, J. T.; Sheng, S.; Rodriguez, A. L.; Katzenellenbogen, J. A.; Katzenellenbogen, B. S.; Greene, G. L. (2004) Allosteric Control of Ligand Selectivity between Estrogen Receptors α and β: Implications for Other Nuclear Receptors, *Mol. Cell 13,* 317-327.

38. Yamamoto, K.; Abe, D.; Yoshimoto, N.; Choi, M.; Yamagishi, K.; Tokiwa, H.; Shimizu, M.; Makishima, M.; Yamada, S. (2006) Vitamin D Receptor: Ligand Recognition and Allosteric Network, *J. Med. Chem. 49,* 1313-1324.

39. Brelivet, Y.; Kammerer, S.; Rochel, N.; Poch, O.; Moras, D. (2004) Signature of the oligomeric behaviour of nuclear receptors at the sequence and structural level, *EMBO Rep. 4,* 423-429.

40. Damstra, T.; Barlow, S.; Bergman, A.; Kavlock, R.; Kraak, G. v. d. (2002) Global Assessment of the

State-of-the-Science of Endocrine Disrupters.

41. Sumpter, J. P. (1998) Xenoendocrine disrupters - environmental impacts, *Tox. Lett. 102,* 337-342.

42. Pillon, A.; Boussioux, A. M.; Escande, A.; Aït-Aïssa, S.; Gomez, E.; Fenet, H.; Ruff, M.; Moras, D.; Vignon, F.; Duchesne, M. J.; Casellas, C.; Nicolas, J. C.; Balaguer, P. (2005) Binding of Estrogenic Compounds to Recombinant Estrogen Receptor-*alpha*: Application to Environmental Analysis, *Environ. Health Persp. 113,* 278-284.

43. Colborn, T.; vom Saal, F. S.; Soto, A. M. (1993) Developmental Effects of Endocrine-Disrupting Chemicals in Wildlife and Humans, *Environ. Health Persp. 101,* 378-384.

44. Danzo, B. J. (1997) Environmental Xenobiotics May Disrupts Normal Endocrine Function by Interfering with the Binding of Physiological Ligands to Steroid Receptors and Binding Proteins, *Environ. Health Persp. 105,* 294-301.

45. Sonnenschein, C.; Soto, A. M. (1998) An Updated Review of Environmental Estrogen and Androgen Mimics and Antagonists, *J. Steroid Biochem. Mol. Biol. 65,* 143-150.

46. Witorsch, R. J. (2002) Endocrine Disrupters: Can Biological Effects and Environmental Risks Be Predicted, *Regul. Toxicol. Pharmacol. 36,* 118-130.

47. Aitken, R. J.; Koopman, P.; Lewis, S. E. M. (2004) Seeds of concern, *Nature 432,* 489-52.

48. Jacobs, M. N. (2004) In silico tools to aid risk assessment of endocrine disrupting chemicals, *Toxicology 205,* 43-53.

49. Paige, L. A.; Christensen, D. J.; Grøn, H.; Norris, J. D.; Gottlin, E. B.; Padilla, K. M.; Chang, C. Y.; Ballas, L. M.; Hamilton, P. T.; McDonnell, D. P.; Fowlkes, D. M. (1999) Estrogen receptor (ER) modulators each induce distinct conformational changes in ER alpha and ER beta, *Proc. Natl. Acad. Sci. 96,* 3999-4004.

50. Iannone, M. A.; Simmons, C. A.; Kadwell, S. H.; Svoboda, D. L.; Vanderwall, D. E.; Deng, S. J.; Consler, T. G.; Shearin, J.; Gray, J. G.; Pearce, K. H. (2004) Correlation between *in Vitro* Peptide Binding Profiles and Cellular Activities for Estrogen Receptor-Modulating Compounds, *Mol. Endo. 18,* 1064-1081.

51. Sumbayev, V. V.; Bonefeld-Jørgensen, E. C.; Wind, T.; Andreasen, P. A. (2005) A novel pesticide-induced conformational state of the oestrogen receptor ligand-binding domain, detected by conformation-specific peptide binding, *FEBS 579,* 541-548.

52. Shiau, A. K.; Barstad, D.; Radek, J. T.; Meyers, M. J.; Nettles, K. W.; Katzenellenbogen, B. S.; Katzenellenbogen, J. A.; Agard, D. A.; Greene, G. L. (2002) Structural characterization of a subtype-selective ligand reveals a novel mode of estrogen receptor antagonism, *Nat. Struct. Biol. 9,* 359-364.

53. Blondel, A.; Renaud, J. P.; Fischer, S.; Moras, D.; Karplus, M. (1999) Retinoic Acid Receptor: A Simulation Analysis of Retinoic Acid Binding and the Resulting Conformational Changes, *J. Mol. Biol. 291,* 101-115.

54. Kosztin, D.; Izrailev, S.; Schulten, K. (1999) Unbinding of Retinoic Acid from its Receptor Studied by Steered Molecular Dynamics, *Biophys. J. 76,* 188-197.

55. Martinez, L.; Sonoda, M. T.; Webb, P.; Baxter, J. D.; Skaf, M. S.; Polikarpov, I. (2005) Molecular Dynamics Simulations Reveal Multiple Pathways of Ligand Dissociation from Thyroid Hormone Receptors, *Biophys. J. 89,* 2011-2023.

56. Martinez, L.; Webb, P.; Polikarpov, I.; Skaf, M. S. (2006) Molecular Dynamics Simulations of Ligand Dissociation from Thyroid Hormone Receptors: Evidence of the Likeliest Escape Pathway and Its Implications for the Design of Novel Ligands, *J. Med. Chem. 49,* 23-26.

57. Adcock, S. A.; McCammon, J. A. (2006) Molecular Dynamics: Survey of Methods for Simulating

the Activity of Proteins, *Chem. Rev. 105,* 1589-1615.

58. Karplus, M.; Kuriyan, J. (2005) Chemical Theory and Computation Special Feature: Molecular dynamics and protein function, *Proc. Natl. Acad. Sci. 102,* 6679-6685.

59. Garcia-Viloca, M.; Gao, J.; Karplus, M.; Truhlar, D. G. (2004) How Enzymes Work: Analysis by Modern Rate Theory and Computer Simulations, *Science 303,* 186-195.

60. Benkovic, S. J.; Hammes-Schiffer, S. (2003) A Perspective on Enzyme Catalysis, *Science 301,* 1196-1292.

61. Åqvist, J.; Luzhkov, V. (2000) Ion permeation mechanism of the potassium channel, *Nature 404,* 881-884.

62. Bernéche, S.; Roux, B. (2001) Energetics of ion conduction through the K^+ channel, *Nature 414,* 73-77.

63. de Groot, B. L.; Grubmuller, H. (2005) The dynamics and energetics of water permeation and proton exclusion in aquaporins, *Curr. Opin. Struct. Biol. 15,* 176-183.

64. Forrest, L. R.; Sansom, M. S. (2000) Membrane simulations: bigger and better? *Curr. Opin. Struct. Biol. 10,* 174-181.

65. Saiz, L.; Klein, M. L. (2002) Computer Simulation Studies of Model Biological Membranes, *Acc. Chem. Res. 35,* 482-489.

66. Hornak, V.; Okur, A.; Rizzo, R. C.; Simmerling, C. (2006) HIV-1 protease flaps spontaneously open and reclose in molecular dynamics simulations, *Proc. Natl. Acad. Sci. 103,* 915-920.

67. Hornak, V.; Okur, A.; Rizzo, R. C.; Simmerling, C. (2006) HIV-1 Protease Flaps Spontaneously Close to the Correct Structure in Simulations Following Manual Placement of an Inhibitor into the

Open State, *J. Am. Chem. Soc. 128,* 2812-2813.

68. Berman, H. M.; Westbrook, J.; Feng, Z.; Gilliland, G.; Bhat, T. N.; Weissig, H.; Shindyalov, I. N.; Bourne, P. E. (2000) The Protein Data Bank, *Nuc. Acids Res. 28,* 235-242.

69. Kalé, L.; Skeel, R.; Bhandakar, M.; Brunner, R.; Gursoy, A.; Krawetz, N.; Phillips, J.; Shinozaki, A.; Varadarajan, K.; Schulten, K. (1999) NAMD2: Greater Scalability for Parallel Molecular Dynamics, *J. Comput. Phys. 151,* 283-312.

70. MacKerell, A. D. J. *et al.* (1998) All-Atom Empirical Potential for Molecular Modeling and Dynamics Studies of Proteins, *J. Phys. Chem. B 102,* 3586-3616.

71. Jorgensen, W. L.; Chandrasekhar, J.; Madura, J. D.; Impey, R. W.; Klein, M. L. (1983) Comparison of simple potential functions for simulating liquid water, *J. Chem. Phys. 79,* 926-935.

72. Pitman, M. C.; Suits, F.; MacKerell, A. D. J.; Feller, S. E. (2004) Molecular-Level Organization of Saturated and Polyunsaturated Fatty Acids in a Phosphatidylcholine Bilayer Containing Cholesterol, *Biochemistry 43,* 15318-15328.

73. Accelrys (2000) Quanta 2000, San Diego, USA.

74. Gilson, M. K.; Gilson, H. S. R.; Potter, M. J. (2003) Fast assignment of accurate partial atomic charges. An electronegativity equalization method that accounts for alternate resonance forms, *J. Chem. Inf. Comput. Sci. 43,* 1982-1997.

75. Darden, T.; York, D.; Pedersen, L. (1993) Particle Mesh Ewald: An *N* *log(*N)* method for Ewald sums in large systems, *J. Chem. Phys. 98,* 10089-10092.

76. Feller, S. E.; Zhang, Y.; Pastor, R. W.; Brooks, B. R. (1995) Constant pressure molecular dynamics simulation: The Langevin piston method, *J. Chem. Phys. 103,* 4613-4621.

77. Humphrey, W.; Dalke, A.; Schulten, K. (1996) VMD: Visual Molecular Dynamics, *J. Mol. Graph.*

14, 33-38.

78. Barlow, D. J.; Thornton, J. M. (1983) Ion pairs in proteins, *J. Mol. Biol. 168,* 867-885.

79. Eiler, S.; Gangloff, M.; Duclaud, S.; Moras, D.; Ruff, M. (2001) Overexpression, Purification, and Crystal Structure of Native ERα LBD, *Prot. Expres. Puri. 22,* 165-173.

80. Leduc, A.; Trent, J. O.; Wittliff, J. L.; Bramlett, K. S.; Briggs, S. L.; Chirgadze, N. Y.; Wang, Y.; Burris, T. P.; Spatola, A. F. (2003) Helix-stabilized cyclic peptides as selective inhibitors of steroid receptor-coactivator interactions, *Proc. Natl. Acad. Sci. 100,* 11273-11278.

81. Schiøtt, B.; Bruice, T. C. (2002) Reaction Mechanism of Soluble Epoxide Hydrolase: Insights from Molecular Dynamics Simulations, *J. Am. Chem. Soc. 124,* 14558-14570.

82. Lie, M. A.; Celik, L.; Jørgensen, K. A.; Schiøtt, B. (2005) Cofactor Activation and Substrate Binding in Pyruvate Decarboxylase. Insights into the Reaction Mechanism from Molecular Dynamics Simulations, *Biochemistry 44,* 14792-14806.

83. Renaud, J.; Bischoff, S. F.; Buhl, T.; Floersheim, P.; Fournier, B.; Halleux, C.; Kallen, J.; Keller, H.; Schlaeppi, J.; Stark, W. (2003) Estrogen Receptor Modulators: Identification and Structure-Activity Relationships of Potent ERα-Selective Tetrahydroisoquinoline Ligands, *J. Med. Chem. 46,* 2945-2957.

84. Kim, S.; Wu, J. Y.; Birzin, E. T.; Frisch, K.; Chan, W.; Pai, L.; Yang, Y. T.; Mosley, R. T.; Fitzgerald, P. M. D.; Sharma, N.; Dahllund, J.; Thorsell, A.; DiNinno, F.; Rohrer, S. P.; Schaeffer, J. M.; Hammond, M. L. (2004) Estrogen Receptor Ligands. II. Discovery of Benzoxathiins as Potent, Selecive Estrogen Receptor α Modulators, *J. Med. Chem. 47,* 2171-2175.

85. Schulman, I. G.; Heyman, R. A. (2004) The Flip Side: Identifying Saml Molecule Regulators of Nuclear Receptors, *Chem. Biol. 11,* 639-646.

86. Rodriguez, A. L.; Tamrazi, A.; Collins, M. L.; Katzenellenbogen, J. A. (2004) Design, Synthesis, and in Vitro Biological Evaluation of Small Molecule Inhibitors of Estrogen Receptor alpha Coactivator Binding, *J. Med. Chem. 47,* 600-611.

87. Mizwicki, M. T.; Keidel, D.; Bula, C. M.; Bishop, J. E.; Zanello, L. P.; Wurtz, J.; Moras, D.; Norman, A. W. (2004) Identification of an alternative ligand-binding pocket in the nuclear vitamin D receptor and its functional importance in 1α,25(OH)2-vitamin D3 signaling, *Proc. Natl. Acad. Sci. 101,* 12876-12881.

TOC-graphics.

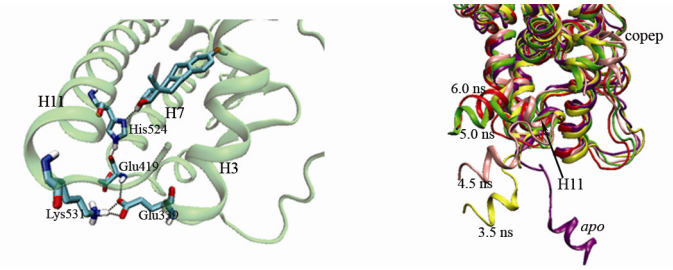

Supporting Information for

Conformational Dynamics of the Estrogen Receptor α: Influence of binding site structure on protein dynamics and biological function studied by MD simulations.

Leyla Celik,[‡] *Julie Davey Dalsgaard Lund,*[§] *Birgit Schiøtt*[‡§]*

[‡]Interdisciplinary Nanoscience Centre (*i*NANO) and [§]Centre for Insoluble Protein Structures (*in*SPIN), Department of Chemistry, University of Aarhus, DK-8000 Aarhus, Denmark

Multiple refined residues.

Two residues were refined to two positions in the *agonist* (Asn359 and His373) and the *apo* (Glu330 and His501) structures. The two positions have equal probability and the second entry was chosen in each case. In the *antagonist* structure four residues were refined to two positions. Two of these (Cys381 and Ser433) had 75/25% occupation. For Cys381 the highest occupied position was chosen but since the lower occupation of Ser433 had the opportunity to form an extra hydrogen bond this was selected. The two other residues (His513 and Met522) had 50/50% occupation and the second entry was chosen for both. Of these eight residues none were closer than 8 Å of the co-crystallized ligand.

Table S1. Histidine protonation:

Protonation of all histidines in ERα MD simulations are tabulated. The decisions are based on the local environments:

Residue Nr.	Protonated on
356	Nε when His524 is charged, otherwise on both.
373	Nδ
377	Nε
398	Nδ
474	Nδ and Nε
476	Nδ and Nε
488	Nε
501	Nδ and Nε
513	Nδ and Nε
516	Nδ
524	See **Table 1** in the paper
547	Nδ and Nε
550	Nδ

Table S2. Residue topology of Estradiol (E2):

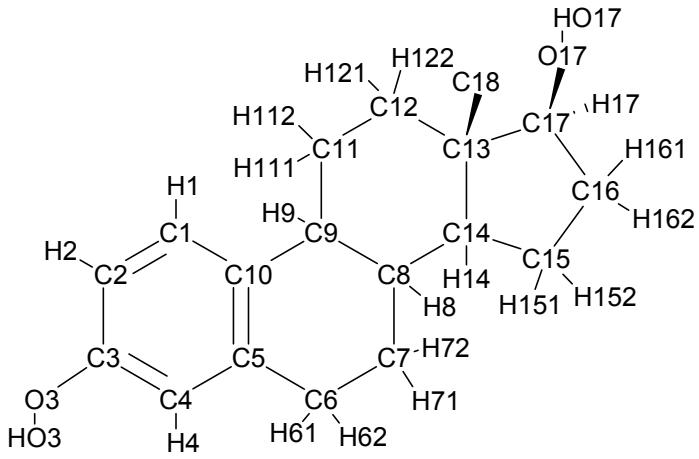

RESI EST 0.000
GROUP

ATOM	C1	CEL1	-0.119984
ATOM	C2	CEL1	-0.123632
ATOM	C3	CEL1	0.120537
ATOM	O3	OH1	-0.521467
ATOM	C4	CEL1	-0.126152
ATOM	H1	HEL1	0.103213
ATOM	H2	HEL1	0.103213
ATOM	H4	HEL1	0.103213
ATOM	HO3	H	0.379540
ATOM	C5	CEL1	-0.017932
ATOM	C10	CEL1	-0.020452
ATOM	C6	CTL2	-0.150425
ATOM	C7	CTL2	-0.168051
ATOM	H61	HAL2	0.084337
ATOM	H62	HAL2	0.084337
ATOM	H71	HAL2	0.084848
ATOM	H72	HAL2	0.084848
ATOM	C8	CTL1	-0.071487
ATOM	C9	CTL1	-0.053861
ATOM	H8	HAL1	0.083704
ATOM	H9	HAL1	0.083193
ATOM	C11	CTL2	-0.168051
ATOM	C12	CTL2	-0.169986
ATOM	H111	HAL2	0.084848
ATOM	H112	HAL2	0.084848
ATOM	H121	HAL2	0.084848
ATOM	H122	HAL2	0.084848
ATOM	C13	CTL1	0.025502
ATOM	C14	CTL1	-0.073422
ATOM	C18	CTL3	-0.269030
ATOM	H181	HAL3	0.085992
ATOM	H182	HAL3	0.085992
ATOM	H183	HAL3	0.085992
ATOM	H14	HAL1	0.083704
ATOM	C15	CTL2	-0.167507
ATOM	C16	CTL2	-0.172585
ATOM	C17	CTL1	0.120331
ATOM	O17	OHL	-0.548188
ATOM	H151	HAL2	0.084848
ATOM	H152	HAL2	0.084848
ATOM	H161	HAL2	0.084848
ATOM	H162	HAL2	0.084848
ATOM	H17	HAL1	0.080529

```
ATOM   HO17 HOL       0.380408
BOND   C1   C2
BOND   C1   C10
BOND   C1   H1
BOND   C2   C3
BOND   C2   H2
BOND   C3   O3
BOND   C3   C4
BOND   O3   HO3
BOND   C4   C5
BOND   C4   H4
BOND   C5   C6
BOND   C5   C10
BOND   C6   C7
BOND   C6   H61
BOND   C6   H62
BOND   C7   C8
BOND   C7   H71
BOND   C7   H72
BOND   C8   C9
BOND   C8   C14
BOND   C8   H8
BOND   C9   C10
BOND   C9   C11
BOND   C9   H9
BOND   C11  C12
BOND   C11  H111
BOND   C11  H112
BOND   C12  C13
BOND   C12  H121
BOND   C12  H122
BOND   C13  C14
BOND   C13  C17
BOND   C13  C18
BOND   C14  C15
BOND   C14  H14
BOND   C15  C16
BOND   C15  H151
BOND   C15  H152
BOND   C16  C17
BOND   C16  H161
BOND   C16  H162
BOND   C17  O17
BOND   C17  H17
BOND   O17  HO17
BOND   C18  H181
BOND   C18  H182
BOND   C18  H183
IMPH   C10  C1   C2   C3
IMPH   C2   C1   C10  C5
IMPH   C1   C2   C3   C4
IMPH   C2   C3   C4   C5
IMPH   C3   C4   C5   C10
IMPH   C4   C5   C10  C1
IMPH   C1   C2   C10  H1
IMPH   C2   C1   C3   H2
IMPH   C3   C2   C4   O3
IMPH   C4   C3   C5   H4
IMPH   C5   C4   C10  C6
IMPH   C10  C1   C5   C9
IC     C10  C1   C2   C3   1.43  119.92    0.07  121.10  1.36
IC     H1   C1   C2   C3   1.08  120.03 -179.98  121.10  1.36
IC     C10  C1   C2   H2   1.43  119.92 -179.94  119.99  1.08
```

IC	C2	C10	*C1	H1	1.40	119.92	-179.96	120.05	1.08
IC	C1	C3	*C2	H2	1.40	121.10	-179.99	118.92	1.08
IC	C1	C2	C3	O3	1.40	121.10	179.87	122.19	1.36
IC	H2	C2	C3	O3	1.08	118.92	-0.12	122.19	1.36
IC	C1	C2	C3	C4	1.40	121.10	-0.36	121.09	1.41
IC	C2	O3	*C3	C4	1.36	122.19	-179.78	116.72	1.41
IC	C2	C3	O3	HO3	1.36	122.19	12.98	109.41	0.96
IC	C4	C3	O3	HO3	1.41	116.72	-166.80	109.41	0.96
IC	C2	C3	C4	C5	1.36	121.09	0.58	117.77	1.40
IC	O3	C3	C4	C5	1.36	116.72	-179.63	117.77	1.40
IC	C2	C3	C4	H4	1.36	121.09	-179.45	120.02	1.08
IC	C3	C5	*C4	H4	1.41	117.77	-179.97	122.21	1.08
IC	C3	C4	C5	C6	1.41	117.77	176.29	114.90	1.52
IC	H4	C4	C5	C6	1.08	122.21	-3.68	114.90	1.52
IC	C3	C4	C5	C10	1.41	117.77	-0.53	122.91	1.40
IC	C4	C6	*C5	C10	1.40	114.90	176.85	122.11	1.40
IC	C4	C5	C6	C7	1.40	114.90	170.08	113.47	1.51
IC	C10	C5	C6	C7	1.40	122.11	-13.07	113.47	1.51
IC	C4	C5	C6	H61	1.40	114.90	-69.84	109.53	1.09
IC	C4	C5	C6	H62	1.40	114.90	50.11	109.45	1.09
IC	C5	C6	C7	C8	1.52	113.47	42.43	109.78	1.53
IC	H61	C6	C7	C8	1.09	107.47	-78.81	109.78	1.53
IC	H62	C6	C7	C8	1.09	107.43	163.55	109.78	1.53
IC	C5	C6	C7	H71	1.52	113.47	162.45	109.47	1.09
IC	C5	C6	C7	H72	1.52	113.47	-77.57	109.49	1.09
IC	C6	C7	C8	C9	1.51	109.78	-64.54	110.17	1.53
IC	H71	C7	C8	C9	1.09	109.33	175.37	110.17	1.53
IC	H72	C7	C8	C9	1.09	109.31	55.58	110.17	1.53
IC	C6	C7	C8	C14	1.51	109.78	177.64	105.32	1.50
IC	C6	C7	C8	H8	1.51	109.78	53.24	109.48	1.09
IC	C7	C8	C9	C10	1.53	110.17	54.18	111.01	1.49
IC	C14	C8	C9	C10	1.50	109.35	169.48	111.01	1.49
IC	H8	C8	C9	C10	1.09	107.30	-64.93	111.01	1.49
IC	C7	C8	C9	C11	1.53	110.17	-176.38	108.95	1.54
IC	C7	C8	C9	H9	1.53	110.17	-75.19	109.45	1.09
IC	C8	C9	C10	C1	1.53	111.01	155.82	121.44	1.43
IC	C11	C9	C10	C1	1.54	116.39	30.45	121.44	1.43
IC	H9	C9	C10	C1	1.09	116.04	-78.40	121.44	1.43
IC	C8	C9	C10	C5	1.53	111.01	-24.18	121.35	1.40
IC	C1	C5	*C10	C9	1.43	117.21	180.00	121.35	1.49
IC	C5	C10	C1	C2	1.40	117.21	0.00	119.92	1.40
IC	C9	C10	C1	C2	1.49	121.44	180.00	119.92	1.40
IC	C5	C10	C1	H1	1.40	117.21	-179.96	120.05	1.08
IC	C1	C10	C5	C4	1.43	117.21	0.25	122.91	1.40
IC	C9	C10	C5	C4	1.49	121.35	-179.75	122.91	1.40
IC	C1	C10	C5	C6	1.43	117.21	-176.34	122.11	1.52
IC	C8	C9	C11	C12	1.53	108.95	61.98	108.32	1.55
IC	C10	C9	C11	C12	1.49	116.39	-171.61	108.32	1.55
IC	H9	C9	C11	C12	1.09	93.72	-50.05	108.32	1.55
IC	C8	C9	C11	H111	1.53	108.95	-177.95	109.55	1.09
IC	C8	C9	C11	H112	1.53	108.95	-57.96	109.50	1.09
IC	C9	C11	C12	C13	1.54	108.32	-62.22	108.79	1.53
IC	H111	C11	C12	C13	1.09	110.06	178.04	108.79	1.53
IC	H112	C11	C12	C13	1.09	109.98	57.42	108.79	1.53
IC	C9	C11	C12	H121	1.54	108.32	57.79	109.48	1.09
IC	C9	C11	C12	H122	1.54	108.32	177.73	109.50	1.09
IC	C11	C12	C13	C14	1.55	108.79	59.94	108.20	1.55
IC	H121	C12	C13	C14	1.09	109.81	-59.86	108.20	1.55
IC	H122	C12	C13	C14	1.09	109.85	179.78	108.20	1.55
IC	C11	C12	C13	C17	1.55	108.79	168.52	116.48	1.54
IC	C11	C12	C13	C18	1.55	108.79	-68.17	114.52	1.53
IC	C12	C13	C14	C8	1.53	108.20	-59.80	111.05	1.50
IC	C17	C13	C14	C8	1.54	97.56	179.06	111.05	1.50

IC	C18	C13	C14	C8	1.53	113.82	68.71	111.05	1.50
IC	C12	C13	C14	C15	1.53	108.20	175.77	100.33	1.53
IC	C12	C13	C14	H14	1.53	108.20	57.89	104.03	1.09
IC	C13	C14	C8	C7	1.55	111.05	178.52	105.32	1.53
IC	C15	C14	C8	C7	1.53	117.05	-67.14	105.32	1.53
IC	H14	C14	C8	C7	1.09	109.49	64.20	105.32	1.53
IC	C13	C14	C8	C9	1.55	111.05	60.15	109.35	1.53
IC	C13	C14	C8	H8	1.55	111.05	-60.75	115.19	1.09
IC	C8	C14	C15	C16	1.50	117.05	-169.99	101.02	1.56
IC	C13	C14	C15	C16	1.55	100.33	-49.79	101.02	1.56
IC	H14	C14	C15	C16	1.09	113.75	60.66	101.02	1.56
IC	C8	C14	C15	H151	1.50	117.05	-49.98	109.49	1.09
IC	C8	C14	C15	H152	1.50	117.05	69.98	109.47	1.09
IC	C14	C15	C16	C17	1.53	101.02	24.82	103.86	1.56
IC	H151	C15	C16	C17	1.09	113.53	-92.27	103.86	1.56
IC	H152	C15	C16	C17	1.09	113.54	141.89	103.86	1.56
IC	C14	C15	C16	H161	1.53	101.02	144.89	109.50	1.09
IC	C14	C15	C16	H162	1.53	101.02	-95.16	109.52	1.09
IC	C15	C16	C17	C13	1.56	103.86	9.05	105.90	1.54
IC	H161	C16	C17	C13	1.09	112.25	-109.14	105.90	1.54
IC	H162	C16	C17	C13	1.09	112.16	127.22	105.90	1.54
IC	C15	C16	C17	O17	1.56	103.86	136.60	113.74	1.41
IC	C15	C16	C17	H17	1.56	103.86	-113.11	116.78	1.09
IC	C16	C17	C13	C12	1.56	105.90	-153.29	116.48	1.53
IC	O17	C17	C13	C12	1.41	115.23	80.06	116.48	1.53
IC	H17	C17	C13	C12	1.09	109.48	-26.58	116.48	1.53
IC	C16	C17	C13	C14	1.56	105.90	-38.57	97.56	1.55
IC	C16	C17	C13	C18	1.56	105.90	78.70	105.20	1.53
IC	C13	C17	O17	HO17	1.54	115.23	56.44	109.49	0.96
IC	C16	C17	O17	HO17	1.56	113.74	-66.11	109.49	0.96
IC	H17	C17	O17	HO17	1.09	95.86	171.21	109.49	0.96
IC	C12	C13	C18	H183	1.53	114.52	60.01	109.48	1.09
IC	C14	C13	C18	H183	1.55	113.82	-65.20	109.48	1.09
IC	C17	C13	C18	H183	1.54	105.20	-170.81	109.48	1.09
IC	C12	C13	C18	H181	1.53	114.52	179.95	109.48	1.09
IC	C12	C13	C18	H182	1.53	114.52	-60.04	109.53	1.09

Table S3. Force Field parameters:

Added parameters for E2:

Bond parameters:

CEL1	OH1	334.300	1.4110	Same as OH1 CA

Angle parameters:

CEL1	CEL1	CEL1	40.000	120.00	35.00	2.41620	Same as CA CA CA
OH1	CEL1	CEL1	45.200	120.0000			Same as OH1 CA CA
CEL1	OH1	H	65.000	108.0000			Same as H OH1 CA
CEL1	CTL1	HAL1	40.0	109.47			HA CT C6R from Accelrys CHARMm
CTL1	CTL1	OHL	45.0	110.50			CT CT OT from Accelrys CHARMM

Torsion parameters:

CEL1	CEL1	CTL1	HAL1	0.01	6	0.0	X CT C6R X from Accelrys CHARMM
H	OH1	CEL1	CEL1	0.9900	2	180.00	Same as H OH1 CA CA

Root mean square deviations for the MD simulations.

Table S4. RMSD for all Cα atoms included in the simulations.

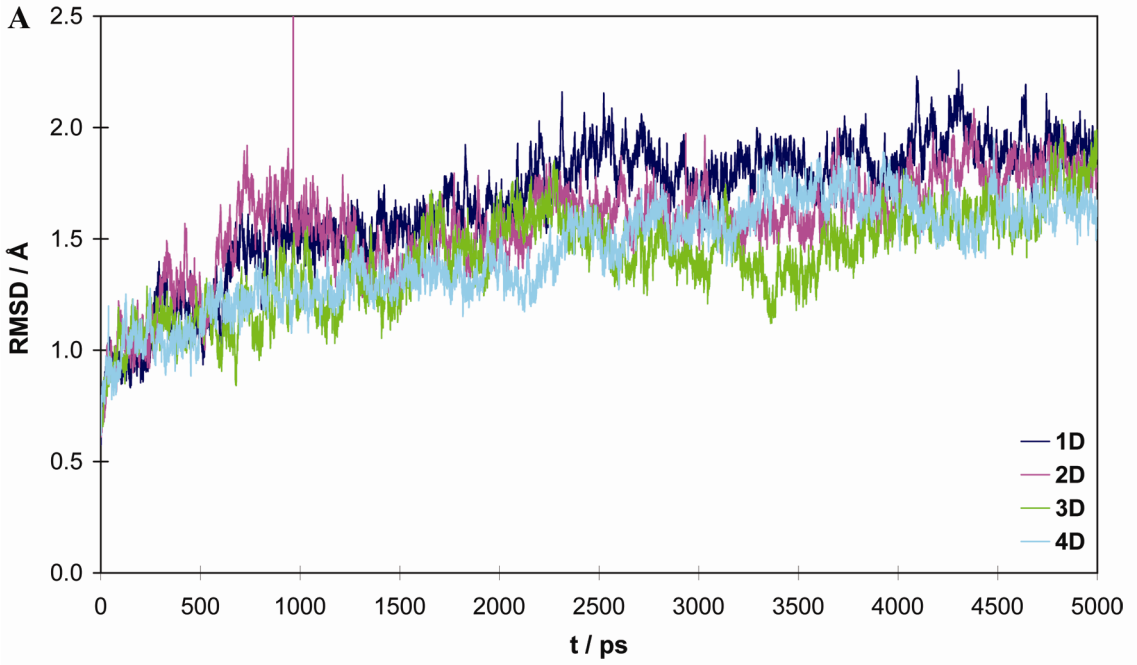

A *Agonist* conformation with His524 protonated on Nδ.

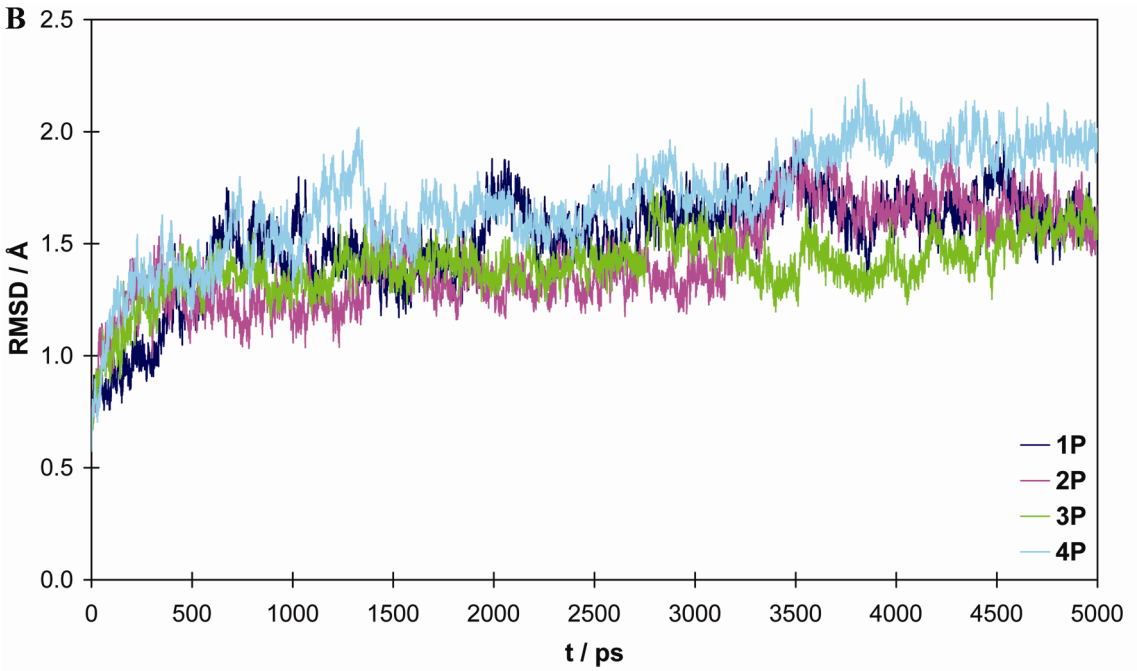

B *Agonist* conformation with His524 charged.

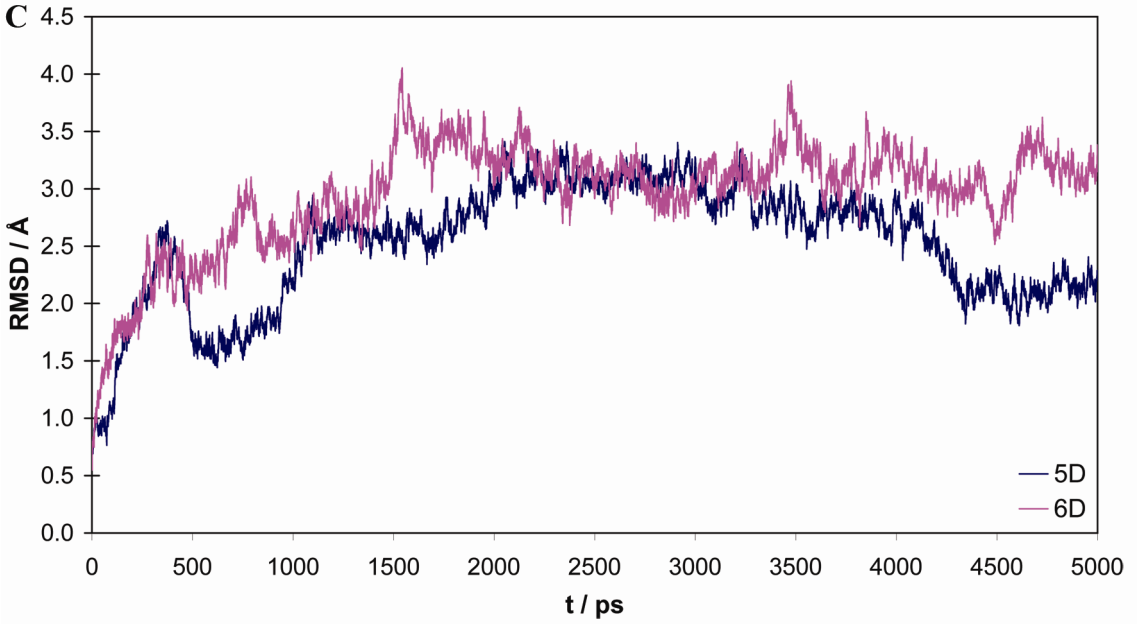

C *Antagonist* conformation with His524 protonated on Nδ.

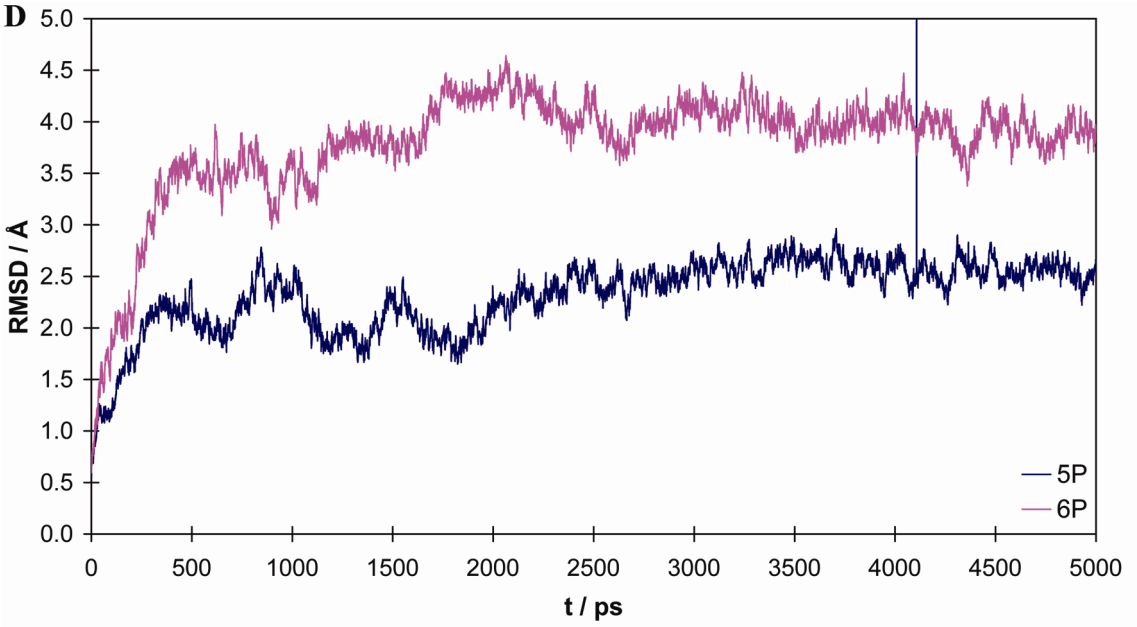

D *Antagonist* conformation with His524 charged.

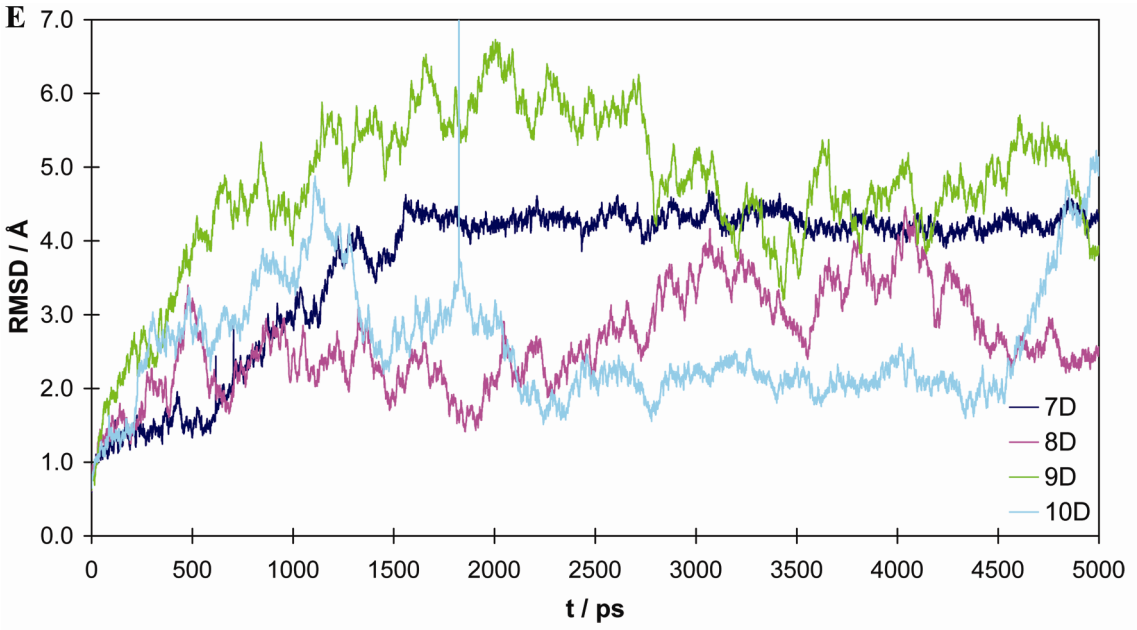

E *Apo* conformation with His524 protonated on Nδ.

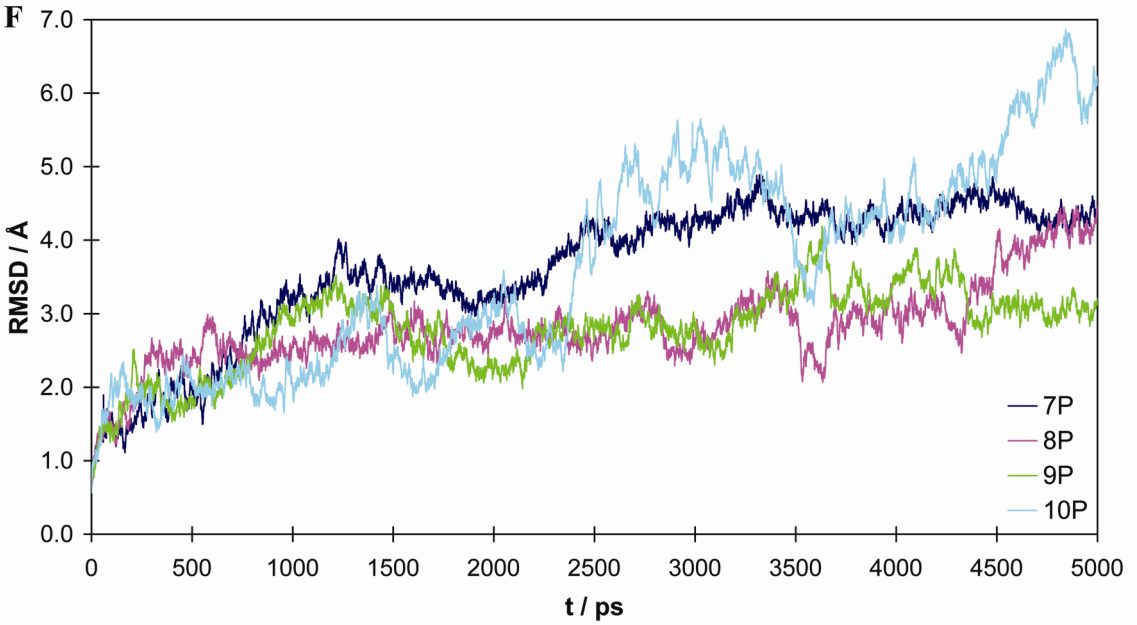

F *Apo* conformation with His524 charged.

Table S5. RMSD for Cα atoms in the core of the protein (residues 306 to 527).

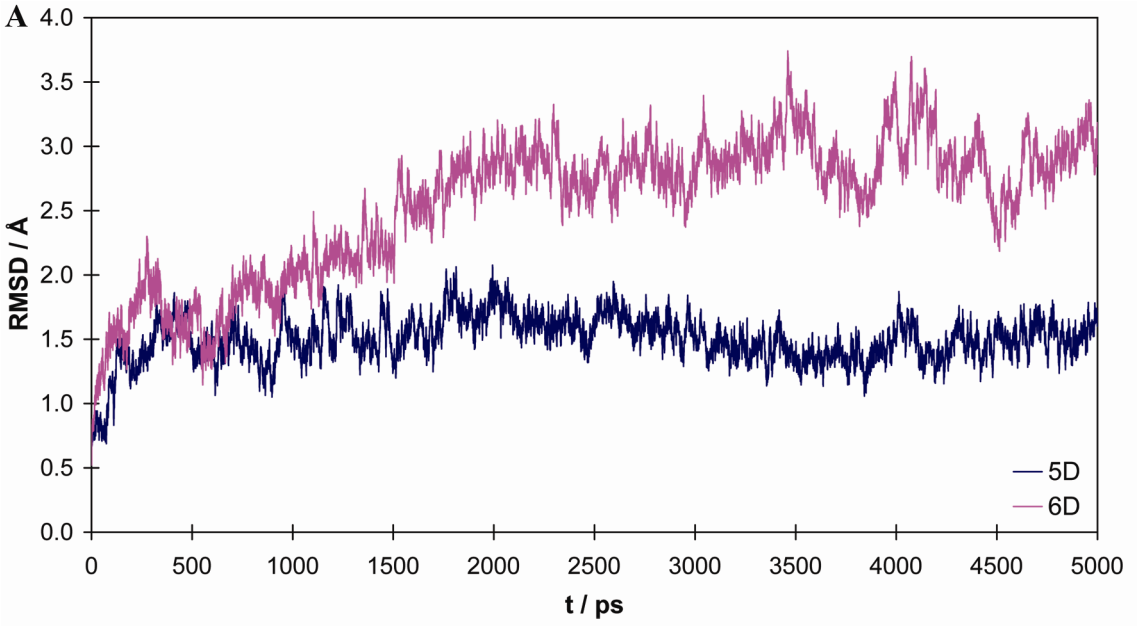

A *Antagonist* conformation with His524 protonated on Nδ.

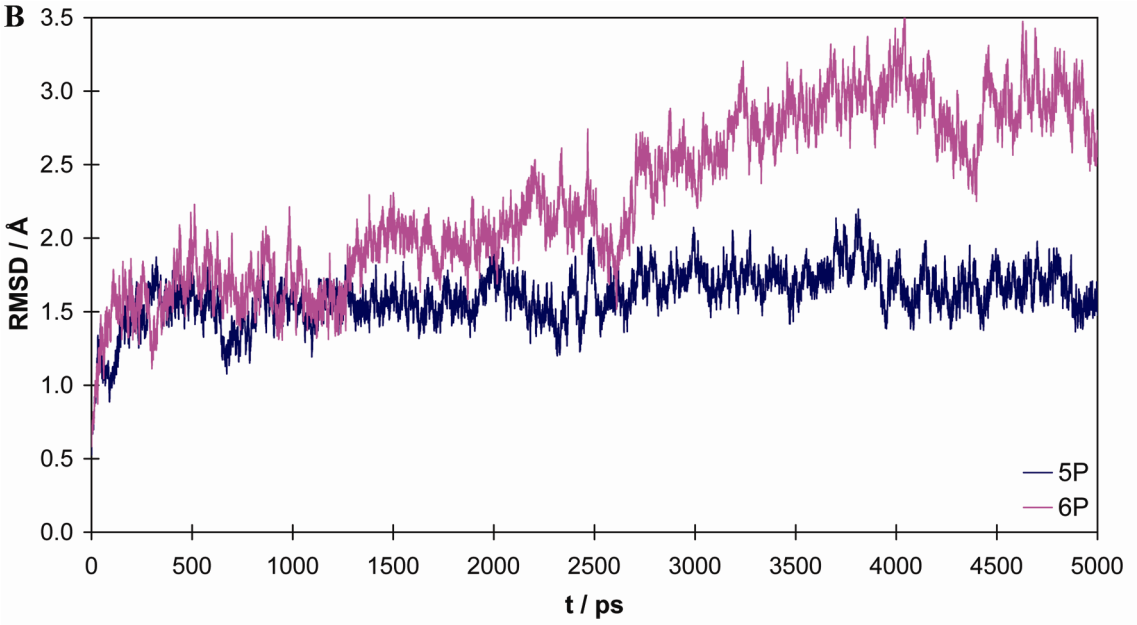

B *Antagonist* conformation with His524 charged.

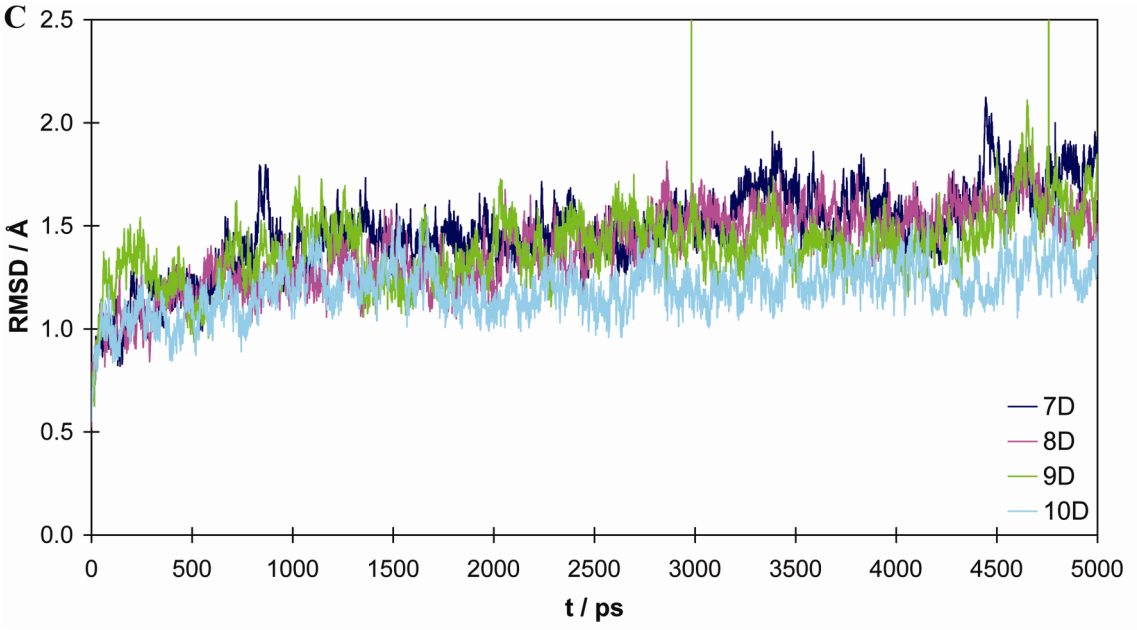

C *Apo* conformation with His524 protonated on Nδ.

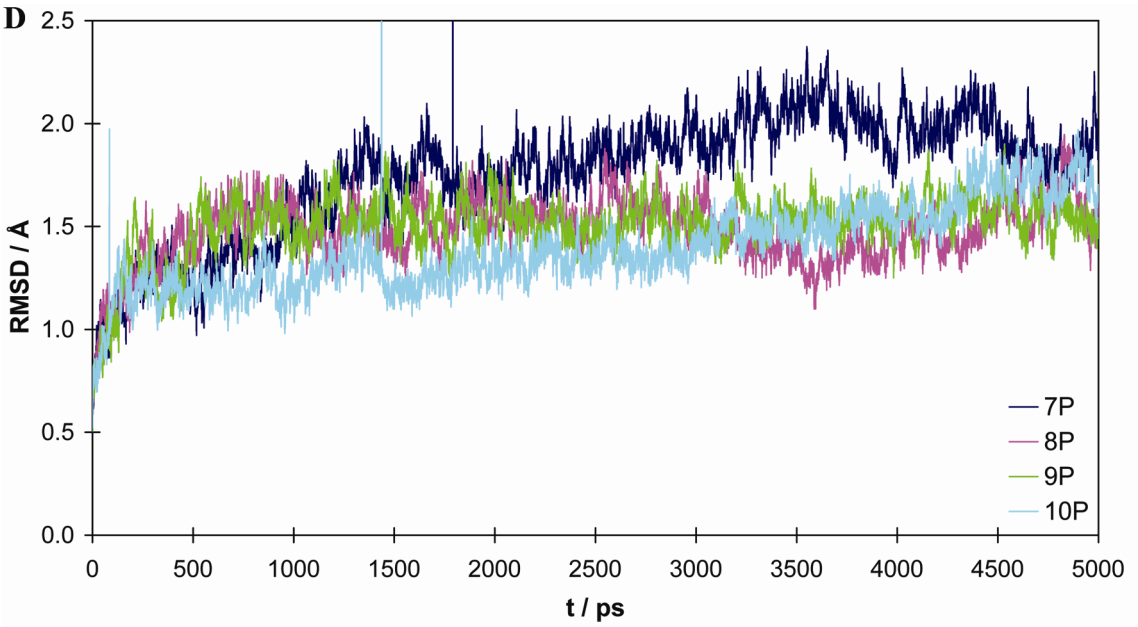

D *Apo* conformation with His524 charged.

Table S6. Hydrogen Bond Zipper

The presence of a hydrogen bond network (zipper) is described by the presence of hydrogen bonds between the following atoms:

Atom	Atom	Dist	Description
His524 (Nδ)	Glu419 (O)	1	Alternative – HB to E2 (O17) in stable simulations.
His524 (Nε)	Glu419 (O)	2	Cannot be present in setups with His524 Nδ.
Glu419 (N)	Glu339 (OE1)	3	These two are equivalent due to rotation of carboxyl-group. Both may be present simultaneously.
Glu419 (N)	Glu339 (OE2)	4	
Lys531 (NZ)	Glu339 (OE1)	5	These two are equivalent due to rotation of carboxyl-group. Both may be present simultaneously.
Lys531 (NZ)	Glu339 (OE2)	6	
Lys531 (NZ)	Glu419 (OE1)	7	These two are equivalent due to rotation of carboxyl-group. Both may be present simultaneously.
Lys531 (NZ)	Glu419 (OE2)	8	

In the tables below statistics for these distances are summed up. For each simulation there are 10.000 snapshots. In each of these the 8 distances are measured and the number of snapshots with distances < 4.00 Å is calculated. While the interactions to His524 are purely of hydrogen bond character the other interactions are also ionic, therefore we have allowed for the atoms to be this far apart. The numbers are summed up for after 1, 2, 3, 4 and 5 ns respectively.

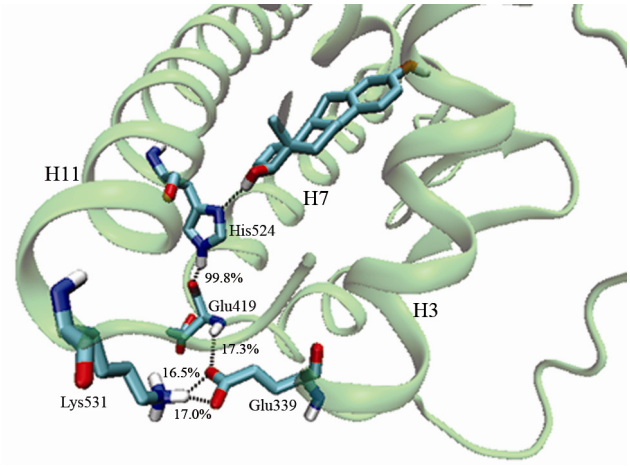

A: His524 as the δ-protonated tautomer

M1

HSD	Dist 1	Dist 2	Dist 3	Dist 4	Dist 5	Dist 6	Dist 7	Dist 8
Total 1ns	23	1169	24	2	0	1	208	166
Total 2ns	23	1227	27	5	0	1	241	213
Total 3ns	23	1227	203	84	0	10	252	234
Total 4ns	23	1227	221	92	17	13	675	660
Total 5ns	23	1227	223	92	17	13	1719	1598

M2

HSD	Dist 1	Dist 2	Dist 3	Dist 4	Dist 5	Dist 6	Dist 7	Dist 8
Total 1ns	2	1377	629	1	0	3	62	32
Total 2ns	2	3085	629	3	0	3	104	91
Total 3ns	4	4688	629	3	0	3	115	135
Total 4ns	4	6180	629	3	82	33	118	136
Total 5ns	4	7413	629	3	82	40	119	136

M3

HSD	Dist 1	Dist 2	Dist 3	Dist 4	Dist 5	Dist 6	Dist 7	Dist 8
Total 1ns	1706	132	45	204	0	0	456	565
Total 2ns	3445	335	216	425	1	3	1197	1593
Total 3ns	5334	494	319	524	1	3	1731	2121
Total 4ns	7190	1114	321	567	350	363	1731	2121
Total 5ns	9004	1552	321	583	1908	2146	1731	2121

M4

HSD	Dist 1	Dist 2	Dist 3	Dist 4	Dist 5	Dist 6	Dist 7	Dist 8
Total 1ns	1875	57	7	122	0	0	1227	1059
Total 2ns	2707	146	147	126	0	1	2241	1878
Total 3ns	3288	720	242	137	7	4	4062	3524
Total 4ns	3627	1175	243	142	227	274	5194	4711
Total 5ns	3893	1407	249	162	239	389	6634	6201

M5

HSD	Dist 1	Dist 2	Dist 3	Dist 4	Dist 5	Dist 6	Dist 7	Dist 8
Total 1ns	126	191	0	0	0	0	0	0
Total 2ns	454	553	0	0	0	0	0	0
Total 3ns	454	555	0	0	0	0	0	0
Total 4ns	648	1170	0	0	0	0	0	0
Total 5ns	872	2481	0	0	0	0	0	0

M6

HSD	Dist 1	Dist 2	Dist 3	Dist 4	Dist 5	Dist 6	Dist 7	Dist 8
Total 1ns	28	82	0	0	0	0	0	0
Total 2ns	28	82	0	0	0	0	0	0
Total 3ns	28	82	0	0	0	0	0	0
Total 4ns	37	126	0	0	0	0	0	0
Total 5ns	38	126	0	0	0	0	0	0

M7

HSD	Dist 1	Dist 2	Dist 3	Dist 4	Dist 5	Dist 6	Dist 7	Dist 8
Total 1ns	568	1093	78	74	1465	1327	26	26
Total 2ns	2120	2096	119	95	3426	3232	26	27
Total 3ns	2715	3418	293	570	5193	5094	110	437
Total 4ns	2715	4890	312	570	7011	6914	110	437
Total 5ns	2715	6400	313	570	7062	6924	110	438

M8

HSD	Dist 1	Dist 2	Dist 3	Dist 4	Dist 5	Dist 6	Dist 7	Dist 8
Total 1ns	1390	724	143	142	840	847	286	327
Total 2ns	1391	2197	143	217	840	848	300	327
Total 3ns	1391	3574	143	219	1001	1061	300	327
Total 4ns	1394	4839	144	220	2801	2776	300	327
Total 5ns	1395	6190	144	221	3126	2840	303	350

M9

HSD	Dist 1	Dist 2	Dist 3	Dist 4	Dist 5	Dist 6	Dist 7	Dist 8
Total 1ns	1490	297	302	155	192	88	151	182
Total 2ns	2992	521	310	250	225	113	151	182
Total 3ns	4649	874	310	256	225	113	151	182
Total 4ns	6258	1101	311	276	229	113	151	182
Total 5ns	8027	1320	311	281	229	113	151	182

M10

HSD	Dist 1	Dist 2	Dist 3	Dist 4	Dist 5	Dist 6	Dist 7	Dist 8
Total 1ns	1821	160	28	262	38	47	235	467
Total 2ns	3645	528	28	263	38	47	235	467
Total 3ns	5317	835	70	270	50	49	235	467
Total 4ns	7149	941	87	303	515	395	235	467
Total 5ns	8918	1028	91	304	558	440	239	467

B: His524 as the ε-protonated tautomer

M1

HSE	Dist 1	Dist 2	Dist 3	Dist 4	Dist 5	Dist 6	Dist 7	Dist 8
Total 1ns	1	1991	170	686	1	0	180	133
Total 2ns	1	3990	835	688	491	486	180	133
Total 3ns	1	5985	1379	1208	987	902	685	633
Total 4ns	1	7982	1380	1428	1517	1407	802	676
Total 5ns	8	9979	1380	1727	1698	1648	804	676

M2

HSE	Dist 1	Dist 2	Dist 3	Dist 4	Dist 5	Dist 6	Dist 7	Dist 8
Total 1ns	0	1995	0	900	0	0	250	268
Total 2ns	0	3993	608	2070	3	1	265	295
Total 3ns	0	5990	1982	2574	6	3	266	295
Total 4ns	0	7986	3465	2575	8	4	266	295
Total 5ns	0	9962	3654	3868	8	6	339	385

M3

HSE	Dist 1	Dist 2	Dist 3	Dist 4	Dist 5	Dist 6	Dist 7	Dist 8
Total 1ns	1341	415	3	1567	7	3	939	593
Total 2ns	2568	959	3	3439	9	4	939	602
Total 3ns	3864	1737	8	3763	13	15	993	626
Total 4ns	5156	2392	71	3763	15	15	1067	744
Total 5ns	6358	2818	74	3765	15	15	1072	753

M4

HSE	Dist 1	Dist 2	Dist 3	Dist 4	Dist 5	Dist 6	Dist 7	Dist 8
Total 1ns	0	1836	230	1012	0	0	269	556
Total 2ns	0	3758	1183	1872	22	23	1619	1925
Total 3ns	0	5640	1885	2322	633	750	2507	2885
Total 4ns	0	7605	1967	4191	2630	2748	3783	3880
Total 5ns	0	9587	1968	6131	4567	4690	5398	4506

M5

HSE	Dist 1	Dist 2	Dist 3	Dist 4	Dist 5	Dist 6	Dist 7	Dist 8
Total 1ns	9	189	0	0	0	0	0	0
Total 2ns	19	717	0	0	0	0	0	0
Total 3ns	317	2330	0	0	0	0	0	0
Total 4ns	445	2898	0	0	0	0	0	0
Total 5ns	466	3407	0	0	0	0	0	0

M6

HSE	Dist 1	Dist 2	Dist 3	Dist 4	Dist 5	Dist 6	Dist 7	Dist 8
Total 1ns	80	559	0	0	0	0	0	0
Total 2ns	84	559	0	0	0	0	0	0
Total 3ns	95	1647	0	0	0	0	0	0
Total 4ns	372	3128	0	0	0	0	0	0
Total 5ns	505	3469	0	0	0	0	0	0

M7

HSE	Dist 1	Dist 2	Dist 3	Dist 4	Dist 5	Dist 6	Dist 7	Dist 8
Total 1ns	0	1997	22	161	1328	1363	9	30
Total 2ns	0	3996	91	204	2734	2809	11	33
Total 3ns	0	5992	114	227	2749	2823	11	33
Total 4ns	0	7964	280	516	2795	2825	11	33
Total 5ns	1	9718	397	962	2795	2825	11	33

M8

HSE	Dist 1	Dist 2	Dist 3	Dist 4	Dist 5	Dist 6	Dist 7	Dist 8
Total 1ns	438	1602	73	390	0	1	50	152
Total 2ns	1482	2654	189	391	0	2	142	373
Total 3ns	2542	3706	677	463	879	905	266	704
Total 4ns	3053	5412	745	478	879	905	266	704
Total 5ns	3584	6906	751	479	879	905	266	704

M9

HSE	Dist 1	Dist 2	Dist 3	Dist 4	Dist 5	Dist 6	Dist 7	Dist 8
Total 1ns	0	1964	0	839	1584	1221	131	265
Total 2ns	6	3915	63	1159	2162	1490	172	291
Total 3ns	123	5722	386	2243	2162	1490	175	304
Total 4ns	238	7496	677	2743	2162	1490	175	304
Total 5ns	239	7507	678	3882	2162	1490	179	304

M10

HSE	Dist 1	Dist 2	Dist 3	Dist 4	Dist 5	Dist 6	Dist 7	Dist 8
Total 1ns	0	1899	81	383	1723	1761	1038	775
Total 2ns	208	3741	84	764	2504	2482	1548	999
Total 3ns	271	4670	85	776	2920	2933	1566	1033
Total 4ns	340	4976	86	778	3292	3336	1716	1149
Total 5ns	770	5205	91	778	5147	5180	2870	2130

C. His524 modelled as the histidinium tautomer

M1

HSP	Dist 1	Dist 2	Dist 3	Dist 4	Dist 5	Dist 6	Dist 7	Dist 8
Total 1ns	431	1216	24	111	0	0	205	158
Total 2ns	432	1591	25	121	1	0	205	158
Total 3ns	447	1695	31	191	16	9	205	158
Total 4ns	559	2769	446	901	16	9	205	158
Total 5ns	669	3657	942	1142	16	9	206	158

M2

HSP	Dist 1	Dist 2	Dist 3	Dist 4	Dist 5	Dist 6	Dist 7	Dist 8
Total 1ns	481	1812	184	294	0	0	730	706
Total 2ns	1612	3722	282	380	0	0	2057	1979
Total 3ns	2330	5664	300	389	0	0	2057	1980
Total 4ns	3200	7032	363	472	0	0	2057	1980
Total 5ns	3570	7964	604	765	0	0	2064	1980

M3

HSP	Dist 1	Dist 2	Dist 3	Dist 4	Dist 5	Dist 6	Dist 7	Dist 8
Total 1ns	521	974	630	1	514	492	475	443
Total 2ns	680	974	643	30	2468	2480	623	609
Total 3ns	927	974	643	331	4446	4480	1684	1433
Total 4ns	1195	974	644	364	6399	6477	1998	1989
Total 5ns	1319	974	644	432	8252	8476	3650	2806

M4

HSP	Dist 1	Dist 2	Dist 3	Dist 4	Dist 5	Dist 6	Dist 7	Dist 8
Total 1ns	218	2000	26	5	0	0	203	196
Total 2ns	586	3597	26	7	0	0	203	196
Total 3ns	1620	5476	26	7	0	0	211	196
Total 4ns	2018	6952	44	79	0	0	218	203
Total 5ns	2388	8295	113	224	0	0	219	204

M5

HSP	Dist 1	Dist 2	Dist 3	Dist 4	Dist 5	Dist 6	Dist 7	Dist 8
Total 1ns	158	318	0	0	0	0	0	0
Total 2ns	407	591	0	0	0	0	0	0
Total 3ns	679	659	0	0	0	0	0	0
Total 4ns	959	697	0	0	0	0	0	0
Total 5ns	1046	797	0	0	0	0	0	0

M6

HSP	Dist 1	Dist 2	Dist 3	Dist 4	Dist 5	Dist 6	Dist 7	Dist 8
Total 1ns	60	62	0	0	0	0	180	200
Total 2ns	185	137	0	0	0	0	180	200
Total 3ns	332	326	0	0	0	0	180	201
Total 4ns	441	345	0	0	0	0	320	254
Total 5ns	623	373	0	0	0	0	325	256

M7

HSP	Dist 1	Dist 2	Dist 3	Dist 4	Dist 5	Dist 6	Dist 7	Dist 8
Total 1ns	0	1996	76	478	1	2	1331	1410
Total 2ns	26	3991	173	1220	1	8	1331	1415
Total 3ns	437	5926	360	1898	1	8	1331	1415
Total 4ns	1342	7493	448	2275	1	8	1331	1415
Total 5ns	1904	7763	468	2347	1	8	1331	1415

M8

HSP	Dist 1	Dist 2	Dist 3	Dist 4	Dist 5	Dist 6	Dist 7	Dist 8
Total 1ns	581	616	224	845	6	0	78	103
Total 2ns	746	1529	1022	1306	6	0	78	103
Total 3ns	1549	2897	1721	2170	6	0	78	103
Total 4ns	2251	3816	1721	2174	6	0	78	103
Total 5ns	2773	4613	1722	2174	6	0	78	103

M9

HSP	Dist 1	Dist 2	Dist 3	Dist 4	Dist 5	Dist 6	Dist 7	Dist 8
Total 1ns	75	1997	58	160	3	1	21	75
Total 2ns	88	3991	965	386	87	31	1011	1172
Total 3ns	90	5985	981	463	89	116	2609	2863
Total 4ns	759	7938	981	463	92	116	3947	4200
Total 5ns	831	9935	987	470	92	116	4093	4440

M10

HSP	Dist 1	Dist 2	Dist 3	Dist 4	Dist 5	Dist 6	Dist 7	Dist 8
Total 1ns	37	609	522	119	550	519	584	130
Total 2ns	37	704	1025	292	2125	1922	1354	614
Total 3ns	37	733	1026	295	2262	1960	1354	616
Total 4ns	161	1112	1027	295	2263	1960	1354	616
Total 5ns	1135	2780	1028	303	2263	1960	1354	616

Table S7. Unwinding of H11

The length of H11 is measured by assuming α-helical structures, implying the presence of hydrogen bonds between the backbone O in residue (n) and the backbone NH in residue (n+4).

In the tables below statistics for these distances are summed up. For each simulation there are 10.000 snapshots. In each of these 12 residues are considered to be the (n+4) residue and distances are measured and the number of snapshots with distances < 3.50 Å is calculated. This distance is slightly longer than the ~ 3 Å preferred distance for hydrogen bonds and is used to allow for "breathing" in the helix. The numbers are summed up for after 1, 2, 3, 4 and 5 ns respectively.

A: His524 as the δ-protonated tautomer

A **M1**

HSD	527	528	529	530	531	532	533	534	535	536	537	538
Total 1 ns	1902	1879	1924	1910	1823	1635	0	0	0	0	0	0
Total 2 ns	3550	3711	3874	3470	3561	2307	0	0	0	0	0	0
Total 3 ns	5420	5570	5851	4791	4809	2307	0	0	0	0	0	0
Total 4 ns	7253	7306	7831	6452	6475	2307	0	0	0	0	0	0
Total 5 ns	8708	9245	9819	8134	8134	2307	0	0	0	0	0	0

M2

HSD	527	528	529	530	531	532	533	534	535	536	537	538
Total 1 ns	1980	1827	1865	1943	1782	1488	0	0	0	0	0	0
Total 2 ns	3954	3799	3752	3940	3613	2944	0	0	0	0	0	0
Total 3 ns	5873	5757	5597	5932	5349	4022	0	0	0	0	0	0
Total 4 ns	7842	7740	7526	7906	7049	5400	0	0	0	0	0	0
Total 5 ns	9811	9728	9405	9895	8697	6959	0	0	0	0	0	0

M3

HSD	527	528	529	530	531	532	533	534	535	536	537	538
Total 1 ns	1968	1891	1634	1996	1894	847	0	0	0	0	0	0
Total 2 ns	3927	3856	3408	3995	3843	1589	0	0	0	0	0	0
Total 3 ns	5876	5690	5293	5992	5617	2381	0	0	0	0	0	0
Total 4 ns	7831	7593	7163	7992	7372	3291	0	0	0	0	0	0
Total 5 ns	9822	9547	9155	9986	7567	3315	0	0	0	0	0	0

M4

HSD	527	528	529	530	531	532	533	534	535	536	537	538
Total 1 ns	1828	1527	1782	1971	1762	748	0	0	0	0	0	0
Total 2 ns	3644	3366	3711	3663	3677	748	0	0	0	0	0	0
Total 3 ns	5452	5213	5647	5298	5374	748	0	0	0	0	0	0
Total 4 ns	7114	7022	7615	6438	6579	748	0	0	0	0	0	0
Total 5 ns	8706	8889	9580	7440	8108	748	0	0	0	0	0	0

M5

HSD	527	528	529	530	531	532	533	534	535	536	537	538
Total 1 ns	911	1879	1841	0	0	0	0	0	0	0	0	0
Total 2 ns	2024	3644	3684	8	0	0	1	0	0	0	0	0
Total 3 ns	3557	5412	5682	118	0	0	6	0	0	0	0	0
Total 4 ns	4833	7353	7682	372	0	0	10	0	0	0	0	0
Total 5 ns	6192	9267	9675	688	0	0	10	0	0	0	0	0

M6

HSD	527	528	529	530	531	532	533	534	535	536	537	538
Total 1 ns	994	1220	203	0	0	0	0	0	0	0	0	0
Total 2 ns	1536	1498	203	0	0	0	0	0	0	0	0	0
Total 3 ns	2996	3015	352	0	0	0	0	0	0	0	0	0
Total 4 ns	4312	4458	846	0	0	0	0	0	0	0	0	0
Total 5 ns	5583	5776	846	0	0	0	0	0	0	0	0	0

M7

HSD	527	528	529	530	531	532	533	534	535	536	537	538
Total 1 ns	1674	1861	1818	1698	1773	1767	96	0	0	0	0	0
Total 2 ns	3197	3861	3762	3442	3721	3722	96	0	0	0	0	0
Total 3 ns	5062	5858	5639	5162	5583	5705	96	0	0	0	0	0
Total 4 ns	6969	7855	7624	7072	7450	7697	96	0	0	0	0	0
Total 5 ns	8947	9855	9590	9049	9369	9697	96	0	0	0	0	0

M8

HSD	527	528	529	530	531	532	533	534	535	536	537	538
Total 1 ns	1324	1949	1983	1237	1005	1753	896	80	2	0	0	0
Total 2 ns	3191	3857	3860	2826	1388	3105	2329	207	2	0	0	0
Total 3 ns	4859	5847	5760	4272	1821	4210	3671	542	2	0	0	0
Total 4 ns	6642	7843	7628	5988	3259	5866	5256	1644	2	0	0	0
Total 5 ns	8348	9842	9258	7543	5000	7474	6313	2148	2	0	0	0

M9

HSD	527	528	529	530	531	532	533	534	535	536	537	538
Total 1 ns	1573	1827	1596	1811	929	0	0	0	0	0	0	0
Total 2 ns	3427	3695	3003	3784	989	0	0	0	0	0	0	0
Total 3 ns	5134	5502	4851	5743	1006	0	0	0	0	0	0	0
Total 4 ns	7052	7341	6452	7644	1722	141	0	0	0	0	0	0
Total 5 ns	8973	9157	7778	8869	2044	183	0	0	0	0	0	0

M10

HSD	527	528	529	530	531	532	533	534	535	536	537	538
Total 1 ns	1662	1528	1718	1660	316	0	0	0	0	0	0	0
Total 2 ns	3505	3148	3058	3334	316	0	0	0	0	0	0	0
Total 3 ns	5414	4920	3681	5330	368	0	0	0	0	0	0	0
Total 4 ns	7224	6644	4371	7231	578	0	0	0	0	0	0	0
Total 5 ns	9058	8431	5437	8995	996	0	0	0	0	0	0	0

B: His524 as the ε-protonated tautomer

B M1

HSE	527	528	529	530	531	532	533	534	535	536	537	538
Total 1 ns	1927	1960	1925	1996	1830	1108	0	0	0	0	0	0
Total 2 ns	3884	3886	3881	3992	3449	2595	0	0	0	0	0	0
Total 3 ns	5807	5871	5860	5879	5296	4559	0	0	0	0	0	0
Total 4 ns	7746	7862	7848	7505	7110	6468	0	0	0	0	0	0
Total 5 ns	9668	9823	9842	9202	8821	8356	0	0	0	0	0	0

M2

HSE	527	528	529	530	531	532	533	534	535	536	537	538
Total 1 ns	1884	1829	1880	1994	1836	895	0	0	0	0	0	0
Total 2 ns	3839	3817	3796	3990	3762	1946	0	0	0	0	0	0
Total 3 ns	5792	5776	5647	5968	5710	3273	1	0	0	0	0	0
Total 4 ns	7726	7714	7456	7950	7708	4529	1	0	0	0	0	0
Total 5 ns	9679	9666	9315	9938	9704	5864	1	0	0	0	0	0

M3

HSE	527	528	529	530	531	532	533	534	535	536	537	538
Total 1 ns	1968	1727	1597	1971	1852	1161	0	0	0	0	0	0
Total 2 ns	3954	3518	3130	3947	3760	2293	0	0	0	0	0	0
Total 3 ns	5926	5343	4785	5936	5723	3444	0	0	0	0	0	0
Total 4 ns	7901	7232	6457	7904	7721	4645	0	0	0	0	0	0
Total 5 ns	9889	9105	7912	9814	9717	5713	0	0	0	0	0	0

M4

HSE	527	528	529	530	531	532	533	534	535	536	537	538
Total 1 ns	1979	1943	1904	1997	1876	826	0	0	0	0	0	0
Total 2 ns	3973	3883	3789	3959	3680	2354	0	0	0	0	0	0
Total 3 ns	5953	5860	5701	5943	5505	3947	0	0	0	0	0	0
Total 4 ns	7938	7853	7670	7933	7461	5811	0	0	0	0	0	0
Total 5 ns	9921	9845	9647	9922	9418	7792	0	0	0	0	0	0

M5

HSE	527	528	529	530	531	532	533	534	535	536	537	538
Total 1 ns	1375	1545	982	0	0	0	0	0	0	0	0	0
Total 2 ns	2936	2604	1074	0	0	0	8	0	0	0	0	0
Total 3 ns	4523	4509	2976	230	0	0	9	0	0	0	0	0
Total 4 ns	6107	6480	4929	386	0	0	10	0	0	0	0	0
Total 5 ns	7830	8342	6882	477	0	0	11	0	0	0	0	0

M6

HSE	527	528	529	530	531	532	533	534	535	536	537	538
Total 1 ns	1387	979	1062	83	0	0	0	0	0	0	0	0
Total 2 ns	2813	1670	1826	130	0	0	0	0	0	0	0	0
Total 3 ns	4311	2079	2598	259	0	0	0	0	0	0	0	0
Total 4 ns	5835	2313	3306	600	0	0	0	0	0	0	0	0
Total 5 ns	6945	2490	4262	745	0	0	0	0	0	0	0	0

M7

HSE	527	528	529	530	531	532	533	534	535	536	537	538
Total 1 ns	1671	1923	1312	1647	240	0	0	0	0	0	0	0
Total 2 ns	3302	3910	3146	2623	259	0	0	0	0	0	0	0
Total 3 ns	4951	5898	5021	2777	262	0	0	0	0	0	0	0
Total 4 ns	6688	7851	7002	2854	268	0	0	0	0	0	0	0
Total 5 ns	8563	9816	8985	2962	268	0	0	0	0	0	0	0

M8

HSE	527	528	529	530	531	532	533	534	535	536	537	538
Total 1 ns	1058	1773	1860	1699	1711	248	0	0	0	0	0	0
Total 2 ns	2502	3733	3813	3393	3255	292	0	0	0	0	0	0
Total 3 ns	4303	5665	5261	5094	4675	292	0	0	0	0	0	0
Total 4 ns	6113	7475	7088	6931	5200	292	0	0	0	0	0	0
Total 5 ns	8063	9436	9046	8207	5219	292	0	0	0	0	0	0

M9

HSE	527	528	529	530	531	532	533	534	535	536	537	538
Total 1 ns	1507	1868	1946	1226	1297	1183	1014	4	0	0	0	0
Total 2 ns	2965	3564	3885	2611	2848	3175	2830	4	0	0	0	0
Total 3 ns	4188	5226	5822	4313	4597	5154	4048	4	0	0	0	0
Total 4 ns	5954	7147	7689	6186	6526	7134	5159	7	0	0	0	0
Total 5 ns	7838	9130	9595	8168	8297	8674	6867	13	0	0	0	0

M10

HSE	527	528	529	530	531	532	533	534	535	536	537	538
Total 1 ns	1783	1891	1776	1516	1212	0	0	0	0	0	0	0
Total 2 ns	3619	3860	3496	3080	2714	542	1	0	0	0	0	0
Total 3 ns	5532	5845	5333	4934	4639	2509	37	0	0	0	0	0
Total 4 ns	7493	7761	7040	6805	6228	4341	158	0	0	0	0	0
Total 5 ns	9463	9756	8481	8534	8058	6232	169	0	0	0	0	0

C. His524 modelled as the histidinium tautomer

C M1

HSP	527	528	529	530	531	532	533	534	535	536	537	538
Total 1 ns	1966	1799	1813	1908	1839	1452	0	0	0	0	0	0
Total 2 ns	3938	3701	3739	3845	3614	3106	0	0	0	0	0	0
Total 3 ns	5893	5613	5715	5828	5401	4599	0	0	0	0	0	0
Total 4 ns	7849	7563	7678	7825	7219	5876	0	0	0	0	0	0
Total 5 ns	9783	9513	9644	9818	9076	7253	0	0	0	0	0	0

M2

HSP	527	528	529	530	531	532	533	534	535	536	537	538
Total 1 ns	1945	1217	1515	1992	1718	1123	0	0	0	0	0	0
Total 2 ns	3928	2869	3399	3990	3475	2273	0	0	0	0	0	0
Total 3 ns	5923	4731	5262	5960	5330	3867	0	0	0	0	0	0
Total 4 ns	7901	6622	7045	7816	7134	5271	0	0	0	0	0	0
Total 5 ns	9851	8350	9027	9774	8594	6793	0	0	0	0	0	0

M3

HSP	527	528	529	530	531	532	533	534	535	536	537	538
Total 1 ns	1874	1894	1959	1979	1655	1254	0	0	0	0	0	0
Total 2 ns	3711	3763	3929	3974	3118	2301	0	0	0	0	0	0
Total 3 ns	5536	5715	5900	5973	4467	2578	0	0	0	0	0	0
Total 4 ns	7409	7539	7885	7925	6087	3904	0	0	0	0	0	0
Total 5 ns	9319	9426	9859	9924	7953	5314	0	0	0	0	0	0

M4

HSP	527	528	529	530	531	532	533	534	535	536	537	538
Total 1 ns	1958	1809	1947	1951	1752	1446	0	0	0	0	0	0
Total 2 ns	3799	3683	3866	3930	3650	2908	0	0	0	0	0	0
Total 3 ns	5657	5582	5860	5923	5612	4501	0	0	0	0	0	0
Total 4 ns	7504	7498	7847	7902	7562	6103	0	0	0	0	0	0
Total 5 ns	9331	9474	9833	9867	9512	7819	0	0	0	0	0	0

M5

HSP	527	528	529	530	531	532	533	534	535	536	537	538
Total 1 ns	1496	1766	1255	0	0	0	0	0	0	0	0	0
Total 2 ns	2872	3635	2571	0	0	0	0	0	0	0	0	0
Total 3 ns	4420	5587	4119	0	0	0	0	0	0	0	0	0
Total 4 ns	5996	7273	6028	0	0	0	0	0	0	0	0	0
Total 5 ns	7397	9185	7600	64	0	0	0	0	0	0	0	0

M6

HSP	527	528	529	530	531	532	533	534	535	536	537	538
Total 1 ns	1095	1555	1723	1263	937	1502	66	0	0	0	0	0
Total 2 ns	2254	2495	3680	3069	1592	3413	232	0	0	0	0	0
Total 3 ns	3848	3739	5255	4850	1932	4423	353	0	0	0	0	0
Total 4 ns	5621	5467	6808	6560	3123	5847	414	0	0	0	0	0
Total 5 ns	7030	6834	8561	8417	4376	7795	531	0	0	0	0	0

M7

HSP	527	528	529	530	531	532	533	534	535	536	537	538
Total 1 ns	1823	1759	1405	1603	1626	1372	115	0	0	0	0	0
Total 2 ns	3453	3661	3099	3220	2944	1909	133	0	0	0	0	0
Total 3 ns	4847	5516	5002	4598	3977	2119	137	0	0	0	0	0
Total 4 ns	6012	7346	6938	6027	4476	2291	147	0	0	0	0	0
Total 5 ns	6844	8264	8932	7942	5388	2442	147	0	0	0	0	0

M8

HSP	527	528	529	530	531	532	533	534	535	536	537	538
Total 1 ns	1523	1111	1802	1498	1134	1682	1268	748	187	0	0	0
Total 2 ns	3321	2171	3745	3492	2896	3368	3089	1864	187	0	0	0
Total 3 ns	5034	3512	5729	5454	4370	4765	4897	3729	187	0	0	0
Total 4 ns	6603	5363	7720	7400	6181	6462	6773	5620	205	0	0	0
Total 5 ns	8442	7210	9650	9363	8089	8361	8627	6862	426	0	0	0

M9

HSP	527	528	529	530	531	532	533	534	535	536	537	538
Total 1 ns	1471	1037	1702	1722	1294	1546	364	0	0	0	0	0
Total 2 ns	3063	2836	3486	3149	2395	3518	810	0	0	0	0	0
Total 3 ns	4922	4589	4955	5032	4192	5464	1080	0	0	0	0	0
Total 4 ns	6487	6544	6417	6831	5947	7399	1604	0	0	0	0	0
Total 5 ns	8169	8524	8362	8712	7681	9029	2064	4	0	0	0	0

M10

HSP	527	528	529	530	531	532	533	534	535	536	537	538
Total 1 ns	1146	1705	1931	1881	419	0	0	0	0	0	0	0
Total 2 ns	2253	3481	3779	3863	610	0	0	0	0	0	0	0
Total 3 ns	3839	5041	5732	5816	680	0	0	0	0	0	0	0
Total 4 ns	5189	6690	7678	7765	713	0	0	0	0	0	0	0
Total 5 ns	7058	8567	9605	9763	832	0	0	0	0	0	0	0

References for Supporting Information

Full reference for ref. (*70*)
MacKerell, A. D. J.; Bashford, D.; Bellott, M.; Dunbrack Jr., R. L.; Evanseck, J. D.; Field, M. J.; Fischer, S.; Gao, J.; Guo, H.; Ha, S.; Joseph-McCarthy, D.; Kuchnir, L.; Kuczera, K.; Lau, F. T. K.; Mattos, C.; Michnick, S.; Ngo, T.; Nguyen, D. T.; Prodhorn, B.; Reiher III, W. E.; Roux, B.; Schlenkrich, M.; Smith, J. C.; Stote, R.; Straub, J.; Watanabe, M.; Wiórkiewicz-Kuczera, J.; Yin, D.; Karplus, M. (1998) All-Atom Empirical Potential for Molecular Modeling and Dynamics Studies of Proteins, *J. Phys. Chem. B 102,* 3586-3616.